

U.S. Environmental
Protection Agency

Electric Power
Research Institute

Topics:
Particulates
Fabric filters
Electrostatic precipitators
Sulfur dioxide
Gaseous wastes
Environment

EPRI CS-4404
Volume 3
Project 1835-6
Proceedings
February 1986



Proceedings: Fifth Symposium on the Transfer and Utilization of Particulate Control Technology

Volume 3

Prepared by
Research Triangle Institute
Research Triangle Park, North Carolina

R E P O R T S U M M A R Y

SUBJECTS	Particulate control / Integrated environmental control / SO _x control	
TOPICS	Particulates Fabric filters Electrostatic precipitators	Sulfur dioxide Gaseous wastes Environment
AUDIENCE	Environmental engineers and operators	

Proceedings: Fifth Symposium on the Transfer and Utilization of Particulate Control Technology

Volumes 1-4

From a speculative discussion of the future regulatory framework in the opening sessions to the detailed treatments of particulate and fugitive emissions control in the following days, this symposium updated the research community on the range of promising technologies. The report includes the more than 100 papers presented.

BACKGROUND	In 1984, EPRI joined EPA as cosponsor of this symposium. The meeting—sponsored in the past by EPA alone—has taken place at 18-month intervals.
OBJECTIVES	<ul style="list-style-type: none">• To promote the transfer of results from particulate control research to potential users of those technologies.• To provide an exchange of ideas among researchers active in the field.
APPROACH	The 430 professionals attending the symposium on August 27-30, 1984, in Kansas City, Missouri, represented utilities, manufacturers, state and federal agencies, educational institutions, and research organizations. From more than 100 presentations, they learned of developments in such areas as electrostatic precipitators, fabric filters, fugitive emissions, and dry SO ₂ control processes. The discussions touched on many aspects of new and old technologies—from economics to operation and maintenance to the development and testing of advanced concepts.
KEY POINTS	The proceedings, which include all formal presentations from the conference, report the research efforts of air pollution control equipment manufacturers, as well as EPA and EPRI. Of particularly broad interest are papers addressing trends in particulate environmental regulations and their possible impacts on those manufacturers, utilities, and the iron and steel industry. Papers having a more detailed focus explore developments in electrostatic precipitator controls and other performance-enhancing technologies, as well as materials and bag-cleaning methods for fabric filters and such new SO ₂ control methods as dry sorbent furnace injection and spray

drying. In addition, several papers consider fugitive emissions control, a growing environmental concern.

EPRI PERSPECTIVE These presentations stimulated new interest in promising technologies, as evidenced by the many requests for further information both at the conference and afterward. Subsequent developments in particulate control will be the focus of the sixth symposium, to be held in February 1986 in New Orleans.

PROJECT RP1835-6
EPRI Project Manager: Ralph F. Altman
Coal Combustion Systems Division
Contractor: Research Triangle Institute

For further information on EPRI research programs, call
EPRI Technical Information Specialists (415) 855-2411.

Proceedings: Fifth Symposium on the
Transfer and Utilization of Particulate Control
Technology
Volume 3

CS-4404, Volume 3
Research Project 1835-6

Proceedings, February 1986

Kansas City, Missouri
August 27–30, 1984

Prepared by

RESEARCH TRIANGLE INSTITUTE
Cornwallis Road
Research Triangle Park, North Carolina 27709

Compiler
F. A. Ayer

Prepared for

U.S. Environmental Protection Agency
Office of Research and Development
401 M Street, SW
Washington, D.C. 20460

Air and Energy Engineering Research Laboratory
Research Triangle Park, North Carolina 27711

EPA Project Officer
D. L. Harmon

Electric Power Research Institute
3412 Hillview Avenue
Palo Alto, California 94304

EPRI Project Manager
R. F. Altman

Air Quality Control Program
Coal Combustion Systems Division

ORDERING INFORMATION

Requests for copies of this report should be directed to Research Reports Center (RRC), Box 50490, Palo Alto, CA 94303, (415) 965-4081. There is no charge for reports requested by EPRI member utilities and affiliates, U.S. utility associations, U.S. government agencies (federal, state, and local), media, and foreign organizations with which EPRI has an information exchange agreement. On request, RRC will send a catalog of EPRI reports.

Copyright © 1986 Electric Power Research Institute, Inc. All rights reserved.

NOTICE

This report was prepared by the Electric Power Research Institute, Inc. (EPRI). Neither EPRI, members of EPRI, nor any person acting on their behalf: (a) makes any warranty, express or implied, with respect to the use of any information, apparatus, method, or process disclosed in this report or that such use may not infringe privately owned rights; or (b) assumes any liabilities with respect to the use of, or for damages resulting from the use of, any information, apparatus, method, or process disclosed in this report; or (c) is responsible for statements made or opinions expressed by individual authors.

ABSTRACT

These proceedings are of the Fifth Symposium on the Transfer and Utilization of Particulate Control Technology, held August 27 to 30, 1984, in Kansas City, Missouri. The symposium was sponsored by EPA's Air and Energy Engineering Research Laboratory (formerly Industrial Environmental Research Laboratory), located in Research Triangle Park, North Carolina, and the EPRI Coal Combustion Systems Division, located in Palo Alto, California.

The objective of the symposium was to provide for the exchange of knowledge and to stimulate new ideas for particulate control with the goal of extending the technology and aiding its diffusion among designers, users, and educators. Fabric filters and electrostatic precipitators were the major topics, but novel concepts and advanced technologies were also explored. The organization of sessions was as follows:

- Day 1
 - Plenary session
 - ESP: Performance Estimating (Modeling)
 - FF: Practical Considerations
 - Economics
 - Novel Concepts
- Day 2
 - ESP: Performance Enhancement I
 - FF: Full-Scale Studies I (Coal-Fired Boilers)
 - Fugitive Emissions I
 - ESP: Performance Enhancement II
 - FF: Full-Scale Studies II (Coal-Fired Boilers)
 - Fugitive Emissions II
- Day 3
 - ESP: Advanced Technology I
 - FF: Fundamentals/Masurement Techniques

--Dry SO₂ Removal I

--ESP: Advanced Technology II

--FF: Advanced Concepts

--Dry SO₂ Removal II

Day 4

--ESP: Fundamentals I

--FF: Pilot-Scale Studies (Coal-Fired Boilers)

--Operation and Maintenance I

--ESP: Fundamentals II

--Advanced Energy Applications

--Operations and Maintenance II

Volume 1 contains 19 papers presented at the Plenary, Advanced Energy Applications, Economics and Novel Concepts Sessions.

Volume 2 contains 33 papers presented at the ESP: Performance Estimating (Modeling), ESP: Performance Enhancement I and II, ESP: Advanced Technology I and II, and ESP: Fundamentals I and II Sessions, plus one unrepresented paper.

Volume 3 contains 24 papers presented at the FF: Practical Considerations, FF: Full-Scale Studies I and II (Coal-Fired Boilers), FF: Fundamentals/Measuring Techniques, FF: Advanced Concepts, and FF: Pilot-Scale Studies (Coal-Fired Boilers) Sessions.

Volume 4 contains 29 papers presented at the Fugitive Emissions I and II, Dry SO₂ Removal I and II, and Operation and Maintenance I and II Sessions.

PREFACE

These proceedings for the Fifth Symposium on the Transfer and Utilization of Particulate Control Technology constitute the final report submitted to EPA's Air and Energy Engineering Research Laboratory (AEERL), Research Triangle Park, North Carolina, and to the Coal Combustion Systems Division, EPRI, Palo Alto, California. The symposium was conducted at the Hyatt Regency Hotel at the Crown Center in Kansas City, Missouri, August 27-30, 1984.

This symposium (the first jointly sponsored by EPA and EPRI) was designed to provide a forum for the exchange of knowledge and to stimulate new ideas for particulate control with the goal of extending technology and aiding its diffusion among designers, users, educators, and researchers. In the opening session, an address was given on the regulatory framework for future particulate technology needs followed by a series of addresses on the impact of coming particulate requirements on the utility industry and the iron and steel industry as well as the viewpoint of large and small manufacturers. There were subsequent technical sessions on electrostatic precipitator performance estimating (modeling), ESP performance enhancement, ESP advanced technology, ESP fundamentals, practical considerations for fabric filters, fabric filter full-scale studies (coal-fired boilers), fabric filter fundamentals/measurement techniques, fabric filter pilot-scale studies (coal-fired boilers), fugitive emissions, dry SO₂ removal, operation and maintenance, and advanced energy applications. Participants represented electric utilities, equipment and process suppliers, state environmental agencies, coal and petroleum suppliers, EPA and other Federal agencies, educational institutions, and research organizations.

The following persons contributed their efforts to this symposium:

- Dale L. Harmon, Chemical Engineer, Particulate Technology Branch, Utilities and Industrial Power Division, U.S. EPA, AEERL, Research Triangle Park, North Carolina, was a symposium co-general chairman and EPA project officer.
- Ralph F. Altman, Ph.D., Project Manager, Coal Combustion Systems Division, EPRI, Chattanooga, Tennessee, was a co-general chairman and EPRI project manager.
- Franklin A. Ayer, Consultant, Research Triangle Institute, Research Triangle Park, North Carolina, was the overall symposium coordinator and compiler of the proceedings.

TABLE OF CONTENTS

VOLUME 1, PLENARY, ADVANCED ENERGY APPLICATIONS, ECONOMICS, AND
NOVEL CONCEPTS

VOLUME 2, ELECTROSTATIC PRECIPITATION

VOLUME 3, FABRIC FILTRATION

VOLUME 4, FUGITIVE EMISSIONS, DRY SO₂, AND OPERATION AND MAINTENANCE

VOLUME 1 PLENARY, ADVANCED ENERGY APPLICATIONS, ECONOMICS, AND NOVEL CONCEPTS

<u>Section</u>	<u>Page</u>
Session 1: PLENARY SESSION	
Everett L. Plyler, Chairman	
The Regulatory Framework for Future Particulate Technology Needs	1-1
Sheldon Meyers	
The Impact of Coming Particulate Control Requirements on the Utility Industry	2-1
George T. Preston	
The Impact of Coming Particulate Control Requirements on the Iron and Steel Industry.	3-1
Earle F. Young, Jr.	
The Impact of Particulate Control Requirements: Large Manufacturer's Viewpoint	4-1
Herbert H. Braden	
Paper presented by Gary R. Gawreluk	
Future Particulate Regulations: The View of the Small Manufacturer	5-1
Sidney R. Orem	
Session 2: ADVANCED ENERGY APPLICATIONS	
George A. Rinard, Chairman	

<u>Section</u>	<u>Page</u>
High-Temperature, High-Pressure Electrostatic Precipitation, Current Status.	6-1
P. L. Feldman* and K. S. Kumar	
Test Results of a Precipitator Operating at High-Temperature and High-Pressure Conditions	7-1
Donald E. Rugg*, George Rinard, Michael Durham, and James Armstrong	
Evaluation and Development of Candidate High Temperature Filter Devices for Pressurized Fluidized Bed Combustion. . . .	8-1
T. E. Lippert*, D. F. Ciliberti, S. G. Drenker, and O. J. Tassicker	
High Temperature Gas Filtration with Ceramic Filter Media: Problems and Solutions	9-1
Ramsay Chang	
The Development and High Temperature Application of a Novel Method for Measuring Ash Deposits and Cake Removal on Filter Bags.	10-1
David F. Ciliberti*, Thomas E. Lippert, Owen J. Tassicker, and Steven Drenker	
Session 3: ECONOMICS	
John S. Lagarias, Chairman	
Economics of Electrostatic Precipitators and Fabric Filters	11-1
Victor H. Belba*, Fay A. Horney, Robert C. Carr, and Walter Piulle	
Estimating the Benefits of SO ₃ Gas Conditioning on the Performance of Utility Precipitators When Burning U.S. Coals	12-1
Peter Gelfand	
Microcomputer Models for Particulate Control	13-1
A. S. Viner*, D. S. Ensor, and L. E. Sparks	
The Impact of Proposed Acid Rain Legislation on Power Plant Particulate Control Equipment.	14-1
William H. Cole	
Session 4: NOVEL CONCEPTS	
Dale L. Harmon, Chairman	

*Denotes speaker

<u>Section</u>	<u>Page</u>
Particle Charging with an Electron Beam Precharger	15-1
J. S. Clements*, A. Mizuno, and R. H. Davis	
Charging of Particulates by Evaporating Charged	
Water Droplets	16-1
G. S. P. Castle*, I. I. Inculet, and R. Littlewood	
Role of Electrostatic Forces in High Velocity Particle	
Collection Devices	17-1
H. C. Wang, J. J. Stukel*, K. H. Leong, and P. K. Hopke	
Hot-Gas Fabric Filtration 500° F - 1500° F, No Utopia but	
Reality.	18-1
Lutz Bergmann	
The Prediction of Plume Opacity from Stationary Sources. . .	19-1
David S. Ensor*, Ashok S. Damle, Philip A. Lawless,	
and Leslie E. Sparks	
APPENDIX: Attendees	A-1

VOLUME 2
ELECTROSTATIC PRECIPITATION

Session 5: ESP: PERFORMANCE ESTIMATING (MODELING)

Leslie E. Sparks, Chairman

Microcomputer Programs for Precipitator Performance	
Estimates.	1-1
M. G. Faulkner*, J. L. DuBard, R. S. Dahlin,	
and Leslie E. Sparks	
Analysis of Error in Precipitator Performance Estimates. . .	2-1
J. L. DuBard* and R. F. Altman	
Use of a Mobile Electrostatic Precipitator for Pilot	
Studies.	3-1
Robert R. Crynack* and John D. Sherow	
Prediction of Voltage-Current Curves for Novel	
Electrodes--Arbitrary Wire Electrodes on Axis.	4-1
Phil A. Lawless* and L. E. Sparks	
Numerical Computation of the Electrical Conditions in a	
Wire-Plate Electrostatic Precipitator Using the Finite	
Element Technique.	5-1
Gregory A. Kallio* and David E. Stock	

*Denotes speaker

<u>Section</u>	<u>Page</u>
Session 6: ESP: PERFORMANCE ENHANCEMENT I	
Ralph F. Altman, Chairman	
A Field Study of a Combined NH ₃ -SO ₃ Conditioning System on a Cold-Side Fly Ash Precipitator at a Coal-Fired Power Plant.	6-1
Robert S. Dahlin*, John P. Gooch, Guillaume H. Marchant, Jr., Roy E. Bickelhaupt, D. Richard Sears, and Ralph F. Altman	
Conditioning of Power Station Flue Gases to Improve Electrostatic Precipitator Efficiency.	7-1
Gernot Mayer-Schwinning* and J. D. Riley	
Pilot-Scale Study of a New Method of Flue-Gas Conditioning with Ammonium Sulfate.	8-1
Edward B. Dismukes*, E. C. Landham, Jr., John P. Gooch, and Ralph F. Altman	
Power Plant Plume Opacity Control.	9-1
J. Martin Hughes* and Kai-Tien Lee	
Pulse Energization System of Electrostatic Precipitator for Retrofitting Application	10-1
Senichi Masuda* and Shunsuke Hosokawa	
Session 7: ESP: PERFORMANCE ENHANCEMENT II	
B. G. McKinney, Chairman	
Practical Implications of Pulse Energization of Electrostatic Precipitators.	11-1
H. Milde*, J. Ottesen, and C. Salisbury	
Laboratory and Full-Scale Characteristics of Electrostatic Precipitators with Rigid Mast Electrodes	12-1
H. Krigmont*, R. Allan, R. Triscori, and H. W. Spencer, III	
Full Scale Experience with Pulsed Energization of Electrostatic Precipitators.	13-1
K. Porle* and K. Bradburn	
New Life for Old Weighted Wire Precipitators: Rebuilding with Rigid Electrodes.	14-1
Peter J. Aa* and Gary R. Gawreluk*	

*Denotes speaker

<u>Section</u>	<u>Page</u>
Pulsing on a Cold-Side Precipitator, Florida Power Corporation, Crystal River, Unit 1	15-1
Joseph W. Niemeyer*, Robert A. Wright, and Wayne Love	
Session 8: ESP: ADVANCED TECHNOLOGY I	
Norman Plaks, Chairman	
Field Study of Multi-Stage Electrostatic Precipitators . . .	16-1
Michael Durham, George Rinard, Donald Rugg, Theodore Carney, James Armstrong*, and Leslie E. Sparks	
Optimizing the Collector Sections of Multi-Stage Electrostatic Precipitators.	17-1
George Rinard*, Michael Durham, Donald Rugg, and Leslie Sparks	
Ceramic-Made Boxer-Charger for Precharging Applications. . .	18-1
Senichi Masuda*, Shunsuke Hosokawa, and Shuzo Kaneko	
Precipitator Performance Enhancement with Pulsed Energization	19-1
E. C. Landham, Jr.*, James L. DuBard, Walter R. Piulle, and Leslie Sparks	
Aerosol Particle Charging in a Pulsed Corona Discharge . . .	20-1
James L. DuBard* and Walter R. Piulle	
Session 9: ESP: ADVANCED TECHNOLOGY II	
Walter R. Piulle, Chairman	
Performance of Large-Diameter Wires as Discharge Electrodes in Electrostatic Precipitators.	21-1
P. Vann Bush*, Duane H. Pontius, and Leslie E. Sparks	
Technical Evaluation of Plate Spacing Effects on Fly Ash Collection in Precipitators.	22-1
Ralph F. Altman*, Gerald W. Driggers, Ronald W. Gray, and James L. DuBard, and E. C. Landham, Jr.	
Electrical Characteristics of Large-Diameter Discharge Electrodes in Electrostatic Precipitators.	23-1
Kenneth J. McLean* and Leslie E. Sparks	
Laboratory Analysis of Corona Discharge Electrodes and Back Corona Phenomena.	24-1
P. Vann Bush* and Todd R. Snyder	

*Denotes speaker

<u>Section</u>	<u>Page</u>
Session 10: ESP: FUNDAMENTALS I	
Grady B. Nichols, Chairman	
The Onset of Electrical Breakdown in Dust Layers	25-1
Ronald P. Young*, James L. DuBard, and Leslie E. Sparks	
Bipolar Current Probe for Diagnosing Full-Scale Precipitators.	26-1
Senichi Masuda*, Toshifumi Itagaki, Shigeyuki Nohso, Osamu Tanaka, Katsuji Hironaga, and Nobuhiko Fukushima	
A Method for Predicting the Effective Volume Resistivity of a Sodium Depleted Fly Ash Layer	27-1
Roy E. Bickelhaupt* and Ralph F. Altman	
Analysis of Air Heater-Fly Ash-Sulfuric Acid Vapor Interactions	28-1
Norman W. Frisch	
Session 11: ESP: FUNDAMENTALS II	
Philip A. Lawless, Chairman	
Experimental Studies of Space Charge Effects in an ESP . . .	29-1
D. H. Pontius* and P. V. Bush	
An Electrostatic Precipitator Facility for Turbulence Research	30-1
J. H. Davidson* and E. J. Shaughnessy	
On the Static Field Strength in Wire-Plate Electrostatic Precipitators with Profiled Collecting Electrodes by an Experimental Method.	31-1
C. E. Akerlund	
The Fluid Dynamics of Electrostatic Precipitators: Effects of Electrode Geometry.	32-1
E. J. Shaughnessy*, J. H. Davidson, and J. C. Hay	
VOLUME 3	
FABRIC FILTRATION	
Session 12: FF: PRACTICAL CONSIDERATIONS	
Wallace B. Smith, Chairman	
Fabric Screening Studies for Utility Baghouse Applications .	1-1
Larry G. Felix* and Randy L. Merritt	

*Denotes speaker

<u>Section</u>	<u>Page</u>
Tensioning of Filter Bags in Reverse Air Fabric Filters. . . .	2-1
Robert W. Tisone* and Gregory L. Lear	
Sound of Energy Savings.	3-1
N. D. Phillips* and J. A. Barabas	
Solving the Pressure Drop Problem in Fabric Filter	
Bag Houses	4-1
Carl V. Leunig	
Session 13: FF: FULL-SCALE STUDIES (COAL-FIRED BOILERS)	
Robert P. Donovan, Chairman	
Emission Reduction Performance and Operating	
Characteristics of a Baghouse Installed on a	
Coal-Fired Power Plant	5-1
David S. Beachler*, John W. Richardson,	
John D. McKenna, John C. Mycock, and Dale Harmon	
Evaluation of Sonic-Assisted, Reverse-Gas Cleaning	
at Utility Baghouses	6-1
Kenneth M. Cushing*, Larry G. Felix,	
Anthony M. LaChance, and Stephen J. Christian	
Sonic Horn Application in a Dry FGD System Baghouse.	7-1
Yang-Jen Chen*, Minh T. Quach, and H. W. Spencer III	
Full Scale Operation and Performance of Two New	
Baghouse Installations	8-1
C. B. Barranger	
Session 14: FF: FULL-SCALE STUDIES II (COAL-FIRED BOILERS)	
Robert C. Carr, Chairman	
Performance of Baghouses in the Electric Generating	
Industry	9-1
Wallace B. Smith* and Robert C. Carr	
Flue Gas Filtration: Southwestern Public Service	
Company's Experience in Design, Construction, and	
Operation.	10-1
John Perry	
Start-Up and Operation of a Reverse-Air Fabric Filter	
on a 550 MW Boiler	11-1
R. A. Winch and L. J. Pflug, Jr.*	

*Denotes speaker

<u>Section</u>	<u>Page</u>
Update on Australian Experience with Fabric Filters on Power Boilers	12-1
F. H. Walker	
Session 15: FF: FUNDAMENTALS/MEASUREMENT TECHNIQUES	
David S. Ensor, Chairman	
Modeling Baghouse Performance.	13-1
David S. Ensor*, Douglas W. VanOsdell, Andrew S. Viner, Robert P. Donovan, and Louis S. Hovis	
Measurement of the Spatial Distribution of Mass on a Filter	14-1
Andrew S. Viner*, R. P. Gardner, and L. S. Hovis	
Laboratory Studies of the Effects of Sonic Energy on Removal of a Dust Cake from Fabrics.	15-1
B. E. Pyle*, S. Berg, and D. H. Pontius	
Cleaning Fabric Filters.	16-1
G. E. R. Lamb	
Session 16: FF: ADVANCED CONCEPTS	
John K. McKenna, Chairman	
Modeling Studies of Pressure Drop Reduction in Electrically Stimulated Fabric Filtration	17-1
Barry A. Morris*, George E. R. Lamb, and Dudley A. Saville	
Flow Resistance Reduction Mechanisms for Electrostatically Augmented Filtration	18-1
D. W. VanOsdell*, R. P. Donovan, and Louis S. Hovis	
Laboratory Studies of Electrically Enhanced Fabric Filtration	19-1
Louis S. Hovis*, Bobby E. Daniel, Yang-Jen Chen, and R. P. Donovan	
Pressure Drop for a Filter Bag Operating with a Lightning-Rod Precharger	20-1
George E. R. Lamb* and Richard I. Jones	
New High Performance Fabric for Hot Gas Filtration	21-1
J. N. Shah	
Paper presented by Peter E. Frankenburg	

*Denotes speaker

<u>Section</u>	<u>Page</u>
Session 17: FF: PILOT-SCALE STUDIES (COAL-FIRED BOILERS) Louis S. Hovis, Chairman	
The Influence of Coal-Specific Fly Ash Properties Upon Baghouse Performance: A Comparison of Two Extreme Examples	22-1
Stanley J. Miller* and D. Richard Sears	
Top Inlet Baghouse Evaluation at Pilot Scale	23-1
Gary P. Greiner* and Dale A. Furlong	
Development of Woven Electrode Fabric and Preliminary Economics for Full-Scale Operation of Electrostatic Fabric Filtration.	24-1
James J. Spivey*, Richard L. Chambers, and Dale L. Harmon	
ESFF Pilot Plant Operation at Harrington Station	25-1
Richard L. Chambers*, James J. Spivey, and Dale L. Harmon	

VOLUME 4
FUGITIVE EMISSIONS, DRY SO₂, AND
OPERATION AND MAINTENANCE

Session 18: FUGITIVE EMISSIONS I Chatten Cowherd, Jr., Chairman	
Technical Manual on Hood Capture Systems to Control Process Fugitive Particulate Emissions	1-1
E. R. Kashdan*, J. J. Spivey, D. W. Coy, H. Goodfellow, T. Cesta, and D. L. Harmon	
Pilot Demonstration of Air Curtain Control of Buoyant Fugitive Emissions	2-1
Michael W. Duncan*, Shui-Chow Yung, Ronald G. Patterson, William B. Kuykendal, and Dale L. Harmon	
Characterization of Fugitive Particulate Emissions from Industrial Sites	3-1
K. S. Basden	
Evaluation of an Air Curtain Secondary Hooding System. . . .	4-1
John O. Burckle Paper presented by William F. Kemner	

*Denotes speaker

<u>Section</u>	<u>Page</u>
Session 19: FUGITIVE EMISSIONS II	
Michael J. Miller, Chairman	
Technical Manual on the Identification, Assessment, and Control of Fugitive Emissions.	5-1
Chatten Cowherd, Jr.*, John S. Kinsey, and William B. Kuykendal	
Quantification of Roadway Fugitive Dust at a Large Midwestern Steel Mill.	6-1
Keith D. Rosbury and William Kemner*	
Evaluation of Street Sweeping as a Means of Controlling Urban Particulate.	7-1
T. R. Hewitt	
Windbreak Effectiveness for the Control of Fugitive-Dust Emissions from Storage Piles--A Wind Tunnel Study.	8-1
Barbara J. Billman	
Evaluation of Chemical Stabilizers and Windscreens for Wind Erosion Control of Uranium Mill Tailings.	9-1
Monte R. Elmore* and James N. Hartley	
Session 20: DRY SO ₂ REMOVAL I	
Richard G. Rhudy, Chairman	
Modeling of SO ₂ Removal in Spray-Dryer Flue Gas Desulfurization System	10-1
Ashok S. Damle* and Leslie E. Sparks	
Fabric Filter Operation Downstream of a Spray Dryer: Pilot and Full-Scale Results	11-1
Richard G. Rhudy and Gary M. Blythe*	
Novel Design Concepts for an 860 MW Fabric Filter Used with a Dry Flue Gas Desulfurization System.	12-1
Michael F. Skinner, Steven H. Wolf, John M. Gustke*, and Donald O. Swenson	
Start-Up and Operating Experience with a Reverse Air Fabric Filter as Part of the University of Minnesota Dry FGD System	13-1
J. C. Buschmann*, J. Mills, and W. Soderberg	

*Denotes speaker

<u>Section</u>	<u>Page</u>
Spray Dryer/Baghouse Experiences on a 1000 ACFM Pilot Plant.	14-1
Wayne T. Davis*, Gregory D. Reed, and Tom Lillestolen	
Session 21: DRY SO ₂ REMOVAL II	
Theodore G. Brna, Chairman	
Design and Operation of the Baghouse at Holcomb Station, Unit No. 1.	15-1
B. R. McLaughlin* and R. D. Emerson	
An Update of Dry-Sodium Injection in Fabric Filters.	16-1
Richard G. Hooper*, Robert C. Carr, G. P. Green, V. Bland, L. J. Muzio, and R. Keeth	
Removal of Sulfur Dioxide and Particulate Using E-SOX.	17-1
Leslie E. Sparks*, Geddes H. Ramsey, Richard E. Valentine, and Cynthia Bullock	
Comparison of Dry Injection Systems at Normal and High Flue Gas Temperatures	18-1
Robert M. Jensen*, William Dunlop, George C. Y. Lee, and Duane Folz	
Acid Rain Control Options - Impact on Precipitator Performance.	19-1
Victor H. Belba*, Fay A. Horney, and Donald M. Shattuck	
Session 22: OPERATIONS AND MAINTENANCE I	
Richard D. McRanie, Chairman	
Comparison of U.S. and Japanese Practices in the Specification and Operation and Maintenance of Electrostatic Precipitators.	20-1
Michael F. Szabo*, Charles A. Altin, and William B. Kuykendal	
Operation and Maintenance Manuals for Electrostatic Precipitators and Fabric Filters	21-1
Michael F. Szabo*, Ronald D. Hawks, Fred D. Hall, and Gary L. Saunders	
An Update of the Performance of the Cromby Station Fabric Filter.	22-1
M. Gervasi*, J. R. Darrow, and J. E. Manogue	

*Denotes speaker

<u>Section</u>	<u>Page</u>
Critical Electrostatic Precipitator Purchasing Concepts. . .	23-1
Charles A. Altin* and Ralph F. Altman	
Reducing Electrostatic Precipitator Power Consumption. . . .	24-1
Joseph P. Landwehr* and George Burnett	
Session 23: OPERATIONS AND MAINTENANCE II	
Peter R. Goldbrunner, Chairman	
Design Considerations to Avoid Common Fly Ash	
Conveying Problems	25-1
Gus Monahu* and Walter Piulle	
Feasibility of Using Parameter Monitoring as an Aid	
in Determining Continuing Compliance of Particulate	
Control Devices.	26-1
Joseph Carvitti*, Michael F. Szabo, and William Kemner	
Air Pollution Control: Maintenance Cost Savings	
from the Washing, Patching and Reuse of Bags Used	
in Fabric Filters.	27-1
Frank L. Cross, Jr.	
Paper presented by Lutz Bergmann	
Optimizing the Performance of a Modern Electrostatic	
Precipitator by Design Refinements	28-1
Donald H. Rullman* and Franz Neulinger	
Weighted Discharge Electrodes - A Solution to	
Mechanical Fatigue Problems.	29-1
John A. Knapik	
PAPER PRESENTED AT THE FOURTH SYMPOSIUM ON THE TRANSFER	
AND UTILIZATION OF PARTICULATE CONTROL TECHNOLOGY BUT NOT	
PUBLISHED IN PROCEEDINGS	
Measurement of the Electrokinetic Transport Properties	
of Particles in an Electrostatic Precipitator.	30-1
Wallace T. Clark III*, Robert L. Bond, and	
Malay K. Mazumder	
UNPRESENTED PAPER	
Electrostatic Precipitator Bus Section Failure:	
Operation and Maintenance.	31-1
Louis Theodore, Joseph Reynolds, Francis Taylor,	
Alan Filippi, and Steve Errico	

*Denotes speaker

Session 12: FF: PRACTICAL CONSIDERATIONS

Wallace B. Smith, Chairman
Southern Research Institute
Birmingham, AL

FABRIC SCREENING STUDIES FOR UTILITY BAGHOUSE APPLICATIONS

Larry G. Felix and Randy L. Merritt
Southern Research Institute
P.O. Box 55305
Birmingham, Alabama 35255-5305

ABSTRACT

A sampling device is described which has been developed under EPRI sponsorship to screen filtration fabrics for utility baghouse applications. The Fabric Filter Sampling System (FFSS) is a portable, reverse-gas cleaned, device designed to extract a sample of flue gas which is kept at stack temperature and conveyed to the fabric under test. Forward and reverse air-to-cloth ratios, filtration and cleaning times are variable. The fabric and collected ash are housed in separate heated enclosures designed for quick access. A variety of operating modes are possible. Results are presented from short-term studies conducted at boilers fired with eastern high sulfur, western low sulfur and Texas lignite coals. These data suggest that fabric performance is ash/flue gas specific.

INTRODUCTION

A sampling system has been developed for the Electric Power Research Institute (EPRI) which can be used to screen filtration fabrics for utility baghouse use under realistic operating conditions(1). The Fabric Filter Sampling System (FFSS) is a portable, reverse-gas cleaned, device designed to extract a sample of flue gas before the inlet of a control device, keep it at stack conditions, and convey it to the fabric under test. Forward filtration and reverse-gas cleaning air-to-cloth ratios and time periods are variable. Ash is collected in a separate heated hopper which can be isolated from the rest of the system for emptying. Two of the FFSS devices have been made. Results are presented from short and long-term studies at various locations which illustrate the usefulness of these devices.

This system was designed in part because laboratory filtration studies cannot duplicate the environment at a baghouse inlet. No technique exists to completely redisperse fly ash so that the original particle size distribution is duplicated; and laboratory studies usually do not attempt to use gas constituencies or temperatures found in boiler exhausts. Further, since

there is evidence that the behavior of a baghouse is closely related to the ash it filters (2,3,4,5), fabric screening and testing should be conducted in an environment as realistic as is possible. The FFSS was designed to overcome the restrictions inherent to laboratory filtration studies by moving the apparatus to the field. Since the air-to-cloth ratio, sampling time, cleaning time, and temperature are variable, a number of cleaning and filtering parameters are available for testing, starting either with a clean fabric swatch or a portion of a seasoned bag removed from an operating baghouse. Finally, such things as particle charging, the injection of gas conditioning agents, and the effect of a multiclone can be tested easily and inexpensively.

SYSTEM DESCRIPTION

Figure 1 shows a schematic diagram of the FFSS. Not shown are the separate water holding tank for the condenser/cooler and silica gel drying columns which follow the condenser/cooler. Figure 2 shows a schematic of the fabric sample holder and ash hopper and Figure 3 shows two photographs of the fabric sample holder. Figure 3(a) illustrates the fabric sample holder in its oven and Figure 3(b) shows the interior of the fabric sample holder. Referring to Figures 2 and 3, one can see the cyclone and ash drop out tray which catch virtually all of the particulate matter which penetrates the fabric. A cyclone was chosen because a compact, low pressure loss technique was needed to keep the exhaust lines clear. Viewports are positioned in front and in back of the fabric sample and in the front of the remote ash hopper. Reverse gas for cleaning is filtered ambient air which is passed through a coiled copper tube heat exchanger in the oven. The FFSS can be operated without the large lower hopper by blanking off the line which connects the upper oven to the lower oven and by replacing the drawer in the lower part of the fabric filter sample holder, as is shown in Figure 3(b). In this configuration, ash must be removed daily.

EXPERIMENTAL RESULTS

The FFSS was first used at the EPRI Arapahoe Test Facility Fabric Filter Pilot Plant (FFPP) on Compartment C, the control compartment cleaned only with reverse gas. The purpose of this test was to determine if pressure loss as a function of time for the FFSS test sample could mimic the behavior of a baghouse. The FFSS was fitted with a swatch of bag material from an FFPP bag (Albany International Q53-S3016 Tricoat) and forward and reverse sampling times used in Compartment C were programmed into the FFSS control unit. The FFSS oven and probe were controlled at the duct temperature at the Compartment C inlet. Figure 4 shows a comparison of pressure drop as a function of time for a single filtering cycle from the FFSS and the FFPP. During this test the FFSS substantially emulated the behavior of Compartment C, starting with fresh bags.

The FFSS was then moved to the inlet of the Public Service Company of Colorado's Arapahoe Unit 3 baghouse. A swatch of the bag fabric used in this baghouse (Menardi Southern 601T) was fitted in the FFSS and tested for 850 hours using typical forward (135 min) and reverse (30 sec) dwell times used for the baghouse. The forward air-to-cloth ratio was set to 1.7 ft/min which

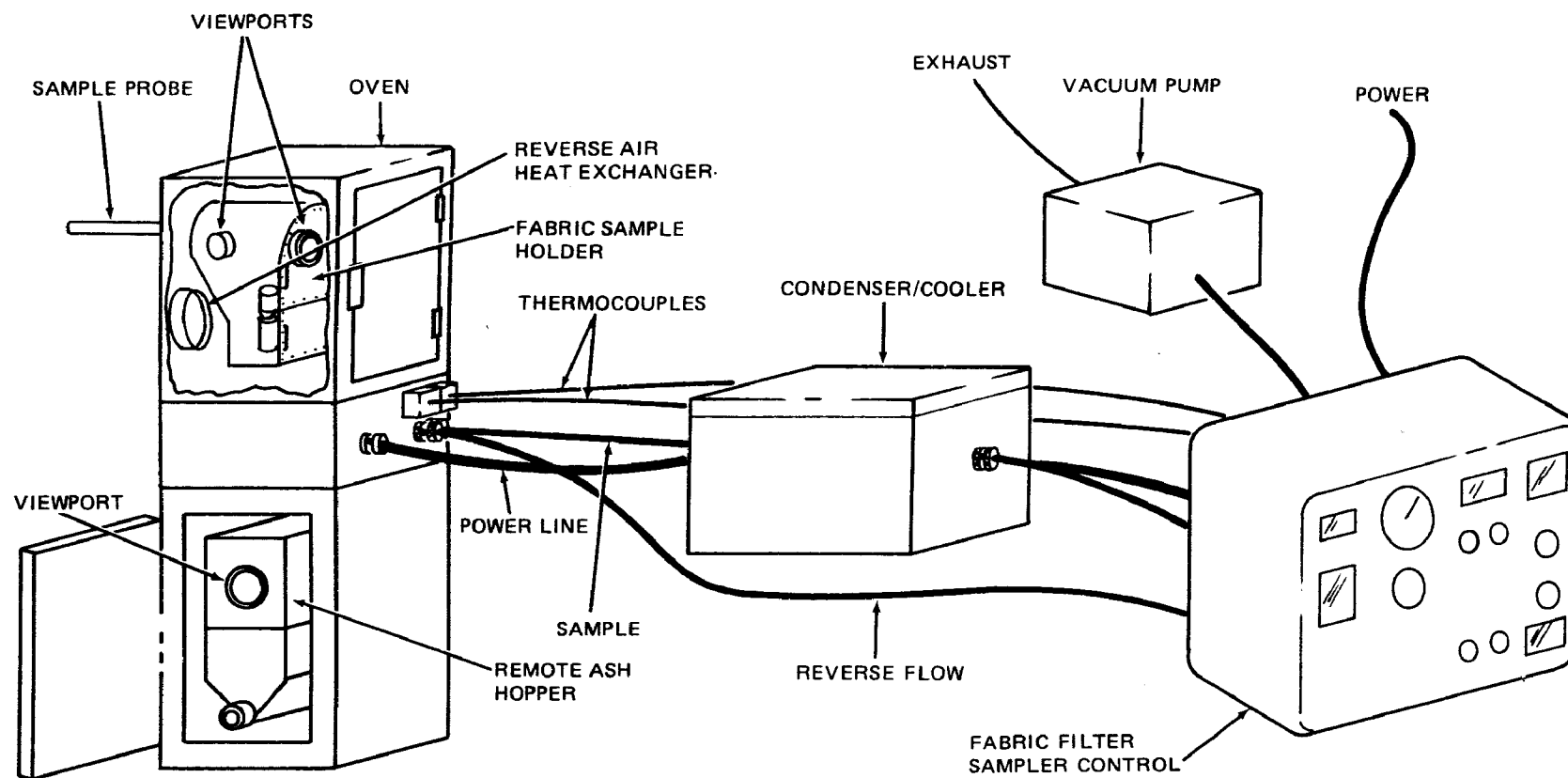


Figure 1. Schematic diagram of the Fabric Filter Sampling System.

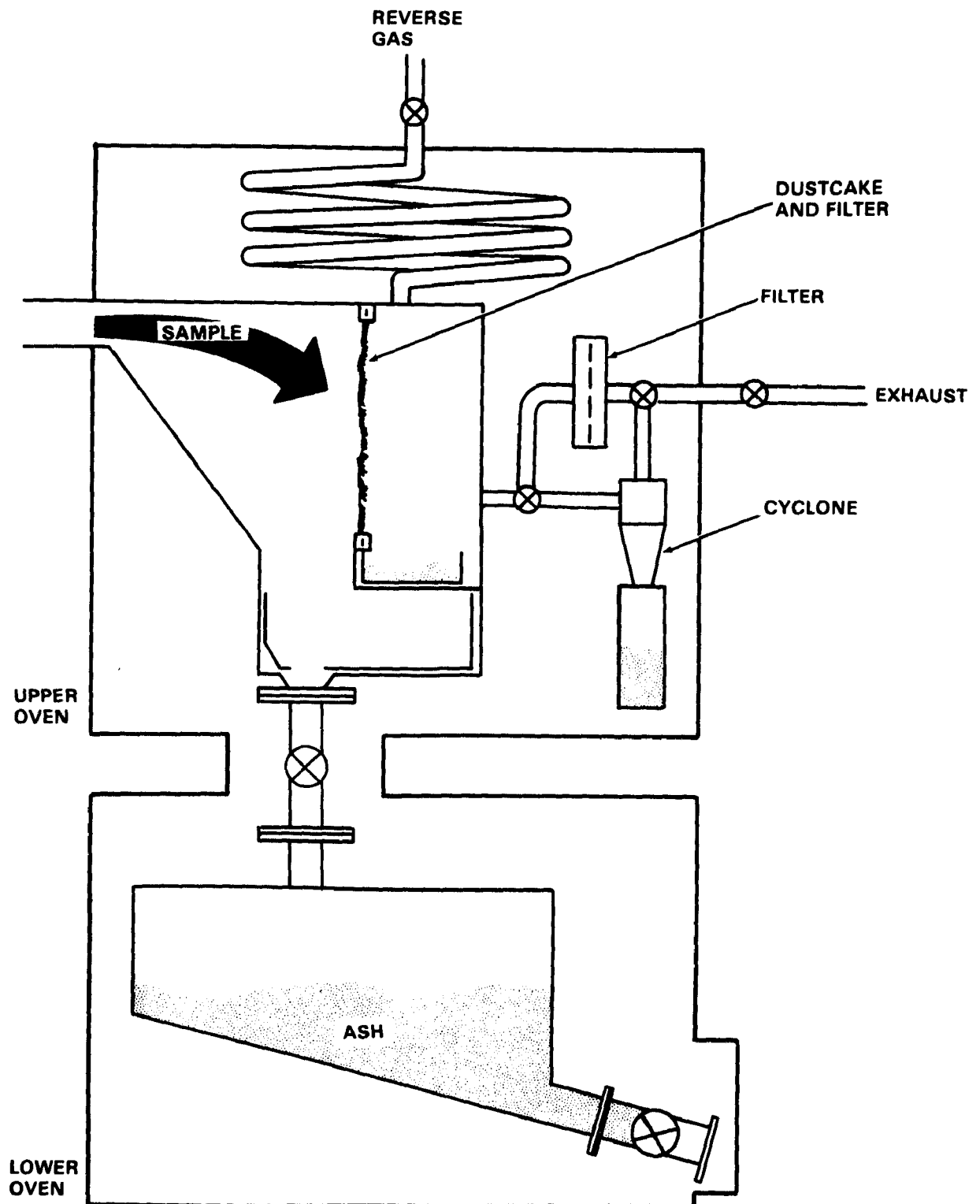


Figure 2. Schematic diagram of the FFSS fabric sample holder and lower remote ash hopper.

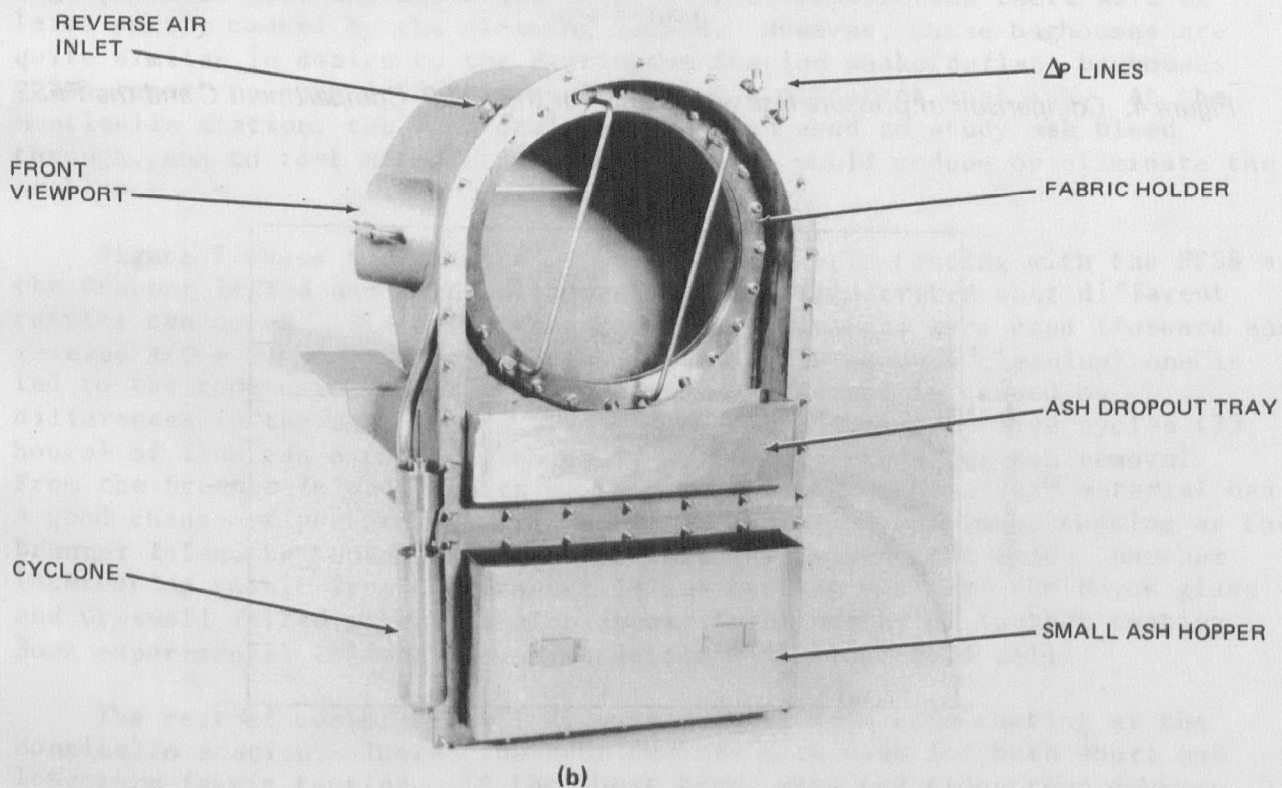
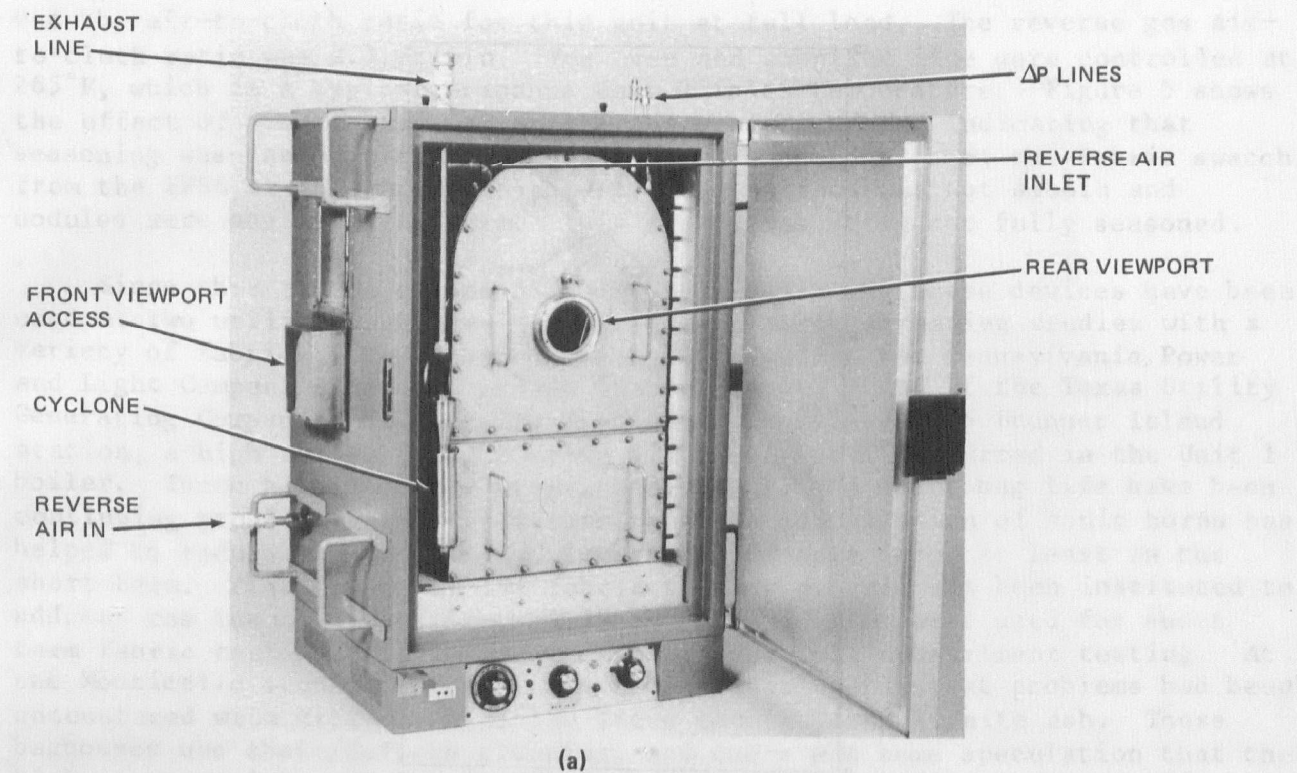


Figure 3. The Fabric Filter Sampling System's fabric sample holder. Oven with sample holder (a). Sample holder with back plates removed (b).

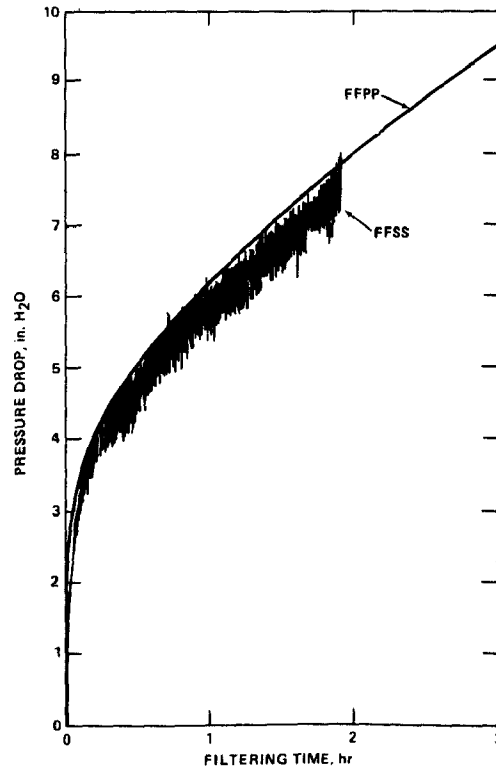


Figure 4. Comparison of pressure loss versus time for the FFPP, Compartment C and the FFSS.

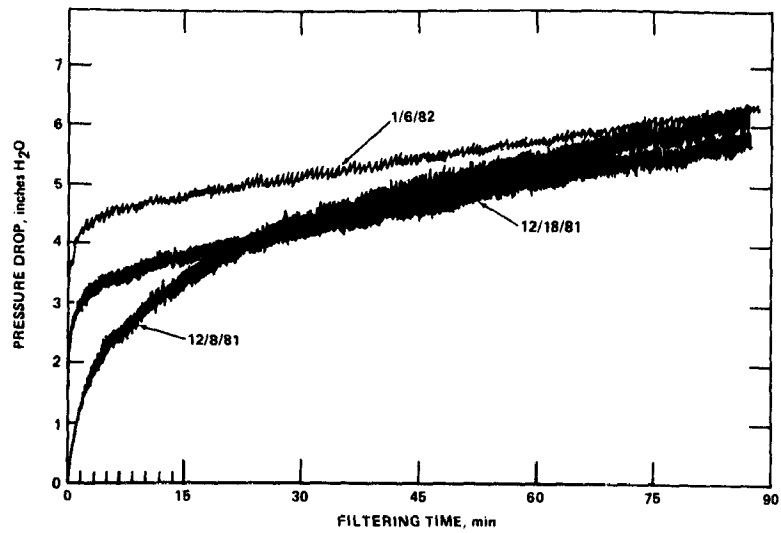


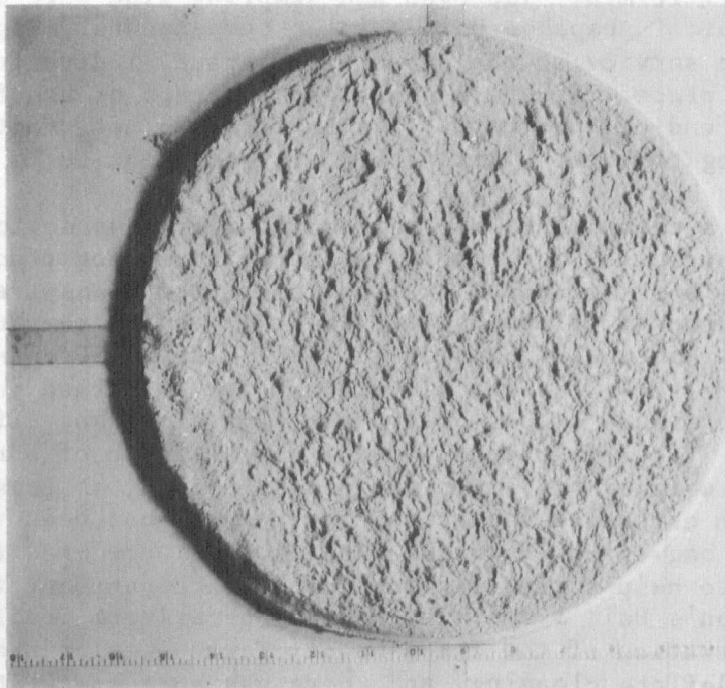
Figure 5. Pressure drop as a function of filtering time for one cycle. Data from 12/9/81, 12/18/81, and 1/6/82. FFSS at Arapahoe, Unit 3.

was the air-to-cloth ratio for this unit at full load. The reverse gas air-to-cloth ratio was 2.7 ft/min. The oven and sampling line were controlled at 265°F, which is a typical Arapahoe Unit 3 inlet temperature. Figure 5 shows the effect of time in service on the shape of ΔP trace, indicating that seasoning was taking place. Figure 6 shows a photograph of the fabric swatch from the FFSS at the end of this test. The surface was not smooth and nodules were beginning to form. This fabric was still not fully seasoned.

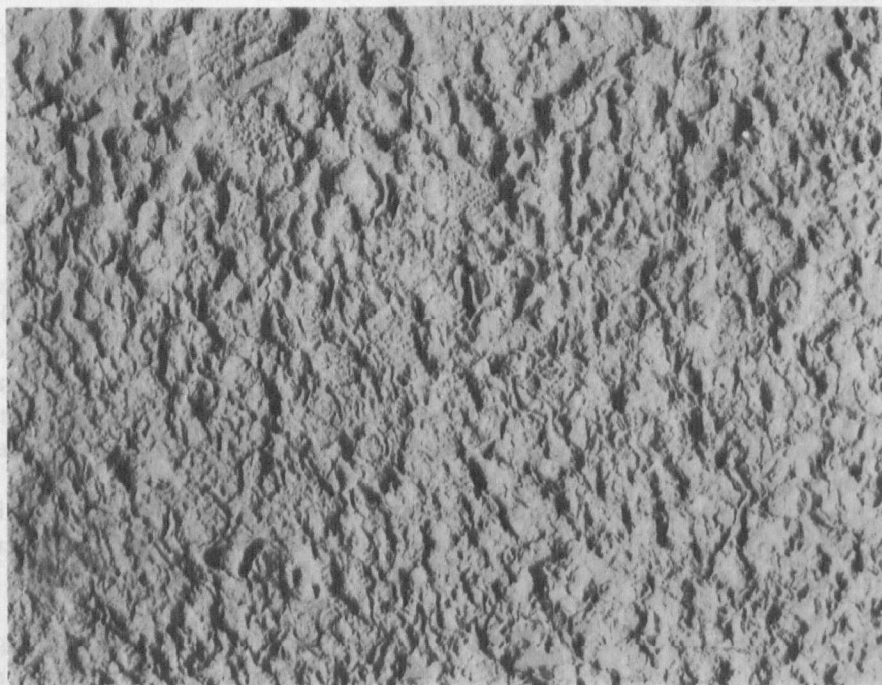
Since this time a second FFSS has been built and these devices have been used at two utility baghouses for extensive fabric screening studies with a variety of fabrics. These baghouses are located at the Pennsylvania Power and Light Company's Brunner Island Station (Unit 1) and at the Texas Utility Generating Companies' Monticello Station (Unit 2). At the Brunner Island station, a high sulfur (~2%) Eastern bituminous coal is burned in the Unit 1 boiler. There high pressure drops, heavy bags, and short bag life have been continuing problems. Bag replacement and the installation of sonic horns has helped to reduce bag weights and lower the pressure drop, at least in the short term. Also, an extensive fabric testing program has been instituted to address the issue of bag life. Here the FFSS devices were used for short term fabric testing to help screen fabrics for full compartment testing. At the Monticello station's Unit 1 and 2 baghouses, persistent problems had been encountered with filtration of the Titus County Texas lignite ash. These baghouses use shake/deflate cleaning, and there was some speculation that the high pressure loss and ash bleed through problems observed there were at least partly caused by the cleaning method. However, these baghouses are quite similar in design to the Harrington Station shake/deflate baghouses which report no such difficulties filtering a different coal ash. At the Monticello station, the FFSS devices have been used to study ash bleed through, and to test methods and fabrics which would reduce or eliminate the problem.

Figure 7 shows the results of short term fabric testing with the FFSS at the Brunner Island and Monticello stations and illustrates what different results can occur. Since the same sampling parameters were used (forward and reverse A/C = 2.0 acfm/ft², 3 hours filtering, 30 seconds cleaning) one is led to the conclusion that the performance difference is caused by differences in the ash. These results are for only twenty-five cycles (75 hours) of flue gas exposure with daily off-line periods for ash removal. From the Brunner Island results we concluded that the Gore-Tex® material had a good chance of performing well. Subsequent full compartment testing at the Brunner Island baghouse has suggested that this may be the case. Another interesting result from the Brunner Island testing was that the Huyck glass and Criswell felted materials also appear to be worthy of further testing. Some experimental Criswell woven materials did not perform well.

The rest of our paper will discuss results from FFSS testing at the Monticello station. There, the FFSS devices were used for both short and long-term fabric testing. In the short term, when the sidestream devices were serviced daily, many of the standard fiberglass filtration fabrics exhibited large ash penetrations. Table 1 summarizes the results of these tests. The fabrics are described in Table 2. From these tests it was clear that:



A. OVERALL VIEW OF FFSS FABRIC SAMPLE



B. CLOSE-UP VIEW OF CENTER SECTION

Figure 6. Filter sample removed from FFSS on 1/19/82. Sample from the Arapahoe Station, Unit 3.

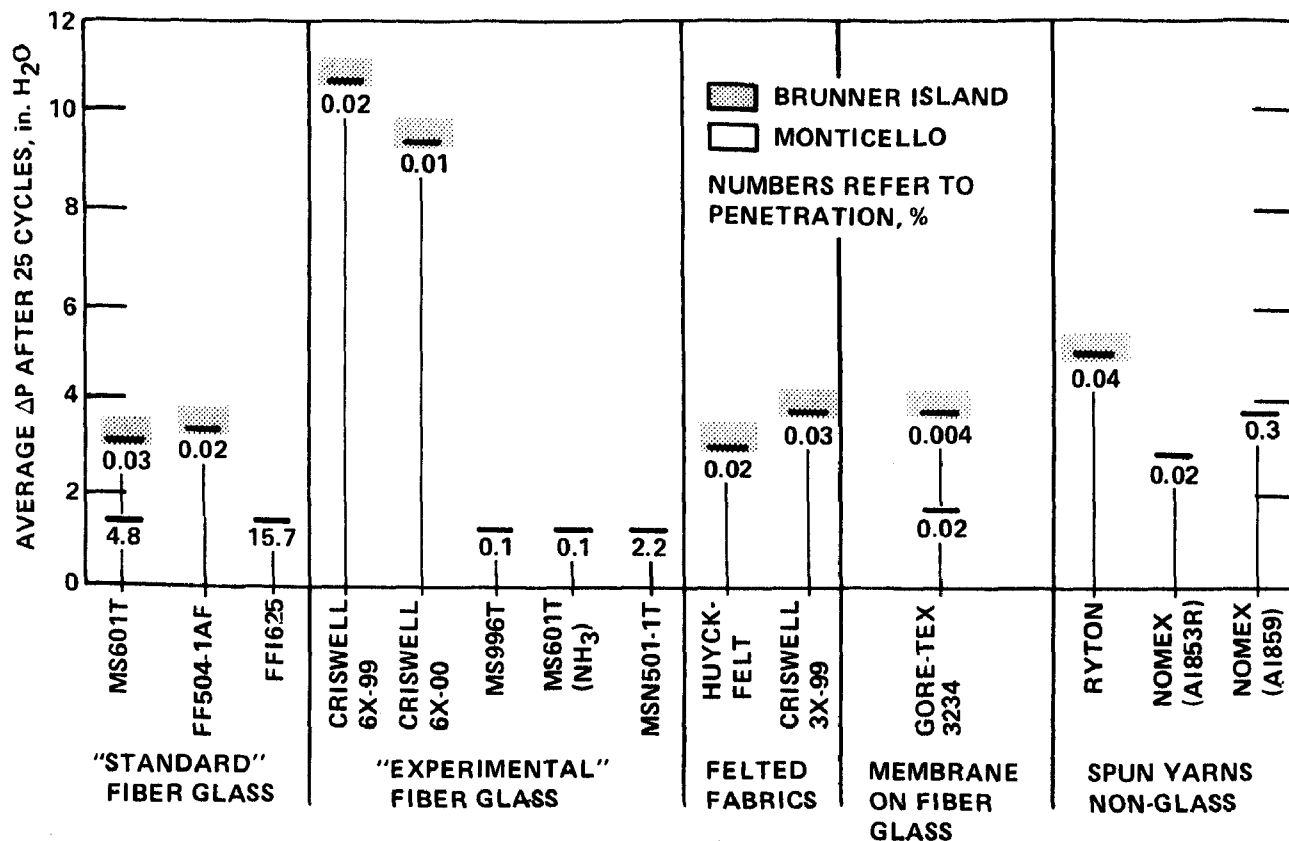


Figure 7. Fabric screening tests at Monticello and Brunner Island using the Fabric Filter Sidestream System (FFSS). After Carr and Smith (4).

TABLE 1. MONTICELLO STATION FFSS SHORT-TERM TESTING SUMMARY*

Fabric	Sample Time (hours)	ΔP Fabric Maximum (in., w.c.)	Penetration (%)
FF	82.0	4.0	15.7
G3234	93.2	5.0	<0.02
G3135†	60.0	5.8	2.1
AI853‡	84.7	6.2	0.02
AI859‡	89.0	7.2	0.29
MS501-I	88.0	2.5	2.2
MS5N9-T	69.7	2.2	7.8
MSN602-1T	87.4	3.0	0.93
MS601-T	104.6	1.2	4.8
MS601-T (250°F)	142.0	2.3	3.1
MS601-T HC	176.9	2.2	4.4
MS996-T‡	156.3	2.5	0.10
MS601-T (NH ₃)	113.0	2.2	0.22

*All fabrics were tested warp-out.

†With sewn-on stainless steel mesh. Leaks occurred around the stitches.

‡Highly texturized filtration surface.

TABLE 2. FABRICS SCREENED AT THE MONTICELLO STATION

Manufacturer/Model No.	Description
Fabric Filters	ECDE glass, 3 x 1 twill, 14.0 oz/yd ² . I625 finish.
Gore-Tex®/3234	ECDE glass, 3 x 1 twill, 9.8 oz/yd ² . Gore-Tex® membrane, non-texturized fabric, 10% Teflon B finish.
Gore-Tex®/3135	ECDE glass, 3 x 1 twill, 9.8 oz/yd ² . Gore-Tex® membrane non-texturized fabric, tri-coat finish.
Albany International/853R	100% Nomex®, 2 x 2 twill, 10.1 oz/yd ² . Woolen systems spun yarn, 39 x 35 count. Calendared fabric. Highly texturized surface.
Albany International/859	100% Nomex® with stainless steel yarn interwoven in a 1 inch x 1/2 inch rectangular matrix. 2 x 2 twill, 10.1 oz/yd ² . Woolen systems spun yarn, 39 x 35 count. Non-calendared fabric. Highly texturized surface.
Menardi Southern/N501T	Napped version of 501-1. ECDE glass, crow-foot weave, 8.4 oz/yd ² , 54 x 52 count, 150-1/2 (warp), 150-1/2 (fill), 10% Teflon B finish.
Menardi Southern/5N9T	Napped version of 509 ECDE glass, 3 x 1 twill, 8.8 oz/yd ² , 54 x 56 count, 150-1/2 (warp), 150-1/2 (fill), napped, 10% Teflon B finish.
Menardi Southern/N601T	Napped version of 601-1. Proprietary yarn construction. ECDE glass, 3 x 1 twill, 9.5 oz/yd ² . 10% Teflon B finish.
Menardi Southern/601T(601-1T)	ECDE glass, 3 x 1 twill, 9.5 oz/yd ² . 54 x 30 count, 150-1/2 (warp), 150-1/4 (fill), 9.5 oz/yd ² . 10% Teflon B finish.
Menardi Southern/601THC	High thread count version of 601-1. Proprietary yarn construction, 3 x 1 twill, 9.5 oz/yd ² . 10% Teflon B finish.
Menardi Southern/996T	ECDE glass, double warp weave, 16.1 oz/yd ² . 50 x 30 count, 37-1/0 texturized + 37-1/0 filament (warp), 75-1/3 texturized (fill), 10% Teflon B finish. Highly texturized surface.

- The ash penetration problem at the Monticello baghouses was not caused by shake/deflate cleaning since the FFSS is reverse gas cleaned.
- Highly texturized filtration fabrics exhibited lower ash penetrations with the Monticello ash.
- The Gore-Tex® membrane coated fabrics worked very well.
- Ammonia injection drastically reduced ash penetration.

Recently, a series of long term fabric tests have been completed at the Monticello station. These tests of Menardi Southern fabric, 601T (warp in and warp out) and 996T (warp out), confirmed and added to the above results. During the periods of ammonia injection, ammonia was injected at the rate of 15 parts per million (ppm) of the flue gas sampled. This injection rate was chosen because it reacted completely with the 2 to 3 ppm of SO_3 present in the flue gas, leaving some slight amount in the FFSS exhaust. The FFSS devices were equipped with the large remote ash hoppers so that daily ash removal was unnecessary. The first result we noted was that for a given fabric, when daily servicings were eliminated, ash penetrations decreased. This is reasonable, since the system was not being taken off line for ash removal so the fabric was not subjected to daily thermal or mechanical shock. The net effect of our daily servicings was probably to overclean the fabric once a day. This conclusion is further supported by the fact that the filtration time for these tests was reduced to 75 minutes, equal to that used at the Unit 2 baghouse.

For these tests, ash penetration was monitored by measuring the amount of fly ash caught in the cyclone in the exhaust line of each FFSS. Figures 8 through 10 show a pressure drop-ash penetration history for each of the three long term tests. In these figures, each before and after cleaning pressure drop data point is averaged over ten filtering cycles. The cyclone was not emptied regularly and ash penetrations are reported in terms of the number of grams of ash per hour retained by the cyclone at the time of measurement. The cyclone D_{50} was about 1.0 micrometers (physical) at these sampling conditions.

Figure 8 gives the pressure drop-penetration history for Menardi Southern 601T fabric, warp-in (~25% texturized). This is the predominant fabric used in the Unit 2 baghouse which has continual opacity problems. Inspection of this figure leads to the conclusion that:

- Ammonia injection substantially reduces the penetration of Monticello ash through a lightly texturized fabric, at the expense of an increased pressure drop.

Figure 9 shows the pressure drop-penetration history for Menardi Southern 601T fabric, warp-out (~75% texturized). Here the ash penetration before ammonia injection is slight, but it is still decreased by more than order or magnitude when ammonia is injected. This time, there was apparently no

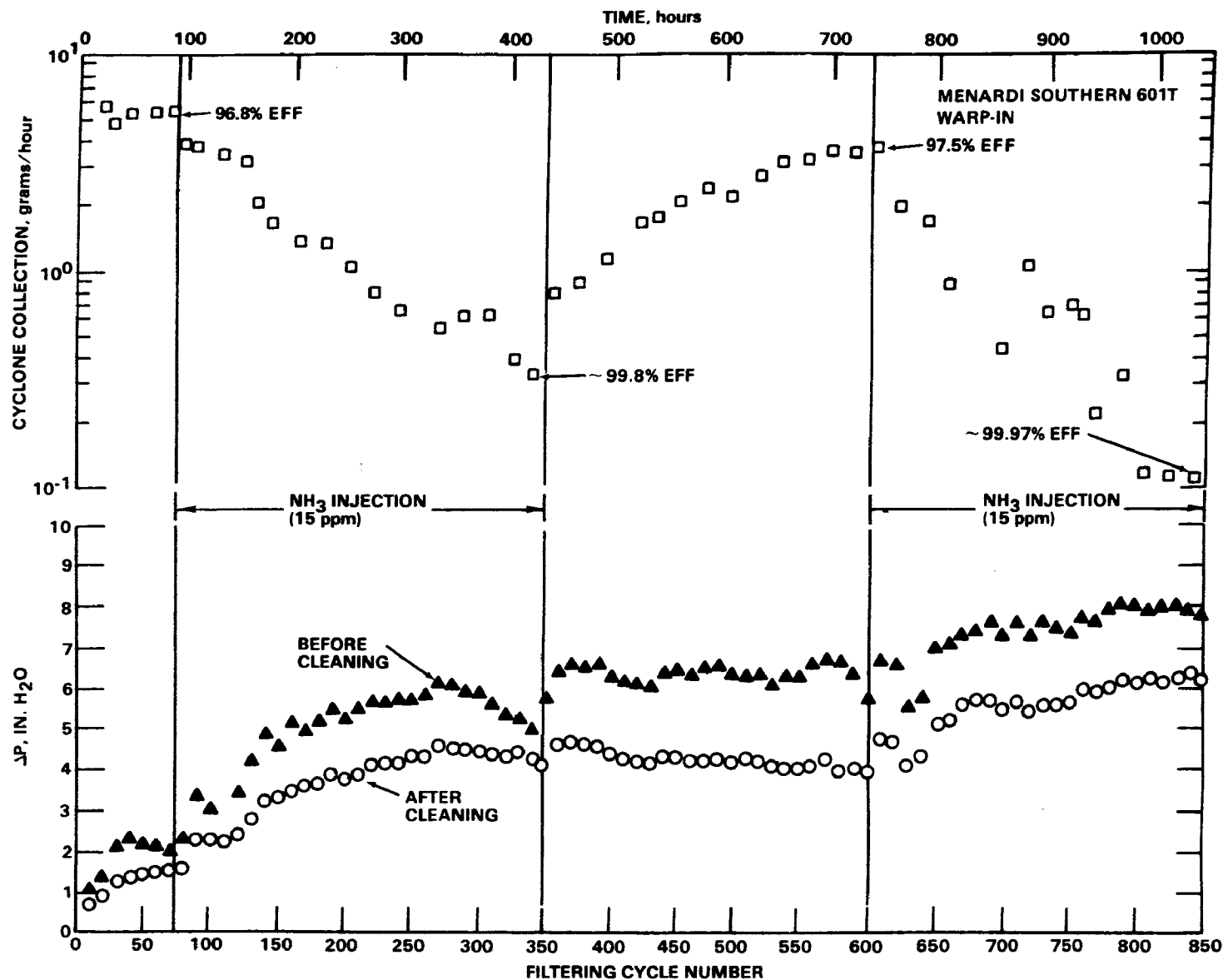


Figure 8. Performance of Menardi Southern 601T(warp in) fabric during sidestream testing at the Monticello Station. The filtering cycle is 75 minutes long with 30 second reverse-gas cleaning. Forward and reverse air-to-cloth ratios are 2.0 acfm/ft². Each ΔP data point is averaged over ten filtering cycles.

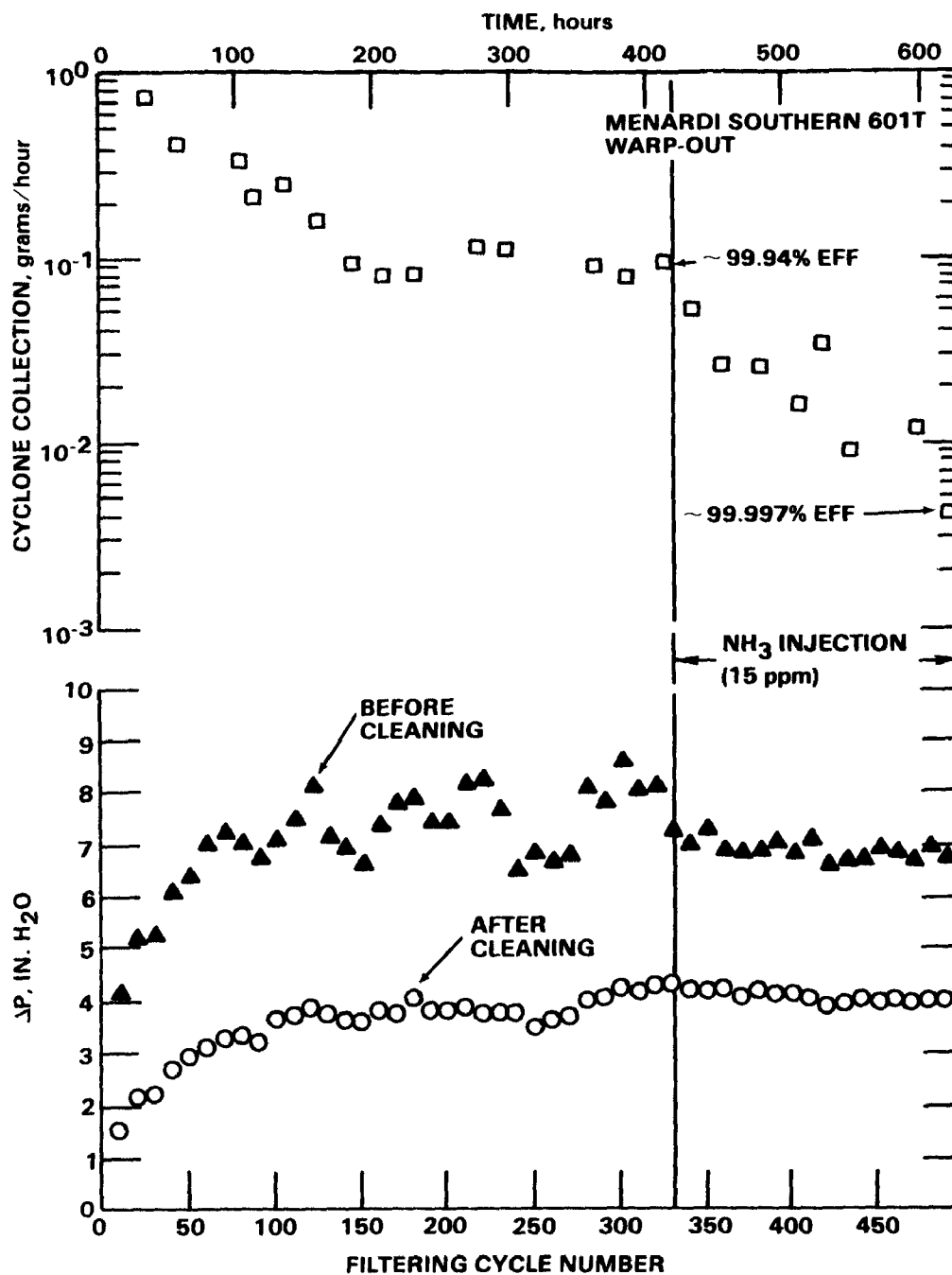


Figure 9. Performance of Menardi Southern 601T (warp out) fabric during sidestream testing at the Monticello Station. The filtering cycle is 75 minutes long with 30 second reverse-gas cleaning. Forward and reverse air-to-cloth ratios are 2.0 acfm/ft². Each ΔP data point is averaged over ten filtering cycles.

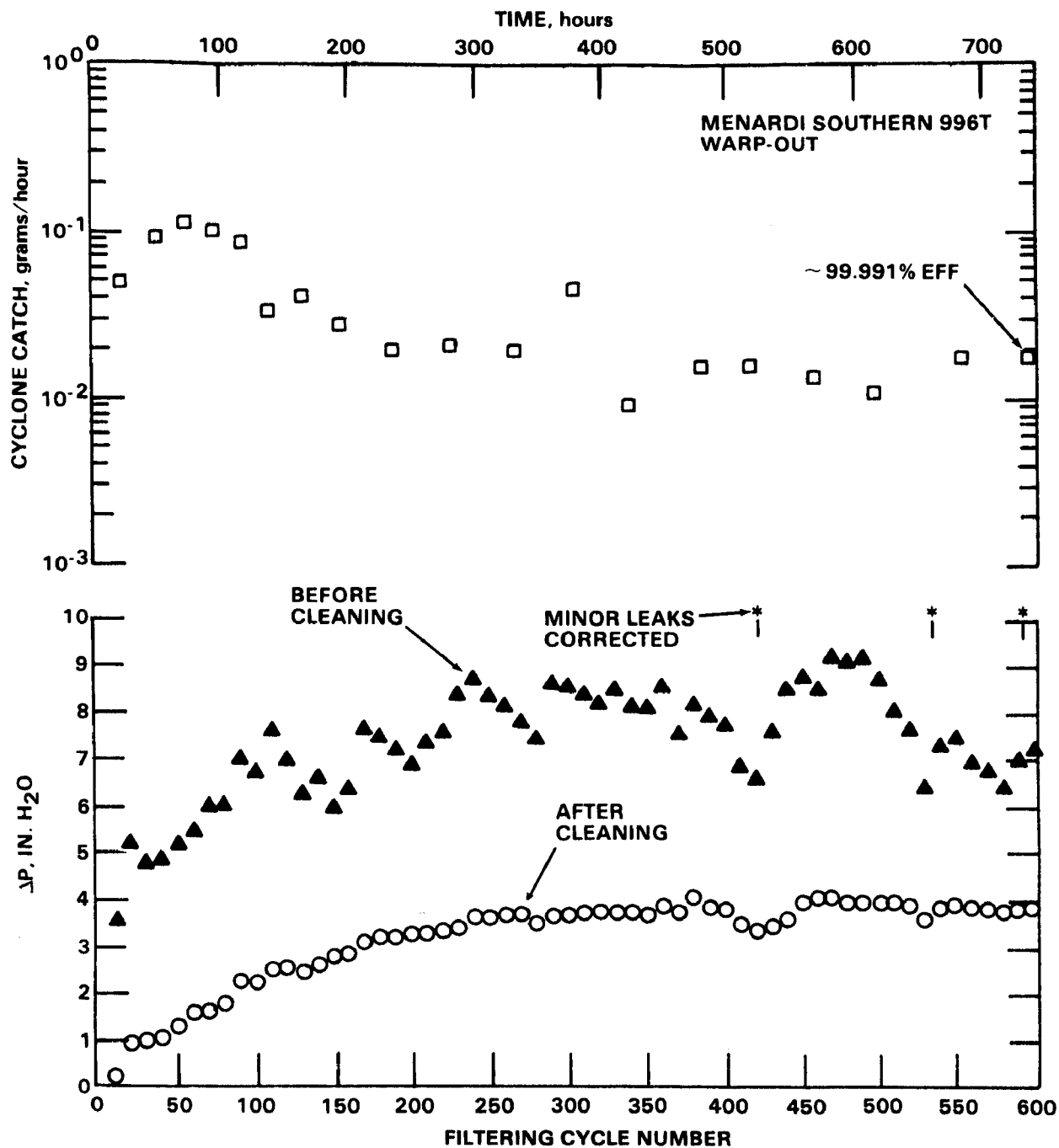


Figure 10. Performance of Menardi Southern 996T (warp out) fabric during sidestream testing at the Monticello Station. The filtering cycle is 75 minutes long with 30 second reverse-gas cleaning. Forward and reverse air-to-cloth ratios are 2.0 acfm/ft². Each ΔP data point is averaged over ten filtering cycles.

pressure drop increase associated with the injection of ammonia. Here we can conclude:

- With more surface texturization, ammonia injection can still reduce Monticello ash penetration with little or no pressure drop penalty.

Figure 10 shows the pressure drop-penetration history for Menardi Southern 996T fabric, warp out. The surface of this fabric is highly texturized and as this figure shows, it can filter with high efficiency at a moderate average pressure drop (~5 to 6 inches of water) without the need for ammonia injection. From these results we can conclude that:

- At high degrees of surface texturization, ammonia injection is not necessary to reduce Monticello ash penetration to an extremely low level (~0.009%).

It must be remembered that these results were obtained in a reverse-gas cleaned sidestream unit and that none of these tests lasted long enough for the fabrics to season. Also, shake/deflate cleaning imparts much more mechanical energy to the fabric surface than does reverse-gas cleaning. Thus, it would be unreasonable to expect that these results could be directly applied to the full scale Monticello baghouse. However, some general conclusions can be made:

- Ammonia gas conditioning combined with increased surface texturization on the filtration fabric has the potential of reducing ash bleed through while maintaining a moderate pressure drop at the Monticello station.
- A very high degree of surface texturization, without ammonia injection, also has the potential of eliminating ash bleed through and maintaining a moderate pressure drop at the Monticello station.

CONCLUSIONS

These and other data suggest that a strong relationship exists between ash chemistry and fabric performance in baghouses associated with coal-fired boilers. Therefore, in order to select the optimum fabric at a particular baghouse, fabric tests should be performed. The portable Fabric Filter Sampling System was developed to aid in the fabric selection process. The usefulness and practicality of this system has been demonstrated in both short-term and long-term testing. For fabric screening and proof testing of a flue gas conditioning agent, these devices represented an economical means of determining whether large scale testing should be considered. Since tests are performed with the actual flue gas, no uncertainty exists as to whether the results of tests conducted with these devices are applicable. In the future, devices such as the FFSS may be used routinely to aid in fabric selection before a baghouse is built.

ACKNOWLEDGEMENTS

The assistance we have received from our utility contacts and plant personnel at the Arapahoe, Brunner Island, and Monticello stations have made this paper possible. Without their help most of the data reported herein could not have been obtained. We would like to particularly thank Mr. Harold Mathes at Arapahoe, Mr. Noel Wagner at PP&L Allentown, Mr. Greg Lear at Brunner Island, Mr. J. L. Martin at the Texas Utility Generating Company, Mr. Dale Dennis, Mr. Robbie Watts and Mr. Lee Hyman at the Monticello Station. The operating data and measurements reported here were taken by Larry Felix, Randy Merritt, and Roger Jefferson of Southern Research Institute. The design and development of the Fabric Filter Sampling System was directed by William Steele. We have benefitted significantly from the support and advice of the Denver on-site EPRI personnel, Richard Hooper and Lou Rettenmaier. Our consultant, Charles Gallaer, has also aided us significantly in this program. This project has been supported under EPRI contract number 1129-8. The Project Officer is Mr. Robert C. Carr.

The work described in this paper was not funded by the U. S. Environmental Protection Agency and therefore the contents do not necessarily reflect the views of the Agency and no official endorsement should be inferred.

REFERENCES

1. Felix, L. G., Merritt, R. L., and Carr, R. C. Performance Evaluation of Several Full Scale Utility Baghouses. Paper 23 presented at the Second Conference on Fabric Filter Technology for Coal Fired Power Plants, Electric Power Research Institute, Denver, CO, March 22-24, 1983. EPRI Report CS-3257.
2. Smith, W. B., Felix, L. G., and Steele, W. J. Analysis and Interpretation of Fabric Filter Performance. Paper 19 presented at the Second Conference on Fabric Filter Technology for Coal Fired Power Plants, Electric Power Research Institute, Denver, CO, March 22-24, 1983. EPRI Report CS-3257.
3. Carr, R. C. and Smith, W. B. Fabric Filter Technology for Utility Coal Fired Power Plants, Part IV: Pilot Scale and Laboratory Studies of Fabric Filter TEchnology for Utility Applications. J. Air Pollution Control Association, 34:399, 1984.
4. Carr, R. C. and Smith, W. B. Fabric Filter Technology for Utility Coal Fired Power Plants, Part III: Performance of Full-Scale Utility Baghouses. J. Air Pollution Control Association, 34:281, 1984.
5. Sears, D. R. and Miller, S. J. Impact of Fly Ash Composition Upon Shaker Baghouse Efficiency. Paper 84-56.6, presented at the 77th Annual Meeting of the Air Pollution Control Association, San Francisco, California, June 24-29, 1984.

TENSIONING OF FILTER BAGS IN REVERSE AIR FABRIC FILTERS

Robert W. Tisone
Environmental Elements Corporation
Baltimore, Maryland 21203

Gregory L. Lear
Pennsylvania Power and Light
York Haven, Pennsylvania 17370

ABSTRACT

A large number of the operational problems currently reported with reverse air fabric filters used in the electric utility industry center on, or are related to, bag tensioning. This paper describes some of these problems and a novel means of bag tensioning by way of a counterweight device which provides constant tension over a wide range of dimensional variations.

The design and development of the counterweight tensioning device as part of a five (5) year fabric filter pilot program, and results of the pilot program are presented.

Full size, commercial operating experience with the counterweight tensioning device is included. Projected cost savings which result from the ease of initial bag installation, elimination of bag retensioning and increased bag life are discussed.

INTRODUCTION

The 1971 New Source Performance Standards (NSPS) and their revisions in 1979 established stringent emission limits for the utility industry (1). To conform to these standards, utilities need gas cleaning systems which can accommodate wide ranges in process variables (2) and provide both high equipment availability and high collecting efficiency. Because SO₂ emission limits are also included in the new standards, the use of low sulfur coal increased significantly. Meeting the lower particulate emission limits while treating the more difficult to precipitate ash from many low sulfur coals required that existing precipitators be upgraded, supplemented with extra equipment or completely replaced with much larger units.

These events prompted the utilities, equipment suppliers and government agencies to look seriously at a major expansion in the use of the fabric filter to control fly ash emissions. In 1977 the total capacity of utility boilers served by fabric filters was less than 1000 MW (1). In response to the needs created by the new laws, Environmental Elements Corporation initiated in 1976 a major program to develop an improved reverse air fabric filter system particularly geared to the utility fly ash application. This effort consisted of a comprehensive engineering and pilot study which produced extensive operational knowledge and improved hardware design (2,3). The purpose of this paper is to present design, operational and maintenance details of a superior bag tensioning device which was developed as part of the fabric filter program.

FABRIC FILTER DEVELOPMENT FACILITY

A two compartment reverse air fabric filter (baghouse) designed for 15 full size (30 feet high x 11.5 inch diameter) bags per compartment was fabricated and installed near boiler #3 at Wagner Station of the Baltimore Gas and Electric Company. A controllable portion of the flue gas from upstream of the existing precipitator serving this pulverized coal fired boiler was ducted to the baghouse, and the cleaned flue gas was returned to the duct before it entered the stack.

The design particulars of the baghouse are given in Table 1, and the completed facility is shown in Figure 1. Boiler fuel during the study was 12,331 BTU/lb. bituminous coal with about 1.4% moisture, 0.83% sulfur and 15% ash.

Some of the major parameters tested and evaluated in the facility included bag tensioning, fabric material, fabric weight, sonic horn cleaning, the influence of particle size on pressure drop and flow distribution. Some dry flue gas desulfurization tests were also conducted.

TABLE 1. FABRIC FILTER DESIGN DATA

Design Gas Volume (ACFM)	2700 TO 5400
Gas Temp. Normal/Maximum ° (F)	Ambient to 500/650
No. of compartments/bags per compart.	2/15
Size of bags: Dia. (in.) x Length (ft.)	8 x 22; 11 x 30
Total bag area (ft. ²)/ air to cloth ratio	1382 to 2708/variable
Bag material	14 oz. woven glass acid resist.
No. of anti-collapse rings	6
Housing & hopper material	3/16 in. carbon steel
Housing W(ft.) x L(ft.) x H(ft.) (incl. hopper)	6.5 x 12 x 45.17
Ash removal	Vacuum system
Reverse air (cfm)/diff. press. (in. w.c.)	0 to 2,000/0 to 10
Rev. air damper dia. (in)/type/operation	12/poppet/pneumatic & electric
Clean air outlet & dirty gas inlet damper: dia. (in.)/type/operation	12/poppet/pneumatic & electric

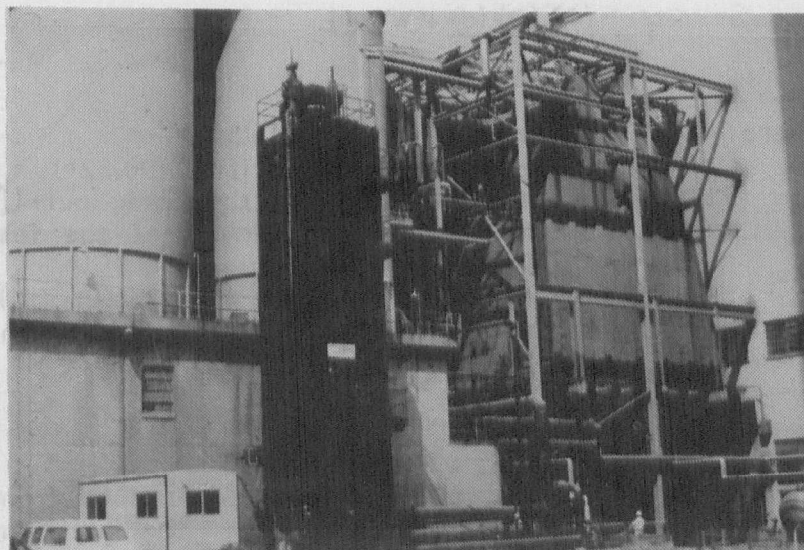


Figure 1. Fabric filter development facility.

BAG TENSION

The study identified bag tension as a significant factor which influences baghouse behavior. Proper tension ranges at various stages of operation for a 30 ft. high x 11.5 inch diameter bag as a function of bag length variations are given in Figure 2. To appreciate the tensioning requirements defined by this figure, the causes and magnitudes of bag length variations at installation and during start up, normal operation and cleaning should be understood. Bag tension beyond the ranges (higher or lower) as shown in Figure 2 has been found to cause bag damage, reduce cleaning effectiveness and increase pressure drop.

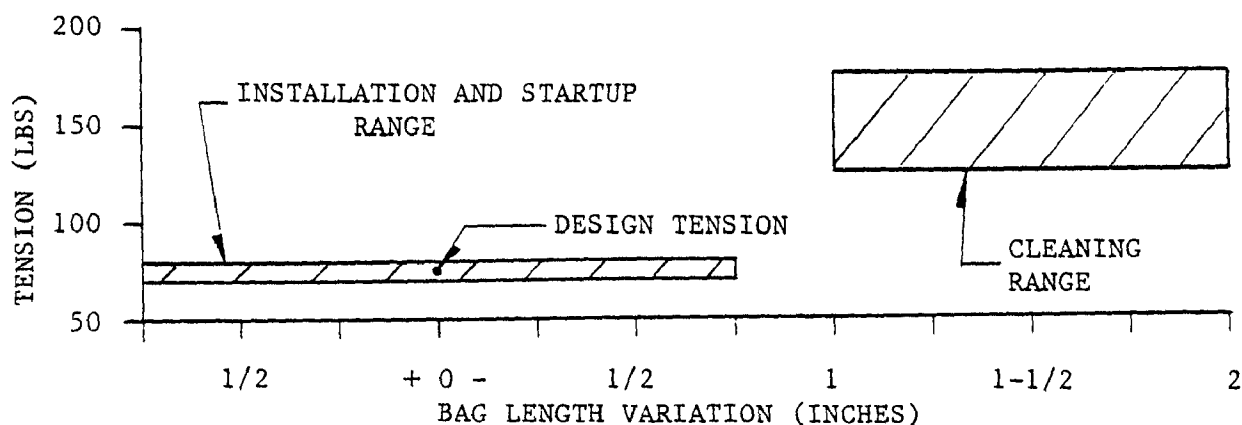


Figure 2. Proper tension ranges vs. bag length variations.

Bag and baghouse manufactures recommend a bag tension which is given typically by an expression of the following form:

$$T = \frac{(A)(D)(d)}{12 \text{ (in./ft.)}} + Wf + L$$

where

- T is the tension required (lbs.)
- A is the gross area of bag (ft.²) (90.32*)
- D is the density of ash on the fabric (pcf) (15*)
- d is the ash layer thickness of the fabric (inches) (0.375*)
- Wf is the weight of the bag without ash (lbs.) (14*)
- L is the required net load at the bottom of the bag (lbs.) (20*)

* values apply for the pilot baghouse

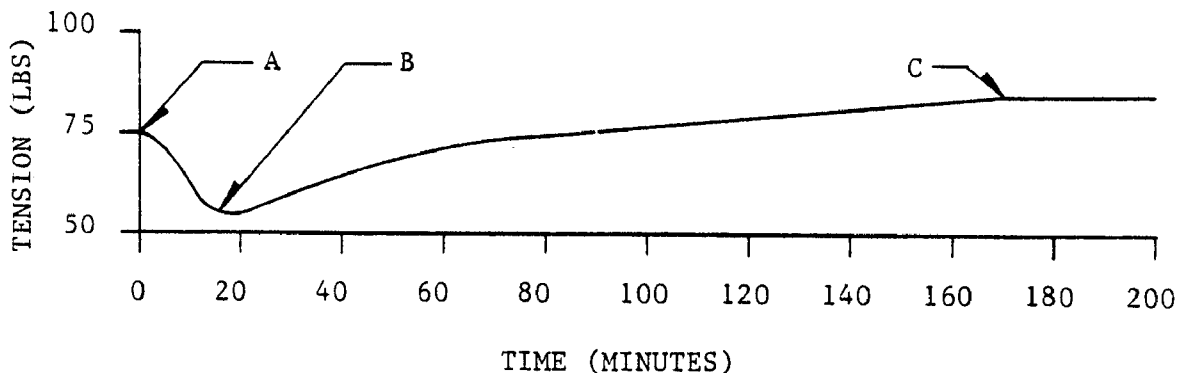
The bag tension for the pilot baghouse as determined from the above information was 76 lbs. Density of the ash (D) on the fabric and ash layer thickness (d) are functions of the ash characteristics and cleaning effectiveness (3). In a baghouse which is cleaning properly, D will vary from 10-25 pcf (4). and d from 1/4 inch to 1/2 inch.

BAG LENGTH VARIATIONS

The real and apparent bag length variations which a bag tensioning device must accommodate at various stages of operation come from numerous sources. At installation, these sources are:

1. Bag manufacturing tolerances (nominal 30ft. long bags typically vary in length about $\pm 1/2$ inch of the nominal length) (5).
2. Variations in the deflection of a bag support system due to mechanical loads (these are estimated to be small).
3. Adjustment increments of the bag tensioning device itself (these vary with the design).

During startup, dimensional variations occur as a result of thermal expansion. Figure 3 shows how the tension for a spring tensioning device varies as the system goes from ambient to steady operating temperature. Note that even though the steel shell has a higher thermal coefficient of expansion than the glass bag ($6.3 \times 10^{-6}/^{\circ}\text{F}$ vs. $2.8 \times 10^{-6}/^{\circ}\text{F}$) the bag grows faster than the shell during the first 15 minutes as evidenced by the reduction in measured tension. This occurs because the hot flue gas totally surrounds the bag, but the shell is exposed to the flue gas only on one side. Once steady operating temperature is reached, tension increases above that measured at ambient temperature indicating that the shell has finally expanded about $3/8$ " more than the 30 ft. long bag.



- A - Start up (outlet gas temperature = 85°F)
B - 15 minutes (outlet gas temperature = 150°F)
C - 170 minutes (outlet gas temperature 350°F)

Figure 3. Bag tension at startup using a spring.

During the first few weeks of service at operating temperature, dimensional variation occurs as the bag elongates (take up) due to the tension applied during normal operation and cleaning (5). This take up is estimated to be about 1/8 inch in the best case for a 30 ft. long bag.

The final dimensional variation which must be considered occurs during the cleaning cycle. To understand the importance of bag tension and the dimensional variation which occurs during cleaning, it is helpful to examine the cleaning mechanisms.

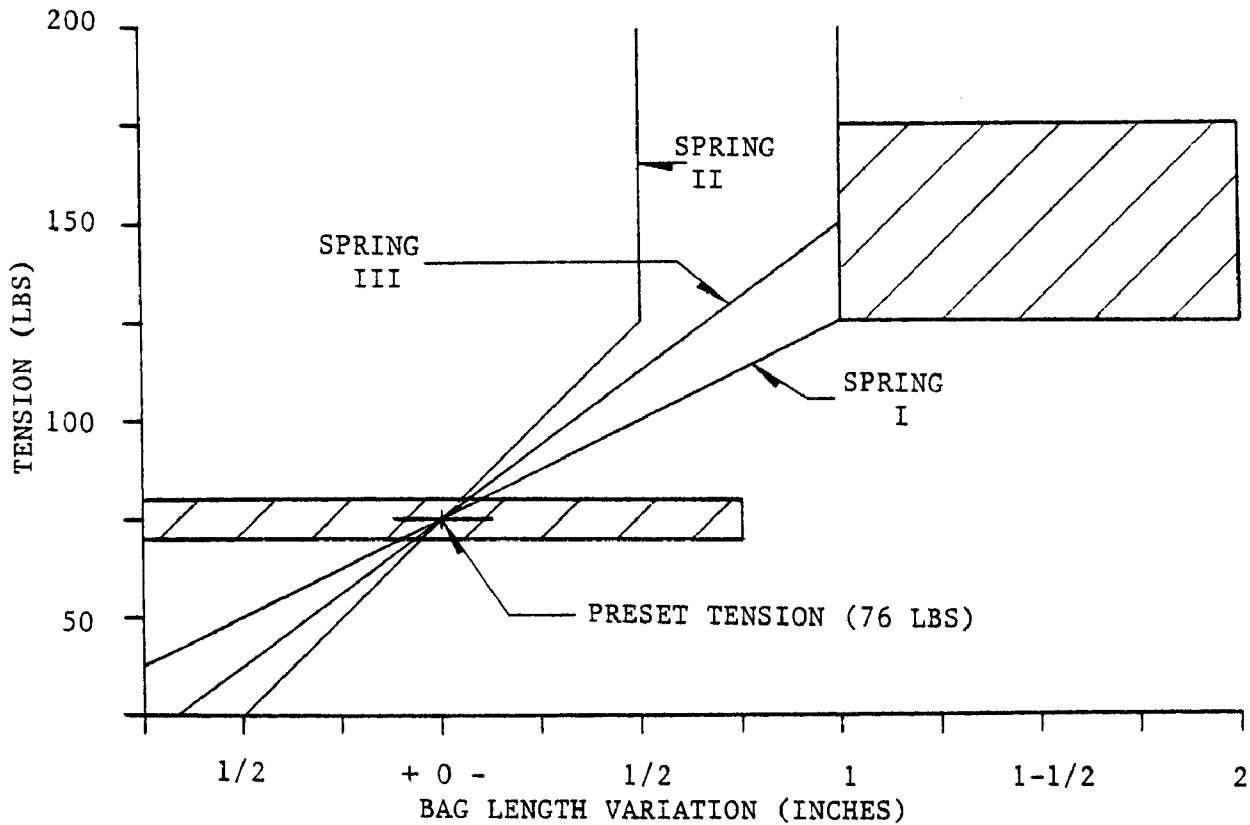
One of the most significant observations consistently made during the study was that the cleaning is not primarily dependent on the amount of reverse air flow. The major cleaning mechanisms were found to be the avalanche effect of the dust as it fell and the secondary air flow through the bag induced by the suction behind the falling dust similar to a piston in a cylinder (2). The primary reverse air starts the avalanche. Similar observations have been reported by other investigators (6, 7). An experiment was conducted without reverse air to confirm the observations about the avalanche cleaning mechanism. After allowing dust to collect under normal operation for about 3 hours, a compartment was taken off line for cleaning. Avalanching was initiated by manually flexing the top portion of the bag causing release of dust at the top only. A pressure tap in the cap of the bag measured a suction of up to 18 inches of water within the bag as the dust fell. The cleaning which resulted was at least as good as that obtained when reverse air initiated the avalanche.

From a dimensional change standpoint, the study indicated that one of the important factors needed to enhance the avalanche effect and promote good cleaning was allowing the bag to deflect (shorten) between 1 and 2 inches during cleaning. This amount of deflection allows the bag to collapse between the anti-collapse rings enough to clean properly without damaging the bag.

TENSIONING DEVICES

SPRINGS

Springs were the first tensioning devices tried during the study. The tension-deflection curves of 3 typical springs used are given in Figure 4.



Spring	I	II	III
Spring rate @ 74°F (lb./in.)	53.33	80.32	78.1
Total height (in.)	3.875	4.3	5.75
Fully compressed height (in.)	1.5	2.8	3.75
Wire material	SS	SS	SS
Wire diameter (in.)	0.171	0.151	0.225
Active Coils	6	14	14

Figure 4. Tension vs. bag length variations for spring tensioners.

None of the springs could satisfy the tension and dimension variation requirements described previously. To get even close to the desired tension conditions with springs during normal operation, the following were required:

1. Very fine adjustment increments were needed during initial tensioning to accommodate bag length differences. Typical support chain link lengths gave too coarse an adjustment to provide reasonably equal tension on all bags.
2. The thermal growth difference between the shell and bag had to be determined and accounted for during initial tensioning to avoid over-tensioning during operation.
3. Once bag take up had reached equilibrium, the bags had to be retensioned.

The desired deflection during cleaning of between 1 and 2 inches could not be achieved because the springs bottomed out. It was concluded that there must be a better way to tension bags.

COUNTERWEIGHT

To satisfy the requirements described previously and others related to installation and maintenance the following design goals were established for a different bag tensioning system:

1. Maintain tension on all bags within the ranges given in Figure 2 while accommodating the following real and relative bag length variations.
 - a) $\pm 1/2$ inch combined bag length and support point deflection differences
 - b) $\pm 1/2$ inch combined thermal expansion difference and bag elongation.
 - c) allow bag deflection during cleaning to be between 1 and 2 inches.
2. One man should be able to connect the bag to the tensioning device and tension the bag without tools or scales.
3. The hardware should last for the life of the baghouse with little or no maintenance.

The device (shown in Figure 5) which was designed to satisfy the above design goals is the patented ENELCO[®] Counterweight. The tension force applied to the bag by this simple lever/weight system is given by:

$$FB = (FA) (X/Y)$$

where FB is the tension force applied to the bag.
 FA is the weight of the counterweight.
 X is the horizontal distance between the counterweight center of gravity and the lever arm pivot point.
 Y is the horizontal distance between the bag centerline and the lever arm pivot point.

ENELCO[®] is a registered trademark of Environmental Elements Corporation, Baltimore, Maryland

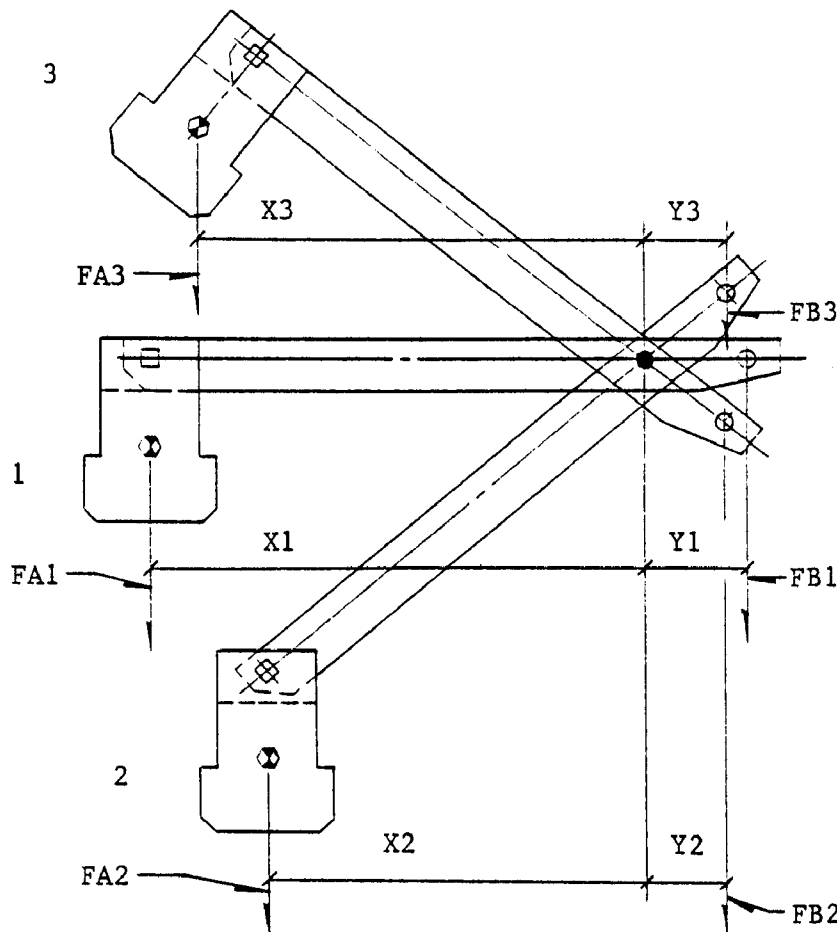


Figure 5. Varying positions of the counterweight and counterarm.

Note that the counterweight is shown in three positions in Figure 5. Positions 1 and 2 demonstrate how, for normal operation, dimensional variations are accommodated while tension is held essentially constant. By allowing the counterweight to be free to pivot on its support pin for the range of lever arm rotation needed to accommodate the desired bag length variations, the X/Y ratio and bag tension remain essentially constant over this range. The third position shown represents the cleaning case. Because it is desirable to apply more tension during cleaning, a stop prevents the weight from further rotation on its support pin when the lever arm rotates to the cleaning position. This causes the X/Y ratio to increase resulting in an increase in force applied to the bag.

Figure 6 shows the tension force applied to a bag by the counterweight system as a function of bag length variations. These data indicated that the desired tension criteria have been satisfied.

The counterweight also satisfies the installation and maintenance design goals. Installation is made easier by disassociating the bag connecting and tensioning processes. The bag and support chain are connected to the counterweight while it is in a relaxed position thus eliminating the need to overcome almost eighty pounds of tension that is required when a bag is connected to a spring system. Once the bag is connected to the lever arm it is only necessary to lower the weight to tension the bag. There are no threaded connections or special tools needed, and field measurements are not required. More important, the tension is right the first time and it remains there. Further, the constant tension feature for dimensional variations eliminates the need to enter the baghouse to retension the bags after a few weeks of service.

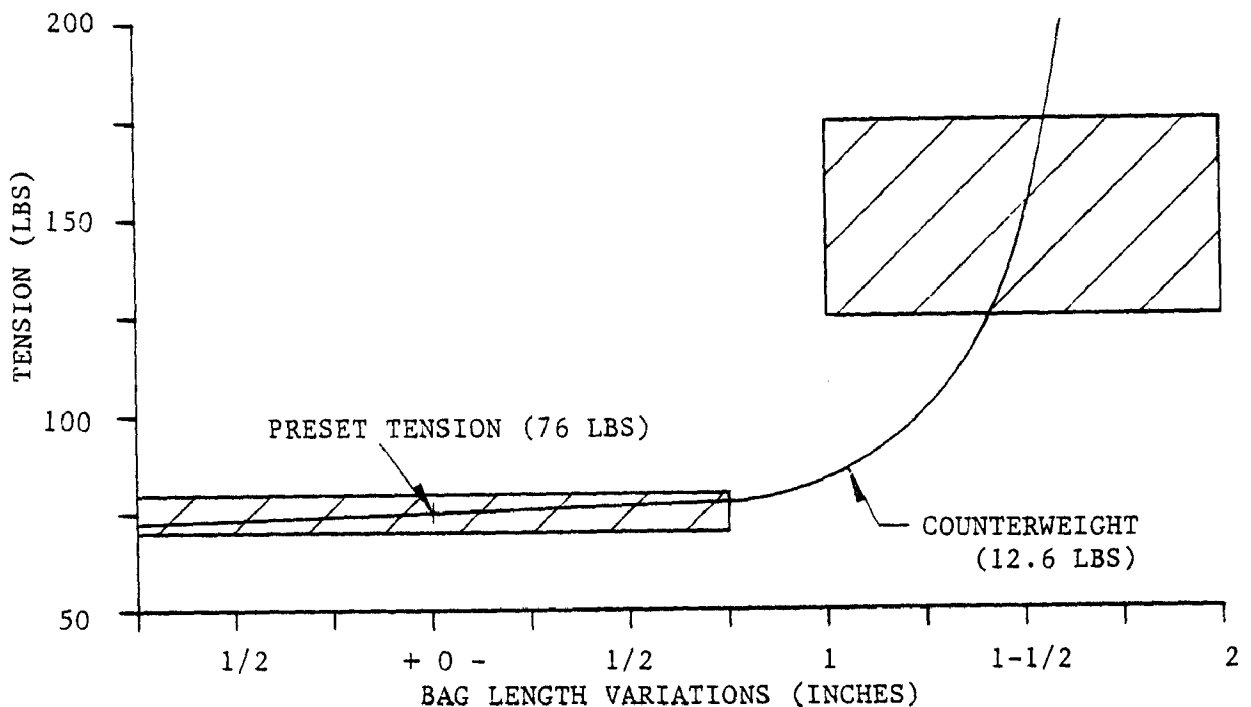


Figure 6. Tension vs. bag length variation for a counterweight bag tensioner.

OPERATING EXPERIENCE

PILOT UNIT

Some of the significant bag tension results and observations obtained from experience with the pilot unit have been cited previously. Following are additional observations:

1. The position of the counterweight is a good indicator of what is going on during the process. Following are two examples:
 - a) During normal operation (when dust is being collected) if the counterweight is above the horizontal axis, the weight of dust on the bag exceeds that used to originally establish the desired tension and thus the weight position indicates that cleaning is required.
 - b) During the cleaning cycle, within two seconds after reverse air is introduced, the counterweight and arm will go to between 60-70 degrees above the horizontal axis. This indicates tension between 150-180 pounds and proper deflection of the bag. Within 4 seconds after reverse air is introduced the counterweight and arm will go to between 35-55 degrees above the horizontal axis, indicating tension between 95-120 pounds and the proper amount of reverse air. This position should be held for the duration of the reverse air flow.
2. With a spring tensioner if (because of improper initial tension or over compensation for thermal expansion) a bag goes slack during operation all of the reverse air applied to the bag during cleaning will go through the bloused portion at the bottom (3). This results in poor cleaning and, ultimately, in bag damage.
3. Bags which deflect more than 2 inches during cleaning will experience excessive fabric flexing and will not be cleaned properly.
4. Bags tensioned by typical spring tensioners which limited deflection during cleaning showed damage in the area of the anticollapse rings after one year of service. For the same conditions, and time bags tensioned by the counterweight showed no such damage.

COMMERCIAL SERVICE

Experience with commercially operating baghouses, including the unit serving Boiler #1 at the Brunner Island Station of the Pennsylvania Power and Light Company, confirmed the shortcomings of spring tensioners. Therefore, in April 1984 the 264 spring tensioners in one compartment were replaced with ENELCO^R Counterweight tensioners. Figure 7 is a photograph of the installed counterweights.

The baghouse compartments are inspected periodically. During an inspection at the end of June, 1984 it was observed that all bags checked in the compartment with the counterweight tensioners had maintained proper uniform tension, whereas in compartments with spring tensioners some slack bags were found.

It is planned to instrument the compartments, including the one with the counterweights, to evaluate pressure drop; however, this work is not complete.



Figure 7. Counterweights installed in the baghouse serving boiler #1 of Brunner Island Station.

PROJECTION OF COST SAVINGS

As noted previously, the counterweight bag tensioning system eliminates the basic installation and maintenance problems associated with a spring tensioning system. The maintenance costs for the counterweight system are, therefore, considerably less than those for a typical spring system. The following example quantifies the savings for a typical case

Assumed Conditions

Gas Volume	1,000,000 ACFM
Gross A/C	1.62
Net A/C	1.80
Net-Net A/C	1.90
Number of Bags/Compartment	324
Number of Compartments	20
Total Number of Bags	6,480

For the above unit equipped with a spring tensioning system it will take about 102 man-hours to complete a bag change out for one compartment (8).¹ If the unit was equipped with a counterweight system the same job could be done in 70 man-hours.¹ Since a spring system typically requires retensioning about 2 weeks after a bag change, an additional 20 man-hours must be included per compartment for this system. Per bag changeout for the complete baghouse using the counterweight system requires about 1040 manhours less than the spring system. At \$25 per manhour, this represents a savings of \$26,000. Assuming a bag change every 3 years and a unit life of 30 years, the saving would be \$260,000. This information is shown graphically in Figure 8.

The above example assumes the same bag life for both tensioning systems. Data from the study indicate that the counterweight system will provide a longer bag life than a spring system. If the counterweight can eliminate one bag change over the life of the unit, and additional saving of about \$520,000 (based on today's bag prices) could be realized.

¹ These numbers were not generated from PP&L, Brunner Island Station.

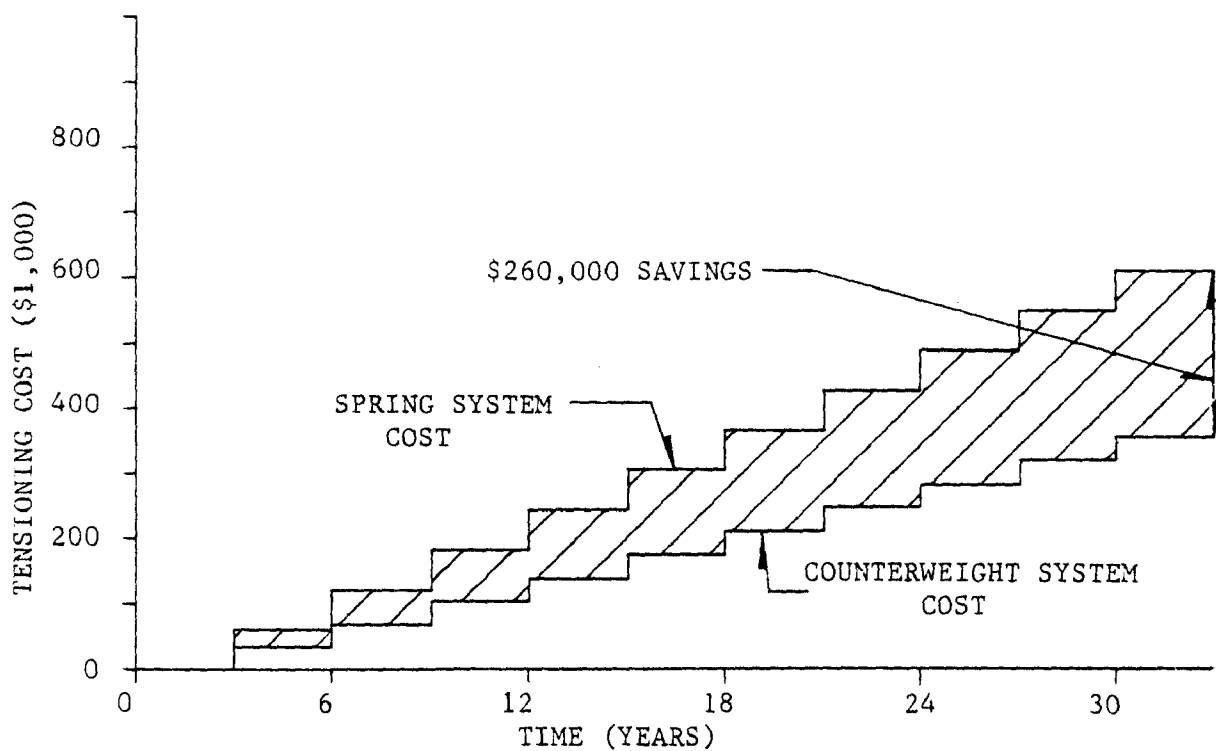


Figure 8. Maintenance cost comparison between counterweight and spring bag tensioners.

The work described in the paper was not funded by the U. S. Environmental Protection Agency and therefore the contents do not necessarily reflect the views of the Agency and no official endorsement should be inferred.

REFERENCES

1. R. C. Carr, and W. B. Smith. Fabric Filter Technology for Utility Coal-Fired Power Plants. In: Journal of the Air Pollution Control Association, February, 84.
2. R. W. Tisone, A. R. Becker, and J. R. Zarfoss. Environmental Elements Report #7376. November, 79.
3. R. W. Tisone and A. R. Becker. Environmental Elements Report #7380. April, 80.
4. R. C. Carr, and W. B. Smith. Fabric Filter Technology for Utility Coal-Fired Power Plants. In: Journal of the Air Pollution Control Association, March, 84.
5. P. R. Campbell. Make Fiberglass Bags Last Longer by Maintaining Proper Tension. In: Power, March, 80.
6. M. G. Ketchuk, M. A. Walsh, O. F. Fortune, M. L. Miller, and M. A. Whittlesey. Fundamental Strategies for Cleaning Reverse Air Baghouses. In: Proceedings of the Fourth Symposium of the Transfer and Utilization of Particulate Control Technology. Houston, Texas 1982.
7. R. C. Carr, and W. B. Smith. Fabric Filter Technology for Utility Coal-Fired Power Plants. In: Journal of the Air Pollution Control Association, April, 84.
8. O. F. Fortune, R. L. Miller, and E. A. Samuel. Fabric Filter Operating Experience from Several Major Utility Units. In: EPA-600/9-82-005A. Third symposium of the Transfer and Utilization of Particulate Control Technology: Volume 1. July, 82.

SOUNDS OF ENERGY SAVINGS

N. D. Phillips
Sr. Project Engineer
Air Pollution Control Engineering
J. A. Barabas
Project Engineer
Research & Development Department
Fuller Company
Bethlehem, Pennsylvania, 18001

ABSTRACT

The concept of sonic energy being used to assist traditional methods of cleaning bags in fabric filter units was started in the late 1950's. Early work was accomplished in the cement kiln baghouse and the carbon black industry with reverse air and shaker units.

During the years of low cost energy from natural gas or oil, there was very little incentive for decreasing pressure drop in baghouses except for wet cement kilns and carbon black applications.

Recent impetus for the use of sonic horns has come from coal fired boiler baghouses which have exhibited the undesirable condition of creeping pressure drop.

Reductions in pressure drop of 1 inch w.g. and greater have been achieved. Depending on the charge rate for power, a 2 inch reduction can pay off the installation in one year.

Present experimenting is aimed at better understanding the phenomenon and determining the method of optimizing the cleaning effectiveness.

Dedication: This paper is dedicated to the memory of W. C. "Charlie" Brumagin, former Chief Product Engineer for Air Pollution Control Equipment of Fuller Company for many years, who was personally involved in the background work of this subject and the initiation of the present day applications. He is sorely missed for his dedicated service.

SOUND OF ENERGY SAVINGS

BACKGROUND

The "Sound of Energy Savings" all started with U. S. Patent No. 2,769,506 by H. Abboud, issued November 6, 1956.

As with all patent concepts that become useful, the hardware must be produced to bring it to fruition. This phase involved several years of development to produce a unit that would achieve the aims of the patent. One phase of testing included a three year simulated environment at 500° F. for life testing.

INTRODUCTION

Sonic energy produces vibrations that may be coupled to receivers from the source. Many instances of secondary vibrations are undesirable, but for the application under discussion the effects are desirable.

Some experimental work has been done to produce agglomeration of small particles into larger ones (1). The effects are dependent on the frequency and sound power. High frequency in the range of 1-4 KHz and at power levels of 600 watts is required for useful effects.

Another use of sonic energy is for cleaning items of hardware in liquid baths. The vibration transmitted through the liquid coupler separates dirt from the specimen. Many commercial systems exist for this process.

The present application of sonic energy cleaning depends on an air coupling between the sonic generator and the dust cake on the surfaces to be cleaned. As will be explained later in the text, sonic energy is not typically the sole cleaning method, it usually assists other methods of cleaning.

SOUND DATA

A typical sonic horn used today as an assist for fabric cleaning consists of two major components. They are a sound generator and a horn or resonator. The driving force for the sonic generator is usually high pressure air. The air quantity and pressure required for a particular sonic horn is a function of its design.

The sound generator usually consists of a cast iron housing that contains a thin, flexible metal plate. This plate is free to vibrate and generate sound. The frequency and intensity of the sound is related to the size and thickness of the plate and the air supply (volume and pressure).

The second major component is the horn section. This acts as a resonator to increase the intensity of the sound that is produced by the generator section. Shapes and sizes of the horn section vary depending on the manufacturer.

Sound in the audible range for these horns has been measured at frequencies from 31.5 to 16,000 Hz. Most sound producing devices have characteristic patterns with a fundamental frequency peak and one or more minor peaks at secondary levels. The sound produced by the present generator is shown in Table 1. These values were measured in free air at various distances.

The dB values are also listed in terms of sound power, W/m², and sound pressure, pascals, Pa., as calculated by the following relationship:

$$\text{dB} = 10 \log_{10} \frac{\text{power}}{10^{-12} \text{ W/m}^2}$$

$$\text{dB} = 20 \log_{10} \frac{\text{pressure}}{.0002 \text{ } \mu \text{ bar}} ; \text{ Pa} = \mu \text{ bar} \times .1$$

Both values have been reported with regard to the effects of sonic energy cleaning fabric filter surfaces in baghouses. It is obvious that horn power should be considered by either of these values rather than dB values.

Sound power within compartments maintains higher values due to the reflection and reverberation. Orientation of the horns in compartments has an effect on the sound levels and this will be discussed later.

Figure 1 shows the frequency peak data for two different pieces of hardware. As is well known, shorter horns on sound generators produce higher frequency values. It has been learned that by varying the air supply pressure on the shorter horns, the frequency peak can be enhanced, as shown in Figure 2 and Table 2.

APPLICATIONS

Early trials with horns in baghouses were purely empirical to determine benefits for bag cleaning. However, a prime concern in developing the useful hardware was to produce equipment with life in excess of 3 years. During early development work many horns were destroyed by the sound power produced. This was corrected by proper choice of materials of heavy gage and welding techniques (2).

The usual installation of horns in baghouse compartments is shown in Figure 3, for practice prior to 1981.

Even though horns have been used since 1959, no published articles are available on the practice prior to 1982 (3 and 4). Since then many articles (5, 6, 7, 8, 9, 10) have appeared describing installations and test work to evaluate performance.

TABLE 1
SOUND LEVEL OF FULLER SONIC HORNS
MEASURED IN FREE AIR

Line Pressure PSIG	Distance Hz	SOUND LEVEL			SOUND INTENSITY			SOUND PRESSURE		
		.5'	15' dB	30'	.5'	15' Watts/m ²	30'	.5'	15' Pascal	30'
90	31.5	89	66	59	--	--	--	--	--	--
	64	103	81	76	--	--	--	--	--	--
	125	142	113	107	163.9	0.18	0.05	252.6	8.4	4.4
	250	151	122	116	1303.1	1.45	0.36	712.3	23.8	11.8
	500	145	116	110	327.7	0.36	0.09	357.2	11.8	5.9
	1000	140	111	105	104.0	0.12	0.03	201.2	6.8	3.4
	2000	127	100	94	5.2	0.01	--	45.0	2.0	--
	4000	112	84	85	--	--	--	--	--	--
	8000	98	78	79	--	--	--	--	--	--
	16000	90	62	59	--	--	--	--	--	--

-- Values below .01

-- Values below 1.0

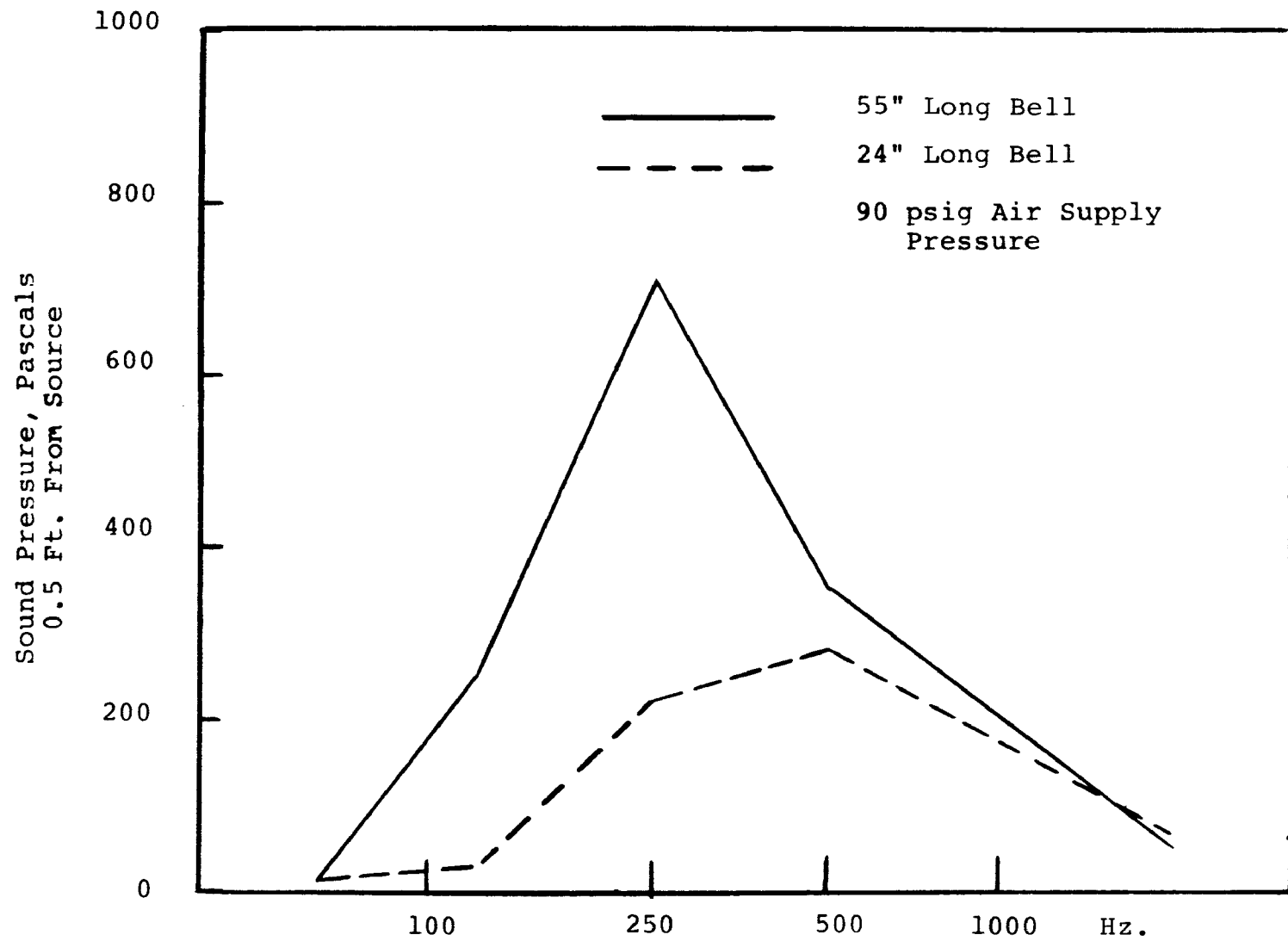


Figure 1. Sound Patterns of Fuller Sonic Horns

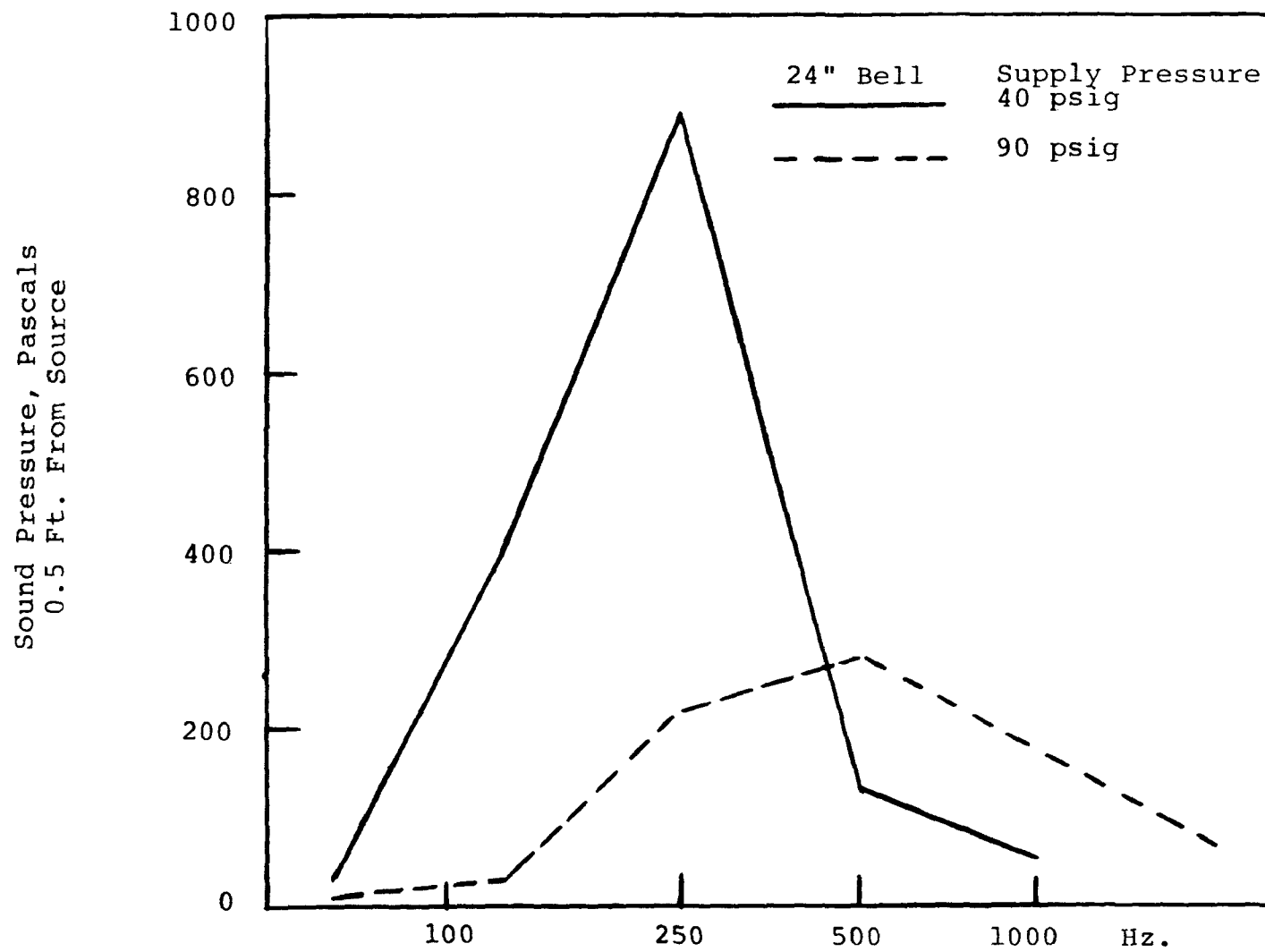


Figure 2. Frequency Changes With Air Pressure Control

TABLE 2
SOUND LEVEL OF SHORT BELL
MEASURED IN FREE AIR

Line Pressure PSIG	Distance Hz	SOUND LEVEL			SOUND INTENSITY			SOUND PRESSURE		
		.5'	15' dB	30'	.5'	15' Watts/m ²	30'	.5'	15' Pascal	30'
90	31.5	--	--	--	--	--	--	--	--	--
	64	124	--	--	2.6	--	--	31.8	--	--
	125	124	--	--	2.6	--	--	31.8	--	--
	250	141	111	106	130.1	0.14	0.04	225.1	7.4	4.0
	500	143	114	108	205.5	0.23	0.06	282.9	9.5	4.8
	1000	138	108	103	65.0	0.07	0.02	159.1	5.2	2.8
	2000	130	100	--	10.4	0.01	--	63.6	2.0	--
	4000	--	--	--	--	--	--	--	--	--
	8000	--	--	--	--	--	--	--	--	--
	16000	--	--	--	--	--	--	--	--	--
40	31.5	--	--	--	--	--	--	--	--	--
	64	124	--	--	2.6	--	--	31.8	--	--
	125	146	117	110	411.0	0.46	0.11	400	13.4	6.5
	250	153	124	118	2065.2	2.29	0.57	896.8	29.9	14.9
	500	136	107	100	41.6	0.05	0.01	127.3	4.4	2.0
	1000	129	100	--	7.8	0.01	--	55.1	2.0	--
	2000	--	--	--	--	--	--	--	--	--
	4000	--	--	--	--	--	--	--	--	--
	8000	--	--	--	--	--	--	--	--	--
	16000	--	--	--	--	--	--	--	--	--

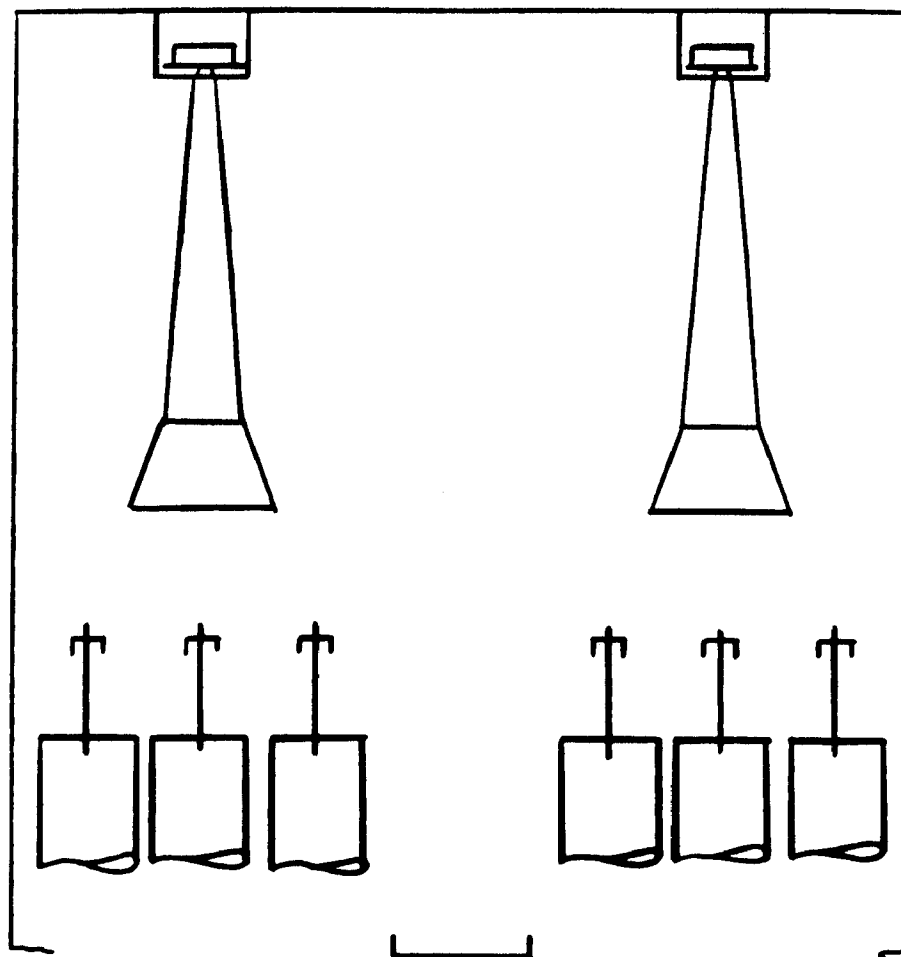


Figure 3. Vertical Arrangement Above Bags

For testing horns in one or two compartments to evaluate potential benefits, three types of data can be acquired, but only one method can be truly indicative of percentage gain in performance.

1. Bag weights
2. Tube sheet pressure drop.
3. Compartment flow.

1. A decrease in bag weight due to better cleaning with sonic horns shows the effect, but it cannot be directly translated to actual savings.
2. Tube sheet pressure drop values can be misleading because increased flow due to better cleaning can increase the pressure drop whereas we would expect a lower pressure drop.
3. The change in air flow through a compartment can be determined by measuring the pressure drop across the outlet poppet valves. Since the poppet valve is similar to an orifice meter, the change in flow through a compartment can be approximated by the change in the square root of the valve pressure drop. We have seen a 30% increase in flow through a test compartment. Other techniques have used pitot tubes in the outlet duct of a compartment. Usually the connection from the compartment to the manifold does not provide this opportunity.

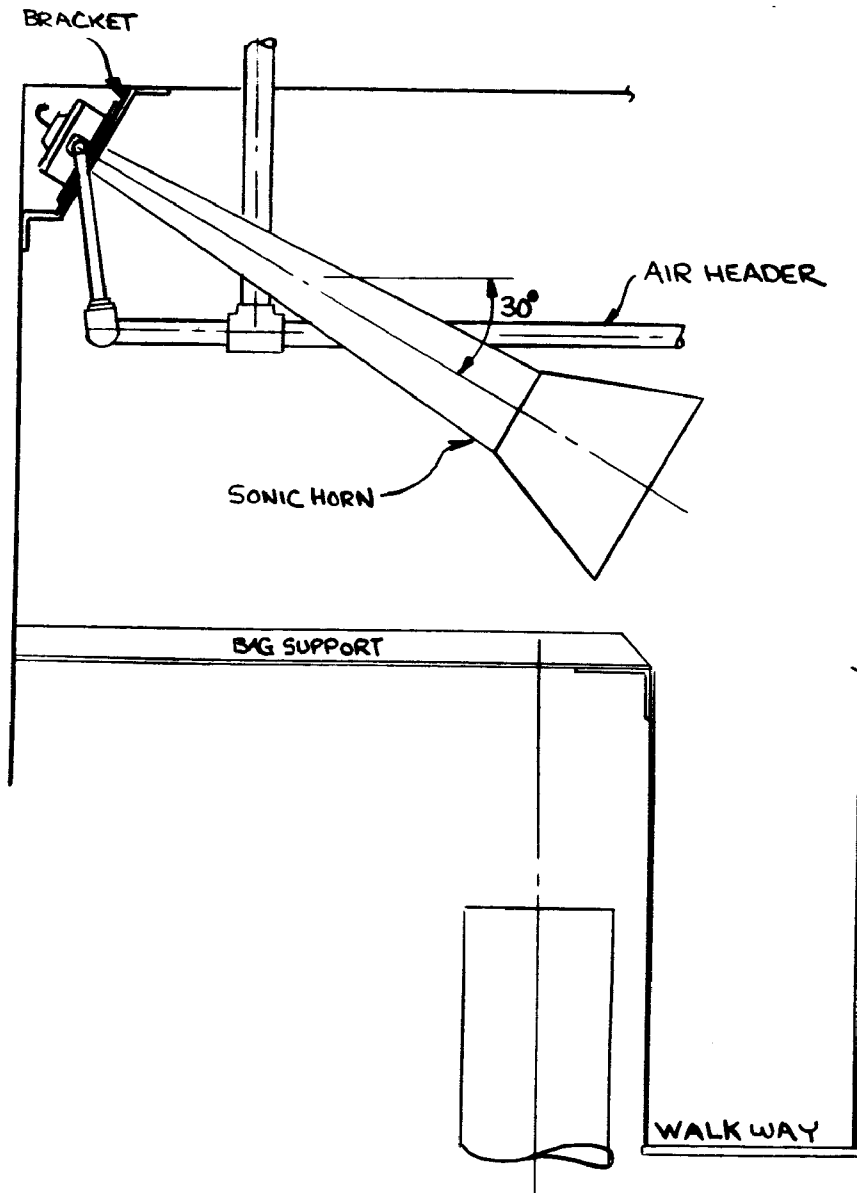
Because of space restrictions, horns were installed on an angle at Bruner Island as shown in Figure 4, (4). The sound level patterns measured [9] with this arrangement indicate that apparently more reflection and reverberation of the sound waves is produced by this arrangement to produce adequate cleaning in conjunction with reverse air. Table 3 shows a comparison between vertical and angular arrangements. The important value is the percent of energy or pressure available at all levels of the compartment.

Since this data has been obtained, the angular arrangement with slopes of 30°, 10°, and 5° from horizontal has been utilized in three full size baghouses and several test installations. The success has been gratifying.

The Fuller Company supplied baghouse at the Holtwood Station of PP&L has maintained approximately 6-1/2" w.c. pressure drop, flange to flange, for over three years with the use of horns. Even though there was evidence of "creeping" pressure prior to installing the horns, this has not occurred since.

Furthermore, with regard to this installation, the original bags are still in use after 3-1/2 years. There does not appear to be evidence of shortened bag life due to the use of horns. Many baghouses in cement kiln applications using sonic horns have equally long bag life but they are not as well documented as at Holtwood.

3-10



SECTION A-A
SECTION B-B

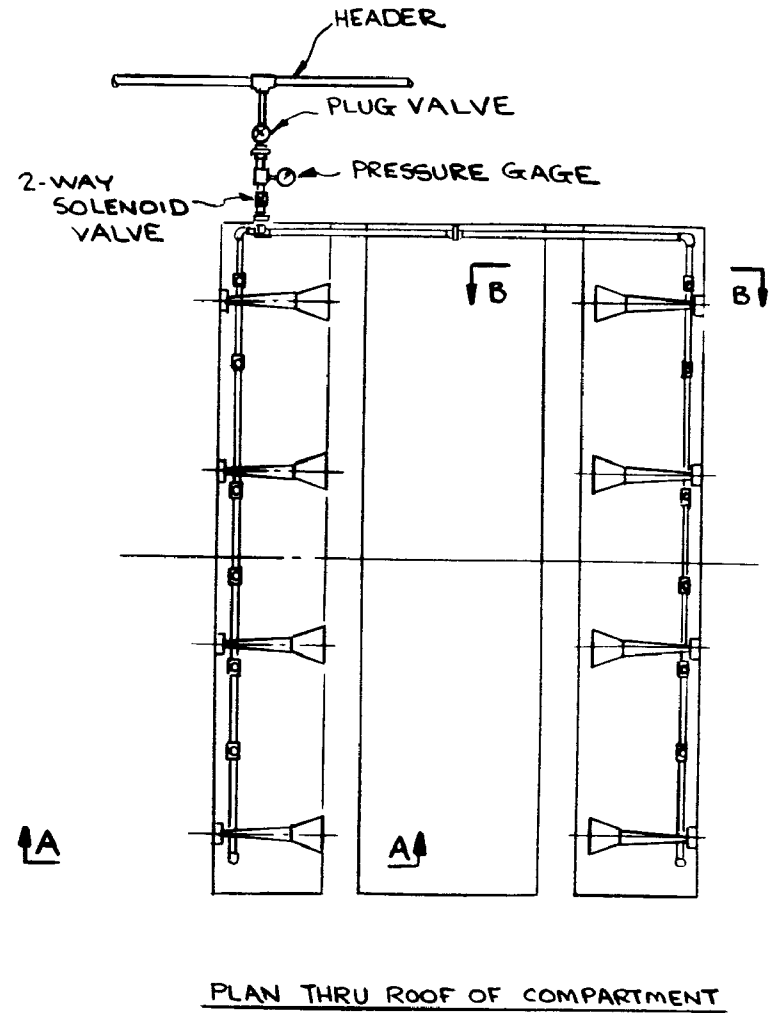


Figure 4. Typical Angular Horn Arrangement

TABLE 3
COMPARISON OF SOUND LEVEL BETWEEN
VERTICAL AND ANGULAR ARRANGEMENTS

Location	dB	Power, W/m ²	% Top Power	Pressure, Pa	% Top Pressure
Number and Arrangement		(2) Top Vertical	Station A		
Top	131.6	14.4	100	76.0	100
Middle	130.6	11.4	79	67.7	89
Bottom	126	4.0	27.7	39.9	52.5
Sq.ft. cloth per horn		4126			
Cu.ft. compartment per horn		3986			

(4) Top Vertical Station A

Top	132.2	16.2	100	81.5	100
Middle	131.3	13.5	83.3	73.5	90.1
Bottom	128.4	6.9	42.6	52.6	64.5
Sq.ft. per horn		2063			
Cu.ft. per horn		1993			

(2) Top (2) Middle Vertical Station A

Top	131.	12.5	100	70.9	100
Middle	130.5	11.2	89.6	66.9	94.3
Bottom	129	8.0	64	56.4	79.4
Sq.ft. per horn		2063			
Cu.ft. per horn		1993			

(8) Top Angular Station B

Top	135.1	32.4	100	113.7	100
Middle	133	20	61.7	89.3	78.5
Bottom	133.9	24.4	75.3	99.1	87.2
Sq.ft. per horn		3409			
Cu.ft. per horn		2851			

(8) Top Angular (4) Middle Vertical Station B

Top	137.2	52.9	100	144.9	100
Middle	135.3	34.1	64.5	116.4	80.3
Bottom	135.6	36.1	68.2	120.5	83.1
Sq.ft. per horn		2275			
Cu.ft. per horn		1900			

At present day costs, the following scenario can be shown:

Approximate installed cost of horn	\$1000 each.
Fan horsepower savings	@ 7¢/KWH
Annual operating savings at 1" ΔP reduction (5000 sq.ft. cloth per horn @ 2 A/C)	\$ 876/horn

Therefore, with a 1" reduction, the installation can be paid for in about one year and with a 2" reduction the capital costs will be recovered in less than one year.

SPECIAL APPLICATIONS

Sonic horns are also being applied to cleaning I.D. fans, tubular air heater tube sheets, economizers, boiler banks, and electrostatic precipitators. These applications are new without confirmed long term benefits, but early results appear favorable. The sonic energy can be useful to break the bond of dust cake build-ups as long as there is a moving gas stream to carry away the dust.

CONCLUSION

Many successful installations have proved that sonic horns can assist reverse air cleaning of the bags in baghouses. The pressure drop reduction and the fan power savings achieved can pay for the installation in one year or less.

The work described in this paper was not funded by the U. S. Environmental Protection Agency, and therefore the contents do not necessarily reflect the views of the Agency and no official endorsement should be inferred.

REFERENCES

1. Volk, M. Jr. and Hogg, R. - Sonic Agglomeration of Aerosol Particles. Technical Report March 1977 CAES Publication No. 465-77.
2. Lincoln, R. L. - Fuller Company files.
3. Wagner, N. H. and Hokkanen, G. G. - Design, Start-up and Operating Experience Of The Holtwood SES Unit 17 Additional Bag House Filter and Related Equipment. PEA Winter Meeting January 21, 1982.
4. Murray, R. W. and Lear, G. L. - Design, Start-Up and Operation To Date Of The Brunner Island Unit 1 Bag Filter. PEA Winter Meeting January 21, 1982.
5. Menard, A. R. and Richards, R. M. - The Use Of Sonic Air Horns As An Assist To Reverse Air Cleaning Of A Fabric Filter Dust Collector. Transferring Utilization Of Particulate Control Technology. Houston, Texas October 13, 1982.
6. Cushing, K. M. et. al. - A Study Of Sonic Cleaning For Enhanced Baghouse Performance. 2nd Conference On Fabric Filter Technology For Coal Fired Power Plants Denver, Colorado March 22-24, 1983.
7. Wagner, N. H. - Present Status Of Bag Filters At Pennsylvania Power and Light Co, ibid Reference No. 6.
8. Menard, A. R. and Richards, R. M. - The Use Of Sonic Air Horns As An Assist To Reverse Air Cleaning Of A Fabric Filter Dust Collector ibid Reference No. 6.
9. Cushing, K. M.; Smith, W. B.; Carr, R. C. - A Study Of Sonic Cleaning For Enhanced Fabric Filter Performance. Paper 84-95.5 presented at the 77th APCA Annual Meeting San Francisco, California 1984.
10. Felix, L. G. and Merritt, R. L. - Field Evaluation Of Sonic Assisted Reverse Gas and Shaker Cleaned Full Scale Utility Baghouses. Paper No. 84-95.7 ibid Reference No. 8.

SOLVING THE PRESSURE DROP PROBLEM IN
FABRIC FILTER BAG HOUSES

Carl V. Leunig
Albany International Corp.
Albany, New York 12201

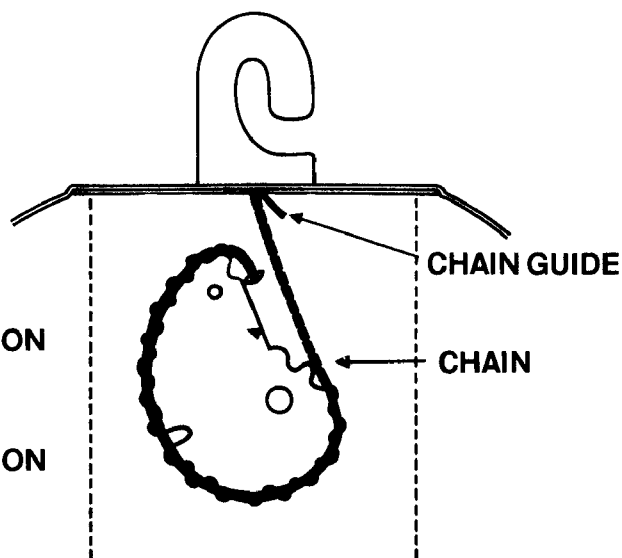
Two years ago at a fabric filter symposium sponsored by Electric Power Research Institute (EPRI), I suggested the use of a constant tension cap to improve the cleaning and extend the life of the bags by preventing cuffing at the lower extremities of the bag. This product development was directed to what was defined as the problem area, the lower extremity of the bag, where failure was most prevalent.

At that time, it was a widely held belief that accurate initial setting of a bag tension would eliminate all kinds of problems. Accepting this simplistic and subjective analysis dictated the need for a tension measuring device to measure bag tension. Many attempts to design such a product met with failure. It was decided that it would be simpler to design a product to give uniform tension at all settings rather than measure what was applied by the crude tensioning devices being used. The Albany International tension device trademarked Tensi-Top^(R) is the result of that effort.

SPRING RATE
40-160#
IN 3/4 REVOLUTION

CAM ½" TO 2"
IN 3/4 REVOLUTION

TRAVEL 6½"



The diagram illustrates the internal components of a Spring Spacer Cup (2). A central vertical shaft passes through the assembly. At the top, a hook is attached to the shaft. Below the hook, a guide is positioned. The assembly is supported by a base plate, which is covered by a fume cap. The base plate is held in place by two brackets. A chain is connected to the shaft and the base plate. A spring is attached to the chain and the base plate. A sprocket cam is mounted on the shaft. A spacer is located between the sprocket cam and the spring. A shaft is also shown, connected to the sprocket cam.

Labels in the diagram include: Hook, Guide, Fume Cap, Bracket (2), Chain, Base Plate, Shaft, Sprocket Cam, Spacer, Spring, and Spring Spacer Cup (2).

Figure 2. Constant Tension End Cap Schematic

To operate as a constant tension device the cam has a linear change of fulcrum the same as the linear rate of the spring. For example, the spring schematically illustrated has a rate which increases from 0 to 160# in 360 degrees. The cam has a fulcrum which increases from 1/2" to 2" in 270 degrees. When pulled to 90 degrees the spring force is 40 pounds. At this point the fulcrum of the cam is 1/2 inch, exerting a force of 80# on the chain. This is the initial setting point on the device. Rotating the cam to 180 degrees increases the spring force to 80 pounds where it now acts through a one inch fulcrum to provide 80 pounds of pull on the chain. At a full 270 degrees the spring force is 160 pounds acting through the two inch fulcrum which still provides 80 pounds of tension to the chain. At any intermediate point the fulcrum arm works in conjunction with the spring rate to provide an 80# pull.

The chain travel is 6 inches from its set point to its fully extended position, more than ample to compensate for thermal expansion, bag stretch and/or relaxation, and installation variables. 80# tension illustrated would accommodate a 70# bag and cake weight and still provide a minimum of 10# tension in the bottom of the bag.

You will notice that the device is mounted inside the bag. While not essential to the operation, this arrangement allows for an increase in bag length of approximately 3% per bag.

The device utilizes a spring of chrome silicon steel which has a service temperature of 425 degrees F (SMI)*. Carbon steel can only be utilized at temperatures below 250 degrees F. For temperatures above 475 degrees stainless steel would be the spring of choice. Operating springs above their service temperatures result in rapid decay of spring force, effective travel (pitch) and free height. At 400 degrees for 100 hours a carbon steel spring tested for this device lost 20% of its free height and almost 30 pounds of its total 160 pound torque.

The initial results in applying a constant tension device to a bag solved only two problems. It eliminated cuffing at the lower extremities and thermal expansion differentials but only marginally improved cleaning. These results dictated a more thorough theoretical analysis of what occurs during the null and cleaning portions of the cycle.

In many reverse air hanging systems a compression spring imparts a tension load on the bag. These spring supports are designed to provide an initial tension compatible with the bag

*Spring Manufacturers Institute

weight and cake weight anticipated. Accurate tension settings are difficult to achieve and spring rates in the order of 40#/inch are generally used. Travel is often limited to 1 or 2 inches after tensioning.

It is obvious that to clean a bag a catenary must form between the anti-collapse rings of the bag. It was hypothesized that the deeper the catenary, the better the cleaning of the bag.

It was obvious that the bag would have to foreshorten to allow the catenary to form. It was also noted that in a conventional hanger system foreshortening would be inhibited since every inch of spring compression would impart an additional 40# of tension on the bag.

Since the bag with its cake load does not impart uniform stresses along the bag length it became apparent that the forces required to form the catenary would vary from a maximum at the top to a minimum at the bottom.

When a new bag is hung the tension in the longitudinal bag fibers is a function of initial tension applied to the bag. The initial bag weight of approximately 10 pounds causes a differential of only 10 pounds from top to bottom in a static condition. During bag house operation the tension on the bag is increased as a function of the pressure drop forces applied to the area of the cap. As cake buildup occurs, the differential from top to bottom increases. With a bag weight of 10 pounds and a cake weight of 60 pounds the vertical fibers see a variation in load of 70 pounds. With the application of reverse air the forces to be overcome will go to 200-260 pounds if 2" foreshortening occurs and a catenary will only form at the lower reaches of the bag and only with high reverse air pressures. Figure 3 shows the bag tension at various stages, using conventional hangers and 8 ring bags.

It becomes obvious that to form a uniform catenary a variable force is necessary from top to bottom. Since the reverse air pressure in the compartment can be assumed to be a constant then the only practical way to overcome the variable tension load is to stagger the ring spacing. Figure 4 shows the condition at various stages for the constant tension device and staggered ring bag.

An iterative approach was used to determine the spacing of the rings to allow for a uniform five inch catenary depth between the rings. It is also possible, if necessary, to design the bag to provide a variable catenary from top to bottom to allow for different cake consistency within the bag from top to bottom.

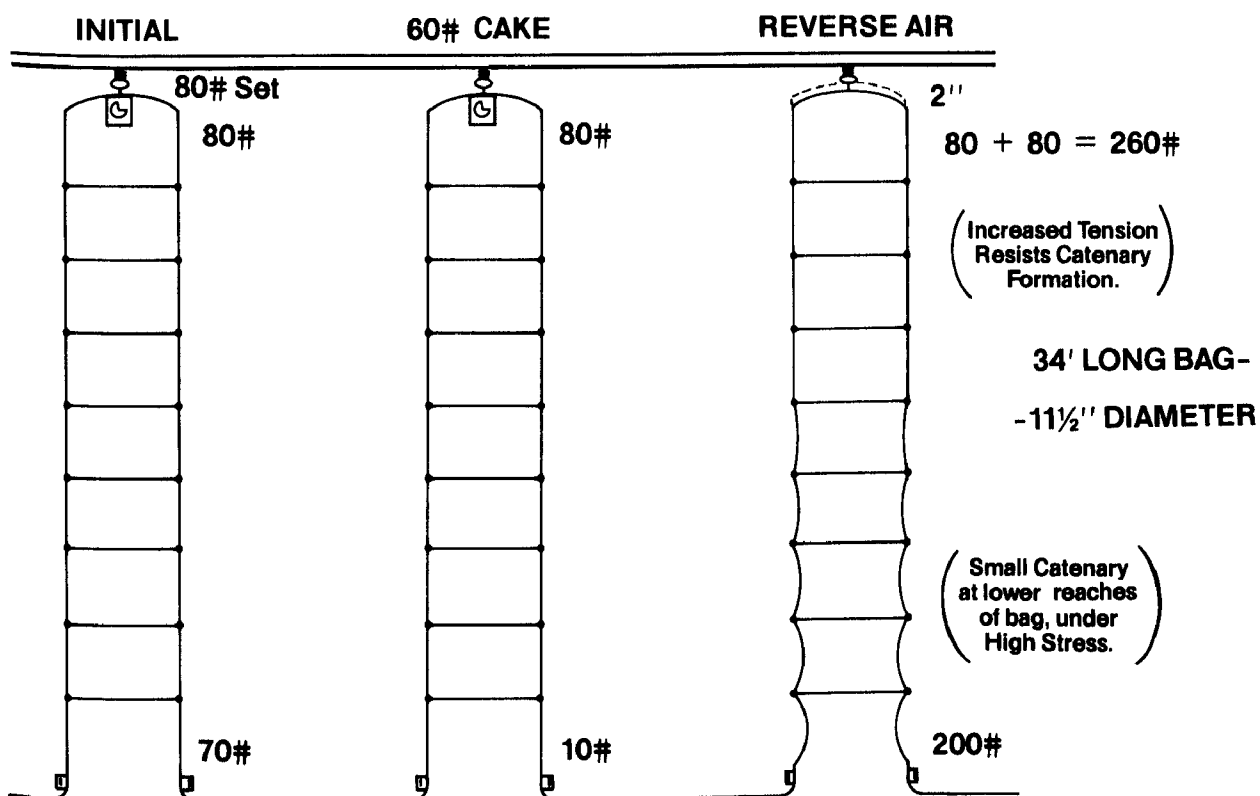


Figure 3. Top and Bottom Loads (Conventional Hangers)

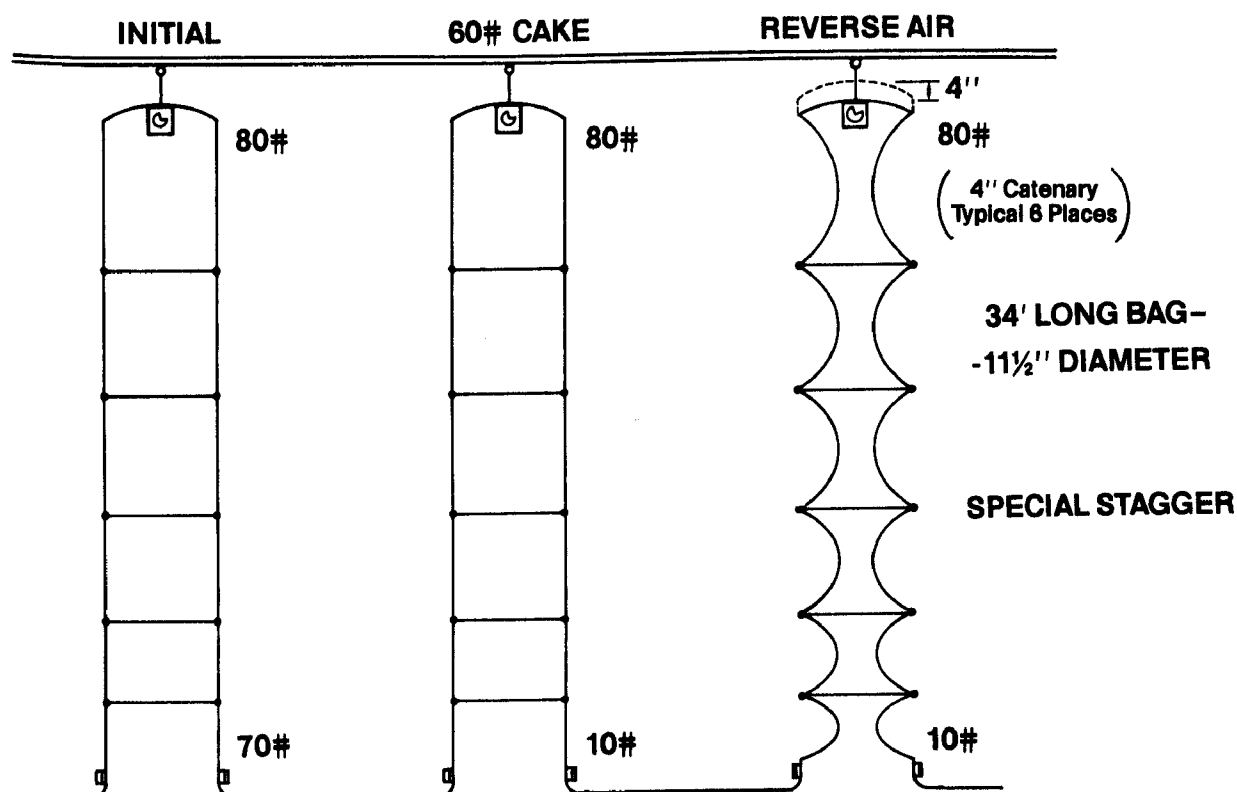


Figure 4. Top and Bottom Loads (Constant Tension)

The resulting bag design had five rings with spacing diminishing from top to bottom instead of the normal eight rings, uniformly spaced. In order for this five inch catenary to form it was calculated that a 5 inch foreshortening would have to occur. In a conventional hanger system this 5 inches would impart an additional 200 pound loading on the bag inhibiting catenary formation. With a constant tension device no additional load is imparted and the catenary can readily form.

An unanticipated benefit was achieved from this 5 ring bag in that in the null mode the bag forms a four cusped hypocycloid or astroid in the upper reaches of the bag, which stresses the cake in the vertical plane. (See Figure 5.)

This formation is sufficient in itself to start cake removal or to facilitate it when reverse air is applied for cleaning.

Since the glass fabric is not extensible or compressible in itself, the catenary formed is not a pure catenary. In order to reduce in diameter some convoluting is formed in the fabric. This convoluting during reverse air application goes from none at the anti-collapse rings to a maximum at the deepest point of the catenary. This convoluting of the bag also contributes to the effective release of the cake from the fabric.

Since an astroid is formed in the null mode it is postulated that this shape convolution or a variant of it will continue to propagate on the application of reverse air along the lines already imposed. This, of course, is dependent on the amount of catenary selected. Figure 6 shows a possible astroid variant.

It has been repeatedly observed that bag cleaning occurs mainly at the lower reaches of the bag. It has also been repeatedly observed that bag failure is concentrated in this area. It is now obvious that this area is the only area where some catenary can form and some cleaning can occur. This also explains why only 10 to 15% of the cake is removed during the cleaning cycle. In excess of 50 pounds of residual cake has been observed in bags removed after cleaning.

Two bags with these staggered rings and Albany International's Constant Tension Cap were installed in a bag house in April 1983 and the results were astounding. No apparent residual cake could be detected anywhere from top to bottom, while the adjacent bags with uniform spacing and conventional hangers exhibited a cake in excess of $3/8$ of an inch at the top and $1/4$ inch at the bottom. This is evidence that any catenary formed in the conventional system is not sufficient to release the cake. These two staggered ring bags and constant tension

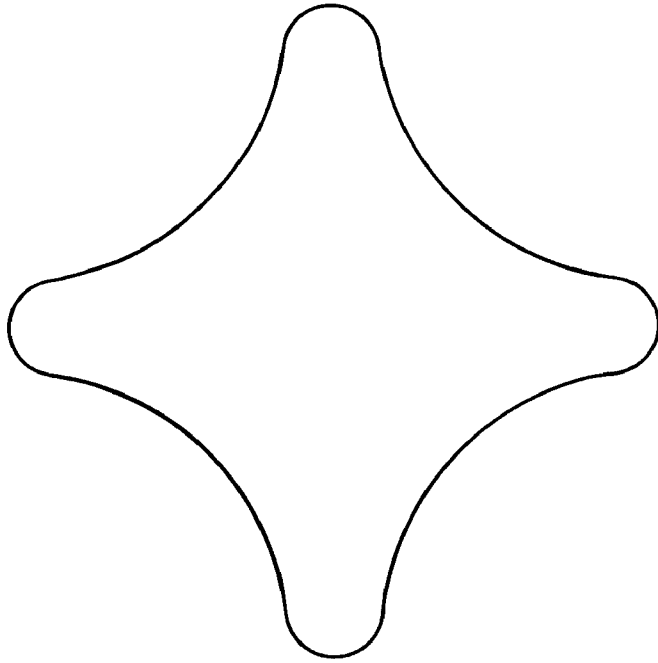


Figure 5. Astroid

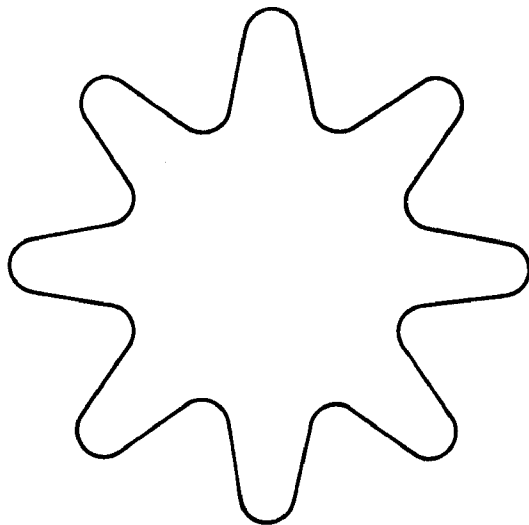


Figure 6. Astroid Variant

tops continued their outstanding performance for over nine months even though they were getting a preferential air flow within the compartment and a much more rapid cake buildup than the conventional bags adjacent to them. In actual use the amount of catenary formed was limited to four inches which causes a foreshortening of about four inches. Catenary formation in both conventional and constant tension modes is shown in Figure 7.

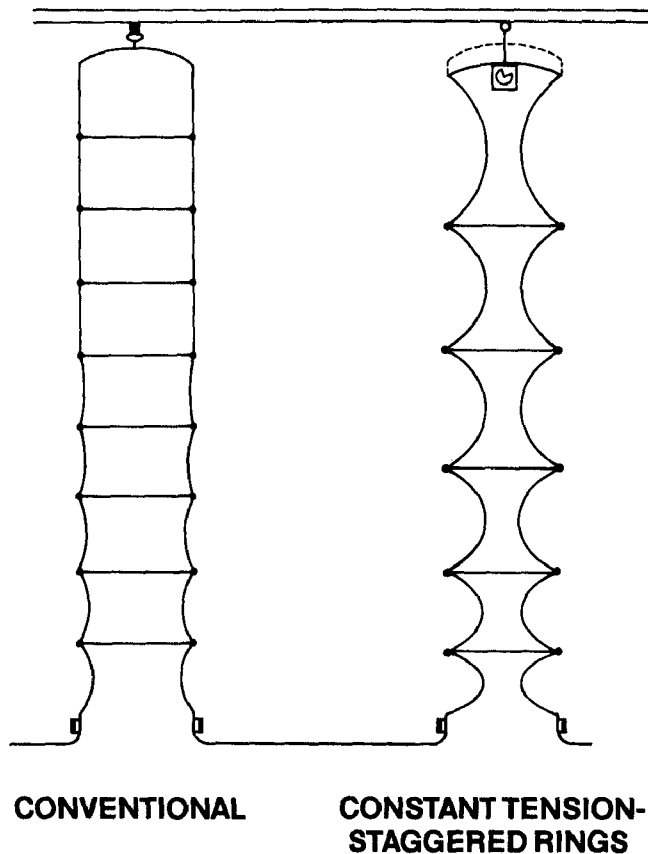


Figure 7. Catenary Formation

Catenary control is obtained during installation. Since the cap has a six inch travel, a two inch initial extension of the chain will allow a foreshortening of only four inches. Bag ring spacing is designed as a function of baghouse operating parameters among which are bag material, cake weight, bag diameter, bag length, and pressure drop.

After a bag is designed the relationship between foreshortening and catenary depth can be readily calculated. For the five ring bag under test the relationship is slightly

greater than one to one, so a four inch foreshortening gives approximately a four and a half inch catenary. Figure 8 .

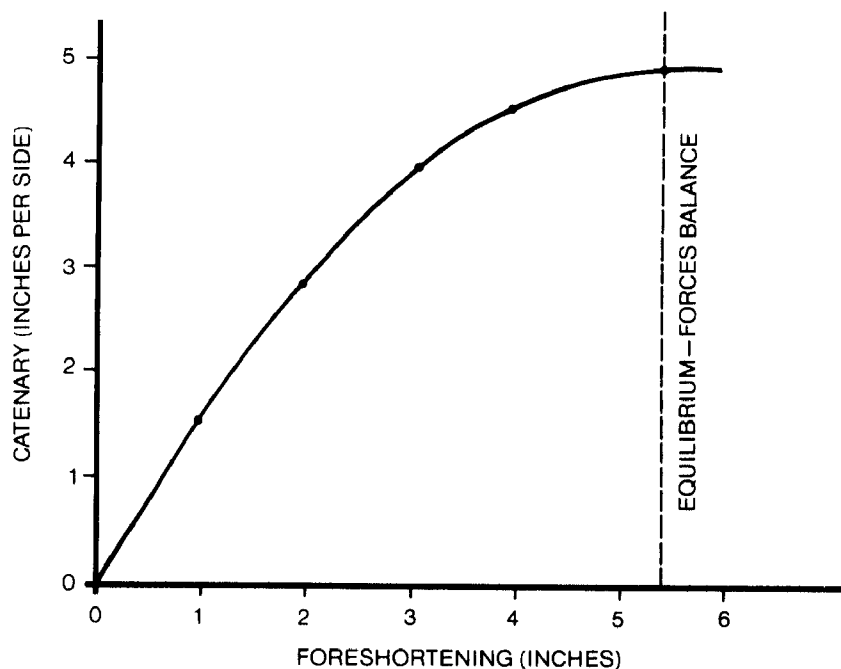


Figure 8. Catenary Formation vs. Foreshortening--34 ft. (408 in.) Constant Tension Cap--5 Ring Staggered Spaced Bag

A full scale compartment will be implemented shortly to determine the magnitude of the pressure drop reduction, and to more thoroughly observe the operation of the bags.

Bag design and tensions can be readily tailored to individual bag house operating parameters. The economic implications for the bag house user for such a dramatic improvement in cleaning with corresponding pressure drop reduction are numerous. Some of the more obvious ones are:

1. Reduction in number of bags required and maintained.
2. Significant energy savings from reduced pressure drop.
3. Longer bag life resulting from reduced bag stress during cleaning.
4. Elimination of mechanical damage due to cuffing.
5. Reduction in load - shedding due to high pressure drop.

In new bag house construction an additional significant capital savings could result from a smaller bag house requirement to handle the anticipated flow.

While most of our attention has been devoted to reverse air bag houses and glass fabric bags, there are indications that a constant tension device could provide many benefits in a shaker bag house using polymer fabric bags.

In a polymeric fabric bag house operating at above ambient conditions a bag will expand significantly more than the bag house. For example, at 250°F. a 35 foot bag would expand over 3 inches, causing a bag to go slack. This affects the shake of the bag. Any slackness can cause cuffing and premature bag failure.

Polymeric bags are also more prone to creep, so a constant tension device will eliminate any need for retensioning.

Any beneficial effects in a shaker bag house at this time is supposition but the possible benefits dictate that these effects be evaluated.

Albany International has been awarded U.S. Patent #4,389,228 for the Tensi-Top(R) cap with patents pending in foreign countries. Patents also have been applied for on the bag designs used in this system.

The device can be affixed within bag caps of 6 inches diameter or larger, or it can be affixed to the bag house structure.

Completion of production tooling is anticipated by late August, after which the full scale compartment trial will be implemented.

Session 13: FF: FULL-SCALE STUDIES (COAL-FIRED BOILERS)

Robert P. Donovan, Chairman
Research Triangle Institute
Research Triangle Park, NC

EMISSION REDUCTION PERFORMANCE AND OPERATING CHARACTERISTICS OF
A BAGHOUSE INSTALLED ON A COAL-FIRED POWER PLANT

David S. Beachler
ETS, Inc.
111 Edinburgh Road
Raleigh, NC 27608

John W. Richardson, John D. McKenna, and John C. Mycock
ETS, Inc.
Suite C-103
3140 Chaparral Drive
Roanoke, Virginia 24018

Dale Harmon
Industrial Environmental Research Laboratory
U.S. EPA
RTP, NC 27711

ABSTRACT

This paper summarizes the field testing results and the operating data recorded from a baghouse installed on a coal-fired power plant. The field tests were conducted at the Pennsylvania Power and Light Brunner Island Station, Unit 1, on two separate occasions. During the field tests, the air flow, temperature, and particulate emissions from the inlet and outlet of the baghouse were measured. Particle size analyses of the inlet and outlet gas streams were also performed. Operating data recorded on strip charts and operating and maintenance data collected by PP&L operators were reviewed. Bag life and pressure drop problems and attempted corrective actions are discussed. The laboratory results from tests performed on a number of bags are also provided.

The information contained in this paper is the result of a program that was funded by the U.S. Environmental Protection Agency, EPA contract 68-02-3649. The research and tests were conducted from November 1980 to October 1982 by ETS, Inc. The EPA project officer for this program was Dale Harmon.

This paper has been reviewed in accordance with the U.S. Environmental Protection Agency's peer and administrative review policies and approved for presentation and publication.

POWER PLANT DESCRIPTION

The Pennsylvania Power and Light (PP&L) Brunner Island Boiler No. 1 produces 350 MW and 2,200,000 lb/hr* of steam. The boiler is a tangentially fired Combustion Engineering boiler designed with controlled circulation, pulverized bituminous coal firing, and divided furnace and reheat.

Coal is pulverized by five Combustion Engineering Raymond bowl mills, each rated at a capacity of 61,400 lb/hr. The boiler is initially fired using No. 2 fuel oil. Oil firing can also be used to supplement coal firing at any boiler load.

The typical flue gas stream conditions and sulfur content of the coal burned in the Brunner Island Boiler No. 1 are:

- Outlet dust loading from boiler - 0 to 10 gr/acf
- Maximum flue gas volume - 1,200,000 cfm
- Maximum flue gas temperature - 500°F
- Normal flue gas operating temperature - 330°F
- Raw coal analysis - 1.1 to 3.0% sulfur (dry basis)

The flue gas from unit No. 1 is ducted to a common stack that is shared with unit No. 2. Two induced-draft (ID) fans are installed on each unit. The ID fans were modified by PP&L to accommodate the baghouse.

Particulate emissions from unit No. 1 were initially controlled by two electrostatic precipitators (ESPs) placed in parallel. One ESP was retired, and flue gas from the boiler is directed through the other ESP (that is de-energized) and into the baghouse. The gas stream is pulled through the baghouse by the ID fans and exits out the stack. The ash handling system of the de-energized ESP is still used to remove any dust that settles in the hoppers. A schematic of the boiler, baghouse, de-energized ESP, fans, and ductwork is shown in Figure 1.

The baghouse was designed, furnished, and erected by the Carborundum Company (Environmental Systems). The specifications of the baghouse are:

- Number of compartments - 24
- Number of bags per compartment - 264
- Total number of bags - 6,336
- Bag diameter - 11½ in.
- Center-to-center bag spacing - 14 in. with three-bag reach
- Bag length - 35 ft. 4 in.
- Effective cloth area per bag - 103.3 ft²
- Cloth area per compartment - 27,271 ft²
- Total cloth area in baghouse - 654,508 ft²
- Reverse air volume - 41,000 acfm
- Air-to-cloth ratios:
 - Gross air-to-cloth ratio without reverse air flow - 1.83:1

* Readers more familiar with metric units are asked to use the conversion factors at the end of this paper.

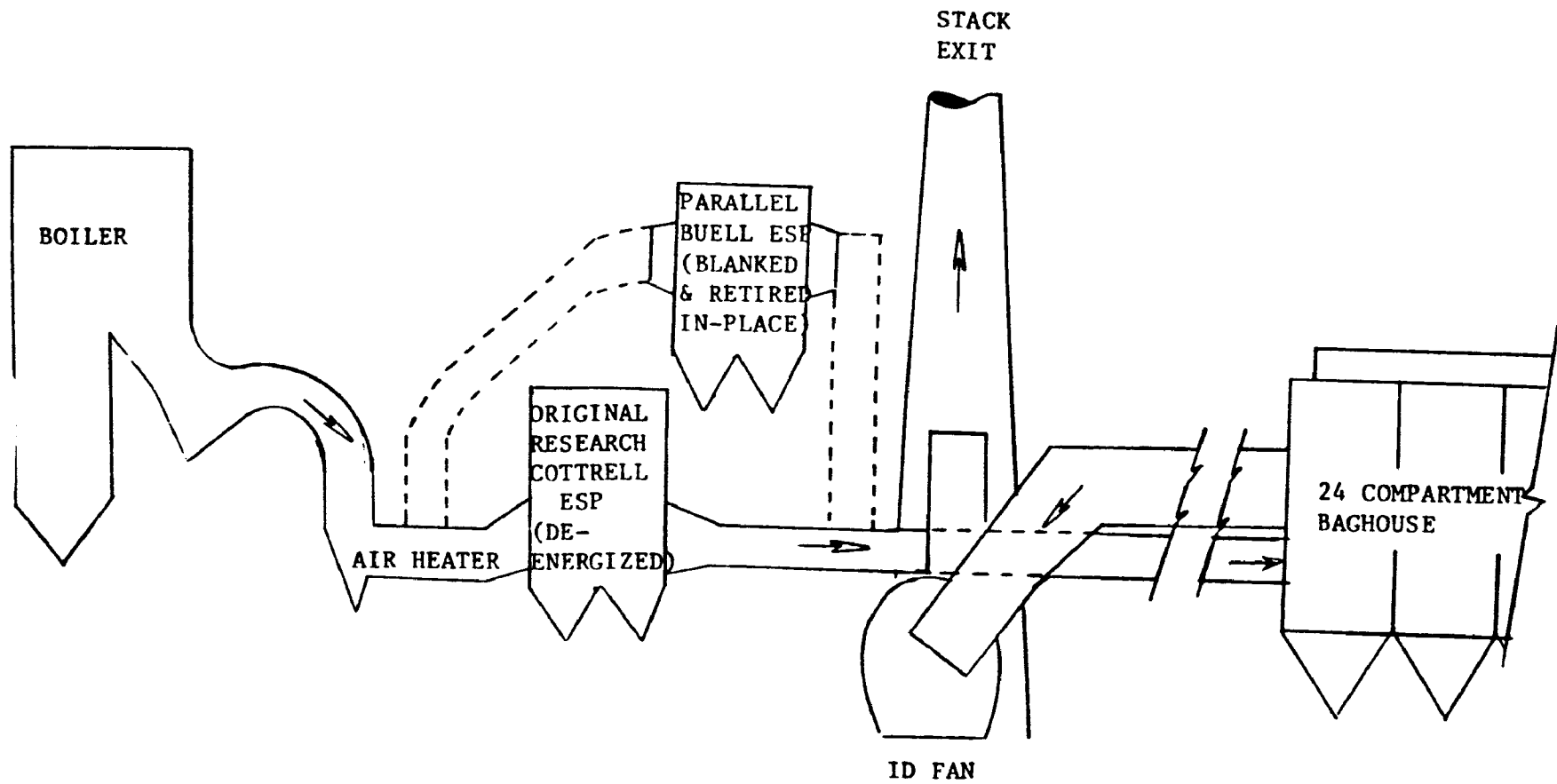


FIGURE 1. Original Equipment and Fabric Filter Arrangement

Air-to-cloth ratios (cont'd)

Net air-to-cloth with reverse air flow and two compartments off line for cleaning - 2.13:1

Net air-to-cloth ratio with reverse air flow and four compartments out of service - 2.3:1

The bags originally installed in the baghouse were manufactured by the Filter Media Division of Carborundum Company. The majority of the bags were made of 9.8 oz fiberglass material coated with Teflon B. Two hundred test bags containing an "acid resistant" coating were installed in one compartment. The bag dimensions and descriptions were:

Bag diameter - 11½ in.

Bag length - 35 ft, 4 in.

Cloth weight - 9.8 oz/yd²

Weave - 3 x 1 twill

Permeability - 40 to 50 cfm/ft²

Top suspension method - chain, compression spring, and disposable cap.

Bottom retainment - compression band sewn into bottom of each bag.

The bag is angled to fit the lower part of the band into a recessed groove near the top of the thimble. The upper part of the band slips over the top of the thimble. Clamps or tools are not required to install the bag onto the thimble.

Bag rings - 3/8-inch diameter cadmium-plated steel rings, quantity eight per bag

Tension - tension is varied by using a chain and clip at the top of the bag. Tension is measured by spring deflection. Initial bag tension was set at 75 lb.

Dust is collected on the inside of the bag and is removed by reverse air cleaning. Two reverse air systems are installed on the baghouse--one for each 12-compartment side of the baghouse. Bag cleaning is initiated either on a continuous-timed cycle or when the pressure drop across the baghouse exceeds a preset value.

An opacity monitor was installed in a straight section of duct on the outlet just ahead of the ID fans. The opacity of the flue gas is continuously recorded onto a strip chart.

TESTING AT PP&L BRUNNER ISLAND, UNIT 1

Particulate emissions tests were performed at the PP&L Brunner Island, Unit 1 on two separate occasions: August 12-16, 1981, and September 2-4, 1982. The tests were conducted according to U.S. EPA Reference Methods 5 and 17 procedures in conjunction with Methods 1, 2, 3, and 4. An Alundum thimble (Method 17) was used for testing on the inlet because the concentration of particulate matter in the gas stream was very high. The EPA contract for this program specified using a Method 5 sampling train for testing on the outlet. Each test included a 49-point traverse with a 5-minute sampling duration at each point, resulting in a total test time of 4 hours and 5 minutes.

SUMMARY RESULTS FOR THE FIRST TEST SERIES

The results for the tests performed August 12-16, 1981, at PP&L Brunner Island, Unit 1, are summarized in Table 1. The average particulate emission rate from the outlet for these five tests was $0.037 \text{ lb}/10^6 \text{ Btu}$. The allowable emission rate, as specified by the Pennsylvania Department of Environmental Resources, is $0.10 \text{ lb}/10^6 \text{ Btu}$.

A total of six tests using a cascade impactor were performed: two inlet, two outlet, and two blank runs. The average mass mean diameters for particles in the flue gas were $13.4 \mu\text{m}$ at the inlet and 7.0 at the outlet.

SUMMARY RESULTS FOR THE SECOND TEST SERIES

The results for the tests performed September 2-4, 1982, are summarized in Table 2. The average particulate emission rate from the outlet for these tests was $0.096 \text{ lb}/10^6 \text{ Btu}$. The outlet emission rate was considerably higher than for the August 1981 test series ($0.037 \text{ lb}/10^6 \text{ Btu}$). However, the emission rate was below the allowable emission rate of $0.10 \text{ lb}/10^6 \text{ Btu}$. Ten tests using an impactor were performed: four inlet, four outlet, and two blank runs. The average mass mean diameter for the particles in the inlet gas stream was $19.0 \mu\text{m}$ and for the outlet was $9.0 \mu\text{m}$.

OPERATION AND MAINTENANCE OF THE BAGHOUSE

Beginning with the start-up of the baghouse on October 19, 1980, and covering the period through September 30, 1982, key data were recorded daily onto log sheets by PP&L operators and also by strip chart recorders. These operation and maintenance (O&M) records were reviewed by ETS engineers.

Initially, baghouse maintenance at Brunner Island, Unit 1, consisted of monitoring the stack opacity and inspecting each baghouse compartment every 2 weeks. A written maintenance schedule was not established. As O&M problems began to occur more frequently, additional maintenance checks were made by the PP&L maintenance crew.

The major maintenance problem at Brunner Island, Unit 1, was very poor bag life. Only six bag failures occurred in the $2\frac{1}{2}$ month operation in 1980. Bag failures rose to 210 in 1981, most of which occurred during the last quarter of the year. By September 30, 1982, 408 bags had failed (in 1982) for a cumulative total of 624 (see Figure 2). As a result, over 6500 man-hours were required for baghouse maintenance in 1982.

PP&L believes that many of the bag failures occurred because the bag tension was improper. It is suspected that insufficient cleaning of the bags also contributed to the bag failure rate.

Increasing pressure drop across the baghouse was the most significant operating problem that occurred during 1981 and 1982. During start-up, and soon after, the month average high pressure drop was about 4 in. of H_2O . Monthly average high values were obtained by taking the highest value

TABLE 1. TEST DATA SUMMARY, TEST SERIES 1, PP&L BRUNNER ISLAND,
UNIT 1, 8/12/81 - 8/16/81

Run & Date	Run 1 8/12/81	Run 2 8/13/81	Run 3 8/14/81	Run 4 8/15/81	Run 5 8/16/81
Particulate Emissions Inlet (lb/10 ⁶ Btu)	16.23	9.52	9.78	11.30	11.74
Particulate Emissions Outlet (lb/10 ⁶ Btu)	0.027	0.018	0.078	0.037	0.026
Baghouse Collection Efficiency (%)	99.8	99.8	99.2	99.7	99.8
Inlet Gas Flow (acfm)	980,000	1,140,000	1,110,000	1,140,000	1,120,000
(dscfm)	600,000	710,000	690,000	710,000	690,000
Outlet Gas Flow (acfm)	1,170,000	1,110,000	1,250,000	1,260,000	1,330,000
(dscfm)	730,000	680,000	780,000	780,000	790,000
Inlet Temperature (°F)	286	290	290	293	300
Outlet Temperature (°F)	294	289	280	282	289
Baghouse Pressure Drop (in. of H ₂ O)	8.0	8.1	7.9	8.3	8.5
Orsat % CO ₂ Inlet	13.1	12.7	12.1	13.0	13.1
Outlet	12.2	12.9	12.9	13.1	13.1
Orsat % O ₂ Inlet	5.4	5.4	5.7	5.3	5.2
Outlet	6.0	5.3	5.3	5.3	5.2
Orsat % CO Inlet	0.0	0.0	0.0	0.0	0.0
Outlet	0.1	0.2	0.1	0.1	0.0
Flue Gas Moisture (%) Inlet	11.0	8.1	9.1	8.1	7.6
Outlet	5.7	7.8	7.6	7.6	6.8
MW Production	337	345	341	340	340

TABLE 2. TEST DATA SUMMARY, TEST SERIES 2, PP&L BRUNNER ISLAND,
UNIT 1, 9/2/82 - 9/4/82

Run & Date	Run 1 9/2/82	Run 2 9/3/82	Run 3 9/4/82
Particulate Emissions Inlet (lb/10 ⁶ Btu)	6.18	7.84	7.82
Particulate Emissions Outlet (lb/10 ⁶ Btu)	0.071	0.104	0.114
Baghouse Collection Efficiency (%)	98.6	98.4	98.3
Inlet Gas Flow (acfm) (dscfm)	1,140,000 670,000	1,230,000 720,000	1,160,000 690,000
Outlet Gas Flow (acfm) (dscfm)	1,370,000 820,000	1,440,000 890,000	1,340,000 820,000
Inlet Temperature (°F)	315	308	314
Outlet Temperature (°F)	318	306	311
Baghouse Pressure Drop (in. of H ₂ O)	8.4	8.0	8.2
Orsat % CO ₂ Inlet Outlet	13.0 13.0	12.8 12.6	12.5 12.5
Orsat % O ₂ Inlet Outlet	6.0 6.0	6.0 6.2	6.3 6.4
Orsat % CO Inlet Outlet	0.0 0.0	0.0 0.0	0.0 0.0
Flue Gas Moisture (%) Inlet Outlet	11.0 5.1	11.1 4.2	9.2 4.8
MW Production	335	335	335

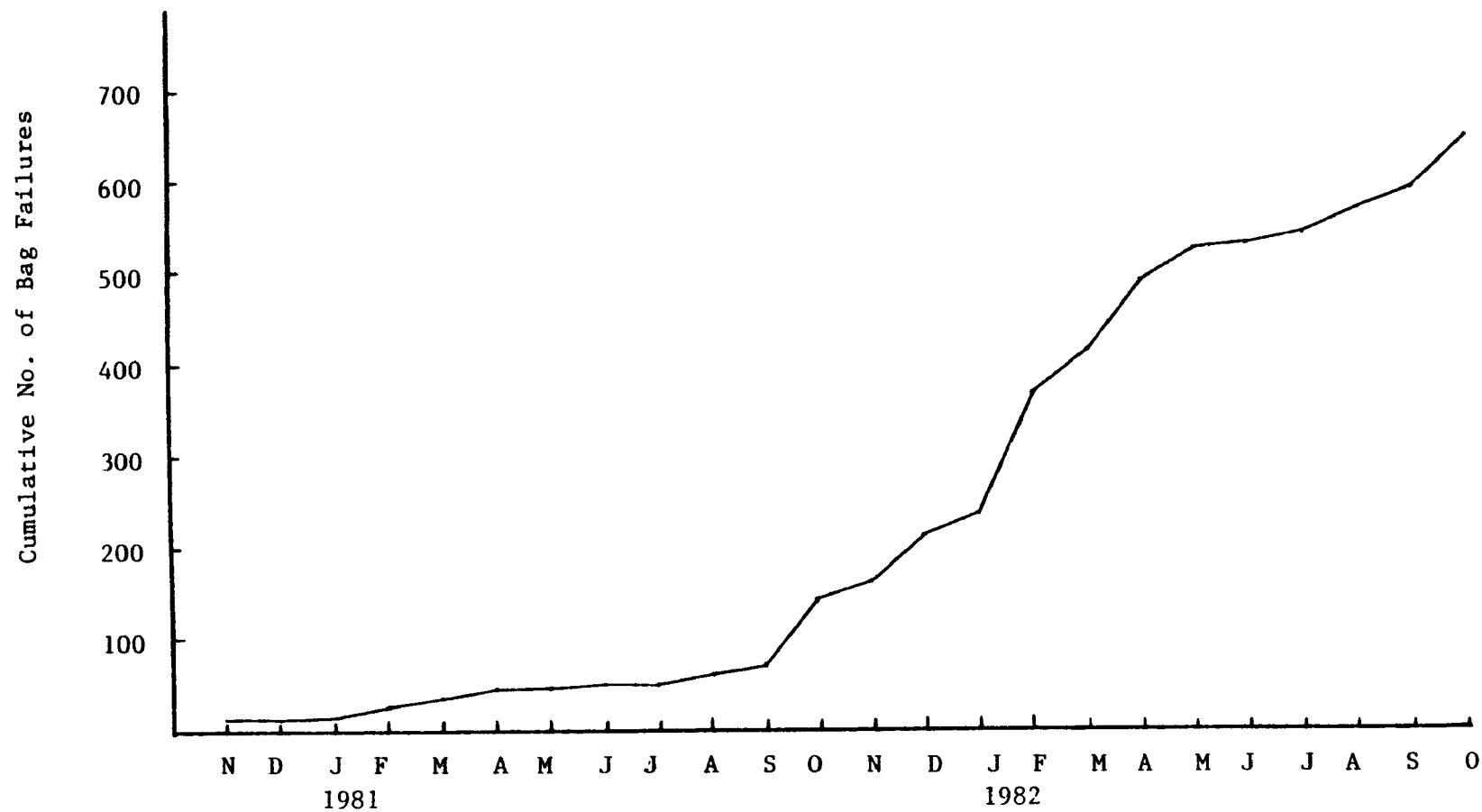


FIGURE 2. Bag Failure History

recorded each day and computing the average of these high values for that month (see Table 3). Pressure drop began to increase in April 1981 to an average high value of 5.2 in. of H₂O. At this time, the cleaning cycle was changed from one that was triggered when the pressure drop across the baghouse reached 4 in. of H₂O to a continuous cleaning cycle where each compartment was cleaned every 30 minutes. In spite of this change, the monthly average-high pressure drops rose to the range of 7 to 8 in. of H₂O by the end of 1981. By early- to mid-1982, the pressure drops across the baghouse exceeded 9.0 in. of H₂O while the plant operated at full load and the baghouse operated with all compartments in service. PP&L believes that the abnormally high pressure drops contributed to the high rate of bag failures that occurred in the baghouse. They also believe that the pressure drop problem was caused by a very thick layer of dust that remained on the bags even after the bags were cleaned and by nodules that formed on the dust cake.

Other operating parameters were recorded daily including SO₂ concentration, baghouse inlet and outlet temperatures, steam flow, air flow into the boilers, and stack opacity. These data were recorded by examining strip charts for each day of operation over a 24-month period. While gathering these data, notes were made by PP&L operators when the data varied significantly from the normal. Operators listed possible reasons for these variances. Boiler downtime was also documented. In addition, a detailed bag failure chart was prepared by the operators. From this chart, it is possible to determine the location of each bag that failed in a compartment, the number of multiple failures that occurred in a compartment, the probable reason for failure, and the failure dates.

Some of the operating data collected were graphed, plotting various parameters versus the time period in which they occurred (e.g., pressure drop, bag failures). Other graphs were created that charted one parameter against another, such as percent opacity versus pressure drop. These figures are presented in Reference (1). One of these is shown in this paper as Figure 3.

It does not appear from examining Figure 3 that the baghouse inlet temperature drops significantly during periods of high pressure drop. However, the data from Table 3 show that several occasions a month in which the pressure drop was high were usually preceded by a month in which the inlet temperature and the resulting outlet temperature fell below some critical point. For example, in December 1980, the average inlet temperature was approximately 274°F, and the average outlet temperature 264°F. In the following month, January 1981, the pressure drop increased to 5.3 in. of H₂O, from the previous month's value of 4.1. Other months of low temperature followed by months of increased pressure drop include 3/81 - 4/81, 7/81 - 8/81, and 12/81 - 1/82. These low temperatures in the baghouse may have allowed the flue gas to reach its dew point. If this occurred, sulfuric acid (in the flue gas) would condense on the fabric, creating wet surfaces on the bags where particles would collect. After drying, the particles would then be difficult to remove using the normal bag cleaning techniques. Consequently, the pressure drop would likely increase as the PP&L maintenance crew observed.

TABLE 3. OPERATING PARAMETERS - MONTHLY AVERAGE OF TYPICAL DAILY VALUES

	F "H ₂ O			SO ₂ PPM			TEMPERATURE °F				STEAM FLOW 1000 ^{lb} _{hr}			AIR FLOW 1000 ^{lb} _{hr}			OPACITY %		
	Hi	Lo	Avg.	Hi	Lo	Avg.	In	Out	Avg.	Diff.	Hi	Lo	Avg.	Hi	Lo	Avg.	Hi	Lo	Avg.
10/80	7.3	5.6	6.5	1400	1140	1270					2170	1930	2070	1920	1510	1720	4.5	3.4	3.9
11/80	4.3	4.0	4.1	1400	1190	1320	297	283	290	13.8	2130	1580	1860	1900	1400	1650	-	-	
12/80	4.1	4.1	4.1	1360	1050	1200	274	264	269	13.4	2230	1670	1950	2210	1650	1930	-	-	
1/81	5.3	4.1	4.6	1260	1020	1150	292	289	289	10.3	1960	1720	1850	1800	1620	1710	7.2	4.1	6.7
2/81	4.6	3.1	3.9	1460	1260	1370	302	285	294	16.8	2200	1500	1900	2000	1370	1710	11.5	7.8	
3/81	4.3	3.1	3.5	1730	1170	1320	294	278	287	16.0	1910	1490	1760	1750	1490	1670	10.6	5.9	7.9
4/81	5.2	3.6	4.2	1380	1090	1250	304	283	293	22.5	1750	1500	1640	1650	1420	1550	7.3	3.8	5.4
5/81				1430	1120	1270	273				2080	1390	1740	1910	1190	1540	9.8	4.9	8.2
6/81				1470	1090	1280													
7/81	5.9	4.6	5.1	1420	1290	1370	304	268	292	23.0	2110	1730	1970	2110	1720	1900	6.9	3.4	5.0
8/81	7.2	5.5	6.1	1500	1240	1370	319	292	306	26.6	2240	1560	1900	2210	1350	1790	6.3	2.9	2.9
9/81	8.5	7.0	7.8	1480	1220	1350	312	286	300	28.5	2250	1700	1970	2270	1670	1970	7.1	4.3	5.3
10/81	6.9	5.9	6.4	1460	1140	1300	310	285	299	27.6	2090	1580	1800	2160	1600	1840	9.5	4.2	7.0
11/81	8.1	7.1	7.6	1380	1220	1300	313	278	296	35.0	2220	1330	1800	2280	1370	1820	7.9	4.7	7.4
12/81	7.1	6.3	6.7	1500	1230	1370	297	277	294	37.0	2230	1650	1940	2280	1580	1940	12.9	7.3	9.9
1/82	10.0	8.3	9.1	1510	1200	1360	311	278	295	33.0	2160	1660	1890	2150	1570	1860	10.4	4.7	7.1
2/82	7.9	7.8	7.9	1700	1220	1430	307	284	295	22.8	2140	1700	1920	2120	1550	1880	6.5	3.4	4.9
3/82	9.8	8.9	9.4	1570	1270	1420	321	295	308	26.7	2240	1670	1950	2210	1650	1930	10.7	6.4	8.6
4/82	7.1	3.8	5.4	1550	1410	1480					2240	1470	1860	2230	1480	1860	7.9	1.8	4.8
5/82	8.9	3.7	6.3	1400	1330	1380	324	297	310	26.0	2240	1400	1820	2120	1320	1740	6.4	0.4	3.4
6/82																			
7/82	8.1	3.5	5.8	1380	1170	1270	319	293	306	26.0	1950	960	1450	1950	1000	1480	13.0	1.4	7.2
8/82	9.0	4.7	6.9	1470	1240	1360	323	296	310	27.0	2210	1290	1760	2110	1240	1690	16.6	2.5	9.6
9/82	8.7	3.9	6.3	1470	1260	1370	314	287	301	26.5	2220	1030	1630	2130	1040	1590	15.5	3.4	9.4

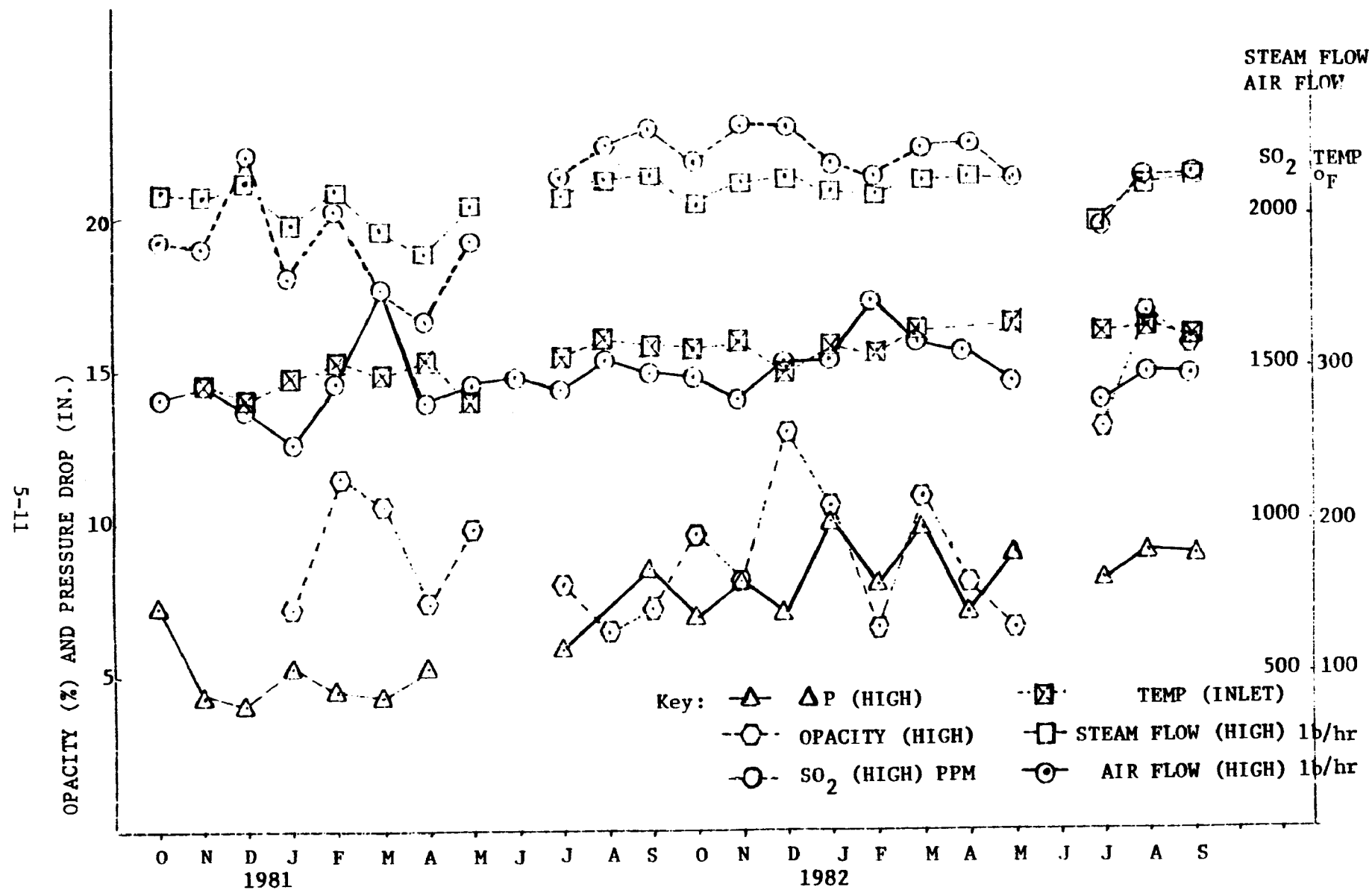


FIGURE 3. Overview of Unit Performance Over 24 Months

PP&L has attempted to correct the high pressure drop problem by changing the cleaning cycle, increasing the flow of reverse air (for bag cleaning), manually cleaning the bags on an intermittent basis, and installing sonic horns that help remove dust from the bags during the cleaning cycle. Eight sonic air horns were placed in compartment 7A in November 1981. Initial data indicate that the horns helped remove the dust cake from the bags and thus increased the gas flow through the compartment by approximately 30 percent. PP&L has installed sonic air horns in the other 23 compartments. The horns have improved bag cleaning and thus decreased the pressure drop across the baghouse.

FABRIC TESTS

Various fabric tests were conducted on four separate occasions by two different testing companies. Fabric tests performed include tensile strength, permeability, Mullen burst, and the MIT flex test. The results of these tests are given in Table 4.

In the data presented from the MIT flex test, the average number of flexes to failure rate on a new bag are in the range from 4000 to 7000. These values are not unusual for this type of bag. Testing of bags after 10 months of exposure showed that the flexes to failure rates were in the range from approximately 300 to 400, which is greater than a 90 percent loss in flex strength. After 14 months of exposure, the bags tested continued to show a flex to failure rate in the 300 to 400 range. While this is a relatively low flex strength level, it is possible that the bags would be usable indefinitely. However, the bags should be continually tested to verify if this strength measurement remains in the 300 to 400 range or if it declines further. A drop below 200 flexes would be considered a significant further reduction and would probably result in a bag failure shortly afterward.

The results of the Mullen burst tests obtained in the ETS laboratory indicate that after 10 months' exposure more than 60 percent of the burst strength still remains. This value is considered satisfactory. The Tex laboratory results show approximately 40 to 50 percent burst strength remaining after 10 months of exposure and approximately 34 percent remaining after 16 months. It should be noted that the single bag tested after 16 months had been cleaned with reverse air and a sonic horn, whereas bags with less exposure were cleaned with reverse air only.

Tensile strength tests indicate that the new bags had fill values ranging from 146 to 230 lb/in. After 14 months of exposure, the bags tested in the ETS laboratory show more than 50 percent strength remaining while the Tex laboratory showed that some of the bags tested with a tensile strength of less than 40 percent.

According to the permeability tests performed on new bags, the permeability was in the range of approximately 30 to 60 cfm/ft² of cloth. The bags that had been used for some time had permeability values from 2.8 to 5.0 cfm/ft² of cloth. These later values are not considered unusual for bags that have been used in baghouses installed on coal-fired boilers. The

TABLE 4. BAG TESTING - LABORATORY RESULTS

TESTING CO. & BAG I.D.	EXPOSURE (MONTHS)	TEST DATE	FLEX	BURST	TENSILE		PERMEABILITY	
			(FILL)		Fill	Warp	Rec'd	Vac.
			No.toFail	lb/in. ²	lb/in.	lb/in.	FPM	FPM
ETS/81-195	New	9/2/81	6,733	490	146	360	32.2	*
ETS/81-196	New	9/2/81	4,207	554	215	350	62.7	*
Tex Lab/	New	N/A	N/A	609	230	447	53.9	*
Tex Lab/#73	7	7/23/81	N/A	393	147	188	3.3	13.2
Tex Lab/#96	7	7/23/81	N/A	398	151	193	2.8	12.4
ETS/81-198	10	9/2/81	420	323	114	197	4.4	19.8
ETS/81-200	10	9/2/81	294	325	112	189	2.9	19.2
ETS/81-197	10	9/2/81	332	327	112	189	4.0	22.0
Tex Lab/#32	10	3/8/82	N/A	332	163	316	3.5	15.6
Tex Lab/#54	10	3/8/82	N/A	404	186	314	3.5	13.8
Tex Lab/#76	10	3/8/82	N/A	241	85	246	3.5	8.8
Tex Lab/#194	10	N/A	N/A	228	133	292	3.6	19.4
ETS/#260	14	6/4/82	305	N/A	121	228	4.8	25.9
ETS/#261	14	6/4/82	422	N/A	120	197	5.0	22.4
Tex Lab/#184	16	3/19/82	N/A	205	88	227	3.4	23.8

N/A - data not available

* - new bags not vacuumed

permeability of the fabric after being vacuumed up to a pressure of 30 in. of H₂O showed permeability values generally less than 50 percent of the new bag values. This indicates that dust lodged in the fabric may be difficult to remove.

In addition to the previously mentioned tests, a Loss of Ignition (LOI) test was performed on two new bags to verify the amount of organic coating present. These tests showed LOI values of 10.6 percent that correspond closely with the specified Teflon coating of 10 percent.

OVERVIEW AND CONCLUSIONS

The particulate emissions from the outlet of the baghouse averaged 0.037 lb/10⁶ Btu for the August 1981 tests while the baghouse collection efficiency was 99.7 percent. The particulate emissions for the September 1982 tests averaged 0.096 lb/10⁶ Btu while the baghouse collection efficiency was 98.4 percent. Both of these average values were below the maximum emission rate of 0.10 lb/10⁶ Btu that is specified by the Pennsylvania Department of Environmental Resources.

The results of the bag tests performed in the laboratory indicate that, while the burst and tensile strengths do not indicate a potential problem, a large percentage (approximately 90%) of the flex strength had been lost after 10 months of use in the baghouse. Any further deterioration in flex strength would indicate potential bag failures. The permeability values of the bags that had been in service do not seem too low. However, the recovery of the permeability after vacuuming at 30 in. of H₂O is relatively low. These low values generally indicate that the increased values of pressure drop are caused by dust lodging in the fabric interstices. Once this happens it is very difficult to remove the dust using conventional bag cleaning techniques.

REFERENCES

1. Richardson, John W., McKenna, John D., Mycock, John C. "An Evaluation of Full-Scale Fabric Filters on Utility Boilers, PP&L Brunner Island Station, Unit 1." Draft Report, EPA Contract No. 68-02-3649, August 1984.

METRIC EQUIVALENTS

Readers more familiar with metric units may use the following to convert to that system.

<u>Nonmetric</u>	<u>Times</u>	<u>Yields Metric</u>
acfm	4.719×10^{-4}	am^3/s
cfm/ft ²	5.08×10^{-3}	$(\text{m}^3/\text{s})/\text{m}^2$
dscfm	4.719×10^{-4}	dsm^3/s
ft	0.3048	m
ft ²	9.29×10^{-2}	m ²
fpm	5.08×10^{-3}	m/s
°F	$(^{\circ}\text{F}-32)(1.8)$	°C
gr/acf	2.29	g/m^3
in.	2.54	cm
in. H ₂ O	249	Pa
lb	0.454	kg
lb/hr	1.26×10^{-4}	kg/s
lb/in.	175	N/m
lb/in. ²	6.89×10^3	Pa
lb/10 ⁶ Btu	430	ng/J
oz	2.834×10^{-2}	kg
oz/yd ²	3.39×10^{-2}	kg/m ²

EVALUATION OF SONIC-ASSISTED, REVERSE-GAS CLEANING AT UTILITY BAGHOUSES

Kenneth M. Cushing, Larry G. Felix, and Anthony M. LaChance
Southern Research Institute
2000 Ninth Avenue South
P.O. Box 55305
Birmingham, AL 35255-5305

Stephen J. Christian
Montana Power Company
Environmental Department
P.O. Box 38
Colstrip, Montana 59323

ABSTRACT

Fabric filters (baghouses) are rapidly gaining acceptance as particulate control devices for the electric utility industry because of their high efficiency and relative insensitivity to coal composition. As a result of their increasing application, means are being investigated to optimize their performance in terms of cost and maintenance. One promising method of effectively removing or avoiding heavy residual dust cakes, which can cause excessive pressure drop and bag failures, is the application of sonic energy.

This paper discusses the first phase of a program sponsored by the Electric Power Research Institute to evaluate sonic-assisted, reverse-gas cleaning at full-scale utility baghouses. Data are presented showing the relationship among number of sonic horns per compartment, their location, and the resulting sound pressure levels. Reductions in residual dust cake weight and system pressure loss are documented for specific sonic horn applications. In addition, applicable research data from pilot scale evaluation of sonic horns are also presented.

INTRODUCTION

Electric utilities have made significant progress in recent years in designing and operating fabric filters. As a result of these advances, in a ten year period baghouses have become an accepted and frequently preferred particulate matter control technology within the industry. This acceptance has been influenced by their high collection efficiency and relative insensitivity to coal composition. As a result of their increasing application, means are being investigated to optimize their performance in terms of cost and maintenance.

At present, over 90% of utility baghouses are cleaned by reverse-gas. In this process, a gentle flow of filtered gas is reversed back into a baghouse compartment and through the bags, causing the bags to partially collapse inward. This partial collapse fractures and dislodges the dust cake. Well maintained units generally have very high particle collection efficiencies (particulate mass collection efficiencies over 99.9% with outlet emissions of approximately $0.004 \text{ lbs}/10^6 \text{ Btu}$), clear stacks (achieving opacities averaging less than 0.1%, equivalent to an in-stack visibility of over 50 miles), and good bag life (averages of over four years). However, reverse-gas cleaning is also characterized by heavy residual dust cakes (from 0.5 to over $1.0 \text{ lb}/\text{ft}^2$, or as much as 20 times the weight of dust accumulated during a single filtering cycle), and a higher than expected tubesheet pressure drop which tends to drift slowly upward with time as the dust cake builds (from an initial low value of 3.0 inches of water to 5.0 to 7.0 inches of water). Heavy residual dust cakes are undesirable because they lead to excessive pressure drop and increased bag failures. One promising method of effectively removing or avoiding heavy residual dust cakes in fabric filter bags is the addition of sonic energy to the bags during reverse-gas cleaning periods. The sonic energy is created by low frequency, vibrating diaphragm, pneumatic horns.

This paper discusses a program sponsored by the Electric Power Research Institute to evaluate sonic-assisted, reverse-gas cleaning at full-scale utility baghouses. Data are presented showing the relationship among number of sonic horns per compartment, their location, and the resulting sound pressures. Reductions in residual dust cake weight and system pressure loss are documented for specific sonic horn applications. In addition, applicable research data from pilot scale evaluation of sonic horns are also presented.

TEST RESULTS

The first installation of horns in a full-scale reverse-gas cleaned utility baghouse occurred in April 1981 at Pennsylvania Power and Light Company's (PP&L) Holtwood station on the Unit 17 baghouse. Subsequently, in late 1981, PP&L installed horns into the Brunner Island Unit 1 baghouse. Both units were retrofitted with horns in an attempt to reduce high pressure drop and heavy residual dust cake weight (1). At approximately the same time as the Brunner Island installation, horns were placed in the Arapahoe Unit 3

baghouse of the Public Service Company of Colorado. Again, the objective was to reduce pressure drop and residual dust cake weight (2).

In cooperation with these utilities Southern Research Institute was able to conduct studies to measure sound pressures from the sonic horns, evaluate the reduction in residual dust cake, and monitor the reduction in pressure loss due to the application of sonic energy.

Initially, measurements were conducted to determine the sound pressures throughout the baghouse compartments where sonic horns had been installed. At the Holtwood and Brunner Island stations several configurations of the number and type of horn were investigated before a final selection was made by the utility. At the Brunner Island station both 8 and 12 200-Hertz horns per compartment were studied. At the Holtwood station 2 and 4 200-Hertz horns per compartment, as well as two 250-Hertz horns per compartment were investigated. At the Arapahoe station only two 200-Hertz horns were evaluated. Sound pressures were measured at three levels in each compartment. These included horizontal planes three feet from the top of the bags, the middle of the bags, and three feet from the bottom of the bags. Horizontally, measurements were conducted at 30 positions in the Holtwood compartments, 90 positions in the Brunner Island compartments, and 60 positions in the Arapahoe compartments. The average sound pressures are summarized in Tables 1 and 2. These data illustrate several features. For vertically mounted horns there is a rather rapid fall off in sound pressure from the top to the bottom of the bags. For the large number of horns mounted at an angle at the Brunner Island station, a much higher sound pressure was maintained throughout the compartments. Although these data are accurate unto themselves, the use of the technique described above may not be the most correct for determining the average sound pressure in a baghouse compartment. Additional data taken at the Holtwood baghouse illustrate this point. Figure 1 shows the sound pressure measured at four positions in Compartment 42 along a one-foot vertical traverse of the bags. The influence on the sound pressure due to standing waves can be clearly seen. The sound pressure oscillates between 25 and 100 Pascal with a dramatic decrease just below the top of the bags. It is encouraging to observe, however, that the previous Compartment 42 average of 63.2 Pascal (130 dB) is supported by these recent data. The oscillations in sound pressure due to standing waves indicate, therefore, that accurate measurement of sound pressure in a baghouse compartment can only be obtained by a detailed traverse along the length of the bags as illustrated in Figure 1.

During the past year data have been obtained from the Brunner Island and Holtwood baghouses to document the reduction in residual dust cake due to the sonic horns. Bag swatches were cut in specific bags at locations where the sound pressure had been measured. These data are summarized in Table 3. The horns had been in service for approximately nine months when these data were taken. Two months before the site visit we had requested that the horns in Compartment 34 be turned off. The results show that the dust cake weight in this compartment had already increased back to the level of Compartment 32, where horns had never been used. The two 200-Hertz horns in Compartment 42 did not cause as large a reduction in residual dust cake as the four 200-Hertz horns in Compartment 35. Even though the average sound pressure in

TABLE 1. DATA SUMMARY FOR PP&L AND ARAPAHOE SONIC HORN EVALUATION

Date	March 14, 1983	March 14, 1983	March 15, 1983	March 15, 1983
Plant	Holtwood Unit 17	Holtwood Unit 17	Holtwood Unit 17	Holtwood Unit 17
Compartment	43	31	35	42
Horn Type	250-Hertz	200-Hertz	200-Hertz	200-Hertz
Number	2	4	4	2
Location	Top Mounted (Vertical)	2-Top Mounted- Vertical 2-Side Mounted- Horizontal	Top Mounted (Vertical)	Top Mounted (Vertical)
Cloth Area per Horn (Ft ²)	4126	2063	2063	4126
Compartment Volume Per Horn (Ft ³)	3986	1993	1993	3986
<u>Average Sound Pressure Pascal (dB)</u>				
Top Level	169.0 (138.5)	70.7 (131.0)	80.5 (132.1)	75.9 (131.6)
Middle Level	113.0 (135.0)	68.9 (130.5)	73.5 (131.3)	67.5 (130.6)
Bottom Level	73.5 (131.3)	56.6 (129.0)	52.5 (128.4)	40.0 (126.0)
Average	126.3 (136.0)	65.1 (130.3)	70.1 (130.9)	63.2 (130.0)

TABLE 2. DATA SUMMARY FOR PP&L AND ARAPAHOE SONIC HORN EVALUATION

Date	March 8-9, 1983	March 10-11, 1983	April 13-14, 1983
Plant	Brunner Island Unit 1	Brunner Island Unit 1	Arapahoe Unit 3
Compartment	8A	7A	4
Horn Type	200-Hertz	200-Hertz	200-Hertz
Number	8	12	2
Location	Top Mounted 30° Below Horizontal	8-Top Mounted 30° Below Horizontal 4-Under Walkways (Vertical)	Top Mounted (Vertical)
Cloth Area per Horn (Ft ²)	3409	2273	5605
Compartment Volume Per Horn (Ft ³)	2851	1900	2768
Average Sound Pressure Pascal (dB)			
Top Level	113.8 (135.1)	145.5 (137.2)	65.1 (130.3)
Middle Level	89.4 (133.0)	116.8 (135.3)	51.0 (128.1)
Bottom Level	98.8 (133.9)	120.2 (135.6)	36.3 (125.2)
Average	101.2 (134.1)	128.1 (136.1)	52.1 (128.3)

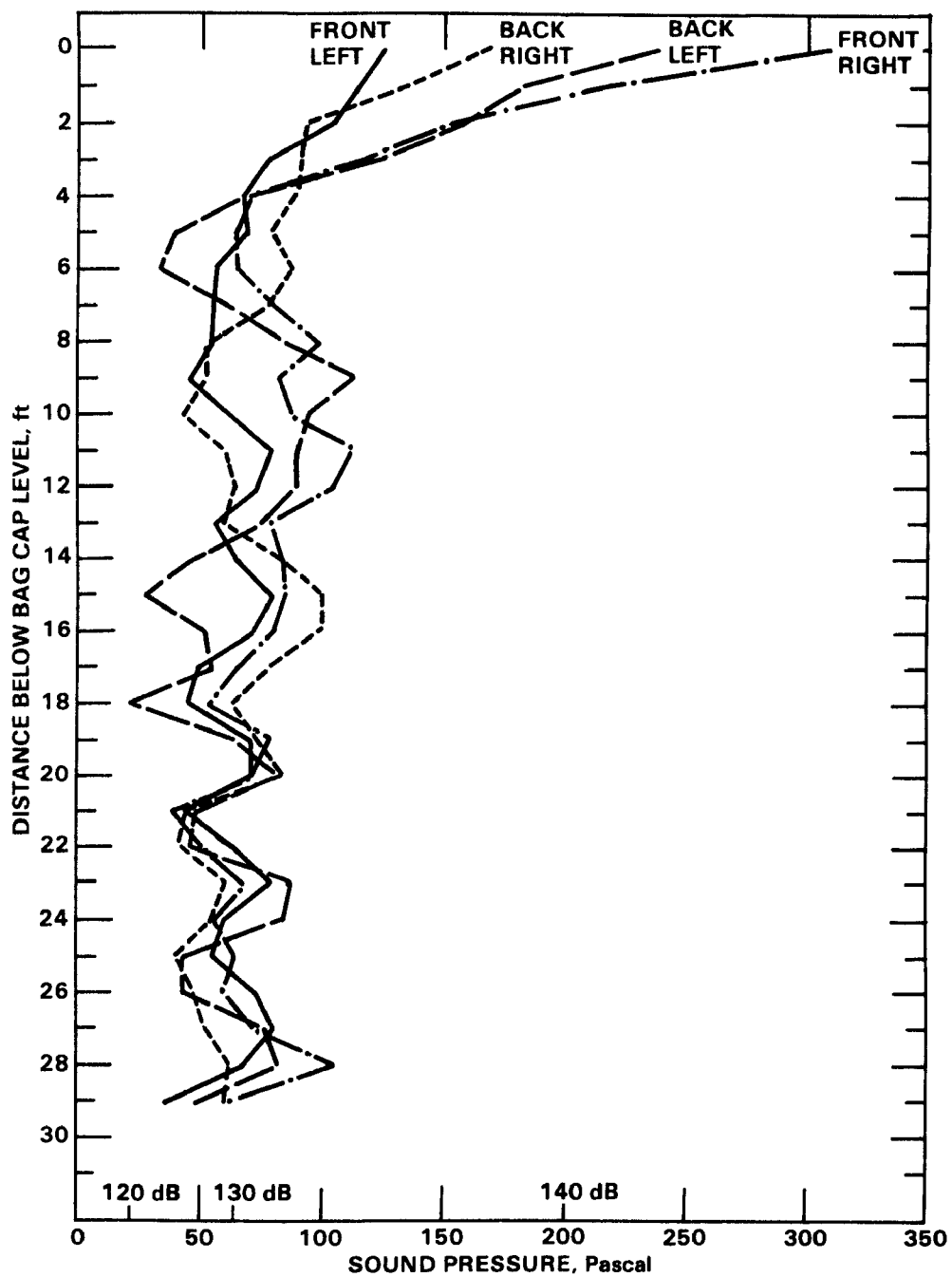


Figure 1. PP & L Holtwood Station Fuller Baghouse Compartment 42. Sound pressure at four positions as a function of the distance below the bag cap level.

TABLE 3. AVERAGE DUST CAKE WEIGHT AT THE
HOLTWOOD UNIT 17 BAGHOUSES

	Reverse-gas Cleaned Baghouse					Shaker-cleaned Baghouse
	32 ^a	34 ^b	35 ^c	42 ^d	43 ^e	Compartment Number 13
Average Dust Cake Weight (lb/ft ²)	1.12	1.06	0.60	0.71	0.75	0.46
Average Sound Pressure (Pascal)			70.1	63.2	126.3	

^aTest compartment, no horns.

^bTwo 200-Hertz horns turned off for two months.

^cFour 200-Hertz horns in regular use.

^dTwo 200-Hertz horns in regular use.

^eTwo 250-Hertz horns in regular use.

Compartment 43 with the two 250-Hertz horns was almost twice as high as any of the 200-Hertz horn compartments, the reduction in residual dust cake was not as large. This indicates that the output of this horn was not concentrated at frequencies best suited for dust cake removal. For comparison, data are shown in this table from the shaker cleaned baghouse in parallel with the sonic-assisted, reverse-gas cleaned baghouse. None of the sonic cleaned compartments were able to reach the low residual dust cake level of the shaker cleaned bags.

Recently, additional data were obtained from the Holtwood baghouse. These data are shown in Figure 2. The trend toward lower residual dust cake for higher sound pressure is significant for the top and middle bag swatches. The bottom swatches are outliers because of the scouring effect due to ash falling from the top of the bags.

During the past year residual dust cake weights have also been measured at the Brunner Island Unit 1 baghouse. Data were obtained from entire bag weights and from swatches cut from bags. Sound pressure values associated with whole bag weights were averaged from measurements along the length of each bag. Individual swatches were cut from specific locations of known sound pressure. The data, shown in Figures 3 and 4, were from compartments containing Menardi-Southern 601T bags. In Compartment 1B the bags were arranged with the warp out (texturized side in), while in Compartment 8B the bags were arranged with the warp in (texturized side out). The difference between the compartments is dramatic. The warp out bags demonstrate the normal reduction in residual dust cake versus an increase in sound pressure. For the warp in bags, however, the sonic horns do not seem to have affected the residual dust cake at all. The conclusion is that the dust cake formed on the non-texturized fabric surface is able to be removed effectively either with or without sonic assist. Further study of this phenomenon is in progress.

Figure 5 summarizes the effectiveness of sonic-assist to reverse-gas cleaning for fly ashes from three coal types. These data are for warp out bags only, with sonic-assist from 200-Hertz horns. Low-sulfur, western coal ashes are most favorably influenced by sonic-assist during reverse-gas cleaning.

The improvements in pressure drop using sonic assist in these baghouses and in EPRI's Fabric Filter Pilot Plant (FFPP) are illustrated in Figure 6. The results are shown as average tubesheet pressure drop versus filtering air-to-cloth ratio and include, for purposes of comparison, the FFPP data for reverse-gas cleaning (shaded region). All of the sonic cleaning data were obtained with 200-Hertz horns and indicate widely varying improvements in pressure drop. For the baghouses filtering fly ash from western low-sulfur coals (Arapahoe Unit 3 and the FFPP) pressure drop reductions of 50-60% were realized. For the baghouses filtering fly ash from eastern, high-sulfur coals, pressure drop reductions of 20-30% were measured. These data support the findings from the residual dust cakes that effectiveness of horns is fly ash dependent.

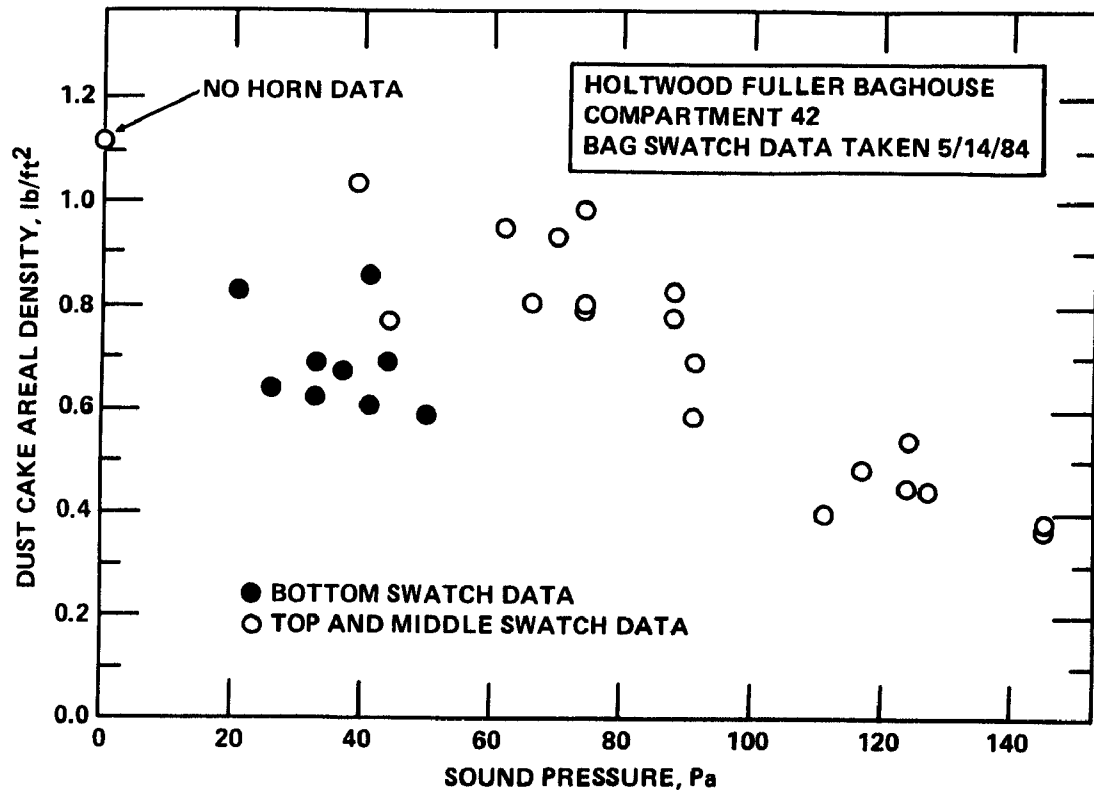


Figure 2. Dust cake areal density as a function of sound pressure at the Holtwood Fuller baghouse, Compartment 42. This compartment has two 200-Hertz sonic horns.

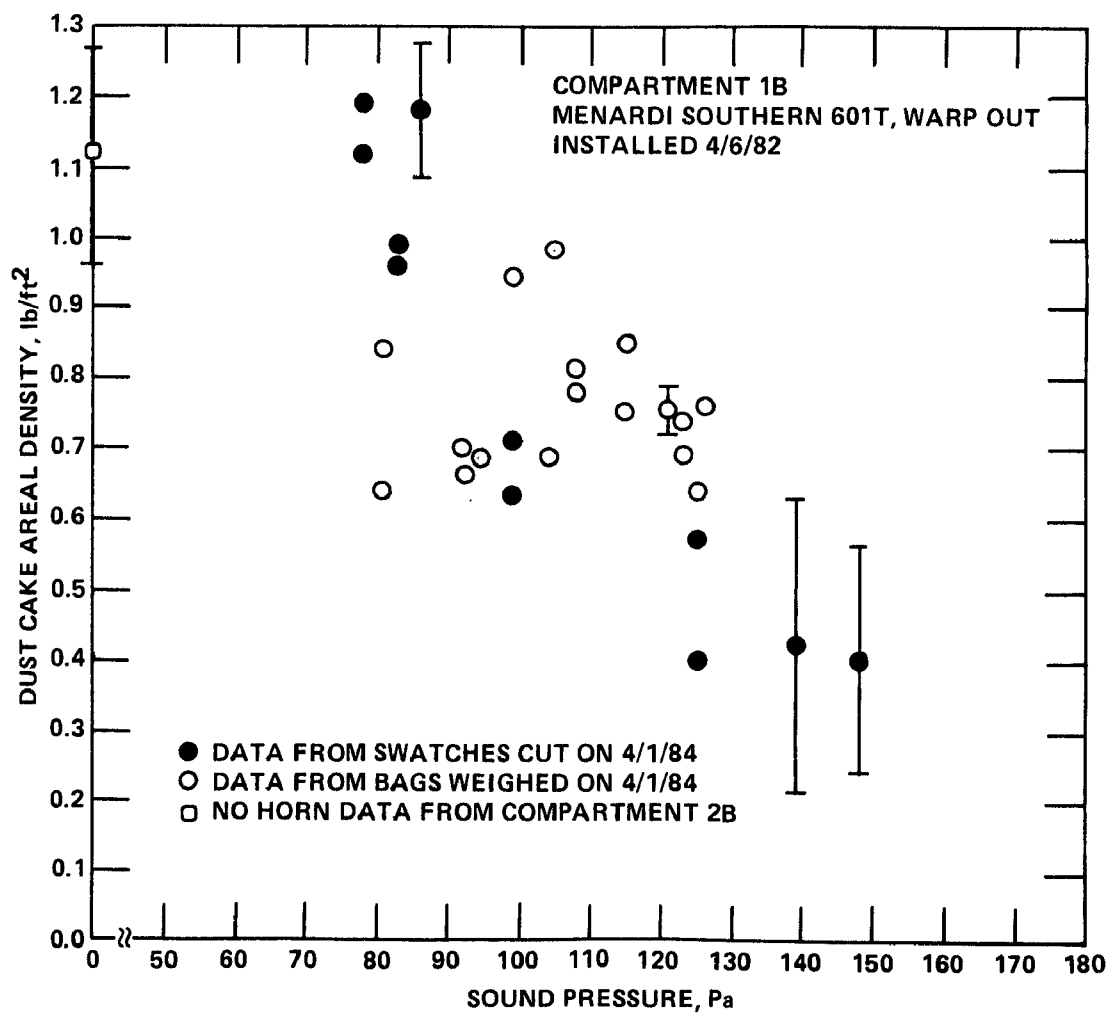


Figure 3. Dust cake areal density versus sound pressure for bags and bag swatches from Compartment 1B of the Brunner Island Unit 1 baghouse.

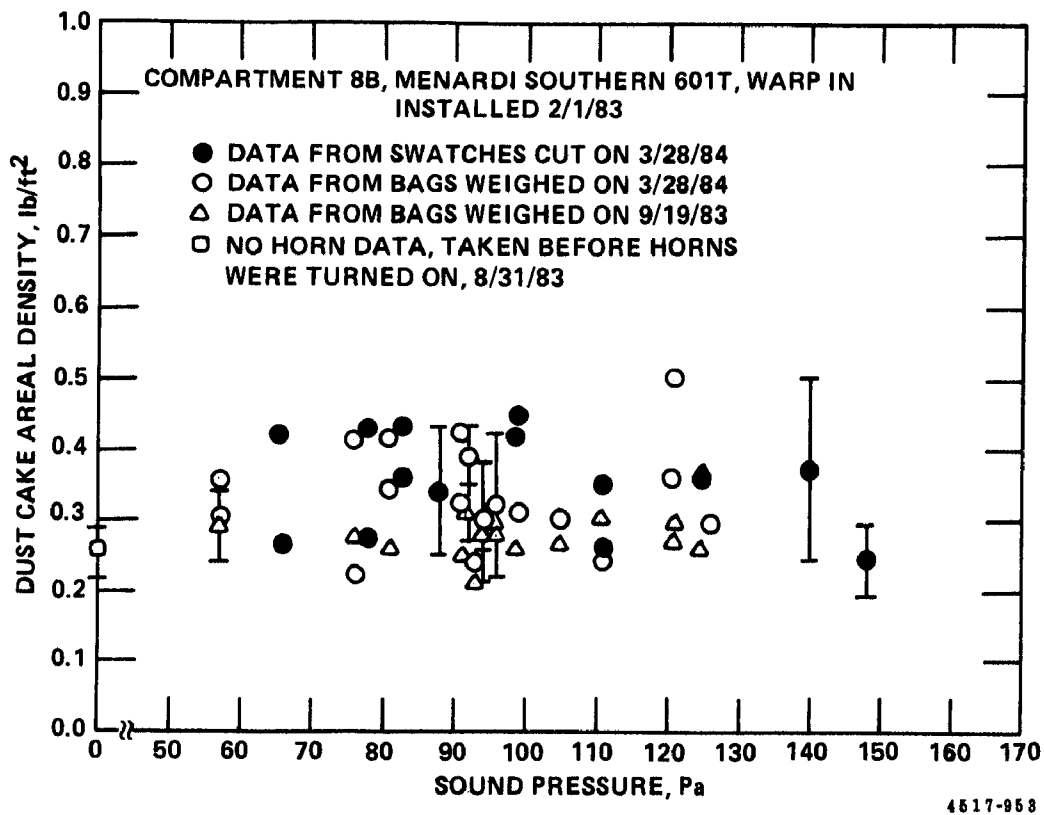


Figure 4. Dust cake areal density versus sound pressure for bags and bag swatches from Compartment 8B of the Brunner Island Unit 1 baghouse.

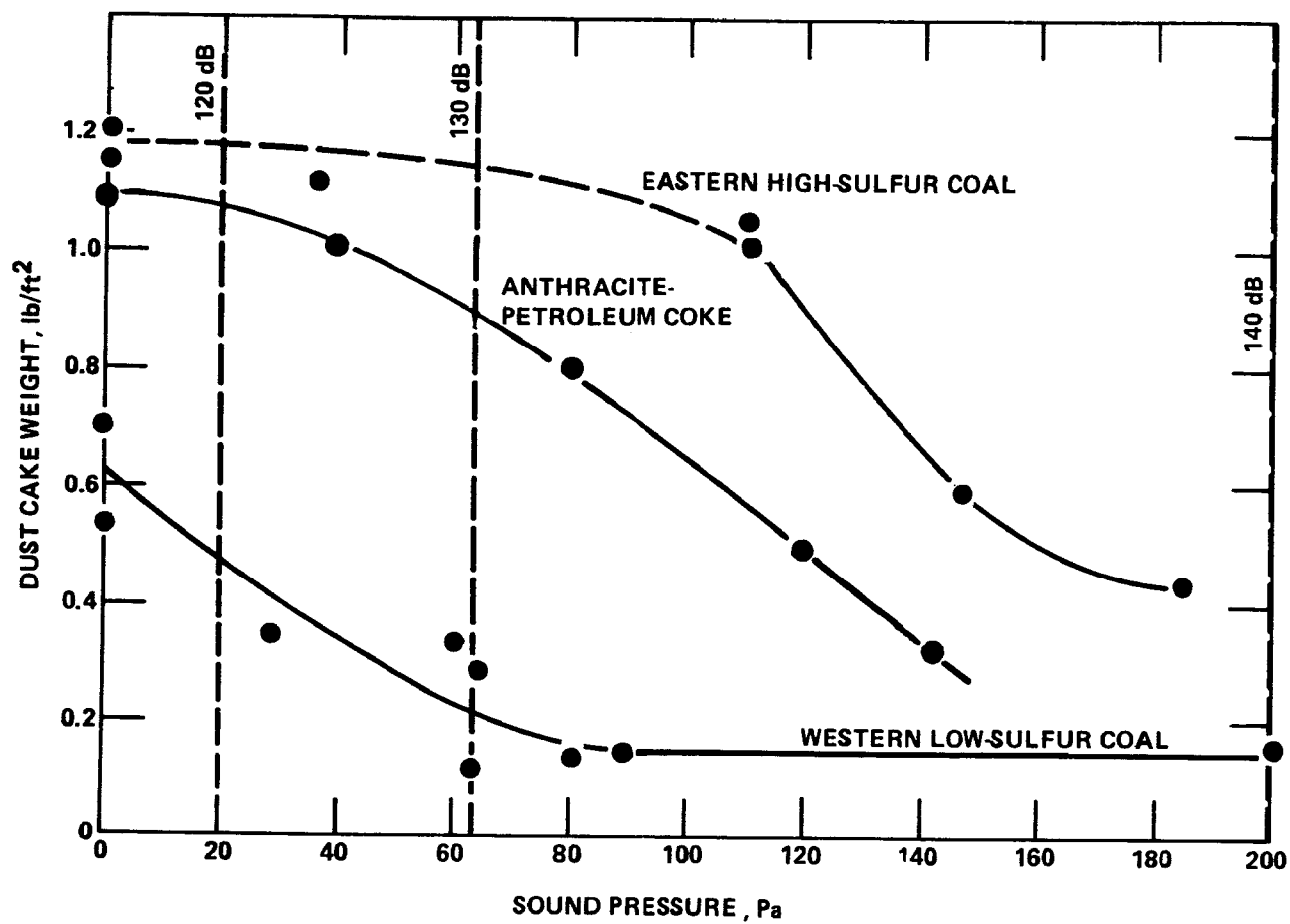


Figure 5. Effectiveness of sonic assist to reverse-gas cleaning for fly ashes from three coal types. (200 Hz)

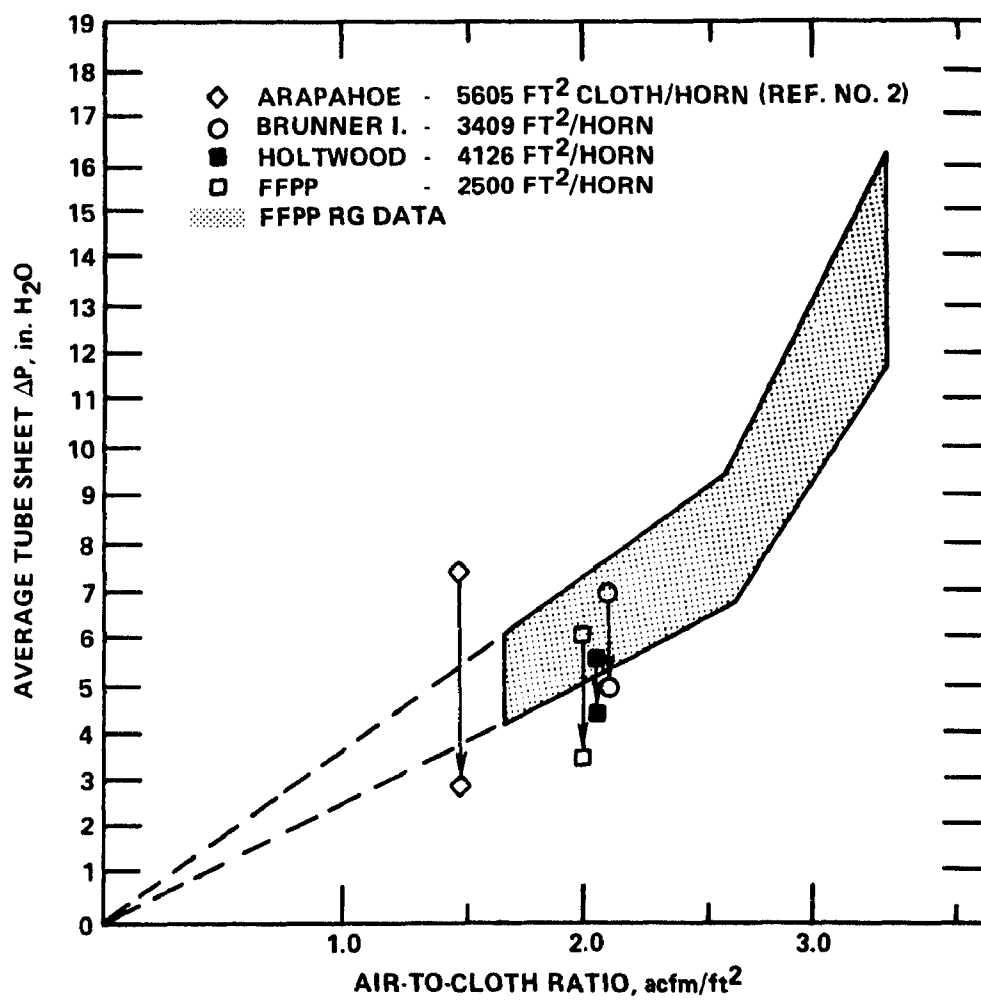


Figure 6. Effectiveness of reverse gas/sonic bag cleaning.

Finally, it is of interest to illustrate the long-term effectiveness of sonic horns. This has been done at the Holtwood Unit 17 baghouse. Figure 7 shows flange-to-flange pressure drop data from all of 1981, 1982, 1983, and early 1984. Horns were installed in the spring of 1981 to aid in meeting a pressure drop guarantee of 6" H₂O. As can be seen, the pressure drop, although initially low after horn installation, has crept back up to, and above the six-inch level. During the spring of this year the baghouse was rebagged. It will be interesting to observe the effectiveness of horns in controlling the increases in residual dust cake and pressure drop in these new bags.

CONCLUSIONS

In summary, the general findings of this field study are that sonic enhancement is an effective method for removing residual dust cakes in reverse-gas cleaned baghouses. Under the best conditions tested with low-sulfur coal fly ash, sonic cleaning can reduce the pressure drop of conventional reverse-gas cleaned baghouses by as much as 60%. This is accomplished through decreases in residual dust cake weight. These data also support the conclusion that the magnitude of the sound pressure adjacent to the bag as well as the surface characteristics of the bag are important parameters governing the effectiveness of sonic cleaning.

Other results from the overall study of sonic cleaning for the Electric Power Research Institute (3,4,5) include the following.

- Commercial horns are often described by a single frequency and power level, but in many instances the majority of their output is distributed over harmonics at higher frequencies.
- Coupling and interactions between horns and baghouse compartments is complex, requiring trial and error to determine the optimum number and location of horns for good spatial energy distribution.
- The combination of reverse-gas and horns is more effective in reducing pressure drop than either method alone.
- Laboratory studies indicate that 60 to 75% of the dust removed during sonic cleaning comes within the first 10 seconds, and that the removal virtually stops after 30 seconds.
- There is a strong dependence of dust cake removal on sound pressure level and frequency, with low frequencies being more effective.
- Particulate emissions from reverse-gas/sonic cleaned bags appear to be approximately equal to emissions from bags cleaned by reverse-gas alone.

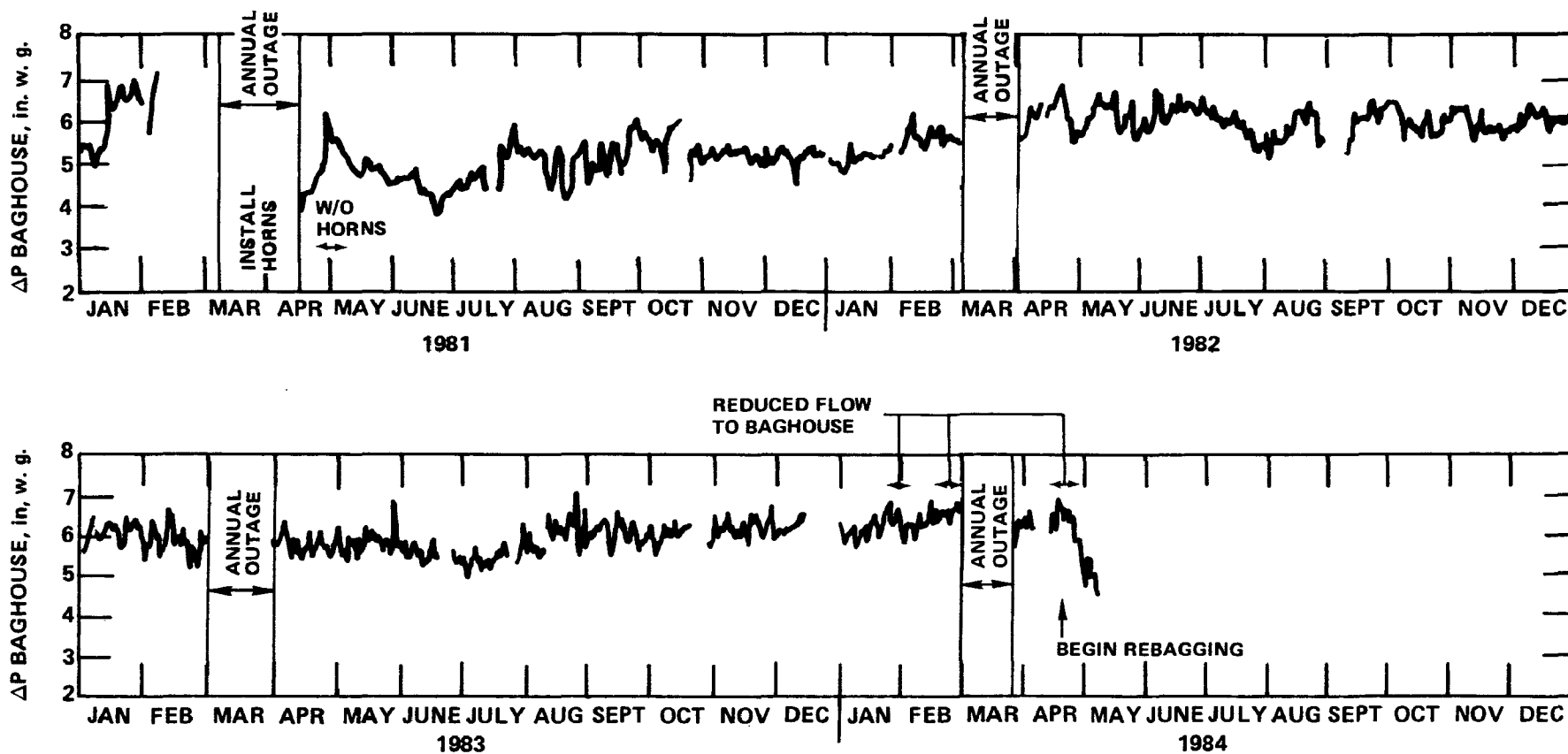


Figure 7. PP&L Holtwood Unit 17 Fuller bag filter, daily flange-to-flange pressure drop for 1981, 1982, 1983, and January through May of 1984. Unit load constant at 79 MW.

ACKNOWLEDGMENTS

We wish to thank Mr. Noel Wagner of Pennsylvania Power and Light Company and, specifically, Mr. Greg Lear at the Brunner Island Steam Electric Station, and Mr. Harvey Smith at the Holtwood Steam Electric Station for allowing us to conduct these tests. We also wish to thank Mr. Harold Mathes at the Arapahoe Generating Station of the Public Service Company of Colorado for his cooperation in our test program. This project has been supported by the Electric Power Research Institute under Contract Number RP1129-8, Mr. Robert Carr, Project Manager.

The work described in this paper was not funded by the U.S. Environmental Protection Agency and therefore the contents do not necessarily reflect the views of the Agency and no official endorsement should be inferred.

REFERENCES

1. N. H. Wagner. "Present Status of Bag Filters at Pennsylvania Power & Light Company," Proceedings: Second Conference on Fabric Filter Technology for Coal-Fired Power Plants, CS-3257, Electric Power Research Institute, Palo Alto, CA, November 1983.
2. A. R. Menard, R. M. Richards. "The Use of Sonic Air Horns as an Assist to Reverse Air Cleaning of a Fabric Filter Dust Collector," Proceedings: Second Conference on Fabric Filter Technology for Coal-Fired Power Plants, CS-3257, Electric Power Research Institute, Palo Alto, CA, November 1983.
3. K. M. Cushing, D. H. Pontius, R. C. Carr. "A Study of Sonic Cleaning for Enhanced Baghouse Performance", Proceedings: Second Conference on Fabric Filter Technology for Coal-Fired Power Plants, CS-3257, Electric Power Research Institute, Palo Alto, CA, November 1983.
4. K. M. Cushing, D. H. Pontius, R. C. Carr. "A Study of Sonic Cleaning for Enhanced Baghouse Performance", Paper Number 84-95.5, Presented at the 77th Annual Meeting of the Air Pollution Control Association, San Francisco, CA, June 24-29, 1984.
5. R. C. Carr, W. B. Smith. "Fabric Filter Technology for Utility Coal-Fired Power Plants, Part V: Development and Evaluation of Bag Cleaning Methods in Utility Baghouses, Journal of the Air Pollution Control Association, Vol. 34, Number 5, May 1984, pp. 584-599.

SONIC HORN APPLICATION IN A DRY FGD SYSTEM BAGHOUSE

Yang-Jen Chen
Minh T. Quach
H. W. Spencer III

Western Precipitation Division
Joy Manufacturing Company
4565 Colorado Blvd.
Los Angeles, California 90039

ABSTRACT

This paper will present the results of sonic horn testing in a dry FGD system baghouse at the Riverside Steam Generating Station of Northern States Power. The sonic frequency and sonic power were measured. The filter drags before and after the sonic horn installation were monitored and compared. The test results conclude that the sonic power reduces the residual drag for this application. The installation of the sonic horn and some of the economic aspects of this sonic horn application will also be discussed.

INTRODUCTION

The stringent emission codes of today have had a tremendous impact on the utilization of the fabric filter as a particulate control device. This device has the capability of producing extremely high efficiencies under varying inlet conditions. However, a potential problem in dry FGD applications is an excessive pressure drop across the fabric, which is generally the result of the inability of standard methods to clean the filter bags. One of the promising methods of reducing an excessive pressure drop caused by a heavy residual dust cake is the use of sonic energy generators to assist the traditional methods of bag cleaning.

Two JOY-Airchime sonic horns Model KM-250 were installed in Compartment Number 4 of the N.S.P. Riverside baghouse in August, 1982. The sonic frequency and sonic power were measured at various locations inside the compartment, and the pressure drop and flow volume through the compartment were recorded.

In this paper, the features of JOY-Airchime sonic horns are discussed. The test results with and without sonic horns in operation are compared. The conclusion is drawn that sonic power reduces the baghouse residual drag in dry FGD applications.

DESCRIPTION AND OPERATION OF THE RIVERSIDE BAGHOUSE

A schematic of the JOY/NIRO 100 MW dry Flue Gas Desulfurization (FGD) Demonstration Facility at Northern States Power, Riverside Generating Station (Minneapolis, Minnesota) is shown in Figure 1. The baghouse, installed downstream from the NIRO spray dryer absorber (SDA), is a JOY THERM-O-FLEX fabric filter. The performance and technical specifications of the baghouse are summarized in Table 1.

The baghouse compartments, as shown in Figure 2, are arranged in two rows, six compartments to a row. Each compartment consists of 250 twelve-inch diameter, thirty-five foot long bags. Total gross filter area for each compartment is 26,775 square feet. Woven fiberglass materials of various specifications are installed in different compartments for testing. The design characteristics for bag type A (which is a 9.3 ounce per square yard, texturized, and teflon-finished woven fiberglass material) are given in Table 2.

The Riverside baghouse was designed to operate with or without the spray dryer in service. The gross air-to-cloth ratio varied from 0.7 to 2.5 ft/min depending on boiler load conditions and number of compartments in service. When the spray dryer is in operation, the baghouse runs at a considerably lower temperature than a non-FGD installation. The operating temperature with the SDA in service has been as low as 18°F above the adiabatic saturation temperature. The dust loading with the SDA in operation (4.27 - 12.1 grain/ACF) is much higher than without the SDA (1.2 - 2.9 grain/ACF).

Since the Riverside power plant is a peaking unit and the dry FGD system is a demonstration facility, the baghouse has been through various operating conditions:

- High load and low load at high temperature without spray drying.
- High load and low load at low temperature with the spray dryer in service.

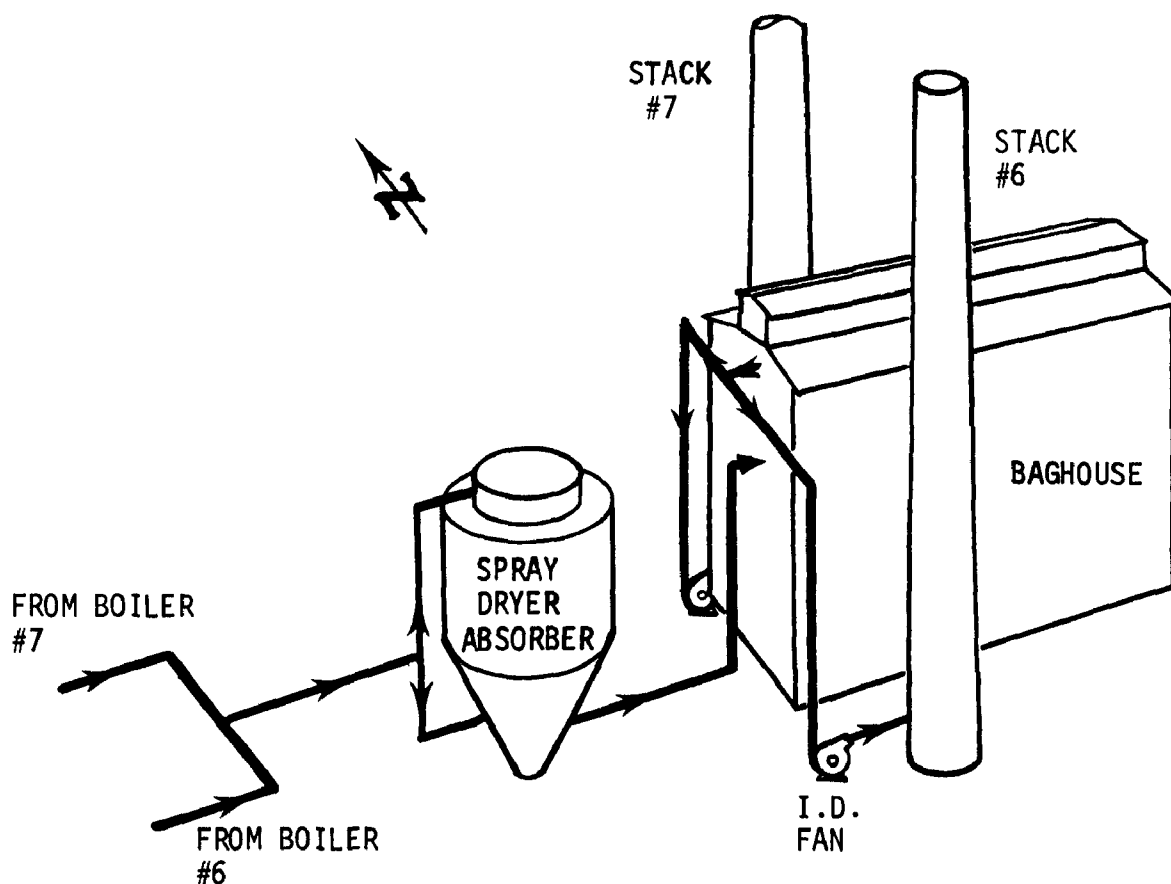
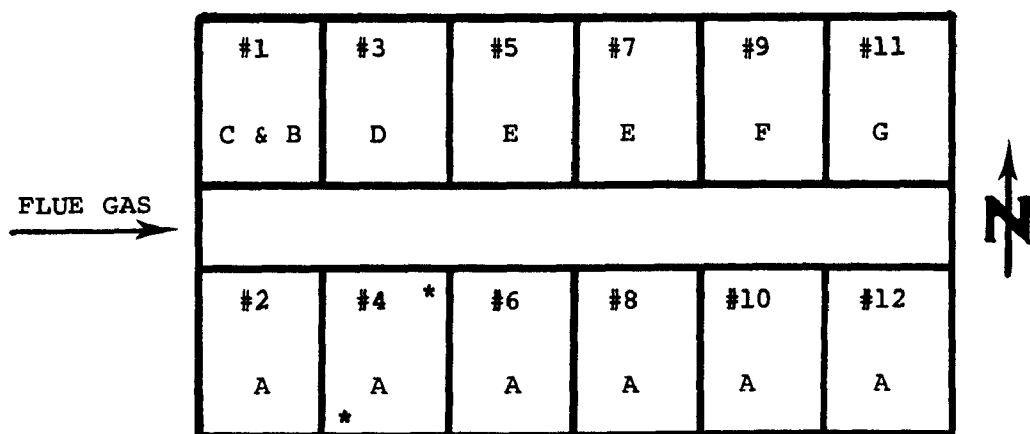


Figure 1. Joy/Niro Dry FGD System at Riverside

Table 1. Joy Therm-O-Flex Baghouse Data Summary

Gas Volume (max acfm)420,000 (540,000)*
Design Temperature (°F)	500
Outlet Loading (lb/10 ⁶ Btu).	0.03
Pressure Drop (in. VWC)	6
Design Pressure (in. VWC).	-30 to +20
Number of Compartments.	12
Number of Bags per Compartment	250
Bag Diameter (in.).	12
Bag Length (ft.).	35

* Value is for non-FGD system operation



* SONIC HORNS

A to G : Woven Fiber Glass Materials with Various Specifications

Figure 2. Location of the Sonic Horns in the Baghouse

Table 2. Type A Material Specifications

Thread Count	53 x 30
Warp Yarn	150-1/2
Fill Yarn	150-1/4 Texturized
Weave	3x1 Twill
Avg. Wt., Oz./Yd ²	9.3
Permeability, CFM/FT ²	65-80
Mullen Burst, psi	595 (450 minimum)
Finish	Teflon
Material	Glass

- Very low load, low temperature during boiler banking.
- Various coals with sulfur contents ranging from 0.8 to 3.5%
- Various additives in the dry FGD process.
- Start-ups with hot or cold flue gas.
- Various cleaning cycles.

During some cold start-up processes, Compartments 2 and 4 were selected to receive the cold flue gas from the boiler initially, then other compartments were put in-service after the flue gas was above the saturation temperature. Since increases in the residual drag in these two compartments were observed, compartment 4 was chosen for sonic horn testing.

JOY-AIRCHIME SONIC HORN MODEL KM-250

After research and evaluation of the commercially-available sonic generators, the JOY-Airchime sonic generator, Model KM-250 was selected for testing. The specifications of the horn are summarized in Table 3. The physical dimension of the KM-250 horn are small, 21-7/8" x 13-1/2", and the weight is 29 pounds. Therefore, the installation of the horn inside the compartment does not require a large space.

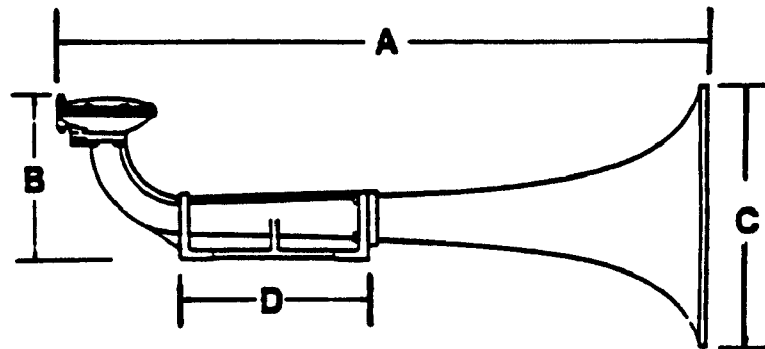
The horn is designed to operate normally at 30-150 psi of air pressure with the air consumption in the range of 20-65 CFM.

The sound pressure level is rated at 144 dB at a distance of 3.3 feet while the horn is operating with 45 psi air pressure. The specially-designed bell and dual diaphragms will generate a fundamental frequency and natural harmonics. The bell of the horn has the following features:

1. It determines the frequency at which the diaphragm will vibrate.
2. It amplifies the fundamental frequency and corresponding harmonic frequencies.
3. It eliminates undesirable and off tone frequencies.
4. It projects the sound waves in an omni-directional pattern.
5. It increases or maintains high sound pressure levels at virtually any operating air pressure.

Table 3. Joy-Airchime Sonic Horn Model KM-250

Basic Frequency	S.P.L. @ 1 Meter	Air Consumption	Air Pressure	Length Overall	Net Weight
250 Hz	144 dB	20-65 CFM	30-150 PSI	21 7/8"	29 LBS



A	B	C	D
21 7/8"	9 3/4"	13 1/2"	6 5/8"

SONIC HORN INSTALLATION AND OPERATION

The sonic horns are located at two diagonal corners at the top of Compartment # 4, facing the center. Each horn is bolted to a pivotable bracket which is mounted on an I-beam of the compartment roof. The air supply to the horns, 90-100 psi, comes from the power plant and is stored in a 60-gallon receiver to prevent a sudden decrease in the line pressure when the horns are turned on. The horn piping schematic is presented in Figure 3. The operation of the horns was controlled using one of the baghouse outlet valve limit switches to initiate timing. Both horns were turned on five seconds after the reverse air flow started and ran for eight seconds during the period of the flow (20 seconds). No other sonic horn operation mode was tested in this phase of the test program. The baghouse cleaning cycle was normally one hour.

TEST RESULTS

A. Sound Pressure Level Measurement

The sound pressure levels were measured at five locations inside Compartment #4 as indicated in Figure 4, using General Radio Precision Sound Level Analyzer Type 1933. At each location, measurements were conducted at an upper level (2 feet below the bag cap) and a lower level (2 feet above the thimble). An additional measurement was performed 10 feet above the thimble at location No. 3.

Typical curves of sound pressure levels versus octave center band frequencies at each test location are shown in Figure 5. The average values of the sound pressure levels inside the compartment are shown in Figure 6. High intensities of sonic pressure were measured not only at the fundamental frequency of the Model KM-250 sonic horn (250 Hz) but also at the corresponding harmonic frequencies, 500, 1K, 2K, and 4K Hz. The background noise, as indicated in Figure 5, does not affect the intensity of sonic sound level measurements based on the instrumentation characteristics (error is less than .5 dB if the difference between the sound level and the background noise is greater than 10 dB).

The sound pressure measurements were also performed with one horn in operation (the other was disconnected). The comparison of the sound pressure levels at the frequency of 250 Hz is shown in Table 4. There was no substantial difference between the sound pressure levels with one horn or two horns in operation. This indicates that the sonic effect inside the compartment with one horn or two horns in operation might be the same, however, additional testing would be required to

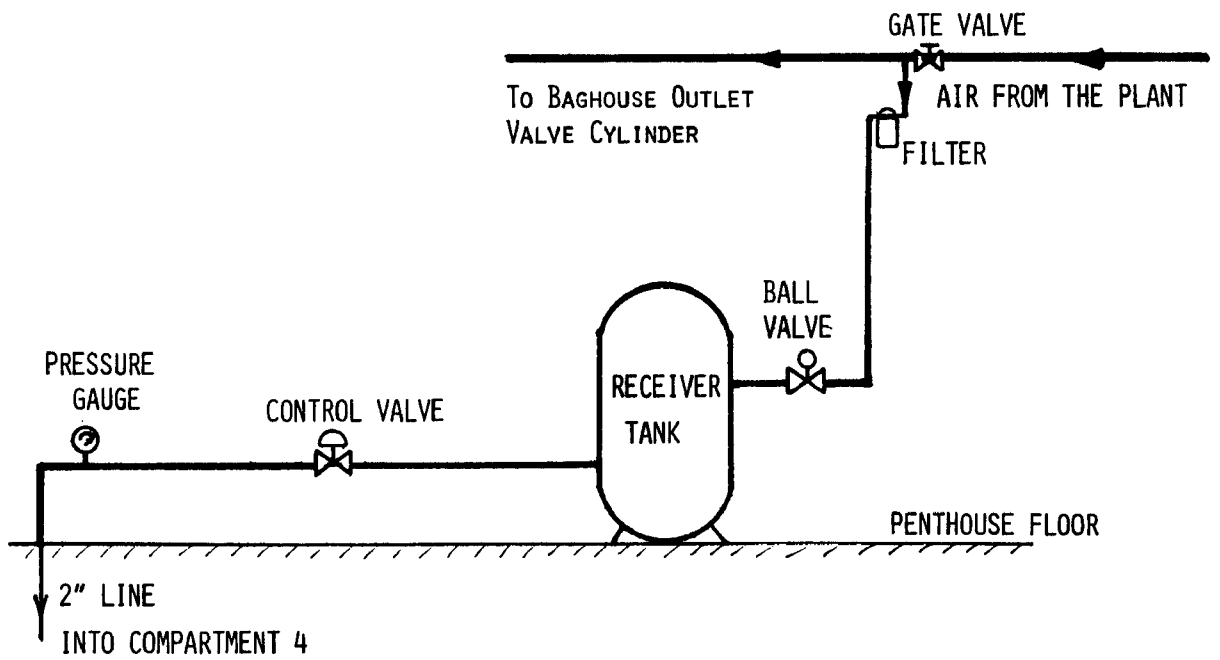


Figure 3. Sonic Horn Piping Schematic

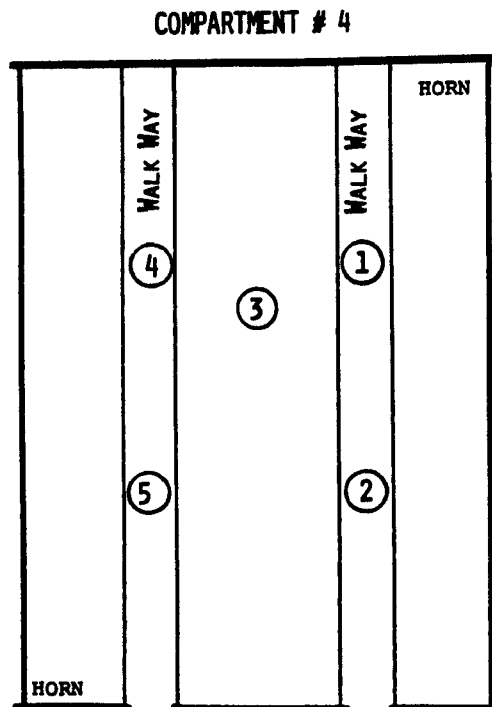


Figure 4. Locations of the Sonic Horns and the Sound Level Test Points

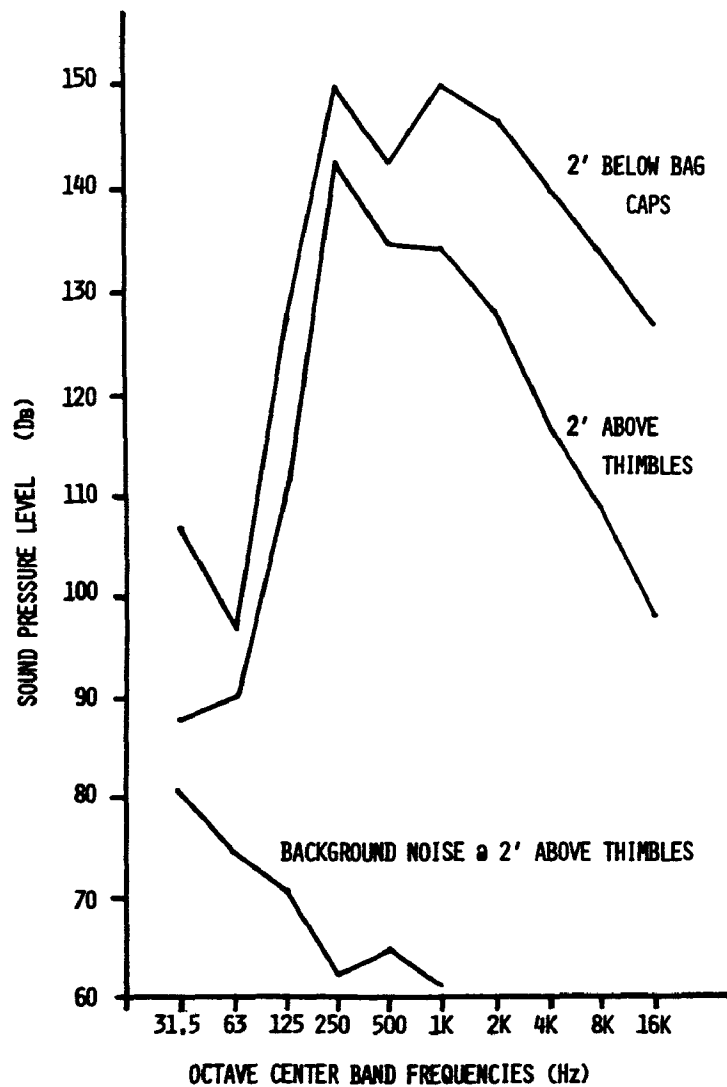


Figure 5. Sound Pressure Level at Location #5

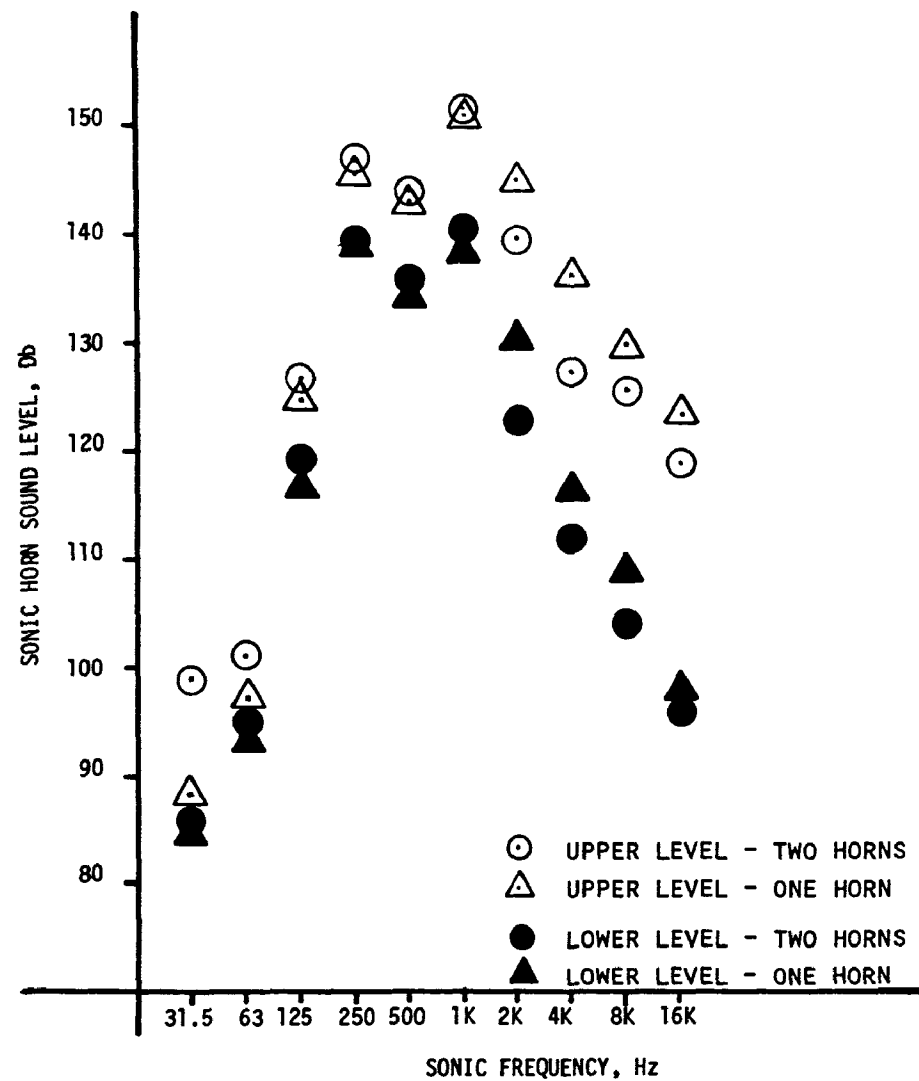


Figure 6. Average Sonic Sound Levels vs. Frequency

Table 4. Sonic Horn Level (Db) @ 250 Hz

LOCATION	1		2		3		4		5	
NO. OF HORNS USED	1	2	1	2	1	2	1	2	1	2
UPPER LEVEL (2' BELOW BAG CAPS)	147	149	144	148	142	141	151	150	143	151
LOWER LEVEL (2' ABOVE THIMBLES)	149	136	130	138	134	133	142	143	140	148
MIDDLE (10' ABOVE THIMBLES)						142				

verify performance.

B. Measurements of Residual Drag, Flow Volume and Residual Dust Cake Weight

The Riverside baghouse was instrumented to measure the pressure drops and flow rates across the individual compartments. The flow volumes through compartments 2, 4, 6, and 8, which have the same fabric material, are compared in Figure 7. With sonic horns in operation, Compartment #4 received a much higher flow rate after cleaning and a greater flow volume during filtration.

The residual filter drag, which is the ratio of the compartment pressure drop to the air-to-cloth ratio after cleaning, was compared in Figure 8. The residual drags in the compartments with the same fabric material are in the same range without sonic effects. Substantial improvement of the residual drag was observed in Compartment #4 after the sonic horns were installed.

In-situ bag weight measurements were also performed with and without sonic horn operation to check the dust buildup trends on the bag surface. Eight bags at various locations inside each compartment were weighed. The average values of these weights are presented in Figure 9. A significant reduction of the residual dust cake on the bag was observed in Compartment # 4 with the sonic horns compared to the compartments without sonic horns. The results support the finding of the substantial improvement in residual drags with the use of sonic horns.

C. Fabric Evaluation

Sample bags removed for examination after one year of sonic horn operation showed no significant degradation. The profiles of the as-received permeability and cloth weight (material and residual dust) along the length of the bag were also investigated. The results, plotted in Figure 10, indicate the uniform distribution of the weight and permeability along the bag.

ECONOMIC ASPECT OF SONIC HORN APPLICATIONS

The pressure drop across the baghouse at a specified air-to-cloth ratio is the prime index for the operating cost. The compartment pressure drop increases and the gas flow to the compartment decreases as the dust cake builds up on the surface of the bag. The average value of the compartment pressure drop (P_a) and the average value of the air-to-cloth ratio (A_c) before and after cleaning are used to represent the performance

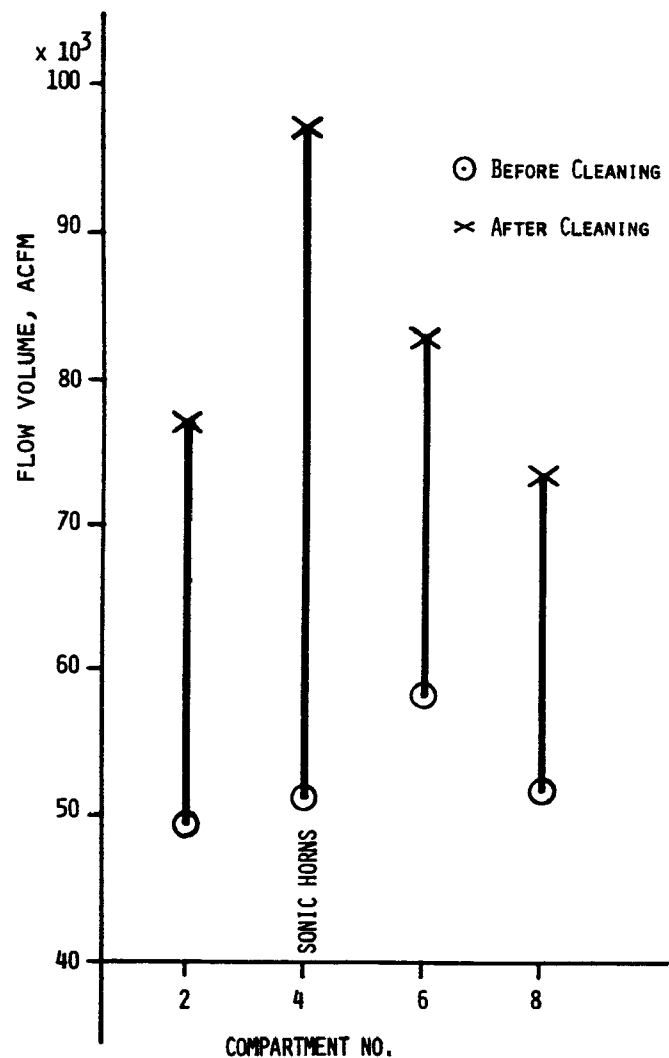


Figure 7. Comparison of the Flow Volumes through the Compartments with and without Sonic Horns

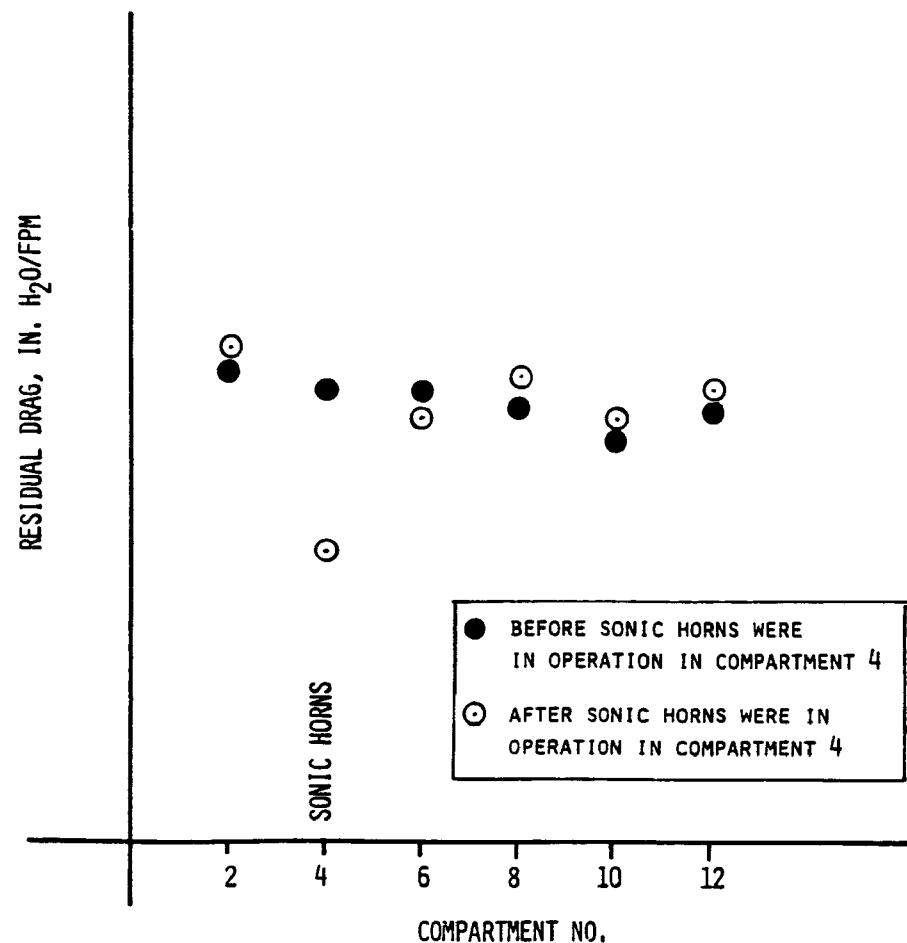


Figure 8. Comparison of the Residual Drags in the Compartments with and without Sonic Horns

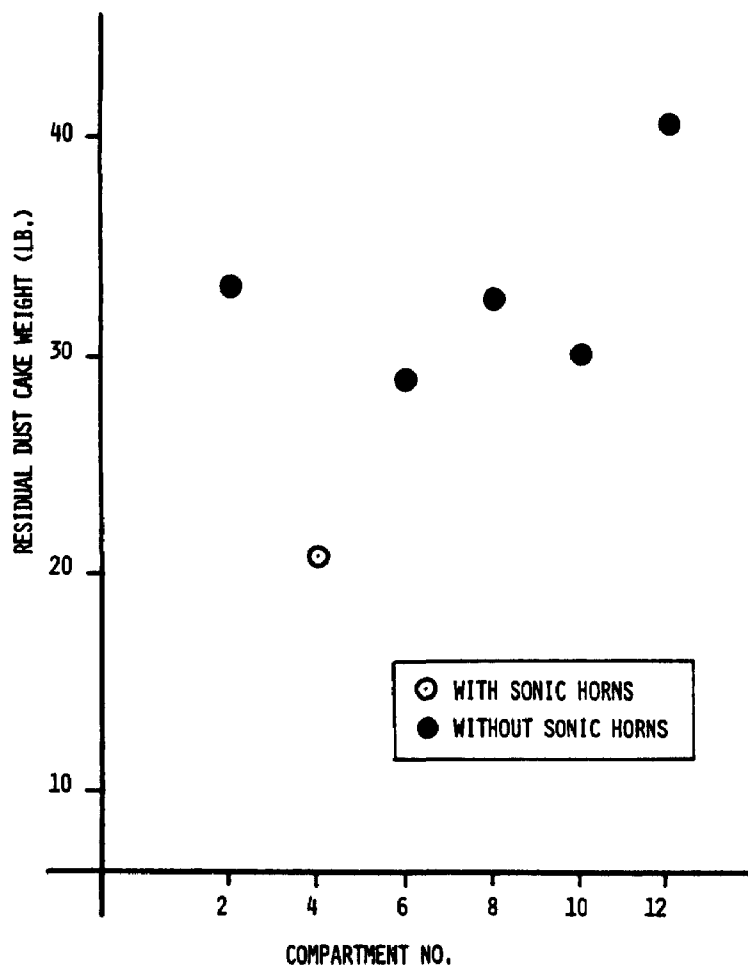


Figure 9. Comparison of the Residual Dust Cake Weights in the Compartments with and without Sonic Horns

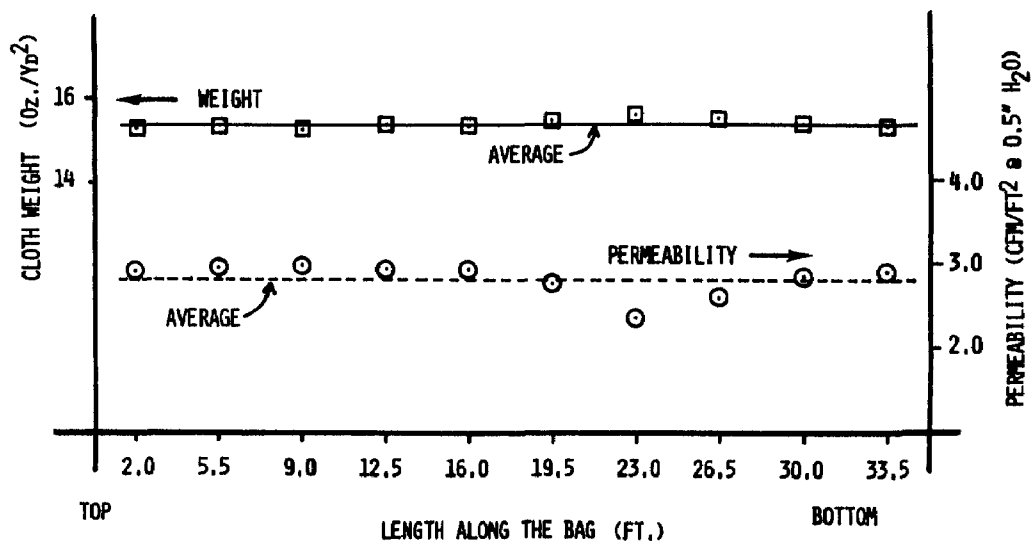


Figure 10. As-Received Cloth Weight and Permeability Along the Bag Removed from the Compartment with Sonic Horns

of each compartment. A performance index, $I = P_a/A_a$, can be defined to indicate the energy requirement during the filtration process. Higher index numbers mean higher I.D. fan power consumption.

The pressure drop and flow volume across Compartment #4 were monitored before and after the sonic horn installation. The performance index prior to operating the horns was 1.90. After the horns were in operation, this value dropped to 1.35; a reduction of almost 30%. This significant improvement corresponds to a reduction in the residual drag indicating a more efficient removal of the dust cake.

SUMMARY AND CONCLUSIONS

Two JOY-Airchime, Model KM-250 sonic horns were installed in Compartment #4 of the Riverside baghouse for testing. Owing to their compactness and rigidity, the horns were installed within a minimum space. With the specially-designed bell and dual diaphragms, the horns generate not only the fundamental frequency and natural harmonics, but also propagate the sound energy in an omni-directional pattern and maintain high sound pressure levels inside the compartment. The test results indicate a reduction in the residual dust cake, improvement in the residual drag, and a uniform dust distribution along the length of the bag. The effectiveness of the sonic horns when applied in a dry FGD system baghouse was demonstrated.

Although a significant improvement in the performance of Compartment #4 at the Riverside baghouse was observed, the effectiveness of sonic-assist cleaning on the other baghouses needs to be evaluated individually. The amount of improvement will be effected by such factors as the characteristics of the residual dust cake, the type of sonic generators utilized, and the individual baghouse operating conditions.

No significant deterioration of the fabric material strengths was observed after one year of sonic horn operation, but the long-term effect of sonic cleaning on the fabric material strengths is still under investigation.

ACKNOWLEDGEMENTS

The authors are grateful to Mike Skinner and Steve Wolf of Northern States Power Company; also, Tom Tarnok and Al Narverud of Joy Manufacturing Company for their review of this paper.

FULL SCALE OPERATION AND PERFORMANCE OF
TWO NEW BAGHOUSE INSTALLATIONS

C. B. Barranger
Flakt, Inc.
Knoxville, Tennessee 37923

ABSTRACT

During 1983 Nevada Power Company began operating a new 250 MW boiler at their Reid Gardner Station. At approximately the same time, Utah Power and Light began operating a new 400 MW boiler at their Hunter Station. Both boilers are pulverized coal fired units burning low sulfur western United States coals. Low ratio reverse air cleaning baghouses utilizing glass filter bags are the devices installed to meet the particulate control requirements of each boiler unit. This paper will describe the design, start-up, operation, maintenance, and actual performance results of these two baghouse installations.

INTRODUCTION

The Nevada Power Reid Gardner Station is located approximately 50 miles northeast of Las Vegas, Nevada, just west of Interstate 15 near Moapa, Nevada. This station consists of four boiler units, three small older units and the new 250 MW-Unit Number 4.

The Utah Power and Light Hunter Station is located approximately 100 miles southeast of Provo, Utah, east of Interstate 15 near Castle Dale, Utah. This station consists of three boiler units similar in size, including the new 400 MW-Unit Number 3.

UNIT DESIGN

Both the Nevada Power and Utah Power and Light boiler units incorporate similar design constraints, i.e., both burn low sulfur western coal, fire with pulverized coal burners, and utilize Ljungstrom type air heaters. Foster Wheeler supplied the Nevada Power boiler unit and Babcock & Wilcox supplied the Utah Power and Light boiler unit. Table 1 describes the design of these boiler units and Tables 2, 3, and 4 show the design coal and ash analyses of the fuels burned.

TABLE 1. DESIGN OF BOILER UNITS

	Nevada Power	Utah Power and Light
Boiler Supplier	Foster Wheeler	Babcock & Wilcox
Boiler Size (Net)	250 MW	400 MW
Type Firing	Pulverized coal	Pulverized coal
Fuel Normal	Low sulfur western coal	Low sulfur western coal
Fuel Start-up	No. 2 fuel oil	No. 2 fuel oil
Draft Control	Balanced draft	Balanced draft
Air Heater Type	Ljungstrom	Ljungstrom

TABLE 2. PROXIMATE COAL ANALYSIS (TYPICALS)

	Nevada Power	Utah Power and Light
Moisture (%)	7.2	4.57
Ash (%)	7.2	11.60
Volatile Matter (%)	43.66	40.16
Fixed Carbon (%)	41.94	44.27
Sulfur (%)	0.52	0.56
Heating Value (BTU/LB)	12,400	11,900

TABLE 3. ULTIMATE COAL ANALYSIS (TYPICAL %)

	Nevada Power	Utah Power and Light
Moisture	7.20	4.57
Carbon	67.50	66.71
Chlorine	0.04	0.01
Hydrogen	5.08	5.21
Nitrogen	1.10	1.12
Oxygen	11.40	10.22
Sulfur	0.52	0.56
Ash	7.20	11.60

TABLE 4. ASH ANALYSIS (RANGE %)

	Nevada Power	Utah Power and Light
Phosphorus Pentoxide	-----	0.01 - 1.2
Silica	56.40 - 60.25	42.5 - 60.6
Ferric Oxide	6.40 - 8.39	0.7 - 8.3
Alumina	12.30 - 15.00	9.9 - 30.0
Titania	0.75 - 0.93	0.7 - 1.4
Magnesium Oxide	0.78 - 1.10	0.2 - 4.6
Lime	7.84 - 12.00	4.9 - 12.5
Sulfur Trioxide	5.49 - 7.60	2.9 - 11.7
Sodium Oxide	0.97 - 1.33	1.5 - 11.5
Potassium Oxide	0.85 - 0.97	0.1 - 2.2
Undetermined	0.84 - 0.96	0.2 - 2.2

AIR POLLUTION CONTROL SYSTEM

In 1979, specifications for the required pollution control systems were developed. Nevada Power hired Fluor Power Services, Chicago, and Utah Power and Light hired Brown and Root, San Francisco, to design the systems. It was determined to design the system for control of both sulfur dioxide gases as well as solid particulates. Based on experience and necessary evaluations, a baghouse was selected to control the particulates and to be followed by a wet scrubber to control the sulfur dioxide gases. Flakt, Inc. was selected as the supplier of these baghouses for both stations. Table 5 lists the major milestone dates achieved as these baghouses were incorporated into the systems.

TABLE 5. BAGHOUSE MILESTONE DATES

	Nevada Power	Utah Power and Light
Specification	September, 1979	March, 1979
Order	February, 1980	November, 1979
Start-Up	June, 1983	May, 1983
Performance Test	September, 1983	October, 1983

Baghouse Design Criteria

The type of baghouse selected was a low ratio, reverse air cleaning baghouse utilizing fiberglass filter bags.

These baghouses designed to control the solid particulate contained in the flue gases are described as follows:

	Nevada Power	Utah Power and Light
Total flue gas flow rate (ACFM)	1,440,000	2,053,544
Flue gas temperature (°F)	273	260
Inlet particulate concentration (Grains/ACF)	2.13	2.47
Outlet particulate concentration (Grains/ACF)	0.008	0.0075
Outlet particulate concentration (LBS/10 ⁶ BTU)	0.03	0.03

	Nevada Power	Utah Power and Light
Quantity of baghouses	1	2
Quantity of casings per baghouse	2	1
Quantity of compartments per casing	8	10
Quantity of filter bags per compartment	432	522
Filter bag material (Table 6)	Fiberglass	Fiberglass
Filter speeds: Gross (FPM)	1.97 ¹	1.87 ³
Net (FPM) ⁵	2.22 ²	2.24 ⁴
Net/Net (FPM) ⁵	2.38 ²	2.52 ⁴
Pressure loss - baghouse (inches of water)	5 Average	5.5 Average
Pressure loss - ductwork (inches of water)	3	1.75
Opacity (max %)	20	10
Reverse air fans	1 + 1 Spare	2 + 1 Spare

TABLE 6. FILTER BAGS

	Nevada Power	Utah Power and Light
Supplier	MIDWESCO	MIDWESCO
Bag diameter (inches)	12	12
Bag length (feet)	35.5	36.5
Construction	3x1 Twill	3x1 Twill
Warp	150 1/2	37 1/0
Fill	75 1/2 Texturized	75 1/3 Tex & Fil
Finish	10% Teflon	7% Teflon
Weight (oz/sq. yd.)	10.3	14.3
Permeability (@ 1/2" W.C.)	30-60	35-60

Baghouse Arrangement

Figure 1 shows the arrangement of the Nevada Power baghouse. There are two primary and two secondary air heater boiler flue gas exit points

¹One compartment off for cleaning.

²One compartment off for cleaning plus one compartment off for maintenance.

³Two compartments off for cleaning.

⁴Two compartments off for cleaning plus two compartments off for maintenance.

⁵Calculations include reverse air flow.

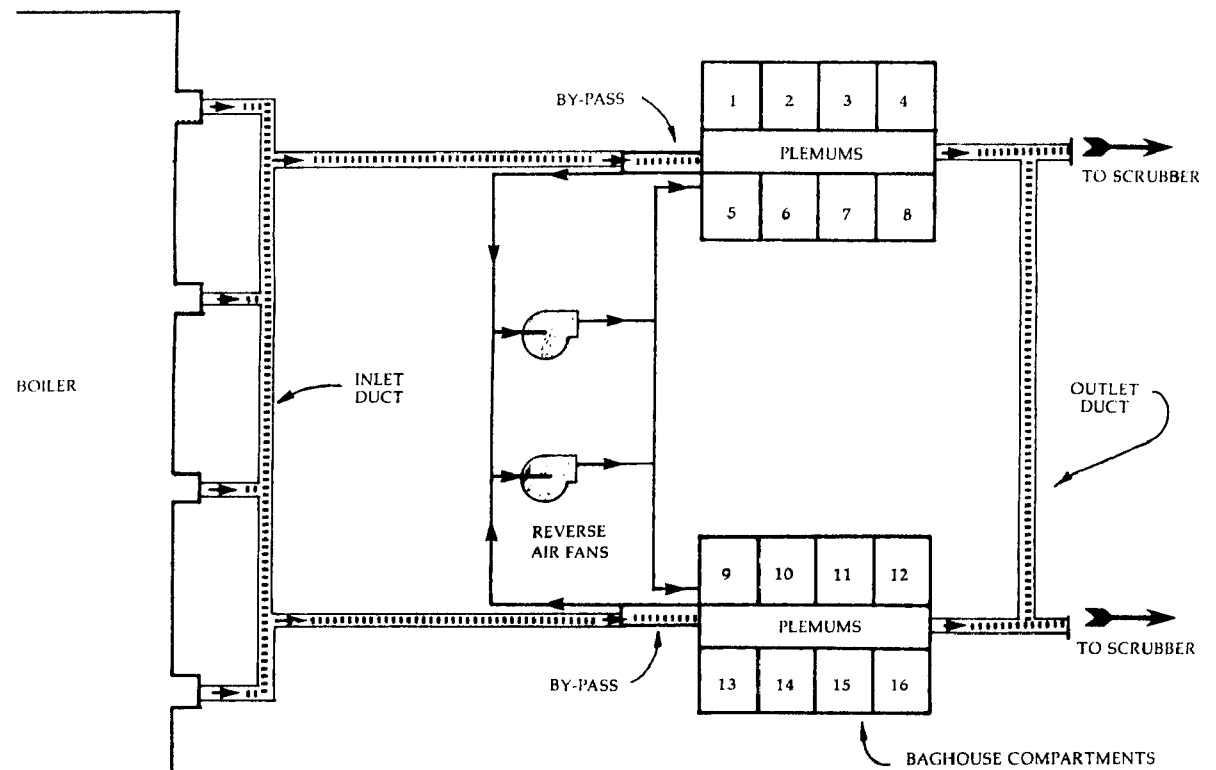


FIGURE 1. NEVADA POWER ARRANGEMENT

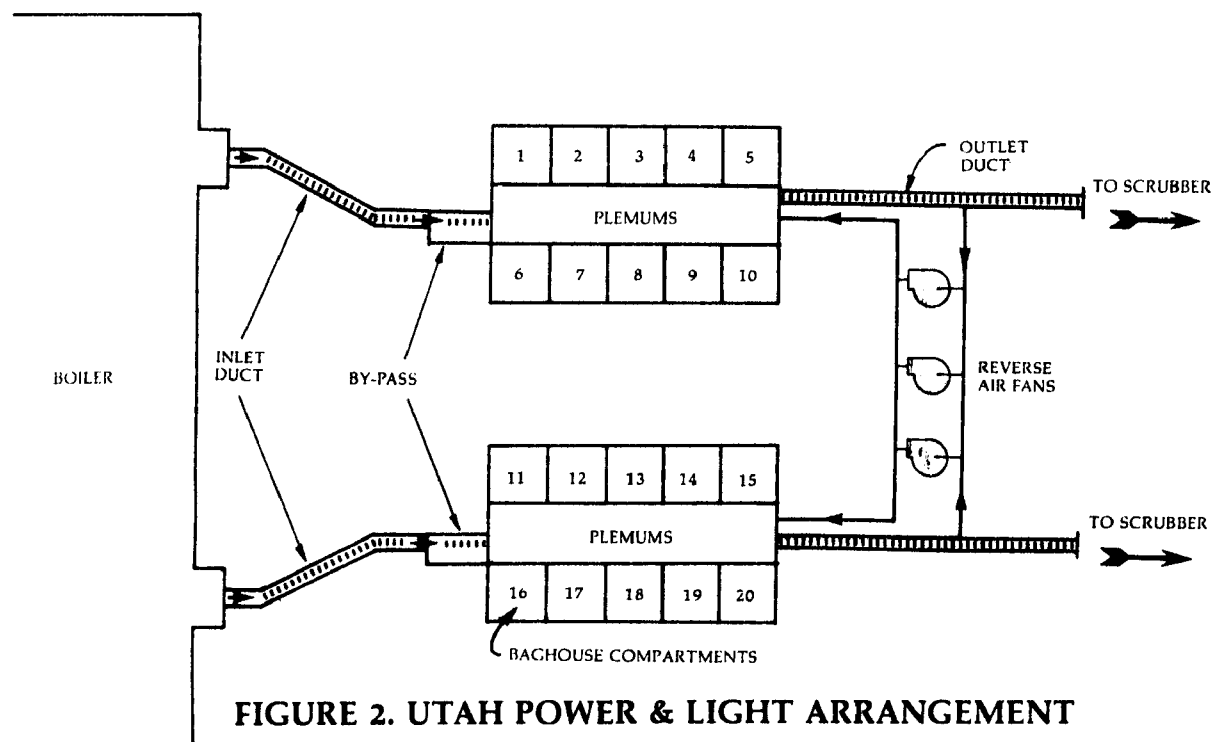


FIGURE 2. UTAH POWER & LIGHT ARRANGEMENT

which are connected together and ducted to two separate baghouse casings. Each casing includes centrally located inlet, outlet, reverse air, and vent air plenums. The reverse air fans are located at the inlet end of the baghouse. Figure 2 shows the arrangement of the Utah Power and Light baghouses. There are two boiler air heater outlets each ducted to a single baghouse. Each baghouse contains centrally located plenums as Nevada Power, and the reverse air fans are located at the outlet end of the baghouse.

Compartments

Each baghouse compartment contains a series gas inlet, gas outlet, reverse air, and vent air dampers. All dampers are poppet type dampers operated by pneumatic air cylinders. This ensures proper gas sealing and quick actuation. The filter bags are placed within the compartment in a normal three bag reach arrangement. Extended one foot long thimbles are welded into the grid sheet and allow a positive clamping surface for the bottom of the filter bags. All compartments are provided with full internal and external fiberglass type heat insulation.

At Nevada Power each baghouse compartment contains one single hopper with 60° valley angle slope design. At Utah Power and Light each compartment contains a double discharge type hopper. All hoppers are electrically heated with blanket type hopper heaters.

Supplementary Systems

Full flow flue gas by-pass, key interlock, and compartment ventilation systems have been installed with both units. All three are basic systems to protect either plant personnel or baghouse equipment. The flue gas by-pass system will automatically divert the flue gas around the baghouse compartments whenever high gas temperatures (above 450°F) are sensed at the baghouse inlet, thus, protecting the filter bags from high gas temperatures. Key interlocks allow personnel access into the compartments or hoppers only when it is safe to enter. To provide maintenance personnel a reasonable working area inside the compartments, a ventilation system purges and cools the inside of the compartment (see Figures 3 and 4).

BAGHOUSE OPERATION

Normal Filtering

Flyash laden gas from the boilers are drawn into the inlet manifolds of the baghouses. The inlet minifold spans the length of each baghouse casing and ducts the gases through inlet poppet valves into all the hoppers of the baghouses. These gases are directed upward into the filter bags of each compartment and particulate is deposited on the interior surface of the filter bags. Gases are filtered as they pass through the dust cake and bag material and are drawn upward through

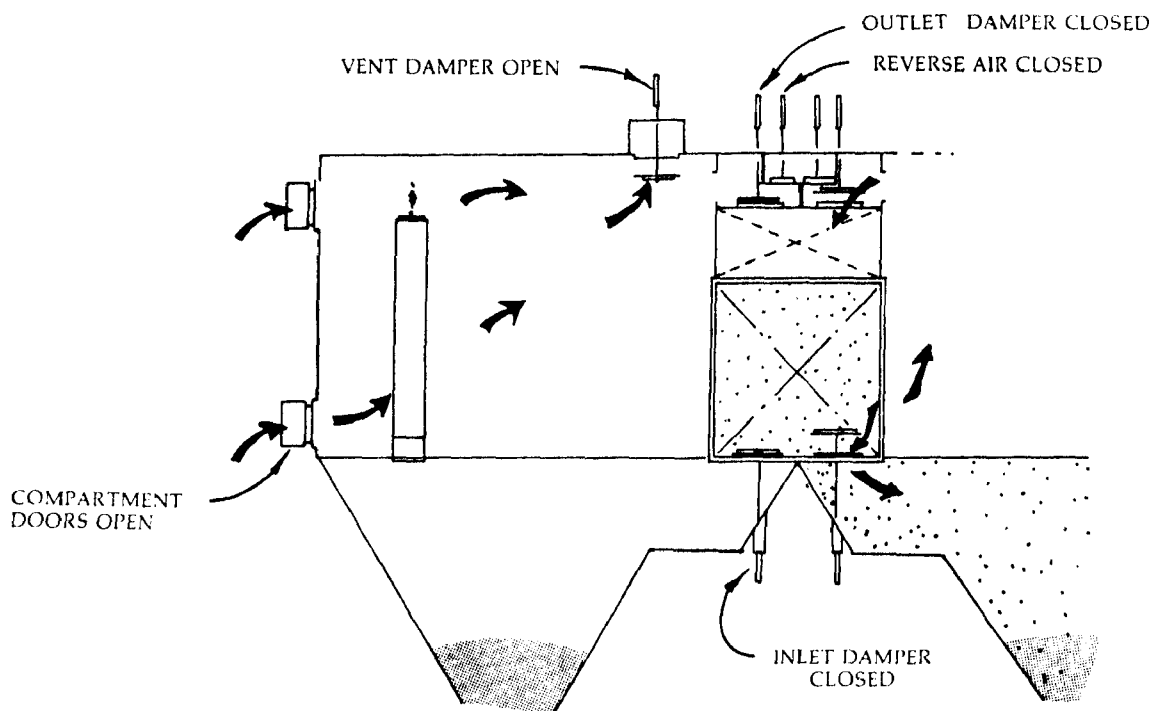


FIGURE 3. ON-LINE MAINTENANCE

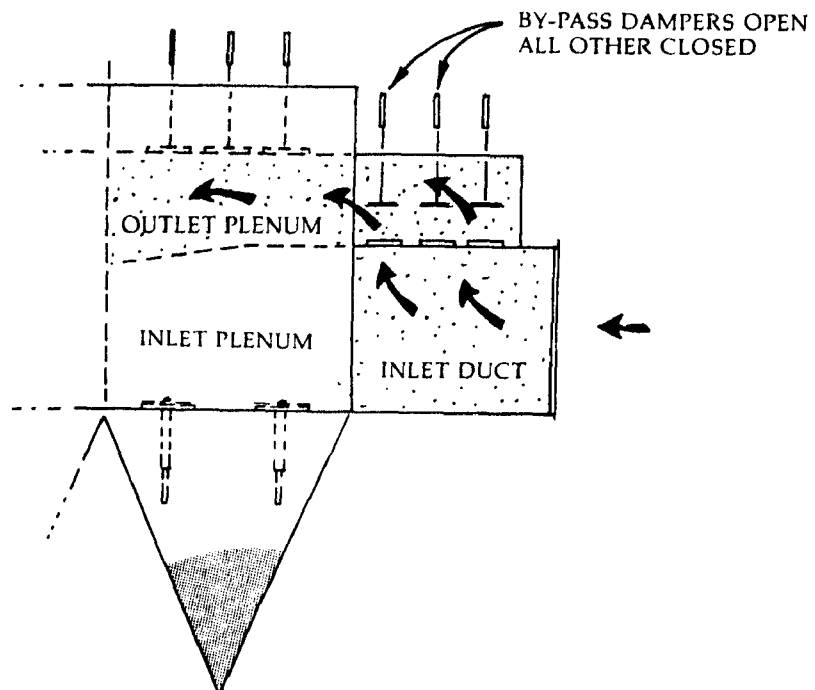


FIGURE 4. FLUE GAS BY-PASS

poppet valves into the common outlet plenum. Filtered gases exit the baghouse through the outlet ductwork, pass through the wet scrubbers, and discharge to the atmosphere through common stacks. During this mode of operation, only the compartment inlet and outlet poppet valves are in their open position (see Figure 5).

Automatic Fabric Cleaning

As particulate is filtered, ash deposits gradually build up on the bag surface. These deposits increase the fabric's resistance to flow, thus increasing the pressure loss across the bags. This ash cake must be periodically removed or the resistance to flow will increase the fabric's pressure to a level too high for the I.D. Fans to overcome. Cleaning these ash deposits is automatic. The filter bag cleaning system is activated by a signal sent by the differential pressure sensor. (Sensors are located across the baghouse inlet and outlet duct.) The indicator is set to activate cleaning once the baghouse differential pressure is sensed at 4.5 to 5.0 inches water gauge. Once the cleaning system is activated, all bags in all compartments are sequentially cleaned one compartment at a time. After the total baghouse is cleaned (approximately 30 minutes) and is operating somewhere below five inches water gauge, the differential pressure indicator is automatically reset and normal filtering resumes. During the automatic baghouse cleaning mode, the only dampers which are opened and closed are the reverse air and compartment outlet dampers, the compartment vent damper remains closed and the compartment inlet dampers remain open (see Figure 6). Energy required to reverse gas clean these filter bags is via a centrifugal fan system. These fans pull clean heated gases from the baghouse outlet duct and push the gas through the bags in a reverse direction. The particulate is dislodged from the bag surface and falls to the bottom of the hopper.

All cleaning time functions are adjustable so that optimum field settings can be attained. If desirable, the pressure activation of the cleaning cycle may be switched to a timing activation cleaning cycle.

Model Studies

To evaluate the aerodynamic design of the baghouses and duct systems, model studies were performed at Nels, Inc. Plexiglass 1/12 scale models of all the ductwork and the baghouses were constructed. Parameters such as velocity and gas flow distribution, pressure losses, and particulate distributions were measured. Baffling, vaning, and design configurations were optimized and incorporated into the actual baghouse designs. The following are the results of the studies:

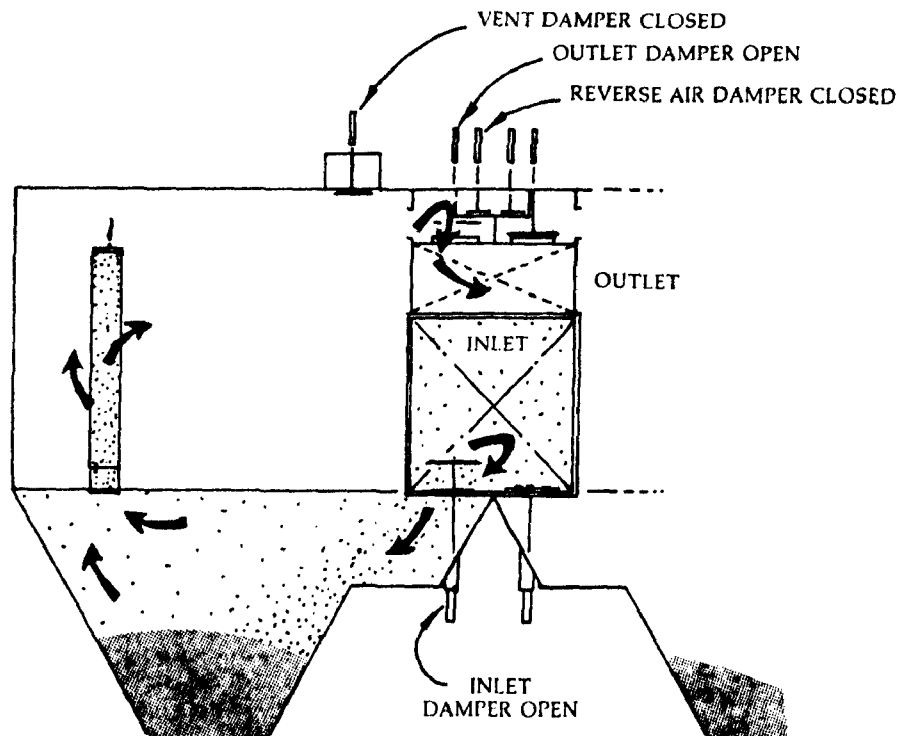
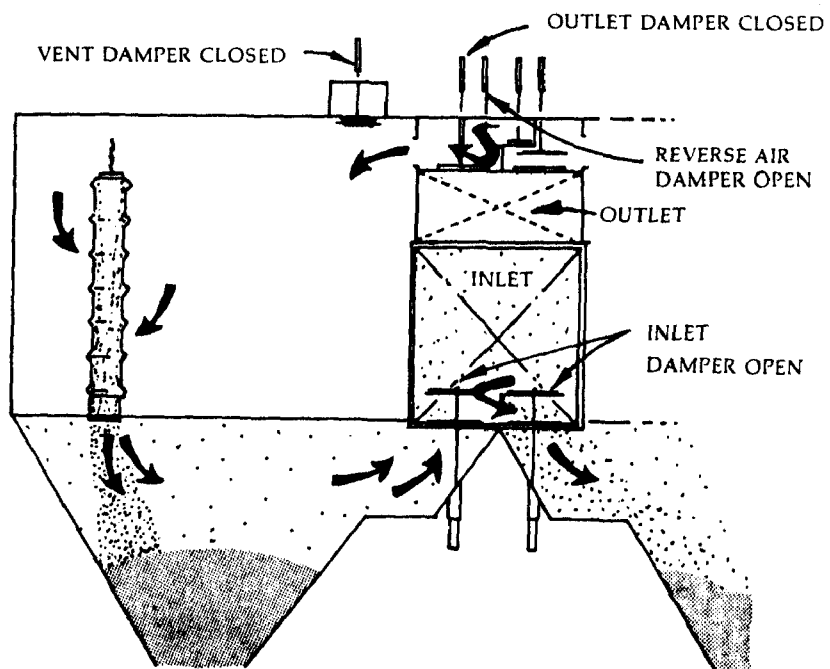


FIGURE 5. NORMAL FILTERING



**FIGURE 6. AUTOMATIC FABRIC CLEANING
REVERSE AIR FLOW**

	Nevada Power	Utah Power and Light
Pressure loss - total system (inches of water)	6.83	7.48
Pressure loss - baghouse (inches of water)	5.96	5.88
Pressure loss - by-pass (inches of water)	5.59	---
Volumetric flow distribution between compartments (% of equal)	+5.0 (-)7.5	+6.0 (-)7.5
Velocity distribution across tube sheet (% RMS deviation)	7.1	4.0
Particulate distributions between compartments (TYP % RMS deviation)	30.5	27.6

Start-Ups

After the baghouses were erected and the bags installed, a visual inspection of the complete system was performed. Filter bag tension was checked and bags requiring retensioning were retensioned. Baghouse compartments, hoppers, and plenums were made clear of all tools and or debris. All mounting bolts were tightened, and all poppet valves were opened and closed and checked for proper sealing and operation. Reverse air and vent fans were checked for proper rotation and vibration. A thirty minute cleaning cycle was set at the timers in the control panel and a dry run of the clean cycle was performed. Minor adjustments were made, and the baghouse was ready for start-up.

At the time of the baghouse contract, it was envisioned the filter bags would be seasoned by externally injecting flyash into the baghouse prior to handling boiler flue gas. However, based on experience and other recent baghouse start-ups, Flakt recommended on-line seasoning of the filter bags.

During the boiler unit start-up period, the baghouse was set on by-pass. This period comprised all initial oil-firing activities including boil-out, critical pipe steam blows, and initial turbine synchronization. Once coal firing began, and the boiler fire stabilized, and oil firing was minimized, the baghouse compartments were put on-line and the by-pass dampers were closed (external pre-coating of the filter bags was not performed). As the boiler load stabilized and began increasing, the bag cleaning pressure activation system was switched on. This system however did not signal the system to clean for several days due to slow build up of baghouse differential pressure loss. Further, the first few bag cleanings were completed with the reverse air fan dampers in the closed position. To date, the Nevada Power cleaning system stabilized and operated during the performance test with the reverse air fan damper in the 10% open position. Utah Power and Light reverse air fan damper remains in the 100% closed position. Baghouse pressure losses now range between 3 and 6 inches water. Also, opacities exit the baghouse are in the non-visible

emission range (5-8%). Bag losses since start-up have been less than 1.5%.

Performance Testing

On 9/83, a performance test was performed on the Flakt baghouse at Nevada Power. A series of six test runs were performed. One month later, Utah Power and Light ran a performance test consisting of nine test runs. Testing was conducted simultaneously at the baghouse inlets and outlets in accordance with EPA Test Methods 1, 2, 3, and 17. The following summarizes the data established through this testing.

	Nevada Power ¹	Utah Power ² and Light
Boiler load average (MW) gross	262	426
Boiler load range (MW) gross	256-273	392-463
Flue gas temperature (°F average)	325	267
Flue gas temperature (°F range)	314-337	255-286
Inlet particulate concentration average (gr/ACF)	3.02	2.73
Inlet particulate concentration range (gr/ACF)	2.41-4.15	2.24-3.25
Outlet particulate concentration average (gr/ACF)	0.0009	0.0018
Outlet particulate concentration range (gr/ACF)	0.0003-0.002	0.0006-0.0028
Outlet particulate concentration average (LB/10 ⁶ BTU)	0.0013	0.0063
Outlet opacity average (%)	7	6.9
Outlet opacity range (%)	5-8	6.8-7.1
Baghouse pressure loss average (inches H ₂ O)	4.1	4.2
Baghouse pressure loss range (inches H ₂ O)	3.0-6.0	3.0-6.0
³ Baghouse filter speed average (FPM)	1.91	2.17
³ Baghouse filter speed range (FPM)	1.69-2.45	1.99-2.50
Time between cleaning cycles (minutes)	90-210	60-300

For coal burned during testing, refer to Table 7.

¹All tests run with one compartment off-line for maintenance.
²All tests run with two compartments off-line for maintenance.
³All filter speeds include reverse air in the calculations.

TABLE 7. COAL ANALYSIS DURING PERFORMANCE TESTS

	Nevada Power	Utah Power and Light
Moisture (%)	9.5	7.0
Ash (%)	7.45	11.0
Volatile Matter (%)	-	39.7
Fixed Carbon (%)	-	42.3
Sulfur (%)	0.33	0.55
Heating Value (BTU/LB)	11,798	11,900

Conclusions

- After over one year of operation, the baghouse performances experienced at Nevada Power and Utah Power and Light can be considered state-of-the-art. Care should be used when reviewing test data submitted here-in. Note outlet emissions tested are extremely low. Testing at such low levels should be considered just that and should not be considered to be the norm for baghouse installations or their design requirements. Due to these extremely low concentrations, the outlet particulate concentrations varied five fold during testing. Further testing after extended use should bear out these high performances.
- Over the past few years there has been some controversy over baghouse compartment sizes. Some insist the compartments designed at Nevada Power and Utah Power and Light are too large. The performance data here-in appear to demonstrate Flakt's concepts with proper gas/ash distributions will enhance baghouse performance.
- Sound design, engineering, construction, and start-up practices result in proper operating baghouses.
- Boiler fuel, proper boiler operation, and diligent maintenance practices impact baghouse performance.
- Conservative filter speeds at a net/net condition (2.4 FPM) result in low maximum operating baghouse pressure losses. However, if the design includes off-line cleaning compartments and redundant maintenance compartments, then the fewer compartments utilized in the design (within reason) will result in lower gross (all compartments on-line) filter speeds and resulting lower average pressure losses during this most normal operating condition. Further, cleaning will be less frequent and bag life should be extended.
- Filter speeds are not the only design considerations when selecting baghouses. Gas and particulate distributions, plenum and inlet

damper velocities, etc. can further affect baghouse performance.

- Baghouses continue to be desirable equipment selections for utility boilers burning low sulfur western coals.

The work described in this paper was not funded by the U.S. Environmental Protection Agency and therefore the contents do not necessarily reflect the views of the Agency and no official endorsement should be inferred.

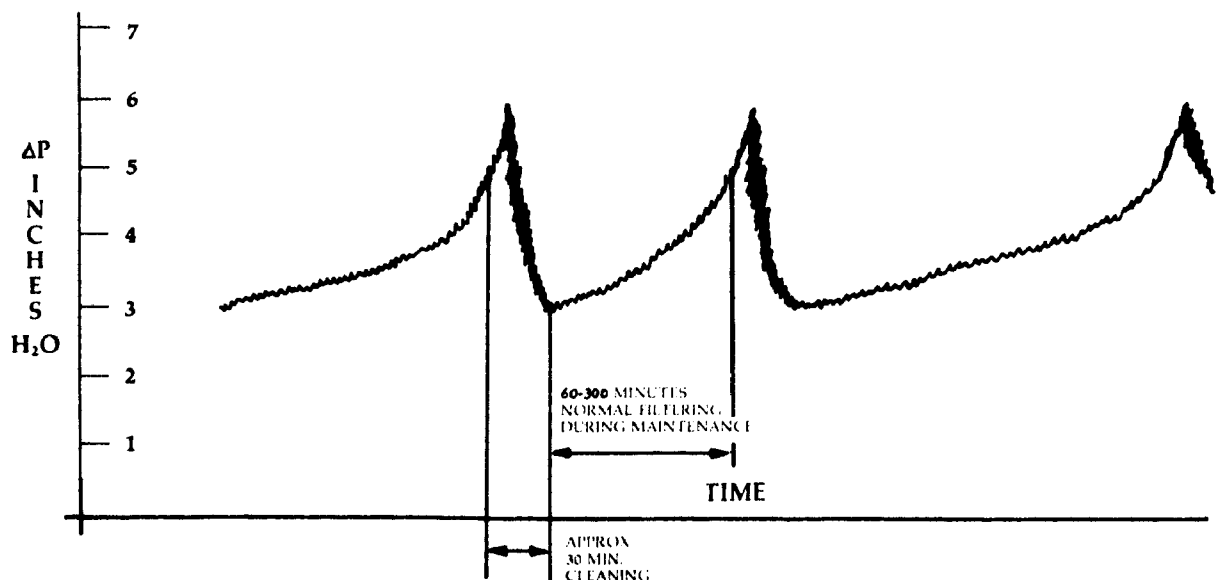


FIGURE 7. BAGHOUSE ΔP VS. TIME

Session 14: FF: FULL-SCALE STUDIES II (COAL-FIRED BOILERS)

Robert C. Carr, Chairman
Electric Power Research Institute
Palo Alto, CA

PERFORMANCE OF BAGHOUSES IN THE ELECTRIC GENERATING INDUSTRY

Wallace B. Smith
Southern Research Institute
P.O. Box 55305
Birmingham, Alabama 35255-5305

Robert C. Carr
Electric Power Research Institute
P.O. Box 10412
Palo Alto, California 94303

ABSTRACT

Results are reported from testing performed to evaluate the performance of four large pilot-scale and twelve full-scale baghouses. One of the pilot units collects ash from high-sulfur coal, the other from low-sulfur coal. The full scale units collect ash from western, low-sulfur, subbituminous coal, eastern bituminous coal, Texas lignite, and mixtures of anthracite silt, eastern bituminous coal, and petroleum coke. Several bag cleaning methods were investigated: reverse gas, reverse gas with sonic assist, and shake/deflate. Measurements of dust cake properties, pressure drop, and efficiency are described and the results related to the ash cake properties and operating modes.

INTRODUCTION

The electric utility industry in the U.S. is presently committed to more than 20,000 MW capacity in baghouse technology for particulate control. Capital and levelized costs can range up to \$70/kW and 3.5 mills/kWh, respectively, but intensive research and development programs are underway and options have already been identified which can reduce those costs substantially. This paper is a brief overview of the first four years of an EPRI-sponsored research program. The program includes pilot-scale, full-scale, and laboratory studies. Most of the work has dealt with baghouses cleaned by reverse gas because that design is dominant in the industry. Studies of sonic-assisted reverse gas cleaning, shake/deflate cleaning, and dry injection for SO₂ control are now in progress. More detailed discussions have been published elsewhere and in companion papers at this conference (1,2,3).

TECHNICAL DISCUSSION

PILOT-SCALE STUDIES

Pilot-scale research has been performed at EPRI's Arapahoe Test Facility using 1 MW, 2.5 MW, and 10 MW (Fabric Filter Pilot Plant, FFPP) pilot plants. These units all collect ash from low sulfur coal (0.7%). Additional research is conducted with a 10 MW (High Sulfur Pilot Plant, HSPP) plant at Gulf Power Company's Scholz station. High sulfur coal (2.7%) is burned there. All the pilot units are completely instrumented for continuous analysis and gas flow is controlled independently of boiler loads. Full-sized bags and hardware are used to yield performance data typical of commercial systems.

As the research program matured, a consistent pattern of behavior emerged which led to a qualitative model of baghouse performance. The filtration process can be divided into three distinct time regimes: filtration by a clean fabric, which occurs only once in the life of a bag, and only for a few minutes; establishment of a residual dust cake, which occurs after many filtering and cleaning cycles, and takes several weeks or months to form; and steady state, in which (with the residual dust cake established on the bags) the quantity of particulate matter removed during the cleaning cycles equals, on average, the amount collected during each filtering cycle.

Within these time regimes, it is possible to discern distinct patterns of pressure drop behavior. First, as shown in Figure 1 for the FFPP, pressure drop during initial startup was fairly low and steady, approximately 2.8 in. H₂O. Presumably, the dust cake is loosely bound and much of it is removed during each cleaning cycle. After this initial startup phase, however, the pressure drop increased rapidly up to a level of approximately 6 in. H₂O. During the following several months, the FFPP was shutdown four times for testing purposes and its bags were manually cleaned to reduce pressure drop and to restore the system to a constant initial starting point. (Even after this manual cleaning, however, a light residual dust cake of approximately 0.1 lb/ft² adhered to the bags.) Despite these shutdowns, and subsequent brief intervals of low pressure drop operation, the FFPP pressure drop consistently and relentlessly increased to approximately 6 in. H₂O. This behavior pattern is now believed to indicate establishment of the heavy residual dust cake characteristic of the second distinct filtration time regime. At the end of the first seven months of operation, residual dust cake weights of 0.6 lb/ft² were measured.

Following establishment of this heavy, residual dust cake, pressure drop at the FFPP settled into a more or less "stable" operating mode for approximately the next 21 months. During this period, a slight upward trend in pressure drop was still observed, but values remained within the range of 5 to 8 in. H₂O. This period is believed to coincide with the third distinct filtration time regime, and was characterized by fluctuating day-to-day pressure drop and seasoned bags with a residual dust cake weight of approximately 0.7 lb/ft². Since residual dust cake weight did not significantly increase over these 21 months, the cyclic pressure drop behavior is believed to be related to subtle changes in residual dust cake

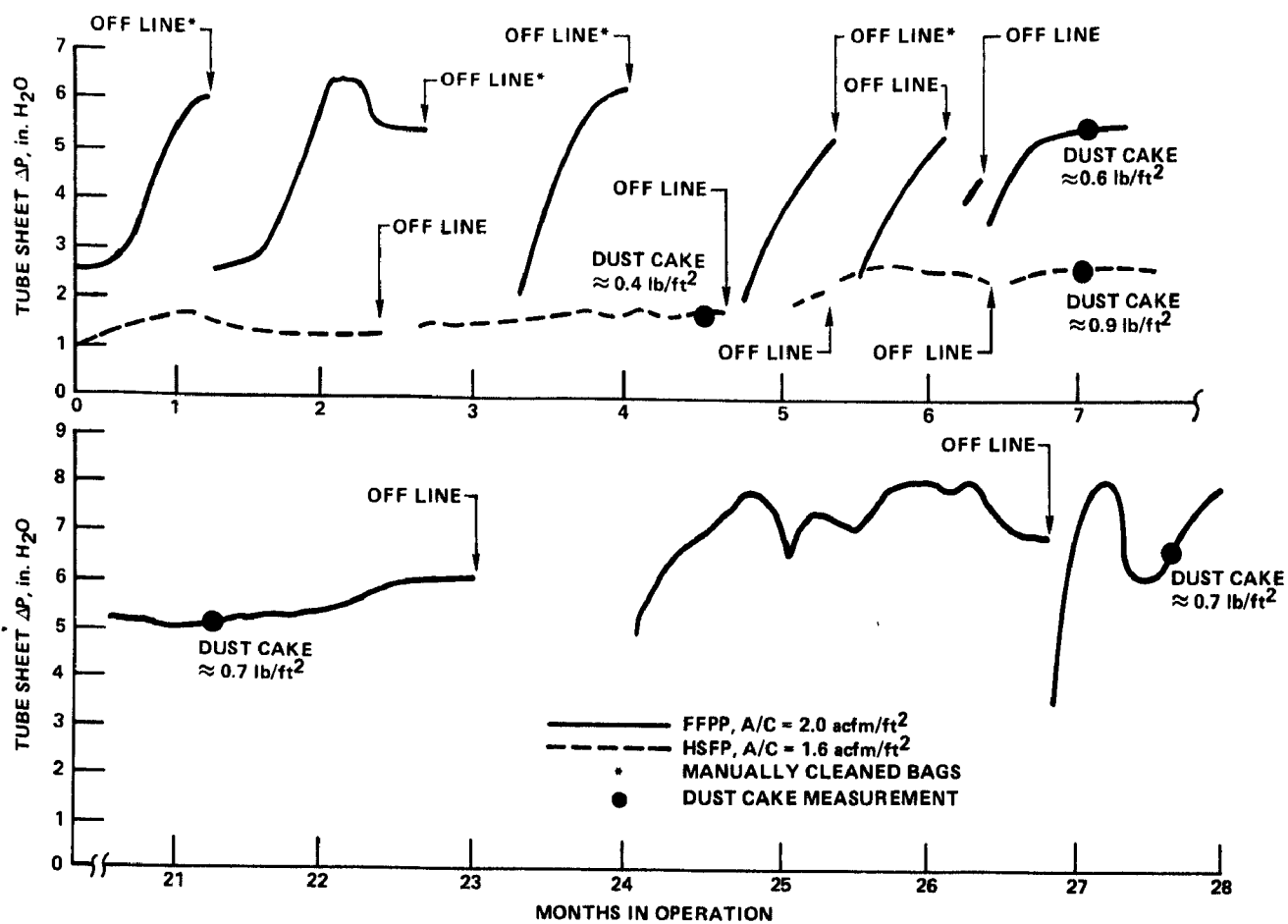


Figure 1. Pressure drop history and residual dust cake evolution for the FFPP and HSFP.

structure. These changes may come as a result of day-to-day variations in fly ash and flue gas composition; boiler load cycling; disturbances during startup and shutdown, where portions of the dust cake may be irregularly and randomly dislodged or disturbed; or perhaps mechanical compaction and continuing reaction of the dust cake with flue gas constituents.

For the HSFP, a similar but somewhat less complicated pattern of pressure drop behavior was observed. As seen in Figure 1, pressure drop for this unit was characterized by a very gradual, but steady, increase over time and a very narrow operating range. For example, during the first eight months of operation pressure drop increased from 1.0 in. H₂O to slightly less than 3.0 in. H₂O. During this same period residual dust cake weight rose to a very high level of 0.9 lb/ft².

From these results it is clear that baghouses filtering fly ash from low-sulfur and high-sulfur coals exhibit distinctly different pressure drop versus time behavior. The most obvious of these is the rapid rise in pressure drop exhibited by the FFPP compared to that of the HSFP. After the first month of operation, for example, the FFPP was operating at 6.0 in. H₂O whereas the HSFP was at 1.5 in. H₂O. As Figure 1 illustrates, and despite the fact the dust cake at the FFPP was significantly lighter than that at the HSFP, this disparity persisted over the period reported here. Moreover, from the onset, pressure drop for the HSFP exhibited a stability only observed at the FFPP after an extended period of operation when seasoned dust cakes were established on the bags. The behavior of the pilot plant can only be explained by examining their individual dust cakes in detail. Some results of that analysis are summarized below in the section on Dust Cake Studies.

Of course, the primary function of a baghouse is to prevent the emission of particulate matter into the atmosphere. Therefore, a substantial part of the pilot-scale studies has been dedicated to measuring, in detail, particulate collection efficiency and opacity. Particulate collection efficiency measurements included both total mass and size-dependent, or fractional, efficiency. A measure of fractional efficiency is particularly useful because it allows investigation of discrete particle-size intervals, it allows detailed comparison with theoretical models, and it allows better interpretation of the responsiveness of baghouses to boiler and ash characteristics. Opacity is a good supplementary measurement because it yields continuous, real-time data which can be related to stack plume visibility—a feature not generally obtained with other particulate sampling instruments.

Figure 2 shows fractional efficiency curves for particles of 0.02-30 μ m diameter for the FFPP and of 0.2-20 μ m for the HSFP. All data were taken with the pilot baghouses operated with reverse-gas cleaning. As these curves illustrate, overall particulate mass collection efficiency is over 99.99 percent, near the sensitivity limits of the measuring instruments. This level of efficiency is extremely high and corresponds to outlet emissions of approximately 0.0004 lb/10⁶ Btu, well below any current particulate emission standard.

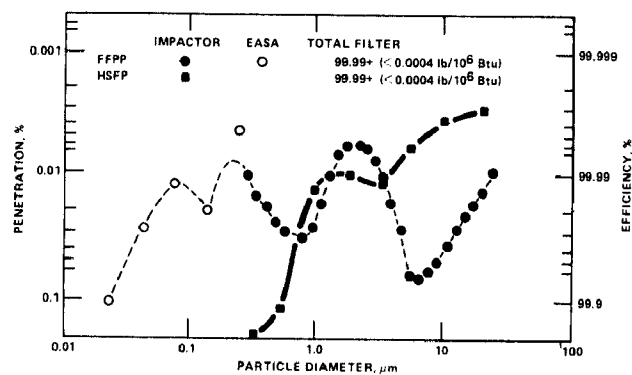


Figure 2. Total fractional efficiency of the FFPP and HSFP operated with reverse-gas cleaning. Measurements were made using cascade impactors, electrical aerosol size analyzers (EASA), and filter samplers.

Figure 3 shows recordings of opacity obtained at the outlet of a single compartment of the FFPP. As these curves indicate, the opacity averages less than 0.1 percent for a 10 m path length, corresponding to an equivalent instack visibility of over 50 miles. This is a remarkable result, indicating that a well-maintained baghouse will reduce the particulate emissions of a coal-fired boiler to less than typical ambient concentrations.

Inspection of Figure 3 also shows that opacity rises sharply when filtration begins immediately after cleaning. A value exceeding one percent is observed for about two minutes, then the magnitude decreases monotonically until the end of the filtering period (in this case, 180 minutes). This indicates that the majority of the emissions occur immediately after cleaning and thus total emissions are dependent on the frequency of bag cleaning.

Figure 4 presents a summary of average tube sheet pressure drop as a function of A/C from the FFPP during reverse-gas operation. To develop this graph, each compartment of the FFPP was operated at a different A/C for several months. Data were obtained at A/C values of 1.7, 2.3, 2.7, and 3.3 acfm/ft². The shaded region encompasses all of the data. The dashed lines below an A/C of 1.7 acfm/ft² are shown to indicate that although pressure drop behavior below this point is unknown, the lines must pass through the origin. Also shown in this figure for approximately six and 24 months of operation are data boundaries which reflect the time dependent nature of pressure drop discussed previously.

The pilot data in Figure 4 indicate that pressure drop is approximately a linear function up to values of A/C near 2.7 acfm/ft². At higher values of A/C, the slope of pressure drop versus A/C is much steeper. While this behavior is not well understood, it may result from differences in permeability of dust cakes formed at different values of A/C. These data again illustrate the time dependent nature of pressure drop. For example, a 60% increase in pressure drop was observed over the intervening 18-month period at an A/C of 2.0 acfm/ft².

The pilot plant data shown in Figure 4 are bounded (below A/C \approx 2.7) by a region defined by the following equation:

$$\begin{aligned} \text{Tube sheet } \Delta P &= 3(A/C) \pm 20\% \\ \text{where A/C is expressed in acfm/ft}^2, \text{ and} \\ \text{pressure drop is expressed in in. H}_2\text{O.} \end{aligned} \tag{1}$$

The lower value obtained would be representative of units with several months to a year of service; the upper value would be representative of units with two years or more of service. For example, assuming an A/C of 2.0 acfm/ft², tube sheet pressure drop of 5 to 7 in. H₂O would be expected. If an additional 2 in. H₂O is added for duct work pressure drop, a system pressure drop of 7 to 9 in. H₂O would be expected. In actual baghouse operation, account must also be made for removing compartments from service for cleaning, and for the reverse-gas flow used to clean out-of-service compartments. The effect of these factors will be manifested in brief, periodic increases in system pressure drop, and the degree of increase will depend upon the cleaning cycle of the specific unit. The pressure drop

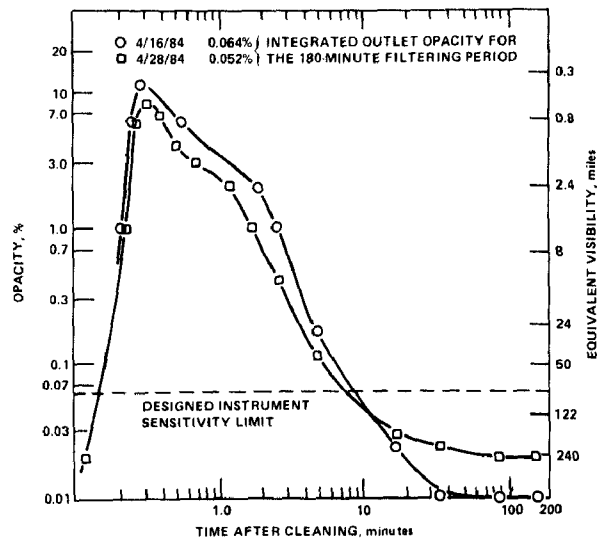


Figure 3. Typical opacity of the emissions from the FFPP operated with reverse-gas cleaning. Opacity is calculated for a 10-meter stack.

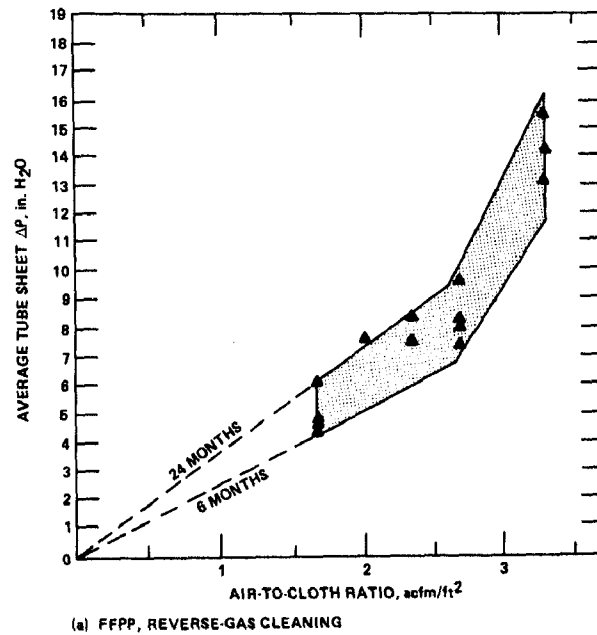


Figure 4. Data of average tube sheet pressure drop as a function of air-to-cloth ratio for the FFPP. Reverse-gas cleaning.

predicted by equation (1) is significantly higher than many manufacturer's guarantees, indicating that the expected (design) values are unrealistically optimistic.

FULL-SCALE BAGHOUSE STUDIES

In this test program, data were acquired at ten utility baghouse installations. These data include characterizations of:

- baghouse designs
- operating modes: air-to-cloth ratio (A/C), cleaning cycle, bag fabrics, etc.
- the type of fly ash being collected, dust cake properties, and
- performance in terms of collection efficiency, in-stack opacity, pressure drop (ΔP), and maintenance requirements.

The baghouses evaluated encompassed a representative sampling of unit size, design, and fuels, and are listed in Table 1. Data taken at the Nucla and Kramer stations reported by Ensor et al. under earlier EPRI sponsorship are included in the table as well (4,5). Also, for comparison with these full-scale units, EPRI's two pilot baghouses—the low sulfur coal fabric filter pilot plant (FFPP) at the Public Service Co. of Colorado's Arapahoe Station in Denver, and the high-sulfur coal fabric filter pilot plant (HSFP) at Gulf Power Co.'s pilot plant (HSFP) at Gulf Power Co.'s Scholz station near Sneads, Florida—are included in the data base. For convenience in reading Table 1 (and Tables 2, 3), units are grouped according to the type of fuel burned at the site. These categories are indicated by the dashed lines. Units 1-7 burn western, low-sulfur subbituminous coal; Unit 8 burns Texas lignite coal; Unit 9 burns eastern, high-sulfur bituminous coal; and Units 10-12 burn moderate- to high-sulfur mixtures containing eastern bituminous coal, anthracite silt, and petroleum coke. Units were selected for testing based on the type of fuel burned at the site and on the cleaning method they use. The FFPP operates on a slip stream from the Arapahoe Unit 4 boiler and allows good comparisons to western, low-sulfur coal units. The HSFP operates on a slip stream from the Scholz Unit 2 boiler and allows comparisons to eastern, high-sulfur coal units.

Of the full-scale baghouses evaluated, nine are reverse-gas cleaned and three are shake/deflate cleaned. All except the Nixon station were retrofitted to existing boilers. Four of the reverse-gas units have been retrofitted with low-frequency horns inside the compartments to improve dust cake removal. Six utilities and six baghouse manufacturers are represented. The boilers served range in capacity from 13 to 575 MW. Some of the boilers operate near peak load almost continuously. Others vary load on hourly, daily, or seasonal time scales.

Table 1 is a detailed list of the most significant baghouse design specifications. For baghouses cleaned by reverse gas, the design values of

Table 1. Baghouse descriptions.

NO.	PLANT NAME	DATE ON LINE	NO. OF COMP.	BAGS PER COMP.	BAGHOUSE DIMENSIONS ^①		CLEANING METHOD	AIR TO CLOTH ^②	REVERSE GAS	FLANGE-FLANGE
					LENGTH (FT)	DIA. (IN.)		GROSS (NET) (ACFM/FT ²)	FLOW (ACFM)	PRESSURE DROP (IN. H ₂ O)
1	ARAPAHOE	1979	14	236	22.5	8.25	REVERSE GAS	2.10 (2.38)	16700	6.5
2	CAMEO	1978	14	236	22.5	8.25	REVERSE GAS	2.0 (2.31)	21350	8.0
3	CHEROKEE	1980	14	290	34.0	12.0	REVERSE GAS	2.03 (2.36)	60000	6.0
4	MARTIN DRAKE	1978	12	198	30.5	11.5	REVERSE GAS	1.85 (2.20)	36000	4.0
5	NIXON	1980	2 x 18	156	31.75	12.0	REVERSE GAS	1.97 (2.08)	30000	5.0
6	KRAMER	1977	10	72	35.0	11.5	REVERSE GAS	1.69 (2.10)	14400	5.0
7	NUCLA ^③	1974	6	112	22.0	8.0	SHAKE/DEFLATE	2.8 (3.58)	5600	5.2
8	MONTICELLO ^③	1979	2 x 18	204	30.75	11.5	SHAKE/DEFLATE	2.74 (2.90)	19600	6.0
9	BRUNNER ISLAND	1980	24	264	35.33	11.5	REVERSE GAS	1.83 (1.97)	41000	6.0
10	HOLTWOOD (RG)	1981	16	90	30.7	11.875	REVERSE GAS	1.78 (2.00)	12400	5.0
11	SUNBURY	1973	14	90	30.0	12.0	REVERSE GAS	1.92 (2.18)	12500	5.0
12	HOLTWOOD (S/D) ^③	1975	16	120	22.0	8.0	SHAKE/DEFLATE	2.27 (2.43)	550	6.5
13	FFPP	1980	4	36	VARIABLE					
14	HSFP	1982	5	42	35.0	12.0	VARIABLE			

① Bags described as "12 inches" in diameter, are generally somewhat less (~11.5) because of constraints in weaving

② GROSS: All compartments in service

NET: One compartment out of service for cleaning including reverse or deflation gas flow

③ Monticello shaker: frequency of 235 cpm, ±0.75 inches displacement, bag lift of 0.03 inches, 7 second duration
Holtwood shaker: frequency of 235 cpm, ±0.80 inches displacement, bag lift of 0.03 inches, 10 second duration
Nucla shaker: frequency of 235 cpm, 10 second duration

Table 2. Fly ash analyses.

PLANT	Al ₂ O ₃ % wt	CaO % wt	Fe ₂ O ₃ % wt	K ₂ O % wt	Li ₂ O % wt	MgO % wt	Na ₂ O % wt	P ₂ O ₅ % wt	SiO ₂ % wt	SO ₃ % wt	TiO ₂ % wt	LOI % wt	SO ₄ % wt	MMD μm	σ _g	RESISTIVITY ohm-cm	Q/M μC/g
1. Arapahoe	27.2	5.3	3.6	1.1	0.03	1.4	0.9	1.4	57.4	0.5	1.4	5.1	0.3	6.8	2.6	1x10 ¹²	
2. Cameo	28.1	6.3	4.8	1.2	0.03	1.9	0.7	1.5	51.2	1.5	1.7	5.7	0.4	5.7	2.7		
3. Cherokee	28.3	5.6	4.6	1.7	0.02	1.9	0.6	1.1	51.3	1.0	1.5	3.8	0.3	6.2	2.7	8x10 ¹¹	
4. Martin Drake	27.4	5.7	4.9	1.6	0.02	1.7	1.1	1.2	52.9	1.2	1.4			5.2	2.6		
5. Nixon	25.7	7.5	5.4	1.7	0.02	2.0	1.9	1.1	51.0	1.3	1.3			5.4	2.6		
6. Krammer (Ref. 5)	25.1	6.5	4.7	1.4		4.8	0.7	0.002	49.3	0.7	0.9	13.0		3	2		
7. Nucla (Ref. 4)	19.1	3.2	9.7	0.6			0.2		32.0	1.7	1.1	30.0		12	4.7		
8. Monticello	18.5	8.3	3.0	0.1	0.02	1.9	0.3	1.1	64.2	0.3	1.8	0.1	0.2	6.6	3.2	2x10 ¹²	-3.8
9. Brunner Island	26.3	1.9	11.1	2.3	0.05	0.8	0.3	0.7	46.2	2.3	2.2	10.9	0.9	6.9	2.5		-1.0
10. Holtwood (RG)	26.5	0.8	7.0	2.7	0.03	0.8	0.4	0.3	55.5	1.0	2.3	2.8	0.3	5.2	2.5		
11. Sunbury	27.1	0.7	8.2	2.7	0.03	0.8	0.4	0.3	52.6	0.9	2.7	2.5	0.3	4.6	2.4		
12. Holtwood (S/D)	26.5	0.8	7.0	2.7	0.03	0.8	0.4	0.3	55.5	1.0	2.3	2.8	0.3	5.2	2.5		
13. FFPP	27.2	5.3	3.6	1.1	0.03	1.4	0.9	1.4	57.4	0.5	1.4	0.4	0.3	7.2	3.1		-0.2
14. HSFP	23.2	0.8	30.3	2.3	0.06	0.8	0.3	0.7	38.4	1.3	2.5	9.1	1.3	5.9	2.6		

Table 3. Measured baghouse performance data.

PLANT	TEST DATE	BOILER LOAD/ FULL LOAD MW	AIR/CLOTH ACFM/FT ²	GAS TEMP °F	TUBESHEET ΔP in. H ₂ O	FLANGE FLANGE ΔP in. H ₂ O	FABRIC TYPE	BAG CLEANING INITIATION	FILTERING CYCLE MIN	CLEANING TIME SEC	DUST CAKE WEIGHT AFTER CLEANING LB/FT ²	EFF./ OPACITY %	REMARKS
1. Arapahoe	1/82	40/46	1.30	255	5.0	6.0	MS601T	Timed	164	30	0.56	26	--/ <1 No Horns
	1/81	46/46	1.51	261	4.2	--	MS601T	--	--	--	--	--	99.98/-- (Ref. 7)
	2/83	46/46	1.48	--	7.6	--	MS601T	Timed	--	--	0.77	36	-- No Horns (Ref. 8)
	2/83	48/48	1.48	--	3.0	--	MS601T	Timed	--	--	0.26	12	--/2 2 Horns/Comp. (Ref. 8)
2. Cameo	10/81	40/44	1.35	293	3.5	4.0	MS601T	4-6 in. H ₂ O	90-330	25-75	0.65	23	--/ <1
3. Cherokee	10/81	140/150	1.37	274	4.0	5.0	Fabric Filter	4-6 in. H ₂ O	70-170	60	0.36	42	--/1-2 (1/84+0.78 lb/ft ²) ②
4. Martin Drake	3/82	63/85	1.24	313	5.7	--	MS601T	4.5 in. H ₂ O	80-140	18	0.49	48	--/ <0.1
5. Nixon	4/81	200/200	1.97	307	5.0-7.0	--	MS601T	Timed	90	30	0.38	40	99.72/-- Clear Stack
	3/82	88/200	1.50	291	2.3	--	MS601T	Timed	--	--	--	--	--
6. Kramer	8/78	--/25	1.24-1.86	365	--	3.0-4.2	FF504-1	Timed	100	10	--	--	99.9+/- <0.1 (Ref. 5)
7. Nucla	11/75	12/13	2.74	210-260	--	3-4.5	C445-04	4.5 in. H ₂ O	23-240	15	--	--	99.9+/-0.02 (Ref. 4)
8. Monticello	4/82	575/575	1.61 ①	340	6.0	8.0	MS601T,C442	Cont.	68	11	0.33	33	--/4-20
	4/82	575/575	2.02	--	8.0	10.0	MS601T,C442	Cont.	68	11	0.33	33	--/4-20
	4/82	575/575	2.32	--	10.0	12.0	MS601T,C442	Cont.	68	11	0.33	33	--/4-20
9. Brunner Island	5/83	335/354	2.07	295	5.0	6.0	MS601T	Cont.	63	25	0.70	72	--/ <0.1 12 Horns/Comp.
	5/83	335/354	2.07	295	7.0	8.0	MS601T	Cont.	63	25	1.15	111	-- No Horns
10. Holtwood (RG)	1/83	79/79	--	--	--	--	FM106E	Cont.	32	2x30	0.60	55	--/ <1 4 Horns/Comp.
	1/83	79/79	2.03	312	4.5	6.0	FM106E	Cont.	32	2x30	0.71	65	1/ <1 2 Horns/Comp.
	1/83	79/79	--	--	5.0	8.5	FM106E	Cont.	32	2x30	1.09	100	-- No Horns (Ref. 8)
11. Sunbury	1/83	88/88	2.29	325	5.3	6.8	MS601T	Cont.	33	48	0.61	56	--/ <1 No Horns
	1/83	88/88	--	--	--	--	MS601T	Cont.	33	48	0.49	45	-- 2 Horns/Comp.
12. Holtwood (S/D)	9/83	79/79	2.35	352	4.5	6.0	C442,MS601T	Cont.	40	15	0.46	21	--/ <1
13. FFPP	2/83	N/A	2.0	270	5.5	6.5	AIQ53-S3016	Timed	180	30	0.2(1/81)	20	99.9+/- <0.1 Low-Sulfur Pilot Plant
											0.6(1/82)	60	99.9+/- <0.1
											0.7(2/83)	70	99.9+/- <0.1
14. HSFP	6/83	N/A	1.6	276	2.5	3.5	Midwesco	Timed	360	30	1.0	100	99.9+/- <0.1 High-Sulfur Pilot Plant

① Various flowrates were obtained by altering the flow split between the baghouse and an electrostatic precipitator in parallel with it.

② Bags weighed during 10/81 test were in service only eight months.

air-to-cloth ratio (A/C) and pressure drop range from 1.7 to 2.1 acfm/ft² (gross) and 4-8 in. H₂O, respectively. For shake/deflate units, the corresponding values are 2.3-2.8 acfm/ft² (gross) and 5.2-6.5 in. H₂O, respectively. Some of the units have large compartments with hundreds of bags. Others have less than 100 bags per compartment. The bags fall into two size groups: nominally 8 in. in diameter by 22 ft in length, or 12 in. in diameter by 30-35 ft in length. The units have been in service from two to ten years. Specifications reflect no systematic relationship to fuel or manufacturer, or even between pressure drop and A/C.

Table 2 gives a summary analysis of fly ash entering the baghouses at the sites evaluated. Constituents which vary significantly among the samples include calcium oxide (CaO: 0.7-8%), ferric oxide (Fe₂O₃: 3-30%), sodium oxide (Na₂O: 0.3-2%), soluble sulfate (SO₄: 0.2-1.3%), and loss on ignition or carbon carryover (0.1-9%). Although it had not been established what specific fly ash constituents play an important role in residual dust cake formation and removal in the bags, these data were collected to explore potential relationships which might explain the variability in pressure drop and bag life being experienced by full-scale units. Certain physical and electrical properties of the fly ash could also conceivably affect the character of the dust cake. Among those thought to be important are: particle concentration, size distribution, electric charge and electric resistivity. These data, along with findings from additional experiments, theoretical studies, and empirical correlations, are being used to search for any important dependencies among fly ash properties, dust cake properties, and baghouse performance.

Table 3 summarizes measured baghouse performance data for the units evaluated. In contrast to the design values given in Table 1, Table 3 shows that several units were operating substantially below their design A/C, and pressure drops were both higher and lower than design with no clear dependence on fuel, baghouse design, or cleaning method. The amounts and variability of dust cake and bag weights was a surprising result of this testing. Indeed, some residual dust cakes on seasoned bags in the units filtering ash from eastern, high-sulfur bituminous coal were as heavy as 150 lb—more than twice the amount of tension normally set to support new bags.

Fabrics installed in all the baghouses tested are of similar construction and use one of the three traditional finishes: silicone/graphite, silicone/graphite/Teflon, or Teflon B. Three different bag cleaning philosophies are used: intermittent or batch cleaning initiated at a predetermined pressure drop, timed cleaning, and continuous cleaning.

Figure 5 is a comparison of the expected drag (ΔP divided by A/C) calculated from Table 1 with the measured values calculated from Table 3. The numbers in the figure refer to plants as indicated in Tables 1-3, and represent data points measured at those sites. For reference, a line of perfect correspondence has been drawn. As the figure shows, ten of the measured values lie higher than the expected value and four lie lower. Consequently, predictions of drag—and hence of pressure drop—in the majority of cases are inaccurate and generally optimistic. This leads to the

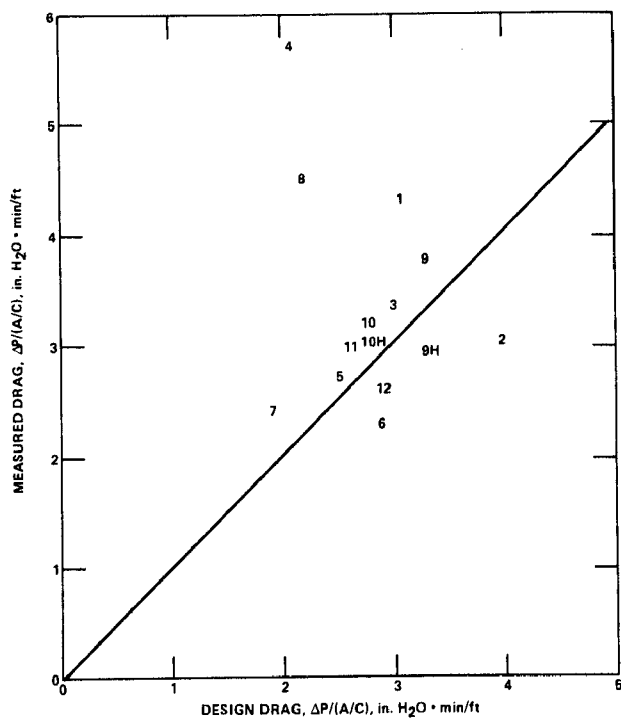


Figure 5. Drag measured during operation compared to the design value.

conclusion that there has been no proven method of predicting the pressure drop to be expected from any one particular baghouse design. Also, the scatter in both measured and design values in the figure is greater than a factor of two, even for units filtering similar ashes. In interpreting this scatter, it is important to consider that time in service and operating experience (i.e., shutdown/startup, boiler upsets, etc.) strongly affect the characteristics of residual dust cakes and therefore, the measured values of pressure drop.

A comparison of the dependence of pressure drop on A/C between the FFPP and several full-scale baghouses is provided in Figure 6. Also shown are data for the HSFP and the 2-1/2 MW pilot baghouse at Arapahoe. The shaded region encompasses the FFPP reverse-gas cleaning data shown in Figure 4. With few exceptions, the data are generally similar for all the reverse-gas baghouses tested. Also, it can be seen that much of the full-scale data are at lower A/C than normally expected. This is a consequence of full-scale unit operation at reduced boiler load and of conservative baghouse designs. Nevertheless, the agreement between pilot- and full-scale data is reasonably good. Some of the data scatter is undoubtedly related to different operating histories and time in service for each unit.

These results suggest that the pilot plant data for the FFPP can be used to estimate pressure drop versus A/C behavior for full-scale, reverse-gas cleaned baghouses with seasoned dust cakes according to equation (1).

DUST CAKE STUDIES

If the residual dust cakes on filter bags were homogeneous in permeability, the drag at any given A/C would be directly proportional to its thickness. The thickness in turn would be directly proportional to dust cake weight. Examination of the cross-sections, however, has shown that the dust cakes are not homogeneous media of uniform thicknesses (6). Main features are large nodular formations, crevices or fissures, and in some instances thinner "fold lines" where the bags deform during cleaning. Also, the dust cakes are very heavy, from about five to 20 times the amount of mass deposited during each filtering period (Table 3). The heavier dust cakes are on bags cleaned by reverse-gas alone (Arapahoe, Brunner Island, Holtwood, and the HSFP), while the lighter dust cakes are on bags cleaned by shake/deflate and sonic-assisted reverse gas (Harrington, Monticello, Holtwood, Arapahoe, and Sunbury). High-sulfur coals also appear to develop heavier dust cakes than low-sulfur coals.

Although the heavier dust cakes tend to have higher drag, there are exceptions and no quantitative relationship appears to exist between drag and thickness. Considering the existence of the low resistance flow paths (fissures and folds), it is not surprising that dust cake thickness alone does not correlate well with drag. Nevertheless, it is clear that practical advantages, both in maintenance and pressure drop, could be achieved by using cleaning methods more energetic than conventional reverse-gas flow to remove the heavy residual dust cakes.

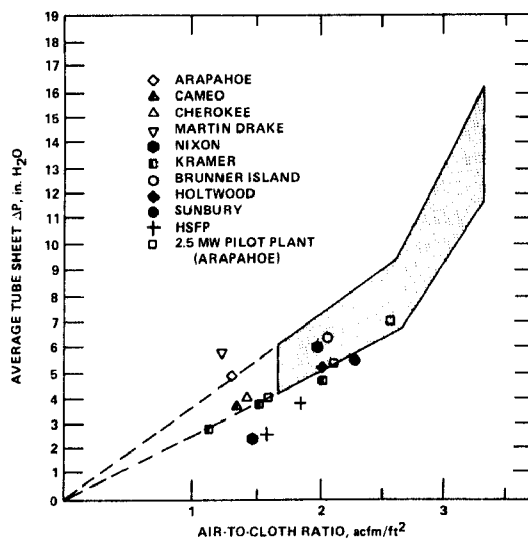


Figure 6. Average tube sheet pressure drop as a function of air-to-cloth ratio for the FFPP, HSFP, 2.5 MW pilot plant and full-scale units.

Figure 7 examines the relationships among dust cake weight, drag, and cleaning methods. Here drag and normalized drag, which is determined by dividing drag by the dust cake weight, are grouped by the type of fuel burned at the baghouse sites evaluated. Drag is shown on the left-hand side of Figure 7. In spite of the systematic differences in dust cake weights between western, subbituminous, low-sulfur coals and eastern, bituminous, high-sulfur coals, variations in drag are greater within these coal categories than between them. Ash from the Texas lignite coal burned at Monticello has high drag values similar to Brunner Island. Shake/deflate cleaning (Harrington and Holtwood) and sonic-assisted reverse-gas cleaning (Arapahoe, Brunner Island, and Holtwood) yield dust cakes of approximately equal drag, while the reverse-gas cleaned units tend to have higher drag (Arapahoe, Cameo, Cherokee, Martin Drake, Brunner Island, and Holtwood).

Normalized drag is shown on the right-hand side of Figure 7. In a homogeneous medium, this normalization would be justifiable and correct. For these data, however, normalization is only approximate since the dust cakes are not of uniform thickness. Nevertheless, the normalized data show that the thinner and thus lighter dust cakes associated with the western coals and Texas lignite tend to be less permeable than the heavier dust cakes associated with eastern coals. This result can be explained by considering the structural features revealed by microscopic examinations (7). The portion of the dust cakes near the fabric surface, and the thinner cakes, are more uniform, have smaller or nonexistent fissures, and are less affected structurally by the bag folding action. At distances several millimeters from the fabric surface, however, the fissures are large and the fold areas contain no ash at all. Clearly there is little resistance to flow there. It can be concluded, then, that the thicker dust cakes are not proportionally higher in drag or pressure drop than the thinner ones, and that the pressure drop is largely determined by the intimately bound dust layer near the fabric surface. The dust caked formed from the Texas lignite burned at Monticello is unique in that the dust has penetrated in and through the fabric interstices creating a structure of rather low permeability.

An important parameter in determining the cohesive and adhesive forces between elements in the fabric/fly ash structure is likely the presence of sulfuric acid on the particle surface which could act as "glue". The combustion of high-sulfur coals results in higher flue gas concentrations of SO_3 which can react with water to form sulfuric acid. The amount of free sulfuric acid available to act as a binding agent is in turn affected by the presence of calcium and other alkalis.

Figure 8 shows the qualitative relationship between the weight and ash chemistry of dust cakes on bags cleaned by conventional reverse gas. Interestingly, the soluble SO_4 value (measured in an attempt to quantify the availability of sulfuric acid) does not correlate well with dust cake weight. Interpretation of these SO_4 data, however, is confused by uncertainties in the analytical measurements, variations in other chemical constituents, and by the observation that the dust cake SO_4 concentration is strongly affected by the time of exposure to the flue gas. For example, measurements have shown that the residual dust cake contains considerably more SO_4 than the hopper ash. Sulfur in the coal, calcium (as CaO) in the ash, sodium (as

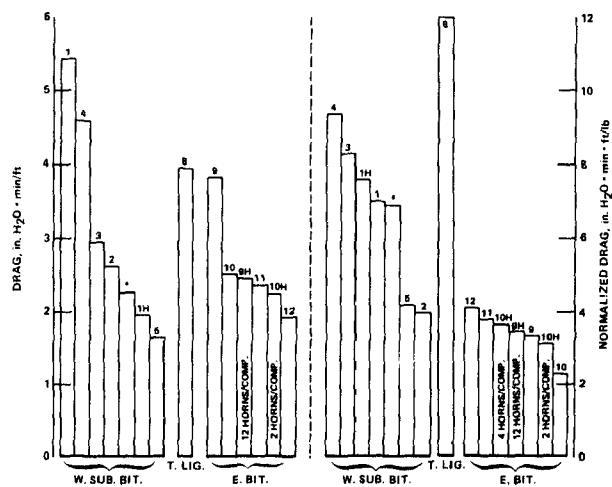


Figure 7. Relationship of drag and normalized drag to bag cleaning method and fuel.

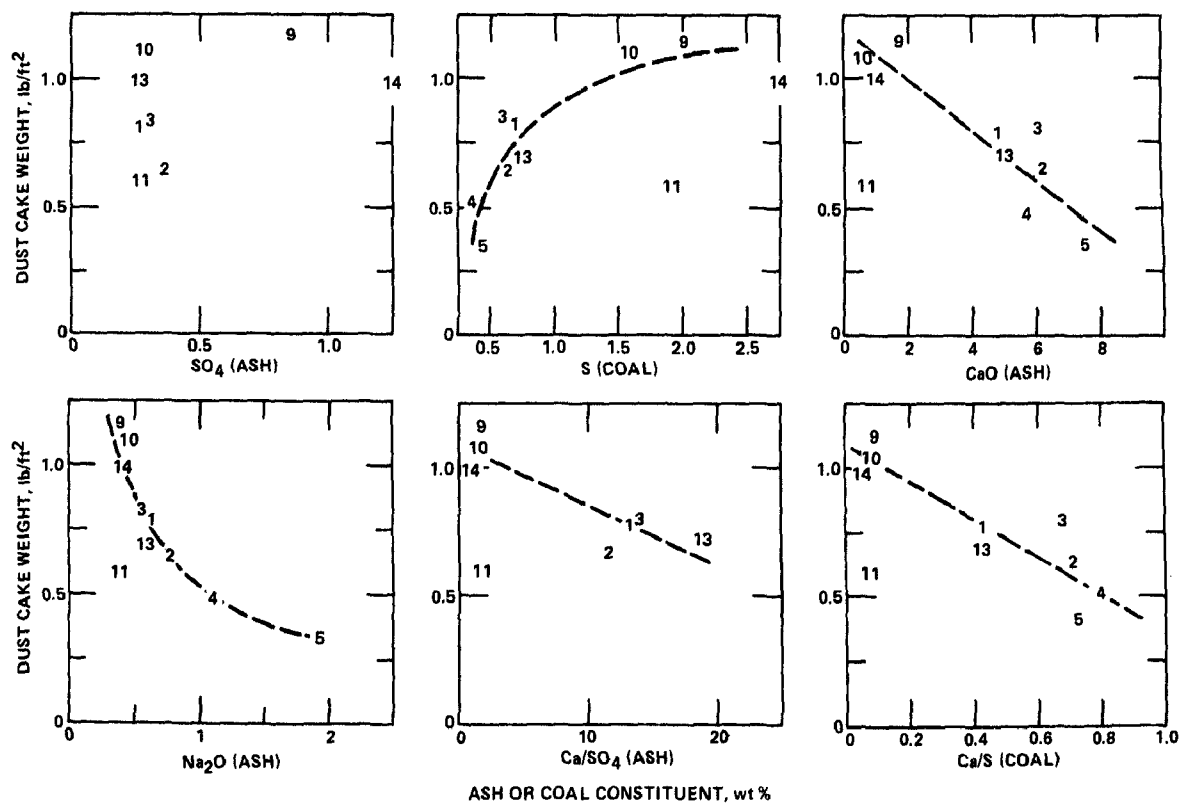


Figure 8. Relationship of residual dust cake weight to coal and ash composition in reverse-gas cleaned baghouses. (Dashed lines indicate qualitative relationships.)

Na₂O) in the ash, calcium-to-sulfate ratio (Ca/SO₄) in the ash, and calcium-to-sulfur ratio (Ca/S) in the coal, all appear to correlate to some degree with dust cake weight. It is possible that the ashes of higher alkali content "scrub" or react with the gaseous SO₃, preventing its condensation as sulfuric acid on the surfaces of the particles. Since S, Ca/SO₄, Na, and Ca all correlate with dust cake weight, they must also correlate with one another. (The parameters were not varied independently.) Data collected in this study indicate that the high-sulfur coals which produce more SO₃, also contain less calcium and sodium than low-sulfur coals. This combination of circumstances appears to favor the formation of a cohesive dust cake which is difficult to remove by conventional reverse-gas cleaning.

The Sunbury dust cake does not show the same degree of correlation as the other fly ashes in Figure 8. As discussed earlier, Sunbury burns an unusual fuel mixture and its anomalous behavior, albeit excellent, cannot be explained without more analyses. Although shake/deflate units are not shown in Figure 8, it has been observed that the Monticello ash, which is unusually noncohesive with a low dust cake weight, contains the highest concentration of CaO (10.6%) of any analyzed. Thus, the Monticello ash behavior is qualitatively consistent with the reverse-gas units shown in the figure. More sophisticated statistical analyses of these data are proceeding in an attempt to develop quantitative, predictive relationships among drag and fuel or ash chemistry, fabric construction and finish, and cleaning method.

A principle concern of baghouse users is that temperature excursions through water or acid dew points will cause dust cakes to adhere more strongly and blind the bags. In fact, when a failure of the FFPP microprocessor controller forced the unit off line during its initial startup phase and the flue gas cooled inside of the compartments without being purged by ambient air, a large increase in pressure drop was observed after the unit was put back into service. Manually cleaning the bags reduced pressure drop to its pre-upset value, but the event indicated the need for further testing of startup and shutdown (cyclical operation) to characterize the potential impacts on system pressure drop performance.

After approximately one year of service at the FFPP, during which a seasoned dust cake was established on the bags, a series of startup/shutdown tests was conducted. For these tests, a compartment was taken off line three times and allowed to cool well below the water and acid dew points without purging the compartments of flue gas. During this period, no deleterious effect on pressure drop was observed. It was therefore concluded that the thicker, seasoned dust cake protected the bags.

To investigate startup/shutdown effects in the more severe environment of a high-sulfur coal baghouse—which generally contains higher flue gas concentrations of SO₃—a test series was performed at the HSFP. Figure 9 summarizes pressure drop and bag weight history for a 250-day operating period at this site. As shown, normal startup/shutdown occurrences are randomly distributed throughout the operating period. In addition, a concentrated series of 25 startups/shutdowns without purging was conducted during the period of 310 to 335 days in service.

For normal shutdowns, the unit was take off line and purged of flue gas. Upon returning to service (without preheating), the pressure drop was generally observed to be lower than before shutdown. Thereafter, both pressure drop and dust cake weight tended to drift slowly upward. Occasionally (e.g., after 186 and 334 days) the bags were vigorously cleaned by hand to remove much of the dust cake. For the concentrated startup/shutdown tests, however, extreme conditions were created to study worst case operation. For these tests, the HSFP was shut down and allowed to cool without purging for 18 hours, and then restarted without preheating and operated for six hours. This cycle was repeated every 24 hours for 25 days.

As indicated in Figure 9, the dust cake weight increased at an accelerated rate during these no-purge tests. During this period, it reached an average of 1.3 lb/ft^2 , attaining a maximum of 1.8 lb/ft^2 . This 1.8 lb/ft^2 value corresponds to a bag weight of 200 lb. And, as shown in Table 3, similar bag weights have been measured at full-scale baghouses collecting high-sulfur coal fly ash. Although pressure drop did not increase proportionately, other operational problems would likely result since many baghouse structures and bag tensioning systems would not be able to accommodate these weights. Further, the tension on the bags would surely result in increased bag failure rates. After returning to continuous service, bag weights did decline, although not to pre-test values. This may be indicative of a loss of volatile constituents collected during the cyclic testing, or a return to an equilibrium residual dust cake thickness.

In these tests, the effect of cyclic operation was manifested by excursions in pressure drop for bags which did not have a seasoned dust cake. For bags with seasoned dust cakes, the predominant effect of cyclic operation was measured to be increased bag weight. In either case, it is concluded that the baghouse should be purged of flue gas following any shutdown to prevent the possibility of undesirable pressure drop or bag weight excursions.

ADVANCES IN BAGHOUSE TECHNOLOGY

At present, over 90% of utility baghouses are cleaned by reverse gas. Well-maintained units generally have very high particle collection efficiencies (particulate mass collection efficiencies over 99.9%, with outlet emissions of approximately $0.004 \text{ lb}/10^6 \text{ Btu}$), clear stacks (achieving opacities averaging less than 0.1%, equivalent to an in-stack visibility of over 50 miles), and good bag life (averages of over 4 years). However, reverse-gas cleaning is also characterized by heavy residual dust cakes (from over 0.5 to over 1 lb/ft^2 , or as much as 20 times the weight of dust accumulated during a single filtering cycle), and a higher than expected pressure drop (ΔP) which tends to drift slowly upward with time as the dust cake builds (from an initial low value of approximately $3.0 \text{ in. H}_2\text{O}$ to 5 to $8 \text{ in. H}_2\text{O}$).

To better predict and control pressure drop and residual dust cake weight, investigations have been made to improve the reverse-gas cleaning process. In addition, several alternative bag cleaning methods have been and

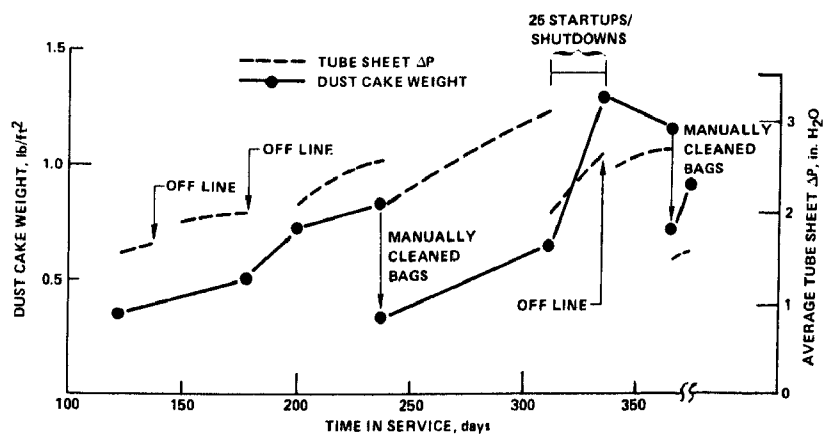


Figure 9. Pressure drop and bag weight history for the HSFP.

are continuing to be evaluated. Primary among these alternatives are sonic assisted reverse-gas cleaning using horns, and shake/deflate cleaning.

The first installation of horns in a full-scale reverse-gas cleaned utility baghouse occurred in April 1981 at Pennsylvania Power and Light Company's (PP&L) Holtwood station on the Unit 17 baghouse. Subsequently, in late 1981, PP&L installed horns in its Brunner Island Unit 1 baghouse. Both units were retrofitted with horns in an attempt to reduce high pressure drop and heavy residual dust cake weight (8). At approximately the same time as the Brunner Island installation, horns were placed in the Arapahoe Unit 3 baghouse of the Public Service Company of Colorado. Again, the objective was to reduce pressure drop and residual dust cake weight (9).

Figure 10 illustrates the improvements in pressure drop obtained using horns in these baghouses and in the FFPP. The results are shown as average tube sheet pressure drop versus A/C and include, for purposes of comparison, the FFPP data for reverse-gas cleaning (shaded region) described earlier. All of these sonic cleaning data shown were obtained with 200 Hz horns and indicate widely varying improvements in pressure drop. For the baghouses filtering fly ash from western, low-sulfur coal (Arapahoe Unit 3 and the FFPP), pressure drop reductions of 50 to 60% were realized. For the baghouses filtering fly ash from eastern, high-sulfur coals, pressure drop reductions of 20-30% were measured.

In addition to the sensitivity of sonic cleaning to fly ash composition, a number of other factors may influence horn effectiveness. In these investigations, for example, the configuration and size of the baghouse compartments tested was significantly different. Horn frequency was not varied, and they were always applied with each reverse-gas cleaning cycle. Also, the horns evaluated were installed exclusively in baghouses where seasoned dust cakes were established using reverse-gas cleaning alone. In this latter regard, it remains to be demonstrated that horns can maintain low pressure drop and low residual dust cake weight in baghouses started up with new bags.

Tests have recently been initiated at the FFPP and HSFP to characterize and optimize shake/deflate cleaning in line with the growing awareness of the advantages the technology offers. Although not retrofittable in most cases, shake/deflate cleaned units are usually designed to operate at significantly higher values of A/C (2 to 3 acfm/ft²) than baghouses using reverse-gas cleaning (1.6 to 2 acfm/ft²), and they promise lower pressure drop and improved operating economics.

Widespread application of shake/deflate cleaning within the utility industry has been retarded because reverse-gas cleaning has historically been considered to be more gentle, thereby contributing to longer bag lives and better equipment reliability. Today, however, concerns about the effect of shaking on bag life and reliability have lessened with improvements in shaker mechanisms and achievement of bag lives in excess of three years in full-scale shake/deflate applications.

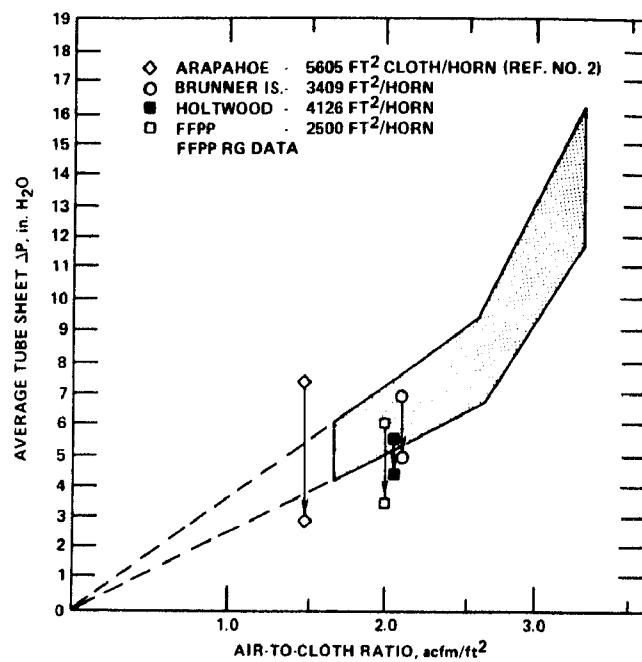


Figure 10. Effectiveness of reverse-gas/sonic bag cleaning.

In Figure 11 pressure drop versus A/C is plotted for four full-scale baghouses and the FFPP, and compared to FFPP data for reverse-gas operation (shaded region). As can be seen, with the exception of Monticello (where a Texas lignite coal is burned yielding fly ash which behaves poorly for either type of bag cleaning) baghouses using shake/deflate cleaning are operating similarly and at much lower values of pressure drop than the reverse-gas data reported for the FFPP. In this figure, the data for the Harrington station are of particular interest in that the two units at that site are large (360 MW); they are representative of state-of-the-art technology; they filter representative fly ash; and, they have performed very well, demonstrating low pressure drops at high A/Cs (nominally 6-7 in. H₂O at 3.0 to 3.4 acfm/ft²) and thin, light, residual dust cakes (typically 0.2-0.5 lb/ft²).

Figure 12 shows, in general terms, the potential improvements in drag (tube sheet ΔP divided by air-to-cloth ratio [A/C]) available with the more energetic reverse-gas/sonic and shake/deflate cleaning methods compared to reverse gas alone. The drag values shown are averages for different coal types from several full-scale baghouses, the Arapahoe fabric filter pilot plant (FFPP), and the Scholz high-sulfur coal pilot plant (HSFP). Since the values shown are averages, they can be expected to vary by as much as 20% depending upon factors such as time in service and specific operating procedures. However, the relative effectiveness of these different cleaning methods is apparent in the trend of progressively greater reductions in drag for reverse-gas/sonic and shake/deflate cleaning, respectively.

Figure 13 shows calculated capital and levelized costs of different air-to-cloth ratios and bag cleaning systems in a hypothetical 500-MW utility baghouse collecting fly ash from the combustion of Powder River Basin coal (10). Interestingly, the most common type of baghouse now in operation in the utility industry, a reverse-gas cleaned unit with an air-to-cloth ratio of 1.6—2.0 acfm/ft², is also the most expensive of those shown in this example. This situation exists because in early utility applications both reverse-gas cleaned units were thought to have unacceptably high operating costs which would offset their lower capital costs. With the former, the concern was with higher system pressure drop; with the latter it was with potentially reduced bag life attributable to this more rigorous cleaning method. Recent research and economic studies have shown that the reduced capital cost of reverse-gas units operating at higher air-to-cloth ratios can outweigh the increased operating cost resulting from their higher pressure drop, and that bag lives of over three years can be attained with shake/deflate units (3). As Figure 13 shows, a shake/deflate cleaned baghouse with an air-to-cloth ratio of 2.7 acfm/ft² offers a lower total cost than comparable or lower air-to-cloth ratio reverse-gas units. Although not calculated, sonic assisted reverse-gas baghouses with high A/C presumably would offer similar cost advantages.

PLANS FOR ADDITIONAL RESEARCH

Substantial progress has been made in understanding and improving baghouse performance. In addition a number of key factors have been identified that warrant further research and development. The EPRI program is continuing and current research is active in the following areas:

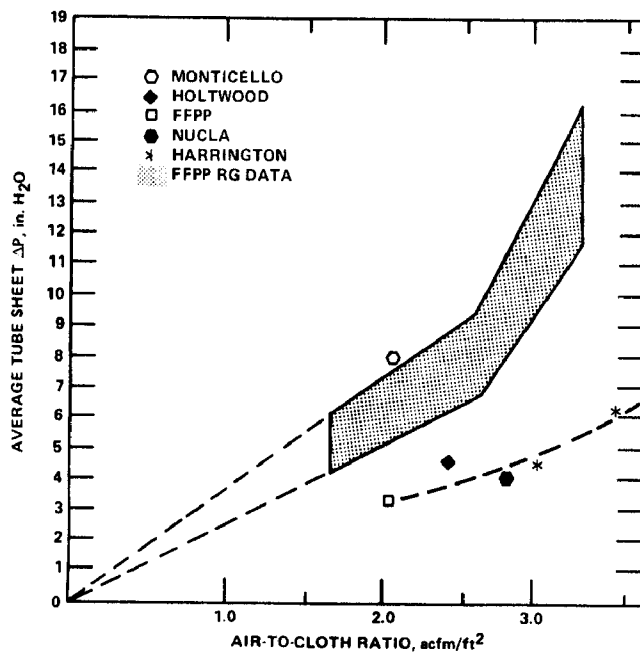


Figure 11. Effectiveness of shake/deflate bag cleaning.

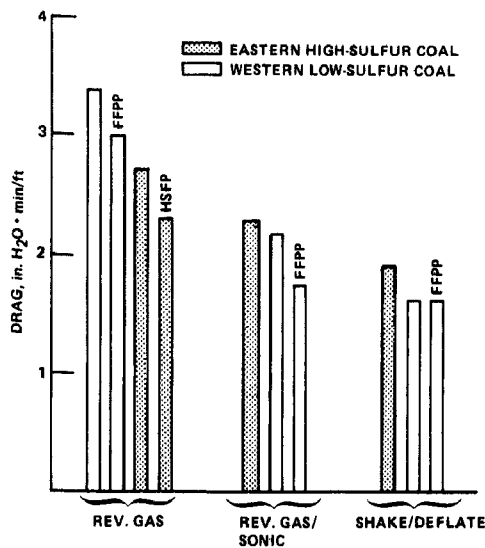


Figure 12. Relationship between drag, coal type, and bag cleaning method for several full-scale baghouses and the pilot-scale units.

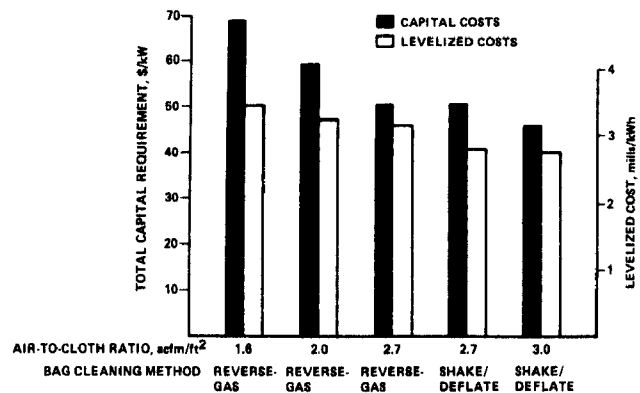


Figure 13. Capital and levelized costs for different air-to-cloth ratios and bag cleaning systems in 500 MW utility baghouses using Powder River Basin coal. After R. R. Mora, R. W. Scheck.¹⁰

- better understanding of residual dust cake properties,
- optimizing bag cleaning methods for specific applications,
- selecting the most suitable fabrics,
- predicting and extending bag life,
- developing baghouse monitoring systems,
- investigating electrostatic effects,
- developing combined SO₂-particulate collection systems, and
- implementing improved systems in full-scale demonstrations.

ACKNOWLEDGEMENTS

The work reported here was supported by EPRI under contracts RP725-12, RP1129-8, RP1129-8, RP1402-13, and RP1867-4. The majority of data were taken by staff members of Southern Research Institute.

The work described in this paper was not funded by the U.S. Environmental Protection Agency and therefore the contents do not necessarily reflect the views of the Agency and no official endorsement should be inferred.

REFERENCES

1. Proceedings: First Conference on Fabric Filter Technology for Coal-Fired Power Boilers, EPRI CS-2238, February 1982.
2. Proceedings: Second Conference on Fabric Filter Technology for Coal-Fired Power Boilers, EPRI CS-3257, November 1983.
3. Carr, R. C. and Smith, W. B. Fabric Filter Technology for Utility Coal-Fired Power Boilers, Parts I-VI, JAPCA, Vol. 34, Nos. 1-6, 1984.
4. Ensor, D. S., Hooper, R. G, and Scheck, R. W. "Determination of the Economic Aspects of a Fabric Filter Operating on a Utility Boiler," EPRI FP-297, Project 534-1, Final Report, Electric Power Research Institute, Palo Alto, CA, November 1976.
5. Ensor, D. S., Cowen, S., Schendrikar, A., Markowski, G., Woffinden, G., Pearson, R., and Scheck, R. "Kramer Station Fabric Filter Evaluation," RP1130-1, Final Report CS-1669, Electric Power Research Institute, Palo Alto, CA, January 1981.
6. Felix, L. G., and Smith, W. B. "Preservation of Fabric Filter Dust Cake Samples," JAPCA 33:1092 (1983).
7. Carr, R. C., and Smith, W. B. "Fabric Filter Technology for Utility Coal-Fired Power Boilers," Part IV. JAPCA, Vol. 34, No. 4, 1984.
8. Wagner, N. H. "Present Status of Bag Filters at Pennsylvania Power and Light Company," Proceedings: Second Conference on Fabric Filter Technology for Coal-Fired Power Plants, CS-3257, Electric Power Research Institute, Palo Alto, CA, November 1983.

9. Menard, A. R., and Richards, R. M. "The Use of Sonic Air Horns as an Assist to Reverse Air Cleaning of a Fabric Filter Dust Collector," Proceedings: Second Conference on Fabric Filter Technology for Coal-Fired Power Plants, CS-3257, Electric Power Research Institute, Palo Alto, CA, November 1983.
10. Scheck, R. W., More, R. R., Belba, V. H. "Economics of Fabric Filters and Electrostatic Precipitators," RP1129-9, Electric Power Research Institute, Palo Alto, CA, March 1984.

FLUE GAS FILTRATION: SOUTHWESTERN PUBLIC SERVICE COMPANY'S
EXPERIENCE IN DESIGN, CONSTRUCTION, AND OPERATION

John Perry
Southwestern Public Service Company
Amarillo, Texas 79170

ABSTRACT

This paper is an overview of Southwestern Public Service Company's experience with Fabric Filters on utility boilers. To date, this consists of two operating shake-deflate baghouses at Harrington Station (370 MW units) and two reverse gas baghouses at Tolk Station (550 MW units), one in operation and one under construction.

Background and current operating status of the operating baghouses will be discussed along with the insight gained in seven and one-half years of baghouse operation. During this time, extensive testing and refinement of the filter bags and operating procedures have increased bag life twofold and reduced pressure drops. All of this has had a substantial effect on the design of Tolk Unit #2 baghouse.

The Tolk Unit #2 baghouse is Southwestern Public Service Company's first fabric filter baghouse to be designed and engineered completely in-house. An extensive discussion of the design details of the unit including some unique features that are a result of years of baghouse operating experience. The items and details that are critical to the satisfactory operation of baghouses will be highlighted for the benefit of newcomers to baghouses. Start-up of this unit is slated for early 1985.

FLUE GAS FILTRATION

Southwestern Public Service Company is an investor owned electric utility serving 52,000 square miles in Texas, New Mexico, Oklahoma, and Kansas. Based in Amarillo, Texas, it has a generating capacity of 3,828,000 kilowatts and serves in excess of 340,000 customers.

Historically, Southwestern Public Service has relied on local natural gas reserves for boiler fuel. Due to increased gas prices, the first coal fired power plant, Harrington Station Unit #1, a 370 megawatt unit, was put into service in July 1976. It uses a cold side precipitator for particulate removal. High ash removal efficiency plus lower evaluated cost lead to the use of baghouse filters on subsequent units. Three more coal fired units have since been brought into service and a fourth is now under construction. All four use baghouse filters behind pulverized coal boilers burning low sulfur Wyoming coal.

Southwestern Public Service Company is different from most utility companies by the fact that it designs and engineers its own power plants. The Generation Plant Design Department of the Company grew from a few engineers and drafters required to design gas fired units to the present department which has designed all of the Company's coal fired generation. The transition from gas fired to coal fired generation required that the Company deal with new and unfamiliar technology. The successful application of baghouses was a part of that learning experience.

Southwestern's first baghouse installation was at Harrington Unit #2 which went on line in June of 1978, followed by the Harrington Unit #3 baghouse in 1980. Both baghouses used the shake/deflate filter bag cleaning system and were designed and fabricated by Wheelabrator-Frye. These two baghouses are of the same design, differing in air to cloth ratio and performance as shown in Table #1. Initially, numerous design and operating problems plagued both units. Upgrading of the design deficiencies and diligence from Southwestern's operating personnel in fine tuning and improving baghouse performance have decreased the average baghouse pressure drop by more than of 15% while increasing filter bag life from one year to better than four years. This performance improvement has provided a savings in excess of \$200,000.00 per year in operating cost.

The filter bag service life increase is due to three factors: decreased wear and tear from the cleaning cycle, lower bag ΔP 's, and better filter media. The present filter bag is a product of years of testing of numerous filter media variations. This testing involved full compartments of bags operated until failure. Compartment pressure drops were recorded as an indication of compartment throughput. Visual inspections were used to detect ash bleed-through and wear problems. All of this data has been used to produce a filter bag specification that spells out the cloth finish and fabrication details of replacement bags. Approximately fourteen variations of filter bags have been tested in the two Harrington units. A similar program has been started for Tolk Station Unit #1, which is the first unit of the Company's second coal-fired power plant.

Another area of performance improvement has been in the cleaning cycle. The duration, amplitude and frequency of the shaker system has been refined to the point of attaining effective cleaning with minimum wear and tear on the filter bags. This change has resulted in a decrease in pressure drop with a substantial increase in the filter bag life. The deflation gas circuit is a reverse gas cycle operated with a minimum flow. This too has been optimized.

TABLE 1

BAGHOUSE DATA SHEET

	<u>Harrington Unit #2</u>	<u>Harrington Unit #3</u>	<u>Tolk Unit #1</u>	<u>Tolk Unit #2</u>
Gas Flow	1,650,000 acfm	1,650,000 acfm	2,400,000 acfm	2,400,000 acfm
Air to Cloth Ratio	Net = 3.4 to 1 Gross = 3.13 to 1	Net = 2.92 to 1 Gross = 2.74 to 1	Net = 2.09 to 1 Gross = 1.94 to 1	Net = 2.09 to 1 Gross = 1.94 to 1
No. of Compartments	28	32	28	28
No. of Bags	5,712	6,528	13,440	13,440
Bag Size	30'-8" x 11½"	30'-8" x 11½"	33'-6"	33'-6"
Δ P Design	5" to 6" W.G.	5" to 6" W.G.	5" W.G.	5" W.G.
Δ P Actual	7" to 8" W.G.	6" to 7" W.G.	5" to 6" W.G.*	N/A
Available Bag Δ P (I.D. Fans)	16" W.G.	16" W.G.	N/A	N/A
Start-up Date	June 1, 1978	June 15, 1980	August 12, 1982	April, 1985
Typical Opacity	2 - 8%	2 - 8%	2 - 8%	2 - 8%**
Cleaning Method	Shake Deflate	Shake Deflate	Reverse Gas	Reverse Gas
Unit Size	370 MW	380 MW	550 MW	550 MW

* One year of operation with no extended full load operation.

** Expected.

Tolk Station consists of two 550 megawatt units located 100 miles southwest of Amarillo, Texas. The baghouse on the first unit was put into service in August of 1982. It is a reverse gas cleaning cycle unit designed and fabricated by Ecolaire Environmental. Design conditions are 2.4 million acfm at 266°F with gross gas to cloth ratio of 1.95 to 1. The unit is presently operating at an average 6" to 8" wg flange to flange pressure drop. Flow modeling of the outlet plenum is now underway in an effort to reduce the pressure drop.

The unit uses 9½ oz Teflon finished fiberglass bags. Six full compartments (480 bags) with different cloth, finish, or anti-collapse ring spacing are being tested to determine the optimum filter bag. Two or three more years will be required before conclusions are reached.

During the erection, start up and initial operation of the Harrington baghouses, a pattern of problems emerged; the first being distortion of x-bracing of the support structure. Further inspection revealed that permanent deformation had occurred in both the hot and cold structures. As a result teflon slide plates failed. The initial start up of the Harrington Station Unit #3 baghouse (the second baghouse erected) demonstrated the nature and magnitude of the problem. The baghouse was outfitted with position indicators on all slide plates. The movement of the hot structure in relation to the cold structure was closely monitored during the heat-up phase. The horizontal movement was close to the predicted values with some binding of guide bolts in the slotted holes. The unexpected movement was a vertical separation of the slide plates under the exterior walls. With these columns carrying no load, the remainder of the columns were overloaded. Even with four inches of high density insulation on the exterior walls, a 50°F temperature difference existed between interior and exterior walls. This produced a bulging effect of the hot structure over the interior walls. Southwestern Public Service Company's Plant Design Department immediately did a thorough structural analysis of the baghouse using finite element techniques. This analysis included dead loads, fly ash dust loads (95 lb/ft³), horizontal loads due to thermal expansion sliding friction (20% of the vertical load, steel on steel), column eccentricity and thermal deformation of the hot structure. Both the hot and cold structures were found to be deficient. The unit remained on line while corrective measures were taken. Columns were stiffened with 4" x½" plate on the ends of each flange. Beams tying the tops of the columns together were replaced with larger members. X-bracing was converted from single to double angle bracing. The hot structure support beams could not be replaced nor could the slide plates. Gussets were added to reinforce the beams and accept the increased loads due to the steel on steel slide plates.

Tolk Station Unit #1 baghouse was well into the engineering phase when the Harrington baghouse thermal expansion problems were resolved. The Company's Generation Plant Design department computer modeled the baghouse using finite element analysis methods. Again, deficiencies in the structure were found. Further checks of the engineering revealed problems in compartment doors, poppet dampers, inlet dampers, and cell plate thimbles. Most of these problems were corrected prior to start-up.

Meanwhile, the second 550 megawatt unit at Tolk was in the early stages of engineering. In most aspects, it was identical to the first unit with a duplicate boiler, turbine-generator, boiler fans, etc. It was decided to evaluate baghouse suppliers again. A full economic evaluation of the in-house engineering and design of the unit versus a vendor-supplied unit was undertaken. The analysis indicated that it would be cost effective to design, in-house, the Tolk Unit #2 baghouse. Other benefits to which no additional value was assigned included Southwestern's conservative design philosophy, increased shop fabrication decreasing the required field labor cost, an operator-oriented design, and direct control of suppliers and fabricators yielding better quality control.

The conceptual design began immediately. Numerous configurations were considered. The fact that the remainder of the plant is essentially a duplication of the first unit restricted layout options. The benefit of interchangeable bags was an incentive to design around the Tolk Unit #1 filter bag. The remainder of the hardware was also designed around these restrictions.

The structural design required the greatest amount of engineering time. The symmetry of the unit in both North-South and East-West planes minimized the computer time required. A finite element analysis computer model of one quarter of one baghouse was used for design. A series of thermal loading conditions were applied to the finite element model. These loads consisted of structural dead loads, internal compartment pressure loads, fly ash live loads, wind loads, frictional forces at the slide plates, and thermal loading. The thermal loading conditions simulated the baghouse under a wide range of normal and abnormal operating conditions. These conditions included the baghouse heated to a temperature of 350°F with various compartments at a reduced temperature of 100°F, representing compartments in an "offline" condition; and the compartments at 550°F with the inlet and outlet ducts at 750°F, representing the condition of an air preheater failure.

This study provided the magnitude and direction of the thermal distortions. From this, the sliding forces, the compartment stresses, and the resulting forces in the "fixed line" supports were calculated. The design requirements for the slide plates and guides were established as well as load conditions for columns and associated steel.

The performance of the baghouse, along with optimizing the reliability of the equipment, was the primary goal of the mechanical design. The performance of a baghouse can be broken into three major categories: filtration efficiency, pressure drop, and bag life. The required filtration efficiency in baghouses has not been a problem. The flange to flange pressure drop is a sum of the fixed or casing losses (plenum, damper, and hopper losses) and the filter bag losses. The fixed losses should be as low as possible (0.5" - 1.5" WG). An inch of pressure drop at Tolk Station costs approximately \$50,000.00 per year in horsepower cost alone. The larger the baghouse, the more difficult it is to design the internals to provide low pressure drop while maintaining uniform dust and gas distribution. The inlet plenum must be designed so that velocities are low enough to provide the

desired pressure drop characteristics and high enough to keep fly ash from settling out under varying boiler loads.

Inlet dampers are used for isolation purposes only. These dampers will go for long periods of time in a dirty gas stream without operating. There is a potential for ash build-up and the consequential failure to operate. The second mode of failure is distortion due to external loads imposed on the damper from thermal expansion of the baghouse. The best way to counter this problem is to design dampers with very rigid frames with ample blade clearance and flexible seals. Poppet dampers also work well under these conditions. A recess in the floor of the inlet plenum over a damper is a prime location for ash build-up with its associated problems. Below the inlet dampers, the entrance to the hopper should be horizontal with very low velocities since the uniform distribution of flue gas to the filter bags is essential to low pressure drop operation.

Hopper design is dictated by the angle of slope required to prevent plugging and bridging of ash, since the storage capacity of the hopper is usually more than required by operating dictates. The Southwestern design uses a minimum 55° valley angle based on previous experience. A decrease in this angle can be tolerated with some types of ash - particularly true of the upper hopper, since the plugging or bridging only occurs in the bottom of the hopper. Significant savings can be made by using the compound angle hopper due to lowering of the overall height of the structure.

Re-entrainment of the fly ash in the hopper can occur under two circumstances. The first circumstance occurs during the normal filtering mode. High inlet velocities directed toward the bottom of the hopper coupled with excessive quantities of ash left in the hopper are usually the cause. This problem can be avoided by low inlet velocities and continuous ash removal. The second type of ash re-entrainment occurs during the reverse gas cycle. The reverse gas flow through the bags into the hopper becomes very heavily ash laden due to the ash falling from the bags into the hopper. The gas carries the ash back into the inlet plenum and deposits it on bags in the downstream compartments. In reverse gas baghouses, this type of re-entrainment cannot be completely avoided, but it can be minimized. The cleaning mechanism of a reverse gas baghouse is not the gas flow through the bag in the reverse direction. Ash removal from the bag is a result of the inward flexing of the filter material, breaking the ash cake and allowing it to fall into the hopper. The ideal situation would be to obtain this flexing with minimum reverse gas flow, so that the ash remains in the hopper and is not carried back into the inlet plenum. The amount of flex produced in a bag by a given reverse differential pressure is a function of the bag tension, which is an induced upward force on the bag to support the maximum weight of the bag. Lesser force will allow the bag to sag and crease and will eventually cause the bag to fail. Springs are generally used to maintain 70 to 75 pounds of tension on a 12 inch diameter, 30 - 34 foot bag. This amount of force is adequate during normal filtration and works well with the six to eight inch springs typically used by vendors, but during the reverse gas cycle, the bags neck down between the anti-collapse rings, resulting in a decrease in bag length in excess of two inches for a nominal 30 foot bag. This shortening produces a large increase of tension on the order of 70 - 90

lbs in a 35 to 45 lb/inch spring if the spring doesn't bottom out first. As a result, the amount of reverse gas flow increases to produce the required bag deflection for filter cake removal. Increased reverse gas flow results in increased ash re-entrainment. The ideal tensioner would be a constant force support mechanism which is commercially available in either counterweight or spring and lever types. The drawbacks to these devices are cost and insufficient travel. After a thorough investigation of these mechanisms, including several of Southwestern's own design, a 16 inches, spring with a low spring constant of 15 lb/inch was selected. This spring is adequate and still reasonable in cost.

The tube sheet for dividing flow between hopper and filter compartment is also a critical element in baghouse design. It must be designed to carry the tremendous loads produced by bag tension plus the load imposed due to differential pressure. Any resulting deflection in the tube sheet changes the floor-to-bag support dimension which results in changes in bag tension.

The lower attachment for bags, the thimble, is mounted in the tube sheet. All thimbles should be seal welded and the tube sheet flooded with water, prior to initial operation, to check for leaks. The "slip on" type thimble that requires no adjustable attachment band is very popular with baghouse vendors and requires much less bag installation time. Dimensional tolerances and bag-to-thimble interface design are very critical in this type thimble. This critical area (see Figure 1) should also be tapered from perpendicular by no more than 4°, and, along with an adequate bead along the top edge, rolled until the top edge is smooth, provides an excellent bag attachment mechanism. In the case of Tolk Unit 2, several sample filter bags and sets of dies were used before a satisfactory thimble was produced.

Filter bags require special attention. Opportunities for mistakes are endless and correction usually requires replacement. On one small order of 500 bags, the fabricator sewed in thimble bands that were 1/8 inch in circumference out of tolerance in half of the bags. As a result, the bags could not be used. To insure compliance, thorough bag specification should be written with any variances from the specification spelled out in writing. The specification should contain acceptable material weave and finish types as well as acceptable fabric suppliers. Complete dimensional data on the bag is required, including length, thimble circumference, and ring placement. Seam, ring cover and cuff construction should be detailed with dimensions and thread type. Quality assurance is worth the expense of hiring an independent lab to verify that the cloth and finish is what has been specified. Bag packaging is as important as bag fabrication. A bag has to be slightly damaged in only one spot to render it useless, and with fiberglass, damage due to mis-handling or packaging is highly likely.

The maintainability of a baghouse is another serious consideration. In Southwestern's 550 megawatt units, a large number of bags are required (13,440). With a four to five year life expectancy on a filter bag, bag change out is the single largest maintenance item. Being more operations-oriented than most baghouse designers, Southwestern included some extra features to minimize maintenance time. Two-bag-reach not only reduces average bag change out time by one-third, but reduces damage to bags next to

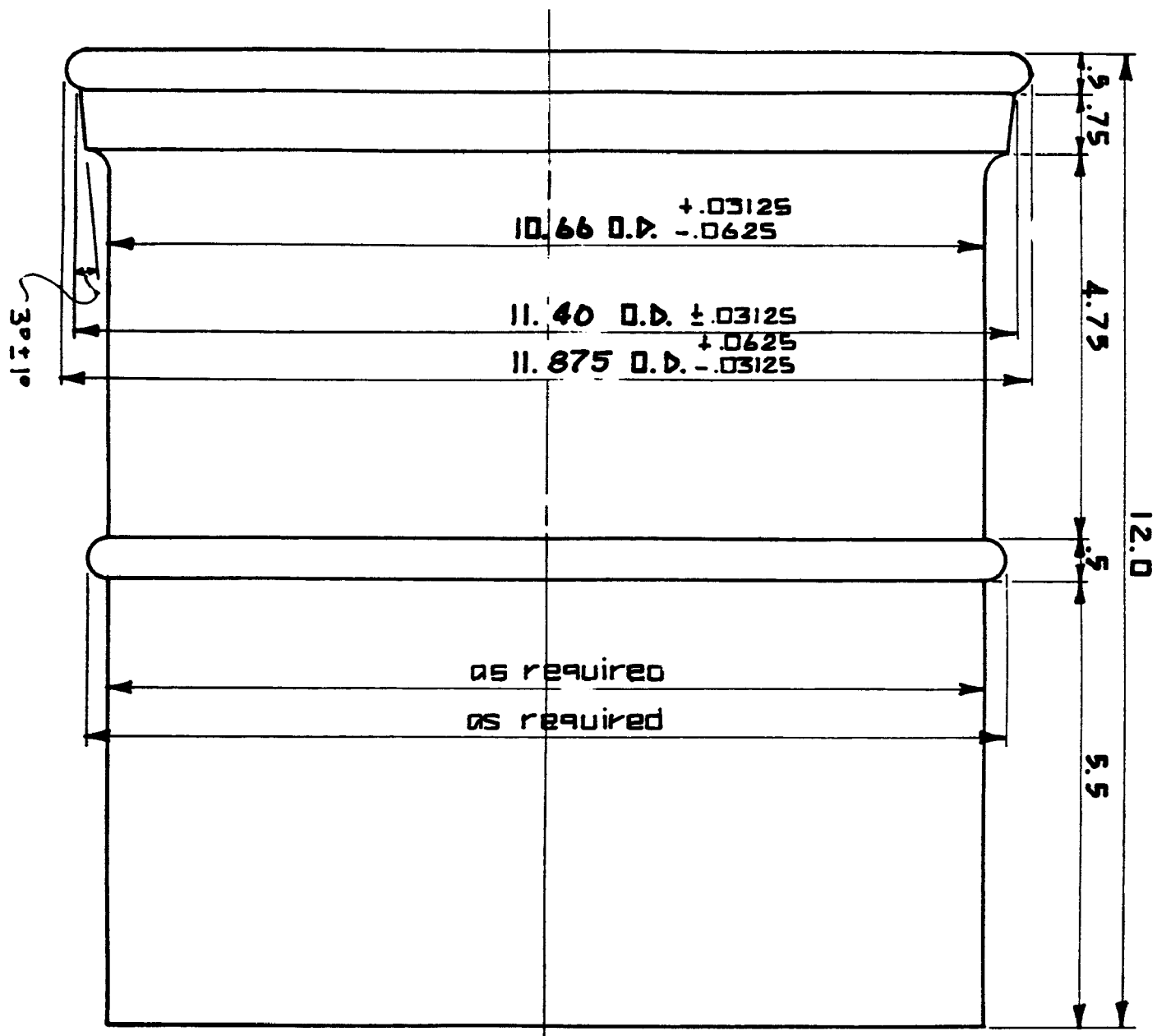


Figure 1. Filter Bag Thimble

the aisles. Properly designed slip-on thimbles are a tremendous time saver, and bag support mechanisms with slip-in pins and a pneumatic spring compressing device make tensioning a one-man job.

The corrosive nature of flue gas should be a serious consideration of design. The higher the sulfur content of the coal burned and the higher the dew point of the flue gas produced, the more serious the problem. Some of the basic considerations are:

- (1) The amount of time in which the unit will operate below the acid dew point.
- (2) Is it possible to bypass the baghouse during these periods?
- (3) What procedures are required to purge flue gas from the baghouse during shut down and compartment isolation?
- (4) Are there any areas of stagnant or low velocity flue gas?

Careful design of doors, dampers, and ducts will minimize air in-leakage and its cooling effect. The reverse gas system is one of the most likely locations for corrosion. The long runs of small diameter ductwork lend themselves to high heat losses. This system should be generously insulated. The design should include a recirculation by-pass so that flow is maintained at all times.

Many other items in Southwestern's present baghouse design have evolved over the last eight years of operation and refinement. The operation and performance of the Tolk Unit 2 baghouse are expected to be successful. Southwestern's trend toward in-house engineering design is expected to continue. This in-house design now includes cooling towers as well as baghouses, and soon will include other, normally vendor-engineered, components of Southwestern's newest proposed facility, South Plains Station.

START-UP AND OPERATION OF A REVERSE-AIR
FABRIC FILTER ON A 550 MW BOILER

R. A. Winch
Houston Lighting and Power Co. Inc.
Houston, TX 77001

L. J. Pflug, Jr.
Research-Cottrell, Inc.
Somerville, NJ 08876

ABSTRACT

Houston Lighting & Power began commercial operation of W.A. Parish unit #8 in December, 1982. The unit is equipped with four parallel Bag-houses for particulate collection, which was the largest such system supplied at the time. Details of the System including: Configuration, Filter Bag description, Control System, Design Parameters, and Coal Characteristics are presented. Cleaning Cycle and Bag Support System modifications are also described. Performance Test results and the effects of sonic horns are then presented.

The W.A. Parish Generating Station of Houston Lighting and Power Company is located in Fort Bend County, near Richmond, TX, approximately 40 miles southwest of Houston. Unit No. 8 is the fourth coal fired unit at the site. It has a maximum, continuous rating of 570 MW and went into commercial operation in December, 1982.

The particulate control system at Parish #8 consists of a Research-Cottrell reverse-air fabric filter. It is the first fabric filter in the HL&P system and was selected after engineering studies determined that fabric filtration would be the most cost effective choice for particulate removal. There are two sources of fuel for WA Parish Station: one is a sub-bituminous, low sulfur coal from Wyoming's Powder River basin supplied by Kerr-McGee; the second is a sub-bituminous, low sulphur, high sodium Montana coal supplied by NERCO. The fabric filter is designed to operate with either 100% Kerr McGee, 100% NERCO or a blend of both.

This paper presents the history of this unit for its first two years of operation. Bag fabric pre-coat, start-up, cleaning cycle adjustments, hardware modifications, test results, and sonic horn installation will be discussed.

EQUIPMENT DESCRIPTION

Steam generation is provided by a single Combustion Engineering balanced draft, pulverized coal fired boiler rated for 4199K lb/hr steam flow. Either natural gas or fuel oil can be fired for ignition and warm up. Power generation is by a Westinghouse tandem compound turbine generator with a nominal rating of 607 MW at VWO 5% over pressure. Four Research-Cottrell baghouses control particulate emissions. Each pair has a common inlet from one of the two air preheaters, while all four exhaust into a common outlet plenum. The system has maximum hourly emissions guarantees of .03 lb/MMBTU heat input, 0.0134 gr/scf at 60°F based on a 24 hour averaging period, and a maximum opacity of 20%. Specific performance guarantees also are to be met for system pressure drop, power consumption and bag life. Design conditions are noted in Table 1.

The four baghouses are arranged in parallel. Each has ten compartments with 324 bags per compartment. Bag row arrangement is an 18-bag wide by 18-bag deep (three walkway) configuration with a three bag reach. Gas flow to each compartment is controlled by inlet butterfly and outlet poppet dampers which are pneumatically operated. Compartment isolation is accomplished with these dampers. Three by-pass poppet dampers are located at the inlet end of each baghouse to provide both high temperature protection for the bags. Bag cleaning is accomplished by reverse air (gas) flow through the filter bags. The reverse air (RA) fans are located at grade near the baghouse inlet. Two fans (one operating, one standby) are provided to clean the 40 compartments. All outlet and RA dampers are located centrally at the top longitudinal axis of each baghouse. To provide weather protection all damper operators are enclosed under a roof and partial side-wall penthouse. Multiple points of access with extensive platform areas allow easy maintenance and inspection at the penthouse, bag suspension and tube sheet levels, hopper level detectors, inlet dampers and ash removal system. An exhausting purge air system is provided to vent an off-line compartment for maintenance.

TABLE 1
DESIGN CONDITIONS
H.L. &P. CO./W.A. PARISH 8

Flue Gas Flow Rate	6.98 x 10 ⁶ lb/hr 2.20 x 10 ⁶ ACFM
Temperature	300°F
Inlet Load	4.9 gr/scf
Coal Type	Sub-bituminous
Coal Analysis:	
Heating Value	8000-9715 Btu/lb
Moisture	21.7-31.3%
Ash	2.26-8.12%
Sulfur	0.20-0.76%

Bags on Unit #8 are woven fiberglass with an acid resistant finish. Weave specifics are as follows: weight- 14 oz./yd., permeability- 35 to 50 cfm/sq. ft., count- 44x24, weave- 3x1 twill, and finish- I-625 (38 compts.), Q78 (1 compt.), Teflon B (1 compt.). Each bag has a 12" diameter and a 32'-9" total length (31'-6" effective length). Bag attachment at both thimble and cap is by a sewn-in, stainless steel snapband; no tools are needed for attachment. Six anti-collapse rings per bag are cadmium-plated carbon steel. When all 40 compartments (12,960 bags) are in service, the gross air-to-cloth ratio is 1.73:1 at a design gas flow rate of 2,200,000 ACFM at 300°F. When two compartments are isolated for maintenance and two compartments are cleaning, the air-to-cloth ratio increases to 2.02:1 with reverse air included. Thirty-eight compartments were initially bagged with acid resistant bags of I-625 finish. As a test for potential replacement bags, the two remaining compartments were filled with Q-78 acid-resistant finish and teflon B finish bags. In February, 1984 another compartment was bagged with Manardi-Southern 9.5 oz./sq.yd. bags as part of HL&P's bag replacement review program.

The baghouse auxiliary systems were specified to provide a high degree of reliability and maintainability. Since WAP #8 would be base loaded, the fabric filter would be required to be maintained on line and still have a low system pressure drop. The 40 compartment configuration allows four compartments to be out of service for maintenance and/or cleaning while the air-to-cloth ratio is still a low 2.02:1. The numerous compartments that resulted are easily inspected and will take a minimum amount of time to rebag. The compartment purge air ventilation system reduces the temperature in any compartment, with adjacent compartments in service, to less than 120°F within two hours of being isolated. The purge air fan pulls ambient air through open compartment doors, through the three purge air poppet dampers at the top of the compartment and via the purge air ducting to atmosphere.

Automatic control of the fabric filter is accomplished by a Modicon 484 programmable controller(PC). It is located in the control panel in the fabric filter control building. The PC is programmed to be dedicated to each baghouse pair. Separate instrumentation on each pair transmits operating parameters to the PC. Initiation of cleaning, cleaning sequence, cleaning cycle timing, alarm conditions, and all normal control/sequencing activities are through the PC. The graphic display panel is supplemented with opacity, inlet pressure, ΔP , inlet and outlet temperature which are indicated and recorded. The graphic display gives operators a visual representation of the fabric filter, and the ability to determine the operating status of system components at a glance.

START-UP ACTIVITIES

Based on past experience and surveys of utility baghouse experience, it was determined that initial bag coating using boiler-generated fly ash was acceptable. One hundred percent Kerr-McGee fuel was being fired during initial unit start-up. This Powder River Basin fly ash does not exhibit the sticky characteristics of the high sodium NERCO fuel. It was determined that controlled admittance of the Kerr-McGee, boiler-generated fly ash would be suitable for initial bag coating. The separate pre-coat piping system

was not used for the initial bag coating.

Initial coating of all forty compartments was accomplished simultaneously with the boiler on line, firing coal at approximately 60% full load. Operating levels during initial coating activities were: 350 MW, 250 °F, 1,740,000 ACFM, and 0.5 in.w.c. Pressure drop increased at a rate of 0.1 in./ hour. Initial coating activities commenced on October 18, 1982, and continued until early October 19, when the baghouse was by-passed due to boiler feed pump difficulties. Feed pump repairs were made and initial coating activities resumed and concluded on October 20. System initial coating was complete when a system ΔP of 2" WG at 80% of design gas flow was achieved. Initial coating was accomplished in about 14 hours of fabric exposure to fly ash.

Boiler load was maintained at 60% of full load during the initial coating procedure. This was done to reduce the velocity of the gas and particulate coming in contact with the virgin bags, and to minimize the risk of high speed impingement of the particles into the interstices of the fabric. The velocity, however, could not be reduced to a point where drop-out of the heavier particulate would occur in the ductwork and hoppers, causing only the extremely fine particles to remain entrained in the gas stream to initially coat the filter bags. An air-to-cloth ratio of approximately 75% of design was maintained to accomplish initial coating.

Once the initial coating activities were completed, boiler load was gradually increased. Reverse air fan 8A was started and the first cleaning cycle on A and B baghouses was initiated on October 20, 1982. The first cleaning cycle on C and D baghouses occurred the next day. Full boiler load was achieved on October 22 at 1:00 PM. Pressure differential was 5-6 in.w.c. at initiation of the cleaning cycle. Following the attainment of full load, boiler output was reduced as planned for a complete shutdown on October 26. All baghouses were by-passed and purged.

Start-up activities were punctuated with frequent compartment outages caused by filter bags slipping off of their respective thimbles. It was determined that incorrect seating of the filter bags had occurred during their initial installation. Approximately 7/10 of one percent (91) of the total filter bags in the unit were affected. Eighty percent of these failures occurred during the first reverse-air cleaning cycle. The remaining 20% occurred with decreasing frequency during the following several weeks of operation. All subject filter bags were reinstalled correctly and no further problems have been encountered.

Detached bags are detected by excursions in opacity, undetectable by eye, but apparent on the opacity monitor located on the outlet of each respective baghouse. When an opacity excursion is noticed on the monitor for one of the four baghouses, an isolation procedure can be performed by the operator assigned to the fabric filter. This procedure is the individual, sequential isolation of each compartment in a baghouse until the opacity drops to its normal operating level. When the problem compartment is located, it is isolated and tagged "out of service". The compartment is purged and the compartment is entered. Bags are then replaced on their thimbles, retentioned, and the compartment is closed and returned to service. Normal operating opacity is 0 to 1 percent. Due to the light-reflecting characteristics of the fly ash, a single detached bag in one baghouse of 3240 bags causes an opacity of 3-4% for that baghouse.

CLEANING CYCLE

The flexibility afforded by the programmable controller made optimization of the cleaning cycle an easy task. After start-up filter bag cleaning was initiated by a baghouse differential pressure setpoint of 5.5 in.w.c. from a differential pressure transmitter located between the inlet and outlet plenums of each baghouse pair. This method was changed to continuous cleaning in October, 1983, then back to pressure drop initiation in July, 1984.

The original cleaning sequence progressed perpendicular to gas flow through each baghouse and alternated between baghouses in each pair. Figure 1 shows how cleaning progressed from compartment A1 to B1 to A6 to B6 to A2, etc. During cleaning in the parallel mode, two compartments were occasionally off-line for cleaning at the same time. However, the sequencing did not allow two reverse-air poppet dampers to be open simultaneously. The original cleaning cycle of two compartments, one in A-B pair and one in C-D pair was: first null 60 sec., R/A application 25 sec., final null 30 sec., and wait between compartments 25 sec. with a 60 second offset, so only one compartment was cleaning at a time. By opening the reverse air dampers one compartment at a time, two benefits result. The first is that only one reverse-air fan is required to clean all 40 compartments. The second is that the incremental gas volume filtered in the baghouse is kept at a lower actual air-to-cloth ratio during cleaning and a lower maximum system ΔP during cleaning. In a 40 compartment arrangement, these effects are minimized since the reverse-air volume is only 2.5% of the filtered gas volume, but they have a positive effect to help keep operating pressure drop to a minimum.

In late 1983, it had become more difficult for HL&P to operate the system below an 8" pressure differential. In order to further improve cleaning cycle efficiency, changes were made to the sequence and cycle timing. With reverse gas cleaning the flue gas used for cleaning exits a compartment through its inlet duct. The gas is then filtered by the other nine operating compartments in the baghouse. It was conjectured that since adjacent compartments cleaned immediately after each other, the dust laden gas could enter a newly cleaned compartment and quickly dirty the filter bags. Although this claim was never substantiated, the cleaning sequence was changed to prevent its occurrence. The new sequence proceeded from compartment A1 to C1, then to A2, instead of A6. Refer to Figure 1 for compartment layout. There was no observable change in pressure drop after the sequence was changed. In addition to changing the sequence, cleaning cycle timing and coordination were changed. In an effort to reduce the overall cleaning cycle duration, cycle times were adjusted in several steps to a final setting of 20 sec. null, 30 sec. R/A application, 10 sec. final null, zero wait between compartments. In addition, the opening of R/A dampers was coordinated to have one R/A damper open as the previous one was beginning to close with two compartments off-line simultaneously. These steps reduced the overall cycle time from 40 to 20 minutes. Pressure drop was not reduced, but operation at full load could now be maintained for a longer time period.

The cleaning cycle remained in this mode until July, 1984 when sonic

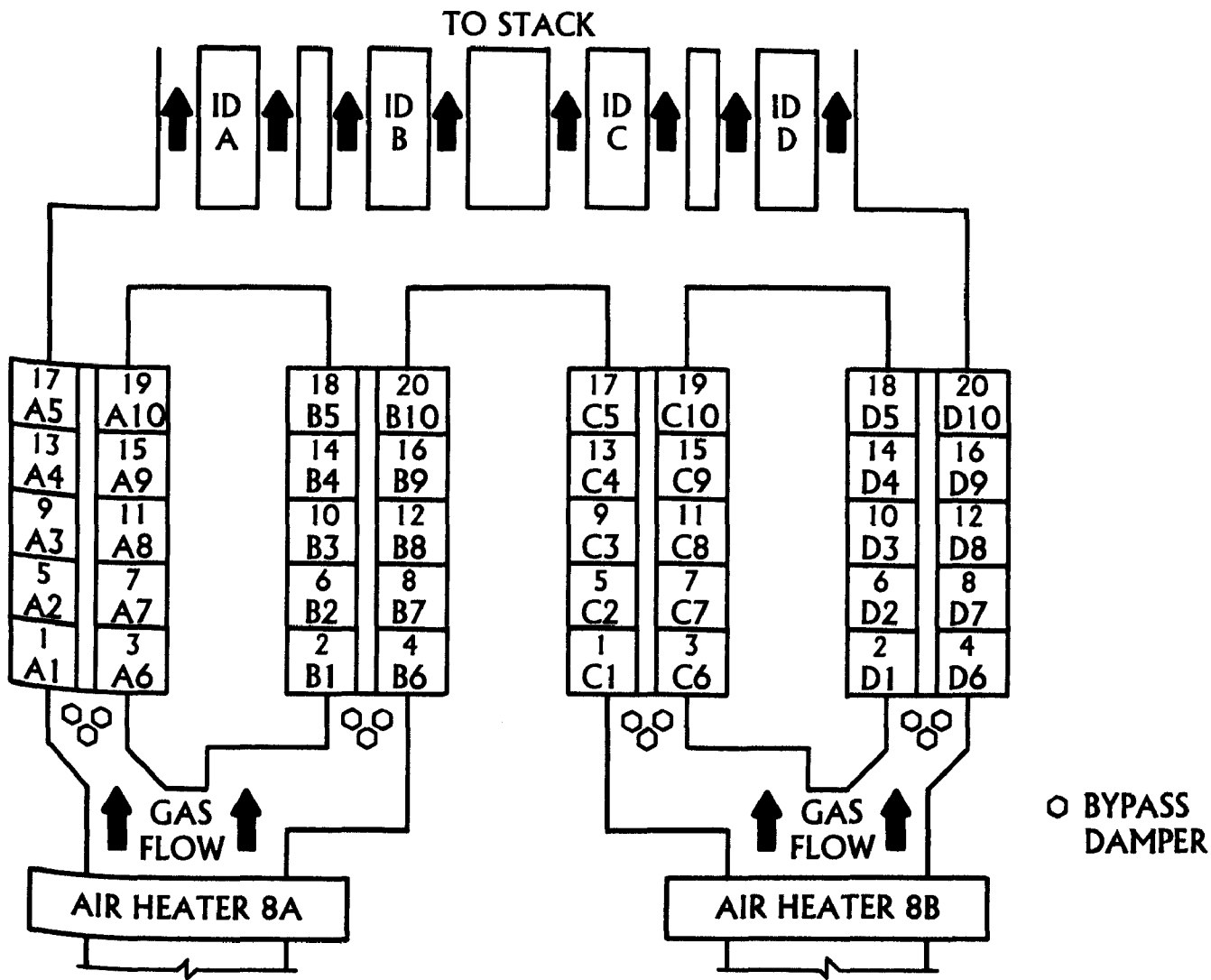


FIGURE 1
BAGHOUSE LAYOUT

horns were put in the baghouse. Following installation of sonic horns in all compartments, further cleaning cycle changes were made. The cleaning cycle times were adjusted to the following: first null 20 sec, R/A application 30 sec., final null 25 sec., and wait between compartments 100 sec. Application of the sonic horns was for 10 sec. within the R/A application, and was done on every third cycle. These settings were established because sonic horn assisted cleaning significantly reduced the pressure drop, and the need for cleaning. In addition, the usage of instrument air to intonate the horns is reduced by using the horns on every third cycle. Finally, continuous cleaning was abandoned in lieu of a 4.5 in.w.c. start of clean.

COMMERCIAL OPERATION

On December 1, 1982, WAP #8 was declared in commercial operation. Since that time, operation has been successful and within compliance with state and federal emissions limits. From a maintenance standpoint, only a few areas needed attention.

During the first year of operation an unusual degree of corrosion was observed on the Reverse-Air (R/A) damper operator, pneumatic shaft and limit switch assembly. The corrosion was due to flue gas leaking past the packing gland and condensing within the damper housing. The problem was traced to low load operation, when the system's static pressure was higher (less negative) and the cleaning cycle was not needed for several hours. During this time, the R/A duct would be stagnant and under positive pressure. Deteriorating packing in the shaft seal allowed flue gas to escape from the R/A duct and enter the cylinder housing. The gas then condensed and caused corrosion of the components. The problem was solved by installing a new type packing material in all shaft stuffing boxes. Replacement of the damaged damper components during the 1983 annual outage resolved this problem.

In March, 1983 during a routine inspection, the No. 3 compartment in 8C baghouse was found to have almost complete bag failure. This compartment was one of two in the system that was initially equipped with other supplier's bags as a test of future alternate bag replacements. Laying on the tube sheet were 245 of the 324 installed bags. Most were solidly packed full of fly ash. The caps from 167 bags were scattered about and 78 caps were hanging bagless from their chains. Strangely, the opacity had not increased, so it could not be determined how long the bags had been in this condition. The inlet damper was found almost closed. The air supply had mistakenly been turned off and the damper had drifted to only 30% open.

In tests later in 1983, it was found that the compartment gas flow is significantly reduced when the inlet duct is only 30% open. Since the permeability of removed bags was a low 1.1 ACFM/FT² at 0.5 in.w.c., the conjecture is that only fines were carried to the bags and caused fabric blinding. Laboratory examination of several failed and unused bags from this lot also revealed an excessively loose connection between the top cap and bag band, and a high bias in the cloth. The bias problem, which means the cloth is not squarely rolled during bag manufacture, caused the bag to pull on the cap harder on the seam side than on the rest of the cap. The loose top band allows the bags to slip off the caps if pulled hard enough. It was concluded that the closing of the damper reduced the gas flow, caused

finer to blind the bags, reduced cleaning effectiveness, allowed dust accumulation and increased the dust load on the bags. The extra dust loading when combined with the normal forces caused by reverse air cleaning and extra load from the blinding of the bags was enough to pull the bag from the unevenly loaded, loose fitting cap. Once the bags fell, their weight on adjacent bags caused them to fall as well. The bag supplier made full settlement for the fabrication problem. The compartment was rebagged with spare bags and has operated since without incident.

Other than the compartment 8C-3 bag replacements, bag failures over the first fourteen months of operation have been minimal. Of the 186 other bag failures (1.4%) almost all were due to a defect in the spring assemblies used to tension and support the the filter bags. Infant mortality failures of the welded bag support chains and "S" hooks also contributed to these failures. The original spring assemblies consisted of a 5 1/4" long spring, compressed by two counter directional drawbars mounted 90° apart inside the spring. Binding of the drawbars against each other and into grooves worn in the spring coil was discovered on many failed bags. Failures due to bags rubbing adjacent bags also began to appear. It was believed that the springs, which collapse during the loading induced by the reverse-air, were binding in the collapsed position which allowed the bags to slacken. Attempts to correct the spring binding were not successful. Therefore, in November, 1983, the bag support assemblies were changed from chains and drawbar springs to J-hooks and springs. Following the change, the bags were tensioned to 90 lb. This modification reduced the frequency of rubbing failures. However, although the rate was lower, it was still not zero. Some residual damage was thought to be causing some of the failures. Analysis of the failed bags then provided the cause for continuing problems. Encapsulation of the bag yarns by sulphate salts was occurring. Permeability was decreasing due to the encapsulation, resulting in poor cleaning. The residual dust layer on the bags was increasing and causing the bottom of the bags to slacken and in some cases rub against adjacent bags. Since unit restart in December, 1983 approximately 66 bags, or 0.5% of the total failed due to this problem, including cascaded failures. The failure rate was gradually decreasing until June, 1984, when sonic horns were installed. The horns eliminated the encapsulation, reduced the dust load on the bags, which allowed them to remain tensioned properly, and eliminated the rubbing and subsequent failures. No bag failures have occurred since the horns were put into operation.

SYSTEM PERFORMANCE TESTING

ACCEPTANCE TEST

In January, 1983, the first of two contractually required performance tests was conducted. Particulate removal was exceptionally good. Table 3 shows a summary of the results. Particulate outlet emissions ranged from 0.0055 to 0.0095 lb/MMBTU vs. a design limit of 0.03 lb/MMBTU. System pressure drop was 7.6 in.w.c. at the tested gas volume of 2,589,000 ACFM. When corrected to the design volume of 2,200,000 ACFM the pressure drop was reported to be 5.2-5.5 in.w.c. which was within the contractual limit of 7.0-7.5 in.w.c. In April, 1984 an error was discovered in the duct dimensions used by the test company to calculate gas volume. The actual gas volume was

2,313,000 ACFM. Recalculating the results later indicated the true pressure drop for these tests were 6.6-7.0 in.w.c. For this test, a Kerr-McGee and Kerr-McGee/NERCO blend was fired for a seven day period. Dust loading is typically higher for Kerr-McGee than for the NERCO fuel. As shown in Table 3, inlet load ranged from 1.192 to 1.663 gr/scf for the Kerr-McGee fuel. With either Kerr-McGee or blended fuels, however, outlet emissions were virtually the same, ranging from 0.003 to 0.0062 gr/scf. There was no statistically significant difference between the fuels (see Table 2). Opacity was also unaffected by fuel supply--always measuring less than 5% during all tests and more typically it was at the 0-2 % level. For fuels of similar nature, the observed outlet emission performance similarities were as expected.

PERFORMANCE TEST

In May, 1983 the second of the two contractual tests was conducted. As in the first, particulate removal was exceptional. Emissions were 0.006-.012 lb/MMBTU vs. 0.03 lb/MMBTU design. Results are shown on Table 4. In evaluating the system pressure drop, however, a discrepancy was discovered in the gas volume passing through the system. The stoichiometric and scrubber inlet volumes were significantly below the baghouse inlet volume. The discrepancy was resolved in April, 1984 when HL&P discovered the error in the duct dimensions used by the test company. In April, 1984 the results were recalculated using the corrected dimensions. The new data showed that the system pressure drop for the May, 1983 test was above the design limit when corrected to design conditions. Both the original and corrected data are shown on table 4. The pressure drop of 8.7 in.w.c. at 2,476,000 ACFM was thought to be only 6.9 in.w.c. when corrected to design conditions. Since the true gas volume was 2,213,000 ACFM, the pressure drop was actually 8.8 in.w.c. It should be noted that pressure drop corrections to design conditions were made using the ratio of the design volume to the actual volume, raised to the 2.0 power. There are various authorities that suggest the exponent should be 1.5 to 1.8 for filter cloth. Since a significant portion of the pressure drop in this case is due to ductwork and transition losses, the exponent of 2.0 was used.

Unlike the acceptance test, NERCO coal was fired exclusively for this test. The higher pressure drop, initially attributed to a higher gas volume for the 100% NERCO fuel, was actually due to a reduction in the filter bag permeability. This problem resulted from nodula encapsulation of the bag fibers which reduced the ash release property of the bags. Continued increases in system pressure drop were observed in late 1983 and were conjectured to be due to the firing of the higher sodium NERCO Coal and the above-design gas volume.

Although the effect of the higher sodium was never substantiated, the pressure drop increase and the discrepancy between the baghouse and scrubber inlet volumes led Research-Cottrell and HL&P to a joint program to confirm the data. A third test was therefore agreed to in late 1983 to determine the true gas volume and pressure drop. Several months of preparation and investigations, interrupted by outages, boiler testing and coal supply problems, lead to the running of the test in June, 1984. This test was conducted with 3-dimensional directional probes which measure yaw and pitch

TABLE 2
COAL ANALYSIS

<u>Parameter</u> <u>% by Weight</u>	<u>Kerr-McGee</u>		<u>NERCO</u>	
	<u>Average</u>	<u>Range</u>	<u>Average</u>	<u>Range</u>
. HHV, Btu/Lb	8,476	8,000-8,785	9,407	8,800-9,636
. Proximate Analysis				
Moisture	28.87	25.98-31.30	24.50	21.17-27.67
Ash	5.87	4.77- 8.12	3.63	2.26- 6.00
Volatile Matter	31.35	28.42-33.36	31.83	28.80-34.61
Fixed Carbon	33.91	31.82-37.04	40.04	36.54-43.64
Sulfur	0.49	0.20- 0.76	0.33	0.08- 0.60
. Ultimate Analysis				
Moisture	28.87	27.39-30.80	24.50	21.17-27.67
Ash	5.87	4.77-10.00	3.63	2.26- 6.00
Sulfur	0.48	0.34- 0.79	0.33	0.08- 0.60
Nitrogen	0.71	0.67- 0.78	0.68	0.35- 0.95
Carbon	48.61	45.05-50.98	54.64	50.91-58.11
Hydrogen	3.56	3.10- 3.81	3.79	3.47- 4.09
Oxygen	11.99	10.40-14.02	12.42	10.38-14.94
Chlorine	0.01	0.01- 0.01	0.01	0.00- 0.03

TABLE 3
BAGHOUSE ACCEPTANCE TEST SUMMARY
H. L. & P. CO. / W. A. PARISH 8

Date	<u>JAN 18</u>	<u>JAN 21</u>	<u>JAN 22</u>	<u>JAN 23</u>	<u>JAN 24</u>	<u>JAN 25</u>
Run Nos.	1,2	3,4,5	6,7,8	9,10,11	12,13	14,15
Unit Load (MW)	430	560	525	440	575	575
Coal	K-M	K-M	K-M	Blend	Blend	Blend

Baghouse Inlet Test Location:

11-12

Temperature (°F)	290	322	342	297	340	311
Static Pressure (In.W.C.)	-7.8	-12.0	-9.1	-8.3	-13.2	-12.4
Gas Flow (ACFM) *	2,550,000	2,600,000	2,486,000	1,973,000	2,704,000	2,609,000
Dust Loading (Lbs/MMBtu)	2.966	3.246	3.831	3.480	3.319	2.697

Baghouse Outlet Test Location:

Temperature (°F)	277	304	323	281	320	311
Static Pressure (In.W.C.)	-13.0	-19.2	-16.7	-12.6	-19.4	-18.5
Gas Flow (ACFM)	1,973,000	2,637,000	2,495,000	2,015,000	2,759,000	2,644,000
Dust Loading (Lbs/MMBtu)	.0126	.0093	.0060	.0071	.0071	.0059
Dust Loading (Gr/Scf)	.0062	.0044	.0030	.0036	.0032	.0030

Baghouse Collection Eff.(%)	99.58	99.71	99.84	99.80	99.79	99.78
*Corrected 4/84 to:(ACFM)	2,278,000	2,323,000	2,221,000	1,763,000	2,416,000	2,331,000
Pressure Drop (in.w.c.)						
Measured		7.55	6.98		8.45	7.48
Adjusted		5.33	5.45		5.48	5.24
Corrected 4/84		6.77	6.85		7.00	6.66

TABLE 4
BAGHOUSE PERFORMANCE TEST RESULT SUMMARY
HOUSTON LIGHTING & POWER COMPANY
W.A. PARISH GENERATING STATION UNIT NO. 8

Date	May 4	May 5
Run Nos.	1,2,3	4,5
Unit Load (MW)	575	612
Coal	Nerco	Nerco
Baghouse Inlet Test Location:		
Temperature (°F)	293	323
Static Pressure (In. W.G.)	-12.0	-13.2
Gas Flow (ACFM)*	2,268,000	2,476,000
Dust Loading (lbs/mmbtu)	2.349	1.864
Baghouse Outlet Test Location:		
Static Pressure (In. W.G.)	-18.4	-20.6
Gas Flow (ACFM)	2,371,000	2,618,000
Dust Loading (lbs/mmbtu)	.012	.006
Baghouse Removal Efficiency (%)	99.49	99.68
Opacity (%)	-----	≤5
Scrubber Inlet volume (ACFM)	2,050,000	2,150,000
Stoichiometric volume (ACFM)	1,790,000	2,025,000
* Corrected in 4/84 to: (ACFM)	2,027,000	2,213,000
Pressure Drop (in.w.c.)		
Measured	7.2	8.7
Adjusted	6.8	6.9
Corrected in 4/84	8.4	8.8

angles of gas flow vectors as well as total and static pressures. The previous tests had been run with S-type pitot tubes and static pressure measurements. The results of the test revealed the gas volumes at both scrubber and baghouse inlets were the same. This was expected as the previous inlet duct dimensional error had been corrected. The test also showed the pressure drop was 8.9 in.w.c. at 1,980,000 ACFM. When corrected to the design volume of 2,200,000 ACFM, the pressure drop would be 11.3 in.w.c. Data for the third test is shown in Table 5.

SONIC HORNS

The continuing increase of system pressure drop in early 1984, and lab evidence of nodula encapsulation of the fabric yarns prompted HL&P and Research-Cottrell to pursue a trial demonstration of sonic horns. Two programs were conducted. Research-Cottrell installed and tested combinations of one to five horns in the D-1 compartment and HL&P installed and tested four horns in the C-1 compartment. These tests lead to the decision to install two horns per compartment throughout the system.

The D-1 compartment, five horn test was intended to show the effect of sonic horns on filter bag permeability. The test plan would establish a baseline, then test one, two, three, four and five horns in succession. The increase in gas velocity through the compartment inlet duct at a constant pressure drop would be used to indicate the effect of the horns. The horns were installed in an "X" pattern in the compartment two feet above the bags facing downward above the catwalks. The horns used were 250 HZ acoustic clean sonic sootblowers.

Tests were conducted over the period of June 5-7, 1984. Baseline data established the compartment inlet velocity at 56.9 fps. Fifteen minutes after cleaning with one horn and reverse air, the velocity had increased to 74.2 fps. This velocity increase corresponds to a 41% reduction in pressure drop. These results were duplicated later the first day. The horns remained off overnight during which time the compartment gas volume returned to its previous level. On the second morning, R/A cleaning with two horns resulted in an increase in gas velocity to 78.2 fps. Two horns would be expected to reduce the pressure drop 47%. Data obtained for 3, 4 and 5 horns showed an insignificant further increase in gas velocity through the compartment. Other limitations on the gas volume, which could pass through the compartment, were limiting the effect of the horns. By increasing the gas velocity by 50%, the pressure drop through the inlet duct, tube sheet and outlet duct increases 225%, which offsets the reduction in cloth pressure drop and prevents further gas volume increase. The only results in this program directly reflecting the horn's effectiveness are from the one horn test. A test on an entire baghouse would be required to determine the pressure drop reduction from more horns. These tests did not substantiate the previous suggestion that four to five horns per compartment would be required. Table 5 summarizes the results of the one to five horn, 8D-1 compartment test.

A second test was conducted in the 8C-1 compartment by HL&P using four horns in a square pattern. These tests were run June 8, 1984, with no horns and with four 150 HZ horns installed two feet above the bags in a square pattern. The baseline velocity on 8C-1 was 64.6 fps. After R/A cleaning

TABLE 5
BAGHOUSE 3-D TEST RESULT SUMMARY
H. L. & P. CO. / W. A. PARISH 8

Date (1984)	June 13	June 14
Run	1,2	3,4
Unit Load (MW)	500	500
Coal	NERCO	NERCO
Baghouse Inlet Test Location		
Temperature (°F)	327	329
Gas Flow (ACFM)	2,003,067	1,953,640
Average Absolute Angle (°)	11.9	10.9
Gas Flow (SCFM)	1,225,280	1,196,992
Scrubber Inlet Test Location		
Temperature (°F)	320	327
Gas Flow (ACFM)	2,034,858	2,018,676
Average Absolute Angle (°)	17.5	18.4
Gas Flow (SCFM)	1,202,543	1,287,843
Pressure Drop (in.w.c.)		
Measured	8.90	8.92
Adjusted (to 2,200,000 ACFM)	10.74	11.32

with four horns, the velocity increased to 84.6 fps. These data suggest a 42% reduction in pressure drop would be realized.

We will not conclude any relative superiority of either horn type based on these tests, as it was not our intent to do so. These tests were conducted to determine the number of horns needed to reduce the pressure drop to acceptable levels. The benefits of sonic cleaning to assist reverse air cleaning are significant and can be concluded to be extremely helpful in dealing with pressure drop problems.

Based on the data obtained in these test programs, HL&P installed two horns per compartment in first the "8A" and "8D" baghouses then in the "8B" and "8C" baghouses in June and July, 1984. Pressure drop across the system was reduced from about 7.5 to about 4.5 in.w.c. with two horns per compartment in use at full load.

Analysis of filter bags removed before and after the 8D1 compartment horn application revealed a substantial (32%) increase in permeability. In addition, permeability had been significantly lower at the top of the bag than at the bottom before sonic cleaning, but after sonic cleaning, permeabilities were nearly the same. In addition, permeability at the bottom increased by 18%. Nodula encapsulation was considered greatly reduced and bag residual dust layer weight was down by 39%. Sulphates, which had been gradually increasing, were 3.76% on the pre-horn bag and 2.61% on the bag that had been cleaned with the horns. There was no indication of over-cleaning of the 8D1 bags which might reduce collection efficiency of the system. Table 6 summarizes typical fabric filter bag parameters. In an additional test twelve bags were weighed after a month of operation with two horns installed in a diagonal pattern. The weight of the bags did not vary more than three pounds. This preliminary data suggests only a minimal correlation exists between horn location and residual dust layer build-up on the bags.

CONCLUSIONS AND RECOMMENDATIONS

1. Bag failures noted initially have declined to almost nil after correction of suspension and dust build-up problems.
2. Sonic horns installed at 16,000 sq. ft. per horn have reduced pressure drop by over 40% on WA Parish 8. The system is operating far below original design pressure drop without noticeable effect on stack opacity.
3. Care must be taken during initial start-up to properly coat the virgin filter cloth with dry ash.
4. Bag fabrication quality assurance procedures must be tightly followed for all size orders to insure acceptable serviceability.
5. Bag suspension systems must be capable of reacting to variable bag and operating conditions without binding or bottoming out.
6. The reverse air system must be maintainable with adequate shaft sealing and condensation protection.

TABLE 6
FILTER BAG ANALYSIS SUMMARY
H. L. &P.CO. / W.A. PARISH 8

		<u>Removed</u> <u>11/3/83</u>	<u>Removed</u> <u>2/14/84</u>	<u>Pre-Horn</u> <u>6/4/84</u>	<u>Post-Horn</u> <u>6/7/84</u>
Weight As Rcv'd (oz/sq.yd)	Top	17.5	20.7	22.1	18.77
	Middle	17.4	20.0	21.8	18.92
	Bottom	17.2	18.4	21.5	18.53
Permeability	Top	2.63	1.43	1.62	2.31
	Middle	2.98	1.94	1.80	2.39
	Bottom	3.17	2.37	2.02	2.46
	Average	2.93	1.91	1.81	2.39
Sulphates (% of Total Extractables)		2.89	3.47	3.76	2.61
PH (Extractable Matter)		10.61	11.20	10.77	10.74

7. Cleaning cycle flexibility is essential in adapting to changing conditions of operation.
8. A replacement bag screening program is expected to help HL&P pick the replacement bags.

The work described in this paper was not funded by the U.S. Environmental Protection Agency and, therefore, the contents do not necessarily reflect the views of the agency and no official endorsement should be inferred.

UPDATE ON AUSTRALIAN EXPERIENCE WITH FABRIC FILTERS ON POWER BOILERS

F.H. Walker, Scientific Services Engineer
Electricity Commission of New South Wales
Sydney, NSW, 2000 Australia

ABSTRACT

The paper reports on recent operating experience with power boiler fabric filters in N.S.W. covering the problems encountered with high and increasing differential pressure, failure of dust to release from the bags and premature bag failure. It reviews the remedial measures taken, their success and the continuing problem areas. The paper also discusses the use of an eight cell pilot plant to identify or develop fabric with more suitable characteristics for the filters. The pilot plant uses full size bags and draws flue gas and dust from a 660 MW Eraring boiler and has a design gas flow of 10,000 c.f.m.

INTRODUCTION

The Electricity Commission of New South Wales is responsible for electricity power generation and high voltage distribution of electricity in the state. It has approximately 10,500 MW of installed thermal plant and 3,960 MW of plant under construction and on order for Bayswater and Mt Piper Power Stations.

The plants all burn black coal with an ash content of the order of 20-30% and a sulphur content of 0.3 to 0.7%. Until 1972 electrostatic precipitators, or in the case of older small boilers mechanical collectors, had been used to remove fly ash from the flue gas but because of the very high electrical resistivity of the fly ash the precipitators necessary to meet the requirements of the Clean Air Regulations required high specific collecting areas and what was regarded as considerable maintenance. Investigations into the practicability of using fabric filters commenced in 1966 and resulted in the successful retrofitting of all boilers in four power stations over a period of ten years. These power stations have a combined output of 850 MW and the performance of the fabric filters has been generally satisfactory.

As a result of these successes a decision was taken to fit fabric filters to new plant then being ordered. As a result shaker type fabric filters using homopolymer polyacrylonitrile woven bags were ordered for the new plant to be supplied by James Howden Australia. The first of these new plants Eraring (4 x 660 MW) completed the commissioning of the fourth unit in May of this year. The next, Bayswater (4 x 660 MW) is expected to commission the first two units in 1985 and the second two units in 1986. Mt Piper (2 x 660 MW) is expected to commission units in 1989, and 1990.

This paper is an update on the paper of similar title by Walker and Floyd at the 1983 EPRI Conference on Fabric Filter Technology for Coal Fired Power Boilers and published in the proceedings of that conference.

HISTORY OF DEVELOPMENT

In the mid 1960's it was clear that acceptable stack emission levels could not be achieved with cyclone type collectors which were installed on some of the early plant and that action would have to be taken to improve the performance of some of the early electrostatic precipitators. These precipitators had been installed before the significance of the high resistivity of N.S.W fly ash was fully appreciated. The decision was made to install a trial fabric filter on one half of a 30 MW Tallawarra boiler and to employ shaker cleaning. Because of the very low sulphur content of N.S.W. coals most of the plant concerned has low backend temperatures certainly below 150° C (300° F) and hence the need for a high temperature resistant fabric was not present. A brief trial period with the then available filter bag materials made it apparent that the most suitable was a woven material made from homopolymer polyacrylonitrile fibre. This material has the trade name of Draylon T and is made by the Bayer Company of Germany. The trial plant proved successful, and a decision was taken to install one

large fabric filter for the whole of the Tallawarra 'A' Station (120 MW). The filter has 12 cells which are not individually isolatable and contains a total of 7,200 filter bags each 165 mm (6-1/2 inches) diameter and 5030 mm (16'-6") long. The face velocity of 0.013 m/sec (gas to cloth ratio 2.6:1) was chosen with a design pressure drop of 1 kPa. The specified outlet burden was to be less than 0.05 g/m³ with an inlet dust burden of 30 g/m³. The plant went into service in June, 1974 and has continued in service as required since that date. The design parameters were chosen on the basis that the Tallawarra 'A' Station was approaching the end of its useful life and the plant would be largely intermittent in operation and hence the higher face velocity could be tolerated. The design pressure drop was chosen on the basis that it was all the I.D. fan capability which was available.

Concurrently difficulties were being experienced with electrostatic precipitators on the 60 MW boilers at Wangi and on the 100 MW boilers at Tallawarra 'B' and increasing effort was being required to enable discharge limits to be met. The precipitators which had been designed in the mid 1950's, were undersized for the high resistivity fly ash, and could not meet the requirements of the Clean Air Regulations without flue gas conditioning. A number of design features and the not infrequent washing down to permit maintenance work contributed to the deterioration of the precipitators to the stage where replacement was essential. It was found that shaker type fabric filters could be fitted into the concrete precipitator casings at Tallawarra 'B' using bags of the same dimensions as the 'A' station but with a lower face velocity of 0.011 m/s (gas to cloth ratio 2.1:1) as the 'B' station was expected to have a much higher duty rating.

At Wangi where the electrostatic precipitators specific collecting area had been much smaller, and hence their performance worse, it was found that if the existing reinforced concrete precipitator casings were to be used a pulse type unit with a gas to cloth ratio of 6.7:1 was the best that could be fitted into the casings and so plants with this gas to cloth ratio were installed at Wangi 'B'. The plants have a face velocity of 0.034 m/sec and use bags 114 mm (4.5 inches) in diameter 3,050 mm (10 ft) long. Each boiler has 4,032 bags and the plant is arranged to pulse each bag for a tenth of a second about each 100 seconds.

The successful performance of these plants resulted in the placing of the orders for fabric filters on new plant at Eraring, Bayswater and Mt Piper. The first of the Eraring units went into service in March, 1982, the second in November, 1982. No. 3 was commissioned in July, 1983 and No. 4 in April, 1984.

In early 1982 Tallawarra 'A' station fabric filter which was causing load limitations because of excessive pressure drop across the filter bags was supplemented by the fitting of a 30 MW pulse clean fabric filter supplied by Flakt Australia to No. 1 boiler. This consists of two casings each containing 648 needlefelt Draylon T bags 130 mm (5.1 inches) diameter and 6000 mm (19ft 8 inches) long giving a face velocity of .024 m/sec (gas to cloth 4.7:1).

The greater than expected increase in the rate of load growth which occurred during 1981 made it obvious that the Sydney Metropolitan power stations would be called on to generate a considerably higher output than had been previously expected, particularly in 1982. These power stations are located in the heart of Sydney and were equipped with electrostatic precipitators which could only meet the legal discharge limits with some difficulty and with load limitations. Therefore the decision was taken to replace these precipitators with fabric filters also and an order was placed with Ducon Micropul Australia. Unlike all the other boilers on the system these boilers had exit gas temperatures of the order of 200°C (390°F). It was decided to fit pulse units in the existing precipitator casings as before but utilising fibreglass (Huyglass) to cope with the high gas temperature rather than attempt air attemperation or flue gas cooling. The Pyrmont installation consists of two cells per boiler each cell containing 1716 bags supported on stainless steel cages. The bags are each 3,660 mm (12 ft) long and 114 mm (4.5 inch) diameter. The White Bay installation is similar with each of the four 25 MW boilers being fitted with 2,208 bags to form one cell per boiler.

Table 1 summarises fabric filter installations in New South Wales power boilers.

TABLE 1

Station Name Boiler No. Type	Rating MW	Filter Type	Year in Service	Nominal Gas Flow m ³ /s per boiler	Number of bags per unit	Gas to Cloth Ratio m ³ /s/m ² (cfm/ft ²)
Tallawarra A No. 4A PF	30	MS	1972	38	1320	.011 (2.1:1)
Tallawarra A Nos. 1 to 4 PF	30	MS	1974	250	7200	.013 (2.6:1)
Tallawarra B No. 5 and 6 PF	100	MS	(b) 1975 (c) 1976	170	5760	.011 (2.1:1)
Wangi A No. 1A and 1B No. 2A and 2B No. 3A and 3B SS	25	MS	1976	123	3760	.018 (3.5:1)
Wangi B No. 4 to 6 PF	60	PJ	(4) 1975 (5) 1976 (6) 1976	124	4023	.034 (6:7:1)

TABLE 1 (CONTD.)

Station Name Boiler No. Type	Rating MW	Filter Type	Year in Service	Nominal Gas Flow m ³ /s per boiler	Number of bags per unit	Gas to Cloth Ratio m ³ /s/m ² (cfm/ft ²)
Tallawarra B Eraring Prototype (No. 5 cell 7)		MS	1978 (cell 7)	18	592	.011 (2.1:1)
Eraring No. 1 to 3 PF	660	MS	(1) 1982 (2) 1982 (3) 1982	990	47360	.0076 (1.5:1)
White Bay Nos. 1 & 2 PF	25	PJ	June, '82	64	2022	.023 (4.6:1)
Nos. 3 & 4	25	PJ	Mar. '82	64		.023 (4.6:1)
Tallawarra A No. 1 PF	30	P	July, 1982	78	1296	.024 (4.7:1)
Pymont No. 1 to 4 PF	50	PJ	(1) 1982	120	3432	0.020 (3.9:1)

LEGEND:

PF - Pulverised Fuel
 MS - Mechanical Shaker
 P - Optipulse
 SS - Stoker Spreader
 PJ - Pulse Jet

TALLAWARRA 'A'

As was pointed out previously, this fabric filter was the first major installation in New South Wales and was installed in 1974, it has a high face velocity for shaker type plant and it is a quite early somewhat primitive design. While it was capable of meeting brief peaks at the design maximum output of 120 MW in the initial stages it was unable to sustain this load for any length of time. This limitation became more severe as the service hours increased and bag blinding became an ever increasing problem. After some 5,000 service hours it was impossible to consistently carry out more than 70 to 80 MW on this plant or to briefly peak at more than 90 MW.

The "Optipulse" plant on No. 1 boiler went into service at the end of June, 1982 and has functioned very well since that date. It has currently achieved 3,500 service hours with 268 starts. The plant is set up to operate with a very small differential pressure range to avoid excessive changes in ID fan operation and to give stable furnace combustion conditions. It is arranged to commence pulsing when the differential pressure reaches 85 mm water gauge (3.3 inches) and to stop pulsing when the differential pressure drops to 70 mm water gauge (2.8 inches). On full load of 30 MW the plant normally pulses 12 times per hour and pulses three rows of bags each time. As there are eighteen rows of bags in each filter this means effectively the whole filter is pulsed on average twice an hour. The plant has a normal emission level of .03 g/m³. There have been 20 bag failures in all, most of which occurred during the initial operating period and were due to faults in the fabric. The failures were entirely random both with regard to location in the filter and the position in the bag and most appear to be caused by the batt coming away from the scrim in small areas with resultant erosion and formation of holes.

The "A" Station normally operates with a clean stack.

TALLAWARRA 'B'

The Tallawarra 'B' plant which went into service in 1975/76 has continued generally to give a clean stack, however the early forecasts of expected bag life have had to be modified in the light of experience. It was initially thought that the differential pressure across the bags would rise to a plateau and then stabilise. This has proved to be incorrect and present experience is that the differential pressure continues to climb over the life of the bags. For this reasons bag blinding as well as bag failure must be taken into account when assessing bag life. As a result of continuing experience it is now reckoned that the effective bag life in Tallawarra 'B' is of the order of 17,000 to 19,000 hours. Towards the end of this period difficulties are experienced both due to high differential pressure and to an increasing rate of bag failure. Figure 1 shows a typical graph of bag failures against service hours at Tallawarra 'B'.

WANGI POWER STATION

Wangi 'B' was equipped with Ducon Micropul pulse fabric filters in 1975 and 1976 and have the high gas to cloth ratio of 6.7:1. These filters have also been shown to be quite capable of producing a clean stack but as at other locations the expectation of a stable pressure drop across the bags has not been realised and the differential pressure across the bags continues to rise with service hours to the point where not only are problems being experienced with bag failures but also with differential pressure causing load limitation on the plant. It is now generally accepted the life expectancy of the bags at Wangi is of the order of 10,000 to 12,000 hours before replacement.

The principal mode of bag failure is a longitudinal fatigue type failure of the fabric usually in the top 600 to 800 mm of the bag length.

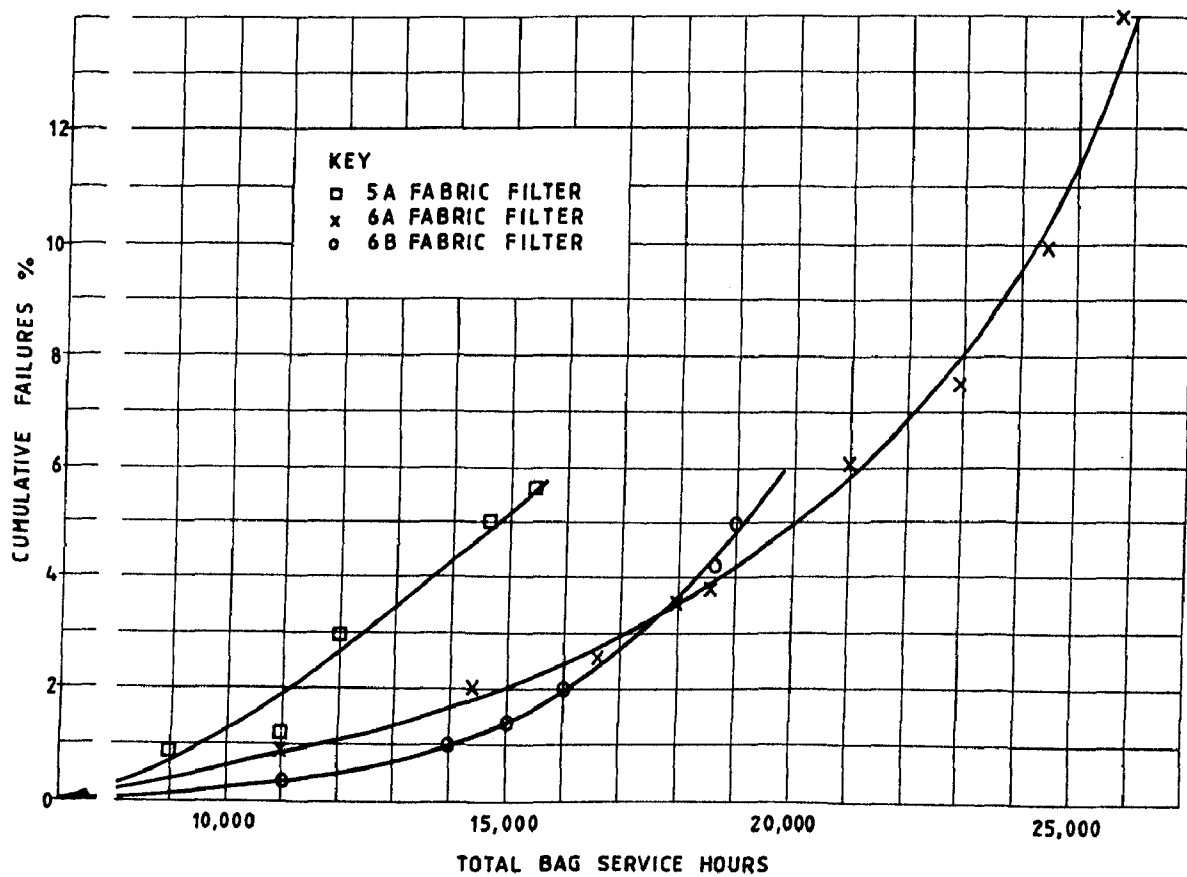


FIG.1 FILTER BAG FAILURES TALLAWARRA

PYRMONT AND WHITE BAY POWER STATIONS

At both power stations the filters are arranged to pulse all bags when the differential pressure reaches a set point currently 0.8 to 1.2 kPa (3.2 - 4.8 inches water gauge). The frequency of pulsing varies considerably but after 1,700 service hours at White Bay is generally three to six times per hour. However, the two filters with the highest service hours have both had periods of high DP and continuous pulsing which have usually occurred on coming into service. After some hours of operation the DP has gradually dropped back to the previous level. The reason for these excursions has not been determined but it is thought to be poor combustion and faulty oil torches when lighting up. The plant being over 30 years old has limited combustion instrumentation.

Since fitting the fabric filters both stations have operated with clean stacks and with an inlet dust burden of some 16 g/m^3 have emission levels of .004 to .02 g/m^3 . A Huyglass bag which was removed for tests after 1,700 service hours and 240 starts showed that its mechanical properties were unchanged from those of the new material.

ERARING POWER STATION

The fabric filter on each of the four 660 MW Eraring Power Station boilers has 40 cells and each cell contains 1,184 bags. Hence the total number of bags for the four boilers is just under 190,000. The gas volume is $990 \text{ m}^3/\text{sec}$ for each boiler. The filter plant was supplied by James Howden and was designed to meet performance guarantees with 10 cells out of service. The bags are woven acrylic and cleaning is by mechanical shaking alone. Figure 2 shows the duct work and cell arrangement in plan. As can be seen each gas path has 10 cells and there are four gas paths.

No. 1 unit at Eraring has operated for 16,000 hours, No. 2 for 11,000 hours, No. 3 for 8,000 and No. 4 for 1,500 hours. The emission levels from the two stacks at Eraring Power Station are satisfactory and both one and two fabric filters met their guaranteed emission levels of less than .05 g/m^3 . A virtually clean stack condition existed until approximately 7,000 service hours when the emission increased to an occasional visible grey haze initially seen as puffs because the bags were showing noticeable bleeding and initial bag failures were being experienced. It is now apparent that the maintenance of a clean stack will depend on the replacement of failed bags as soon as they occur. This also of course requires a decision on the rebagging of complete cells when the number of failures per cell rises to a level where the maintenance requirements of replacing individual bags becomes untenable. Experience has shown that the faulty cells can be easily recognised by studying the smoke density monitor recordings as the cells come out of service for shaking.

However while the Eraring fabric filters have comfortably complied with the emission guarantees considerable problems have arisen with differential pressure and both 1 & 2 fabric filters have failed to meet their guaranteed pressure drop at 8500 hours. Although the boiler outlet gas temperature is

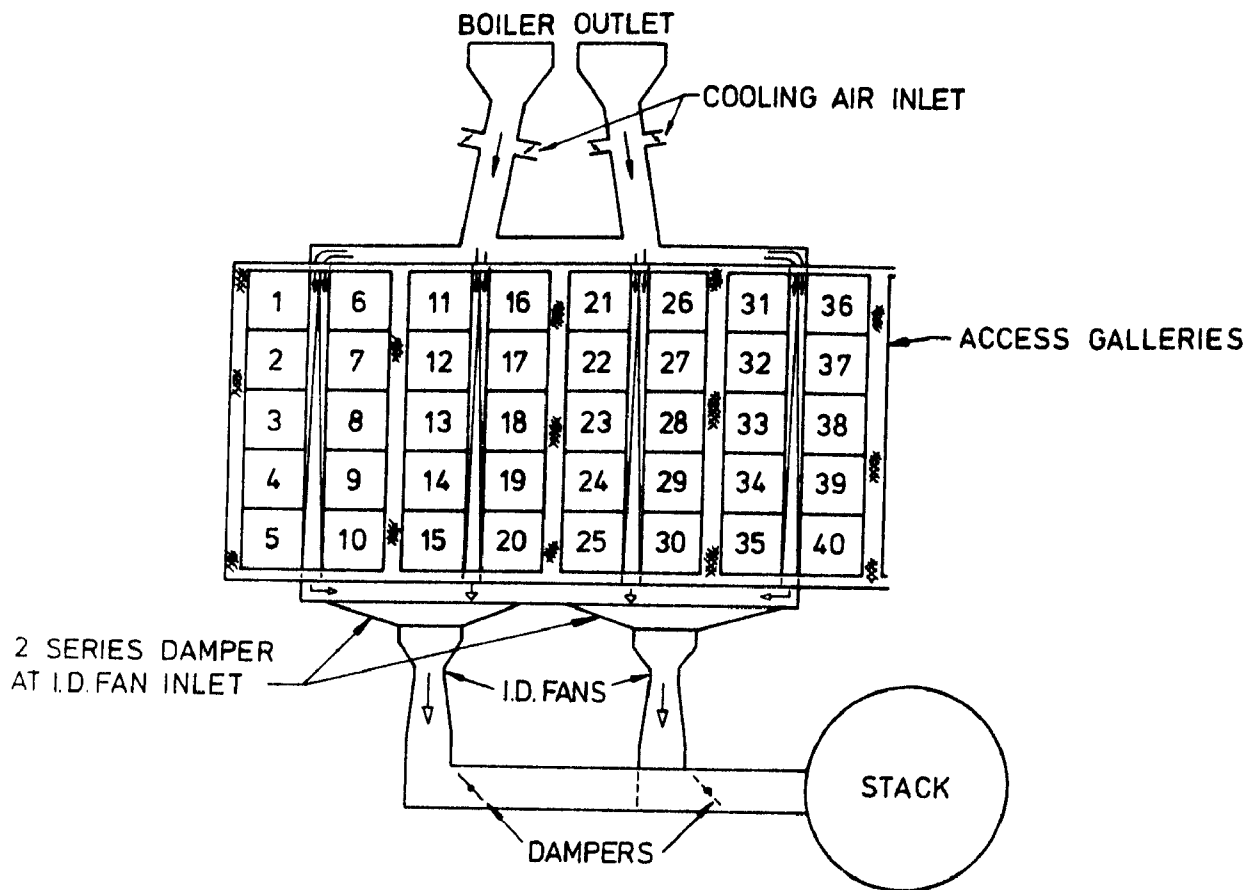


FIG. 2 DUCTWORK AND CELL ARRANGEMENT

higher than expected and results in additional attemperating air flow when ambient temperatures are high, the total gas volume is normally below the 990 m³/s specified for the plant.

The differential pressure across the fabric filters has continued to increase in an irregular pattern on each four boilers since coming into service. Figure 3 shows the variation of differential pressure with time. In an attempt to obtain a more meaningful graph and to compensate for load variations and variations in the number of cells in service the differential pressure has been divided by megawatts and corrected for cells in service and the resulting curves smoothed.

When the problem of excessive pressure drop first became apparent the options of varying the cell shake period settings and increasing shaking time were tried in several variations and with only limited improvement. The early shaker period was 95 seconds being made up of a 10 second dwell, 30 second shake and 55 second post shake dwell. The present period is 112 seconds comprising a 2 second dwell 60 second shake and 50 second dwell. This gives a slip time of 45 seconds. The Contractor also tried variations in shaker frequency. It was found that increasing the frequency to about 9 Hz from the standard 7 Hz had a short lived effect of a minor improvement in the DP while decreasing the frequency to about 4 Hz produced effectively no cleaning at all.

The amplitude of shaking was then increased from the normal 20 mm peak to peak to 30 mm peak to peak and this had a somewhat more marked affect but did not reduce the pressure drop by a significant amount or arrest the gradual long term DP increase. It also produced a number of failures in the shaker mechanism and the amplitude has been restored to the original 20 mm.

A major feature at Eraring is the inability of the shake to dislodge the dust from the bags. The result is that a bag which has been in service for some thousands of hours at Eraring will weight between 10 to 15 kg whereas a similar bag at Tallawarra with an identical shaker system weighs between 3.5 and 5 kg. A clean bag weighs 1.5 kg. An extensive series of tests involving weighing 104 bags in each of the 40 cells showed that the bag weights varied widely within each cell as did the mean weights between different cells.

Investigations into the cause of the DP problem are proceeding however the magnitude of the pressure drop across the filter on No. 1 boiler reached a level where the Commission decided to rebag the 10 worst cells in May, 1983 after 8,500 service hours to ensure that the boiler could operate at full load throughout the winter and not be load limited by bag differential pressure. The complete rebagging of No. 1 commenced in December, 1983 and the process is continuing. Bag failure levels were also causing concern and the first cells rebagged have been done because of excessive bag failure rates as well as high pressure drop. There is great variability in failure rate between cells. In the worst cell, 24.7% of bags failed and in several cells there were effectively no failures. The high and low failure rate cells show no pattern across the filter. The total failure rate at 16,000

12-11

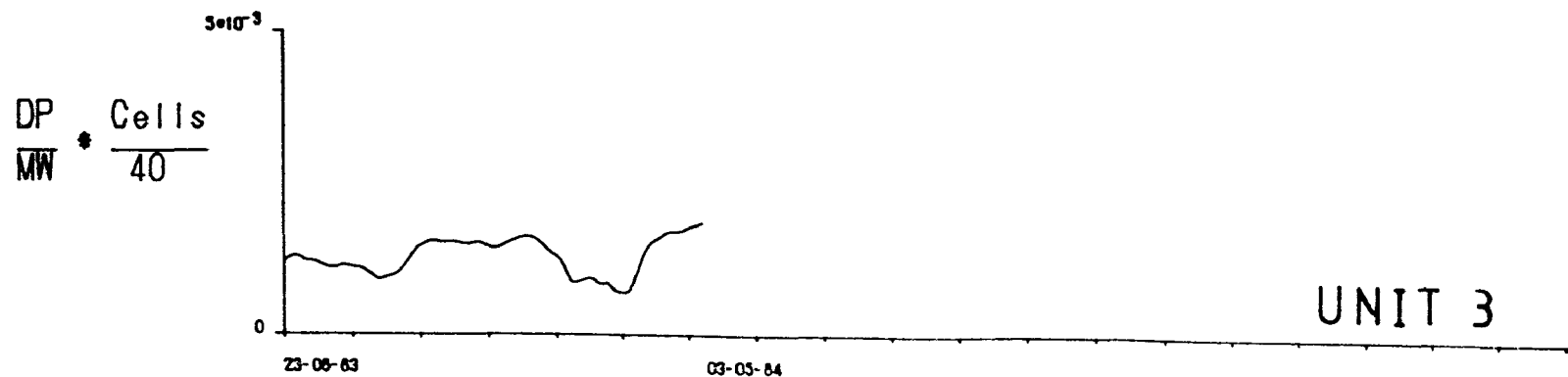
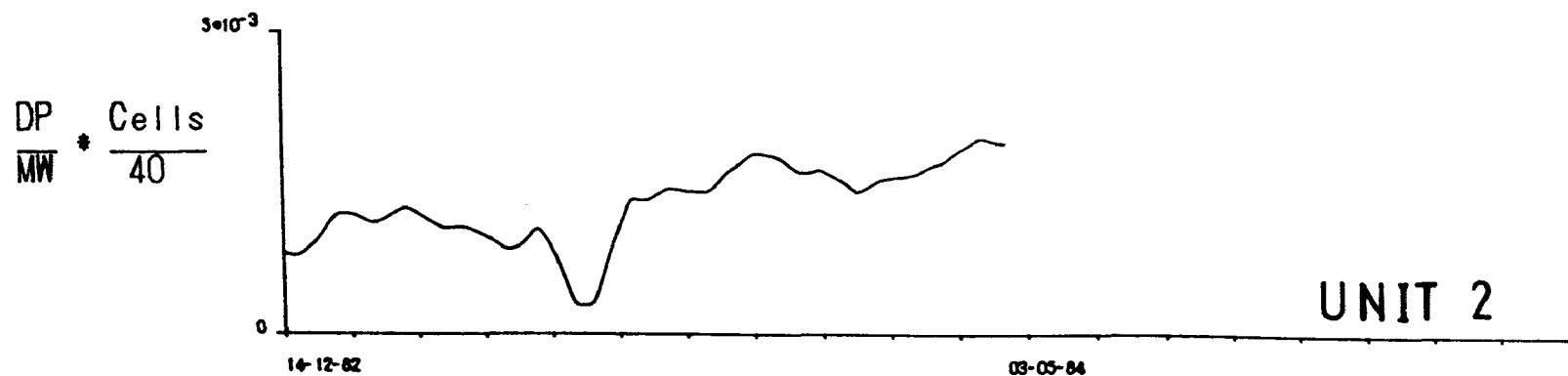
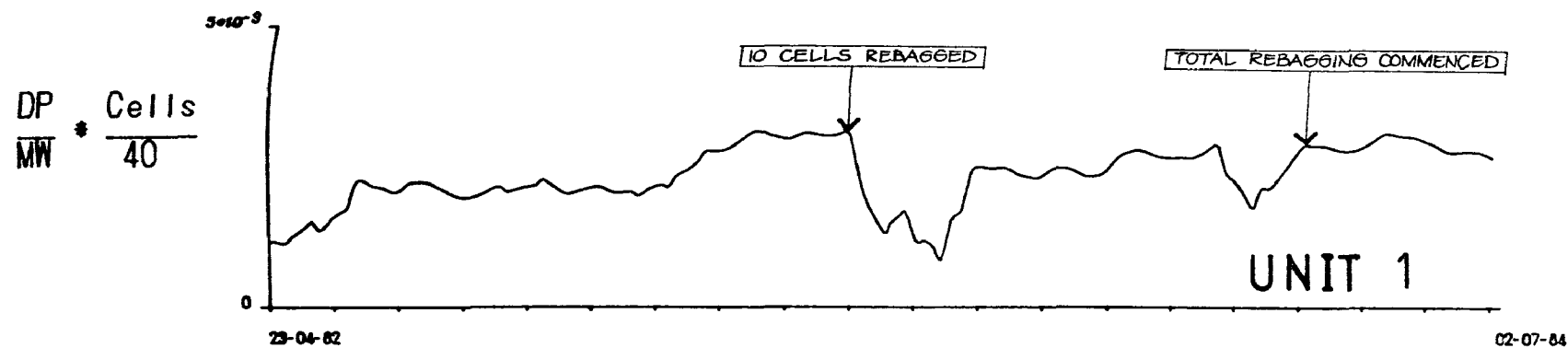


FIG. 3 ERARING UNIT FABRIC FILTER DATA (SMOOTHED)

hours is in excess of 4.9%. This figure is confused by the fact that 25% of the cells were replaced for high DP at 8,500 hours. Figure 4 shows bag failure rates in three of the worse cells and the total bag failure rate for No. 1 fabric filter. The fabric filter on No. 2 boiler has followed a very similar pattern with differential pressure and it is likely that rebagging of that unit will commence towards the end of this year. The pattern for No. 3 boiler fabric filter is also very similar except that the differential pressure appears to be marginally lower, however this position is clouded by the fact that No. 3 Unit has had far more low load operation than the other two units due to system requirements.

No. 4 unit which has recently gone into service has cells of singed bags and it is expected that this unit will operate with improved DP.

Although extensive model tests were carried out to ensure even flow distribution to all cells when the plant was designed the variation in flow between cells on the plant is excessive with some cells having up to three times the flow of others on the same boiler. Dust distribution to the individual cells also varies considerably. Some initial tests have been done in an endeavour to measure the dust catch in each cell and work is at present going on to refine methods so that better assessment of this factor can be made. Due to the plant layout it is effectively impossible to measure the dust concentration in the gas entering each individual cell. There is no obvious pattern to flow distribution at this stage with low and high flow cells at times being adjacent but there is a trend for the cells towards the front of the collector to have higher flow. There is also a similar disposition of low and high flow cells on both 1 and 2 fabric filters.

It was originally assumed that poor flow distributions were due to poor dust distribution. As the common inlet manifold makes measurement of inlet dust burden to individual cells impossible tests have been carried out measuring the dust collected in individual cells of the gas pass during a cleaning cycle and the samples so collected have been sized. However, the tests so far have showed little correlation between the various parameters and attempts to correlate average cell bag weight with cell DP and with bag failure rates have been unsuccessful.

A study has been made of dust characteristics in an endeavour to determine reasons for the different behaviour between Tallawarra and Eraring. For reasons which are yet unexplained a considerable build up of dust up to 25 mm thick occurs on the inlet spigots of the bags at Eraring whereas no such build up occurs at Tallawarra.

A considerable suite of chemical analyses of dust from both locations has been made and typical analyses are shown on table 2.

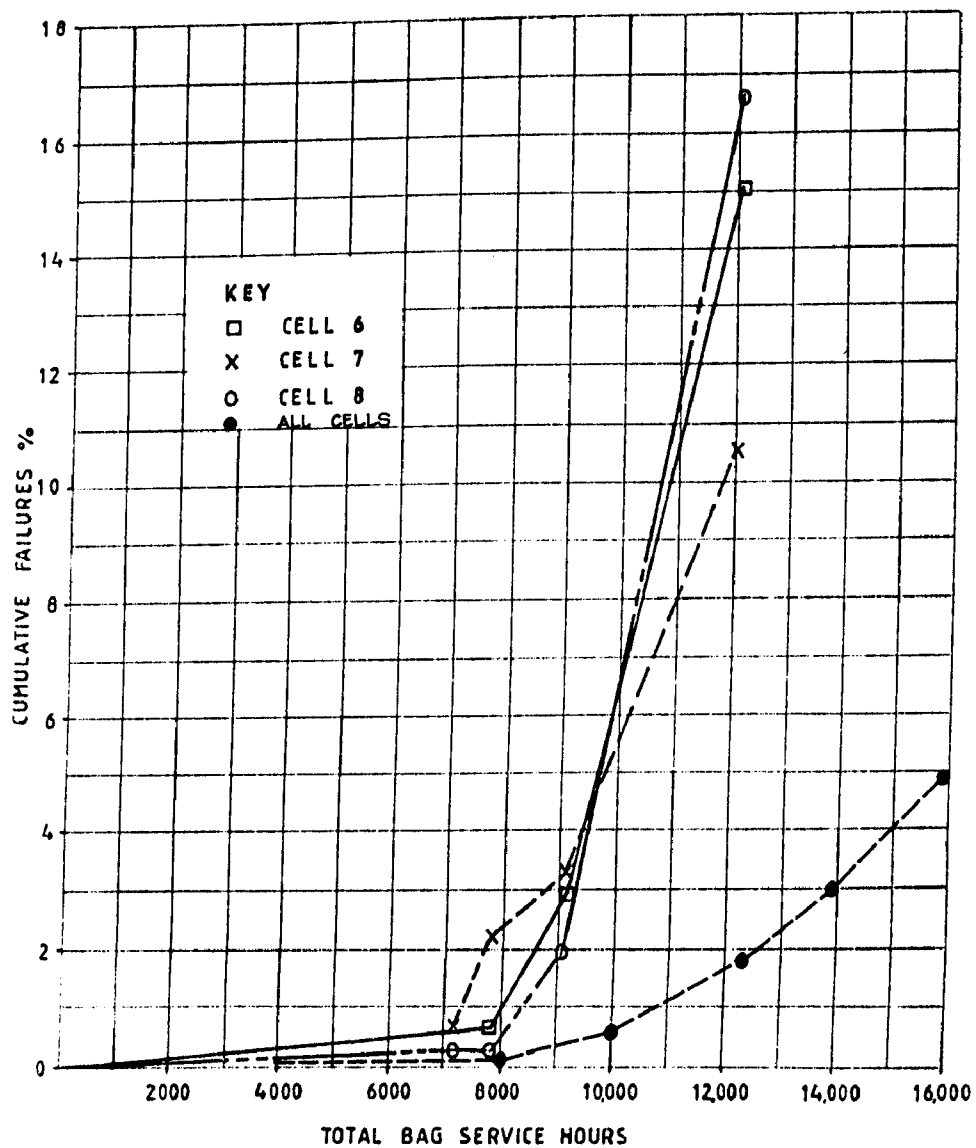


FIG.4 FILTER BAG FAILURES -UNIT 1 ERARING

TABLE 2
CHEMICAL ANALYSIS OF ERARING AT TALLAWARRA FLY ASH

Element	Eraring	Tallawarra
Combustible	2.04	2.50
Al ₂ O ₃	27.54	21.30
BaO	0.05	0.07
CaO	0.71	0.75
Cr ₂ O ₃	0.01	0.01
CuO	0.01	0.02
Fe ₂ O ₃	3.43	5.90
K ₂ O	1.06	1.10
MgO	0.60	0.48
Mn ₂ O ₄	0.08	0.14
Na ₂ O	0.39	0.05
NiO	0.01	0.01
P ₂ O ₅	0.10	0.05
Rb ₂ O	0.01	0.01
SiO ₂	62.38	66.50
SrO	0.03	0.03
TiO ₂	1.16	0.88
V ₂ O ₅	0.03	0.02
ZnO	0.01	0.01
ZrO ₂	0.05	0.05
SO ₃	0.03	0.07
TOTAL	<u>99.70</u>	<u>99.85</u>

From this table it will be observed that there are no dramatic differences in dust composition. Similarly dust sizing has been carried out on many samples from both Eraring and Tallawarra and again there is little difference in the sizing.

Table 3 shows typical sizing of isokinetically sampled dust from Eraring and Tallawarra.

TABLE 3
DUST SIZING
ERARING AND TALLAWARRA FLY ASH

<u>Size</u>	<u>Eraring</u>	<u>Tallawarra</u>
-176 um	97.4%	99.6%
-125	95.4	98.0
-88	89.8	91.0
-62	83.1	85.9
-44	72.8	74.5

TABLE 3 (CONTD.)

<u>Size</u>	<u>Eraring</u>	<u>Tallawarra</u>
-31	60.1	58.8
-22	48.0	41.3
-16	37.8	26.3
-11	27.2	14.8
-7.8	18.5	7.4
-5.5	12.8	4.0
-3.9	6.7	1.5
-2.8	2.2	0.7

A study of the water soluble components in the isokinetically sampled dust from both stations has also been made and the results are tabulated in Table 4.

TABLE 4

	<u>Range ug/g</u>		<u>Mean ug/g</u>	
	<u>Eraring</u>	<u>Tallawarra</u>	<u>Eraring</u>	<u>Tallawarra</u>
Calcium	387-1320	714-746	926	730
Magnesium	0.53-11.6	12.0-29.3	2.49	20.6
Sodium	14.7-26.7	4.9-13.3	19.0	9.1
Potassium	5.9-17.6	18.4-42.7	11.2	30.6
Sulphate	680-2120	986-1520	970	1253
Total Alkalinity ug CaCO ₃ /g	880-2066	240-986	1523	613

While there are obvious differences in soluble components the significance, if any, of the differences is at yet unknown.

Work by Dr. P. Arnold at Wollongong University on dust flow characteristics has shown that there are considerable differences between the dusts from the various power stations with the Tallawarra dust being much more free flowing than that at Eraring.

Investigations are proceeding into the physical and chemical properties of the dust in the hope that better understanding of the filtration process can be achieved.

The prospect of improving plant performance by changes to fabric characteristics is also being investigated.

One attempt to improve plant performance by reducing the dust loading on the fabric was the use of the original fabric singed on one side to give a smoother inside surface to the bag. Early bag weights are promising as are the early differential pressure figures, however the tests have not run for sufficient time to establish if this is a long term solution to the problem.

In a further endeavour to improve fabric performance generally, an eight cell pilot plant was moved to Eraring and placed in service drawing flue gas and dust from No. 3 boiler. This pilot plant consists of eight cells each of which contains 20 full size bags. The plant is arranged so that the gas flow is controlled to each cell to give a constant gas to cloth ratio of 2:1 and is set up to record gas inlet temperatures, differential pressure on each cell and other parameters.

One half of the pilot plant is owned by the contractor and the other half by the Electricity Commission. The plant is being used to assess new fabrics prior to cell scale trials in the main plant and at least one promising development in addition to the singed version of the fabric which was used in the original bags has already come to light.

The singed fabric when tried in the pilot plant carries a dust load about 50% of that of the unsinged bag while one of the development fabrics carries a dust load of about 25% of the unsinged material. Also currently under trial are two laminate type fabrics both of which are showing considerable early promise.

CONCLUSIONS

Operating experience at five EC of NSW power stations has underlined the fact that even with coals with very similar characteristics and ash analyses the long term performance of identical fabrics in similar plants in different power stations can vary widely and at this stage unpredictably. However, the EC of NSW remains committed to fabric filters as the long term answer for particulate emission control.

ACKNOWLEDGEMENTS

The assistance of The Electricity Commission of New South Wales Generation Division staff and Power Projects/Design Group staff who are involved in the various fabric filter projects and who have contributed in the preparation of this paper is thankfully acknowledged.

The work described in this paper was not funded by the U.S. Environmental Protection Agency and therefore the contents do not necessarily reflect the views of the Agency and no official endorsement should be inferred.

REFERENCE

1. F.H. Walker and G.J. Floyd "Operating Experience in Asutralia with Fabric Filters on Power Boilers" Second Conference on Fabric Filter Technology for Coal-fired Power Plants March 22 - 24, 1983.
2. A.N. Lamb and G.W. Rigden "Fabric Filters for Cleaning the Flue Gases from Ten 660 MW Coal Fired Boilers in New South Wales, Australia" Sixth World Congress on Air Quality of the International Union of Air Pollution Prevention Associations - May, 1983.
3. G.J. Floyd and A.TH.M Vanderwalle "Australian Experience with Fabric Filters on Power Boilers" EPRI Conference on Fabric Filter Technology for Coal Fired Power Plants, Denver, Colorado, July, 1981.
4. F.H. Walker, A.N. Lamb, C. Robertson and B. Any "Experience with fabric filters in New South Wales Power Stations". The 8th International Clean Air Conference, Melbourne, May, 1984.

Session 15: FF: FUNDAMENTALS/MEASUREMENT TECHNIQUES

David S. Ensor, Chairman
Research Triangle Institute
Research Triangle Park, NC

MODELING BAGHOUSE PERFORMANCE

David S. Ensor, Douglas W. VanOsdell, Andrew S. Viner,
and Robert P. Donovan

Research Triangle Institute

P.O. Box 12194

Research Triangle Park, North Carolina 27709

Louis S. Hovis

U.S. Environmental Protection Agency

Industrial Environmental Research Laboratory

Research Triangle Park, NC 27711

ABSTRACT

A mathematical model to predict the performance of a baghouse is desirable to allow design of industrial-scale equipment and as a research tool. The important modeling approaches taken in the past are reviewed, and some of the critical issues identified. An important part of a filtration model is the description of the particle deposit on the filter. The areal permeability and mass distribution are the primary unquantified parameters. Mathematical approaches taken in the current modeling effort are summarized.

This paper has been reviewed in accordance with the U.S. Environmental Protection Agency's peer and administrative review policies and approved for presentation and publication.

INTRODUCTION

OBJECTIVE OF RESEARCH

Fabric filtration is simple mechanically but depends on complex physical phenomena to remove particles from the gas stream. The fabric acts as a support for deposited particles which in turn collect particles from the gas stream. The ultimate goal of the present research is a predictive model for baghouse design based on fundamentals of aerosol science. Currently the design of baghouses is based on pilot-plant data or experience on full-scale units collecting similar emissions. A computer model developed by EPA (1) has received limited use in aiding design largely because of the lack of data taken specifically as model inputs and the inability to describe the properties of the ash-fabric system.

OVERVIEW OF PAPER

This paper traces the development of concepts in filtration science and indicates their application to air emissions control. The current approach taken by RTI in filtration model development is reviewed. This paper is limited to reverse-air and shake/deflate designs. The major emphasis will be on pressure drop through the filter. Usually the collection efficiency is more than sufficient to meet existing air pollution limitations

and is not a limiting factor in the application of filtration in air pollution control. Also, a recent review of baghouse modeling by Viner et al. (2) indicated that the currently available design model is a reasonably good predictor of particle collection efficiency but less reliable for pressure drop prediction. In addition, the potential approaches for future research are indicated.

FABRIC FILTER MODELING

PRESSURE DROP IN A POROUS MEDIA

Darcy's Law

The observation of the proportionality of the flow rate of a liquid through a sand bed to the pressure head across the bed was reported in 1856 by Darcy (3). Darcy's law forms the basis of porous media fluid dynamics. The law is valid for a homogeneous porous media under conditions of laminar flow, typical of most applications of fabric filtration. Darcy's law is invalid for liquids at high velocities and for gases at both very low and very high velocities.

Darcy's law is given by:

$$Q/A = k (P_2 - P_1)/h \quad (1)$$

where

Q = the flow rate

A = the area of the bed

Q/A = the face velocity (V)

k = the permeability of the porous media

P_2, P_1 = the pressures at the top and bottom of the bed (ΔP), respectively

h = the bed height.

Modifications of Darcy's Law for Fabric Filtration

In fabric filtration, the exact height of the deposit of dust is very difficult to measure because of the fragile nature of the deposit. The filtration equation has been modified by replacing bed height with more easily measured properties (4):

$$h = W/\rho_r = W/\rho_p (1 - \epsilon) \quad (2)$$

where

h = the dust cake thickness

W = the mass of dust per unit area

ρ_r = the bulk density of the dust deposit

ρ_p = the bulk density of the material making up the particles

ϵ = the dust cake porosity.

The porosity is given by:

$$\epsilon = \frac{\rho_p - \rho_r}{\rho_r} \quad (3)$$

Equations (1) and (2) can be rearranged to yield the following for $P_2 - P_1$ (or ΔP):

$$\Delta P = \frac{W V}{k \rho_p (1 - \epsilon)} = K_2 W V \quad (4)$$

where

K_2 = the specific cake resistance

V = the face velocity.

Because the fabric is cleaned to reduce pressure drop, as suggested by Stephan et al. (5), the equation is often written:

$$\Delta P/V = S = S_e + K_2 W \quad (5)$$

where

S = the drag of the system

S_e = the residual drag of the fabric and dust

$K_2 W$ = the drag of the layer of particles.

Equation (5) is a re-expression of Darcy's law resulting from only some algebraic manipulations to simplify application. The permeability is contained in the specific resistance, K_2 , which is the slope of the drag versus mass concentration curve. The residual drag, or the point where the dust can no longer be cleaned from the fabric, represents a lower limit of drag. In practice, it is very difficult to determine the boundary between the filter cake and fabric because of the projection of fibers from the fabric. Also it is not often apparent in which range on this curve a given baghouse is operating. The system drag after an ineffective cleaning may be greater than the possible residual drag for the filter.

This well-known derivation was reviewed to show where the important assumptions lie in the application of Darcy's law. Also, some confusion exists in the air pollution field as to the relationship of Darcy's law with the accepted fabric filtration equations. Two critical issues should be considered: (1) the accuracy of prediction of K_2 from fundamental properties of the particle deposit, and (2) the assumption of a homogeneous dust bed.

ACCURACY OF PREDICTION OF K_2

A fundamental aspect of filter modeling is the accuracy of the pressure drop prediction through a uniform layer of particles. This is accomplished by drawing upon previous work in applying fluid dynamics theory to porous media. Rudnick and First (6) presented an extensive review of theoretical K_2 prediction. They presented a basic equation:

$$K_2 = R \left[\frac{1}{\tau C} \right] \quad (6)$$

where

R = the resistance factor

τ = the particle relaxation time

C = the slip-correction factor.

The quantity τ in the above equation is defined by Stokes' law as:

$$\tau = \frac{\rho_p D^2}{18 \mu} \quad (7)$$

where

ρ_p = the particle density

D = the particle diameter

μ = the viscosity of the fluid surrounding the particle.

In Equation (6), the quantity in brackets represents the drag per unit mass on a single particle in an infinite medium. This is the minimum value of K_2 that is physically possible. The resistance factor, R , is always greater than 1.0, accounting for the fact that, as the distance between particles decreases, the drag on each particle increases. As the porosity (or void volume) of the dust cake decreases, K_2 will increase. The solution of the Navier-Stokes equations has been reported for a number of idealized geometries such as parallel capillaries through the media, the Kozeny-Carmen model (7), and cells formed by the void spaces between the particles, the cell or free surface model (8,9). The Kozeny-Carmen equation is given by:

$$K_2 = \frac{\mu k S^2 (1 - \epsilon)}{\rho_p \epsilon^3} \quad (8)$$

where

S = specific surface of bed (the surface area of the particles divided by the volume of the particles).

The Happel (9) solution for the cell or free surface model is:

$$R = \frac{3 + 2(1 - \epsilon)}{3 - 4.5(1 - \epsilon)^{1/3} + 4.5(1 - \epsilon)^{5/3} - 3(1 - \epsilon)^2} \quad (9)$$

This equation has no empirical constants and allows the computation of the pressure drop directly. It is currently used in the EPA model (10), although the Kozeny-Carmen expression was used in the earlier version of the EPA model (1). The two models yield different specific bed resistances at high porosities.

The diameter D suggested by Carmen (7) is the volume-surface mean or Sauter mean diameter. Happel also supported the use of the volume-surface mean in the free surface model. However, Rudnick (11) showed that the applicable model for the free surface model is the volume-length diameter defined by:

$$D_{vl} = \frac{\sum_i^n (D_s^3)_i}{\sum_i^n n_i (D_s^2)_i} \quad (10)$$

where

D_{vl} = the volume-length mean diameter

D_s = the Stokes diameter.

Rudnick (11) demonstrated with filtration experiments conducted with Arizona road dust that good agreement within 20 percent can be obtained with experimental K_2 's (from Equation (5)) and K_2 's obtained (Equations (6), (7), (9)) with measured particle size distribution and porosity. Dennis and Dirgo (12) reported that K_2 's (from Equation 5)) were 3.3 times larger than the values obtained with Equations (6), (7), and (9). Dennis and Dirgo (12) had little explanation other than to recommend experimental values of K_2 . However, based on Rudnick's good agreement between the Happel equation and experimental data, we believe that the primary problem lies not in the theory but in the ability to measure the ash properties needed in Equations (6), (7), and (9). This conclusion is illustrated with the following error analysis of K_2 prediction.

The Happel equation was evaluated over the range of possible experimental error in the various parameters. It was assumed that the particle size distributions could be described by the log-normal equation. The parameters considered were the mass mean particle diameter (MMD), geometric standard deviation (σ_g), and the porosity (ϵ). The error analysis was conducted assuming that the errors affected only one parameter at a time; the other two were held constant. From Equation (7), the particle diameter is expected to affect the K_2 value with some amplification as shown in Figure 1. The MMD* represents the "true" mass mean diameter of a dust sample, and MMD represents the "measured" value. Similarly, K_2^* represents the "true" value, and K_2 represents the value predicted from Equations (6), (7), and (9). If the measured MMD is 5 percent larger than the true MMD, then the predicted K_2 will be roughly 9 percent less than the correct value. If the measured MMD is 5 percent less than the true MMD, then the resulting error in predicted K_2 is roughly 11 percent.

A similar approach was taken with the measured (σ_g) and true (σ_g^*) standard deviations shown in Figure 2. However, the sensitivity of K_2 to the error in σ_g depends on the magnitude of σ_g^* . The larger the σ_g^* , the greater the error of K_2 .

The effects of errors in the measured porosity on K_2 are shown in Figure 3. Although the amplification of error in K_2 from errors in porosity also depends on the magnitude of the real porosity (ϵ^*), the predictions of K_2 are most sensitive to errors in the measured porosity (ϵ^*). In fact, as shown in Figure 3, the reported discrepancy between measured K_2 's and K_2 's computed from the particle properties can possibly be accounted for by errors in the measured porosity.

Other reasons have been cited for the differences between theoretical and experimental K_2 values. A log-normal size distribution was assumed by Dennis and Klemm (10) in the baghouse model. As reported by McElroy et al. (13), fly ash may have two log-normal distributions with distinct modes instead of the assumed single-mode distribution. Application over too broad a particle size distribution may not have a deposit with the well-defined model geometry used in the derivation (14,15).

PARTICLE SPATIAL MASS DISTRIBUTION

The fundamental assumption in Darcy's law is a uniform porous media. However, the particle deposit may develop a very nonuniform structure after the cleaning segment of the filtration cycle. Dennis et al. (16) reported that collected dust tended to shed from the filter in patches. Carr and Smith (17) similarly observed that the particle deposit after cleaning was nonuniform; the reverse-air cleaning of bags tended to reduce the particle depth along the folds of the fabric.

It should be pointed out that these observations do not invalidate Darcy's law but do drastically change the appropriate application. The law should be applied to small elements of the filter and then integrated over the whole area of the filter. This approach requires the introduction of the spatial ash distribution to account for the heterogeneous filter cake.

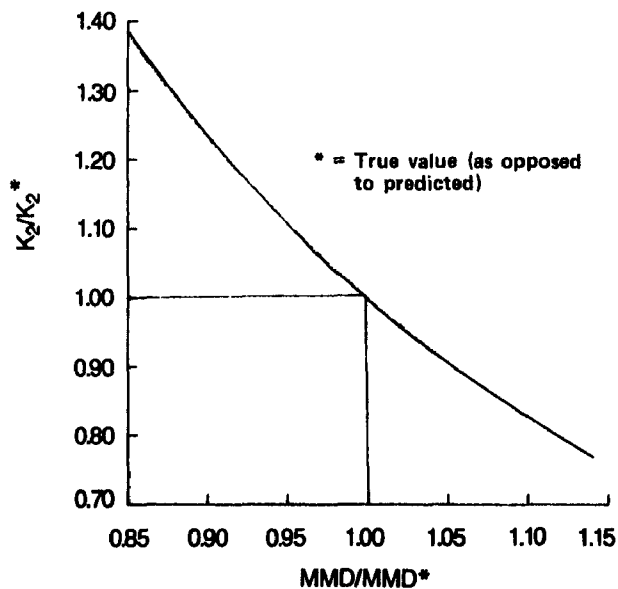


Figure 1. Effect of error in mass mean diameter on K_2 .

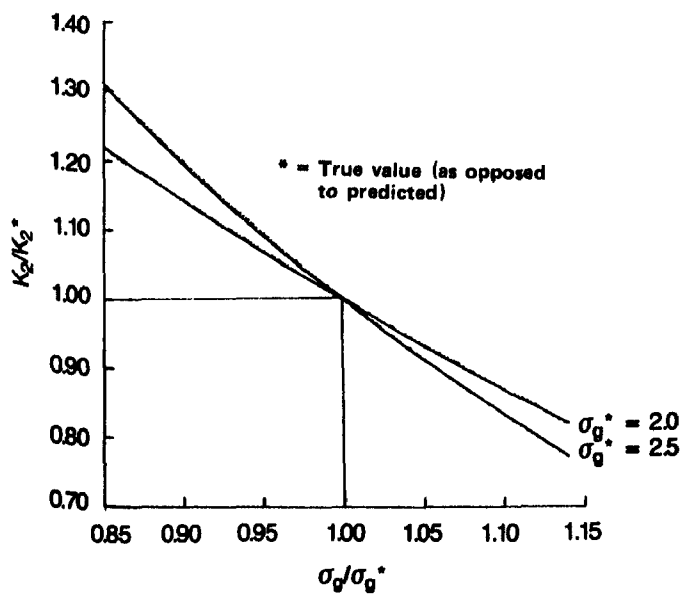


Figure 2. Effect of error in geometric standard deviation on K_2 .

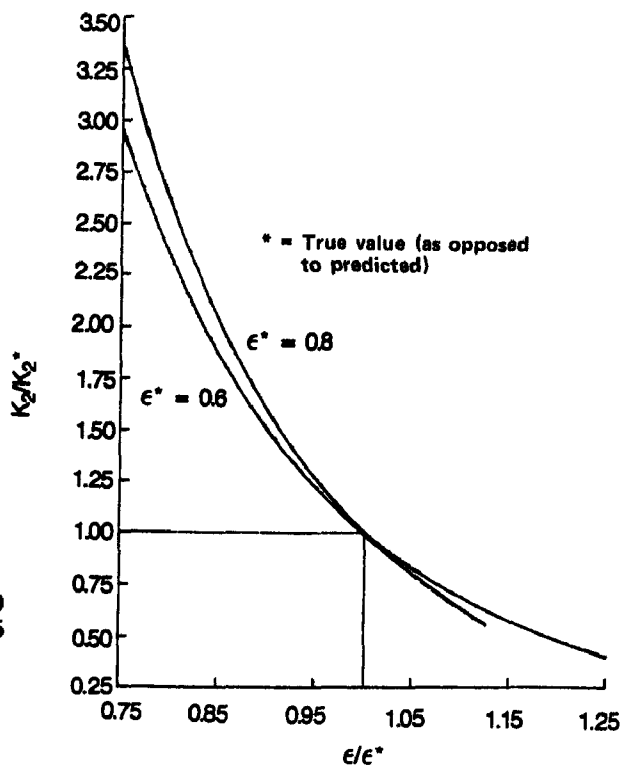


Figure 3. Effect of error in porosity on K_2 .

A similar approach has been suggested in porous media modeling as pointed out by Lyczkowski (15).

Therefore, the particle mass distribution and ash properties need to be examined at a small scale on the fabric. The EPA model (10) assumes that the ash with the deepest layer is removed as a patch. The area of the patch depends on the cleaning energy and fabric loading. In effect, as the calculation progresses, a mass distribution of ash on the surface of the bag is computed. A baghouse model suggested by Morris and Millington (18) uses drag as a function of position on the fabric, $S(x,y)$, as a primary parameter. The importance of the ash distribution function in the filtration equations was pointed out by Cooper and Riff (19) as an adjustment to mean properties of the filter ash deposit. A conceptual diagram of the shape distribution functions of deposited ash is shown in Figure 4. The ash layer during the filtration part of the cycle tends to approach a uniform layer with a narrow distribution because the thin areas offer a lower resistance to the dust-laden gas and are preferentially built up by depositing particles. When the fabric is cleaned, the ash mass distribution will broaden and will be lowered because the easily cleaned areas will lose more ash than other areas.

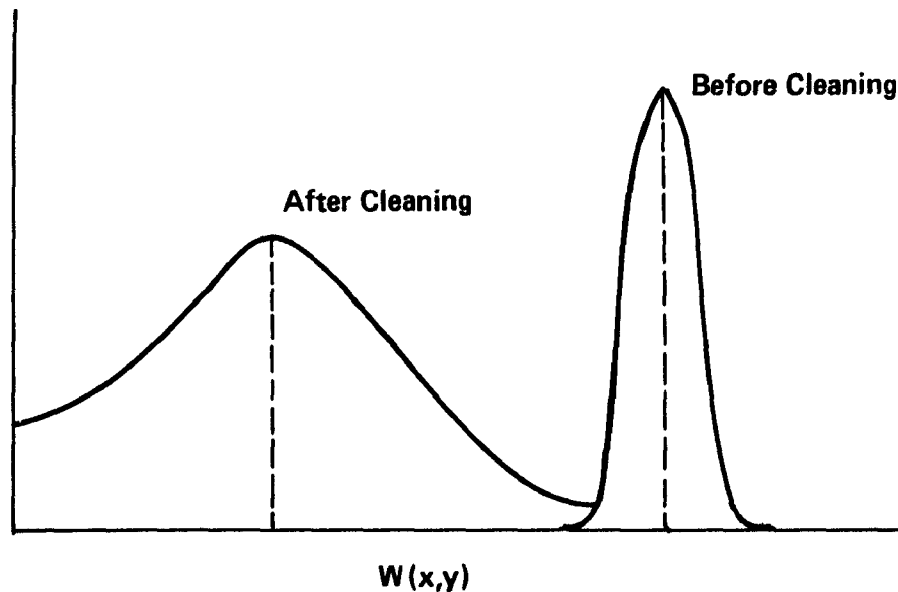


Figure 4. Hypothetical mass distribution history on bag fabric.

Incorporation of this concept into baghouse design will require determining the mass distributions and relating them to baghouse operation. Pressure drop is computed by a numerical integration over the surface of the bag. The design equation is given by:

$$\Delta P = \Delta P_{\text{filter}} + AV \left[\int_x \int_y \frac{1}{S(x,y)} dy dx \right]^{-1} \quad (11)$$

where

ΔP_{filter} = residual pressure drop

A = filter area

V = face velocity

$S(x,y)$ = spatial drag distribution.

The point drag $S(x,y)$ is a function of the cleaning process and the filtration cycle.

The EPA baghouse model is a special case that tends to produce a triangular-shaped mass distribution function. The exact shape of drag and mass distribution under various conditions is the subject of ongoing research. Viner et al. (20) describe the development of a beta gauge for mapping mass distributions on filters which will ultimately be used in new baghouse predictive models.

PARTICLE DEPOSITION MODELING

The deposition of particles on the filter is fundamental to the performance of the filter. It has been the practice of filter investigators to treat the filter as a deterministic system. In reality, fabric filtration is a stochastic process with a behavior at any given time that is related to the previous history of the system. This is partially true because of the effects of fibers protruding through the dust layer, adhesion of particles, and the effects of electrostatic charges and fields. The present investigation incorporates the use of an "instructional model," one that is developed to learn about a process rather than serve as a definitive physical or design model.

RANDOM PACKING MODEL

The random packing of spheres is of wide interest in the physical sciences such as metallurgy, ceramics, soil science, physics, and chemistry. Monte Carlo simulations of packing utilize a random initial location of a particle and then the subsequent application of a series of rules to simulate the physical system (21).

The key to the present model is development of rules that correspond to general attributes of physical processes. These rules are summarized in Table 1 and are applied after the "particle" is released at a random location at the top of the computer screen. The particle drops to the bottom of the screen.

TABLE 1. PACKING RULES

Figure	Physical simulation	Logic guiding dropping particle
5	Nonsticky particles	<ul style="list-style-type: none"> • If a stationary particle is not present at next lower position, advance dropping particle
6	Sticky particles	<ul style="list-style-type: none"> • If a stationary particle is not present at next lower position, advance dropping particle • If a stationary particle is present at either or both sides of next lower position, stop dropping particle
7	Sticky particles with attraction	<ul style="list-style-type: none"> • If a stationary particle is not present at next lower position, advance dropping particle • If a stationary particle is present at either or both sides of next lower position, advance dropping particle • If a stationary particle is present two units at either side of next lower position, move dropping particle one unit toward stationary particle

PROGRESSION OF PACKING RULES

Only a few of the large number of different combinations of the packing rules will be presented. In Figure 5, the case of nonsticky particles (NOR logic) is shown with a corresponding porosity of 0. In Figure 6, the case of sticky particles (OR logic) is shown with a porosity of 0.6. The effects of interparticle attraction are shown in Figure 7. Interparticle attraction increases the roughness of the deposit. The pressure drop under these conditions could be reduced without a significant change in porosity because direct passageways through the deposit are created by clumping of the particles.

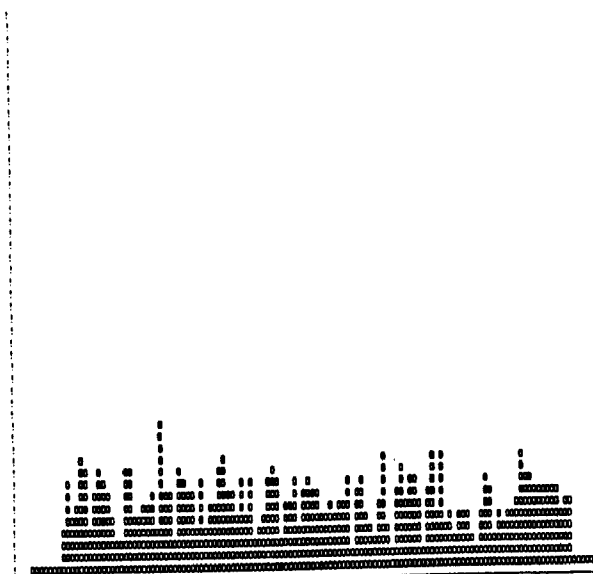


Figure 5. Particle packing with NOR logic (nonsticky particle).

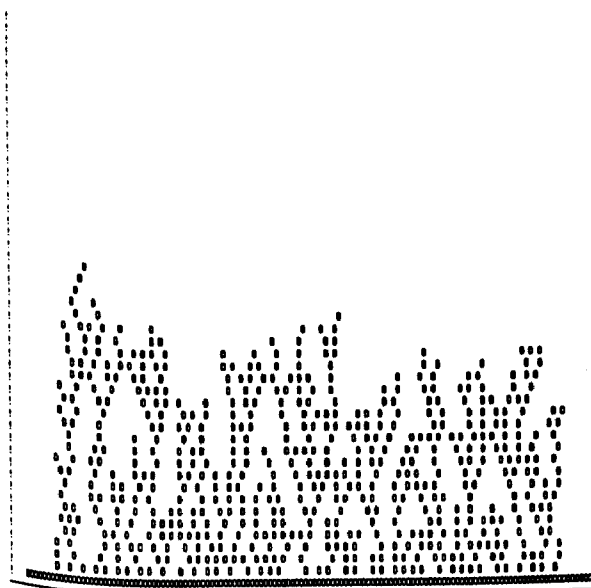


Figure 6. Particle packing with OR logic (sticky particles).

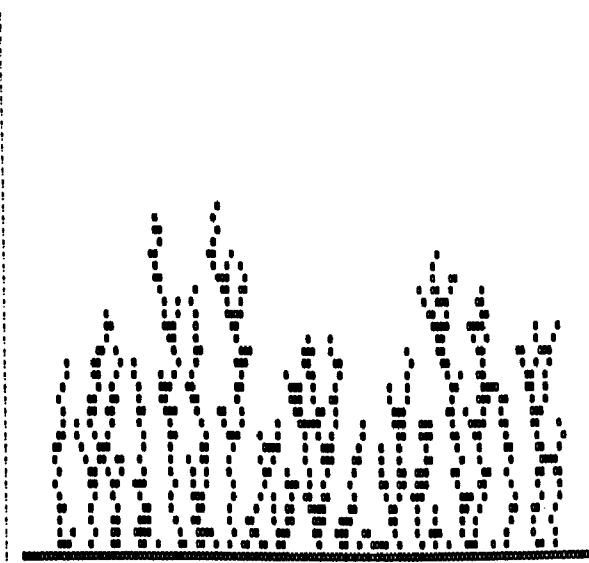


Figure 7. Particle packing with OR logic and short-range attraction (sticky particles with electrostatic attraction).

OBSERVATIONS

The deposition modeling has qualitative agreement with observations about fabric filtration. The possibility that nonsticking tends to increase the pressure drop (presumably by reducing the porosity of the deposit) has been mentioned by Felix et al. (22) to explain a problem associated with the collection of ash from the combustion of certain lignitic coals. The simulation of electrical effects with short-range attraction produces a similar change in appearance in the deposit from smooth to rough as reported by Chudleigh (23) and Mori et al. (24) during filter precharging experiments.

The Monte Carlo modeling has the promise of allowing the introduction of porosity-altering parameters into the baghouse model. At present, it is a parallel effort to the filter cake characterization effort.

SUMMARY AND CONCLUSIONS

The current effort to develop mathematical models of fabric filtration baghouses has been directed at investigations of the deposit of the ash on the fabric. Currently, modeling is limited by the ability to measure critical information about the deposit such as local mass loadings, porosity, and specific resistance. Distribution functions of these parameters will form an important part of future models.

The fragile nature of the deposit offers a challenge in the measurement of suitable physical properties. A new beta gauge to automatically measure spatial mass distributions is under development to obtain some of these data.

The deposition of particles on a filter is a stochastic process. Qualitative simulations of the effects of particle adhesion and electrostatic effects have been obtained.

ACKNOWLEDGMENTS

This work was supported by EPA cooperative agreement CR808936-01-0.

REFERENCES

1. Dennis, R., et al. Filtration Model for Coal Fly Ash with Glass Fabrics. EPA-600/7-77-084 (NTIS PB 276489), August 1977.
2. Viner, A. S., Donovan, R. P, and Ensor, D. S. Comparison of Baghouse Test Results with the GCA/EPA Design Model. JAPCA 34, 872-880. 1984.
3. Scheidegger, A. E. The Physics of Flow Through Porous Media, 3rd ed. Univ. of Toronto Press. 1974.
4. Williams, C. E., Hatch, T., and Greenburg, L. Determination of Cloth Area for Industrial Filters. Heating, Piping, and Air Conditioning, 12, 259-263. 1940.

5. Stephan, D. G., Walsh, G. W., and Herrick, R. A. Concepts in Fabric Air Filtration. Amer. Ind. Hyg. Assn. J., 21, 1-14. 1960.
6. Rudnick, S. N., and First, M. W. Specific Resistance (K_2) of Filter Dust Cakes: Comparison of Theory and Experiments. In Third Symposium on Fabric Filters for Particulate Collection. EPA-600/7-78-087 (NTIS PB 284969), June 1978, 251-288.
7. Carmen, P. C. Fluid Flow Through Granular Beds. Trans. Institution of Chem. Engs. 15, 150. 1937.
8. Happel, J. Viscous Flow in Multiparticle Systems: Slow Motion of Fluids Relative to Beds of Spherical Particles. AIChE J 4, 197. 1958.
9. Happel, J. Viscous Flow Relative to Arrays of Cylinders. AIChE J 5, 174. 1959.
10. Dennis, R., and Klemm, H. A. A Model for Coal Fly Ash Filtration. JAPCA 29, 230--234. 1979.
11. Rudnick, S. N. Fundamental Factors Governing Specific Resistance of Filter Dust Cakes. ScD Dissertation Harvard School of Public Health, Countway of Medicine, 10 Shattuck Street, Boston, MA 02115. 1978.
12. Dennis, R., and Dirgo, J. A. Comparison of Laboratory and Field Derived K_2 Values for Dust Collected on Fabric Filters. Filtration and Separation, 18, Sept/Oct., 394-396. 1981.
13. McElroy, M. W., Carr, R. C., Ensor, D. S., and Markowski, G. R. Size Distribution of Fine Particles from Coal Combustion 215 13-19. 1982.
14. Carmen, P. C. Flow of Gases Through Porous Media. Academic Press, New York, N. Y. 1956.
15. Lyczkowski, R. W. Modeling of Flow Nonuniformities in Fissured Porous Media. Can. J. Chem Eng. 60, 61-75. 1982.
16. Dennis, R., Cass, R. W., and Hall, R. R. Dust Dislodgement from Woven Fabrics Versus Filter Performance. JAPCA 28, 47-52. 1978.
17. Carr, R. C., and Smith, W. B. Fabric Filter Technology for Utility Coal-Fired Power Plants. JAPCA 34, 694-699. 1984.
18. Morris, K., and Millington, C. A. Modeling Fabric Filters. Filtration and Separation. Nov/Dec 478-483. 1982.
19. Cooper, D. W., and Riff, M. Predicted Effects of Filter Inhomogeneities on Flow Rate and Pressure Drop. JAPCA 33, 770-772. 1983.

20. Viner, A. S., Gardner, R. P., and Hovis, L. Measurement of the Spatial Distribution of Mass on a Filter. 5th EPA Symposium on the Transfer and Utilization of Particulate Control Technology, August 27-29, Kansas City, MO. 1984.
21. Visscher, William, M., and Bolsterli, M. Random Packing of Equal and Unequal Spheres in Two and Three Dimensions. Nature 239, 504-507. 1972.
22. Felix, L. G., Merritt, R. L., and Carr, R. C. Performance Evaluation of Several Full-Scale Utility Baghouses. Paper 23, In Proceedings: Second Conference on Fabric Filter Technology for Coal-Fired Power Plants. November 1983.
23. Chudleigh, P. W. Reduction of Pressure Drop Across a Fabric Filter by High Voltage Electrification. Filtration and Separation, May/June, 213-216. 1983
24. Mori, Y., Shiomi, T., Katada, N., Minamide, H., and Iinoya, K. Effects of Corona Precharger on Performance of Fabric Filter. J Chem Eng. of Japan 15, 211-216. 1982.

MEASUREMENT OF THE SPATIAL DISTRIBUTION OF MASS ON A FILTER

Andrew S. Viner
Research Triangle Institute
P.O. Box 12194
Research Triangle Park, NC 27709

R. P. Gardner
Department of Chemical Engineering
North Carolina State University
P.O. Box 7909
Raleigh, NC 27695-7909

L. S. Hovis
Industrial Environmental Research Laboratory
U.S. Environmental Protection Agency
Research Triangle Park, NC 27711

ABSTRACT

A device has been constructed for the measurement of the spatial distribution of mass in a dust cake. The device employs a collimated beta source and a Geiger-Mueller tube calibrated for different test masses. A digital plotter was converted for use as an x-y positioner to allow automatic scanning of the filter surface. The digital plotter and the control instrumentation for the Geiger-Mueller tube were controlled by a laboratory computer to permit automation of the data collection process.

The apparatus was found to work quite well for the measurement of filter dust distributions. Average filter masses were measured within 5 percent of independently measured values. The apparatus performed trouble free for the two sample filters that were analyzed. Improvements in the hardware and software for the device are suggested.

This paper has been reviewed in accordance with the U.S. Environmental Protection Agency's peer and administrative review policies and approved for presentation and publication.

INTRODUCTION

A recycling filter such as a baghouse goes through two stages in every cycle. The first stage is the filtering stage and the second stage is the cleaning stage. During the filtering stage of the cycle, dust is removed from the gas passing through the filter. As a result, the pressure drop across the filter increases as the filtering stage progresses. During the cleaning stage, the flow through the filter is stopped and the dust is removed from the filter. (Note that it is rare that all of the dust on the filter is removed during the cleaning stage.) The cleaning stage is initiated in one of two ways: either when a fixed filtration time has elapsed or when the pressure drop across the filter exceeds some pre-set value.

When a new filter is installed in a recycling filter, there is usually a "break-in" period during which the dust deposition and pressure drop vary from cycle to cycle. After the break-in period, the filter is in a steady-state mode. In this mode the pressure drop at any time, t , in the filtration stage of the cycle is identical to the cycles preceding and following it. Since the pressure drop across the filter attains a steady state, one can infer that the mass on the filter also attains a steady state of some sort. Therefore, if the steady-state characteristics of the dust mass on the filter were known, then it would be possible to predict the pressure drop throughout the cycle.

Dennis et al. (1) and Carr and Smith (2) have shown that at the beginning of the filtration cycle the dust on a filter bag is distributed very unevenly. The amount of dust on a given area of the filter ranges from very light up to very heavy loadings. This nonuniform mass has important consequences for the resulting pressure drop, as noted by Dennis et al. and Chiang et al. (3). Most importantly, Carr and Smith have pointed out that the residual dust mass (i.e., the dust mass on a filter bag at the beginning of the filtration stage) governs the pressure drop that results from operation at a given face velocity. Therefore, if the distribution of the residual mass on a filter were known, it should be possible to predict the filter pressure drop for a given face velocity at any time, t .

This paper describes a device that has been developed to measure dust distributions on filter surfaces. For development purposes, only simple filter samples consisting of redispersed fly ash collected on a 10-cm square section of a glass fiber filter were used. The dust mass was measured at every point on the filter surface (within the resolution of the instrument), and the mass frequency distribution was tabulated. The development of the device and the attendant data analysis techniques will be described in the sections that follow.

INSTRUMENTATION

Several criteria were considered in selecting the measurement technique to be used. It was desirable to use a nondestructive method so that experiments could be repeated. Also, since it was desired to measure the mass at every point on a filter, the device should have a high degree of resolution (at least within 6 cm). Lastly, since a large number of points were to be measured (256 or more), the method should lend itself to computer control to allow automation.

These considerations led to the conclusion that radiogauging was the best technique for this application. The attenuation of beta particles by a filter mass is directly related to the amount of mass between the beta source and detector. Therefore, it is possible to correlate the attenuation of beta particles with the amount of dust on a filter. By collimating the beta source, it is possible to achieve a high resolution and get a detailed picture of the distribution of dust on a filter surface. This technique also lends itself to computer automation, thus simplifying the task of data acquisition and analysis.

The prototype of the "beta gauge" apparatus is sketched in Figure 1. Six components make up the apparatus:

- Beta particle source
- Geiger tube (detector)
- Digital x-y positioner
- Pulse counter
- Controller/interface device
- Laboratory microcomputer.

The particle source used in this study was a strontium-90 source with a half life of 28.1 years. The source was enclosed in an aluminum housing with a 0.75 mm diameter hole drilled in one end to allow the beta particles to escape. The detector was an EG&G Ortec Model 903 end-window, halogen-filled, Geiger-Mueller tube. The x-y positioner was actually a Houston Instruments DMP-2 digital plotter turned upside down and fitted with a carriage for holding the filter samples. The pulses from the Geiger tube were counted by an EG&G Ortec Model 773 Timer-Counter under the control of a Model 879 Interface/Controller unit (also from Ortec). The interface/controller unit was connected to a TRS-80 Model 4 microcomputer by way of an RS-232C interface. Software was developed to allow control of the x-y positioner and the interface/controller unit.

EXPERIMENTAL

The first step in the development of the beta-gauge apparatus was to determine its spatial resolution. The procedure for determining the resolution was to mount a lead shield with a straight, flat edge in the sample holder carriage of the x-y positioner. In this way, the shield could be moved under computer control in 0.025 cm steps. The shield was placed between the source and detector such that the irradiated area was far from the edge of the shield. The number of beta particles reaching the detector in a 30 s interval was measured and recorded and then the shield was moved to a new position so that the irradiated area was closer to the edge of the shield. This procedure was repeated at a series of points, each point being closer to the edge of the shield than the previous point. As the edge of the shield came within the irradiated area, the number of beta particles reaching the detector increased. The shield was moved farther, so that the irradiated area extended beyond the edge of the shield, and the number of counts increased rapidly. Eventually, the irradiated area was unobstructed by the shield and the number of beta particles reaching the detector during a given period remained essentially constant. The results of this experiment are illustrated in Figure 2.

In the figure, the ordinate is the percentage of beta particles that are emitted by the source and subsequently detected by the Geiger Mueller

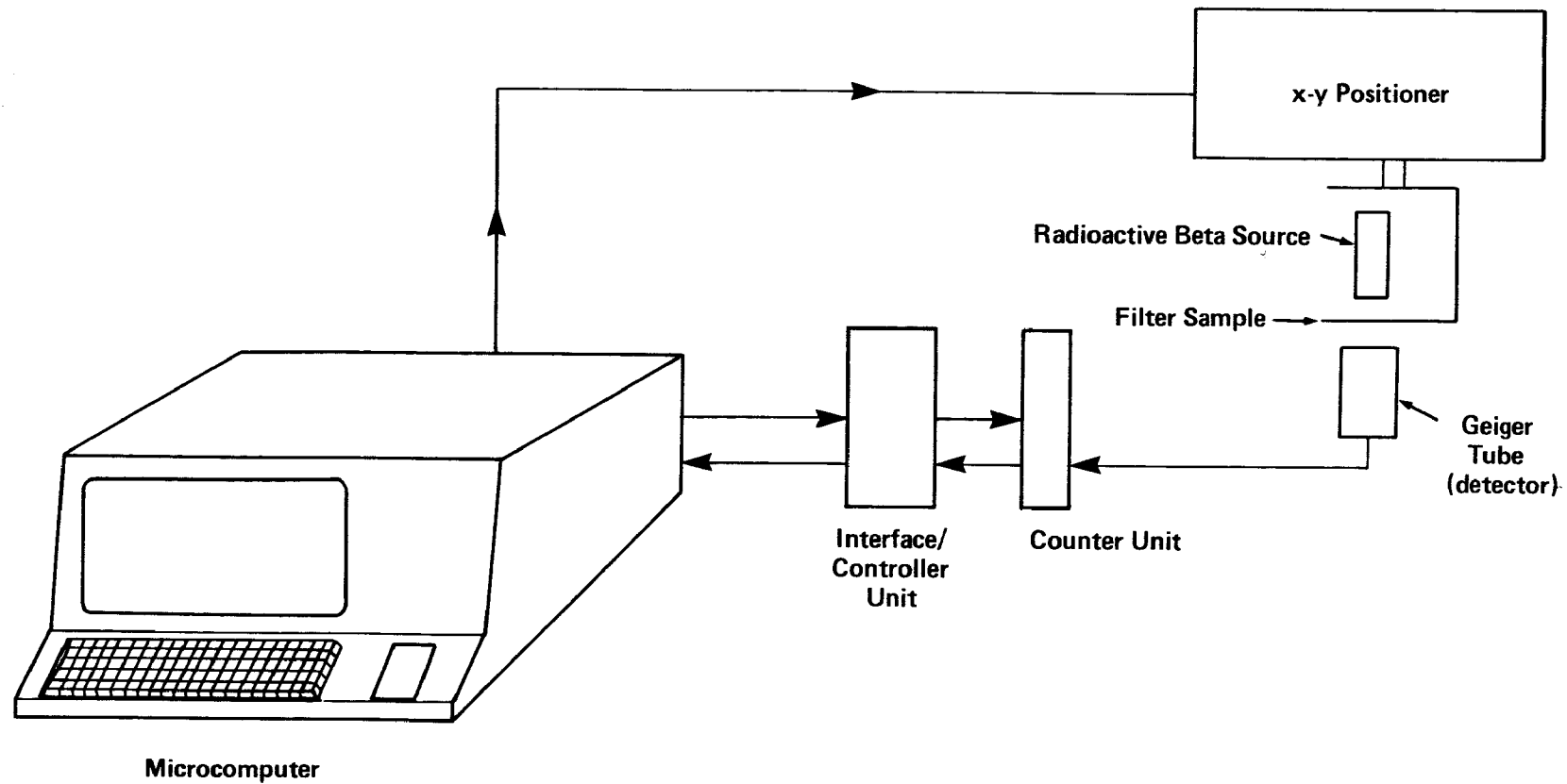


Figure 1. Experimental setup.

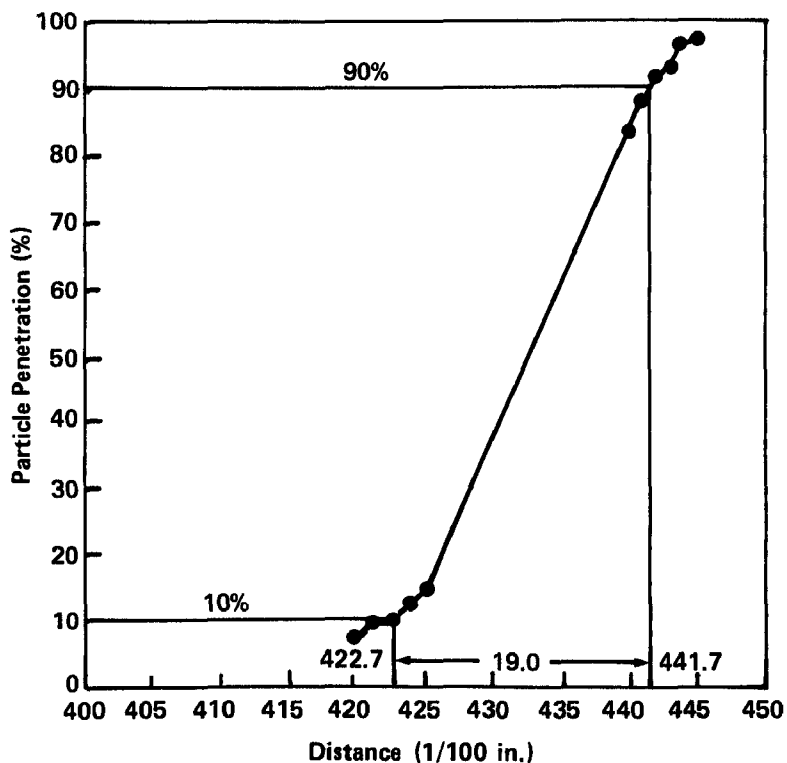


Figure 2. Beta-gauge data for estimation of resolution.

tube. Along the abscissa is a measurement of distance defined relative to an arbitrary starting point. The exact position of the plate edge is not known, but from the figure it can be assumed that the edge occurs at about location 432 in the figure (50 percent penetration). Arbitrarily defining the diameter of resolution as the distance between the points where the penetration increases from 10 percent to 90 percent yields a diameter of 0.48 ± 0.025 cm. Hence, the irradiated area has a diameter of 0.48 cm. This resolution allowed the measurement of over 400 adjacent points on a 10×10 cm filter.

It should be noted that since the irradiated area is essentially a circular cross section of a cone shaped beam, the resolution of the device could be improved by putting the filter sample closer to the beta source. This means that the resolution of the device is only limited by the distance between the source and the sample.

The second step in the development of the mass measurement device was calibration for measurement of local mass loadings on the filter. In general, the relationship between the attenuation of beta particles from a monoenergetic source and the mass on the filter is given by the Beer-Lambert law:

$$-\ln(I/I_0) = \mu \cdot w \quad (1)$$

where

I = the intensity of the radiation penetrating through the filter sample (counts/s)

I_0 = the intensity of the incident radiation (counts/s)

μ = the absorption coefficient characteristic of the radiation source (cm^2/mg)

w = the mass within the irradiated area (mg/cm^2).

Once the absorption coefficient is known, the local mass per unit area (w) can be inferred from the measured values of I and I_0 . This relationship is based on the assumption that the radiation is monoenergetic. This relationship is only approximate for strontium-90 sources which tend to emit particles with a distribution of energy levels, but Equation (1) should apply over the range of mass loadings encountered.

The calibration of the system was further complicated by the nature of the beta particle source. A strontium-90 source decays to yttrium-90 and emits a beta particle. The yttrium-90 also decays, emitting a beta particle and some gamma radiation. These two elements emit particles with different energy levels. As a result, a strontium-90 source cannot be considered as a single source but as a combination of two sources (^{90}Sr and ^{90}Y). If we let component 1 of the particle source be strontium and let component 2 be yttrium and treat each source independently, the attenuation can be expressed mathematically as:

$$I_1 = I_{0,1} \exp(-\mu_1 w) \quad (2)$$

$$I_2 = I_{0,2} \exp(-\mu_2 w) \quad (3)$$

The total radiation reaching the detector is the sum of the independent contributions:

$$I = I_1 + I_2 \quad (4)$$

The particle penetration is computed as the ratio of I to I_0 :

$$\frac{I}{I_0} = \frac{I_1 + I_2}{I_{0,1} + I_{0,2}} \quad (5)$$

or

$$\frac{I}{I_0} = f_1 \exp(-\mu_1 w) + f_2 \exp(-\mu_2 w) \quad (6)$$

where

$$f_1 = I_{1,0}/I_0$$

$$f_2 = I_{2,0}/I_0$$

$$f_1 + f_2 = 1$$

It was mentioned above that the absorption coefficient (μ in Equation (1)) is characteristic of the radioactive source material. An empirical relation for calculating μ based on the maximum energy of the source is presented by Gardner and Ely (4):

$$\mu = \frac{22}{(E_{\max})^{1.33}} \quad (7)$$

where

E_{\max} is tabulated in standard references of radioactive decay.

The authors warn that Equation (7) is only empirical since μ will depend to some extent on the material being irradiated and on any coatings placed on the source. For best results they recommend calibrating the source/detector combination for the material to be sampled. Since the objective here is to measure fly ash mass distributions, the proper material to use in the calibration would be fly ash. Unfortunately fly ash would be difficult to use for measurement of μ because of its heterogeneous nature. As a result, it is necessary to find a material that is "similar" to fly ash but is readily available and can be handled easily. The absorption coefficient for this material could be determined and used as an approximation to the absorption coefficient for fly ash. It is known that μ depends on the chemical composition of the irradiated material, so the candidate material must have a composition similar to fly ash. Fly ash consists of a number of different minerals and trace elements, the principal ones being silica (SiO_2), alumina (Al_2O_3), and iron oxide (Fe_2O_3). Typical compositions are silica--50%; alumina--20%, and iron oxide--10%. The high silica content of the fly ash suggested that glass would be a suitable substitute. Consequently, glass coverslips for microscope slides were chosen as test masses for determination of the mass extinction coefficient in the calibration procedure.

The calibration procedure was:

1. The particle count per unit time was measured while there was no mass (except ambient air) between the beta particle source and detector. This measurement was repeated several times at regular intervals throughout the calibration procedure to get a representative value of I_0 .
2. The masses of 21 round glass coverslips were individually measured on an electrobalance to within ± 0.01 mg. It was

assumed that the coverslips were uniformly shaped and the density of the glass was constant throughout so that the mass per unit area (w) was constant. The diameters of the coverslips were measured to within ± 0.05 mm. The mass per unit area (w) was calculated by dividing the measured mass by the calculated area.

3. The coverslips were combined into 6 different groups to yield a range of test masses for the calibration. Group number 1 consisted of one coverslip; group number 2 consisted of 2 coverslips; etc.
4. A series of measurements was made in which a test mass was chosen at random and mounted between the source and detector. The test mass was irradiated for 30 s and the number of particles penetrating through the test mass during that interval was recorded. This measurement was performed 3 times for each of the 6 test masses for a total of 18 measurements.

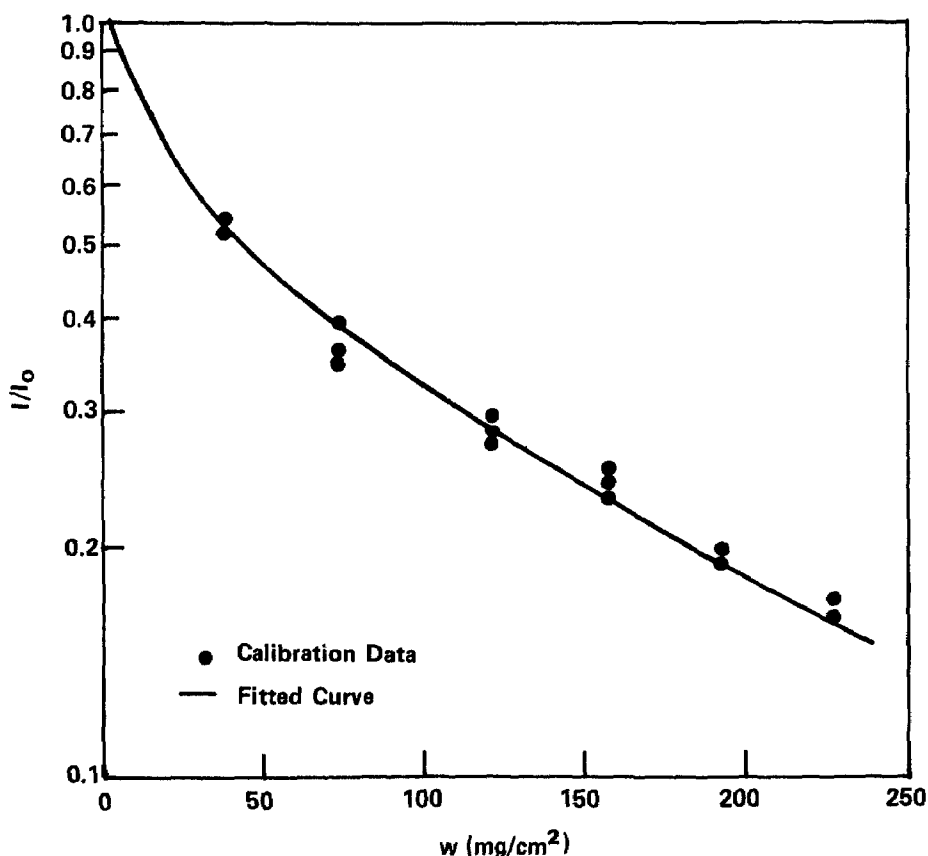


Figure 3. Beta-gauge calibration data using glass cover slides.

The data from the calibration run are presented in Figure 3. The constants f_1 , μ_1 , and μ_2 were determined by minimization of the χ^2 value:

$$\chi^2 = \sum [(y - y_i)^2/y] \quad (8)$$

where

$$y = (I/I_o)_{\text{measured}} \text{ and}$$

$$y_i = \exp(-\mu_2 w) + f_1 [\exp(-\mu_1 w) - \exp(-\mu_2 w)]$$

The value of f_2 was obtained by difference. The results of the data fit are shown in Table 1 and the resultant curve is shown as the solid line in Figure 3. As a further check on the validity of the calibration constants, the calculated values are compared with the empirical values derived from Equation (7). The agreement between the two sets of numbers seems reasonable. The curve in Figure 3 seems to fit the points quite well.

TABLE 1. REGRESSION FIT TO CALIBRATION DATA

	μ_1 (mg/cm ²)	μ_2 (mg/cm ²)	f	χ^2
Regression results	0.0525	0.00565	0.426	0.01136
Empirical correlation	0.0492	0.00744	---	

The test runs of the beta-gauge device were commenced after the calibration was complete. The test procedure was:

1. The filter sample was clamped horizontally (with the dust side up) in a carriage that was attached to the x-y positioner. The x-y positioner (under computer control) moved the sample filter between the beta source and detector.
2. The counter and quartz clock were zeroed by the microcomputer and started simultaneously. The counter accumulated the particle counts detected by the Geiger Mueller tube for a period of 5 s.
3. The count was transmitted to the microcomputer where it was stored in memory and on floppy disk for later analysis.
4. The microcomputer directed the x-y positioner to move the filter to a new location, thereby changing the irradiated area to a new spot on the filter, and restarting the cycle.

This procedure was repeated at all points on the filter (as determined by the resolution of the beta source/detector combination).

RESULTS AND DISCUSSION

The analysis of the data required the inversion of Equation (6) to get an expression for w as a function of I and I_0 . Since Equation (6) is nonlinear, the values of w had to be determined by iteration. After the data were reduced, the mean and variance of the local masses were calculated. As an independent check of the beta-gauge apparatus and experimental procedure, the mass of each filter was determined on a triple beam balance and divided by the collection area of the filter to get a "measured" value of the mean mass per unit area. A comparison of this measured average mass with the average inferred from the beta-gauge data is shown in Table 2. Since the dust on the samples was deposited evenly, it was expected that the measured values of w would be normally distributed. The estimated mean and variance were used to calculate an expected mass distribution. The measured distribution was divided into 30 "bins" defined by equally spaced values of w to generate a frequency distribution. This frequency distribution was compared with the expected distribution in a χ^2 test for goodness of fit. The expected and measured distributions are compared in Figures 4 and 5. Although the agreement between the measured points (histogram) and the normal distribution (curve) appears to be good in both cases, the amount of discrepancy between the observed and expected values in the tails of the distributions yields high values of χ^2 . That is, statistically speaking, the histograms cannot be considered to be normal distributions because the critical values of χ^2 are exceeded.

TABLE 2. COMPARISON OF MASS MEASUREMENTS

Run number	Average loading (mg/cm ²)			Total mass (mg)	
	Triple beam balance	Beta gauge	(σ^2)	Triple beam balance	Beta gauge ^e
F2	21.45	20.66	(19.54)	2214.6	2132.2
F6	18.00	18.04	(12.64)	1857.6	1862.8

Although it was incorrect to assume that the measured distributions shown in Figures 4 and 5 were normal, the value of the beta-gauge mass measurement has been demonstrated. The advantage of the normal distribution is that it provides an analytical function for calculating the fraction of area on the filter whose mass per unit area is w . The failure of the normal distribution only means that the distribution function cannot be easily described, thereby creating more work for modeling of the filter pressure drop performance.

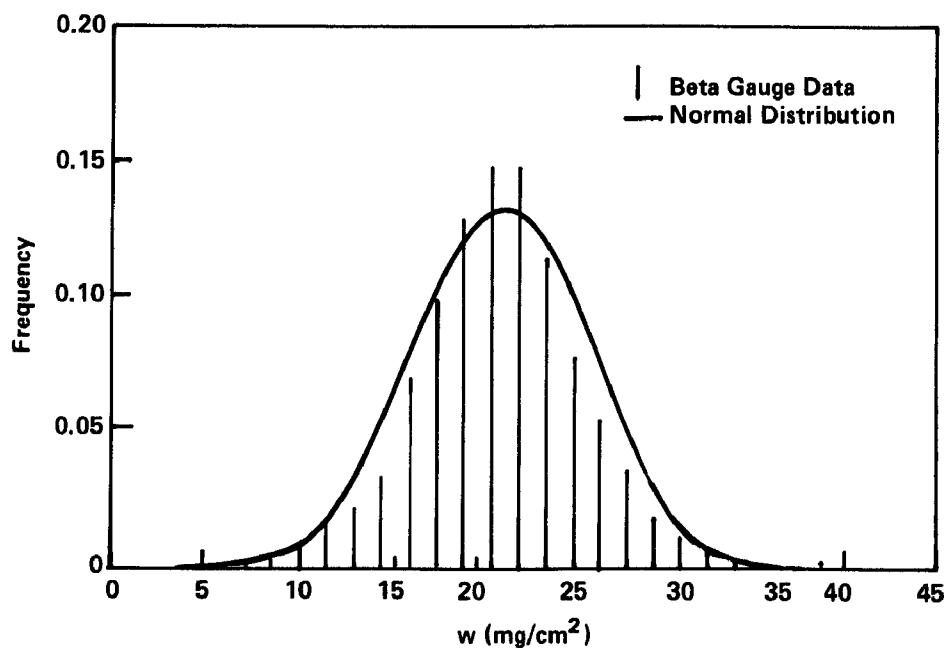


Figure 4. Comparison between the measured distribution and a normal distribution for filter sample F2 ($\chi^2 = 1770$).

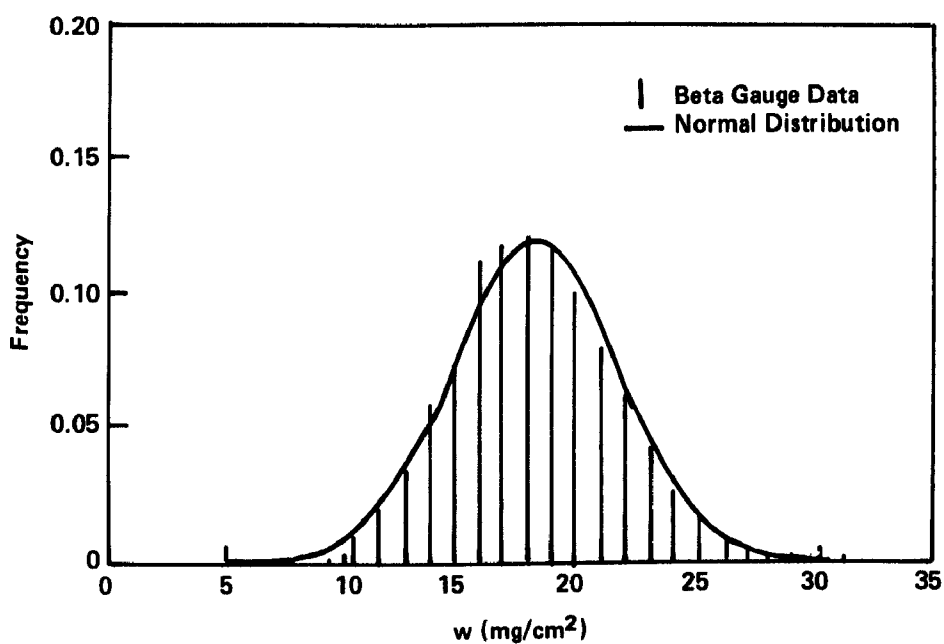


Figure 5. Comparison between the measured distribution and a normal distribution for filter sample F6 ($\chi^2 = 278$).

CONCLUSIONS

In summary, an apparatus for the measurement of dust mass distributions on filter surfaces has been built and tested. The apparatus has been shown to be capable of accurate measurement of the mean mass on the filter. Also, the device seems well suited for the measurement of the mass distribution. Only minor problems were encountered with the apparatus. In particular, the filter positioning apparatus was slightly unstable. As a result, dust could be shaken from the filter sample. That did not occur in the present study, but in order to prevent any future problems, the apparatus is being redesigned so that the particle source and detector are moved rather than the filter sample. Also, the software for the apparatus will be updated to include automatic calibration of the system. Once these features have been added to the beta-gauge system, the apparatus should prove to be quite a valuable research tool.

REFERENCES

1. Dennis, R., et al. Filtration Model for Coal Fly Ash with Glass Fabrics. EPA-600/7-77-084 (NTIS PB 276489), August 1977.
2. Carr, R. C., and Smith, W. B. "Fabric Filter Technology for Utility Coal-Fired Power Plants." JAPCA, 34, January 1984, pp. 79-89.
3. Chiang, T., Samuel, E. A., and Wolpert, K. E. "Theoretical Aspects of Pressure Drop Reduction in a Fabric Filter with Charged Particles," In: Third Symposium on the Transfer and Utilization of Particulate Control Technology: Volume III. Particulate Control Devices. EPA-600/9-82-005c (NTIS PB 83-149609), July 1982.
4. Gardner, R. P., and Ely, Jr., R. L. Radioisotope Measurement Applications in Engineering. Reinhold Publishing Corporation, New York, NY. 1967.

LABORATORY STUDIES OF THE EFFECTS OF SONIC ENERGY ON
REMOVAL OF A DUST CAKE FROM FABRICS

B. E. Pyle, S. Berg, and D. H. Pontius
Southern Research Institute
P.O. Box 55305
Birmingham, Alabama 35255-5305

ABSTRACT

The objective of the experiments described in this report was to identify the sound intensity and frequency which would most efficiently clean fabric filter bags in a baghouse. The frequency and intensity were found to vary between one baghouse facility and another apparently due to variations in the cohesion of the dust cake produced by ashes of differing compositions.

Sonic irradiation tests have been carried out using bag swatches taken from the High-Sulfur Fabric Filter Pilot Plant at the Scholz facility, Sneads, Florida, the Low-Sulfur Fabric Filter Pilot Plant at Arapahoe Station, Denver, Colorado, and other full-scale baghouses. In these tests the sonic cleaning efficiencies (the mass fraction of the dust cake removed) were measured at frequencies of 60, 100, 200, 500, and 800 Hz and at sound pressure levels (SPL) of 95, 105, 115, 125, 130, and 135 dB. Cumulative exposure times for each of these tests ranged from 10 seconds to 90 seconds. The results of these tests show that the sonic cleaning efficiencies were generally greater for the Western low-sulfur samples than for the Eastern high to moderate-sulfur samples. Also, for all types of dust cakes, lower frequency sound removed more of the dust layer than higher frequencies at a given SPL and exposure time.

INTRODUCTION

The first application of sonic assisted cleaning in a full-scale reverse-gas cleaned utility baghouse was in 1981 (1). Since that time interest in the use of sonic horns has greatly increased. However, there have been little or no guidelines developed for the selection and installation of sonic generators. Southern Research Institute (SoRI), under contract to the Electric Power Research Institute (EPRI), is conducting a research program to assist the utility industry in the selection and use of sonic devices. This program includes: pilot-scale tests of commercial and prototype horns, field evaluations of full-scale baghouse applications of sonic assisted cleaning, and laboratory studies to assess the effects of sound intensity and frequency under controlled conditions (2). It is the latter effort to which this paper is addressed.

METHODS

A systematic study of the effects of frequency, intensity and duration of monotonic sound on the removal of dust cakes from fabric filters is being carried out in the laboratory. The general objective of the study is to determine correlations between the variables listed above and the effectiveness of dust removal. The work is being performed in an acoustic isolation chamber, using electronically generated sound, and samples of dust-laden fabric taken from various field sites. In the initial sequence of tests, monotonic sonic energy alone was applied. Additional tests are planned that will include the use of forward and reverse-gas flow in conjunction with sound, and the use of composite, or polytonic sound waves.

An acoustic isolation chamber was constructed to carry out the sonic experiments. The chamber, illustrated in Figure 1, has a usable volume of 450 ft³ and is lined on all six walls with 4 inches of glass wool insulation covered with burlap. Sound pressure levels (SPL) of 200 Pa (140 dB) or more can be generated inside the chamber without causing a significant disturbance outside. Inside the chamber are located a speaker and a smaller enclosure containing a microphone, TV camera, and light source. A sample from a bag swatch cut from a utility baghouse is held in a rectangular clamp much like an embroidery hoop. The clamp seals one end of the box. Normally, the dust-laden side of the swatch faces the interior of the box, while the back side is exposed to the speaker. The exposed sample area is 0.26 ft². The axis of the speaker is placed normal to the plane of the sample, approximately 2 inches from the backside of the swatch. The centerline of the box and speaker is skewed from the principal axes of the sound chamber to avoid standing waves. The speaker, a cabinet mounted Electro-Voice Model EVM-15L Pro-line, has a power capacity of 400 watts and is capable of producing SPL values of 45 Pa (127 dB) at 4 feet and more than 200 Pa (140 dB) at 2 inches. The TV camera is focused on the dirty side of the swatch, and a pan is placed under the swatch to catch dust removed by sonic cleaning. There is a door on the box to provide access to the interior. The box is also padded inside with four inches of glass wool insulation wrapped in burlap to reduce reflection.

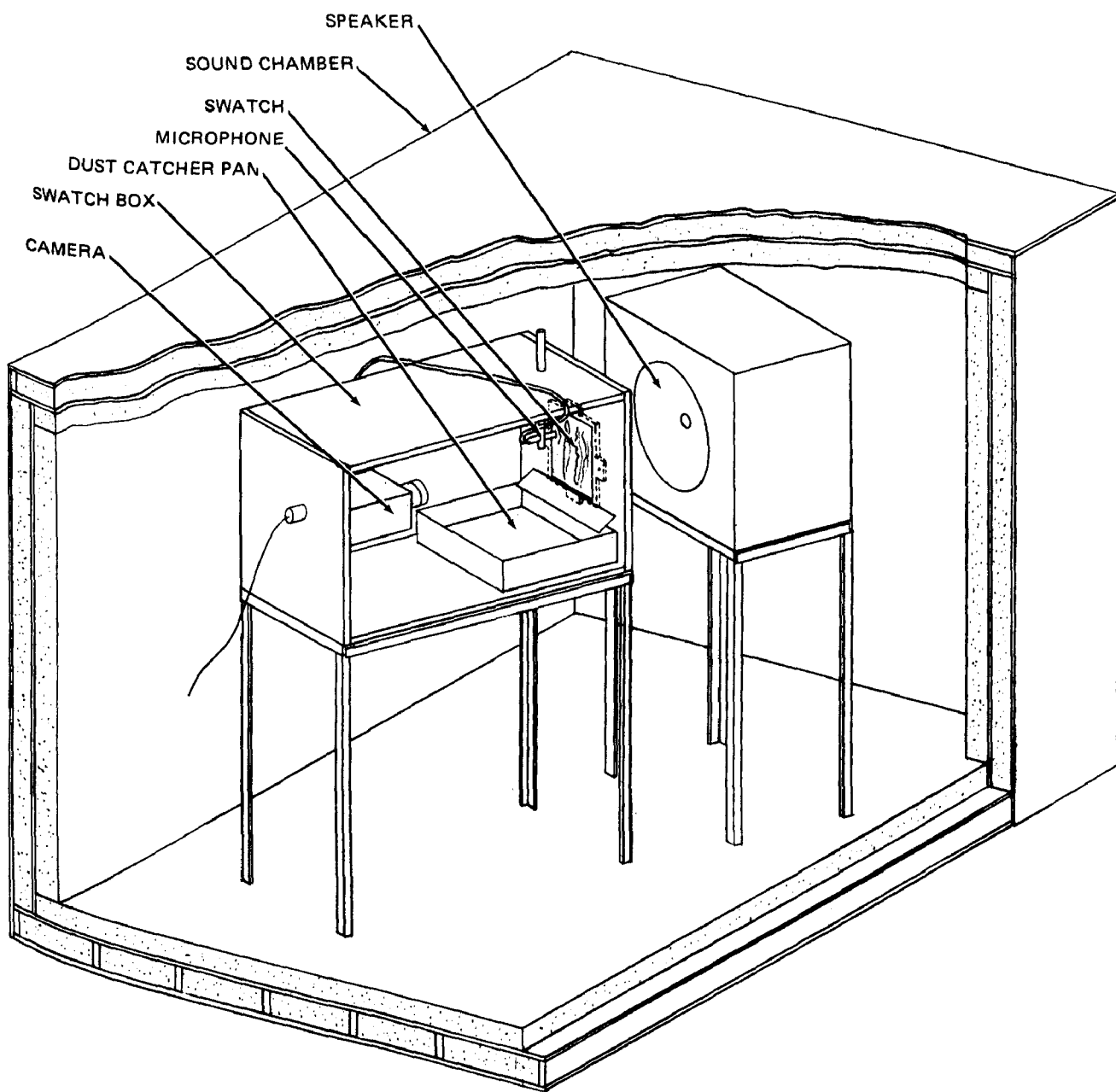


Figure 1. Sound chamber used for sonic experiments.

Each cleaning experiment is video taped for later analysis. Power to the speaker is supplied by a B&K Model E-310B Sine/Square Wave Generator driving a Hafler DH500 power amplifier. For the purposes of this report, only sinusoidal signals of a single frequency were applied to the amplifier. A sound level meter attached to the microphone inside the box monitors the sonic intensity behind the swatch and thus provides a measure of the attenuation by the swatch during testing. A chart recorder monitors the response of the sound level meter.

The sound pressure level is preset before testing by increasing or decreasing the voltage output of the signal generator. The signal to the amplifier is applied through an adjustable interval timer. In the deenergized mode the amplifier input is grounded to reduce the sound intensity inside the chamber to near background levels. By activating the timer the preset sound levels are immediately applied to the sample for a preselected exposure interval. Mapping of the sound pressure level over the swatch placement area indicated that the sonic intensity distribution was uniform to within 1.7 dB.

Before testing, a swatch previously cut from a utility baghouse is weighed and measured to obtain its areal dust loading in lbs/ft^2 . A smaller sample is cut from this to fit in the swatch holder. During a given test the sample was exposed to sonic energy of a single frequency and at a specific sound pressure level. The exposure was divided into four time intervals: 10, 20, 30, and 30 seconds. After each interval the amount of dust removed from the sample was determined by weighing. From these data both the fractional and cumulative reductions in the dust cake areal density were calculated. These were then normalized to the initial areal density and expressed as a percentage of the dust removed.

RESULTS

Sonic tests have been carried out using bag swatches cut from the following installations:

- Public Service Company of Colorado, Arapahoe Station Unit 3 Baghouse, reverse-gas cleaning with sonic assist, ash produced from combustion of Western low-sulfur subbituminous coal.
- EPRI's Fabric Filter Pilot Plant (FFPP) at Public Service Company of Colorado, Arapahoe Station, reverse-gas cleaned, ash produced from combustion of Western low-sulfur subbituminous coal.
- EPRI's High-Sulfur Coal Fabric Filter Pilot Plant (HSFP) at Gulf Power Company, Scholz Station, reverse-gas cleaned, ash produced from combustion of Eastern high-sulfur bituminous coal.

- Pennsylvania Power and Light, Brunner Island Station, reverse-gas cleaned with sonic assist, ash produced from combustion of Eastern high-sulfur bituminous coal.
- Pennsylvania Power and Light, Holtwood Station, Unit 17, reverse-gas cleaned with sonic assist, ash produced from combustion of Anthracite/Pet. Coke mixture.

More detailed information about these installations has been published (3).

A typical plot of the cumulative 200 Hz sonic cleaning efficiencies for low-sulfur ash is shown in Figure 2. The dust cake was obtained from the FFPP and illustrate the ease with which this type ash can be removed by sonic means. It is seen that at the higher SPL values, the greatest fraction of the ash is removed within the first 10 seconds of exposure. Repeated exposures were in general much less effective in removing dust. Also from Figure 2 it is seen that SPL values less than approximately 20 Pa (120 dB) were insufficient to remove any significant fraction of the dust cake.

A similar plot of the results obtained with samples from the HSFP is shown in Figure 3. It is apparent that the sonic cleaning efficiencies are significantly lower than those of Figure 2. For the HSFP samples, the lower limit of SPL values for significant cleaning action were approximately 36 Pa (125 dB). It is important to note that the results shown in Figures 2 and 3 are for a sonic frequency of 200 Hz. At higher frequencies the cleaning effectiveness was greatly reduced for both types of ash. This will be illustrated later.

A series of tests were also carried out to determine the repeatability of the experimental measurements. The results indicate that at a given frequency and SPL, the uncertainty in the laboratory measured sonic cleaning efficiency is on the order of $\pm 3\%$. The results of these repeatability tests are shown in Figure 4.

Similar tests were carried out at other sound frequencies and for other bag samples. The results of these tests are summarized in the following figures. In Figures 5, 6, and 7, the sonic cleaning efficiencies are plotted as functions of the sound frequency for sound pressure levels of 36 Pa (125 dB), 63 Pa (130 dB), and 112 Pa (135 dB), respectively. For the Holtwood and Brunner Island samples, tests of the sonic cleaning were carried out on samples as received and on samples that had been baked for 8 hours at 300°F. This was done because of the hygroscopic nature of these ashes and the fact that during the cutting of these samples in the field, atmospheric relative humidity was extremely high. For the Brunner Island samples, there was essentially no difference in the sonic cleaning properties. However, the ambient or as-received Holtwood samples exhibited a higher sonic cleaning efficiency than the dried Holtwood samples. This was particularly true at the higher sound pressure levels and at the 200 and 500 Hz frequencies. It is apparent that the drying process altered the cohesive properties of the dust cake. However, the exact mechanism is not understood at this time.

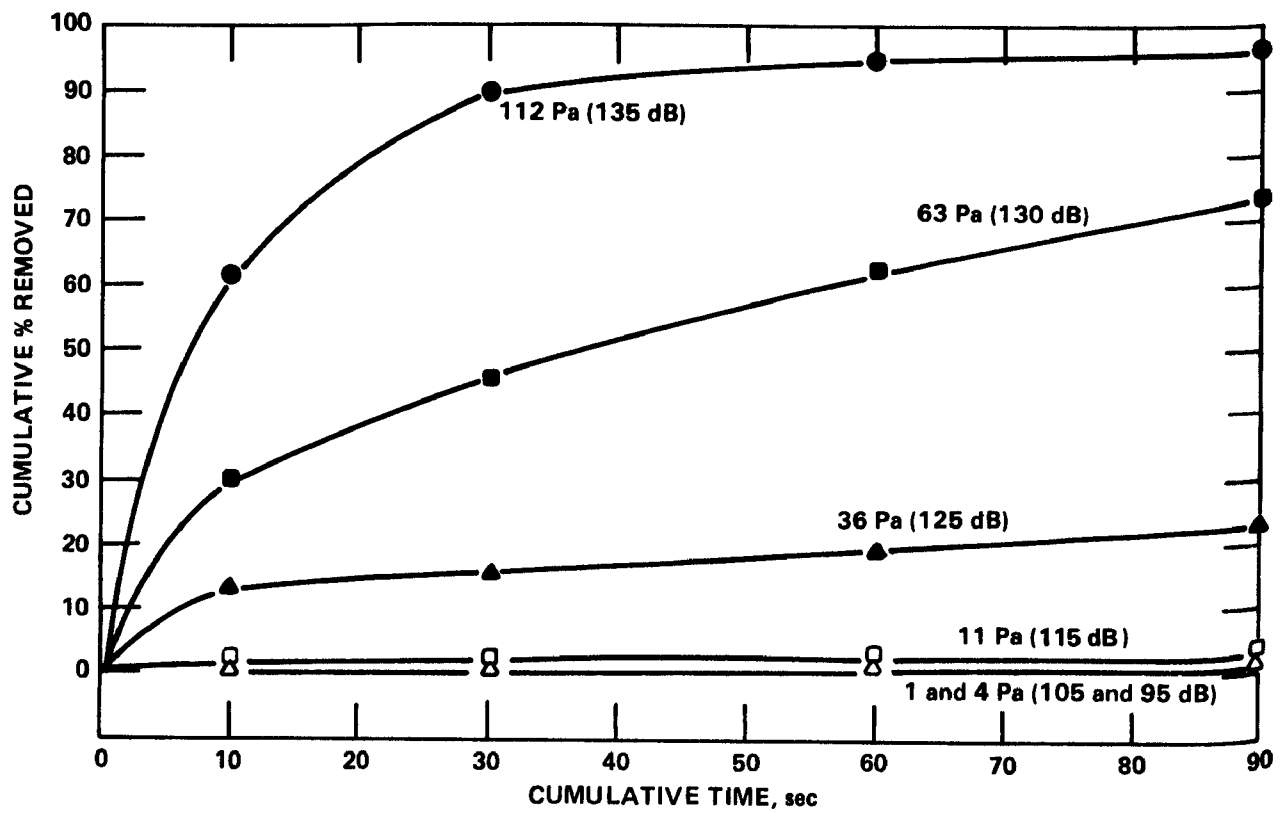


Figure 2. Cumulative percent of the dust cake removed versus cumulative sonic exposure time at 200 Hz. Dust cake produced by combustion of Western low-sulfur coal.

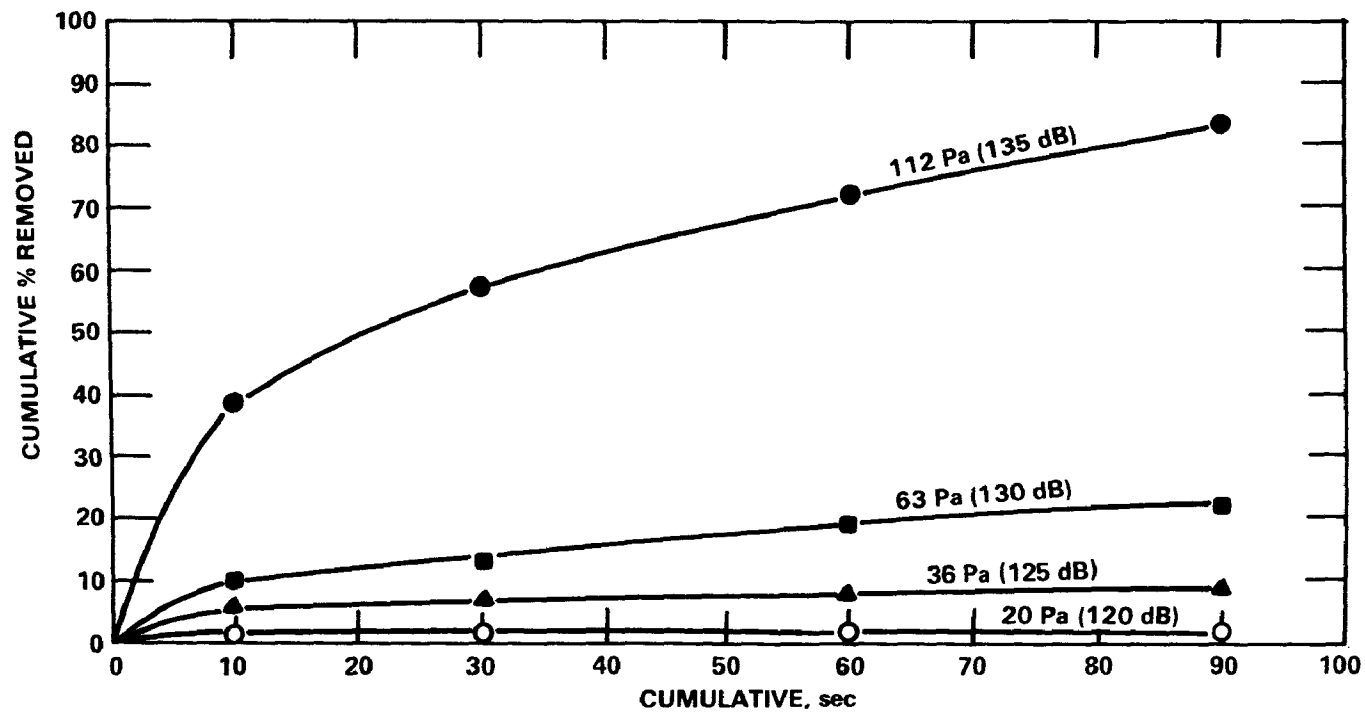


Figure 3. Cumulative percent of the dust cake removed versus cumulative sonic exposure time at 200 Hz. Dust cake produced by combustion of Eastern high-sulfur coal.

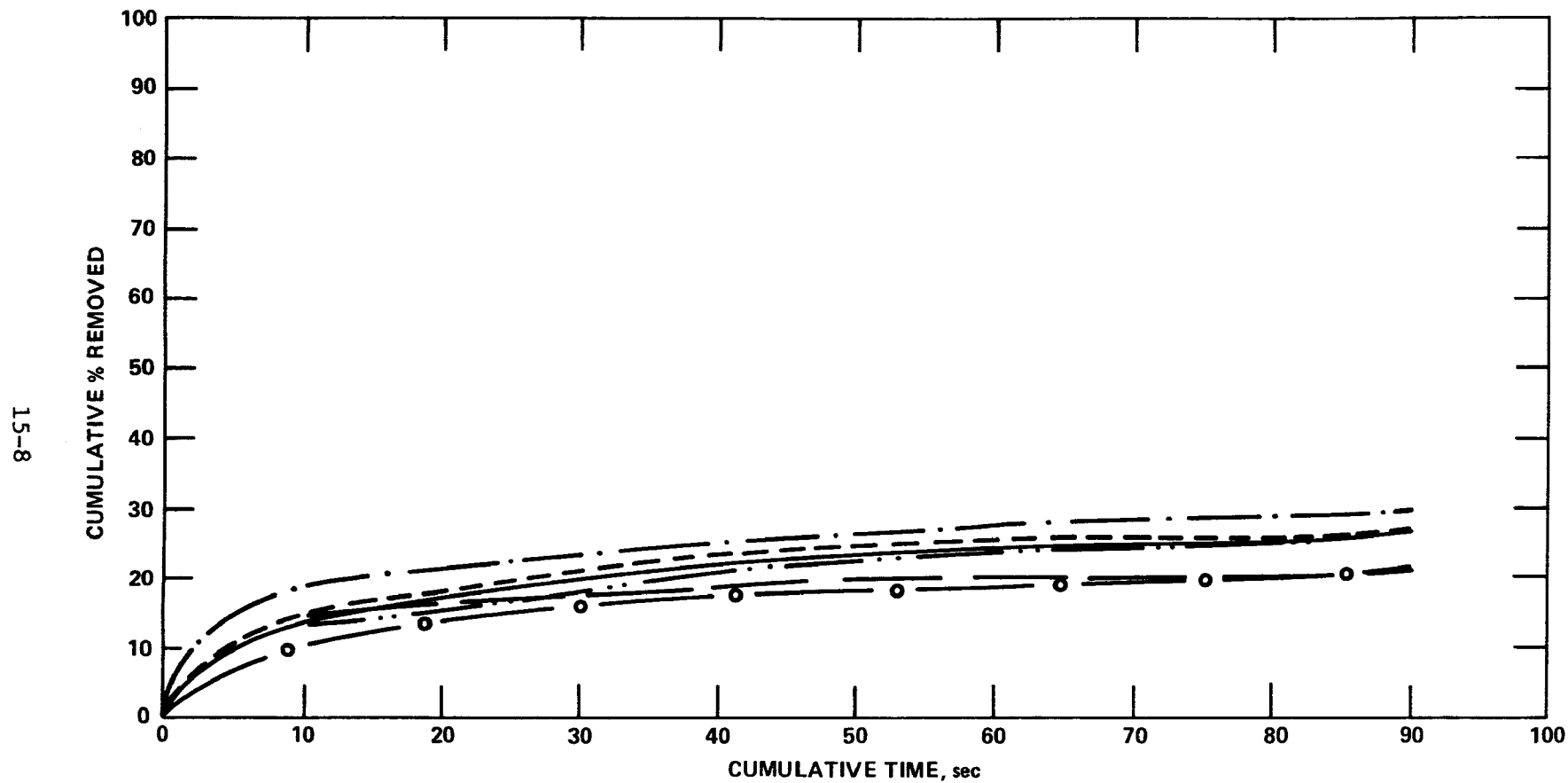


Figure 4. Repeatability of cumulative percent of the dust caked removed versus cumulative sonic exposure time at 200 Hz and at a sound pressure level of 63 Pa (130 dB). Dust cake produced by combustion of Eastern high-sulfur coal.

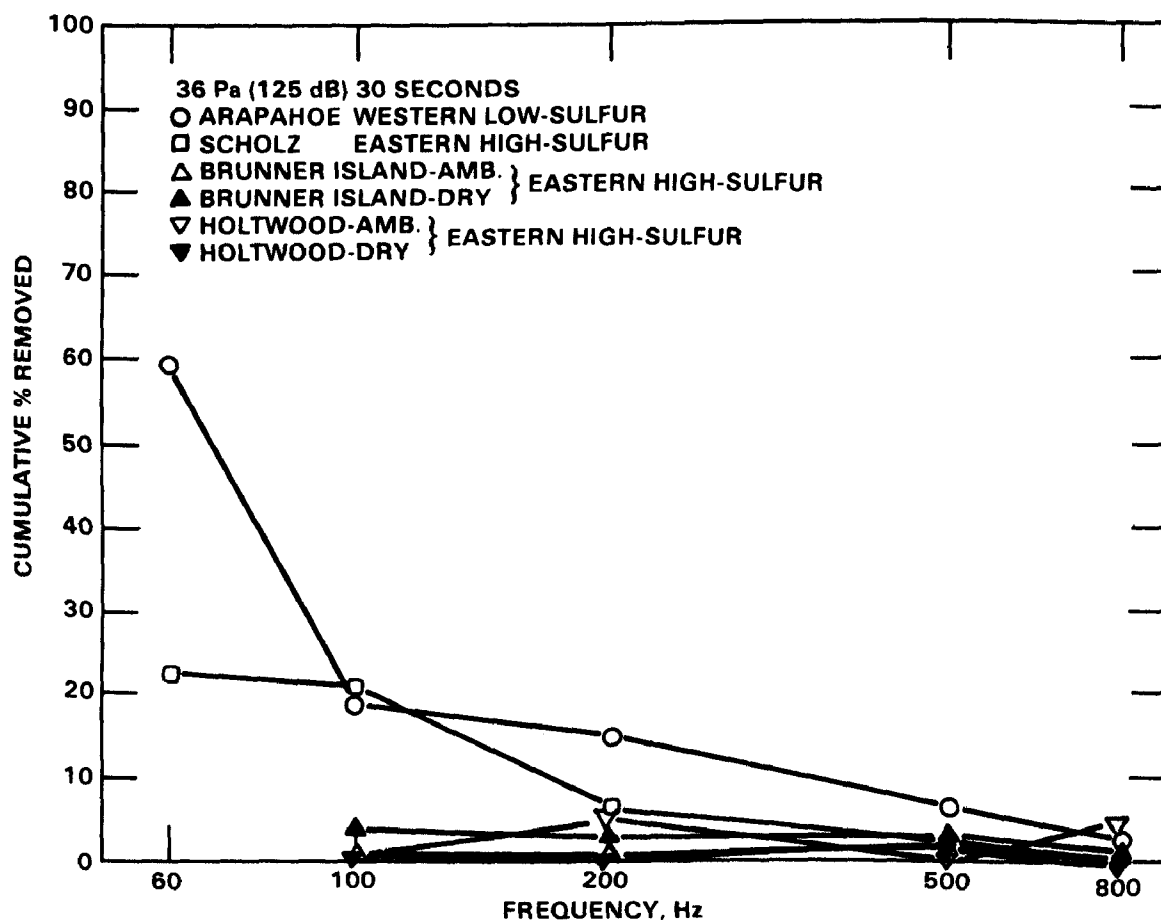


Figure 5. Frequency dependence of the efficiency of sonic cleaning for various types of dust cakes.

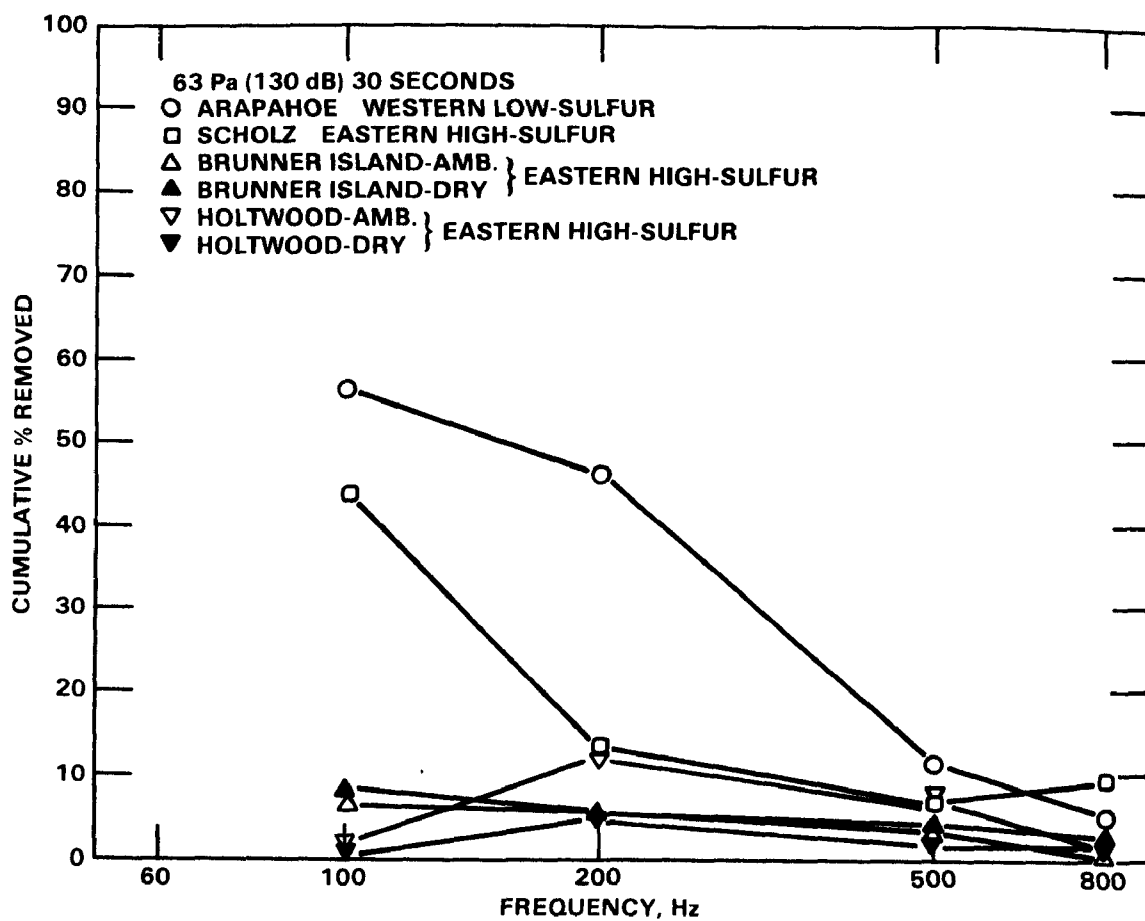


Figure 6. Frequency dependence of the efficiency of sonic cleaning for various types of dust cakes.

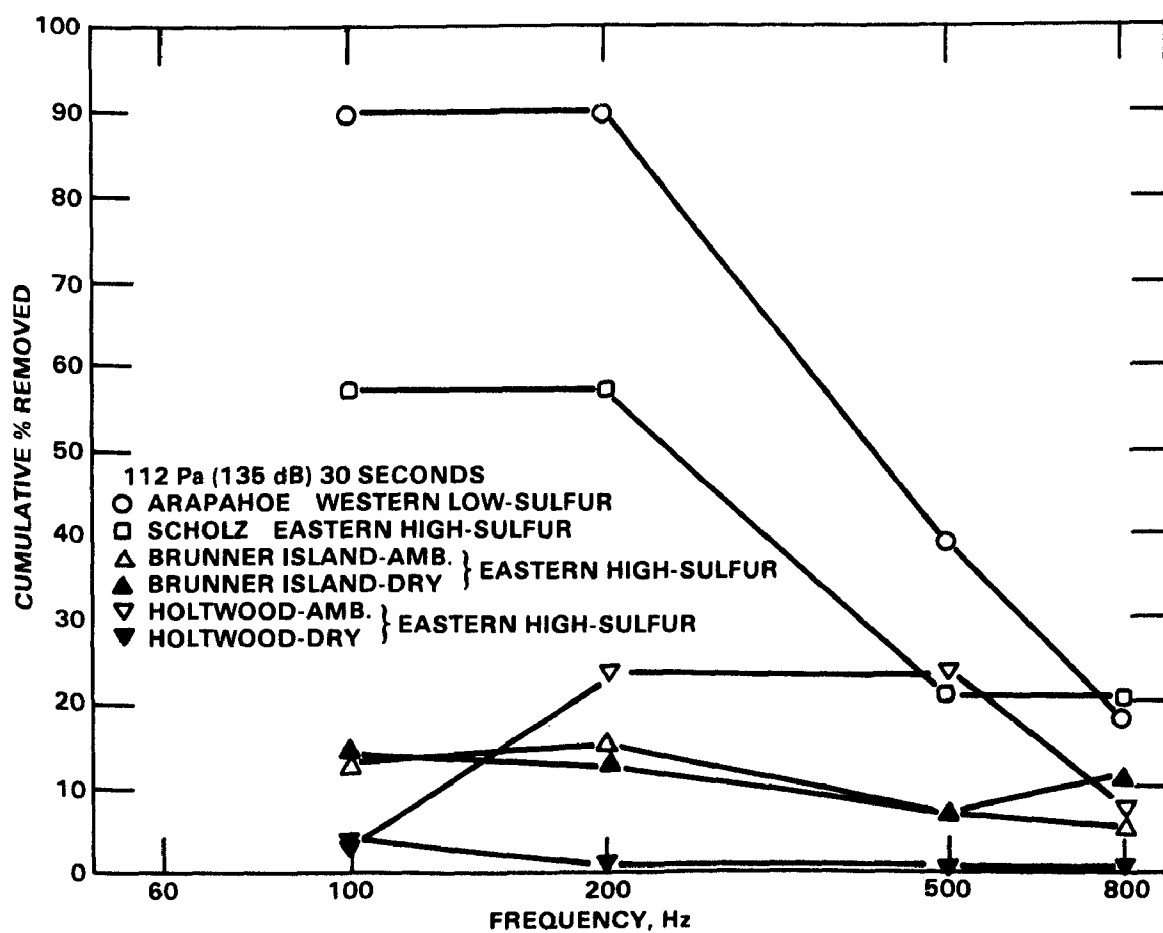


Figure 7. Frequency dependance of the efficiency of sonic cleaning for various types of dust cakes.

The effects of sound pressure level upon the sonic cleaning efficiencies can be seen more clearly in Figures 8 through 11. In each of these figures the frequency of the sonic energy is held constant, and only the sound pressure level and dust cake type is varied. It is evident that the Western low-sulfur dust is more easily removed than the Eastern moderate to high-sulfur dust. This is especially true at sound frequencies below 500 Hz. At higher frequencies there is little or no cleaning action.

For the lower frequencies and higher SPL values shown in Figure 8, more than 50% of the Arapahoe and Scholz dust cakes are completely removed from the fabric surface. Although this is desirable in terms of reducing the pressure drop across the fabric, it might lead to increased penetration of the bag by the dust during the next filtering cycle. Further studies need to be carried out to determine the magnitude of this penetration.

CONCLUSIONS

From the results shown in these figures the following conclusions can be drawn:

- Dust cakes produced by combustion of Western low-sulfur subbituminous coal are easier to remove by sonic means than those produced from Eastern moderate to high-sulfur coal ash.
- At sound pressure levels of 63 Pa (130 dB) or less, the sonic cleaning efficiency for Western low-sulfur ash and some Eastern high-sulfur ashes can be improved by lowering the frequency of the sonic energy.
- At sound pressure levels of 112 Pa (135 dB) or higher, little or no increase in cleaning efficiency is achieved by lowering the sonic frequency below approximately 200 Hz.
- The greater fraction of the dust cake is removed within the first 10-30 seconds of application of sonic energy. Continued applications are less effective in removing the dust.

The results and conclusions drawn from this laboratory study of the effects of sonic energy on the removal of dust cakes from fabrics show trends that in general agree with field data obtained from operating baghouses (3). For example, field measurements show that the reductions in dust cake weights brought about through the use of sonic horns are much less for high-sulfur ashes than for low-sulfur ashes. In fact, for the Eastern high-sulfur coal ashes, substantial amounts of the dust cake are removed only at sound pressure levels exceeding those attainable in the laboratory (3). The correlations between field and laboratory results were found to be quite good despite the fact that for the laboratory data: the dust cake samples were at ambient temperatures and gas compositions rather than of flue gas conditions, the sample geometries were flat rather than cylindrical, and the sound source was monotonic rather than polytonic.

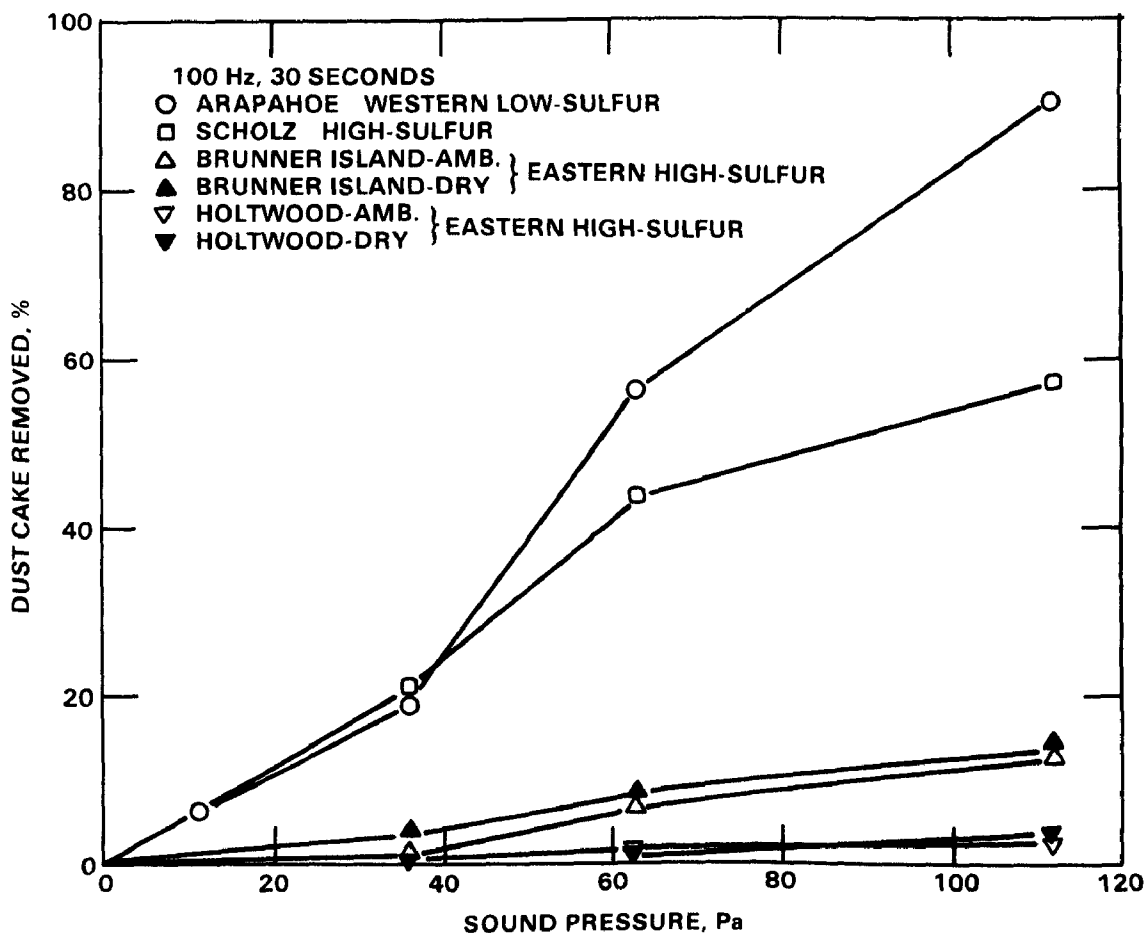


Figure 8. Sound pressure dependence of the efficiency of sonic cleaning for various types of dust cakes.

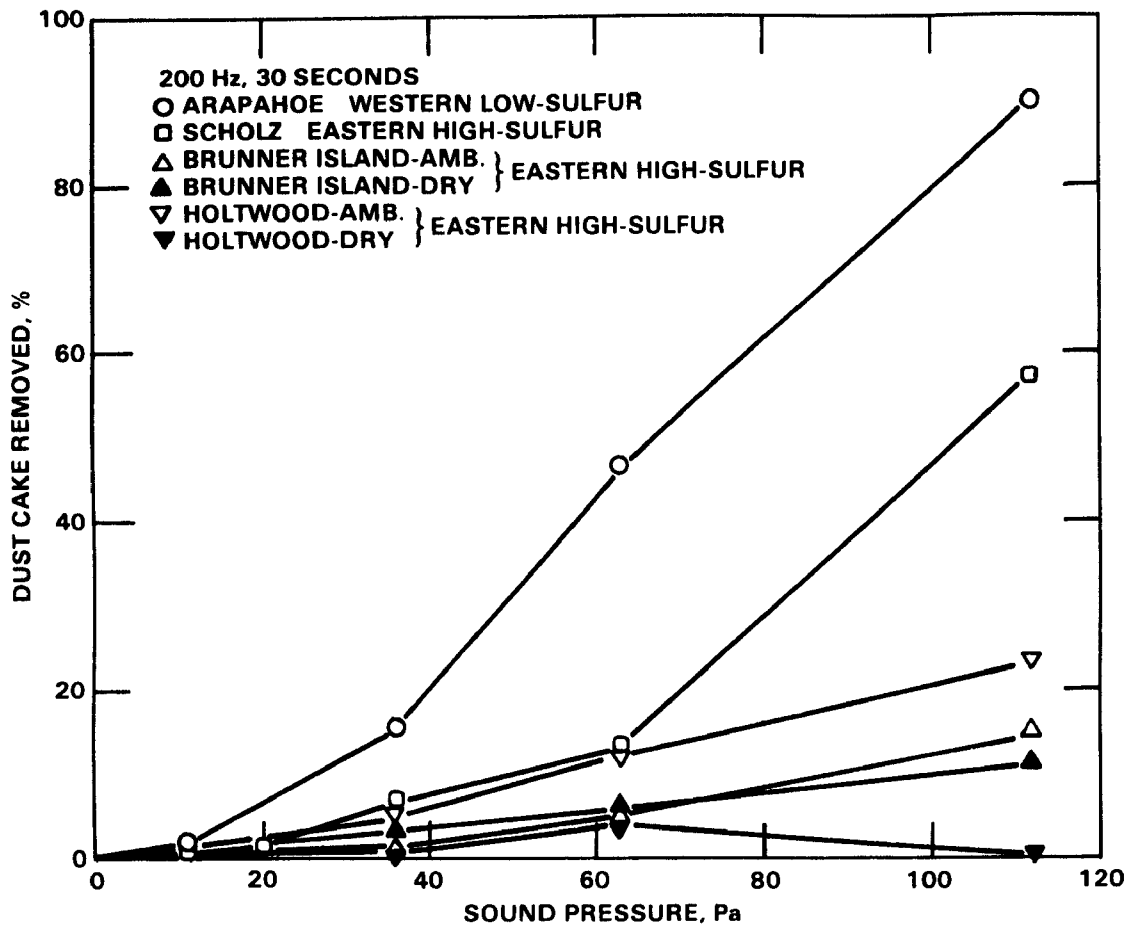


Figure 9. Sound pressure dependence of the efficiency of sonic cleaning for various types of dust cakes.

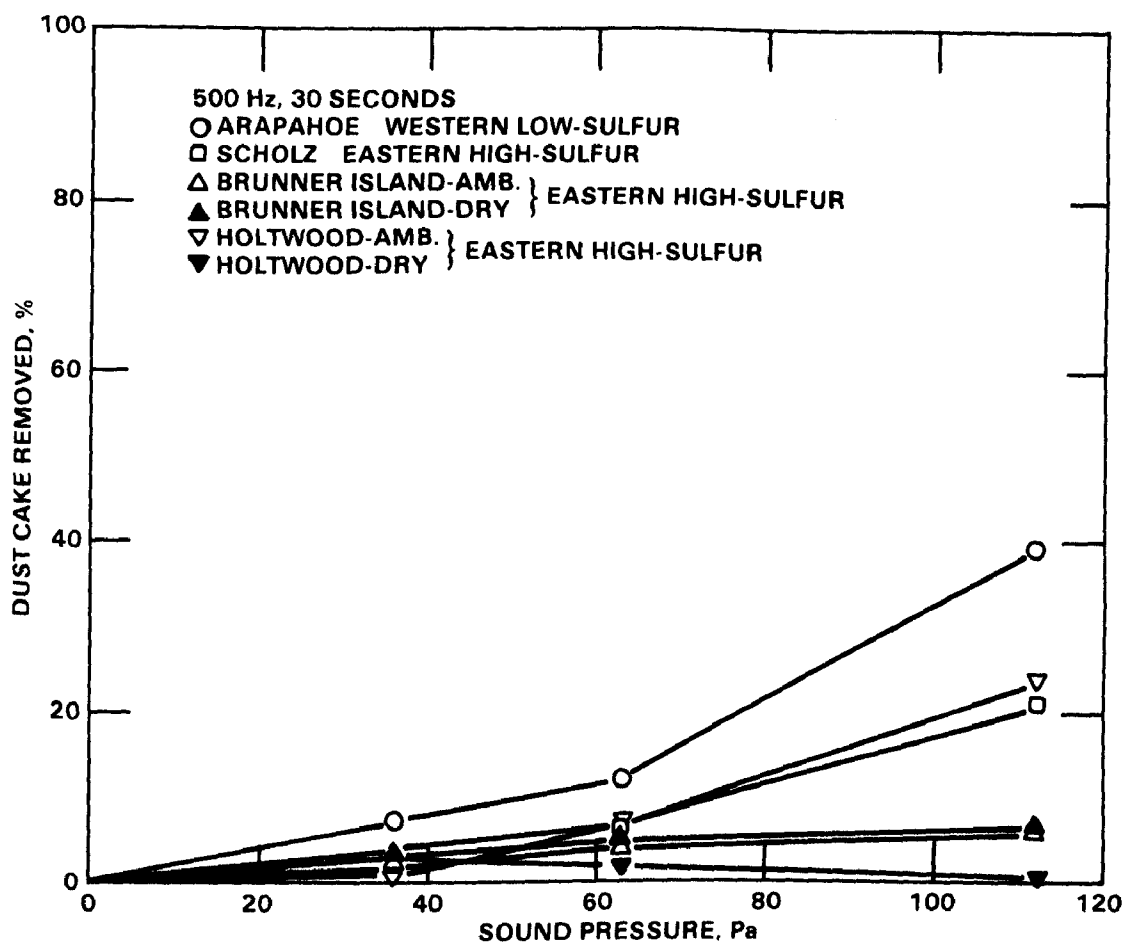


Figure 10. Sound pressure dependence of the efficiency of sonic cleaning for various types of dust cakes.

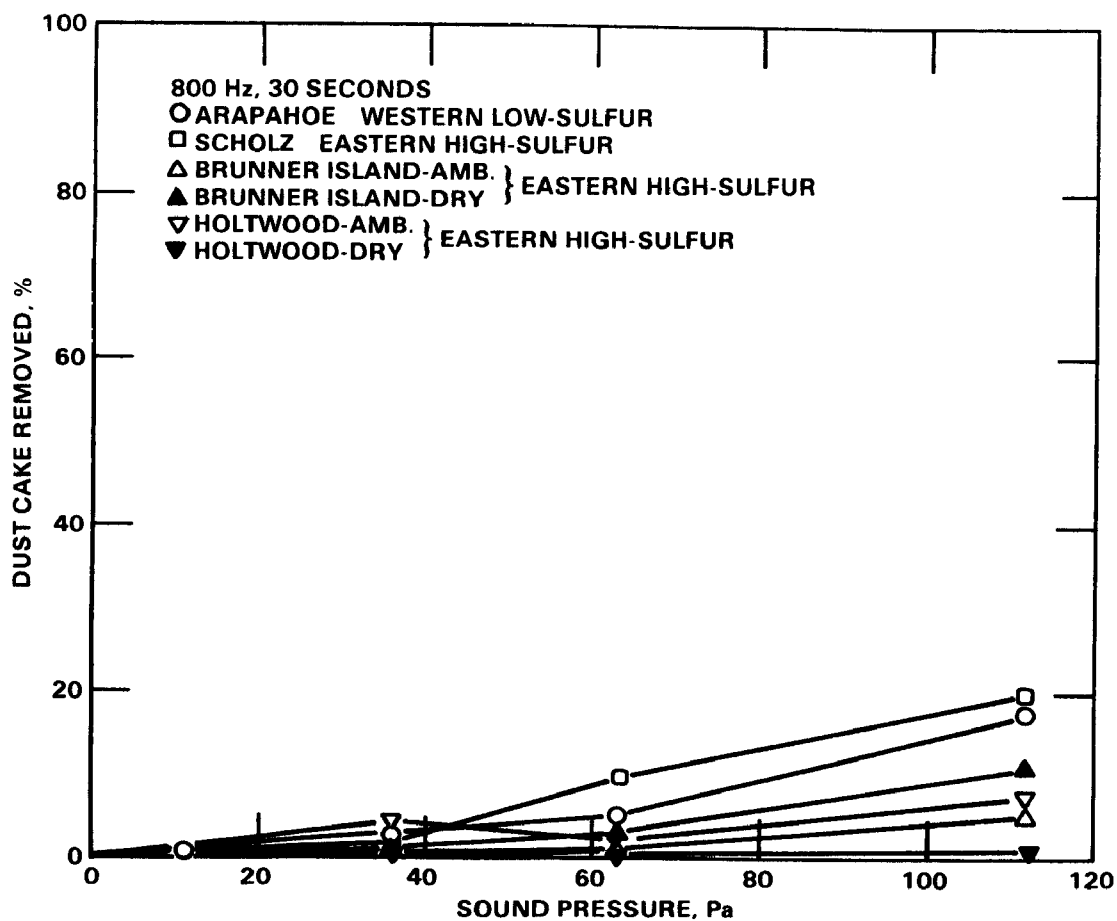


Figure 11. Sound pressure dependence of the efficiency of sonic cleaning for various types of dust cakes.

These laboratory results also indicate a strong possibility of being able to develop empirical equations to predict the response of a given dust cake to sonic energy. However, more work needs to be, and is being, done before this degree of predictability can be achieved.

ACKNOWLEDGMENTS

The data reported here were taken by D. K. Armstrong and O. D. Parker of SoRI. The work described in this paper was supported by EPRI Contract Number RP1129-8, Mr. R. C. Carr, Project Manager. The work described was not funded by the U.S. Environmental Protection Agency and therefore the contents do not necessarily reflect the views of the Agency and no official endorsement should be inferred.

REFERENCES

1. Wagner, N. H., Present Status of Bag Filters at Pennsylvania Power & Light Company. Proceedings: Second Conference on Fabric Filter Technology for Coal-Fired Power Plants, CS-3257, Electric Power Research Institute, Palo Alto, CA, November 1983.
2. Carr, R. C., W. B. Smith, Fabric Filter Technology for Utility Coal Fired Power Plants: Part V, Development and Evaluation of Bag Cleaning Methods in Utility Baghouses, JAPCA, 34:584-599 (1984).
3. Carr, R. C., W. B. Smith, Fabric Filter Technology for Utility Coal Fired Power Plants: Part III, Performance of Full-Scale Utility Baghouses, JAPCA, 34:281-293 (1984).

CLEANING FABRIC FILTERS

G. E. R. Lamb
Textile Research Institute
Princeton, New Jersey 08542

ABSTRACT

The effectiveness of filter bag cleaning can become a critical factor during filtration at high velocities, since, as velocity increases, dust removal becomes more difficult. Indeed, the efficiency of cleaning places practical limits on the gas flow rate. Measurements of pressure drop and penetration for several filter bags at higher-than-normal face velocities indicate that with cleaning methods involving mechanical impact (e.g., pulse-jet or reverse air with shaking), there is a trade-off between excessive pressure drop at low impact energies and excessive penetration at high energies. It would seem, then, that improvements should come from better directed application of cleaning energy into stressing the bond between fabric and dust cake. Two novel substitutes for shaking during reverse air cleaning were tried: the application of an electric field to the filter, and shearing the bag fabric by twisting the bag support. From exploratory experiments it appears that, while neither approach gave significant improvement over shaking, it should be possible to arrange conditions of twisting so as to provide substantial advantages. It is likely that future systems will employ a combination of methods.

This paper has been reviewed in accordance with the U. S. Environmental Protection Agency's peer and administrative review policies and approved for presentation and publication.

INTRODUCTION

A recent study has shown that, in order to enhance the economic advantage of fabric filtration over other methods of dust control, operations should be conducted at the greatest possible face velocity (1). The area of filter cloth needed to process a certain flow of gas is inversely related to the face velocity, and a smaller cloth area would be accompanied by decreased hardware sizes and consequently lower capital costs. As a rule of thumb, costs vary inversely as face velocity.

An increase in face velocity, however, usually results in increased pressure drop and particle penetration, so that for a given set of conditions - fabric, dust composition and concentration, temperature, - there is a velocity limit beyond which pressure drop and/or penetration become unacceptable. In seeking means to allow higher velocity operation, several approaches have already been taken. The potential of electrostatic aids for decreasing the penalty in Δp and penetration has been documented (1-3). Studies of fabric structure have shown how performance may be improved by using fibers having modified geometry (4) and layered fabrics (3). A third area of potential value is filter cleaning, a topic that has received minor attention yet is relevant in this context, since the excessive pressure drop developed at higher velocities is usually the result of failure of the cleaning procedure to remove a mass of dust equal to that just collected. The retained dust mass thus increases gradually from cycle to cycle and leads to poor performance. There is a tendency for this to happen no matter how low the velocity, so that pressure drop increases as the filter becomes "conditioned." The concept of conditioning carries the implication that eventually a steady state is reached, but in reality, the pressure drop continues to increase approximately in proportion to log of time, and the rate of increase is greater at higher face velocities. Ideally, it should always be possible, no matter what the face velocity, to design a cleaning procedure that, by being sufficiently energetic and prolonged, would return the pressure drop to the same value. In practice it may be assumed that such vigorous cleaning is precluded by cost, by possible bag damage, and perhaps by a lack of information as to the best procedure to follow.

The success of a cleaning method in removing dust accumulation should also affect penetration. A woven fabric benefits from a certain amount of dust cake buildup because the weave has many pinholes that at first allow leakage. When these pores are partially blocked with particles, there is a decrease in penetration. If, however, a dust cake is formed of sufficient thickness to cause a high pressure drop, local collapse of the cake may occur and penetration will again increase. With felts the effect of pinholes is minor, but with these materials seepage effects become more pronounced as the fabric becomes loaded with dust. Effective cleaning should thus be important in maintaining low penetration.

This paper describes an investigation of filter bag performance at higher-than-normal face velocities and of the effectiveness of some unconventional methods of cleaning.

PRESSURE DROP AND PENETRATION AT HIGH FACE VELOCITY WITH PULSE-JET AND REVERSE AIR CLEANING

Three sets of measurements were made: the first with a Teflon® felt bag cleaned by pulse-jet, the second with a J. P. Stevens type 648 woven glass bag also cleaned by pulse-jet, and the third with a Teflon® felt bag cleaned by reverse air with shaking. All three bags were virtually unused so that the trials began with a period of conditioning.

In all three cases, the procedure was to run the baghouse at different face velocities and measure pressure drop (Δp) and penetration at each velocity. The first run was at 3 cm/s (6 ft/min), and the air speed was increased in steps of 1.5 cm/s until either Δp or penetration moved out of an acceptable range. The speed was then reduced and increased again in the same steps to examine the ability of the bag to recover the better performance associated with lower speeds.

It was decided to do the pulse-jet cleaning off line. To do this, the timers were connected so that (a) the main flow was interrupted just before the pulse, and (b) the pulse valve remained open for a few seconds after pulsing. The first measure was expected to allow dust blown off by the pulse to fall to the hopper before the next filtering cycle began. If the main flow is not interrupted, the dust is immediately redeposited on the bag a short distance below the point where it was dislodged. This redeposition, as might be expected, becomes more severe at higher face velocities, until eventually almost all the dust cake is redeposited, so that the pulse becomes ineffectual and pressure drops rise to large values. At the same time, it was expected that the second measure might eliminate the "carpet beater" effect. It has been shown that penetration in pulse-jet bags is a maximum just after the pulse when the bag is driven back against the cage by the main flow. The impact appears to loosen the dust cake structure and promote seepage. Leith et al. (5) showed that this effect could be reduced by a secondary flow of air following the pulse which prevents the bag from rapidly collapsing onto the cage.

PULSE-JET RUNS

Results for the Teflon felt and woven glass bags with pulse-jet cleaning were so similar that they will be discussed together. The same conclusions apply to both.

Figures 1 and 2 show average Δp (i.e., $\frac{1}{2}[\Delta p_f + \Delta p_i]$) vs. face velocity; the values reached are reasonable in view of the rather high velocities. Face velocities were varied up and down between 3 and 7.5 cm/s, and the figures show that there is a certain time effect, but that after ~200 hours the "hysteresis" loops have narrowed, indicating that some kind of steady state has been approached.

On the other hand, inspection of the penetration curves (Figures 3 and 4) reveals an unexpected situation, because as time progresses, penetration levels continue to increase with time, and by the time the runs were stopped, had

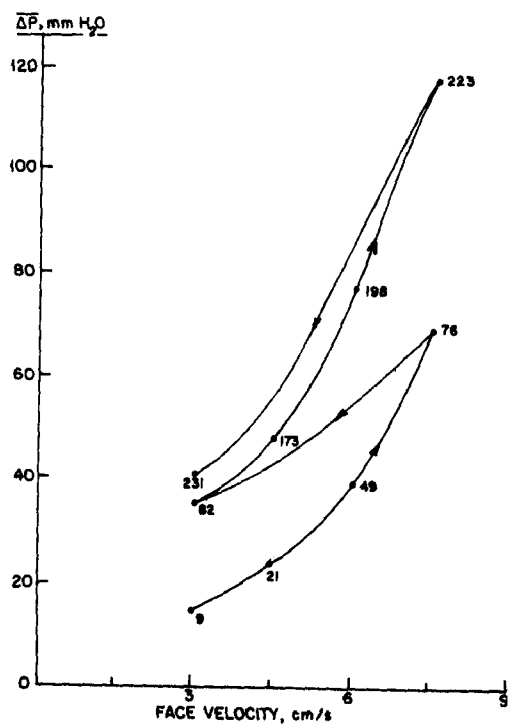


Figure 1. Dependence of average pressure drop on face velocity and running time. (Numbers near points in this figure and in Figures 2-7 indicate running time in hours.) Teflon® bag cleaned by pulse-jet.

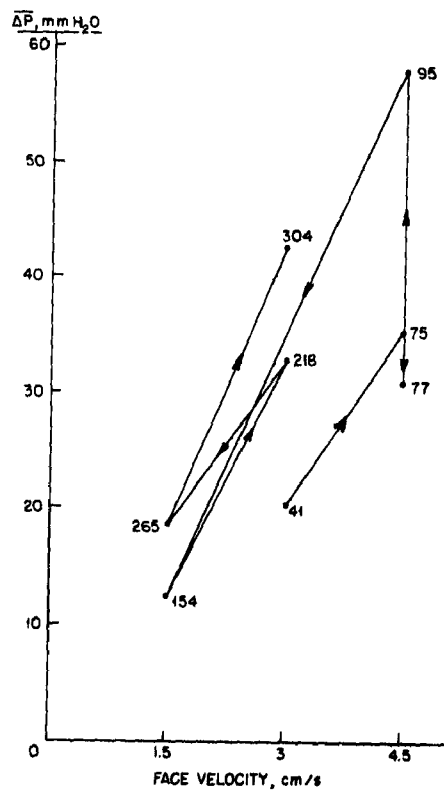


Figure 2. Dependence of average pressure drop on face velocity and running time. Woven glass bag cleaned by pulse-jet.

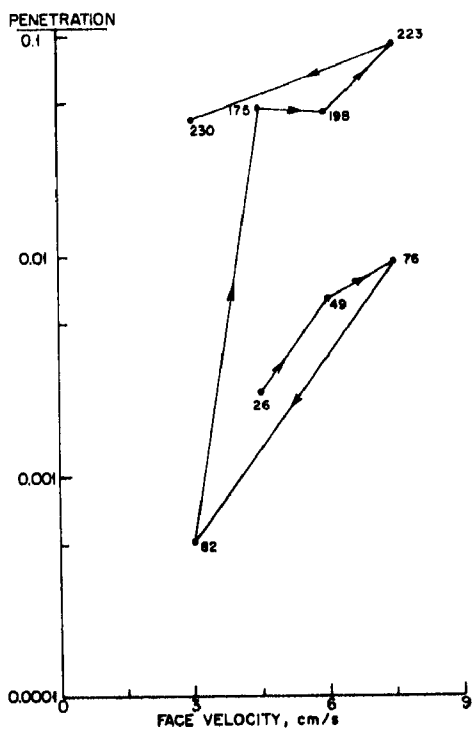


Figure 3. Dependence of penetration on face velocity and time for the conditions corresponding to Figure 1.

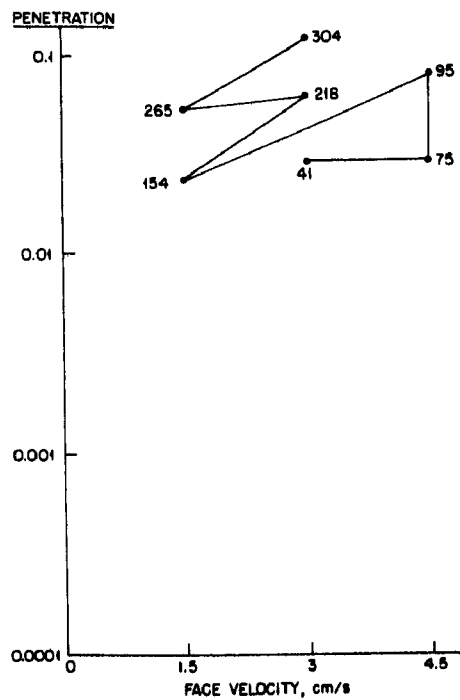


Figure 4. Dependence of penetration on face velocity and time for the conditions corresponding to Figure 2.

reached the region of 5 to 10%. Reducing the face velocity to the regular operating range of 3 cm/s did not always bring about a reduction in penetration, which means that the accumulated dust causes a permanent change in the penetration mechanism. This could conceivably involve interfiber spaces being "wedged" open by dust aggregates, or some other unknown reason for the breakdown in the process whereby dust is normally captured. This phenomenon is worth studying more closely because it appears to provide evidence of a penetration mechanism different from the "carpet beater" effect described by Leith (5).

REVERSE AIR RUNS WITH SHAKING

Measurements of Δp and penetration were made with the Teflon bag in the same type of sequence used with the pulse-jet runs. Face velocities were increased in 1.5 cm/s steps beginning at 3 cm/s, and reverse air velocities were made equal to the forward velocities.

Qualitatively, the results are roughly opposite to those obtained with pulse-jet, where penetration increased to high levels with time and increasing face velocity, but Δp levels reached quasi-steady states. In contrast, with shaker-reverse air, penetration remained below 1%, as can be seen in Figures 5 and 6, but pressure drops rose to high levels and did not approach steady states. Figure 7 shows how even with electrical stimulation (ESFF) and pre-charging the dust (+4,-15), Δp reached 400 mm of water at 5.5 cm/s face velocity. The drop in Δp between 260 and 288 hours was the result of adjustment of the shaker mechanism.

In conclusion, there was a large difference in the performance of the same fabric depending on whether it was cleaned by pulse-jet or by shaking with reverse air. There is a large difference in the energy input for the two methods. With the shaker used in our baghouse, the energy release per shake was 0.4 J or about 1 J/m² of fabric. Since cleaning involved 8 shakes, the total energy was of the order of 10 J/m². This may be contrasted with the energy of a 30 psi pulse, which was calculated to be 350 J/m² for the dimensions of our pulse-jet unit.

These results are in general agreement with those of Dennis and Wilder (6), who report that penetration for pulse-jet cleaned bags is 10 to 100 times higher than for reverse air, mechanically shaken systems. They also found that penetration increased with the pulse energy. It appears, therefore, that cleaning methods that use some form of mechanical impact permit only a trade-off between excessive pressure drop or excessive penetration, depending on whether the impact energy is low or high. It would seem profitable then to inquire whether cleaning methods based on different principles might offer more rewarding alternatives.

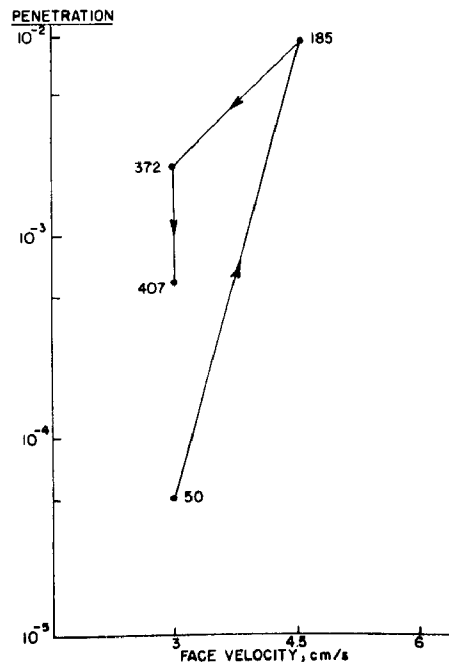


Figure 5. Dependence of penetration on face velocity and running time. Teflon® bag cleaned by reverse air.

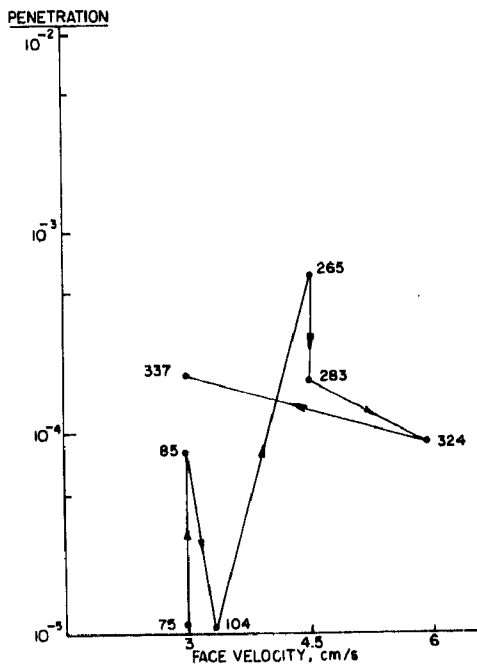


Figure 6. As Figure 5, but with 4 kV/cm average field on bag, -15 kV on precharger (+4, -15).

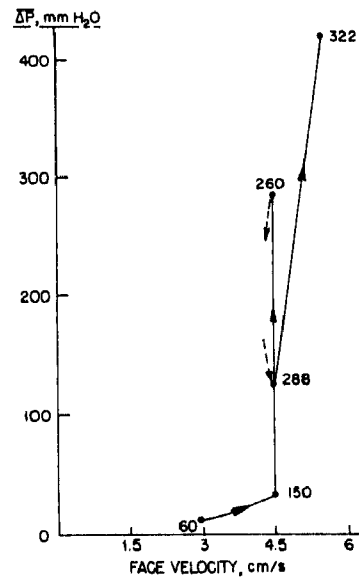


Figure 7. Dependence of average pressure drop on face velocity and running time for the conditions corresponding to Figure 6 (+4, -15).

NOVEL CLEANING METHODS

ELECTROSTATIC CLEANING

If a bag is to be operated with electrostatic enhancement, or ESFF, it has to be fitted with electrodes of some design. It would clearly be of further advantage to use the same electrodes to impart some electrostatic force to the dust cake while the bag was being cleaned, or possibly to provide all the force required to remove the cake. Such a cleaning method would eliminate the stresses on the bag due to shaking or pulsing and would consequently increase bag life. It might also prove to be less costly in energy than conventional methods.

Initial measurements were made with patch filters 10 cm in diameter. The electrodes in the filter were coupled to a high voltage relay. The relay allowed the electrodes to be connected to one or another of two power supplies. Thus, if one power supply were set to a positive and the other to a negative voltage, the applied field at the filter could be changed in magnitude and direction by throwing a switch.

The polarity was reversed during reverse air cleaning of the filter. Previous observations supported the belief that cleaning might be aided by electrostatic means because brief application of a large voltage resulted in the shedding of accumulated dust. This was seen both at the macroscopic level, where dust was removed from a bag, and at the microscopic level, where particles were seen to fly off single fibers to which they were adhering. For the experiments reported here, the extent of cleaning was gauged from the magnitude of the residual pressure drop (Δp_i) in the cycle following cleaning. Values of Δp_i were measured after cleaning with and without electrostatic assistance and with filtering at various levels of applied field.

In a study of the effect of the duration of the reverse polarity field applied during cleaning, it was found that 1.5-s and 15-s applications gave equivalent effects, so that time appears to play a minor role.

Results for the effects of the magnitude of the reverse voltage obtained with patches of woven glass fabric are shown in Figure 8a. There is clearly a significant effect on the initial pressure drop. Similar results were obtained with a woven glass bag (Figure 8b). However, the value of these results is diminished by two observations: The effectiveness of the voltage reversal is less when a voltage is applied during filtering (Figure 8a), which is the likely condition seeing that the electrodes are present in the fabric for the purpose of providing electrostatic enhancement. Secondly, although significant reductions in the value of the residual pressure drop (Δp_i) are seen, the final pressure drop, after the dust cake has been built up again, is the same as when no voltage reversal is used to aid cleaning. This indicates that voltage reversal only clears a small space near the electrodes in which the dust cake quickly builds up again. A similar explanation accounts for the first observation; with an applied voltage a thinner dust cake forms near the electrodes which is less affected by voltage reversal. Both these effects severely limit the value of electrostatic aid in cleaning by the method described.

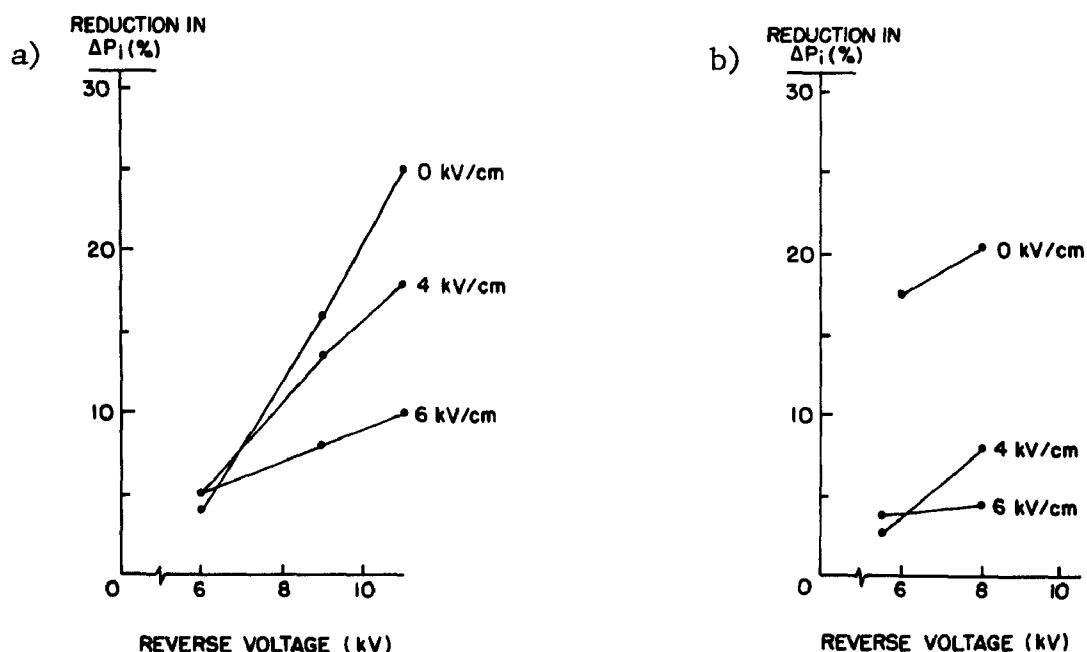


Figure 8. Effect of reverse polarity voltage during cleaning on initial pressure drop in following cycle.

- a) Patch experiments using woven glass fabric at several filtering voltages.
- b) Results for bag made of the same woven glass fabric.

A different insight into these events is derived from the data plotted in Figures 9 and 10. These were obtained by conditioning a woven glass filter patch for many cycles, and monitoring the pressure drop continuously and the mass of captured dust at intervals. The results confirm and simplify the previous observations. As the filter conditions, the mass of dust retained after cleaning (the "residual" dust) increases, and so does the residual pressure drop (lower points in Figure 9). The slope of the broken line may be taken as the specific cake resistance of "residual" dust; this is much lower than the slopes of the solid lines which are due to the dust deposited during filtering (the "filtered" dust). This difference is due to the location of the dust: residual dust is assumed to be deeper in the fabric. The specific cake resistance K_2 associated with the filtered dust also increases as the filter conditions (Figure 10). These observations are consistent with a model in which the residual dust is trapped in small pores, so that it has a small effect on permeability. Whether the two kinds of dust have different composition or particle size is not known, but it is reasonable to expect that residual dust contains smaller particles.

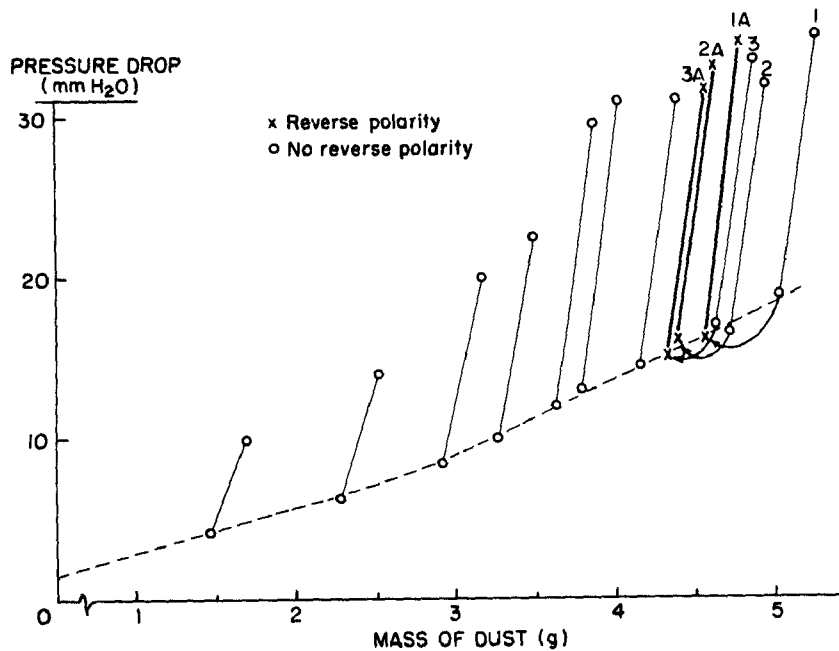


Figure 9. Initial (lower points) and final (upper points) pressure drops while conditioning a woven glass filter. The points marked x were obtained after reversal of ESFF voltage polarity during reverse air cleaning. The difference between "conditioning" (broken lines) and "filtering" cake resistance (full lines) is clearly seen. Constant field of 4 kV/cm; face velocity 6 cm/s.

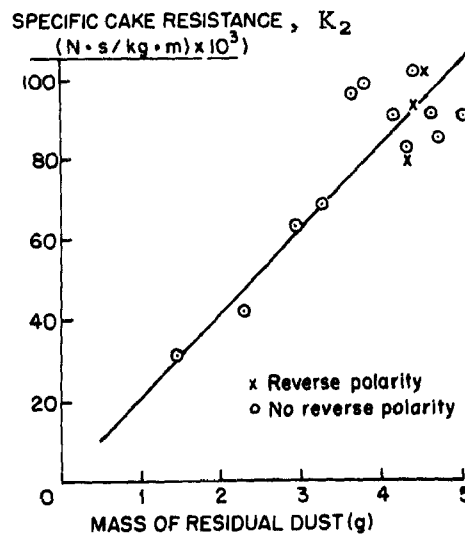


Figure 10. Dependence of "filtering" cake resistance (slope of solid lines in Figure 9) on mass of "conditioning" dust (mass at beginning of cycle, lower points in Figure 9).

It appears that unless the structure of the dust deposits can be drastically changed, the only way to reduce pressure drop is by operating in a region closer to the origin in Figure 9, i.e., by reducing the amount of accumulated residual dust. In this regard, it is clear that the reversal of polarity achieves only minor results in this direction if the reversal is applied to a filter that is already conditioned. In Figure 9 the points following polarity reversal are shown in heavier lines. Three pairs of cycles are shown. For example, after the conditions of cycle 1 were recorded, polarity reversal yielded cycle 1A. The same occurred with cycles 2 and 2A, and 3 and 3A. The resulting reduction in pressure drop is consistent with the other data points and amounts to only a few millimeters of water.

CLEANING BY BAG SHEARING

The data in Figure 9 illustrate what is intuitively reasonable, namely that residual pressure drop is due to dust lodged within the structure of the fabric, while the rise in pressure drop during filtration is due to more superficial dust. To dislodge the residual dust without shaking, a technique was explored which involved shearing of the bag fabric. In addition to being potentially harmful to the bag, shaking has the drawback of not cleaning every portion of the bag since nodes may occur where the shaking intensity is a minimum. If a baghouse is operating with ESFF, it may be a further disadvantage that contact between neighboring bags and consequent short circuiting may occur. The function of shaking is to provide a mechanical supplement to the cleaning action of the reverse air flow. There is thus no reason why mechanical modes other than shaking should not be equally effective.

One such mode consists of applying a shear strain to the bag. Since the bag is a cylinder, this can be done simply by turning the top support about the bag axis. The advantage of this procedure is that it is potentially less traumatic and theoretically affects every element of the bag equally. When a fabric is sheared, especially a woven fabric, each elemental space bounded by two neighboring warp and fill yarns will be transformed from a rectangle to a parallelogram. If the space were filled with dust accumulation, the shearing strain would tend to crush the dust aggregate and allow it to be more easily removed by the reverse air flow.

To twist the top bag support, it was encircled with strings which passed through a small hole in the baghouse wall and could be manipulated from the outside. The distance through which the strings had to be pulled to give a certain twist angle was determined beforehand. The shaker was disconnected.

The results of tests performed at different twist angles and numbers of twists are shown in Table 1. These measurements were made after only three cycles and are therefore far from representing steady state conditions. The values in the table refer to the effects of twist cleaning on residual and final pressure drops. Each twist consisted of turning the bag support through the listed angle, first clockwise, then counterclockwise to a negative value of the same angle, and back to the starting point. This was repeated for measurements marked two twists. The results show that "twice" was significantly more effective than "once", and that a larger twist angle reduces pressure drop more than a smaller one.

TABLE 1. RATIO OF PRESSURE DROP AFTER TWISTING TO THAT WITHOUT TWISTING AT SEVERAL TWIST ANGLES AND NUMBERS OF TWISTS

Twist angle	One twist		Two twists	
	Δp_i	Δp_f	Δp_i	Δp_f
2.1°	0.81	0.97	0.60	0.85
4.1°	0.80	0.97	0.64	0.84
6.2°	0.55	0.91	0.44	0.81

Further results, obtained after ten cycles at each condition, are given in Table 2. Here a comparison is made with shaker cleaning, and it can be seen that mechanical agitation, whether twisting or shaking, is an important component of the cleaning procedure. It can also be seen that twisting is as effective as shaking.

TABLE 2. COMPARISON OF PRESSURE DROPS AFTER SHEAR AND SHAKER CLEANING

Cleaning method	Δp_i , mm H ₂ O	Δp_f , mm H ₂ O	Δp $=\Delta p_f - \Delta p_i$, mm H ₂ O
Twist, 2x, 2.1°	10.6	38.1	27.5
Twist, 2x, 4.1°	8.5	35.1	26.6
Twist, 2x, 6.2°	7.3	32.8	25.5
Shake	7.8	32.9	25.1
No shake, no twist	12.2	41.7	29.5

CONCLUSIONS

The performance of a filter bag depends markedly on the method and intensity of cleaning. It follows that significant benefits might derive from research into cleaning principles other than those currently used. Of two such novel approaches explored briefly - subjecting the bag fabric to electric field reversal or to shear during reverse air flow, - shearing appears to merit further study.

REFERENCES

1. Van Osdell, D. W., Ranade, M. B., Greiner, G. P., and Furlong, D. F. Electrostatic Augmentation of Fabric Filtration: Pulse-Jet Pilot Unit Experience. EPA-600/7-82-062 (NTIS PB83-168625), November 1982.
2. Penney, G. W. . Electrostatic Effects in Fabric Filtration Vol. I. EPA-600/7-78-142a (NTIS PB 288576), September 1978.
3. Lamb, G. E. R. and Costanza, P.A. Role of Filter Structure and Electrostatics in Dust-Cake Formation, Textile Res. J. 50, 661-667 (1980).
4. Lamb, G. E. R. and Costanza, P.A. Influences of Fiber Geometry on the Performance of Nonwoven Air Filters. Part III: Cross-Sectional Shape, Textile Res. J. 50, 362-370 (1980).
5. Leith, D., First, M.W., and Gibson, D.D. Effect of Modified Cleaning Pulses on Pulse Jet Filter Performance, Filtration and Separation 15, 400 (1978).
6. Dennis, R. and Wilder, J. Fabric Filter Cleaning Studies. EPA-650/2-75-009 (NTIS PB240372), January 1975.

Session 16: FF: ADVANCED CONCEPTS

John K. McKenna, Chairman
ETS, Inc.
Roanoke, VA

MODELING STUDIES OF PRESSURE DROP REDUCTION
IN ELECTRICALLY STIMULATED FABRIC FILTRATION

Barry A. Morris

Textile Research Institute, Princeton, New Jersey 08542,
and Department of Chemical Engineering, Princeton University,
Princeton, New Jersey 08544

George E. R. Lamb

Textile Research Institute

Dudley A. Saville

Textile Research Institute, and Department of Chemical
Engineering, Princeton University

ABSTRACT

In electrically stimulated fabric filtration, the presence of an applied electric field reduces the pressure drop across the dust-laden filter. One possible explanation is that the electric field changes the dust cake structure by shifting the dust mass distribution towards upstream regions of the fabric where the porosity is greater. Experimental evidence and a mathematical model developed to calculate the pressure drop across a fibrous filter where both the porosity and the dust mass distribution are nonuniform show that the greater pore sizes in the upstream regions can accommodate more dust without plugging, thereby reducing the overall resistance of the filter.

This paper has been reviewed in accordance with the U. S. Environmental Protection Agency's peer and administrative review policies and approved for presentation and publication.

INTRODUCTION

In electrically stimulated fabric filtration (ESFF), an electric field is used to improve the performance of baghouse filters (1). Electric potentials of several kilovolts are applied across wire electrodes placed a few centimeters apart on the upstream surface of the fabric, generating an electric field parallel to the fabric plane. The application of the electric field results in both an increase in fiber capture efficiency (an order of magnitude or more) and a reduction in pressure drop across the dust cake (50% and greater). The former phenomenon is understood to be a surface charge effect (2). The latter phenomenon is important economically in that it may lead to significant savings in capital and operating costs. Mechanisms for this behavior are discussed below.

Lamb et al. (3) showed that the electric field alters the dust deposition on the bag from the almost uniform deposition when no field is present. The dust preferentially deposits near the entrance of the bag and on or near the wire electrodes, setting up a skewed dust distribution in both the lengthwise and tangential directions of the tubular bag. Using the concept of parallel resistors, one would suspect that these mechanisms play an important role in the observed reduction in pressure drop.

However, there is evidence that these are not the only mechanisms involved. Measurements of the local permeability taken around the circumference of the bag show that there is no correlation between the amount of dust deposited and resistance to flow (4). Somehow, the dust cake in the region of greater deposition is more porous. In addition, experiments have shown that fluffing up the surface of the fabric reduces the pressure drop further (5). This leads to the following hypothesis involving deposition of the dust within the depth of the fabric: in a typical fabric there is a lower fiber number density at the surface than in the interior. With no field present the dust penetrates the low density surface region and deposits below the surface where the fibers are closer together; plugging of pores occurs rapidly. The application of the electric field increases the capture efficiency of the fibers so that the dust is captured in the surface region. The dust distribution is effectively shifted upstream where the fibers are farther apart, and plugging of the pores occurs less rapidly.

For the hypothesis to be valid we must show that: 1) a fiber number density distribution exists, 2) the electric field shifts the dust upstream, and 3) the new placement of the dust results in an overall reduction of the pressure drop. In this paper we present both experimental evidence and the results of some mathematical modeling which support the hypothesis.

EXPERIMENTS

The first condition to be satisfied is the fiber number density distribution. Figure 1 shows a photomicrograph of the cross section of a polyester needled fabric. The depth of the fabric is 2.0 mm, and each fiber is 20 μm in diameter. The picture was sectioned into 0.1 mm increments, and the number of fibers in each interval counted. The results are plotted on the histogram on the right. This shows quantitatively that there are fewer fibers near the surfaces of the fabric than in the interior.

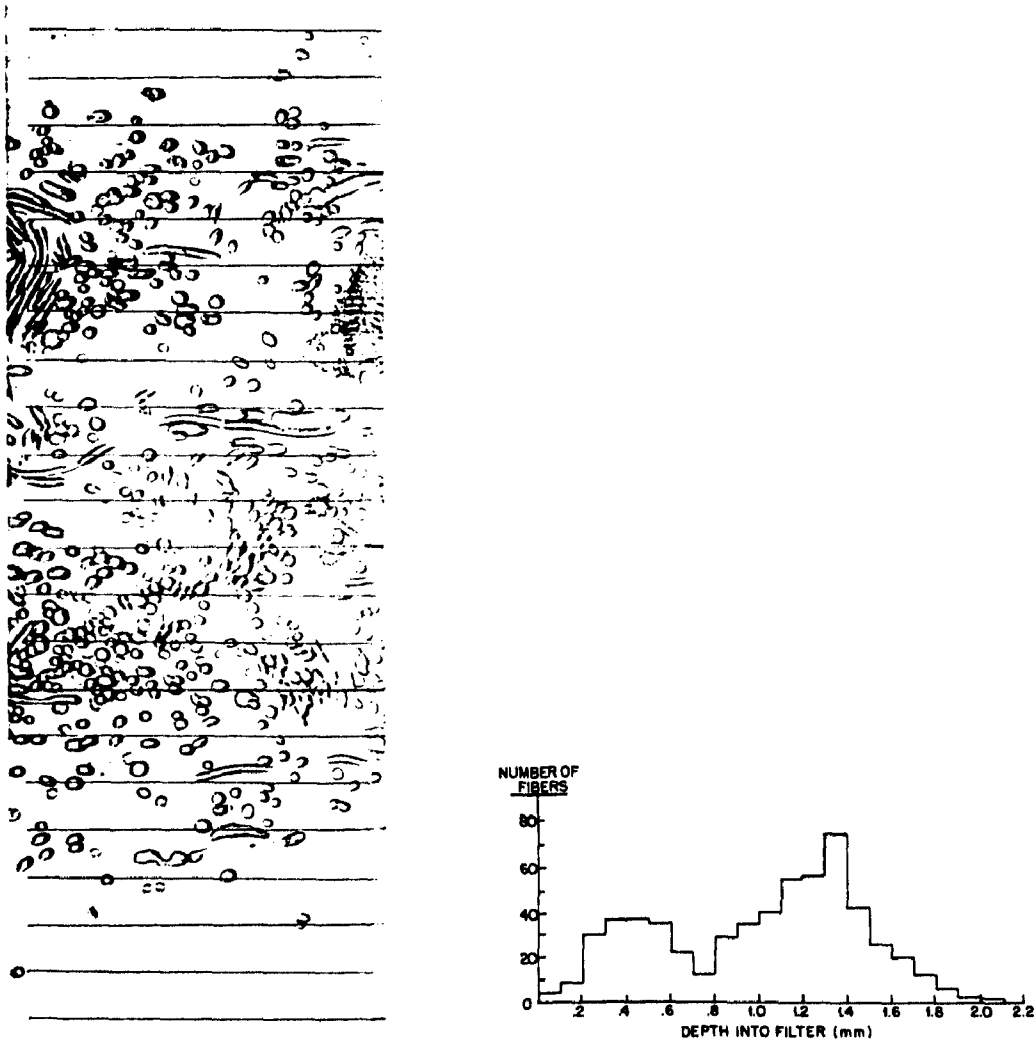


Figure 1. Cross section of polyester needled fabric 2.0 mm thick, and fiber counts in designated 0.1-mm intervals.

To observe any shift in the dust distribution due to the electric field, dust was deposited onto a filter under controlled conditions using the apparatus shown schematically in Figure 2. The filters had a planar geometry, rather than the tubular geometry of a baghouse filter, to eliminate the contribution of axial and tangential distributions to the pressure drop reduction. The filters were usually multilayered to emphasize the fiber distribution effect. Typically, a filter consisted of an upstream layer of carded 3 denier polyester fibers of solidity 0.015-0.020 and a needled polyester downstream layer of solidity 0.23. (The solidity is the volume fraction of fibers and is equal to 1 minus the porosity.) An array of electrodes was placed on the upstream surface so that the electric field was parallel to the fabric surface. The dust was flyash, which ranges in particle size from submicron to $\sim 20\text{ }\mu\text{m}$. The aerosol was generated by dispersing the flyash with a jet of compressed air into the filtering chamber, where a pump forced the aerosol through the fabric. Usually a face velocity of 3 cm/s was used, giving a Reynolds number less than unity (based on the fiber diameter). The design of the apparatus allows for control of the face velocity, electric field strength, and dust loading.

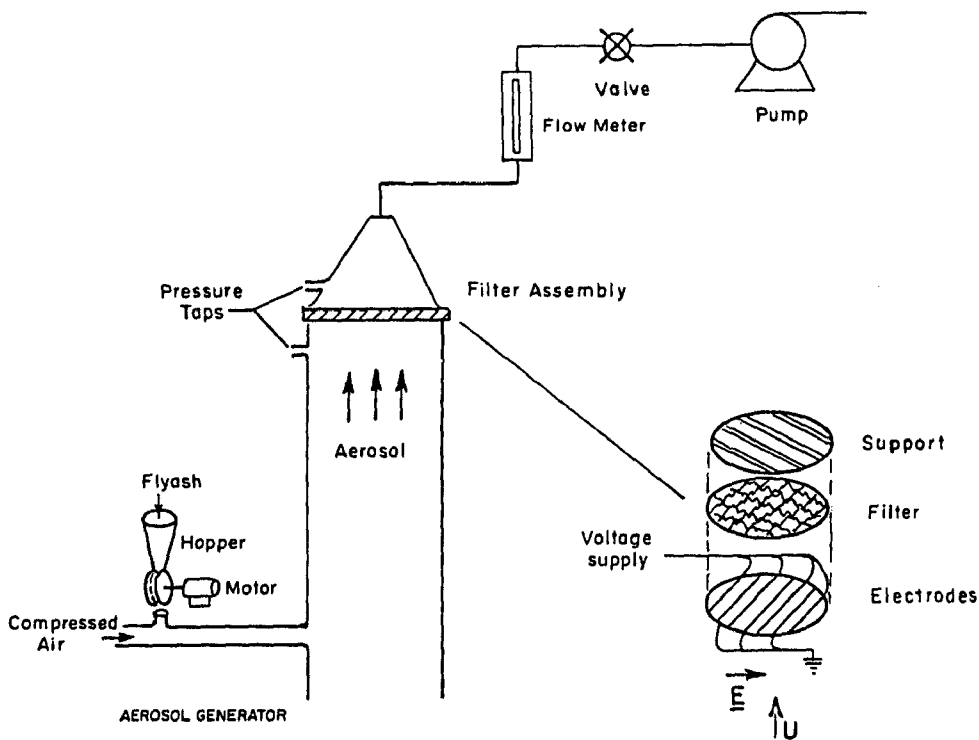


Figure 2. Apparatus to deposit flyash on planar filters.

A crude but useful description of the dust distribution within the depth of the filter was obtained by weighing each layer of the two-layer model before and after deposition. A plot of the fraction of dust in the upstream layer for a loading of 11.9 mg/cm^2 vs. the applied potential is given in Figure 3a. Although there is some scatter in the data, the results show quantitatively that the dust distribution is shifted upstream to regions of lower solidity in the presence of a strong electric field.

Figure 3b shows the corresponding reduction in pressure drop as a function of applied potential. The reduction is greater than what would be observed in real filters since we have added the low density upstream layer.

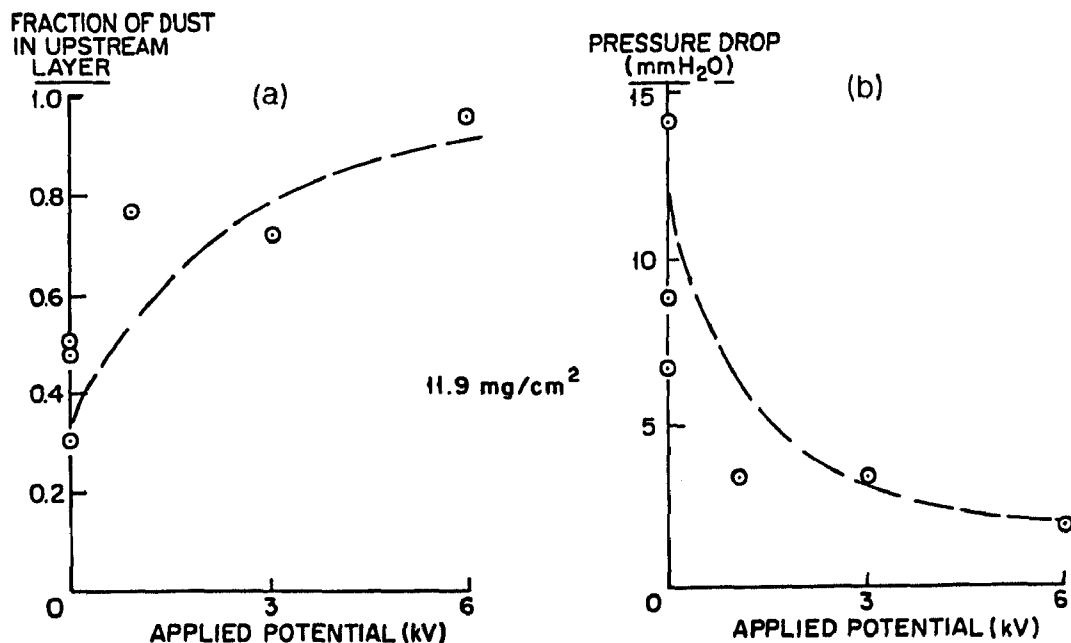


Figure 3. Effect of applied potential on the fraction of dust deposited in the low solidity upstream layer of a two-layer filter (a), and the corresponding effect on pressure drop across the composite (b).

These studies tell us nothing about the structure of the dust cake. Our modeling, described in the next section, points out the importance of knowing how the dust deposits in the filter for predicting the pressure drop. To observe the cake structure we need to look at cross-sectional views which has, in the past, been impossible because of the fragility of the dust cake. Any attempt to section the filter destroys the dust cake. Felix and Smith (6) developed a technique to embed a dust-loaded filter with a low viscosity epoxy. They were looking at strongly bound residual dust, however. The loosely bound "first cycle" dust on our filters is much more fragile and cannot withstand the viscous and surface tension forces of the embedding medium. Attempts to embed them with an epoxy were not successful.

A new technique was developed which eliminates this problem by first fixing the particles in place with the vapor of cyanoacrylate, the active ingredient of some instant adhesives. Cyanoacrylate polymerizes in the presence of water and so it must be kept dry until it comes into contact with the filter. Dry nitrogen is used as the carrier gas (see Figure 4). The sample usually is exposed to steam before the fixation process is begun to provide moisture for polymerization.

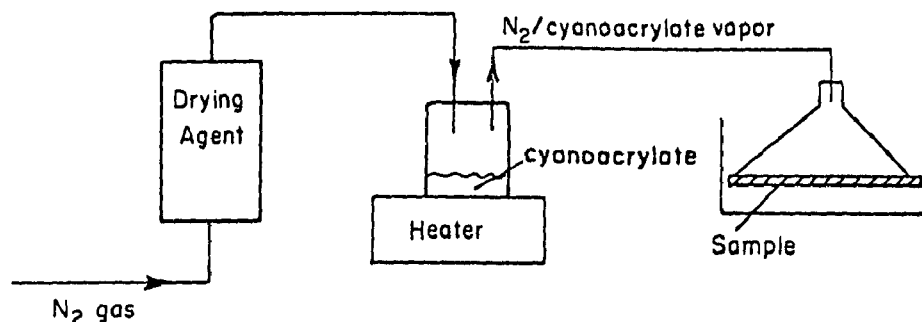


Figure 4. Apparatus for fixing dust cake with cyanoacrylate vapor.

Once the dust has been fixed in place with the cyanoacrylate, the filter is embedded with a low viscosity epoxy, cured, and sliced using standard microscopy techniques. Examples of cross-sectional views are shown in Figures 5 and 6.

Figure 5 is the control case; no electric field has been applied. The filter is comprised of two layers: the top layer of solidity 0.017 and depth 1.6 mm, and a bottom layer of solidity 0.23 and depth 1.7 mm. The fibers in both layers are approximately 20 μm in diameter. The aerosol flow was from top to bottom in the picture and the dark areas represent deposited flyash. For this particular run, 13.8 mg/cm^2 of dust was collected, and the increase in pressure drop due to the dust was 12.8 mm H_2O . The aerosol face velocity was 3.7 cm/s.

Figure 6 shows a similar filter under the same conditions except that an electric field of nominal strength 4 kV/cm was present. Here, 17.3 mg/cm^2 of dust was deposited, but the increase in pressure drop was only 0.4 mm H_2O .

These photographs show the strong difference in dust placement due to the electric field. Without a field almost all the dust penetrates the low density upstream layer and deposits in an almost continuous structure where the dense layer begins. The pores are plugged. When the field is present, very little dust penetrates the upstream layer. The dust deposits around individual fibers, creating a very porous structure.

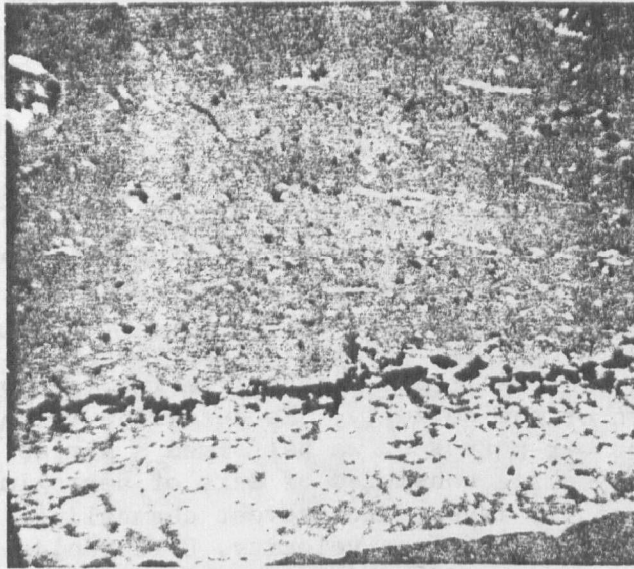


Figure 5. Cross section of two-layer filter, the upper layer of low solidity (fibers white), with dust particles (black) deposited with no electric field.

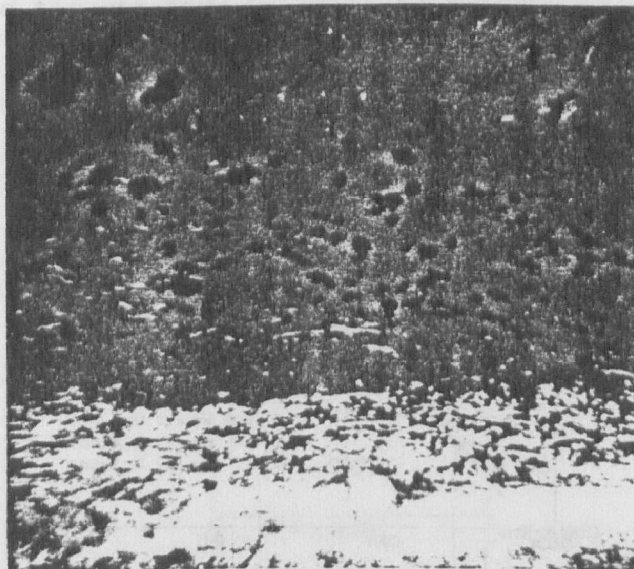


Figure 6. Same as Figure 5, but dust deposited with a 4-kV/cm field applied.

MODELING

The experiments verified that the first two conditions of the hypothesis are true, namely that there is a fiber number density distribution (fewer fibers at the surface) and that the electric field shifts the dust to the upstream region of lower number density. To determine if this shift is responsible for at least part of the observed reduction in pressure drop, a mathematical model was developed. The utility of the model is that, given a particular fiber number density distribution and dust distribution, it predicts the pressure drop. The model was developed by first selecting an appropriate clean filter model from the literature and modifying it to account for both the fiber distribution and the presence of the dust.

There are many theoretical and empirical relationships for the pressure drop across a clean fibrous filter, each differing in how the pressure drop varies as a function of the solidity. To determine which relationship is most appropriate for our purposes, we performed a series of experiments on a packed column. The packing consisted of mats of approximately randomly oriented fibers carefully layered to prevent channeling. The pressure drop was measured as a function of face velocity, U (Reynolds number was always <1); fiber radius, a ; depth of packing, h ; and solidity, c (volume fraction of fibers). The results are plotted in Figure 7 as a dimensionless pressure drop vs. solidity. The fact that the results fit on a single curve verifies that:

$$\Delta p \propto \frac{\mu U h}{a^2} .$$

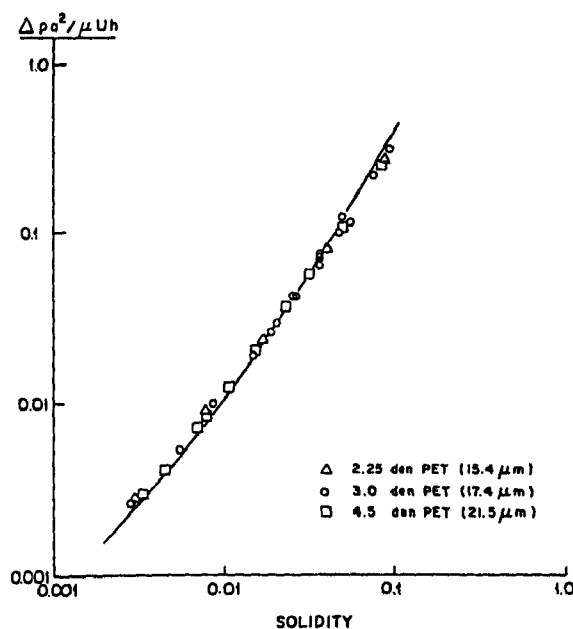


Figure 7. Effect of solidity in a group of polyester (PET) filter fabrics on dimensionless pressure drop (points). Curve calculated using the Happel cell model (7).

One approach to mathematical modeling of the pressure drop across fibrous media is the so called cell model. The disturbance to the flow due to the presence of a fiber is assumed to be confined to an imaginary envelope or cell around the fiber, the diameter of the cell being related to the porosity. The equations of motion are solved inside the cell assuming no slip at the fiber surface. Somewhat arbitrary boundary conditions are imposed at the cell boundary to take into account hydrodynamic interactions between fibers. The drag on a single fiber is computed from the flow field solution, and the pressure drop obtained by summing the drag on all the fibers. The cell models are not rigorous; they were developed for mathematical convenience, but they do seem to predict the right form for the Δp vs. solidity behavior. The Happel cell model (7), which fits our packed column results very well (see Figure 7), assumes zero shear stress at the cell boundary. More importantly, however, it assumes that the fibers are all parallel to the flow, which is totally inconsistent with the more or less random configuration of the fibers in the experiments. We are currently trying to resolve this discrepancy and derive a more rigorous clean filter model. We use the Happel cell model here purely because it empirically fits our data. It may be written:

$$\frac{\Delta p^2}{\mu U h} = \frac{4c}{-\ln c + 2c - (c^2/2) - (3/2)} ,$$

where c = solidity (volume fraction of fibers).

The next step in developing a model to predict the pressure drop across dust-laden filters is to take into account the fiber number density distribution. This was done quite simply by representing the experimental filters as three layers of uniform solidity (see Figure 8). The top layer in the model corresponds to the low density upstream layer and the surface region of the downstream layer in the experiments. This is followed by a thin high density layer in the model representing the thin region near the surface of the downstream layer where most of the dust collects when no electric field is applied (see Figure 5). The third layer in the model represents the remainder of the downstream layer. It is assumed that no dust deposits in the third layer; this is consistent with experimental observations.

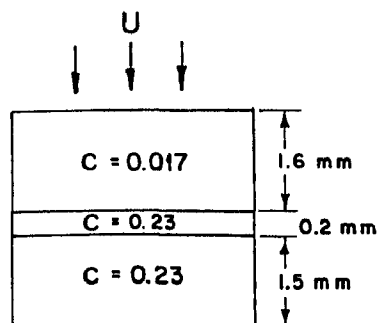


Figure 8. Three-layer representation of filters used in model calculations.

Finally, the presence of the dust is assumed to increase the solidity and the effective diameter of the fibers, both parameters of the clean filter model. The effective diameter of the dust/fiber combination depends on the dust cake structure. Again, a simple approach is taken to represent the dust cake structure. At one extreme one might expect the dust particles to deposit uniformly around each fiber, as shown in Figure 9a. Using this representation, the model predicts pressure drops an order of magnitude too low. At another extreme, based on single fiber deposition studies (2), the particles might deposit as particle-particle chains known as dendrites (Figure 9b). With this representation, the model predicts an order of magnitude too high. In a real filter, the deposition pattern lies somewhere in between, so we combine the uniform and dendrite representations with an adjustable parameter called the dendrite fraction (DFR). We can determine the DFR by fitting experimental results with the model.

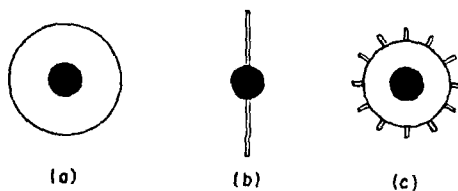


Figure 9. Representations of mode of dust deposition on a single fiber.

(a) Uniform deposition. (b) Dendrite model. (c) Combined model.

Figure 10 shows that a DFR of 0.25 fits the data well. In Figure 10, the dimensionless pressure drop is plotted versus the fraction of the dust in the upstream layer, and the experimental points were obtained by varying the electric field strength. A DFR of 0.25 is consistent with dust cake structure observations. Figure 11 shows how well the model predicts the pressure drop behavior at other dust loadings using the fitted DFR. Reasonable agreement is obtained considering the simplicity of the model.

Even in this simple form, the model shows two important things. The pressure drop is very sensitive to the microstructure of the dust cake. A small decrease in DFR results in a significant reduction in pressure drop. This underscores the importance of the cross-sectional view studies which may lead to a priori prediction of DFR. Moreover, the DFR is likely to be a function of electric field strength, which in itself would be a pressure drop reducing mechanism.

Finally, the model shows that varying only where the dust is collected leads to a substantial pressure drop reduction, clearly supporting the hypothesis. The shift of dust upstream to regions of lower fiber number density can indeed be an important mechanism behind the reduction of pressure drop in ESFF.

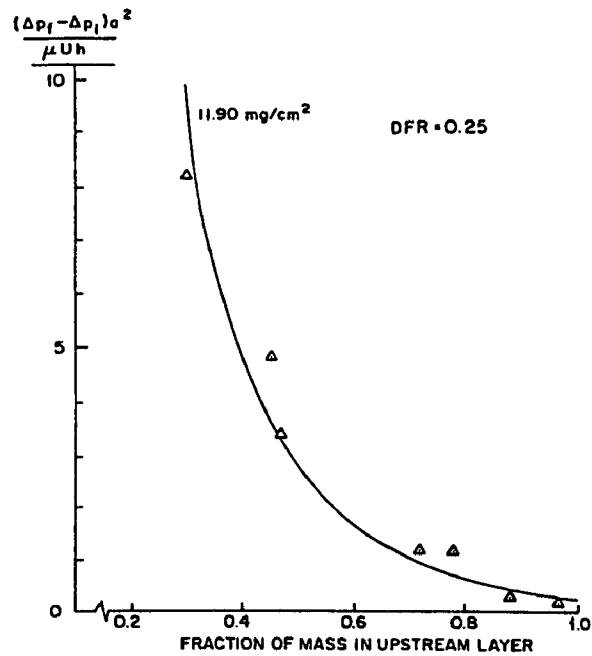


Figure 10. Dimensionless pressure drop vs. fraction of dust in the upstream layer for various applied potentials (points), and curve calculated using the model and dendrite fraction 0.25.

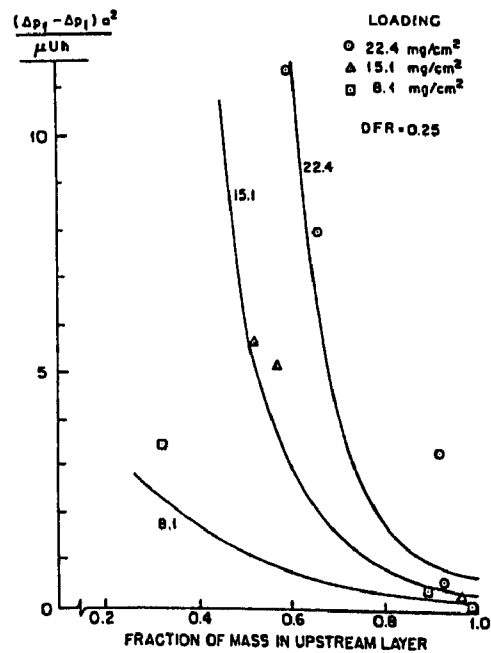


Figure 11. Same as Figure 10 for several additional dust loadings.

REFERENCES

1. Van Osdel, D. W., Greiner, G. P., Lamb, G. E. R., and Hovis, L. S. Electrostatic Augmentation of Fabric Filtration. In: Third Symposium on the Transfer and Utilization of Particulate Control Technology, Volume I, EPA-600/9-82-005a (NTIS PB83-149583), July 1982.
2. Oak, M. J. Fibrous Filtration in the Presence of Electric Fields. Doctoral Dissertation, Department of Chemical Engineering, Princeton University, 1981.
3. Lamb, G. E. R., Jones, R. I., and Lee, W. B. Electrical Stimulation of Fabric Filtration: Enhancement by Particle Precharging. Fourth Symposium on the Transfer and Utilization of Particulate Control Technology, Houston, Texas, 1982.
4. Lamb, G. E. R. and Jones, R. I. Pressure Drop for a Filter Bag Operating with a Lightning-Rod Precharger. Fifth Symposium on the Transfer and Utilization of Particulate Control Technology, Kansas City, Missouri, 1984.
5. Lamb, G. E. R. and Costanza, P. A. Role of Filter Structure and Electrostatics in Dust Cake Formation. In: Second Symposium on the Transfer and Utilization of Particulate Control Technology, Volume III, EPA-600/9-80-039c (NTIS PB81-144800), September 1980.
6. Felix, L. G. and Smith, W. B. Preservation of Fabric Filtered Dust Cake Samples. J. Air Pollution Control Assoc. 33, 1092 (1983).
7. Happel, J. Viscous Flow Relative to Arrays of Cylinders. AICHE J. 5, 174 (1959).

FLOW RESISTANCE REDUCTION MECHANISMS FOR
ELECTROSTATICALLY AUGMENTED FILTRATION

D. W. VanOsdell and R. P. Donovan
Research Triangle Institute
Research Triangle Park, North Carolina 27709

Louis S. Hovis
Industrial Environmental Research Laboratory
U. S. Environmental Protection Agency
Research Triangle Park, North Carolina 27711

ABSTRACT

Electrostatically augmented (EA) filtration has been studied at laboratory, pilot, and nearly full scale over the past several years because of its potential for improving the performance of industrial baghouses. The results of the various experimental studies have not been completely consistent except in the overall result that EA filtration generally leads to reduced pressure drop and improved particle collection efficiency.

The lack of consistency is not surprising when the wide range of experimental conditions and methods of obtaining EA filtration is considered. A number of mechanisms have been suggested to account for the effects of EA filtration, and it is possible that more than one competing mechanism may be operating during any given experiment. The three principal mechanisms are increased collection on the higher porosity upstream surface of the filter, nonuniform dust deposits across the filter surface due to EA, and increased dust cake porosity due to EA. The available experimental data and observations will be used to evaluate these mechanisms through comparison with computer models. Emphasis will be placed on EA filtration of naturally charged fly ash utilizing an external electric field parallel to the fabric surface at normal utility baghouse operating conditions.

This paper has been reviewed in accordance with the U. S. Environmental Protection Agency's peer and administrative review policies and approved for presentation and publication.

INTRODUCTION

EA filtration has been widely studied during the past decade and has been reported to reduce fabric filter pressure drop and to improve particle collection efficiency by a number of researchers.(1-8) In addition, fundamental studies of the interaction of particles and fibers in the presence of electrical fields have been reported(9-13), generally indicating that fiber collection efficiency is increased and that the particle deposits tend to form chain-like structures or dendrites. Despite the widespread study of the phenomenon, the actual mechanisms by which EA filtration reduces pressure drop in an operating fabric filter are not well understood. The purpose of this

paper is to evaluate the three principal models by comparing their pressure drop predictions with actual pilot plant data and observations.

EA filtration can be obtained through a number of filter designs and operating strategies. The dust may be deliberately charged, the filter may be subjected to an external electric field, or both may be done at once. If an electric field is applied to the filter surface, it may be parallel or perpendicular to the fabric surface. The data to be used for comparison in this paper were all obtained at the EPA EA filtration pilot plant, operating on a slipstream from a pulverized coal industrial boiler.(7) The electrical field was applied parallel to the fabric surface, and the particles were not artificially charged (as with a corona charger). This form of EA filtration is known as electrostatically stimulated fabric filtration (ESFF).

In the first model examined below, the multilayer filter model, it is postulated that the effect of the electrostatic forces is to cause increased particle collection in the upstream region of a filter at the expense of collection in the main body of the filter. As the surface typically is less dense than the rest of a filter, dust collection in this region leads to reduced pressure drop. The second model discussed (nonuniform areal dust density model) postulates that the reduced pressure drop is due to nonuniform dust deposition on the filter surface, with the dust tending to separate from the fluid paths due to electrostatic forces. This nonuniform dust cake has been shown to have a reduced pressure drop. The third model (porosity change model) proposes that the cause of the reduced pressure drop is an increase in the porosity of the collected dust due to electrical forces, which can affect both the physical character of the dust deposit and the ability of the dust deposit to resist compression by fluid forces.

These models are compared with pilot plant results for dust cake flow resistance on the basis of normalized pressure drop rise versus time plots. Because the models express the effect of a particular dust cake structure on pressure drop, their applicability is independent of the particular form of EA filtration being studied. Comparison with the ESFF pilot unit is valid because dust cakes like those postulated by the models may form. Each is examined as a "pure" or independent mechanism, standing alone with no interaction with other mechanisms.

ESFF FILTRATION PILOT UNIT RESULTS

The ESFF filtration pilot unit was operated over a period of approximately 2 years on a slipstream from an industrial boiler house(7) in both pulse-jet and reverse-air cleaning modes. A typical pressure drop versus time plot for the pulse-jet operation is shown as Figure 1. Both the residual pressure drop and the rate of increase of pressure drop are seen to be reduced for the ESFF filter. To evaluate the EA filtration models in this paper, only effects on the dust cake flow resistance were considered. Changes in the residual pressure drop were not modeled. The pressure drop rise over one cleaning cycle was the parameter modeled. This pressure drop rise was normalized by dividing by the final pressure drop for the conventional baghouse. The result of this normalization for the pilot plant data is shown in Figure 2. Normalization was necessary because the filtration models studied were

not sufficiently accurate to predict the actual values of pressure drop for either the conventional or the EA filter. The normalization allowed evaluation of the ability of the model to predict the relative behavior of the conventional and EA filters without regard to the actual pressure drop value predicted.

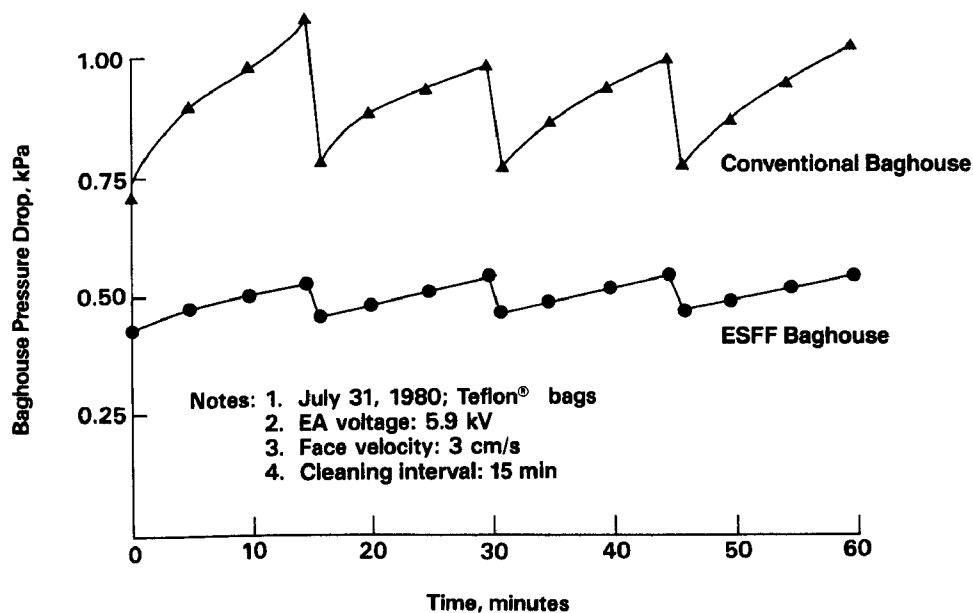


Figure 1. Pressure drop comparison for conventional and ESFF pilot pulse-jet baghouses.

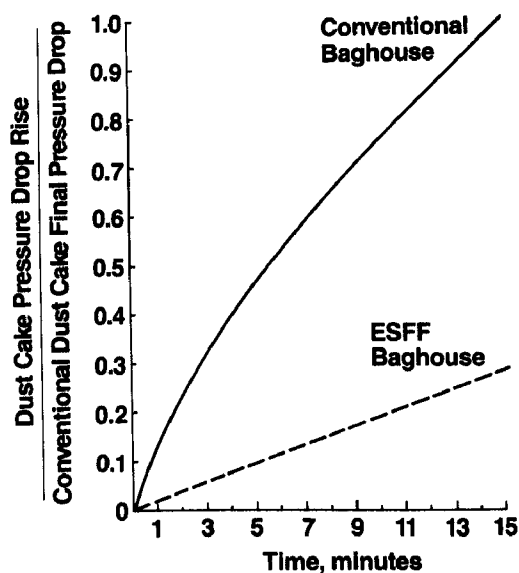


Figure 2. Normalized pressure drop rise for conventional and ESFF pilot pulse-jet baghouses.

EA FILTER MODELS

MULTILAYER FILTER MODEL

Miller et al.(14,15) have shown experimentally that the application of an electric field to a filter causes the dust mass distribution to shift toward the upstream surface of the filter and that the packing density of a fabric filter is not uniform but varies from a very low density at the upstream surface to a more typical value in the body of the fabric. It has also been shown(6) that improved performance of an EA filter results when the filter has a comparatively low surface density. Based on these results, Morris, Lamb, and Saville(16) propose that the pressure drop reduction obtained with EA filtration is caused by a shift in the dust cake mass distribution toward increased dust collection in the upstream surface layer of the filter. This is said to result in reduced pressure drop because the surface of a filter normally is less dense than the inner portions of the filter. Dust collection in the low density region leads to reduced dust cake pressure drop.

The model presented by Morris, Lamb, and Saville treats a filter as being made up of three regions: an upstream, very low packing density region; a middle, higher packing density region; and a downstream, high density region. The surface layer was assigned a packing density of 0.02, and the middle and final layers a packing density of 0.2. The total filter thickness was divided, with 20 percent in the surface layer, 20 percent in the middle layer, and the balance in the downstream filter layer. Ten percent of the total dust mass was assumed to collect in the final layer, and the remaining dust was divided between the surface and middle layers as an adjustable parameter. Figure 3 illustrates the arrangement of the various regions of the filter and their respective packing densities.

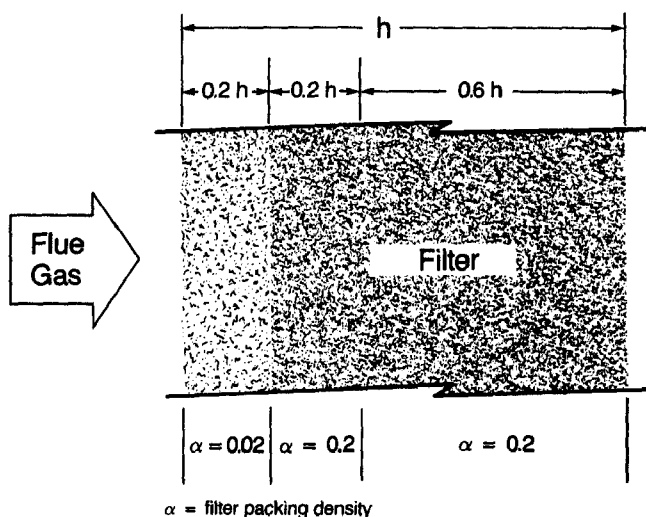


Figure 3. Multilayer filter model.

The basic pressure drop relationship presented by Morris, Lamb, and Saville, in dimensionless form, is:

$$\frac{\Delta P R^2}{\mu U h} = 4K \alpha \frac{(1 - \epsilon)}{\epsilon^3}, \quad (1)$$

where: ΔP = filter pressure drop, Pa;

R = filter effective fiber diameter, m;

μ = gas viscosity, kg/m-s;

U = filter face velocity, m/s;

h = filter thickness, m;

K = hydrodynamic factor =

$$\frac{\epsilon^3}{(1 - \epsilon)[- \ln(1 - \epsilon) + 2(1 - \epsilon) - (1 - \epsilon)^2/2 - 3/2]};$$

α = filter packing density, dimensionless; and

ϵ = porosity of dirty filter, dimensionless.

The strong dependence of the model on the filter porosity and the effect of filter thickness can be seen in Equation 1. As originally derived, by Happel(17), this model was for constant fiber size and, thus, negligible filter loading. Morris, Lamb, and Saville modified Happel's expression to account for two limiting cases: (1) increasing fiber diameter as particles collected in a uniform sheath-like deposit, and (2) changing effective fiber diameter due to particle collection in dendrites one particle thick. Both types of particle collection were used in a weighted average to obtain the final pressure drop expression. Increasing fiber diameter was incorporated by the definition of ϵ as the porosity of the dirty filter and the effect of dendrites by modifying the definition of fiber radius to include the dendrites in a weighted average fiber diameter.

As applied for this paper, the model was similar but not identical to that presented by Morris, Lamb, and Saville in that the pressure drop as a function of time was calculated for conditions which approximated those at the EA filtration pilot unit.

Predictions of this model for 10, 30, 50, and 70 percent of the total dust load collected in the upstream layer are presented in Figure 4. Ten percent of the dust mass in the upstream, low density layer was taken to be the conventional case. Data reported by Morris, Lamb, and Saville indicate that the upstream layer with no applied electric field may collect from 10 to 30 percent of the incoming dust. Figure 4 shows that application of the multilayer model can result in significant theoretical pressure drop reductions. The greatest change in pressure drop occurred as the particle loading was shifted from 10 to 50 percent of the dust on the upstream layer, and

little change occurred for further dust mass distribution shifts. The upward concave shape of the model pressure drop curve in Figure 4 is probably not significant given the overall low accuracy of the model.

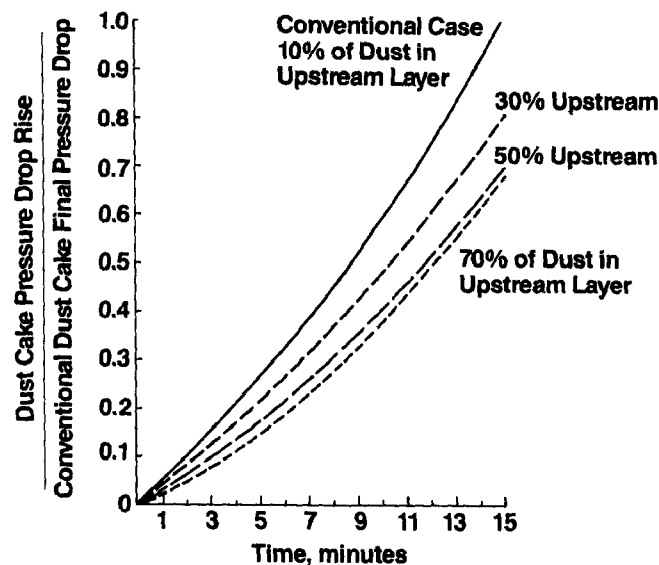


Figure 4. Normalized pressure drop rise for multilayer filter model.

The multilayer model is consistent with observations of the detailed structure of a filter dust cake under EA conditions(14), especially for lightly loaded fabrics where the dust cake interacts to a large extent with the fabric surface. The magnitude of the pressure drop changes predicted by the model is not sufficient to account for all the observed EA filtration pressure drop effects.

NONUNIFORM DUST DEPOSITION ON FILTER SURFACE

Another model which has been proposed to explain EA filtration is that of nonuniform dust deposition on the filter fabric surface. This model has been described by Chiang, Samuel, and Wolpert(18) for charged particle EA filtration, but the same principles apply to filter pressure drop calculation for any nonuniform deposition situation. They argue that the electrostatic forces, rather than the aerodynamic forces, dominate the location of particle deposits on the EA filter surface. Because strong electrostatic forces exist, the self-leveling tendency of a fabric filter--which tends to bring more dust to a high flow region of the filter and reduce flow through that region--no longer applies. Thus, it is possible for dust to accumulate in high areal mass density regions and for the gas flow to proceed through the low density regions. For the cake to be nonuniform, it is only necessary that the areal density be a function of position; the dust cake specific flow resistance is taken to remain constant over the entire filter. Because parallel paths having different resistances are available for gas flow, the overall resistance of the filter is reduced.

Chiang, Samuel, and Wolpert apply the model in two forms: (1) a dust deposition pattern with half the filter being subject to a low deposition rate and half to a high deposition rate, and (2) a smoothly distributed nonuniform dust mass deposition pattern on the filter. They show that application of this model produces pressure drop results comparable to their laboratory EA filter final pressure drop values and consistent with their experimental evidence of nonuniform dust deposits.

Further evidence in favor of the model proposed by Chiang, Samuel, and Wolpert can be found in filter deposits observed by VanOsdell et al.(19) on a small EA filter. Figure 5 is a photograph of two of these filter deposits. The top filter deposit was collected with no electric field applied to the filter, while the lower deposit was collected with the electric field applied to naturally charged dust. The contrast is striking and suggests that long range electrical forces (Coulombic) are dominating the collection process. Despite this clear evidence of nonuniform deposits in the laboratory, examination of the pilot unit pulse-jet dust deposits did not reveal any nonuniform deposits. As the pulse-jet unit was cleaned while the laboratory filter was not, the difference may have been in the cleaning and dust redeposition. While the electric field was not turned off during cleaning, the bag was inflated away from the electrodes. Presumably the dust began to redeposit while the bag was not in contact with the electrodes.

The model of Chiang, Samuel, and Wolpert was modified slightly to allow variation of the areas of the thick and thin deposits on the filter and was applied using dust and filter cake parameters from the EA filtration pilot unit data shown in Figure 1. The principal parameters of the model are the fraction of "thin" dust cake area and the deposition rate ratio, which is the mass of dust collected in the high mass (thick cake) region compared to the low mass (thin cake) region. The pressure drop equations derived were:

$$\Delta P_{\text{uniform}} = K_2 C U^2 \Delta t, \text{ and} \quad (2)$$

$$\Delta P_{\text{nonuniform}} = K_2 C U^2 \Delta t \left[\frac{n}{(n+1)[r^2(n+1) - 2r + 1]} \right], \quad (3)$$

where: uniform and nonuniform refer to the dust cake;

ΔP = pressure drop rise, Pa;

K_2 = specific dust cake flow resistance, s^{-1} ;

C = gas dust loading, kg/m^3 ;

U = filtration velocity, m/s;

Δt = elapsed time in filter cycle, s;

n = deposition rate ratio, thick/thin; and

r = areal fraction of thin cake.

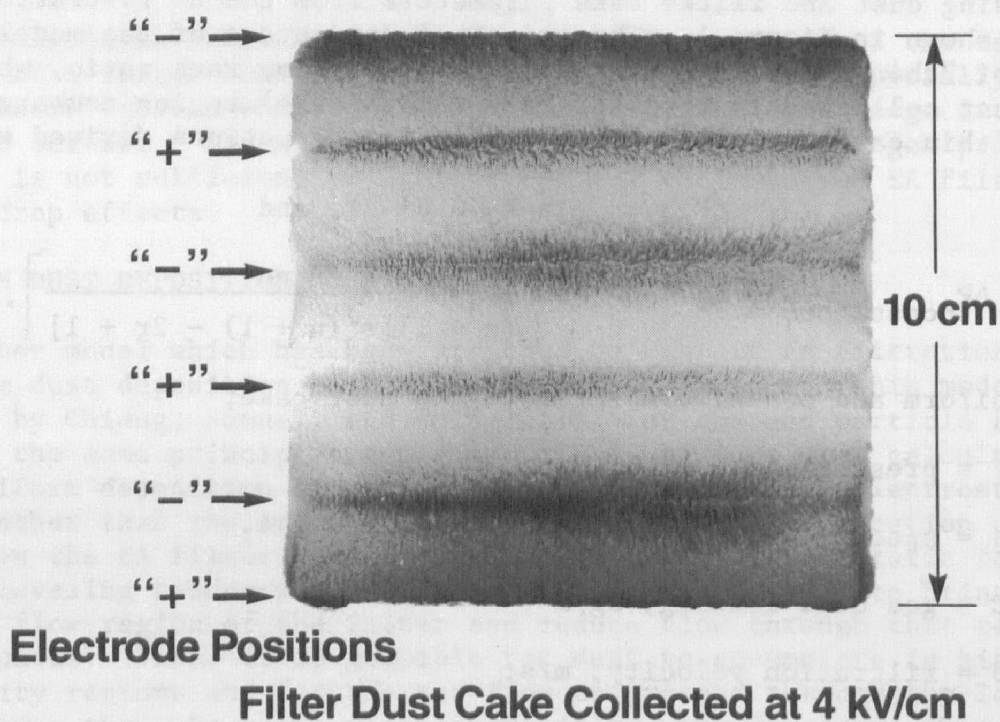
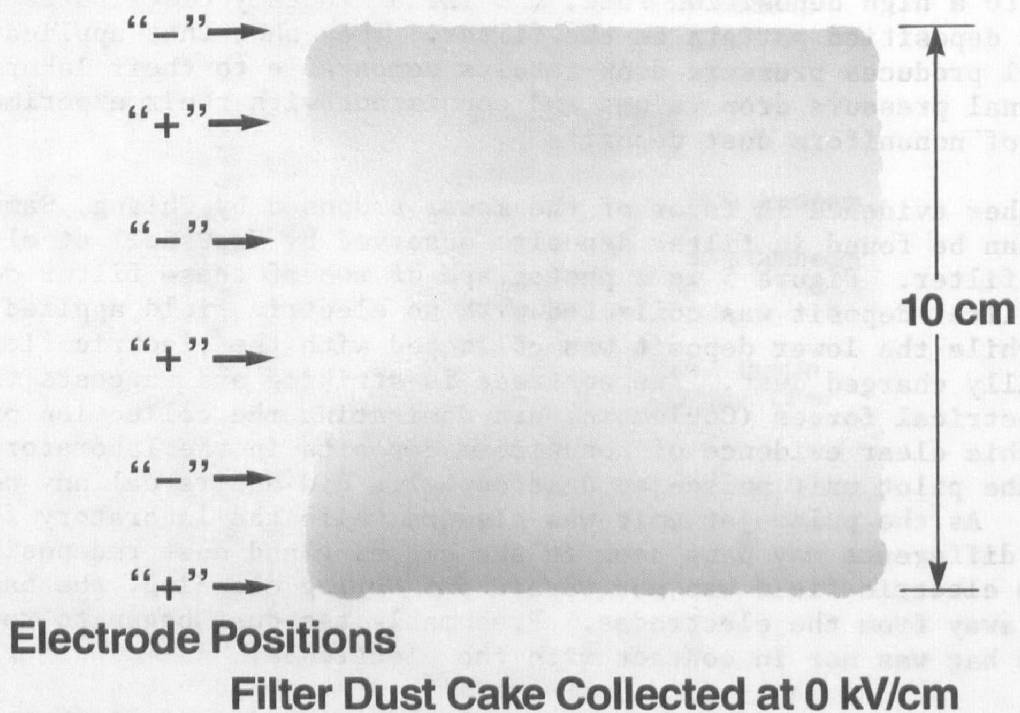


Figure 5. Laboratory filter dust deposits for 0 and 4 kV/cm electric field strength.

Figure 6 shows the results of applying the model for a constant fraction of thin dust cake area while varying the deposition rate ratio. At a deposition rate ratio of between 2 and 3, the model predicts reductions in pressure drop rise which are comparable to those observed at the EA pilot unit. As expected, further increasing the deposition rate ratio causes additional reduction in the pressure drop rise. Figure 7 shows the effect of changing the fraction of thin dust cake while holding the deposition rate ratio constant at 3:1.

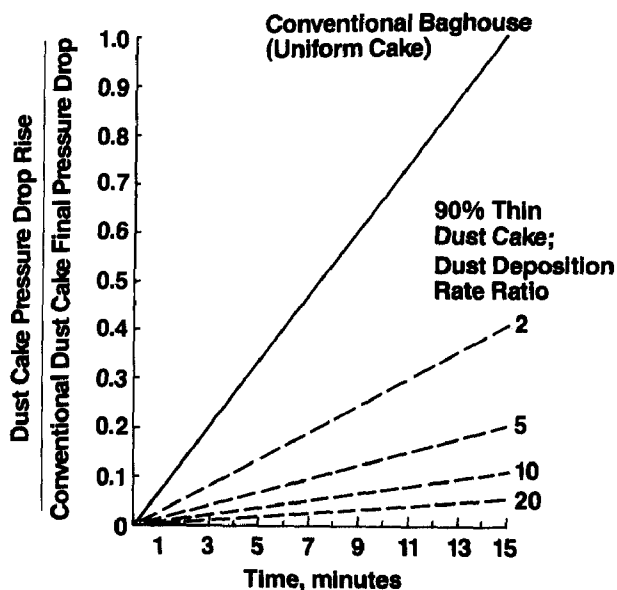


Figure 6. Normalized pressure drop rise for nonuniform dust cake model: thin dust cake over 90 percent of filter with different dust deposition rate ratios.

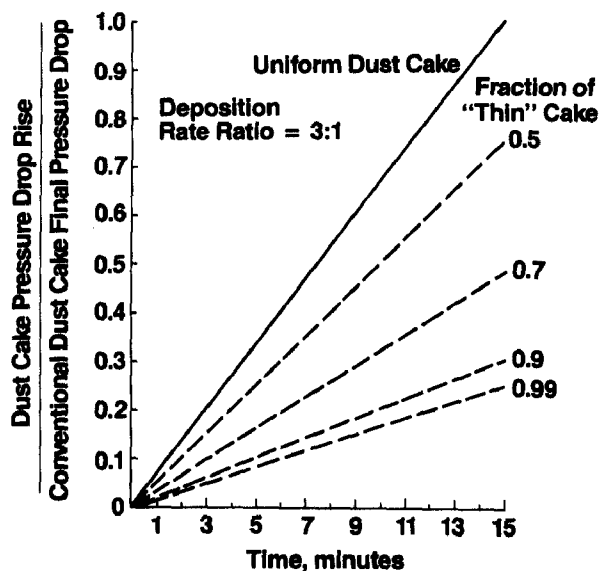


Figure 7. Normalized pressure drop rise for nonuniform dust cake model: deposition rate ratio of 3:1, varying thin cake fraction.

In summary, the nonuniform deposit model can predict a reduction in the dust cake flow resistance, using reasonable values of all parameters, which agrees well with the effects observed at the EA filtration pilot unit. Laboratory EA filtration experiments have produced nonuniform filter deposits with apparent deposition rate ratios and thin/thick area ratios that match up well with the model. However, actual pilot plant dust deposits have been relatively uniform, without any readily visible thick or thin regions.

CHANGE IN DUST CAKE POROSITY

The flow resistance of particle beds is known to depend, in part, on the porosity of the particle deposit. A detailed application of fluid mechanics to the prediction of filter dust cake specific flow resistance has been presented by Rudnick.(20) It has been observed that the dust collected in the EA baghouse hopper has a lower bulk density than the dust collected at the same time in the conventional baghouse.(7) The bulk density of the EA baghouse dust was 0.23 g/cc, while that of the conventional baghouse hopper dust was 0.27 g/cc. The packing density of the EA filter hopper dust and conventional baghouse hopper dust were calculated to be 0.085 and 0.10, respectively, based on the known true particle density of 2.7 g/cc. The dust cake was assumed to be both uniform throughout its depth and uniformly distributed over the filter surface. K_2 was then calculated using the form of the Happel equation suggested by Dennis and Dirgo(21):

$$K_2 = \frac{18 \mu}{d_p^2 \rho_p C_c} \left[\frac{3 + 2 \alpha^5}{3 - 4.5 \alpha^1 + 4.5 \alpha^5 - 3 \alpha^2} \right], \quad (4)$$

where: d_p = Sauter mean particle diameter, m;

ρ_p = true particle density, kg/m³; and

C_c = slip correction factor, dimensionless.

This K_2 value was substituted into Equation 2 to obtain an expression for filter pressure drop as a function of dust cake porosity.

Figure 8 presents the results of this calculation. The normalized pressure drop reduction obtained for the porosity variation observed at the EA pilot unit is seen to be considerably less than that observed at the pilot unit. The EA filter normalized pressure drop is approached only after an unrealistically high porosity is reached. However, the porosity of the fly ash collected in the conventional baghouse is unusually high at the ESFF pilot unit, so this mechanism could be more important for fly ashes of lower porosity in standard operation.

CONCLUSIONS

Of the models examined in this paper, only the nonuniform deposition model, in its pure form, predicts improved pressure drop performance at the scale observed experimentally when reasonable values are chosen for the input parameters. In addition, nonuniform dust cakes have been observed in the

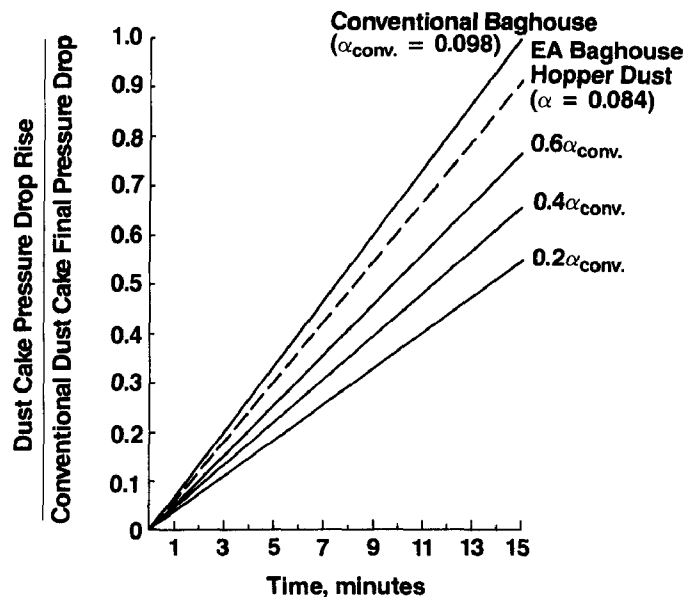


Figure 8. Normalized pressure drop rise for variation in dust deposit porosity based on ESFF pilot unit data.

laboratory. However, because the deposition pattern of the pilot unit pulse-jet EA filter did not appear to be nonuniform, serious reservations must be held as to the adequacy of the nonuniform deposition model. Strong experimental evidence supports both the porosity change and multilayer models, but neither appears to adequately account for the observed EA filtration pressure drop effects.

The pressure drop rise reduction produced by EA filtration is probably due to a combination of the three mechanisms: nonuniform deposition, porosity change, and multilayer deposition. Further detailed study will be required to isolate the effects.

REFERENCES

1. Penney, G. W. Electrostatic effects in fabric filtration: fields, fabrics, and particles (annotated data). Volume I. EPA-600/7-78-142a (NTIS No. PB 288576), U. S. Environmental Protection Agency, September 1978.
2. Ariman, T. and Helfritch, D. J. Pressure drop in electrostatic fabric filtration. In: Second Symposium on the Transfer and Utilization of Particulate Control Technology, Volume III. EPA-600/9-80-039c (NTIS No. PB81-144800), U. S. Environmental Protection Agency, Research Triangle Park, North Carolina. September 1980. Pp. 222-236.
3. Bergman, W. et al. Electrostatic filters generated by electric fields. UCRL-81926, Lawrence Livermore National Laboratory,

P. O. Box 808, Livermore, California, 94550, July 23, 1979.
(Presented at the Second World Filtration Congress, London, England,
September 18-20, 1979).

4. Chudleigh, P. W. and Bainbridge, N. W. Electrostatic effects in fabric filters during build-up of the dust cake. *Filtration and Separation*. 17(July/August): 309-311, 1980.
5. Donovan, R. P. et al. Electrostatic augmentation for particulate removal with fabric filters. In: Fifth International Fabric Alternatives Forum Proceedings. American Air Filter Company, Inc., 215 Central Avenue, Louisville, Kentucky, January 1981. Pp. 12-1 to 12-24.
6. Lamb, G. E. R. and Costanza, P. A. A low-energy electrified filter system. *Filtration and Separation*. 17(July/August): 319-322, 1980.
7. VanOsdell, D. W., et al. Electrostatic augmentation of fabric filtration: pulse-jet pilot unit experience. EPA-600/7-82-062 (NTIS No. PB83-168625), U. S. Environmental Protection Agency, Research Triangle Park, North Carolina, November 1982.
8. Greiner, G. S., et al. Electrostatic stimulation of fabric filtration. *JAPCA*. 31(10): 1125-1130, (October) 1981.
9. Bhutra, S. and Payatakes, A. C. Experimental investigation of dendritic deposition of aerosol particles. *J. Aero. Sci.* 10: 445-464, 1979.
10. Nielsen, K. A. and Hill, J. C. Particle chain formation in aerosol filtration with electrical forces. *AIChE J.* 26(4): 678-680, (July) 1980.
11. Oak, M. J. Fibrous filtration in presence of electric fields. Ph.D. thesis, Princeton University, Department of Chemical Engineering, September 1981.
12. Wang, C. S., et al. Effect of electrostatic fields on accumulation of solid particles on single cylinders. *AIChE J.* 26(4): 680-683, (July) 1980.
13. Zebel, G. Deposition of aerosol flowing past a cylindrical fiber in a uniform electric field. *J. Colloid Sci.* 20: 522-543, 1965.
14. Miller, B. et al. Studies of dust cake formation and structure in fabric filtration: second year. EPA-600/7-79-108 (NTIS No. PB297581), U. S. Environmental Protection Agency, April 1979.
15. Miller, B. et al. Studies of dust cake formation and structure in fabric filtration. EPA-600/9-81-023 (NTIS No. PB83-259986), U. S. Environmental Protection Agency, August 1983.
16. Morris, B. A., Lamb, G. E. R., and Saville, D. A. Electrical stimulation of fabric filtration part V: model for pressure drop reduction. *Textile Res. J.* 54(6): 403-408, (June) 1984.

17. Happel, J. Viscous flow relative to arrays of cylinders. *AIChE J.* 5:174-177, (June) 1959.
18. Chiang, T. K., Samuel, E. A., and Wolpert, K. E. Theoretical aspects of pressure drop reduction in a fabric filter with charged particles. In: Third Symposium on the Transfer and Utilization of Particulate Control Technology, Volume III. EPA-600/9-82-005c (NTIS No. PB83-149609), U. S. Environmental Protection Agency, July 1982. Pp. 250-260.
19. VanOsdell, D. W., et al. Permeability of dust cakes collected under the influence of an electric field. Paper presented at the Fourth Symposium on the Transfer and Utilization of Particulate Control Technology, Houston, Texas, October 1982.
20. Rudnick, S. N. Fundamental factors governing specific resistance of filter dust cakes. Ph.D. thesis, Harvard University, August 31, 1978.
21. Dennis, R. and Dirgo, J. A. Comparison of laboratory and field derived K_2 values for dust collected on fabric filters. *Filtration and Separation.* 18(5): 394-396, 417, (September/October) 1981.

LABORATORY STUDIES OF ELECTRICALLY ENHANCED FABRIC FILTRATION

L. S. Hovis and
Bobby E. Daniel
U.S. EPA/IERL-RTP
Research Triangle Park, N.C. 27711

Yang-Jen Chen
Joy Industrial Equipment Co.
Los Angeles, CA 90039

R. P. Donovan
Research Triangle Institute
P.O. Box 12194
Research Triangle Park, N.C. 27709

ABSTRACT

Laboratory studies of electrically stimulated fabric filtration (ESFF) in a newly designed and built fabric filtration test facility have shown that the magnitude of the electrically enhanced fabric filtration of fly ash remains relatively constant over the temperature range of 250° to 375° F (120° to 190° C). The influence of an external electric field on the filtration of spray dryer solid byproduct (chiefly calcium salts and fly ash) is small until the temperature and moisture conditions of field operation are simulated. Then the electrical enhancement becomes greater than any yet seen in the EPA test program, making the application of ESFF to fabric filters located downstream from spray dryers appear very attractive.

This paper has been reviewed in accordance with the U.S. Environmental Protection Agency's peer and administrative review policies and approved for presentation and publication.

INTRODUCTION

A new, experimental baghouse facility at the EPA Industrial Environmental Research Laboratory in Research Triangle Park, N.C., was placed in operation in 1983 to fulfill the need for versatile laboratory baghouses which could duplicate field conditions with respect to temperature and at the same time accommodate innovations, especially electrostatic augmentation. This paper is primarily concerned with some of the initial results from experiments carried out in these baghouses, but also includes a brief description of the equipment and its operation.

This laboratory test facility consists of two one-bag compartments, one cleaned by reverse air and the other by pulse-jet action. These two compartments were built with independent controls which means that experiments can be carried out in each compartment at the same time. One of the first assignments for the reverse-air compartment was to perform experiments to answer the question related to an ESFF-temperature dependence which had been raised by reviewers at a 1983 peer review of ESFF. Since those initial experiments, the facilities have been used to test different fabrics, different dusts, precharging, electrode configurations, and other fabric filter and ESFF parameters. This paper reports only on the temperature dependence of fly ash ESFF and the application of ESFF to spray dryer byproduct solids.

DESCRIPTION OF EQUIPMENT

Each compartment of the baghouse test facility is based on the model used by Lamb and coworkers at Textile Research Institute (1), but has been designed to include high temperature operation and allow easy modification for nonstandard operating configurations. Each compartment can hold one bag up to 4 feet (1.2 m) long and about 8 inches (20 cm) in diameter. The compartments operate off one blower which delivers 100 cubic feet of air/minute ($2.8 \text{ m}^3/\text{min}$). Dust is injected into the inlet air stream just before it enters the baghouse. Two separate feed hoppers are maintained, one for each compartment. A bypass system on the blower permits control of the gas flow independently to each compartment. A schematic diagram of the baghouse is shown in Figure 1. As shown in the figure, space for prechargers has been provided for, and, in fact, both corona wire prechargers and Masuda's Boxer Chargers (2) have been tried at these locations. Heating is provided by strip heaters on the baghouse proper, including the doors, and by pipe heaters clamped around the recirculating piping system. The whole system is well insulated except for the blower which is covered by a wooden box to cut down noise and to provide for some minimal thermal insulation. Figures 2 and 3 show the outside of the baghouse and the piping system, respectively. The blower cover and the control panel for the baghouse can be seen in Figure 3. Near atmospheric pressure is maintained by venting part of the system air to the room. So far this has worked well, but obviously the venting system would have to be changed if future experiments involved noxious gas addition to the air stream. Other than particulate matter, only water or steam has been injected into the air up to this time. Flow regulation and temperature control are automatic. The dust feeding system has not been automated, but this has not presented a major problem.

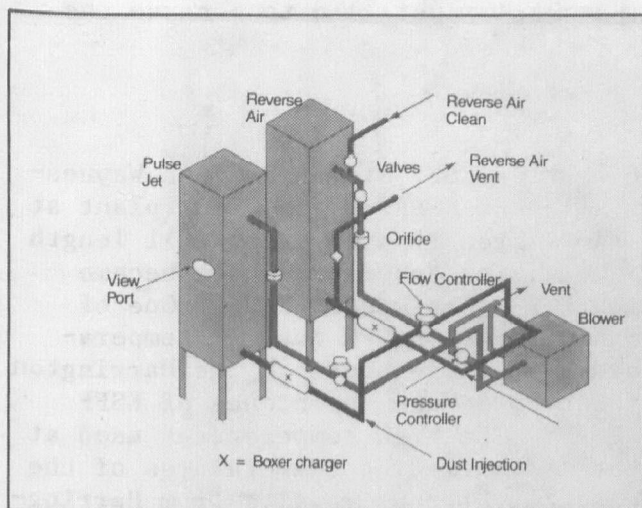


Figure 1. Sketch of EPA high temperature experimental baghouse.

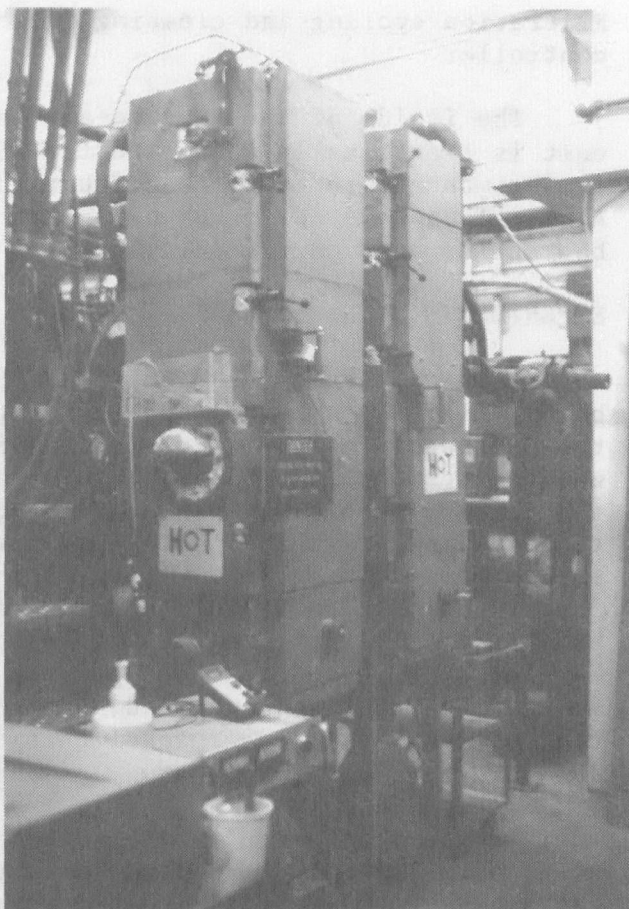


Figure 2. Baghouse photograph.

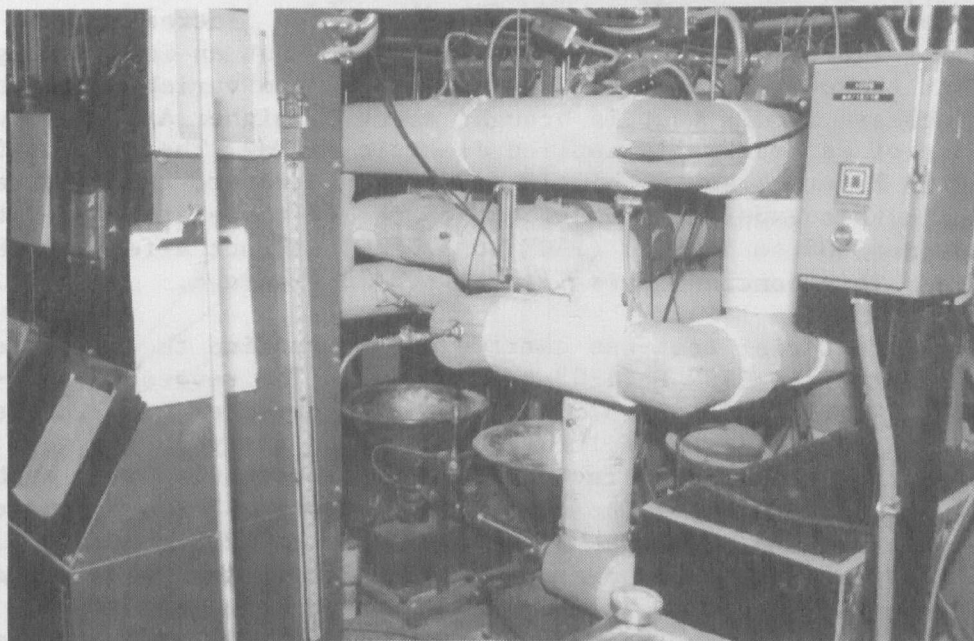


Figure 3. Insulated lines and control panel.

Filtration cycling and cleaning pulses are controlled by a Xanadu card controller.

The inside of the reverse-air compartment is shown in Figure 4. The unit is electrically connected for ESFF in the figure. Obviously both compartments were designed so that they could be electrified for ESFF. Also, glass covered sight ports with wipers were installed to observe the bag and/or dust during filtration.

EXPERIMENTS WITH FLY ASH

With completion of the pilot plant work on ESFF at the Du Pont Waynesboro, Virginia, site (3) and the installation of ESFF in the pilot plant at the Southwestern Public Services (SPS) Harrington Station using full length woven electrode bags (4), the in-house facilities described above became the primary laboratory scale unit for further experimental ESFF. One of the first experiments involved evaluation of ESFF on SPS dust at temperatures below 400° F (205° C), the standard test temperature at the Harrington Station pilot plant. The question of the temperature dependence of ESFF had arisen earlier at a peer review of ESFF. The high temperatures used at Harrington were judged to be greater than the operating temperatures of the majority of utility baghouses, and it was thought that results from Harrington could be biased because of this deviation. The reviewers recommended a supplementary laboratory study of temperature effects.

The initial study was a factorial experimental design involving temperature at two levels, gas velocities at two levels, and electrode field voltage at three levels (including zero voltage). The results of the experiment were predictable as far as velocity and electric field were concerned. Using the net pressure drop, ΔP_D , ($\Delta P_D = \Delta P_{\text{final}} - \Delta P_{\text{eff}}$) across the filter as the primary response, both gas velocity (A/C) and electric field had significant effects. The latter is the ESFF effect, in which ΔP_D decreases with increasing electric field. Increasing the gas velocity will increase ΔP_D in a given time cycle, but an interesting point here is that there is an interaction between the two variables in that the relative increase in ΔP_D that is brought about by higher A/C is reduced by the presence of an externally applied electric field. The plot of ΔP_D versus A/C in Figure 5 shows this interaction. However, the important new conclusion in this experiment is that a change in temperature over the range studied (300° to 350° F) (150° to 177° C) did not affect the ESFF performance. This conclusion is illustrated in Figure 6.

A second factorial test was carried out to examine the wider temperature range of 250° to 375° F (120° to 190° C). (The reverse-air in-house baghouse has a limit of about 375° F (190° C) because of heat losses through the fan.) The length of the filtration cycle and gas velocity were also varied as part of this second factorial test. The results were much the same. Figure 7 is a plot of the average ΔP_D across all the parameters versus temperatures in the range of 250° to 375° F (120° to 190° C) with power on (2 kV/cm field) and power off. The plot shows a lack of dependence of ΔP_D on temperature and no interaction of temperature and field. The conclusion reached by these experiments with fly ash is that high tempera-

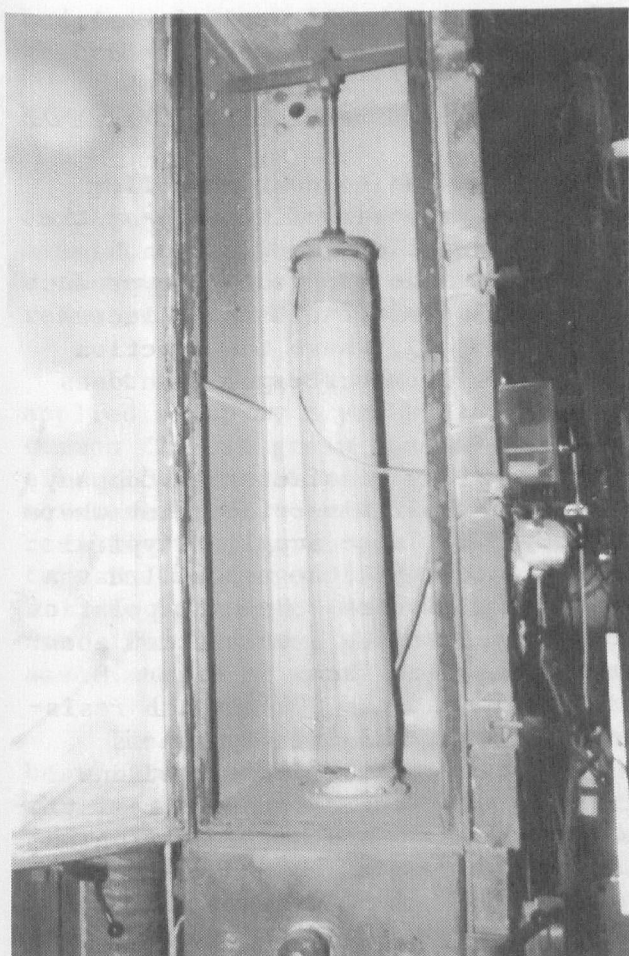


Figure 4. Reverse air bag mounting.

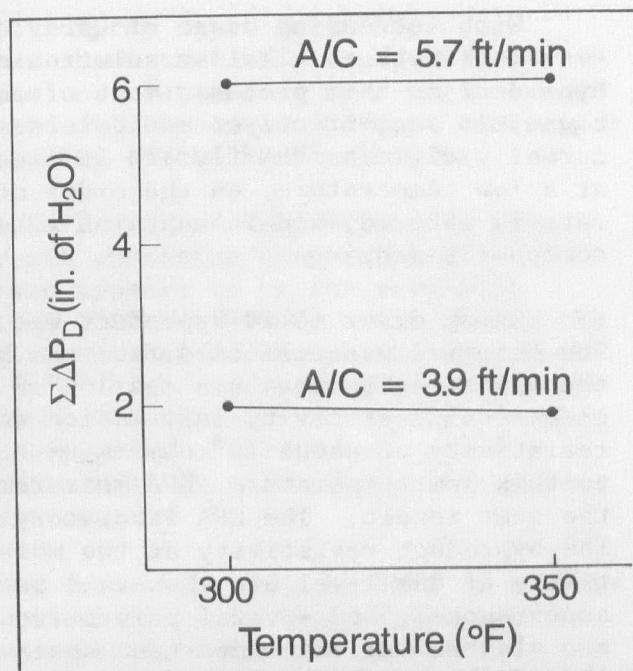


Figure 6. Temperature independence of electrical enhancement (reverse air, SPS fly ash).

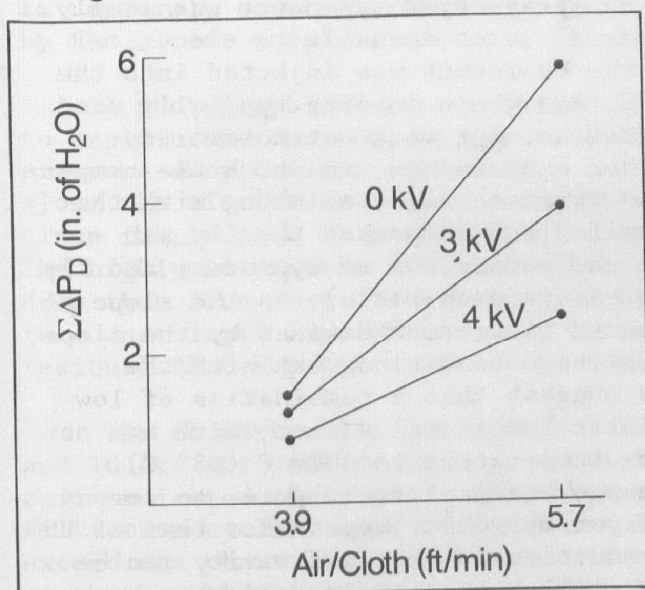


Figure 5. Net pressure drop at various face velocities and applied electrode voltages (reverse air, SPS fly ash).

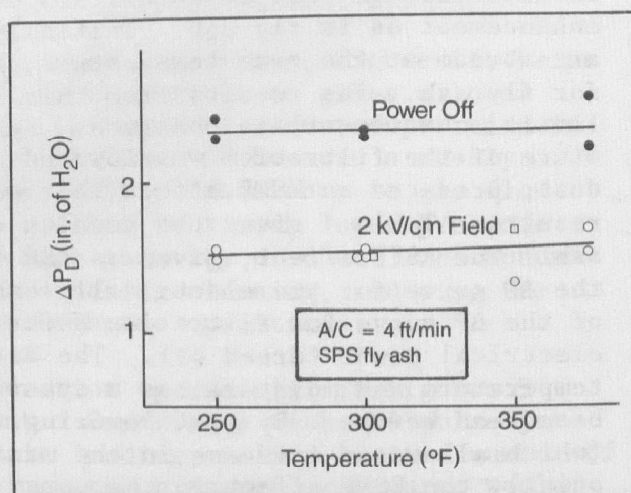


Figure 7. Extended temperature range data (reverse air, SPS fly ash).

ture operation of the Harrington Station pilot unit should not compromise the conclusions.

ESFF APPLIED TO SPRAY DRYER SOLID BYPRODUCT

With increasing usage of spray drying techniques to contact boiler emissions with an alkaline solution or slurry to remove sulfur oxides, the byproduct of this process, most often removed from the flue gas by a baghouse, is an attractive candidate dust for ESFF. The spray dryer byproduct normally differs from fly ash in electrical resistivity. It is collected at a low temperature, on the order of 150° F (66° C), where the reaction rate is favored, and it contains a larger amount of water vapor than does common fly ash.

Spray dryer solid byproduct was supplied by Joy Manufacturing Company. The material was collected from the baghouse at their Riverside Plant where the operating temperature was 160° F (71° C). They also supplied typical electrical resistivity information which indicated that the material has a resistivity of about 10^8 ohm-cm with 12 percent moisture. By extrapolation to this low temperature, EPA measurements of resistivity also yielded about the same result. The EPA laboratory measurements are shown in Figure 8. The byproduct resistivity at two moisture levels and the SPS fly ash resistivity at one level are shown. A reference plot of SPS dry fly ash is superimposed, and several points from the Joy resistivity determinations are also shown. The important observations are the big changes in resistivity of the byproduct with moisture and temperature. This has a bearing on the ESFF measurements to be described below.

COMPARISON WITH FLY ASH

The reason for applying ESFF to the spray dryer byproduct was simply to determine if filtration of this material is as amenable to electrical enhancement as is fly ash. Initially the byproduct was injected into the air stream at the same temperature, A/C, and grain loading typically used for fly ash. The results from this first attempt were not noteworthy: little enhancement was observed. Further experiments, in which the temperature of the filtration was lowered and moisture injected along with the dust, produced an ESFF effect that equalled and surpassed the fly ash results. Table 1 gives the results of the comparison of byproduct and fly ash. The ESFF effect, given as PDR (pressure drop ratio), is the slope of the ΔP curve for the electrically enhanced filtration divided by the slope of the ΔP curve for filtration under the same conditions but with the electrical power turned off. The data suggest that a combination of low temperature and moisture has a synergistic beneficial effect which has not been seen before. By just lowering the temperature to 200° F (93° C) (which allows an increase in the maximum electrical field prior to corona onset), the ESFF effect in the spray dryer byproduct approaches that of the fly ash at 300° F (149° C). Further reduction in the resistivity can be accomplished by moisture addition, and still higher fields can then be maintained, and consequently a lower PDR is achieved. These observations showed spray dryer byproduct to be compatible with ESFF. Other experiments were then carried out to determine the magnitude of electrical enhancement

under conditions approximating realistic operating conditions and are described next.

EXPERIENCE WITH SPRAY DRYER SOLID BYPRODUCT

EPA in-house application of ESFF to a spray dryer solid byproduct supplied by Joy Manufacturing Company has shown that this material can benefit from electrical enhancement. The correlations of ESFF performance with temperature and electrical field and its dependence on dust electrical resistivity have promoted basic understanding of the ESFF mechanism.

It has already been mentioned that ESFF was not very effective when applied to spray dryer byproduct at fly ash operating temperatures and common fly ash grain loadings. One reason appears to be the very high electrical resistivity of dry byproduct at 300° F (149° C). Increasing the moisture level to near actual operating conditions decreases the byproduct resistivity significantly. A combination of high moisture and low temperature in the range of 150° to 170° F (66° to 77° C) resulted in PDRs in the 0.15 to 0.2 range--well below the range typically observed even for fly ash. Furthermore, this response to ESFF held up at the high grain loadings associated with spray dryer outlet conditions.

The extremely good response of spray dryer byproduct to ESFF is perhaps best illustrated by pressure drop comparisons taken directly from recorder charts. Figures 9 and 10 are reproduced from the pulse-jet recorder. Figure 9 shows two ΔP curves with power off followed by three curves with power on (ESFF). The first curve after a field has been applied to the electrodes is still under the influence of the conventional cycle which has just preceded turning power on. One pulse of compressed air has not been sufficient to completely clean the bag which, without the electric field, is uniformly covered with dust. Two pulses did clean sufficiently as shown by the almost complete recovery of the first ESFF curve in Figure 10.

A photograph of dust deposited under ESFF conditions, Figure 11, helps to explain why dust deposition with the electric field on gives a lower pressure drop buildup with time. As seen in Figure 11, dust deposition is along the electrodes. This accounts for the lower ΔP because a nearly clean fabric path is provided which offers little resistance to gas flow. The highly nonuniform dust distribution results in a much lower pressure drop than a uniform distribution of the same quantity of dust. The nonuniform dust layer also proves easy to remove during cleaning, reducing the residual ΔP creep characteristic of most baghouse operations.

The ΔP curves for conventional filtration (power off) in Figures 9 and 10 are not reproducible or consistent. Experience with the pulse-jet unit indicated that, under this high grain loading, only a limited number of filtration cycles could be performed before the pressure drop curve would exceed the chart limit. This is a consequence of inadequate cleaning (5); increasing the cleaning energy might have kept the ΔP on the chart. Under ESFF, however, these same cleaning pulses provided sufficient cleaning energy to give a stable reproducible ΔP plot. Because PDR is based on a comparison of ESFF and conventional ΔP 's, the PDR's reported herein are based only on the average of a limited number of conventional cycles.

**TABLE 1. ESFF RESULTS: COMPARISON
OF FLY ASH AND SPRAY DRYER BYPRODUCT**

Baghouse	Dust Type	Water Added, %	Temperature, °F	Electric Field, kV/cm	Loading, grains/ft ³	Effect (PDR)
Pulse Jet	Fly ash	0	300	6	2.5	0.4-0.5
	Byproduct	0	300	6	2.5	1
	Byproduct	0	200	6.5	2.5	0.67
	Byproduct	6	300	7	2.5	0.4
	Byproduct	5	200	7.5	2.5	0.26
Reverse Air	Fly ash	0	300	2	2.5	0.5-0.6
	Byproduct	0	300	2	2.8	0.85
	Byproduct	0	200	2	2.8	0.74
	Byproduct	5	250	2	2.3	0.6
	Byproduct	5	200	2.5	2.3	0.29

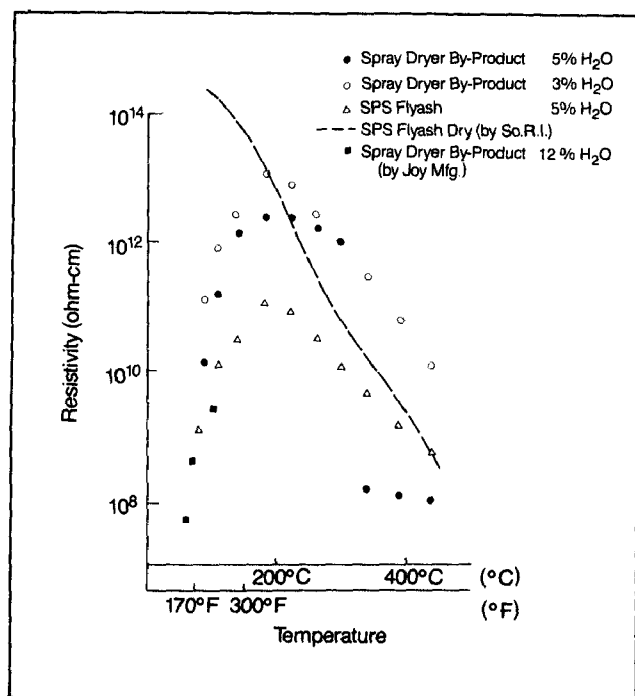


Figure 8. Fly ash electrical resistivity.

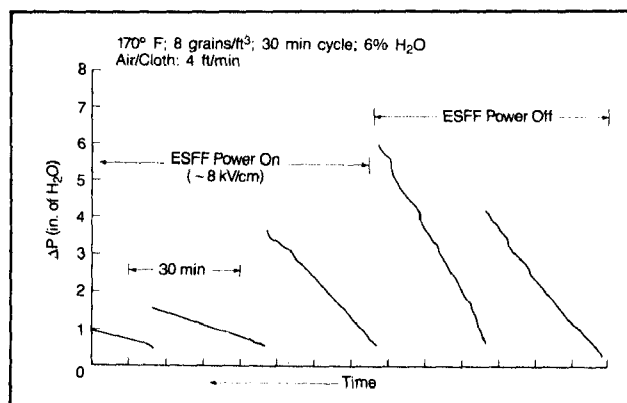


Figure 9. Change in ΔP brought about by turning the electric field on (pulse jet, spray dryer byproduct).

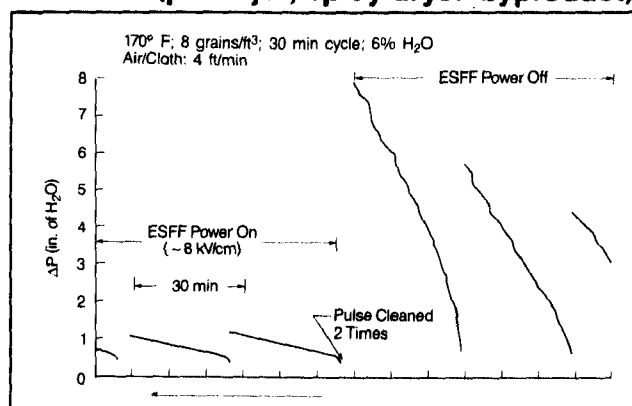


Figure 10. Change in ΔP brought about by turning the electric field on (pulse jet, spray dryer byproduct, with two cleaning pulses).

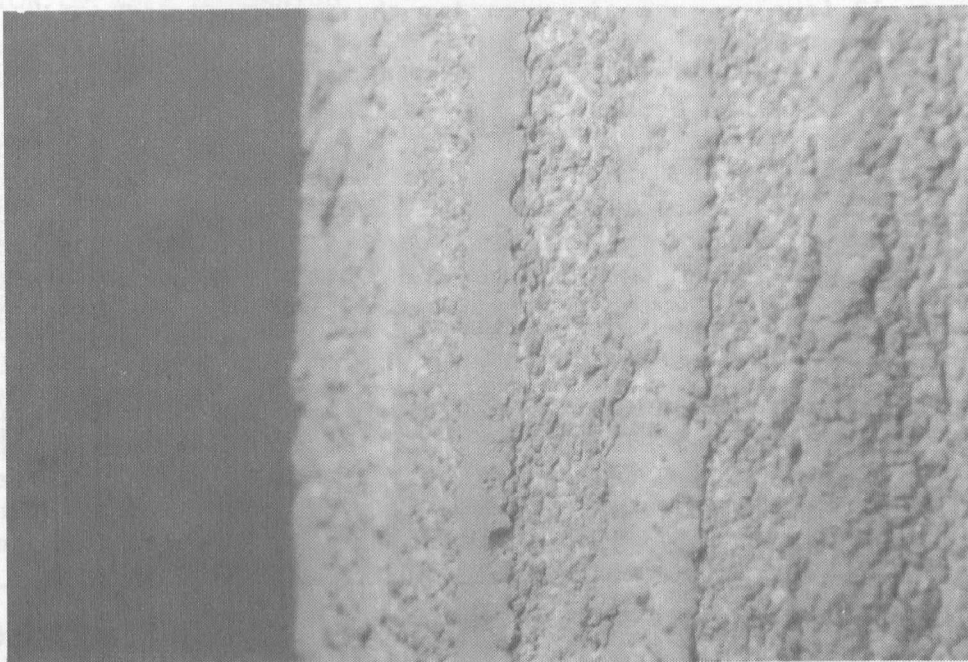


Figure 11. Spray dryer byproduct deposit on electrified bag (pulse jet cleaning).

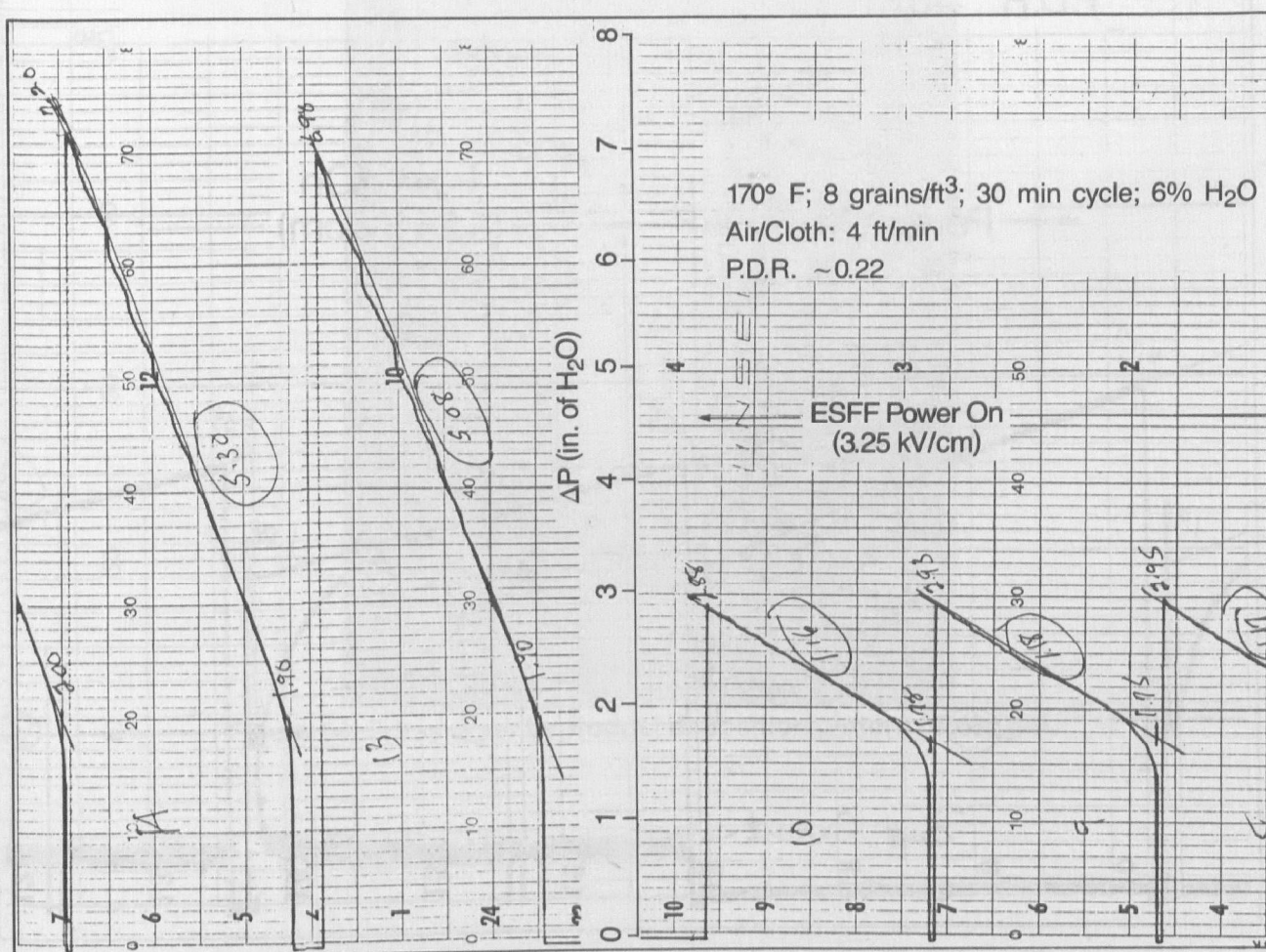


Figure 12. Electric field effect on spray dryer byproduct filtration (reverse air).

Figure 12 is a reverse-air recorder chart comparison similar to the one for pulse-jet just reviewed. The PDR values are extremely good here also, being in the range of 0.2 to 0.3. Dust deposition along the electrodes is not readily observed because of the inside-the-bag nature of filtration. However, there is no reason to think that the mechanism for achieving a low pressure drop differs from that of the pulse-jet case. The record of ΔP indicates that, for the cycling shown in Figure 12, there is sufficient cleaning energy to remove the uniform layer of dust under conventional filtration because the ΔP curve is reproducible. The pressure drop rose above the chart limit for the power-off condition only when the filtration cycle time was doubled.

The striking difference between the power-on and power-off curves of Figures 9 and 10 (pulse-jet) and Figure 12 (reverse-air) can be appreciated by comparing them with similar curves for fly ash (Figure 13, reverse-air). The ESFF effect, while clearly evident, is much less pronounced in the Figure 13 data which yield a PDR typically in the 0.4 to 0.6 range.

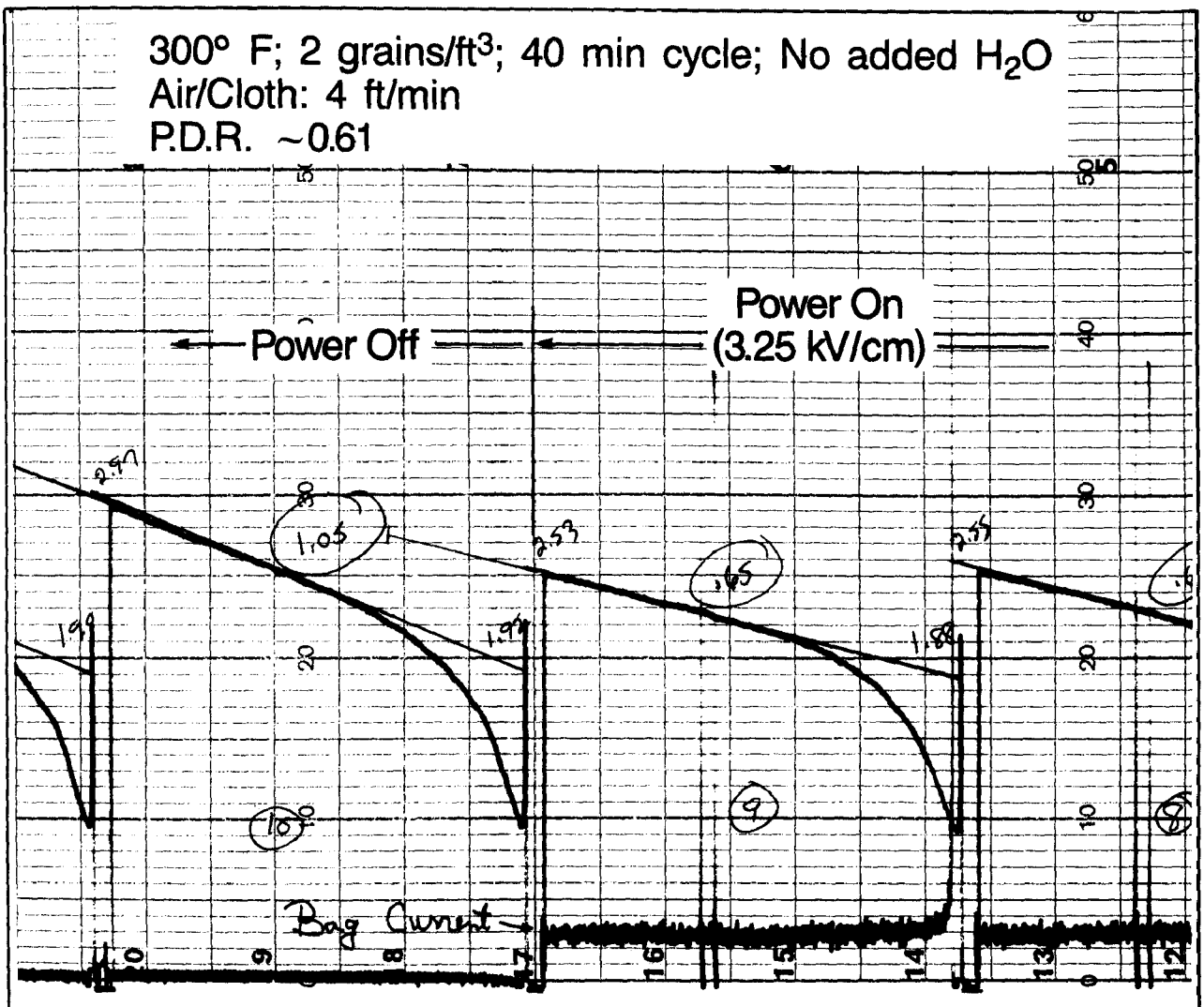


Figure 13. Electric field effect on SPS fly ash filtration.

VERIFICATION OF ESFF MECHANISM

The nonuniform dust deposition pattern, alluded to in describing the lower ΔP_d , and the ease of cleaning were readily observed through the port on the pulse-jet baghouse. The nonuniform dust deposition pattern, which was emphasized by the large grain loading in the case of spray dryer byproduct, is most likely a consequence of relatively long range coulomb forces exerted on the dust (6). Charged particles are attracted to either the positive or negative electrode with more depositing on the electrode of polarity opposite to the charge on the majority of particles. Other mechanisms (7, 8) may play a role, but the nonuniform deposition clearly dominates. Figures 11 and 14 show the buildup of dust along the electrodes. That the dust can be adequately removed from the bag, as evidenced by a stable, low value of residual ΔP , also contributes to the effectiveness of ESFF.



Figure 14. Spray dryer byproduct deposition pattern (pulse jet).

MAXIMIZING THE ESFF EFFECT

It has been concluded that the spray dryer byproduct, because of the conditions under which it is filtered, is a likely candidate for ESFF. Although the dust has a very high electrical resistivity when dry, a combination of low operating temperature and high moisture lowers this resistivity into a favorable range for ESFF. Both high moisture and low temperature are necessary. Figure 15 shows a pulse-jet response to a reduction in filtration temperature versus a reduction in temperature with added moisture. The lower PDR response to temperature is measurable, but it takes the added moisture to observe the impressively low values of PDR. There is no intended implication that electric field is held constant in Figure 15. The Figure 15 data were collected at "maximum" allowable electric field--that value of electric field just below corona onset. This value of field increases with increasing moisture and decreasing temperature. Thus, the low-temperature, high-moisture data of Figure 15 were collected under higher values of applied electric field than the low-moisture, high-temperature data.

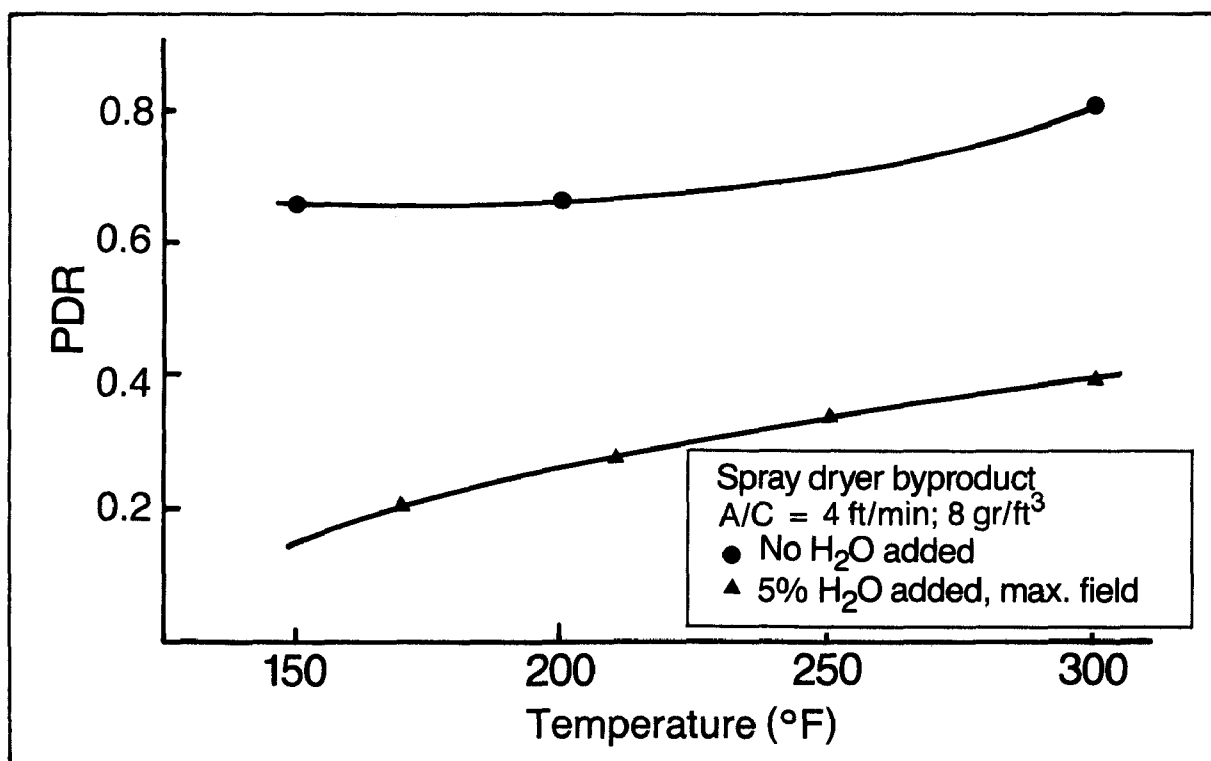


Figure 15. Pressure drop reduction attributable to reduced temperature and increased moisture (spray dryer byproduct, pulse jet).

This field dependence is demonstrated for pulse-jet operation in Figure 16 and for reverse-air operation in Figure 17. It is interesting to note that an applied electrode voltage of approximately 11 kV (5.5 kV/cm) and approximately 4 kV (2 kV/cm field) for pulse-jet and reverse-air, respectively (at this temperature and moisture condition), gives an ESFF result comparable to SPS fly ash at 300° F (149° C) and low moisture. Data are not available to confirm this, but it is surmised that electrical resistivities are nearly the same for the two products at these conditions.

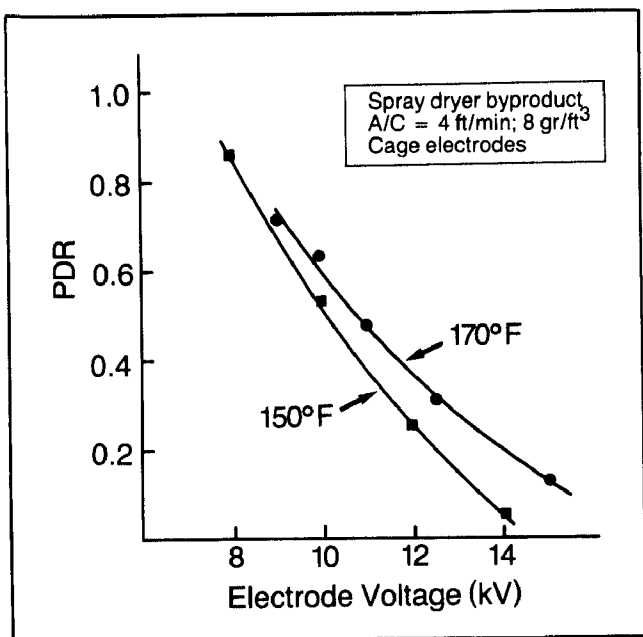


Figure 16. Field dependence of pressure drop reduction (spray dryer byproduct, pulse jet).

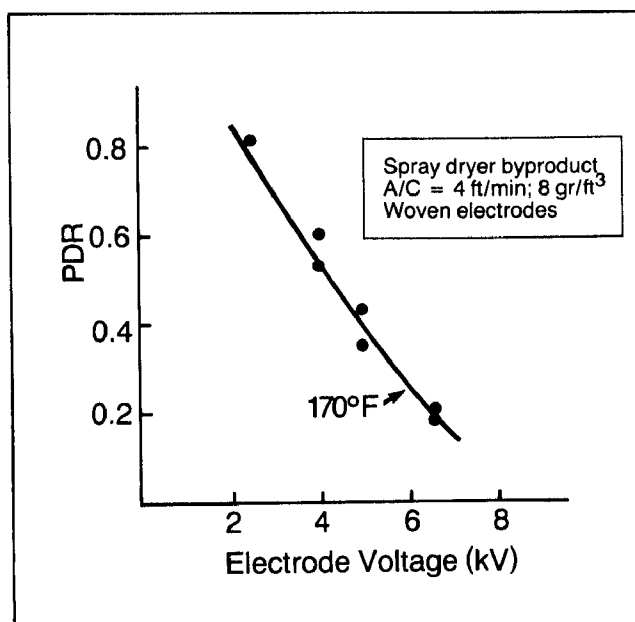


Figure 17. Field dependence of pressure drop reduction (spray dryer byproduct, reverse air).

CONCLUSIONS

New, versatile high-temperature baghouses recently installed in the EPA Industrial Environmental Research Laboratory at Research Triangle Park have already proven their worth in evaluating ESFF at varying temperatures and in testing ESFF on spray dryer byproduct. The use of this equipment to investigate other aspects of fabric filtration will be reported later. Conventional and nonconventional fabrics have been tested, and alternative electrode configurations have been studied in a continued search for lower cost and more easily maintained fabric filtration.

METRIC CONVERSIONS

$$1 \text{ in. of H}_2\text{O} = 249 \text{ Pa}$$

$$1 \text{ grain/ft}^3 = 2.29 \text{ g/m}^3$$

$$1 \text{ ft/min} = 0.5 \text{ cm/s}$$

REFERENCES

1. Lamb, G. E. R., Costanza, P. A., and O'Meara, D. J., Electrical Stimulation of Fabric Filtration. Part II: Mechanism of Particle Capture and Trials with a Laboratory Baghouse. Textile Research Journal 48. No. 10, Oct. 1978, pp. 566-573.
2. Masuda, S., Nakatani, H., and Mizuno, A. Boxer-Charger Mark III and its Applications in ESP's. In: Third Symposium on the Transfer and Utilization of Particulate Control Technology. Vol. II, EPA-600/9-82-005b (NTIS PB83-149591), July 1982, pp. 380-389.
3. Greiner, G. P., Furlong, D. A., VanOsdell, D. W., and Hovis, L. S. Electrostatic Stimulation of Fabric Filtration. JAPCA 31, No. 10, Oct. 1981, pp. 1125-1130.
4. Chambers, R. L., Spivey, J. J., and Harmon, D. L. ESFF Pilot Plant Operation at Harrington Station. Paper 86, Fifth Symposium on the Transfer and Utilization of Particulate Control Technology. Kansas City, MO, Aug. 1984.
5. Leith, D., and Ellenbecker, M. J. Theory for Pressure Drop in a Pulse Jet Cleaned Fabric Filter. Atmospheric Environment. No. 14, 1980, pp. 845-852.
6. Chiang, T. K., Samuel, E. A., and Wolpert, K. E. Theoretical Aspects of Pressure Drop Reduction in a Fabric Filter with Charged Particles. In: Third Symposium on the Transfer and Utilization of Particulate Control Technology. Vol. III, EPA-600/9-82-005c (NTIS PB83-149609), July 1982, pp. 250-260.
7. Morris, B. A., Lamb, G. E. R., and Saville, D. A. Modeling Studies of Pressure Drop Reduction in Electrically Stimulated Fabric Filtration. Paper 69. Fifth Symposium on the Transfer and Utilization of Particulate Control Technology. Kansas City, MO, Aug. 1984.
8. VanOsdell, D. W., Donovan, R. P., and Hovis, L. S. Flow Resistance Reduction Mechanisms for Electrostatically Augmented Filtration. Paper 70, Fifth Symposium on the Transfer and Utilization of Particulate Control Technology. Kansas City, MO, Aug. 1984.

PRESSURE DROP FOR A FILTER BAG OPERATING WITH A LIGHTNING-ROD PRECHARGER

George E. R. Lamb and Richard I. Jones
Textile Research Institute
Princeton, New Jersey 08542

ABSTRACT

It has been shown that, when a filter bag is fitted with electrodes carrying a potential of several kilovolts, and when the dust entering the bag is acted on by a corona precharger, pressure drop is greatly reduced. Dust cake mass distributions have been measured for such a case, and the altered distribution can account for the observed pressure drop reductions. However, measurements with a permeability scanner also show that the permeability of a dust cake is greater when it is formed in the presence of an electric field. Thus the reduction in pressure drop is due to two main effects - mass redistribution and a more permeable dust cake, the former being dominant in the case considered. Calculations of particle trajectories inside a bag yield results consistent with the observed deposition patterns, and support the view that electric enhancement effects are due to Coulomb forces.

This paper has been reviewed in accordance with the U. S. Environmental Protection Agency's peer and administrative review policies and approved for presentation and publication.

INTRODUCTION

A previous paper (1) has described measurements with a one-bag laboratory baghouse in which enhanced performance was obtained by the use of high electrical potentials applied to electrodes in the wall of the bag. In addition, the dust entering the bag through the bottom opening was charged by a charger resembling a lightning rod. The special feature of this precharger was that, because of its location, practically all the dust that became charged entered the bag, unlike what occurred with other prechargers described in the past. It was possible, therefore, to attribute any changes in pressure drop entirely to changes in the structure or distribution of the dust deposit without having to allow for effects of lower dust load. With this combination of charged bag electrodes and precharged dust, considerable reductions in pressure drop and in penetration were obtained.

For these measurements, a textured woven glass bag was made with a seam that was held closed by clamps rather than being stitched, and was also secured with a quick-release clamp at the upper end for easy removal from the baghouse. It was thus possible to remove the bag and to open it for examination without disturbing the dust deposit. It was found that the areal density of the dust cake became heavily skewed so that a large fraction of the deposition occurred near the bag entrance at the bag bottom. In addition, dust accumulation occurred mainly on and near the electrode wires, with heavier deposition on the positive wires than on the ground wires when the dust had been negatively charged. It was also seen that, where small pieces of adhesive tape had been placed over the wires, dust deposited as heavily as where there was no tape. This indicated that movement of dust particles near the wires was controlled almost entirely by electrical forces, since there was no air velocity component normal to the tape. The present paper describes further measurements made to interpret the dust deposition patterns and the accompanying changes in pressure drop.

MAPPING OF DUST DEPOSITS

A map of the areal density distribution of a fly ash dust cake was obtained by aspirating the dust from 8 mm x 120 mm areas at various locations on the bag after it had been opened and laid on a table. The dust from the following locations was collected on a membrane filter and weighed: the positive wires, the ground wires, and the space between wires, at each of five distances from the bottom of the bag. The dust cake areal densities for the 15 representative bag locations, shown in Table 1, show the shift toward the bottom of the bag discussed previously (1). However, the distribution of dust mass with respect to the electrodes is somewhat different from what might be expected. In the case (+4,-15) where the dust has been given a negative charge, there is a clear preponderance of collection on the positive electrode. (The substantial amount that collects on the ground electrode has been assumed to be dust that, being first collected at the positive wire, acquires a positive charge and is then reentrained. This hypothesis is supported by the fact that the fraction of the total dust deposited that collects on the ground wire is greater at the bag top than at the bottom.) In the case of (+4,+15) where

TABLE 1. DISTRIBUTION OF DUST AREAL DENSITIES (mg/cm²) ON REVERSE AIR BAG
ON POSITIVE, GROUND, AND BETWEEN ELECTRODE WIRES

Distance up bag (cm)	(0,0) ^a			(+4,+15) ^a			(+4,-15) ^a		
	Pos. wire	Ground wire	Betw. wires	Pos. wire	Ground wire	Betw. wires	Pos. wire	Ground wire	Betw. wires
20	12.2	12.2	12.2	7.02	5.76	2.03	13.57	1.87	0.16
40	13.0	13.0	13.0	3.16	6.44	3.05	6.26	2.67	0.28
60	12.2	12.2	12.2	3.95	3.00	0.75	2.46	1.76	0.15
80	11.8	11.8	11.8	1.82	3.15	1.93	1.63	1.26	0.11
100	10.9	10.9	10.9	2.14	2.92	0.53	1.10	0.84	0.07
$R^b = [\sum \frac{1}{R_i}]^{-1}$									
		0.80			0.13			0.022	
PDR ^c (calc)									
					0.16			0.028	
PDR ^c (meas)									
					0.21			0.040	

^a First numeral = potential gradient between electrodes (kV/cm).
Second numeral = potential on precharger (kV).

^b R = total resistance to air flow; R_i = air flow resistance of area i.

^c PDR = pressure drop ratio = ratio of pressure drop with applied field and precharging to that without either.

the dust was charged positively, however, the expected preferential deposition on the ground wire is not seen. In both cases, the amount between wires is small, especially for the (+4,-15) case.

The resistance R to air flow for the entire bag was calculated assuming that the resistance R_i for each small area was linearly proportional to the areal density of dust deposit, and that, in analogy with the rule for electrical resistances,

$$R = \left[\sum \frac{1}{R_i} \right]^{-1} .$$

The quantity PDR, or pressure drop ratio, is the ratio of the pressure drop buildup during a filtering/cleaning cycle when electric stimulation is applied to the corresponding pressure drop buildup without the applied field. Values of PDR calculated as the ratio of the R values determined for the electrified cases to R for the (0,0) case are compared in Table 1 to the measured PDR values. The degree of agreement obtained indicates that the reductions in pressure drop due to bag electrification and precharging under the conditions of these experiments can in large measure be explained by dust redistribution.

PERMEABILITY SCANNING

Pressure drop reductions observed with electrically stimulated fabric filtration (ESFF) are commonly attributed to two different factors: increased porosity of the dust cake and nonuniform dust deposition. The latter mechanism is analyzed in the previous section, and supported by Chiang et al. (2) as the primary reason for pressure drop reduction. A simple permeability scanning experiment was devised to discriminate between the two mechanisms. The method consisted of depositing a fly ash dust cake on a bag (6 ft/min, 15 min filtering, 32 g total deposition), then opening the bag flat. A metal tube of 0.5 cm i.d. was connected to a source of compressed air and the flow from the tube adjusted so that the air velocity was 3 cm/s (6 ft/min). The calibration was made with a bubble flowmeter. The end of the tube was pressed against the dust cake at 15 tightly spaced locations spanning three adjacent electrodes. Arrangements were made to ensure a good seal so that the excess pressure in the tube (measured by a manometer) was the full pressure drop needed to drive the air through the small area of dust cake covered by the tube. In this way the distribution of dust cake permeability around the electrode wires was mapped for the filtering conditions (+4,-15). The results are plotted in Figure 1.

Several features of these plots are notable. One is the discrepancy between the plotted points and the pressure drop for the bag, indicated as a double horizontal line. This was probably due to the pressure that must be exerted on the fabric to effect a seal around the scanner tube. The compressed fabric should have a lower permeability, and this is reflected in the estimated 4 mm of water increase over the bag pressure. Differences in cake permeability should not be affected by this compression.

The second, more meaningful feature of the plots is the difference between the permeability patterns and those expected from the visual appearance

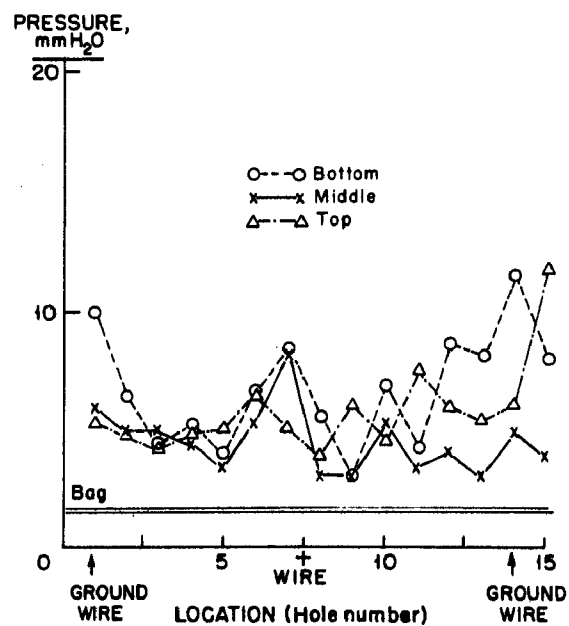


Figure 1. Permeability of dust cake deposited with (+4,-15) at various filter bag locations and for the bag as a whole (double line).

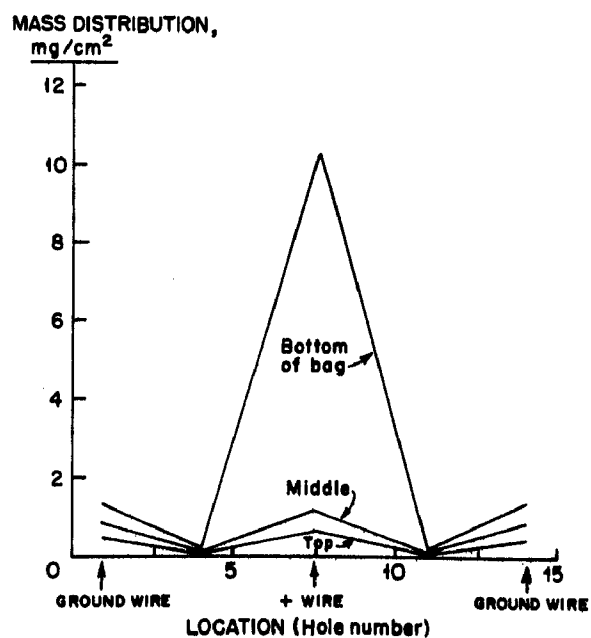


Figure 2. Dust cake mass deposited with (+4,-15) at various locations on the inner surface of the filter bag.

and measured mass distribution of the dust cake. Figure 1 clearly shows the variations of pressure drop with dust deposition, but the relative heights of the maxima and minima do not match the pattern in Figure 2 which shows the mass distributions. It can be seen that, although the mass collected on the positive wires is several times greater than on the ground wires, the pressure peak is lower on the positive wires. Again, although the mass on the positive wire at the bottom of the bag is much larger than at the top, the pressure drops at these two locations (and at the middle) do not show the same relationship. Lastly, the mass collected at the bottom of the bag is greater for (+4,-15) than for (0,0), but even on the positive wires where the heaviest deposition occurred, the pressure drop at (+4,-15) does not exceed that at (0,0) which is nowhere less than 15 mm of water.

All these facts point to strong differences in dust cake structure and permeability depending on the conditions of deposition. In particular, the dust cake formed with a strong electric field is much more permeable than without the field. These results appear to be in disagreement with the findings of the preceding section which indicated that reductions in pressure drop were chiefly due to dust cake redistribution, but in fact the two sets of results need not be inconsistent because the resistance of a number of resistors in parallel is controlled by the lowest. Thus once pressure drop is reduced by establishing a pattern of thick and thin dust cake regions, any increase in the porosity of the thick regions will make only a small difference to the total resistance. In any case, from these results it may be concluded that pressure drop is reduced by both redistribution and by increased dust cake porosity, but that the first effect is the dominant one under the conditions studied.

THEORETICAL APPROACH TO DUST DEPOSITION PATTERNS IN ESFF

In order to explain the observed patterns of dust deposition in the filter bag in terms of the electrical forces that give rise to them, some knowledge of the shape and strength of the electric field and of the particle charge was needed. These could then be used to compute particle trajectories and locations where the dust would deposit. The following two sections give accounts of experiments and computations designed to obtain this information.

MEASUREMENT OF PARTICLE CHARGE

A Faraday cage was mounted on the outer wall of the baghouse, fed by a pipe which pointed into the tube sheet opening as illustrated in Figure 3. It consisted of a filter on which the dust collected, backed by a porous metal plate connected to a Keithley electrometer. Charges on the dust leaked to the metal plate and to the electrometer, which measured the leakage current.

To make the measurements, the baghouse was run without a bag, so that when all the systems, including the precharger, were turned on, a stream of charged fly ash aerosol came through the hole in the tube sheet. Isokinetic 1-minute samples of the dust on the Faraday cage filter were weighed, and the corresponding electrometer current readings recorded. The resulting charge/mass values are plotted in Figure 4. They are slightly larger than values obtained by Donovan et al. (3), probably because of differences in the experimental arrangements and in the fly ash used.

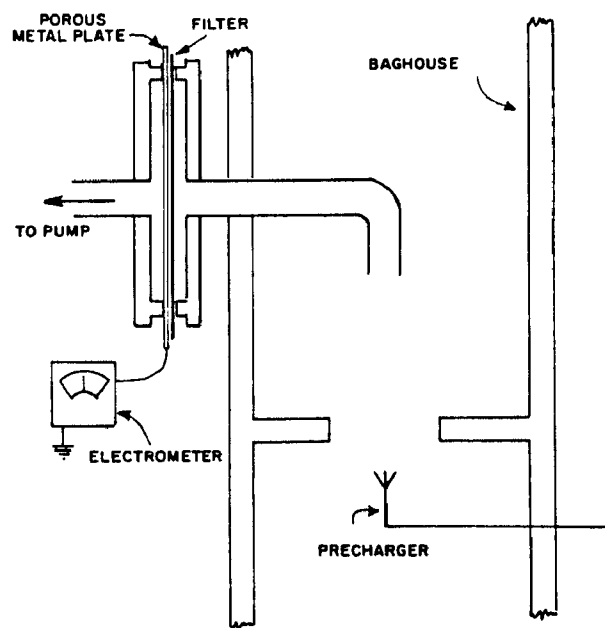


Figure 3. Faraday cage for the measurement of particle charge due to precharging.

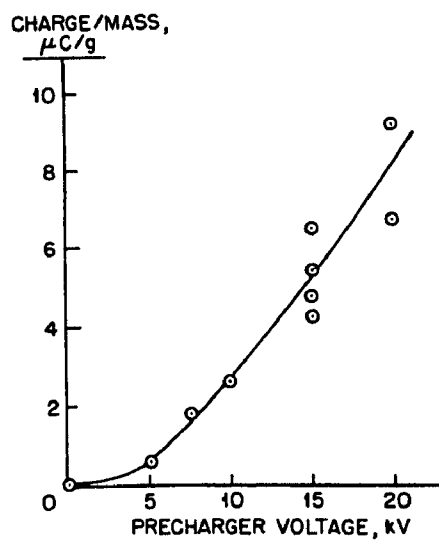


Figure 4. Charge/mass ratio as a function of precharger voltage for a fly ash aerosol stream.

The object of measuring charge/mass ratios, q/m , is to assign values of this parameter to various particle size ranges. Ideally, q/m ratios should be measured for each size range, but since this is significantly more difficult, the assumption was made that particle charge is proportional to particle surface area. On this basis, the average charge of $5 \mu\text{C/g}$ obtained with a pre-charger potential of 15 kV (Figure 4) was distributed as shown in Figure 5. The mass fraction in each size range had previously been determined, the size ranges corresponding to those captured on the various stages of an AIR impactor (Aerostatics Instrumentation & Research, Logan, Utah).

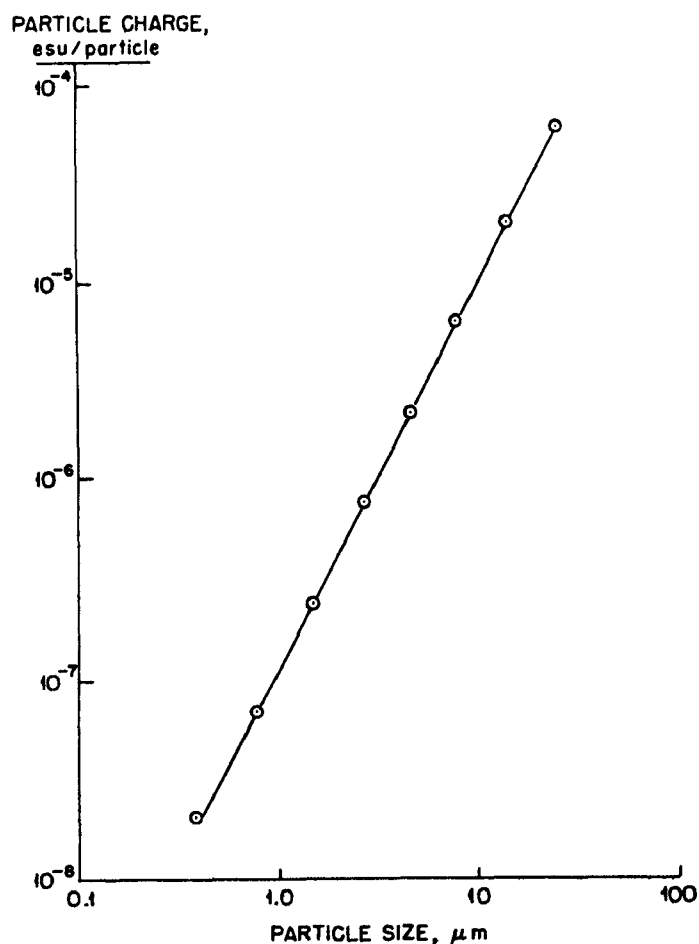


Figure 5. Particle charge as a function of particle size.

The approximate theoretical maximum charge q_p acquired by a particle of diameter d is given by (4)

$$q_p = 0.75 E d^2,$$

where E is the field near the particle, and all units are cgs and esu. The value to be assigned to E in the present case is uncertain, since, as it passes the precharger, a particle travels through regions of different field intensity.

It follows that particle charge levels would depend not only on their size but also on how close they pass to the charger. However, some self-leveling mechanisms may be provided by the fact that particles in a high field region quickly move away from the charger to a region of lower field. This should narrow considerably the spread of charge levels for each particle size. These considerations mean that the relationship in Figure 5, though valid, can only be taken to give average values of charge and that in fact the line in that figure occupies the center of a band of unknown width. The results reported in a later section must consequently also be rendered more diffuse.

CALCULATION OF ELECTRIC FIELD AND PARTICLE TRAJECTORIES IN AN ESFF BAG

The electric field inside a bag fitted with electrodes is due to the charge which appears on the electrodes when a potential is applied to them. The field E at a distance r from a straight wire carrying a charge q per unit length is

$$E = \frac{2q}{r} .$$

If a number of electrodes are involved, the field will be the vector sum of all contributions. In the case considered here, the electrodes are parallel to the bag axis and are alternately grounded and raised to a high potential. The problem then is to find the charge on each wire. An analysis for one pair of parallel wires is available (5), but extension of the treatment to cover nonplanar arrays of more than two wires was not attempted.

A more direct approach was taken - namely, experimental measurement of the capacitance of wire arrays. The instrument used was a bridge type capacitance meter (General Radio Co. Type 740). The meter was tested against a number of known capacitors ranging from 10^{-5} to 10^2 μ F, and the measured values were found to match the rated capacitances within roughly 10%; the capacitors themselves do not have a guaranteed accuracy much better than this.

The capacitance C of two parallel cylindrical conductors of radius a , separated by a distance b , is given by

$$C = \frac{k}{2 \ln \left[\frac{b + \sqrt{b^2 - 4a^2}}{b - \sqrt{b^2 - 4a^2}} \right]} \quad \text{esu/cm,}$$

where k is the dielectric constant, which is roughly unity for air. A straight cylindrical conductor of radius a held horizontally a distance h above an infinite grounded plane also has a capacitance-to-ground C_g given by

$$C_g = \frac{k}{2 \ln \left[\frac{h + \sqrt{h^2 - a^2}}{a} \right]} .$$

When the diameter of the conductors is 0.025 cm and their length 11 m, C is $6 \times 10^{-5} \mu\text{F}$. If the distance h is 2 m, C_g is likewise $6 \times 10^{-5} \mu\text{F}$. In practice, both effects will operate simultaneously, but because of interference, the total capacitance will be less than the sum of C and C_g . Nevertheless, it can be shown (6) that the ratio of the charge carried by the positive wire to that on the grounded wire differs negligibly from 2, so that the capacitance of the system is still effectively the sum of two equal capacitances, allowing the charge distribution shown in Figure 6.

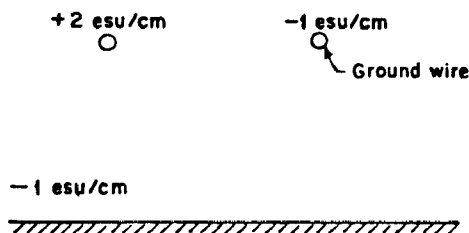


Figure 6. Charge distribution assumed for calculations leading to trajectories in Figures 7, 8, and 9.

The capacitance of a model electrode system was then measured. A cage was built by stringing 18 alternately coupled parallel wires between two plexiglass disks, 1.22 m apart, to form a cylindrical array; the distance between wires was 2 cm. The spacing was identical with that of the electrodes in the bag shown in Figure 10. As in the bag, alternate wires were grounded and the others connected to the positive terminal of the capacitance meter. The cage wires were equivalent to a pair of wires 11 m long. The capacitance of the cage was found to be $7.8 \times 10^{-5} \mu\text{F}$, or 70 esu. When the potential difference between wires is 9 kV, or 30 esu of potential, the total charge is 2100 esu and the charge per unit length of wire is thus ~ 2 esu/cm. The capacitance of a pair of straight wires 11 m long was also measured and found to be $7.2 \times 10^{-5} \mu\text{F}$, or, within experimental error, almost equal to that of the cage.

The charge per unit length just obtained and the specific charges plotted in Figure 5 were now used to plot particle trajectories within a bag. A computer program was written that summed the x and y components of the field due to the charge on each of the 18 electrodes at a point in the bag. From this and the charge and size of a particle near the bag axis, the particle velocity was calculated, and hence its position 0.1 s later. The calculation was repeated starting from this new point, and stopped when the particle reached the bag wall. A face velocity of 3 cm/s was assumed, which gave the particle a basic radial velocity of $3R/5.8$ cm/s, where R was the radial position of the particle and the bag radius was 5.8 cm. Such calculations were made for 1, 3, and 10 μm particles, which had q/d ratios of 1.5×10^{-3} , 3.33×10^{-3} , and 11.2×10^{-3} esu/cm, respectively.

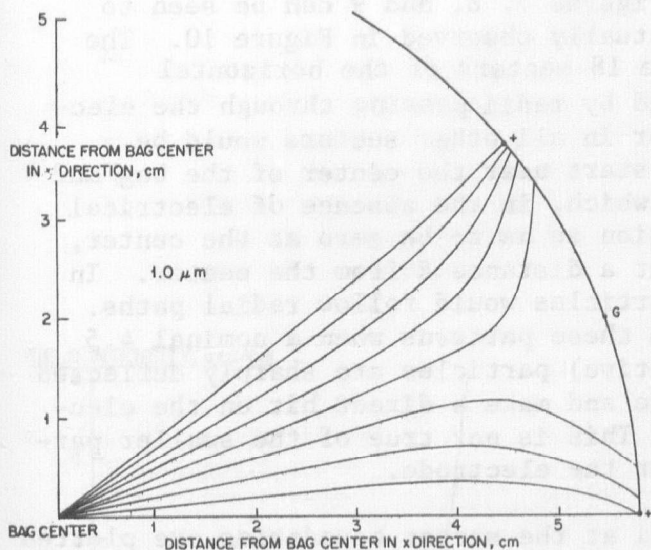


Figure 7. Trajectories of particles 1 μm in diameter with charge/diameter ratio $q/d = 1.15 \times 10^{-3}$ esu/cm.

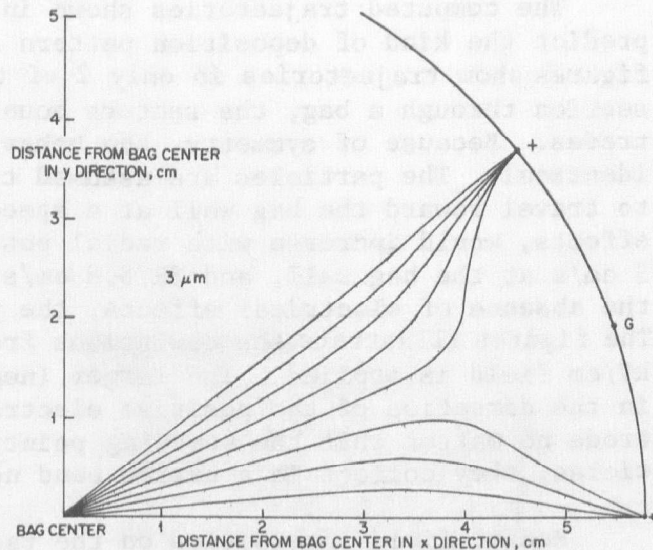


Figure 8. Trajectories of particles 3 μm in diameter with $q/d = 3.3 \times 10^{-3}$ esu/cm.

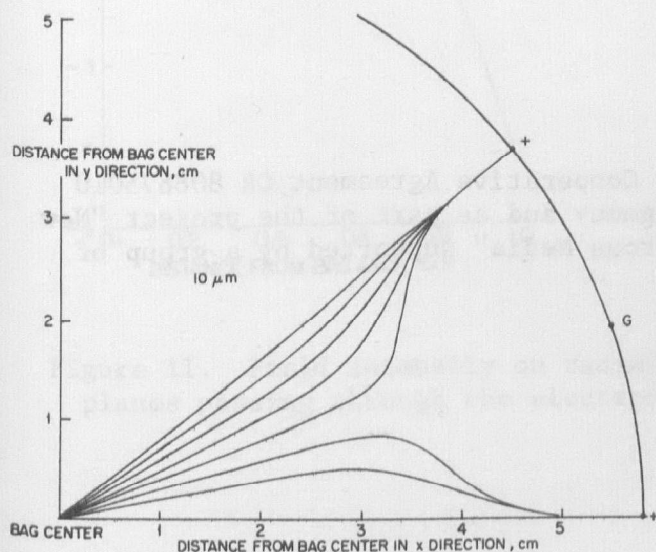


Figure 9. Trajectories of particles 10 μm in diameter with $q/d = 1.12 \times 10^{-2}$ esu/cm.

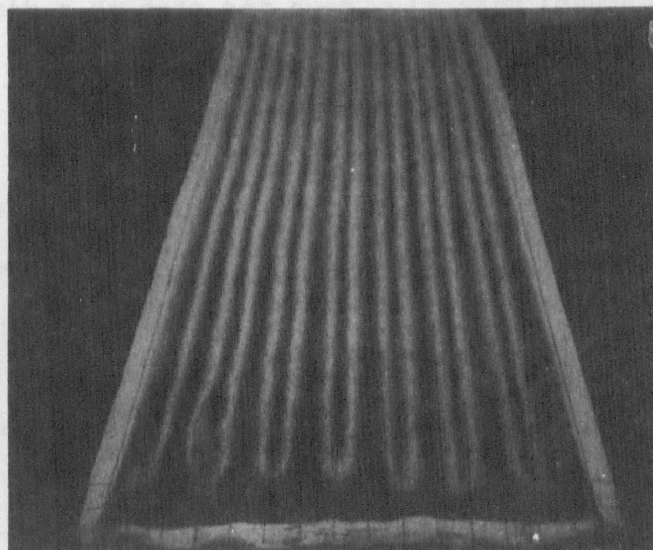


Figure 10. Photograph of dust deposits on inner bag surface after filtration with combined bag electrode field and precharging.

The computed trajectories shown in Figures 7, 8, and 9 can be seen to predict the kind of deposition pattern actually observed in Figure 10. The figures show trajectories in only 2 of the 18 sectors of the horizontal section through a bag, the sectors bounded by radii passing through the electrodes. Because of symmetry, the behavior in all other sectors would be identical. The particles are assumed to start near the center of the bag and to travel toward the bag wall at a speed which, in the absence of electrical effects, would increase with radial position so as to be zero at the center, 3 cm/s at the bag wall, and $3R/5.8$ cm/s at a distance R from the center. In the absence of electrical effects, the particles would follow radial paths. The figures illustrate the deviations from these patterns when a nominal 4.5 kV/cm field is applied. The larger (negative) particles are sharply deflected in the direction of the positive electrode and make a direct hit on the electrode no matter what the starting point. This is not true of the smaller particles; they collect in a narrow band near the electrode.

Radial field intensities on the radii at the sector boundaries are plotted in Figure 11. It is interesting to note how, at radial positions as far from the center as half the bag radius, the intensities are near zero. This accounts for the appearance of the trajectories in Figures 7, 8, and 9, which begin to deviate from radial directions only when the particle moves beyond half the bag radius.

Velocities of particles moving along these sector boundary radii are plotted in Figure 12. For these particles, the symmetry of the field will cause radial acceleration only. Here it can be seen that the particles approaching a positive electrode (top three curves) will be accelerated to rather high velocities, but those traveling towards a ground electrode (lower three curves) will slow down and stop at a distance that depends on the q/d value for the particle.

Acknowledgements

These studies were carried out under Cooperative Agreement CR 808875010 with the U. S. Environmental Protection Agency and as part of the project "New Technology for Filtration of Gases by Fibrous Media" supported by a group of TRI Participants.

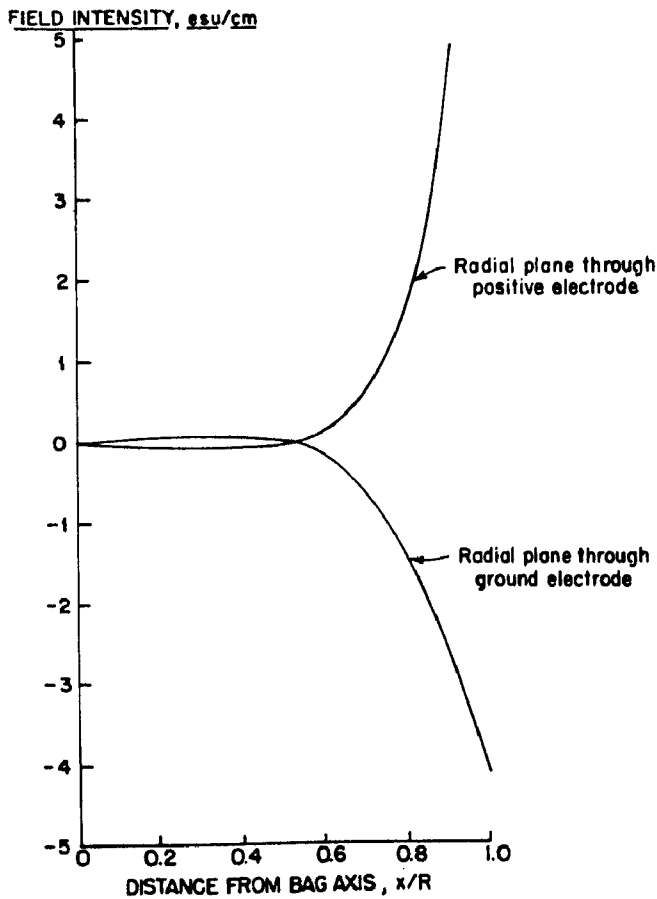


Figure 11. Field intensity on radial planes passing through the electrodes.

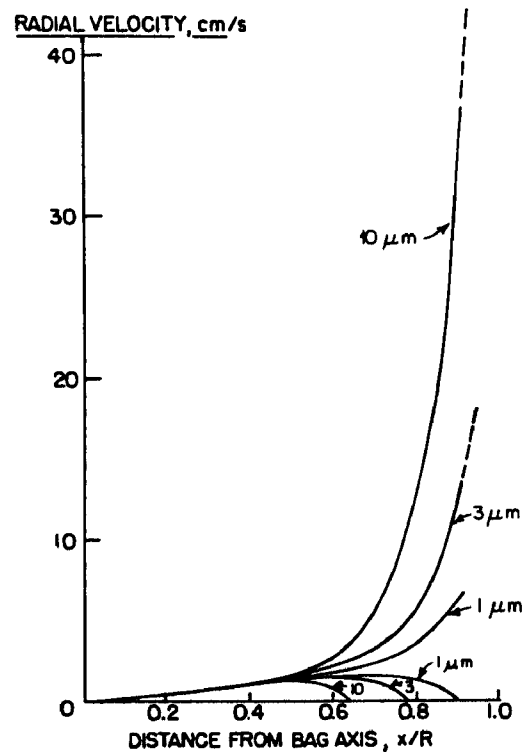


Figure 12. Radial velocities for particles of indicated diameters moving in radial planes through electrodes.

Upper 3 curves:
plane through positive electrode.
Lower 3 curves:
plane through ground electrode.

REFERENCES

1. Lamb, G. E. R., Jones, R. I. and Lee, W. Electrical Stimulation of Fabric Filtration. Part IV: Enhancement by Particle Precharging. Textile Res. J. 54: 308-314, 1984.
2. Chiang, T., Samuel, E. A. and Wolpert, K. E. Theoretical Aspects of Pressure Drop Reduction in a Fabric Filter with Charged Particles. In: Third Symposium on the Transfer and Utilization of Particulate Control Technology, Volume III, EPA-600/9-82-005c (NTIS PB83-149609), July 1982.
3. Donovan, R. P., Hovis, L. S., Ramsey, G. H. and Abbott, J. H. Pulse-Jet Filtration with Electrically Charged Flyash. In: Third Symposium on the Transfer and Utilization of Particulate Control Technology, Volume I, EPA-600/9-82-005a (NTIS PB83-149583), July 1982.
4. Cooper, D. W. and Rei, M. T. Evaluation of Electrostatic Augmentation for Fine Particle Control. EPA-600/2-76-055 (NTIS PB253381), March 1976.
5. Page, L. and Adams, N. I., Jr. Principles of Electricity, Second Ed., D. Van Nostrand Co., Inc. New York, 1949. p. 102.
6. Myers, D., TRI Research Fellow, private communication, 1984.

NEW HIGH PERFORMANCE FABRIC FOR HOT GAS FILTRATION

J. N. Shah
E. I. Du Pont de Nemours & Co., Inc.
Wilmington, DE 19898

ABSTRACT

The development of new filter media designed for reduced baghouse operating costs via increased filtration capacity and/or reduced pressure drop is discussed. The development steps from defining industry needs, product optimization through laboratory tests and industrial baghouse evaluations are reviewed. Results show a significant improvement in baghouse performance, i.e., reduced ΔP and emissions and increased A/C ratio compared to incumbent filter media. Small scale tests comparing performance of various state of the art and new filter media, and the potential impact on baghouse operating cost are reviewed.

INTRODUCTION

The market for fabric filters in the U.S. and abroad has grown rapidly in the 1970's and is forecast to grow at an annual rate of 15% in the 1980's. Market studies by various groups suggest that the portion of the fabric filter market requiring higher temperature capabilities and greater gas throughput while providing very low particulate leakage (e.g., coal fired boiler baghouses) could increase at an even higher rate.

Currently, woven glass filter bags dominate reverse air cleaned, utility baghouses. That trend is expected to continue for the foreseeable future because of low cost and adequate filtering efficiency at air/cloth ratios <2.5 . Smaller, pulse cleaned industrial baghouses have used various types of filter media such as from Teflon* TFE fluorocarbon fiber, Huyglas**, Woven Glass, etc. Each has some advantages as well as some deficiencies when compared to each other. The goal for any baghouse operator is to satisfy Federal and State emission requirements at the lowest possible operating and maintenance cost. Any baghouse upsets, e.g., high pressure drop, high leakage or premature bag failures, whether due to improper boiler operation or inadequate bag/baghouse design, are intolerable.

NEW TEFAIRE* FELT FILTER MEDIUM

Our goal in designing a new filter medium, therefore, was to provide the industry with the most "forgiving" dust filter medium. One that would survive physical abuse in a pulse cleaned coal fired boiler baghouse for up to 4 years and one that would maintain acceptable pressure drops and particulate leakage at $>400^{\circ}\text{F}$ gas temperatures. To accomplish this, we blended fine diameter glass fiber with Teflon* fiber. The carded batt from an intimate blend of these two fibers was needled into a woven scrim of 100% Teflon* TFE fluorocarbon multifilament fiber and then heat set at very high temperatures. The resulting filter medium, trademarked as TEFAIRE* felt, met the required goals. Results from laboratory and field trials are detailed in the remaining section of this paper.

LABORATORY RESULTS

A series of felts containing blends of Teflon* and glass fibers, ranging from 3% to 90% glass fiber content in the fleece, were prepared by needle punching intimately blended batts into woven scrims of Teflon*. The felts were heat set at $\geq 550^{\circ}\text{F}$ to achieve dimensional stability.

* DuPont registered trademark

** Trademark of Huyck Corp.

Filtration tests conducted on a Laboratory Panel tester (6" x 8" samples) as well as in a pilot baghouse using fly ash from a stoker coal-fired boiler showed that at equivalent A/C ratios, the blended felts had a significantly lower particulate leakage than the control felts of 100% Teflon* fiber. In addition, the blended felts were able to filter at A/C ratios up to 15-20/1 with acceptable ΔP while control felts blinded very quickly. Blending of small glass fiber with large Teflon* fiber reduced the initial porosity of the felt and increased the total fiber surface area resulting in higher efficiency. We also suspect that these two fibers, having dissimilar tribo-electric characteristics, develop built-in electrostatic properties responsible for surface rather than in-depth filtration. It was found that filtration efficiency improved as the glass content increased up to 20-30%. At glass levels above 30%, the incremental improvement in efficiency was far less significant, while flex and abrasion resistance of the felt dropped. Additionally, glass content greater than 30% resulted in significantly increased processing difficulties. Therefore, an optimum fiber blend of about 75% Teflon* and 25% glass was selected for baghouse testing.

BAGHOUSE APPLICATIONS (COAL FIRED BOILERS)

GENERAL MOTORS (HAMILTON, OHIO)

One of three side stream separator baghouses (designed to filter approximately 15% of the total flue gases) operating at A/C ratio of 5-6 was clothed with filter bags of 21 oz/yd² TEFAIRE in October, 1982. The two other baghouses contained filter bags made from 100% Teflon* and Ryton**, respectively. After more than one year exposure, the filtration performance of the bags of TEFAIRE continues to be significantly superior to the other products. Furthermore, the improved efficiency was accomplished at lower ΔP and with less frequent bag cleaning. (see Table 1). These differences are even more significant in view of shorter baghouse exposure time for the bags of RYTON**.

* DuPont trademark

** Trademark of Phillips Petroleum Co.

TABLE 1

"TEFAIRE FELT" AT GM

Bag Material	In Baghouse (Months) Exposure/Operation	Leakage (Grains/ACF)		ΔP (inch.H ₂ O)	Pulse Frequency (Minutes)
		Inlet	Outlet		
"TEFAIRE"	15/5	.1680	<.0001	2.5	45
Teflon*	15/6	.1198	.0599	7.5	6
RYTON**	10/2	.3601	.0214	6.5	6

DU PONT POWERHOUSE

One of six compartments of the baghouse was clothed with filter bags of 21 ozs/yd² TEFAIRE felt while the remaining five compartments contained filter bags made from felt of 100% Teflon*. Air flow and ΔP across each compartment were monitored periodically during the 12-month test period. Results show that Average Drag Index ($\Delta P/A.C.$ ratio) for bags of TEFAIRE was 30% lower than for bags of 100% Teflon*. In a direct comparison to the compartment located directly across from that containing the bags of TEFAIRE (to normalize the baghouse), the Drag Index was almost 65% lower.

The filter bags were removed periodically and were analyzed in the laboratory for physical properties and filtration performance (panel tester). Results (Table 2) consistently showed that:

- Particulate leakage through TEFAIRE felt was significantly lower (more than an order of magnitude) compared to felt of Teflon* TFE fiber.
- Pressure drop across TEFAIRE felt was significantly lower despite its higher filtration efficiency.
- Physical properties suggest no abnormal bag wear predictive of premature bag failure.

* DuPont trademark

** Trademark of Phillips Petroleum Co.

- Air permeability and cross sectional Scanning Electron Photomicrographs showed lower dust penetration through TEFAIRE felt. This could explain higher in-use porosity and, therefore, lower ΔP and higher gas throughputs.

In December 1983, the one compartment test with TEFAIRE felt was extended to a full baghouse containing 1344 bags. Initial performance has confirmed results of the earlier one compartment test. Additional tests are planned to confirm the increased gas throughput capabilities of TEFAIRE felt by gradually reducing the number of compartments in service.

TABLE 2

DU PONT POWERHOUSE BAGS

	EXPOSURE MONTHS			
	5		13	
	<u>TEFAIRE</u>	<u>TEFLON®</u>	<u>TEFAIRE</u>	<u>TEFLON®</u>
<u>LABORATORY PANEL TESTER</u>				
LEAKAGE (GR/ACF) AT				
A/C = 7	.0050	.0015	.00016	.019
11	.0010	.050	.00037	.075
ΔP (INCH. H ₂ O) AT				
A/C = 7 (CLEAN/DIRTY)	.2/2.7	.5/3.9	.4/4.1	1.0/10+
11 (CLEAN/DIRTY)	.9/10+	1.9/10+	.2/10+	2.0/10+
MULLEN BURST STRENGTH (PSI)				
	206 (210 NEW)	223 (240 NEW)	178	208
BREAK. STR. (LBS./IN)				
MD/XD	68/62 (68x58 NEW)	94/82 (76/79 NEW)	62/56	90/84

KERR BLEACHER (TRAVELLERS RES, S.C.)

Filter bags of TEFAIRE having a range of felt basis weights were exposed to adverse baghouse operating conditions for more than two years. These included several boiler upsets, routine weekend shut downs and pulse hardware problems. The testing was supervised by ETS Inc. of Roanoke, Va. The air/cloth ratio during the test period ranged from 5 to 12. Periodic analysis of filter bags removed from the baghouse showed no signs of blinding or premature bag failure until a baghouse fire destroyed the majority of the bags. Based on performance and physical properties of the felt (as shown in Table 3), a 4 year useful life is anticipated for filter bags of TEFAIRE under normal baghouse operation.

Baghouse Application (Incineration)

A six-month baghouse test was conducted in a Municipal incineration plant. Although no bag related problems were detected initially, the test was terminated due to poor temperature controls, (>600°F) and frequent sparks. Additional tests in incineration baghouses are planned.

TEXTILE RESEARCH INSTITUTE TEST

Filter bags removed from an industrial coal fired boiler baghouse after 6 months exposure were tested in the laboratory for performance. Small patches from the "exposed" bags were installed on a laboratory filtration tester at Textile Research Institute to measure the filtration efficiency and pressure drops for filter media of Teflon* and TEFAIRE at A/C ≈ 18 . Results indicated that:

- The presence of glass fiber reduced dust penetration by almost an order of magnitude (99.81% vs. 98.47% efficiency) at equivalent ΔP .
- TEFAIRE felt had remarkably higher filtering efficient of sub-micron size dust particles, as measured by an air cascade impactor (Results in Figure 1).

* DuPont trademark

TABLE 3

BAGS OF TEFAIRE FROM KERR
(Laboratory Analysis)

<u>Filtration Panel Tester</u>	<u>TEFAIRE New</u>	<u>TEFAIRE After Exposure Months</u>				
		<u>2</u>	<u>4.5</u>	<u>10</u>	<u>17</u>	<u>20</u>
Leakage (Gr/ACF) @						
A/C = 7	.001	.001	.002	.002	.0017	.0052
11	.001	.0002	.001	.001	.002	.0009
15	.001	.0001	.001	.0007	.0006	.0003
ΔP (inch H ₂ O) at						
A/C = 7 (clean/dirty)	0/0	0/.8	.1/1.2	.1/.9	.2/4.9	0/1.2
11 (clean/dirty)	.1/.35	.4/3.9	.3/5.1	.4/3.1	1./10+	.2/3.9
13 (clean/dirty)	.2/1.0	.7/9.6	.6/10+	.8/10+	3.1.10+	.8/7.7
<u>Properties</u>						
Breaking Strength (lbs)	71	73	73	74	86	72
Elongation (%)	30	28	36	39	33	37
Air Permeability (Ft ³ /min/ft ²)						
As Received	30	7.0	7.6	-	8.5	6.7
Vacuumed	30	15.8	21.5	11.4	16.2	11.4
Mullen Burst (psi)	243	215	211	220	233	187

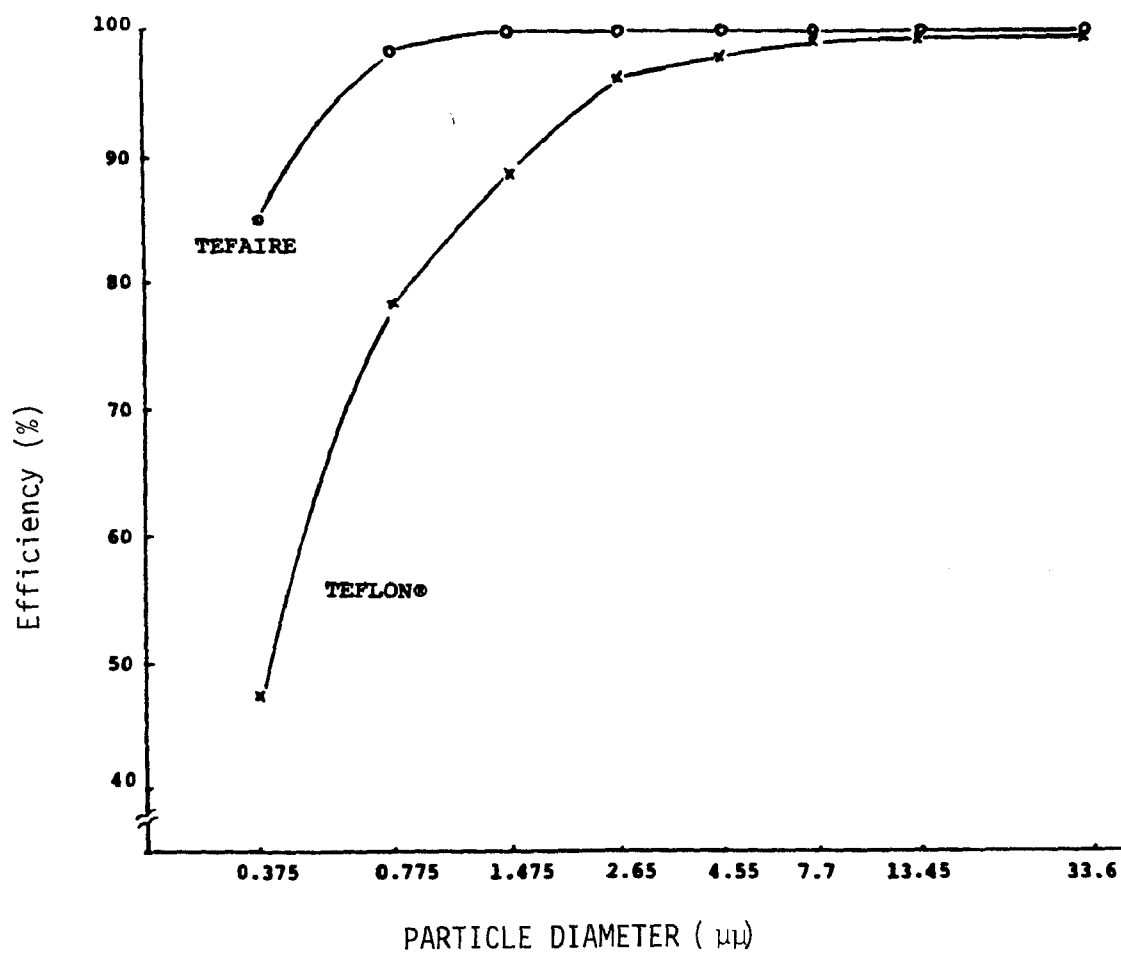


FIGURE 1. FILTRATION EFFICIENCY VS. PARTICLE SIZE

COMPARATIVE PERFORMANCE STUDY

In order to assess the relative performance of various filter media (e.g. TEFAIRE, Woven Glass, HUYGLASS, RYTON and PBI available for pulse cleaned baghouses, a test was conducted by ETS Inc., a consulting and testing company, using a side stream baghouse from a pulverized coal boiler in Waynesboro, VA. The objective of the test was to determine maximum gas throughput possible while maintaining acceptable ΔP and emission. Results of this test were as follows:

- At baghouse temperatures of $<300^{\circ}\text{F}$ and A/C ratios of >10 , TEFAIRE bags exhibited 20-30% lower drag index vs. RYTON and HUYGLAS filter bags. The effects at higher baghouse temperatures ($>350^{\circ}\text{F}$) will be assessed later.
- TEFAIRE filter bags had the lowest particulate leakage while woven glass bags leaked the most (20X compared to the felt candidates) with only half the air throughput.

In a separate test, TEFAIRE filter bags displayed 50% lower drag index compared to bags made from PBI filters.

VALUE-IN-USE MODEL

A model was developed and used to determine comparative operating costs for different filter media. The model takes into account variables such as filter bag cost, bag life, A/C ratio, ΔP , bag changing and cleaning costs, and depreciation. The results, in terms of baghouse system and baghouse operating costs can be used to determine value-in-use of various filter media. Figure 2 shows that:

- In existing baghouses, a \$95 filter bag (9 ft. long x 6" dia.) having a 4-year bag life will be just as cost effective as \$25, \$50, \$75, and \$120 bags having 1, 2, 3 and 5 year bag life respectively. Assuming equal filtering capacity and ΔP , relative costs of different filter media can be compared.
- In new baghouse installations, the increased A/C ratio (smaller size baghouse) and lower ΔP (less fan power) obtainable with TEFAIRE felt would significantly reduce baghouse size, investment and operating cost. Alternatively, in retrofit, the higher filtering capacity of TEFAIRE felt can permit the use of fewer filter bags and thereby reduce the effective cost of filter bags of TEFAIRE.

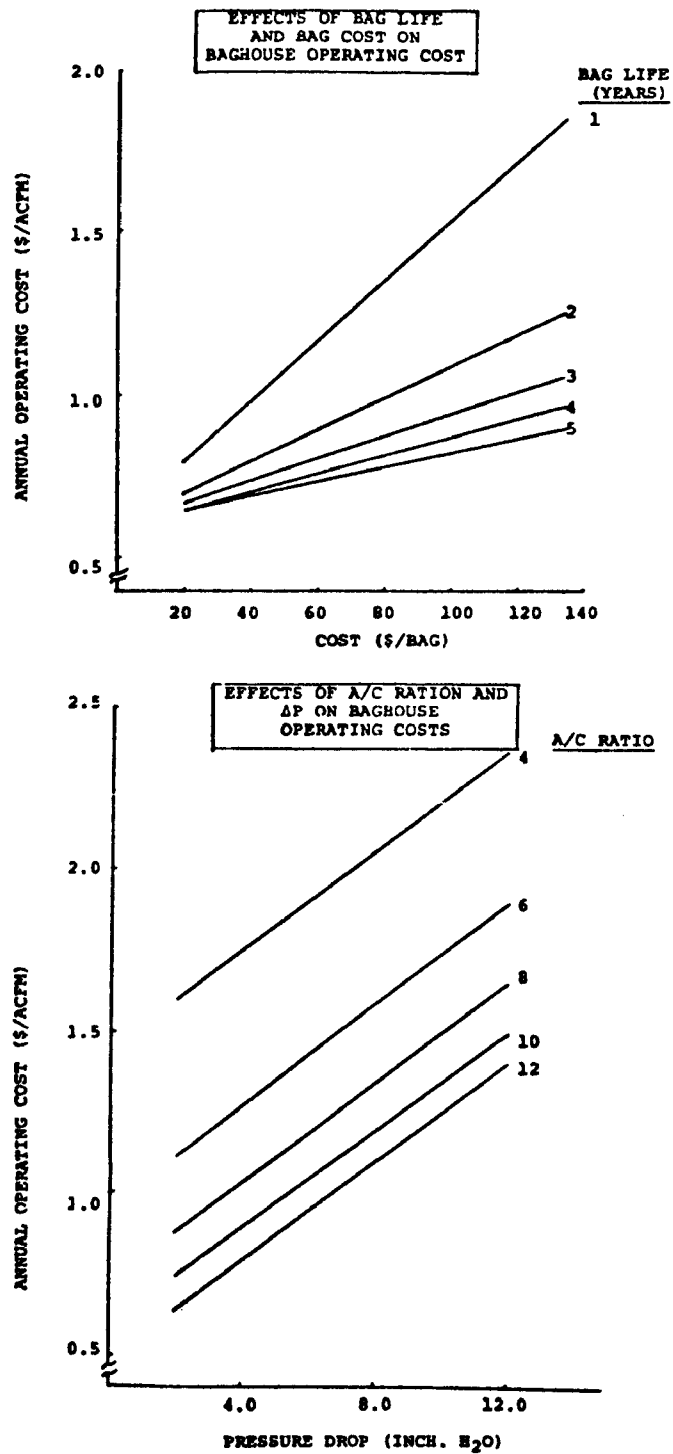


FIGURE 2. FACTORS AFFECTING BAGHOUSE COST

SUMMARY

Results to date indicate that TEFAIRE felts can provide superior baghouse performance with extremely low particulate leakage and pressure drops at conventional gas throughputs. Laboratory and small scale baghouse tests have indicated potential to double the gas throughputs while maintaining acceptable baghouse performance. Filter bags of TEFAIRE are expected to survive up to 4 years in highly corrosive, high temperature baghouse environment which could make them one of the most cost effective filter media in recent years.

NOTICE

The work described in this paper was not funded by the U.S. Environmental Protection Agency and therefore the contents do not necessarily reflect the views of the Agency and no official endorsement should be inferred.

Session 17: FF: PILOT-SCALE STUDIES (COAL-FIRED BOILERS)

Louis S. Hovis, Chairman
U.S. Environmental Protection Agency
Air and Energy Engineering Research Laboratory
Research Triangle Park, NC

THE INFLUENCE OF COAL-SPECIFIC FLY ASH PROPERTIES UPON BAGHOUSE
PERFORMANCE: A COMPARISON OF TWO EXTREME EXAMPLES

Stanley J. Miller and D. Richard Sears
University of North Dakota Energy Research Center
Grand Forks, North Dakota 58202

Work Performed Under Cooperative Agreement No. DE-FC21-83FE60181
For U.S. Department of Energy
Morgantown Energy Technology Center
Grand Forks Project Office
Grand Forks, North Dakota 58202

ABSTRACT

Pilot plant data with a large number of lignite and subbituminous coals have demonstrated that shaker baghouse efficiency is highly coal specific with large differences in baghouse penetration for different coals. A previous report has presented these findings along with an observed correlation between elemental fly ash composition and baghouse penetration.

This paper presents a further investigation of the relationship between fly ash properties and baghouse penetration with woven glass fabric and shaker cleaning. The focus will be on two coals which represent the good and poor extremes of filter performance. The coal and ash properties of a lignite showing good filter performance are compared with the properties of a lignite demonstrating very poor performance. An examination of both chemical and physical ash properties which include elemental compositions as a function of size, particulate size distribution, particle surface morphology, and other physical descriptors is presented in an attempt to determine causes of grossly different baghouse performance.

The work described in this paper was not funded by the U.S. Environmental Protection Agency and therefore the contents do not necessarily reflect the views of the Agency and no official endorsement should be inferred.

INTRODUCTION

The use of fabric filters for control of particulate emissions from utility coal fired boilers has been increasing in recent years. In most cases, baghouses are able to meet or exceed current New Source Performance Standards (NSPS); however, there are some cases in which emissions from utility baghouses have been higher than expected. The fact that some baghouses have higher than acceptable emissions and the possibility of future regulation of fine particle emissions indicate a need for a better understanding of the causes of higher emissions from some fabric filters. The need is not only to achieve high removal efficiency of fine respirable particulate matter but also to accomplish it by an economical method. A better understanding of cause and effect relationships between ash properties and baghouse penetration will facilitate the most economical design of fabric filter collectors that can achieve high removal efficiency of fine particulate matter for any given coal. If, for example, a given coal produces fly ash which is easier to collect than ash from another coal, then the particulate collector should be properly designed for each specific case. Applying the same design approach to both cases could result in overdesign for an easily collected ash with higher than necessary costs, while for the difficult to collect ash, it could result in higher than acceptable emissions.

The particulate characterization project at the University of North Dakota Energy Research Center (UNDERC) has focused on identifying and quantifying those particulate characteristics of low-rank coals that are critical to control device performance and the environment. The long range goal of the work is to develop an increased understanding of coal and collector specific emissions of fine particulate matter that will permit higher levels of particulate control by economical methods.

EXPERIMENTAL APPROACH

Baghouse removal efficiency was measured for 26 fuels with constant baghouse conditions using the same woven glass fabric (Filter Media Products 601E). The pilot baghouse filtered flue gas produced by a 550,000 Btu/hr pulverized coal (pc) fired combustor. A detailed description of both the combustor and baghouse has been presented in a previous paper (1) and will not be repeated here. It should be noted, however, that the pc-fired combustor was specifically designed to generate fly ash representative of large scale pc-fired boilers. When fly ash from the pilot combustor has been compared with fly ash from a large boiler burning the same coal, there appear to be no major differences. The baghouse has three modes of cleaning including the shaker chamber with tube sheet mounted bags, and pulse jet and low pressure expansion, both with cage mounted bags.

The shaker chamber was used with a constant cleaning cycle for the 26 tests reported in Table 1. Most of the test runs were "one day" runs with 8 to 16 hours of steady state baghouse operation. With some coals,

TABLE 1
EFFICIENCY AND FLY ASH ANALYSIS FOR 26 FUELS

Name	Symbol	Coal		Inlet Dust Loading grains/SCF	Baghouse Removal Efficiency, %	Baghouse Penetration, %	Fly Ash Analysis Pct Concentrations as Oxides									
		Source	Rank				SiO ₂	Al ₂ O ₃	Fe ₂ O ₃	TiO ₂	P ₂ O ₅	CaO	MgO	Na ₂ O	K ₂ O	SO ₃
Big Brown	BB1	Freestone, Co., TX	Lignite	5.0	76.0	24.0	53.6	17.7	7.4	1.6	0	14.7	3.0	0.44	0.9	1.2
Big Brown	BB2	Freestone, Co., TX	Lignite	6.4	83.5	16.5	53.0	19.7	7.7	1.6	0	13.3	3.0	0.37	1.1	0.7
Phillips "A"	PA	Panola Co., TX	Lignite	5.3	86.3	13.7	59.2	13.8	11.9	1.4	0	9.8	1.7	0.81	1.2	0.9
Choctaw (washed)	CW	Choctaw Co., AL	Lignite	2.7	89.6	10.4	25.2	12.6	19.1	1.0	0.2	26.7	2.4	0.70	0.7	11.7
Pike Co.	PK	Pike Co., AL	Lignite	3.6	90.0	10.0	34.4	18.8	6.9	1.6	0.1	27.5	1.9	0.71	0.3	8.5
WB Coal	WB	Western USA	Bituminous	2.0	91.9	8.1	62.0	22.6	4.9	1.2	0.6	3.0	1.4	1.3	2.4	0.5
Choctaw (unwashed)	CA	Choctaw Co., AL	Lignite	4.6	92.2	7.8	32.2	13.2	26.8	0.9	0.1	13.8	2.5	0.54	1.1	9.4
Naughton	NT	Lincoln Co., WY	Subbit.	1.6	93.6	6.7	56.4	15.9	8.3	0.9	0.1	7.7	3.2	0.20	1.7	0.8
Falkirk	FK	McLean Co., ND	Lignite	4.0	94.7	5.3	42.2	12.1	12.6	0.9	0	20.8	7.0	0.60	1.5	1.8
Arapahoe	AR	Routt Co., CO	Subbit.	2.8	95.5	4.5	58.4	24.8	3.9	1.2	0.7	6.4	2.1	0.60	1.6	0.9
San Miguel	TL1	Atascosa Co., TX	Lignite	12.0	99.1	0.9	60.2	20.1	3.7	1.1	0.04	5.4	1.1	3.6	2.6	1.2
Antelope High Na	AN max	Wyoming	Subbit.	1.5	99.1	0.9	35.9	10.4	7.1	1.2	0.5	28.6	6.1	2.4	0.6	7.3
Beulah Low Na	BW	Mercer Co., ND	Lignite	3.2	99.3	0.7	38.2	7.4	12.1	1.7	0.2	19.3	5.2	5.8	0.2	9.7
Velva	V5	McLean Co., ND	Lignite	2.5	99.4	0.6	32.9	13.2	6.6	1.3	0.1	30.3	6.4	3.2	0.6	5.3
San Miguel	TL2	Atascosa Co., TX	Lignite	6.2	99.4	0.6	47.8	16.5	8.3	1.0	0	13.1	1.7	5.3	2.2	3.8
Antelope Low Na	AN low	Wyoming	Subbit.	2.8	99.4	0.6	47.7	19.7	4.1	2.0	1.3	17.6	4.2	1.1	0.6	1.8
Caballo/ Spring Creek	NE/SP	Cambell Co., WY	Subbit.	1.9	99.5	0.5	37.6	15.1	6.6	2.0	0.6	26.2	4.3	2.4	0.4	4.7
Velva	V3	McLean Co., ND	Lignite	1.9	99.5	0.5	18.4	10.7	6.4	0.7	0.4	42.2	9.9	3.2	0.1	8.2
Antelope Medium Na	AN med	Wyoming	Subbit.	1.7	99.5	0.5	29.7	14.0	8.8	1.4	0.7	30.9	6.3	1.3	0.4	6.5
Sarpy Creek	SC	Big Horn Co., MT	Subbit.	3.5	99.65	0.35	36.1	16.3	6.8	1.2	0.2	26.2	2.9	5.0	0.8	4.0
Wyodak	WD	Cambell Co., WY	Subbit.	2.4	99.69	0.31	36.2	15.7	7.4	1.7	0.9	27.3	5.5	1.7	0.4	3.4
Indian Head	13	Mercer Co., ND	Lignite	2.5	99.7	0.3	29.2	12.4	11.5	1.0	0.4	20.6	5.3	10.2	1.1	8.3
Antelope/ Spring Creek	AN/SP	Wyoming	Subbit.	1.6	99.8	0.2	36.9	13.1	7.5	1.3	0.6	25.5	5.2	3.1	0.5	6.5
Velva	V4	McLean Co., ND	Lignite	2.0	99.8	0.2	14.8	9.5	7.6	0.8	0.5	41.4	9.4	4.3	0.1	11.7
Beulah High Na	BA	Mercer Co., ND	Lignite	2.1	99.8	0.2	25.5	12.3	11.2	1.1	0.5	18.1	4.3	13.7	0.6	12.9
Beulah	BU	Mercer Co., ND	Lignite	3.2	99.9	0.1	22.8	19.2	8.8	1.1	0.6	22.6	5.2	11.5	0.1	13.2

however, 100-hour runs have been completed in order to assess subtle longer term changes in performance. In these cases, pressure drop has remained quite steady and efficiency has had only minor fluctuations. One example is with Naughton subbituminous coal where the average efficiency was only 93.6%. This was a 5-day run with dust loadings measured each day. Measured efficiency for the first day was low and it did not improve by the end of the week. Another example is with Velva, North Dakota, lignite for which measured first-day efficiency was 99.8%, where it remained for the duration of the 98-hour run. This shows that differences among coals can be detected with one day tests. It does not imply that all long term effects (as in large scale reverse air baghouses in which high residual dust cakes can take months to stabilize) can be studied in one day tests. It is important to recognize, however, that with the shaker chamber tests the cleaning action is vigorous leaving a light residual dust cake. Because of this, the time required for stable operation is much less for shaker cleaning than for conventional reverse air.

The question of whether this shaker baghouse is comparable to baghouses used in industry will be addressed here. The most similar method of cleaning used in the utility industry would be shake-deflate cleaning. The only two examples of this type of baghouse on a utility pc-fired boiler burning a western coal are the Monticello station which burns a Wilcox group Texas lignite and the Harrington station which burns a subbituminous coal from Cambell County, Wyoming. The reported removal efficiency at Harrington (2,3) has ranged from 99.3 to 99.7%, which meets current NSPS. Monticello, on the other hand, is reported to have severe bleed through problems resulting in a low removal efficiency (4,5). Although we have not tested coals from the specific mines supplying these sites, we have tested coals that are similar. Our tests with Wyodak coal which is also from Cambell County, Wyoming, resulted in a removal efficiency of 99.7% which is in the range reported for Harrington. When we tested Big Brown coal, another Wilcox group Texas lignite, the results showed low removal efficiency similar to the experience at Monticello. At least in these two cases results from pilot tests with shaker cleaning can be compared with results from large scale baghouses using shake-deflate cleaning.

In addition to the 26 shaker chamber tests with a single fabric, some tests have been conducted with other fabrics and/or cleaning modes, in order to determine if the extreme differences in results noted during shaker tests would also be observed with other fabrics and cleaning cycles.

RESULTS AND DISCUSSION

PENETRATION AND ASH COMPOSITION

Ash composition, baghouse penetration, and inlet dust loading, are presented for the fuels listed in Table 1. A previous report (1) showed

that the strongest correlation between baghouse penetration and individual elemental concentration was with sodium. Since that report additional data have been added which continue to show the strong relationship between sodium and penetration. In order to quantify the effect of sodium on penetration and to determine if other elements in Table 1 have significant correlations with penetration, regression analysis was completed for each of the elements. Eight two parameters functions were applied to each element and the coefficient of determination, R^2 , was calculated for each case. The results of the regression analyses are presented in Table 2. The mathematical relationship that gave the highest R^2 value for each element is given along with the calculated R^2 value for the 26 data points. It is apparent that the correlation between sodium and penetration with an R^2 of 0.73 is far better than for any of the other individual elements. The next best correlation was with phosphorous with an R^2 of 0.41 followed by potassium, sulfur, silicon, and magnesium. All of these correlations except for silica show that as concentrations of these elements increase baghouse penetration decreases. With silica the relationship is opposite; as silica concentration increases baghouse penetration also increases. Calcium, aluminum, iron, and titanium all showed weaker correlations indicating a much smaller effect on baghouse penetration. It was found that when several elements were combined in a linear combination, the correlation was significantly improved. For example, the combination of $\text{Na}_2\text{O} + 0.4 \text{ MgO}$ resulted in an R^2 value of 0.79 compared to 0.73 for Na_2O alone. When $2.8 \text{ P}_2\text{O}_5$ was added to Na_2O , the correlation was still better with $R^2 = 0.82$. The combination of $\text{Na}_2\text{O} + 0.4 \text{ MgO} + 2.8 \text{ P}_2\text{O}_5$, however, resulted in the best observed correlation with an R^2 of 0.88. The sodium-penetration relationship is plotted in Figure 1 and the combination of sodium, magnesium, and phosphorous is shown in Figure 2. Attempts to improve the correlation by adding different forms of other elements such as sulfur were not successful.

It needs to be reemphasized that all tests were intentionally performed with the same fabric, at the same temperature and air to cloth ratio (A/C), and with the same cleaning cycle parameters. Therefore, any significant differences in removal efficiency among the various ashes must be regarded as originating in differing fuel or ash characteristics. The resulting mathematical models are for the one set of constant conditions. Changing the fabric, A/C, or cleaning cycle would likely change the form of the mathematical relationships. The value of the model at this point is not in predicting baghouse penetration in general for various fabrics and cleaning modes but rather in documenting the influence that ash composition can have on baghouse emissions.

ADDITIONAL BAGHOUSE EFFICIENCY DATA

The penetration data shown in Figures 1 and 2 were for a single fabric and cleaning cycle, however, a number of tests have also been completed for both Beulah and Big Brown coals with other fabrics and cleaning modes. Table 3 presents comparative data for these two coals with three different cleaning modes and several fabrics. Two shipments of each of these coals have been tested to ensure that unique results

TABLE 2
CORRELATIONS BETWEEN ELEMENTAL COMPOSITION AND BAGHOUSE PENETRATION

<u>Elemental Concentration, X</u>	<u>Mathematical Relationship Between Penetration, y, and Elemental Concentration, X</u>	<u>Coefficient of Determination, R²</u>
SiO ₂	$y = 0.081 e^{.071 X}$	0.33
Al ₂ O ₃	$y = 0.117 e^{.162 X}$	0.16
Fe ₂ O ₃	$y = 0.609 e^{.088 X}$	0.07
TiO ₂	$y = 8.34 - 4.67/X$	0.03
P ₂ O ₅	$y = 1.21 - 1.19 \ln X$	0.41
CaO	$y = 7.35 e^{-.082 X}$	0.25
MgO	$y = 10.2 X^{-1.56}$	0.30
Na ₂ O	$y = 2.84 X^{-1.25}$	0.73
K ₂ O	$y = X/(0.48 + 0.73 X)$	0.38
SO ₃	$y = 1/(0.136 + 0.322 X)$	0.34
Na ₂ O + 0.4 MgO	$y = 17.9 X^{-1.96}$	0.79
Na ₂ O + 2.8 P ₂ O ₅	$y = 5.56 X^{-1.42}$	0.82
Na ₂ O + 0.4 MgO + 2.8 P ₂ O ₅	$y = 37 X^{-2.15}$	0.88

were not caused by non-representative coal. In the shaker cleaning mode two woven glass fabrics, the 601E and 648E, both with 10% teflon B coating, were tested for both coals. In addition, a woven glass PTFE membrane fabric was tested with Big Brown coal. Test results show that for both woven glass fabrics the removal efficiency for Big Brown was very low while that for Beulah was high. The measured removal efficiency for Big Brown using a PTFE membrane fabric was 99.0%; however, there were indications of some leakage past loose fitting snap bands in the tube sheet. With tight fitting snap bands the removal efficiency may have been even higher but the test does show that control of this ash may be improved by applying a specialized fabric.

Tests were also completed with pulse jet cleaning at an A/C of about 9 to 1 with the same 648E fabric and a glass felt fabric, the 0100. As one would expect, the felted fabric performed much better than the woven glass

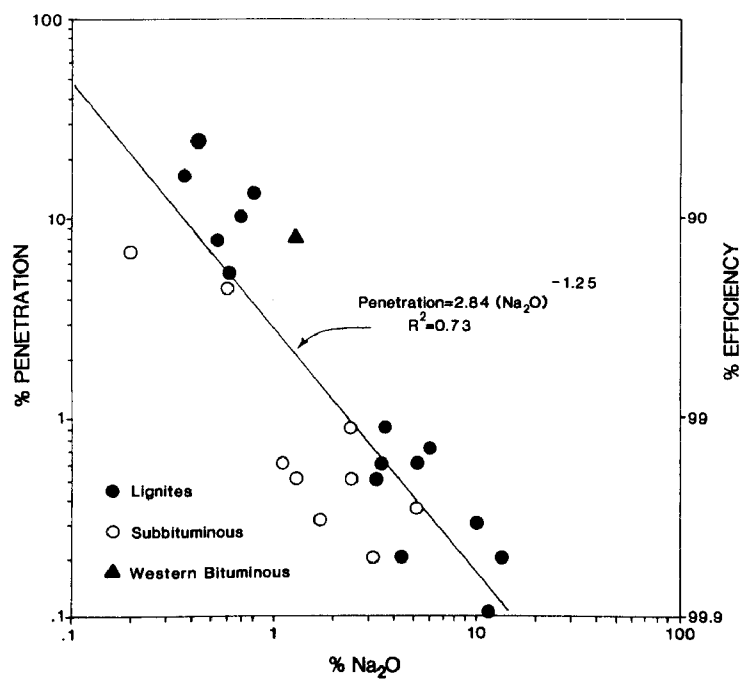


Figure 1. Penetration as a function of Na₂O in the fly ash.

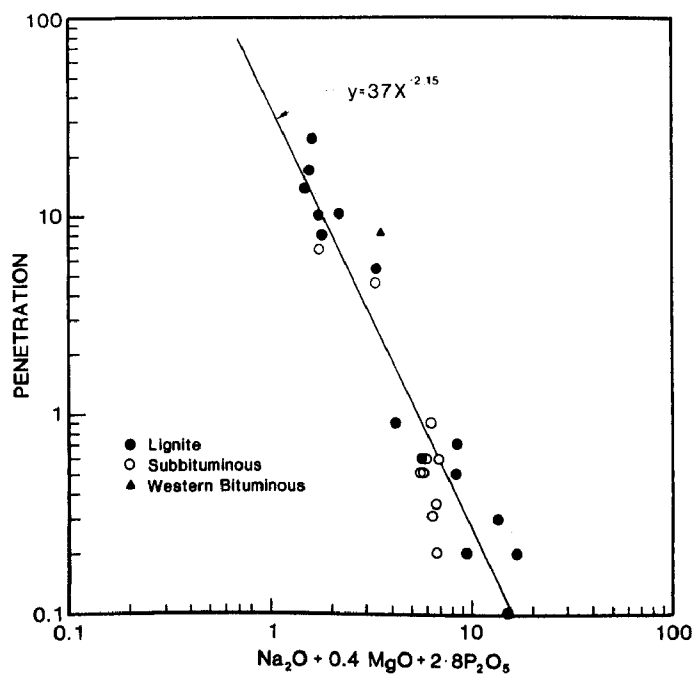


Figure 2. Penetration as a function of (Na₂O + 0.4 MgO + 2.8 P₂O₅).

TABLE 3

BAGHOUSE RESULTS FOR BIG BROWN AND BEULAH

<u>Coal</u>	<u>Sample</u>	<u>PTC Run</u>	<u>Fabric*</u>	<u>Cleaning Mode</u>	<u>Air/Cloth ft/min</u>	<u>ΔP inches WC</u>	<u>% Removal Efficiency</u>
Big Brown	BB1	212	601E	Shaker	3.3	5.1	76.4
Big Brown	BB2	253	601E	Shaker	3.2	2.0	83.5
Big Brown	BB1	208	648E	Shaker	3.3	8.9	86.5
Big Brown	BB2	252	648E	Shaker	3.4	3.8	93.2
Big Brown	BB2	254	PTFE Membrane	Shaker	3.3	4.4	99+ [#]
Big Brown	BB1	210	648E	Pulse Jet	8.2	8.2	55.0
Big Brown	BB1	211	0100	Pulse Jet	8.8	5.8	95.6
Big Brown	BB2	255	0100	Pulse Jet	8.8	6.5	92.0
Big Brown	BB1	209	648E	Reverse Air	4.5	7.1	92.7
Beulah	BA	216	601E	Shaker	3.3	4.3	99.8
Beulah	BU	261	601E	Shaker	3.4	4.2	99.9
Beulah	BA	218	648E	Shaker	3.2	6.0	99.7
Beulah	BA	215	648E	Pulse Jet	8.8	11.0	98.1
Beulah	BA	217	0100	Pulse Jet	8.6	6.0	99.2
Beulah	BA	237	648E	Reverse Air	4.3	10.0	99.7

* All fabrics except the PTFE membrane one are the manufacturer's designation, Filter Media Products, MIDWESCO, Winchester, Virginia.

There may have been some leakage past the snap bands in the tube sheet due to a loose fit.

for both coals, but again the Beulah ash was collected with a much higher efficiency than the Big Brown ash. Finally, tests with reverse air cleaning (low pressure expansion of cage-mounted bags) also resulted in a much lower collection efficiency for Big Brown. Since these tests with several fabrics and three different cleaning modes clearly show the Big Brown ash to be more difficult to collect by fabric filtration than Beulah ash, it can be concluded that the differences in collectibility must originate with differences in fuel characteristics. These differences will be explored in the remaining sections of this paper.

COAL AND FLUE GAS ANALYSIS

Since these two coal ashes have different filtration characteristics, one must ask, "What coal characteristics are causing the observed differences in collectibility." Before ash characteristics are considered in the next sections, coal and flue gas analysis will be presented here. Table 4 gives coal analysis data for both the Big Brown and Beulah coals as well as the corresponding flue gas analysis from the pilot combustion tests. Two Big Brown coal samples, BB1 and BB2, obtained in separate shipments were tested. For the two Big Brown samples, the analyses are similar. Small differences include the slightly higher hydrogen and corresponding flue gas moisture for the BB2 sample compared to BB1. Tests with Beulah lignite also include two coal shipments, BA and BU. Comparing the BU Beulah sample with the BA sample, the ultimate analysis appears to be about the same. The coal and flue gas moisture for the BU sample, however, is much lower because this coal had been dried prior to testing.

When Big Brown lignite is compared to Beulah lignite the two coals also appear to be quite similar. Both are western low-rank coals which are low in sulfur and high in moisture. The most obvious difference is the 18% to 20% ash (moisture free) for Big Brown compared to 10% to 12% ash for Beulah. Total carbon, sulfur, and heating value (moisture free) are somewhat higher for Beulah than Big Brown. The as-burned fuel moisture for both coals is about the same except for the dried Beulah sample. Flue gas O_2 and CO_2 levels are in the same range indicating that both fuels were fired at the same excess air level. Average SO_2 concentrations for all but one Beulah test were somewhat lower than for Big Brown even though the Beulah coal had a higher sulfur content. This is caused by the much higher alkali concentration in the Beulah coal resulting in a greater sulfur retention which is confirmed by higher SO_3 concentration in the Beulah fly ash. NO_x concentrations for the Big Brown tests were somewhat higher than for Beulah, but this was most likely caused by the higher fuel nitrogen for Big Brown.

In comparing the Beulah and Big Brown coals along with the resulting flue gas analysis from the test burns, there are no obvious differences that would explain the noted differences in ash collectibility. Since the heating value, fuel moisture, and the resulting flue gas analysis for the two fuels were similar, the flame conditions would also be similar. This indicates that differing particulate characteristics resulted from

TABLE 4
COAL AND FLUE GAS ANALYSIS FOR BIG BROWN AND BEULAH

Coal-Run No.	Coal Analysis (moisture free)								Coal Moisture %	Flue Gas Analysis (dry)				Flue Gas Moisture %
	C	H	N	S	by diff.	Ash	VM	Btu/lb		% O ₂	% CO ₂	ppm SO ₂	ppm NO _x	
BB1-208	57.80	3.63	1.12	1.07	17.92	18.5	42.5	10096	26.9	5.0	13.7	893	879	12.3
BB1-209	58.50	3.58	1.11	1.08	16.17	19.6	41.5	10015	27.9	5.2	13.4	923	984	11.4
BB1-210	58.27	3.72	1.11	1.06	16.19	19.7	42.7	9975	24.2	4.8	14.2	919	861	12.8
BB1-211	59.40	3.83	1.03	0.91	16.48	18.4	43.3	10137	22.1	4.1	15.1	944	904	12.9
BB1-212	59.24	3.86	1.02	0.88	16.15	18.8	41.1	9862	27.3	4.3	14.9	996	1002	12.2
BB2-252	56.84	4.09	1.14	1.06	17.51	19.7	42.1	9907	26.6	4.5	13.8	890	1075	14.9
BB2-253	57.74	4.21	1.15	1.04	16.33	19.5	41.9	9873	25.8	4.1	15.0	949	839	14.6
BB2-254	58.43	4.02	1.35	1.09	16.05	19.1	42.6	10005	26.0	4.3	14.2	868	871	14.3
BB2-255	57.48	4.04	1.30	1.06	17.94	18.2	42.3	10121	26.3	4.3	14.5	876	1000	13.7
BA-214	63.45	2.93	0.93	1.62	18.92	12.2	41.2	10392	27.6	4.6	14.8	1036	804	12.4
BA-215	61.35	2.77	0.74	1.46	22.70	11.0	41.6	10566	27.2	4.2	15.4	986	740	12.7
BA-216	63.44	3.37	0.87	1.27	20.07	11.0	42.6	10560	34.5	4.5	14.6	639	761	12.5
BA-218	63.10	3.33	0.86	1.33	19.18	12.2	42.4	10484	28.7	4.9	14.0	769	789	12.6
BA-234	64.45	4.67	0.89	1.36	17.23	11.4	42.5	10442	27.2	4.3	14.8	709	698	13.3
BU-261	63.05	4.20	0.84	1.32	20.21	10.4	47.8	10376	14.3*	4.5	14.5	730	673	7.9*

* Coal was dried for this test.

TABLE 5
FLY ASH ELEMENTAL COMPOSITION AS A FUNCTION OF PARTICLE SIZE

		SiO ₂	Al ₂ O ₃	Fe ₂ O ₃	TiO ₂	P ₂ O ₅	CaO	MgO	Na ₂ O	K ₂ O	SO ₃
Big Brown Run 209	Bulk Ash	53.6	18.0	7.1	1.6	<0.1	14.5	3.1	<0.5	0.9	1.2
	Stage 1 > 10 μm	53.7	17.3	7.4	1.8	<0.1	15.1	2.6	<0.5	1.0	1.1
	Stage 2 3-10 μm	52.1	20.2	6.5	1.6	<0.1	14.0	3.2	<0.5	1.0	1.4
	Stage 3 1-3 μm	45.4	23.0	7.7	1.9	<0.1	16.6	2.7	<0.5	0.7	2.0
Beulah Run 220	Bulk Ash	26.4	12.4	11.3	1.1	0.4	18.2	4.5	13.0	0.6	12.2
	Stage 1 > 10 μm	28.1	12.7	13.8	1.1	0.2	21.1	4.9	10.5	0.5	6.9
	Stage 2 3-10 μm	25.8	13.2	8.7	1.2	0.5	16.3	3.9	17.6	0.8	14.2
	Stage 3 1-3 μm	21.9	12.9	5.8	1.4	0.8	10.4	2.4	19.2	1.3	24.1

differences in the inorganic constituents of the two coals rather than different flame conditions.

ELEMENTAL CONCENTRATION AS A FUNCTION OF PARTICLE SIZE

The correlations presented relating baghouse emissions to elemental concentrations were for bulk fly ash composition only. However, there may be additional differences in elemental concentrations as functions of particle size. Previous research at UNDERC (6) has shown that for Beulah, North Dakota, lignite both sodium and sulfur not only increase in bulk concentrations with decreasing particle size but also occur in higher concentrations on the surface of larger particles. Damle et al. (7) has also noted varying degrees of elemental enrichment with decreasing particle size and Keyser et al. (8) has also shown surface enrichment of certain elements on fly ash.

Table 5 gives major elemental concentrations for size fractionated fly ash samples for both Beulah and Big Brown ashes. The samples were collected in an Acurex high volume stack sampler which has three cyclone stages and a back-up filter. Gram size or larger samples were collected in all three cyclone stages which enabled x-ray fluorescence analysis to be performed on the size fractionated samples as well as on the bulk ash. The D₅₀ cut points of the three cyclones are 10, 3, and 1 μ m.

Looking at Table 5, it is evident that there is substantial enrichment of sodium and sulfur with decreasing particle size for the Beulah ash. For both elements, the larger particles have lower concentrations than the bulk ash while the small particles have higher concentration than the bulk ash. The sodium values for Big Brown are below the 0.5% detection limit for the x-ray fluorescence EDS analyzer; however, both NAA and SEM/microprobe analysis indicate that there is also some enrichment in sodium with decreasing particle size for Big Brown. Even for the stage 3 sample, though, the sodium oxide concentration was less than one percent. Sulfur also is enriched in the finer particles for Big Brown but even for stage 3 it makes up only 2% of the ash. Potassium is enriched in the fines for the Beulah ash while it shows no clear trend for Big Brown. Other elements that show enrichment with decreasing size for Beulah are titanium and phosphorous. For Big Brown, titanium shows no clear trend while phosphorous values are all below the 0.1% detection limit of the instrument. Iron, calcium, and magnesium are all reduced in concentration by more than 50% with decreasing particle size for Beulah while they show no clear trend for Big Brown. Silica is somewhat depleted in the fines for both the Beulah and Big Brown ashes. Aluminum on the other hand is somewhat enriched in the fines for Big Brown while it remains fairly constant for Beulah.

Clearly there are different enrichment or depletion trends with decreasing particle size for these two ashes. Of special interest is sodium since it appears to have the strongest individual effect on penetration for these tests. The mechanism by which this occurs is still unclear but the fact that sodium is substantially enriched in the fines

would indicate that it may play an important role in fine particle formation and particle surface morphology (more will be said about this in later sections). Sulfur is another element that may be important in fine particle formation since it is enriched by more than 300% in the fines. Even though there was a much weaker correlation between penetration and sulfur, it is one of the major differences between the Beulah and Big Brown ashes and may be part of the explanation for the gross differences in collection efficiency.

COAL MINERALOGY

The physical and chemical properties of the fly ash will be determined by distribution of inorganic material in the coal, the minerals present along with their particle size, and the time-temperature effect of combustion. It is useful, therefore, to attempt to identify major mineral components of the coals and the association of inorganic materials. Several methods have been employed at UNDERC to identify the forms that inorganic material is present in low-rank coals. One method is to separate denser mineral fractions from the bulk coal using float-sink techniques with high specific gravity liquids. Subsequent analysis of the sink fraction by x-ray diffraction and x-ray fluorescence identifies which minerals and elements are present in this denser part of the coal. Table 6 gives the analysis of the sink fractions for Beulah and Big Brown. The Beulah sink fraction has highest concentrations of iron, silicon, and sulfur. Iron is present as pyrite; silicon is present as quartz, kaolinite, and plagioclase, and sulfur is present as pyrite and gypsum. The Big Brown sink fraction has highest concentrations of silicon and aluminum which are present in the mineral forms of quartz and kaolinite. The primary difference appears to be the much higher iron content (pyrite) in the Beulah sink fraction and the higher silica and alumina content (quartz and kaolinite) in the Big Brown sink fraction. One other interesting difference in the two sink fractions is with sodium. The Beulah sink fraction has a very low sodium concentration compared to the Beulah fly ash, while the Big Brown sink fraction has a higher sodium concentration than Big Brown fly ash. This implies that the sodium in Beulah is associated primarily with the low density organic phases and in Big Brown with the denser mineral phases.

Another method which gives information on the distribution of inorganic material in coal is chemical fractionation, a technique in which sequential extractions of the coal are performed using 1M ammonium acetate and 1M HCl. The first solution removes ion-exchangeable cations and soluble salts; the second solution dissolves carbonates and acid soluble oxides. Unaffected pyrite and silicates remain in the solid residue. Chemical fractionation of Beulah-Zap and Wilcox group lignites reveal the Beulah-Zap lignite to have relatively more of its calcium in unextractable form, presumably calcium aluminosilicates such as plagioclase. By contrast, relatively more of the iron minerals in Beulah-Zap lignite are found in acid soluble species. However, the fuels are alike in having almost all of the sodium in ion-exchangeable form. For Beulah, over 60% of the total ash was removed by the ion exchange reagent NH_4Atc ; for the

TABLE 6

COMPOSITIONAL DIFFERENCES BETWEEN CCl_4 SINK FRACTIONS OF BEULAH,
NORTH DAKOTA, LIGNITE AND BIG BROWN, TEXAS, LIGNITE

Chemical Analysis	<u>Beulah</u>		<u>Big Brown</u>	
	Sink Fraction	Fly Ash	Sink Fraction	Fly Ash
SiO_2	29	26	68	54
Al_2O_3	8	12	20	18
Fe_2O_3	33	11	3	7
TiO_2	1	1	0.9	1.6
P_2O_5	0.7	0.5	0	0
CaO	6	18	0.8	15
MgO	0.3	4	0	3
Na_2O	0.7	14	3	0.4
K_2O	1	0.6	2	0.9
SO_3	20	13	2	1.2
<u>Mineralogical Analysis</u>				
	Quartz		Quartz	
	Kaolinite		Kaolinite	
	Pyrite		Illite	
	Calcite			
	Gypsum			
	Plagioclase			

Wilcox group lignite, only 33% was soluble. This indicates that coal from the Beulah-Zap bed has a higher percent of its ash in organically bound ion exchangeable form.

SURFACE MORPHOLOGY

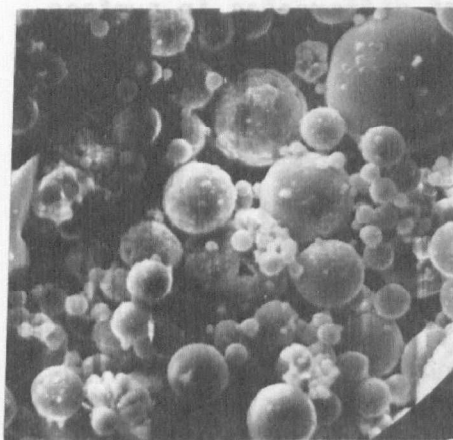
One of the ash characteristics that will likely have an effect on the ash cohesiveness, dust cake formation, and collectibility is the surface morphology of the ash. Even though fly ash from pc-fired combustion consists primarily of spherical particles, there are several different aerosol formation mechanisms which contribute to a variety of particles present. Damle (7), for example, reviewed these and Fisher (9) has defined 11 major classes of coal fly ash particles. The particles formed will depend on the elemental and mineralogical composition of the coal as well as on combustion conditions. If the chemical composition for two ashes is grossly different, one might expect some physical differences as well since some elements may form more volatile products or promote different particle formation mechanisms.

To compare surface morphology for Beulah and Big Brown ashes, SEM micrographs were taken of size fractionated multicyclone samples from the baghouse inlet as well as of cascade impactor deposits from the baghouse outlet. Figure 3 compares stage 1 SASS train cyclone samples which have aerodynamic diameters $\geq 10 \mu\text{m}$. For both ashes there are mostly spherical particles with some irregular shapes. The major difference is the large amount of surface deposits on the Beulah ash while the Big Brown particles are relatively free from surface deposits. Examination of micrographs from later multicyclone stages and of impactor plates (not shown here) reveals that this difference holds true for particles down to about $2 \mu\text{m}$ in size. For smaller particles, there appears to be another difference between these two ashes, as shown in Figure 4, which compares multicyclone backup filters for particles $\leq 1 \mu\text{m}$ in size. Here it can be seen that the Big Brown particles appear to be mainly spherical while the Beulah sample of submicron particles are generally nonspherical with cylindrical and irregular shapes. Outlet impactor samples show this same difference for particles in the size range of 0.3 to $1 \mu\text{m}$. However, impactor backup filters with particles of about 0.1 to $0.2 \mu\text{m}$ reveal that both Big Brown and Beulah particles are spherical again.

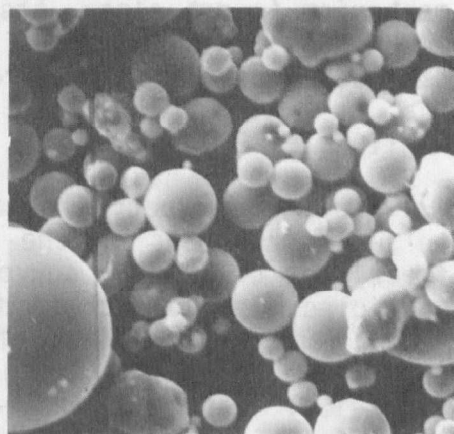
Results clearly show there are two major differences in particle morphology between Big Brown ash and Beulah ash. First, for larger particles in the range of 2 to $20 \mu\text{m}$, there are surface deposits on the Beulah fly ash which are noticeably absent in Big Brown ash. This results in a rough surface texture for the Beulah ash compared to a very smooth surface for Big Brown. Second, for particles in the size range of 0.3 to $1 \mu\text{m}$, the Beulah ash consists of largely nonspherical and irregular shapes while the Big Brown ash consists of spherical particles. Since the rough surface texture is noted with the ash that is easily collected, one can speculate that this makes the particles more cohesive and consequently enhances particle collection. The smooth surface texture of the Big Brown ash, on the other hand, may inhibit agglomeration of particles on the fabric surface so that particles slide over one another and eventually work their way through the fabric, contributing to high emissions.

Carr and Smith (10), in their review series of Fabric Filter Technology for Utility Coal-Fired Power Plants, also note that fly ash from the Monticello station, which has proven to be difficult to collect, has a smooth surface texture compared to more typical fly ashes which usually have surface deposits. The Monticello station burns a Wilcox group Texas lignite which is similar to the Big Brown Wilcox group lignite burned in our pilot plant tests.

The explanation for the differences in surface morphology is not clear but one can speculate that the much higher concentration of sodium and sulfur, especially in finer particles, promotes surface deposition on the larger particles. The particle size distribution of the Beulah ash reveals that there are more fine particles available for surface deposition on larger ones. Another explanation may be that the finer particles that are present in the Big Brown ash are less cohesive and do not stick to the larger ones like the Beulah particles. Even though the




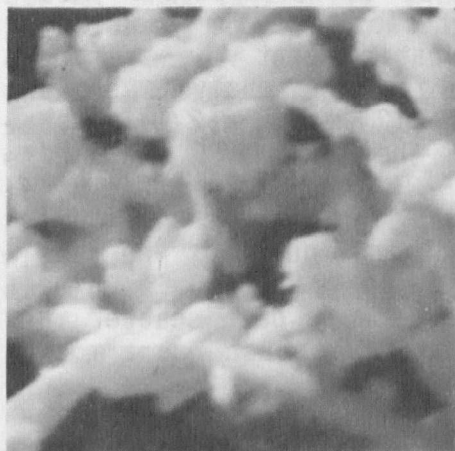
BEULAH



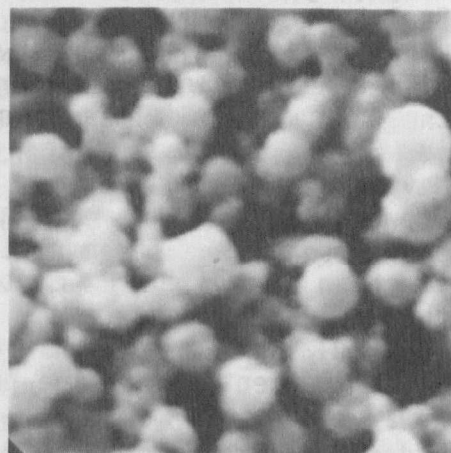
BIG BROWN

Figure 3. Fly ash from sass train cyclone 1 samples.

1000 X  10 μ M

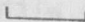


BEULAH



BIG BROWN

Figure 4. Fly ash from multicyclone backup filters.

10,000 X  1 μ M

mechanism is not clear, these results indicate that differences in surface morphology may be part of the explanation for the large difference in baghouse penetration test results for these two ashes.

PARTICLE SIZE DISTRIBUTION

One would expect the particle size distribution (PSD) of the fly ash to have an effect on the penetration characteristics of the ash, since fractional efficiency curves for fabric filters in general show that fine particles are collected with a lower efficiency than larger particles (10). The total effect of PSD on collection efficiency is difficult to determine, however, since other parameters such as ash composition, electrical effects, and ash cohesiveness may also affect collection efficiency. Frazer and Davis (11) showed that when precleaners were installed ahead of a glass fabric filter the collection efficiency was significantly reduced indicating that a finer PSD was more difficult to collect. Their tests using redispersed fly ash in air demonstrate the dramatic effect PSD can have on collection efficiency for a given ash.

Stack PSD measurements for Big Brown and Beulah ash were done using SASS train multicyclones, SoRI and Flow Sensor multicyclones, and University of Washington Mark III impactors. Coulter Counter analyses of bulk baghouse ash were also completed. Figure 5 gives a comparison of the aerodynamic PSD for Beulah and Big Brown ashes. For Beulah ash both multicyclone and impactor data are included since there was good agreement between them. For Big Brown, however, only the multicyclone data is shown since the impactor data indicated a large amount of particle bounce or reintrainment of the deposits. The impactor results demonstrate another observed difference between these two ashes - that Big Brown ash appears to be more subject to particle bounce in an impactor than Beulah ash. Comparing the PSD for the two ashes in Figure 5, it is apparent that Beulah has a much higher mass percent of particles $< 3 \mu\text{m}$ than Big Brown. At $10 \mu\text{m}$, the two plots converge indicating that the primary difference is with the finer particles. Coulter counter analysis shows the mass median diameter (mmd) for Big Brown to be $12 \mu\text{m}$ ($\sigma_g = 2.1$) which is close to $11 \mu\text{m}$ ($\sigma_g = 2.4$) for Beulah. The geometric standard deviation, σ_g , however, is noticeably different. The smaller σ_g for Big Brown indicates a more narrow distribution than for Beulah. This is confirmed by the steeper slope of the Big Brown PSD in Figure 5. The mass fraction less than $1 \mu\text{m}$ for the Big Brown ash is from 0.2 to 0.5% while the Beulah ash is from 1.5 to 6%. Although there is more data scatter in the Beulah PSD plot, the results clearly show that Beulah ash has a much higher percentage of fine particles than Big Brown.

In this case, the ash with a larger percent of fine particles was collected with a much higher efficiency than the ash with fewer fines. This is contrary to what one might expect; however, the composition of the finer particles may also be important. If, for example, the finer particles were more "sticky" or cohesive than the bulk of the particulate matter, the presence of more fine particles could enhance collection efficiency. This may be the case with the Beulah ash. The micrographs of

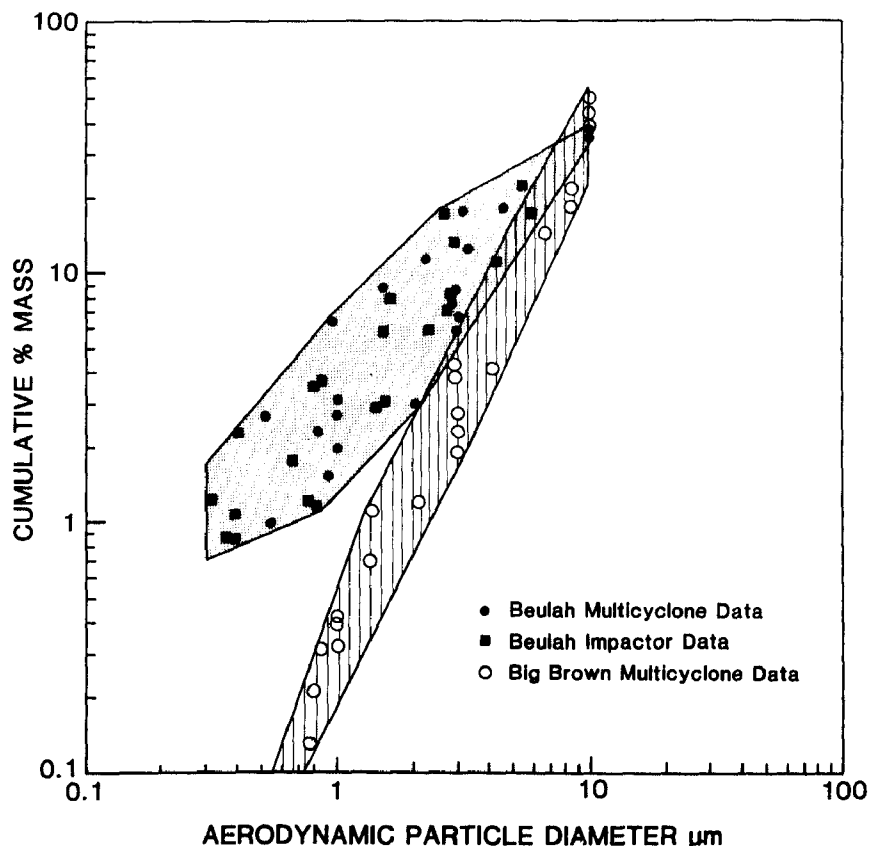


Figure 5. Particle size distribution for Beulah and Big Brown fly ash.

Beulah ash indicates that larger particles are coated with finer particles. Composition data as a function of size shows that both sodium and sulfur are enhanced significantly in the finer particles for Beulah ash. Higher concentrations of these two elements (either combined or separately) in the finer particles may make this ash more cohesive and easier to collect in a fabric filter. Particle size distributions previously reported (1) for other ashes show that there is a wide range of PSD's among the coals forming easily collected ash as well as the coals with difficult to collect ash. This indicates that the explanation for differences in ash collectibility is more complex than PSD alone.

ASH COHESIVENESS

The adhesive and cohesive nature of the ash is also important in fabric filtration. Initially, in starting with a new fabric, ash particles must adhere to the fabric fibers and build up on the fabric in such a way that larger openings in the fabric structure (such as occur in woven glass fabrics) are bridged over resulting in reduced particle penetration through the fabric. Once a dust cake is heavy enough to cause

high pressure drop, the fabric must be cleaned by reverse air, pulse jet, or mechanical shaking. It is desirable, especially for woven fabrics, to operate a cleaning cycle so that enough of the dust cake is removed to lower the pressure drop, but not too much to cause a serious decrease in removal efficiency. In other words, the cleaning cycle should be optimized to maintain an adequate residual dust cake which in turn is dependent on the adhesive and cohesive nature of the ash. Tests with Beulah, North Dakota, lignite show that high-removal efficiencies of 99.9+% can be achieved in a few hours from starting with new fabric, indicating that only a very light residual dust cake is necessary for this ash. Apparently the adhesive/cohesive nature of this ash gives it excellent filtration properties. Tests of coals with difficult to collect ashes indicate that an adequate residual dust cake is not maintained with the same cleaning cycle as the Beulah tests. One longer test showed that this did not improve even after 100 hours of operation. This indicates that the adhesive/cohesive nature of difficult to collect ash is very different. We have also observed that the Big Brown ash will not adhere well to a glass dust loading filter, indicating a lack of adhesion between the glass filter and the dust cake. One of the problems in trying to study the adhesive/cohesive properties of the ash, however, is the lack of a standard measuring technique. It would be desirable to measure quantitatively the cohesiveness of fly ash in the laboratory and determine the correlation with observed differences in particle emissions from a fabric filter. Smith (12) reported the development of a device to determine the relative shear strength of ash as a measure of cohesiveness. Preliminary tests, with this device, however, were not as sensitive or reproducible as desired.

To quantify ash cohesiveness, we have taken a somewhat different approach. The method involves forming a disc shaped ash pellet (30 mm diameter by 5 mm in thickness) in a high pressure press and then applying a force to the center of the pellet as it is supported at the edge. The force required to break the pellet is a measure of the pellet strength which we believe to be dependent on the ash cohesiveness. Preliminary results indicate that the test is quite reproducible for a given ash. Tests with Beulah and Big Brown reveal that Beulah ash forms pellets which are about ten times stronger than Big Brown ash indicating that the Beulah ash is much more cohesive. Strength tests were completed on 16 different ashes and the results were compared with baghouse penetration to check for significant correlations. The strongest correlation was again of the form $y = ax^b$ with a R^2 value of 0.57 with the more cohesive ashes having lower penetration values. The amount of data scatter, however, would indicate there are other factors that influence penetration or that the method is not accurate enough to detect small differences in cohesiveness which may influence penetration. These early results are encouraging and suggest that a laboratory test such as this could be useful in predicting dust cake behavior on a filter bag.

CONCLUSIONS AND RECOMMENDATIONS

Results clearly show that baghouse emissions are highly coal specific for the woven glass fabric, A/C, and cleaning cycle tested. Furthermore, there is a strong correlation between elemental fly ash composition and penetration with sodium exhibiting the best correlation for an individual element. Additional tests with several fabrics and three different cleaning modes confirm that the Big Brown ash is much more difficult to collect in a fabric filter than Beulah ash. A detailed comparison of the Big Brown and Beulah ashes revealed that the Beulah ash is much higher in sodium and SO_3 - especially in the finer particles. There are indications that these differences contribute to the smooth surface of Big Brown ash particles compared to the rough textured surface for Beulah ash. Particle size distributions reveal the Beulah ash to have higher concentrations of particles $< 3 \mu\text{m}$ indicating that an ash with more fine particles is not always more difficult to collect. The difference in ash collectibility for these two ashes apparently cannot be explained by differing particle sizes alone. Laboratory testing of ash pellets indicate that the Beulah ash is much more cohesive than Big Brown ash. Only a very light residual dust cake is necessary to achieve high removal efficiency for Beulah Ash. It would appear that the smooth surface texture for Big Brown makes this ash less cohesive and more difficult to collect on a fabric filter. The surface morphology and cohesiveness of the ash are likely to be affected by the particle size distribution and elemental composition of the ash.

One ash characteristic that has not been addressed by this study is electrical effects. The role of electrical effects in conventional fabric filtration has not been established but studies with electrostatic stimulation of fabric filtration show that electrostatics can have significant effects. Ash resistivity and particle charge may, for example, be part of the explanation for differences in baghouse penetration. It is recommended that future studies relating fabric filter performance to coal specific ash characteristics include an evaluation of electrical effects. Other items that remain unanswered by this study include the question of how sensitive these coal specific effects are to air/cloth ratio and cleaning cycle. It is also not known if low ratio reverse gas baghouses with heavy residual dust cake will demonstrate this coal specific behavior. It is known that low ratio reverse air baghouses can achieve high removal efficiency of low sodium ashes but the optimum weight for the residual dust cake has not been determined.

This study clearly shows that fly ash properties can have significant effects on fabric filter performance, but there is a need for a better understanding of particle formation mechanisms and dust cake properties so that fabric filters can be optimized for each specific coal.

REFERENCES

1. Sears, D.R. and Miller, S.J. Impact of fly ash composition upon shaker baghouse efficiency. Paper 84-56.6 presented at the 77th Annual Meeting of the Air Pollution Control Association, San Francisco, California, June 24-29, 1984.
2. Ladd, K.L., Chambers, R.L., Plunk, D.C., and Kunka, S.L. Fabric filter system study: second annual report. EPA 600/7-818-037. U.S. Environmental Protection Agency, Research Triangle Park, North Carolina, 1981, 104 pp.
3. Piulle, W., Carr, R., and Goldbrunner, P. 1983 Update, operating history and current status of fabric filters in the utility industry. In: Proceedings of the Second Conference on Fabric Filter Technology for Coal Fired Power Plants. EPRI CS-3257, Palo Alto, California, 1983, p. 1-1.
4. McIlvane Co., Fabric Filter Newsletter, No. 91:3, 1983.
5. Carr, R.C. and Smith, W.B. Fabric filter technology for utility coal-fired power plants, part III: performance of full scale utility baghouses. Journal of the Air Pollution Control Association. 34:281, 1984.
6. Benson, S.A., Rindt, D.K., Montgomery, G.G., and Sears, D.R. Microanalytical characterization of North Dakota fly ash. Industrial Engineering Chemistry Product Research and Development. 23:252, 1984.
7. Damle, A.S., Ensor, D.S., and Rande, M.B. Coal combustion aerosol formation mechanisms: a review. Aerosol Science and Technology. 1:119, 1982.
8. Keyser, T.R., Natusch, D.F.S., Evans, C.A., and Linton, R.W. Characterizing the surfaces of environmental particles. Environmental Science and Technology. 12:768, 1978.
9. Fisher, G.L., Prentice, B.A., Silbermen, D., Ondov, J.M., Biermenn, A.H., Fagani, R.C., and McFarland, A.R. Physical and morphological studies of size-classified coal fly ash. Environmental Science and Technology. 12:447, 1978.
10. Carr, R.C. and Smith, W.B. Fabric filter technology for coal fired power plants, part IV: pilot-scale and laboratory studies of fabric filter technology for utility applications. Journal of the Air Pollution Control Association. 34:399, 1984.

11. Frazier, W.F. and Davis, W.T. Effects of fly ash size distribution on the performance of a fiberglass filter. In: Proceedings of the Third Symposium on the Transfer and Utilization of Particulate Control Technology, U.S. Environmental Protection Agency, Research Triangle Park, North Carolina, 1981.
12. Smith, W.B., Felix, L.G., and Steele, W.J. Analysis and interpretation of fabric filter performance. In: Proceedings of the Second Conference on Fabric Filter Technology for Coal Fired Power Plants. EPRI CS-3257, Palo Alto, California, 1983, p. 19-1.

TOP INLET BAGHOUSE EVALUATION AT PILOT SCALE

Gary P. Greiner* and Dale A. Furlong
ETS, Inc.
3140 Chaparral Drive, S.W., Suite C-103
Roanoke, VA 24018-4394

Paper Not Cleared for Publication

DEVELOPMENT OF WOVEN-ELECTRODE FABRIC AND PRELIMINARY ECONOMICS
FOR FULL-SCALE OPERATION OF ELECTROSTATIC FABRIC FILTRATION

James J. Spivey
Research Triangle Institute
Research Triangle Park, NC 27709

Richard L. Chambers
Southwestern Public Service Company
Amarillo, TX 79170

Dale L. Harmon
Industrial Environmental Research Laboratory
U.S. Environmental Protection Agency
Research Triangle Park, NC 27711

ABSTRACT

The Research Triangle Institute (RTI) has undertaken a project for Southwestern Public Service (SPS) to design and fabricate electrostatic fabric filtration (ESFF) hardware and to work with vendors in the development of an ESFF system. The purpose of this project was to determine the technical feasibility of ESFF on a large scale.

This project represents two first-ever achievements: the first application of ESFF to a commercial-size fabric filter bag, and the first demonstration of a woven-in electrode fiberglass filtration fabric for ESFF of this scale.

Material for the fiberglass fabric filter bags was woven by J.P. Stevens (Greenville, SC). This material contained fine woven-in stainless steel electrodes. The design and weaving of this type of fabric was considered essential to the ultimate commercial viability of ESFF. The woven-electrode fabric is 16-oz/yd²* Teflon-coated J.P. Stevens pattern 648 with electrodes on 0.79 in. centers. Six bags that were made from this material by Menardi Southern Corporation (Torrance, CA) have been in operation since start-up in May 1983.

ESFF bags have consistently shown a 40-percent reduction in operating pressure drop relative to the experimental control bags (identical to the woven-electrode bags in every respect except that they do not contain the electrodes) at air/cloth ratios of 2.0 to 4.0 ft/min. Importantly, the

*Readers more familiar with metric units are asked to use the conversion factors shown in Section 5.0.

ESFF filter bags have demonstrated the ability to operate at a stable pressure drop at air/cloth ratios of up to 4.0 ft/min. This compares to typical design air/cloth ratios of about 1.6 ft/min. Additionally, there has been no indication of premature fabric wear for these bags.

The economic implications of this reduced pressure drop are significant. A sample calculation for a 550-MW boiler producing 2.2×10^6 acfm of flue gas shows that, while the total capital cost of a new conventional reverse-air baghouse designed at a gross air/cloth ratio of 1.56 ft/min is \$35.5 million (\$64.54/kW), the total capital cost for an ESFF baghouse operating at the demonstrated air/cloth ratio of 3.4 ft/min, corresponding to an average pressure drop of 4.0 in. H₂O, is \$20.9 million (\$38.00/kW). Also, the total annual cost is less for the ESFF system at these air/cloth ratios--\$4.31 million (\$7.84/kW) versus \$6.95 million (\$12.64/kW). It is also important to note that ESFF can be applied to an existing baghouse as a retrofit to reduce excessively high pressure drop. This is especially important where space for additional baghouse compartments may be limited. The total capital cost for the retrofit installation of ESFF to a 550-MW boiler producing 2.2×10^6 acfm of flue gas is estimated to be \$3.12 million (\$5.68/kW) with a total annual cost of \$1.74 million (\$3.16/kW). In many cases, this is less than the cost of alternative means of reducing the average pressure drop by approximately 40 percent as demonstrated in tests to date.

This project began on May 12, 1982. Installation and start-up of the reverse-air ESFF system occurred on May 12, 1983. Six ESFF woven electrode and six non-electric bags (identical to the ESFF bags with the exception of the woven electrodes) were installed in each of two parallel compartments of the pilot unit. The ESFF woven-electrode and non-electric bags were still in operation as of August 1984.

This paper has been reviewed in accordance with the U.S. Environmental Protection Agency's peer and administrative review policies and approved for presentation and publication.

1.0 INTRODUCTION

The use of fabric filters to remove particles from gas streams is a well-established industrial practice and is currently the most cost-effective particulate control device for many coal-fired electric utilities. The imposition of standards for particulate emissions has forced these utilities to install devices to remove fly ash from their flue gas.

Electrostatic fabric filtration (ESFF) consists of applying a nonionizing electrostatic field at the fabric/dirty-gas interface. The residual and operating pressure drops are reduced with apparently no loss in collection efficiency. Previous laboratory- and pilot-scale studies have consistently demonstrated this reduced pressure drop.

The original concept of ESFF was developed by Lamb and Costanza (1977) of Textile Research Institute (TRI) (1). Continuing extramural

research under the sponsorship of the U.S. Environmental Protection Agency (EPA) has encompassed:

- Laboratory experiments at TRI and RTI to develop a more basic understanding of the fundamental mechanisms of ESFF.
- Pilot studies of pulse-jet and, to a much smaller degree, reverse-air ESFF applied to an industrial boiler at a du Pont facility in Waynesboro, Virginia.

In addition, EPA has continued in-house research on ESFF at the laboratory- and small pilot-unit scale.

As a logical extension of previous work, the application of ESFF to a full-scale electrical utility was undertaken. The purpose of the project at SPS was to demonstrate the technical feasibility of the commercial-scale application of ESFF to a coal-fired electric utility flue gas that was being cleaned by reverse-air fabric filtration. The pilot baghouse facility at SPS utilizes bags of the same dimensions as the main unit. SPS experience has shown that results from its pilot unit are generally directly related to full-unit performance.

The scope of the project included:

- Design, construction, and installation of an electrical hardware system to supply and control the electrical power to the reverse-air fabric filter bags.
- Coordinating and directing the work of vendors (Menardi Southern, Bekaert, and J.P. Stevens) to develop ESFF fabric filter bags with woven-in electrodes.
- Assistance in the start-up and operation of the electrostatic fabric filtration (ESFF) system including onsite troubleshooting, preparation of operation manuals, and assistance in test planning and interpretation of results.

2.0 ESFF SYSTEM FOR SPS

2.1 GENERAL SITE DESCRIPTION

Southwestern Public Service's Harrington Station is a nominal 1,080-MW pulverized-coal-fired electrical generating station consisting of three 360-MW boiler units. The pilot fabric filter test facility is located on Unit 2.

The coal used at Harrington is a low-sulfur (about 0.4 wt%) Powder River Basin western coal mined at Gillette, WY, and transported by rail to the Harrington Station. A Wheelabrator-Frye baghouse is located on the flue gas stream of Unit 2 and consists of 28 compartments, each of which contains 204 filter bags. Each fabric filter bag is approximately 30 ft 9 in. long

and 11.5 in. in diameter at 60 lb tension. The main baghouse cleans by shake/deflate and operates at a nominal air/cloth ratio of 3.4 ft/min. Nominal dust loading of this flue gas is about 2.0 gr/scf. However, the air/cloth ratio and dust loading vary with boiler load.

2.2 PILOT TEST FACILITY

The pilot test facility is located on a slipstream from the flue gas going to the main baghouse. A schematic flow diagram is given by Ladd et al. (2) and is shown in Figure 1.

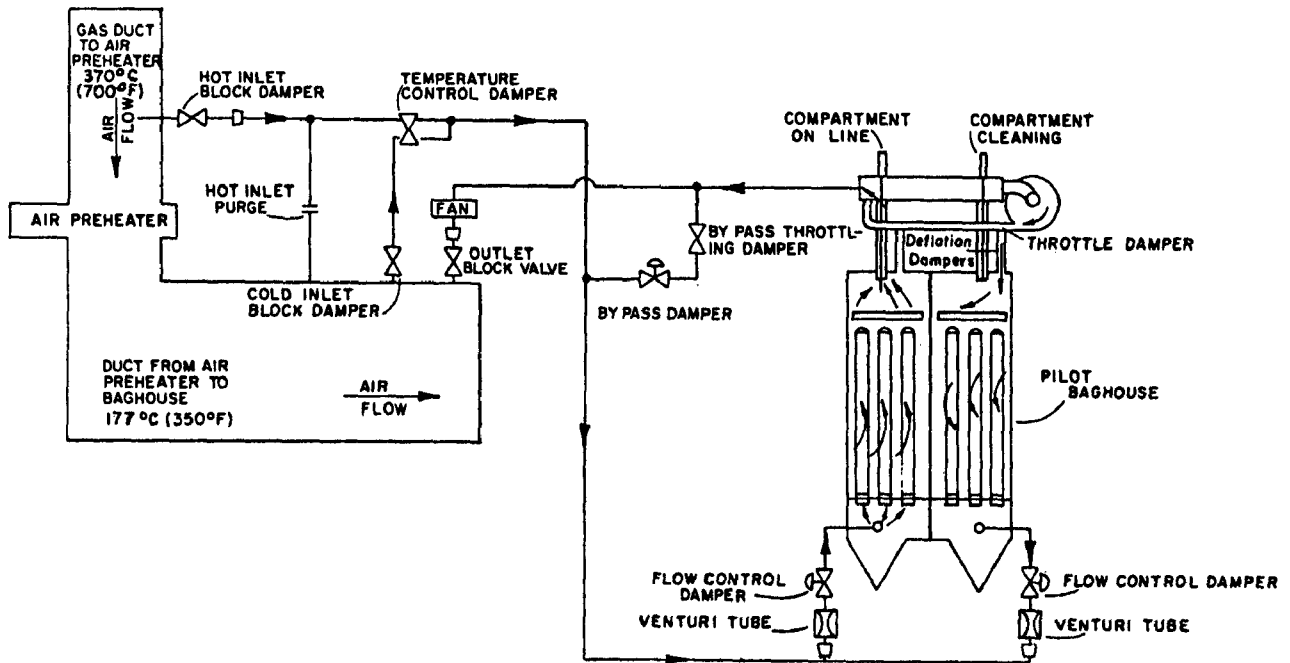


Figure 1. Schematic of Southwestern Public Service pilot fabric filter unit.

The pilot unit at SPS was modified slightly to accommodate the installation of the ESFF electrical hardware and voltage control system. The system was designed based on typical operating voltages for the ESFF system of -5 to -6 kV and a total power consumption of about 0.1 W/ft² of filter surface area. A significant portion of the electrical design involved safety interlock systems to ensure that maintenance and operating personnel are not exposed to high voltage. The ESFF electrical system for this project was designed and custom-fabricated by RTI from off-the-shelf components.

2.3 DESIGN OF FILTER BAGS

There are three basic cleaning mechanisms for fabric filters: reverse air, pulse jet, and shake/deflate. Since the ESFF concept has been proven in other studies for pulse-jet and reverse-air cleaning at a somewhat smaller scale, and since most electric utilities have installed baghouses using this

cleaning method (3), reverse air cleaning was chosen for this ESFF application. In addition, the choice of reverse air reflects concern that shake/deflate cleaning would cause premature fabric failure due to abrasion between the woven-in electrodes and the fiberglass fabric.

This choice of cleaning method had important consequences for the design of the electrical hardware, the design of the filter bag, and the method of producing the electrostatic field at the fabric interface. A reverse-air ESFF bag with integral (woven-in) electrodes had not been fabricated prior to this project but was considered essential to demonstrate the applicability of ESFF on a commercial scale. Other conceivable configurations, including cylindrical rigid conducting cages located outside conventional bags, were considered. At SPS's suggestion, the woven-electrode fabric was considered preferable since it would be much more easily adapted to commercial baghouses. Design and construction considerations for the woven-electrode bag included that the bag should:

- Be made of fabric woven on conventional looms.
- Be sewn on conventional equipment.
- Use nonconductive anticollapse rings.
- Incorporate suitable electrical connectors and buses.
- Be easily installed in the field.
- Have an adequate service life.

After considering the various options available within the constraints of this project, it was decided that a J.P. Stevens 648 fiberglass fabric with Bekaert VN22/1x90 stainless steel electrodes located on 0.8 in. centers would be used to make the reverse-air fabric filter bag. Reasons for the choice of this fabric, electrode, and construction pattern include:

- J.P. Stevens 648 fabric is the only commercially available fiberglass filtration fabric that has texturized warp yarns. Weaving a metal electrode into a fiberglass fabric resulted in pinholes during early weaving test runs prior to this program. It was important to ensure that these pinholes, where penetration of particulates during filtration occurred, were minimized or eliminated. This was accomplished by "piggybacking" the stainless steel electrode with the texturized warp yarn. This also required an electrode small enough to fit into the same space in the loom as the texturized warp yarn (this space is called a "dent").
- Bekaert VN 22/1x90 was the smallest flexible stainless steel yarn that could be made by the vendors contacted. This yarn is not a stock item and required a special production run. It consists of 90 ends, each 22 μ m in diameter with single-ply construction. Stainless steel was chosen as the material of construction to minimize any acid corrosion problems.

- The electrodes were spaced on 0.8 in. centers as a tradeoff between high potential requirements and arcing. If the electrodes are spaced too far apart, the high electrical potentials needed to develop adequate electrical field strengths in the interelectrode region (5 to 10 kV/in.) create electrical fields above the corona onset at the steel filament surface. If the electrodes are too close together, electrical arcing between the electrode filaments becomes a problem. An electrode spacing of 0.79 in. was selected as an appropriate compromise between these two undesirable conditions.

Approximately 200 yd of woven-electrode fabric with a width of 38.5 in. was woven by J.P. Stevens. Figure 2 shows a magnified view of the fabric.

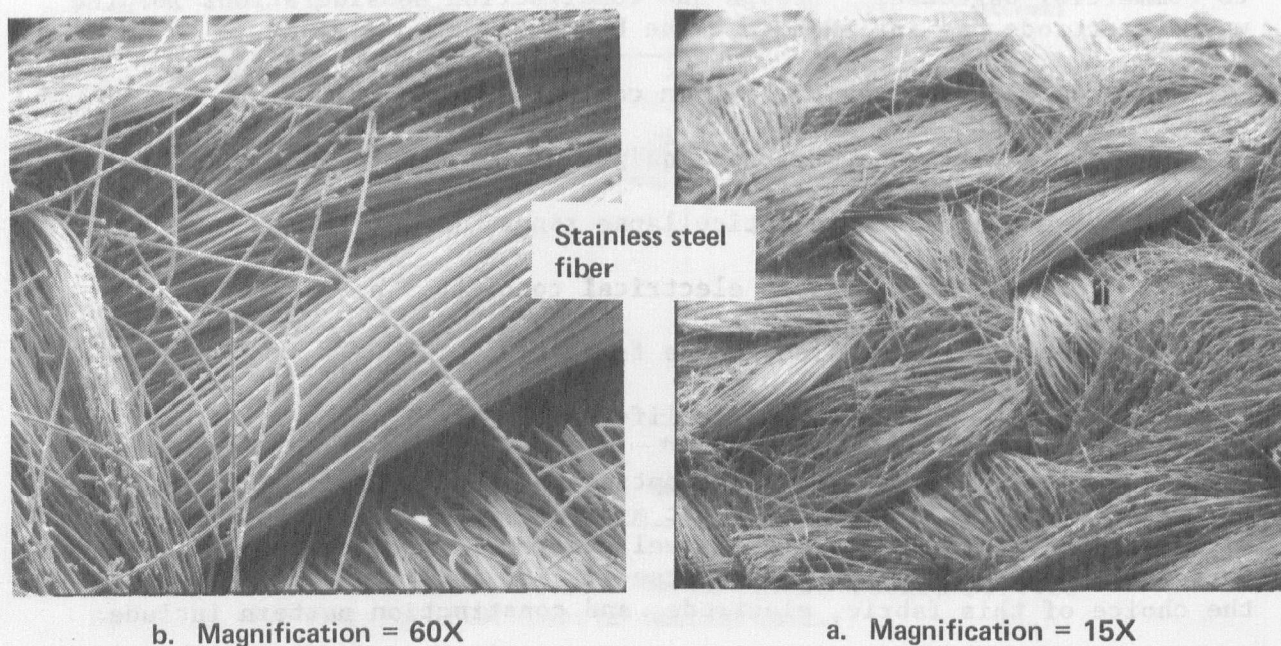


Figure 2. Woven-electrode fabric showing stainless steel fiber electrode.

Although great care was used in making the woven-electrode fabric, defects in the woven electrodes were present in the fabric as it came off the loom. Figure 3 shows photographs of typical defects. These defects were corrected by hand at the fabric plant prior to shipping the fabric to the bag manufacturer.

2.4 BAG CONSTRUCTION AND TESTING

The fabric was made into filter bags at Menardi Southern Corporation in Torrance, CA. A total of 16 bags were constructed as shown in Figure 4. The purpose of the attached cuff was to ensure that there was no electrical contact between the woven electrodes and the metallic thimbles to which the bag is attached.

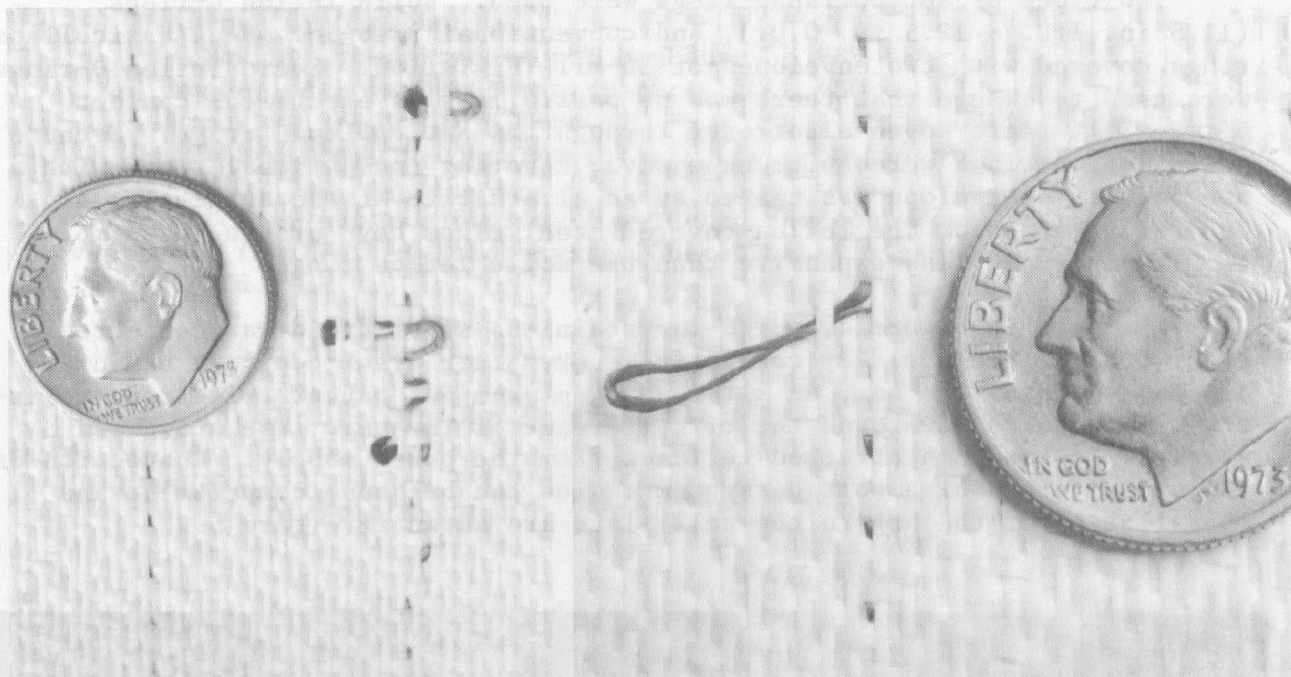


Figure 3. Typical woven-electrode fabric weaving defects.

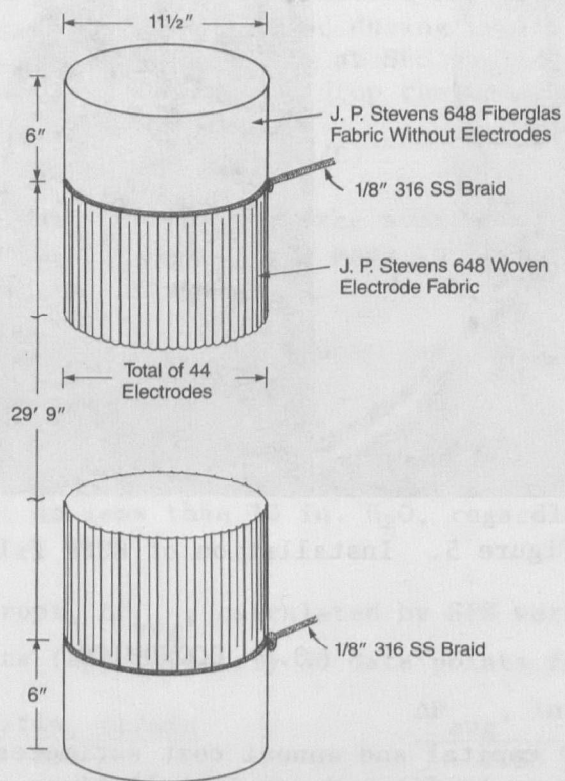


Figure 4. Construction of the woven-electrode bags.

Two types of anticollapse rings were used: solid Teflon O-rings (11.5 in. I.D. \times 12.5 in. O.D.), and conventional 3/16-in. steel anticollapse rings covered with two envelopes of 30-mil TFE Teflon. Solid Teflon O-rings were used to ensure that there was no possibility of electrical contact between alternate woven electrodes through the anticollapse rings. Because these Teflon rings were quite expensive, covering conventional rings with a nonconductive envelope was tested as an alternative at the suggestion of Menardi personnel. The Teflon-covered steel rings have proven to be more satisfactory and less expensive than the solid Teflon rings.

As shown in Figure 4, a 1/8-in. stainless steel braid was connected to every other electrode. By connecting every other electrode to a braid at opposite ends of the bag, an alternating plus-minus pattern electrode polarity was established around the circumference of the bag. The stainless steel braid was then attached to leads from the power supply. Connection of the braid to the high voltage system inside the baghouse compartment and installation of the bag to the cell plate are shown in Figure 5.

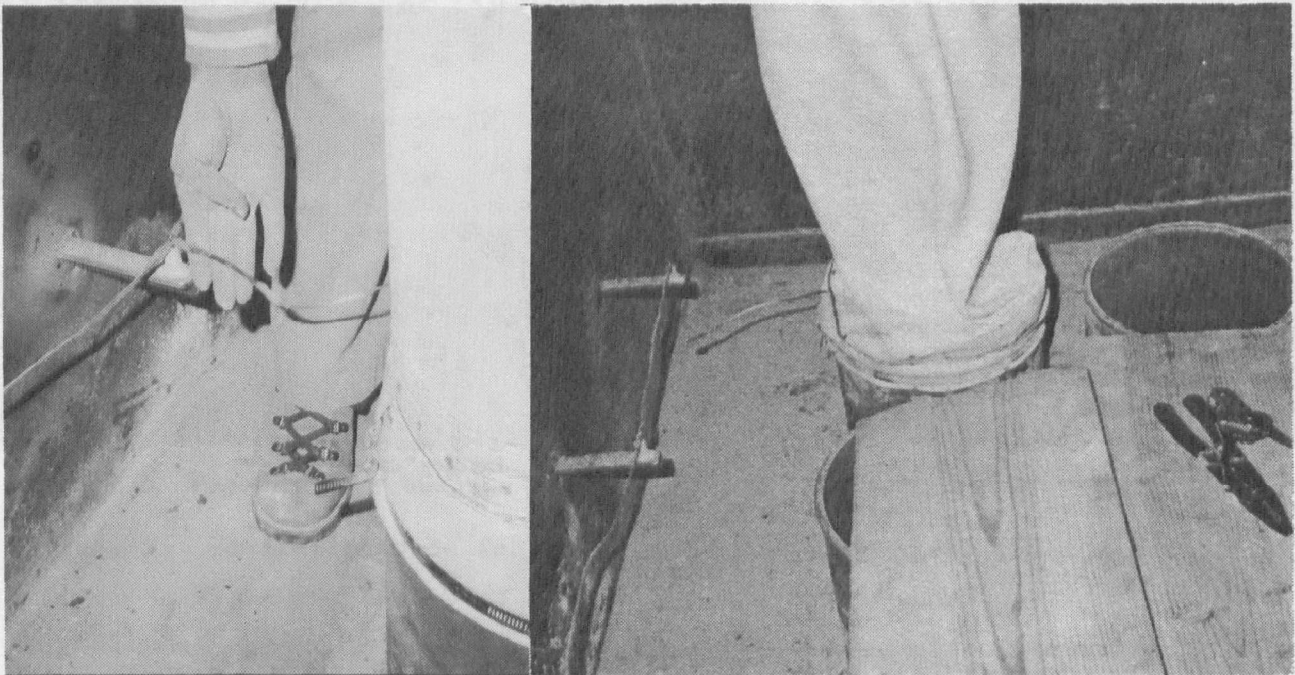


Figure 5. Installation of ESFF filter bags.

3.0 ECONOMICS

Preliminary capital and annual cost estimates (± 30 percent) have been developed for the retrofit and new installations of ESFF on a 550-MW boiler. ESFF can be applied to a baghouse either as a retrofit (to reduce pressure drop) or new (to reduce baghouse size) installation. The specific design basis for this example case is:

Gas volume	2.2×10^6 acfm/min
Number of baghouses	2
Number of compartments per baghouse	28
Number of bags per compartment	480
Bag size (diameter \times length)	11.5 in. \times 33.75 ft
Filter area per compartment	50,517 ft ²

Variable air/cloth ratios were selected for cost comparisons with a conventional fabric filtration system operating at a gross air/cloth ratio of 1.56 ft/min.

3.1 NEW COSTS

Assumptions for the cost of a new ESFF installation based on the above are:

Air/cloth ratio	2.3 ft/min
	3.1 ft/min
	4.0 ft/min
Average pressure drop	
@ 2.3 ft/min	2.0 in. H ₂ O
@ 3.1 ft/min	3.5 in. H ₂ O
@ 4.0 ft/min	5.5 in. H ₂ O

Note that the average pressure drops selected for the cost calculations are based on actual pilot plant data obtained during cyclical testing from October 25, 1983, through November 21, 1983, at SPS's pilot unit. Based on test data, the average (over time) pressure drop can be approximated as:

$$(\Delta P_{\text{avg}})_{\text{ESFF}} = 0.43 (A/C)^{1.84} \quad (1)$$

This relationship is used to calculate the average pressure drops at 2.3 and 3.1 ft/min.¹ Additional assumptions made to calculate the cost of a new ESFF installation include:

- The value of ΔP_{avg} from the pilot unit data is directly transferable to the full-scale system.
- A design pressure drop for the main ID fan, ΔP_{max} , should be 1.5 times ΔP_{avg} , but no less than 10 in. H₂O, regardless of the actual

¹Daily average pressure drops, ΔP_{avg} , calculated by SPS were averaged, with the following results (approximately 30 data points for each value):

<u>A/C ratio, ft/min</u>	<u>ΔP_{avg}, in. H₂O</u>
2.0	1.53
3.0	3.25
4.0	5.96

Equation (1) is a mathematical fit of the above three data points.

average operating pressure drop (ΔP_{avg}). This is an arbitrary value selected to be certain that the fan has adequate capacity for periods of operational problems.

Table 1 shows the input data required for the cost estimation program that is used to calculate the costs of the nonelectric and ESFF baghouses (2,3).

TABLE 1. INPUT VARIABLES FOR COST ESTIMATION

Input variable	Value chosen	Units	Basis
Cost of the ESFF bags	1.50	\$/ft ²	Assuming a cost of about \$65-\$70 for a typical 90-ft ² reverse-air bag (i.e., \$67.50/90 ft ² = \$0.75/ft ²), an ESFF bag is assumed to cost about twice as much and is based on discussions with vendors
(ΔP_{avg}) ^{ESFF}	@2.3 ft/min, 2.0 @3.1 ft/min, 3.5 @4.0 ft/min, 5.5	in. H ₂ O	Based on actual pilot plant data
(ΔP_{max}) ^{ESFF}	10	in. H ₂ O	It is assumed that, regardless of the value of ΔP_{avg} , the baghouse owner would purchase a fan of this size for periods of operational difficulty, start-up, or boiler upsets
(ΔP_{avg}) ^{nonelectric}	@2.3 ft/min, 3.4 @3.1 ft/min, 5.9 @4.0 ft/min, 9.3	in. H ₂ O	Calculated values from the period 10/25/83-11/21/83 for the SPS pilot unit
(ΔP_{max}) ^{nonelectric}	@2.3 ft/min, 10 @3.1 ft/min, 10 @4.0 ft/min, 14	in. H ₂ O	ΔP_{max} is selected as 1.5 times ΔP_{avg} , with a minimum of 10 in. H ₂ O
Bag life	For ESFF, 3 For conventional, 4	yr	Based on SPS experience
Cost of electricity	3	¢/kWh	Based on SPS experience

This program calculates capital costs in five categories:

- Collectors and supports
- Ducting and supports
- Insulation
- ID fan
- Miscellaneous (control equipment, ash handling system, etc.)

A sixth category, ESFF hardware and installation, is added whenever ESFF costs are estimated. The sum of these five (or six) items is the total field cost (TFC). To this sum are added engineering costs (20 percent TFC) and a contingency (20 percent TFC). The TFC plus engineering costs plus contingency is the total capital cost (TCC). The TCC is indexed for inflation using the Chemical Engineering Plant Cost Index (1957-9 = 100; 1983, ~310.0). The annual costs are calculated as the sum of:

- Fixed operating costs (operating labor, including fringe benefits, and supplies)
- Variable operating costs (maintenance labor and supplies including bags)
- Cost of electricity (for hopper heaters, controls, and ESFF if used).

To the sum of these three items is added:

- Annual capital cost (cost of money, estimated herein as 10 percent for 10 years, or 16.275 percent of TCC).

The total annual cost (TAC, which does not account for taxes) is then computed as the sum of the fixed and variable operating costs, cost of electricity, and annual capital cost.

For the nonelectric bags, the daily average pressure drops for the period October 25, 1983, through November 21, 1983, are:

<u>A/C ratio, ft/min</u>	<u>ΔP_{avg}, in. H₂O</u>
2.0	2.49
3.0	5.72
4.0	9.31

From these values, ΔP_{avg} can be calculated as a function of air/cloth ratio (A/C) in the same manner as for equation (1) with the following result:

$$(\Delta P_{avg})_{nonelectric} = 0.67 (A/C)^{1.91} \quad (2)$$

Note that the nonelectric bags used in this test have demonstrated a significantly lower pressure drop than typical (say, 10-oz/yd²) reverse-air filter bags now in use at, for example, the SPS--Tolk Station. A comparison

to those typical bags would be even more favorable to ESFF. For this report, since a direct comparison of ESFF and those typical bags has not been made, the performance of the nonelectric bags has been used as the experimental (and cost) control.

Equations (1) and (2) are plotted in Figure 6 to show the expected difference in performance between ESFF and nonelectric bags.

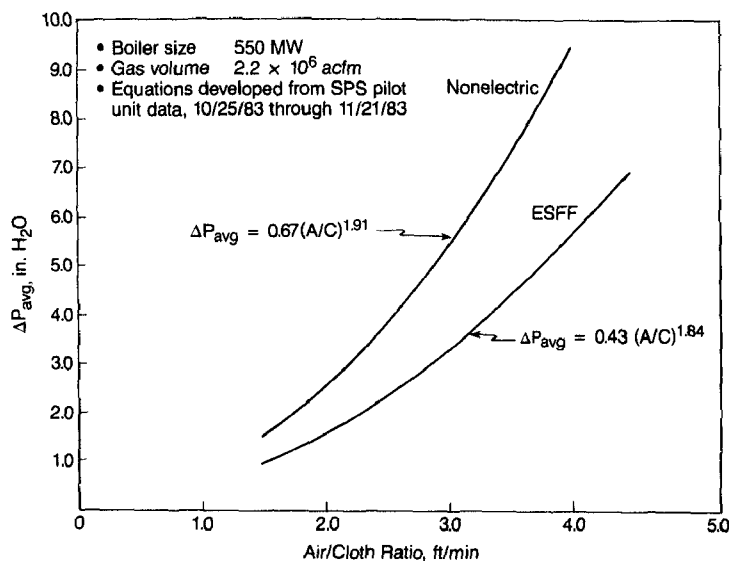


Figure 6. Daily average pressure drop versus air/cloth ratio.

Figures 7 and 8 and Table 2 show the TCC and TAC for ESFF and conventional reverse-air fabric filters applied to a 550-MW boiler, with a gas volume of 2.2×10^6 acfm and other input parameters as specified above.

The primary conclusions to be drawn from Figures 7 and 8 are:

- The total capital cost of a new ESFF installation is only slightly higher than that of a conventional system at the same air/cloth ratio.
- As expected, the total capital cost decreases dramatically with air/cloth ratio, with the most rapid decrease in cost being at the lower air/cloth ratios from about 1.6 ft/min to 2.5 ft/min.
- The total annual cost (a better comparison of the real cost of a system over time since it includes the effects of both the capital cost and all operating costs) for ESFF is higher than for a conventional system until the air/cloth ratio reaches 4.0 ft/min. At 4.0 ft/min, the total annual costs for both conventional and ESFF systems are equal at about \$3.9 million, or \$7.09/kW of capacity.
- The total electricity costs are less for ESFF than for conventional systems at all air/cloth ratios, reflecting the decreased

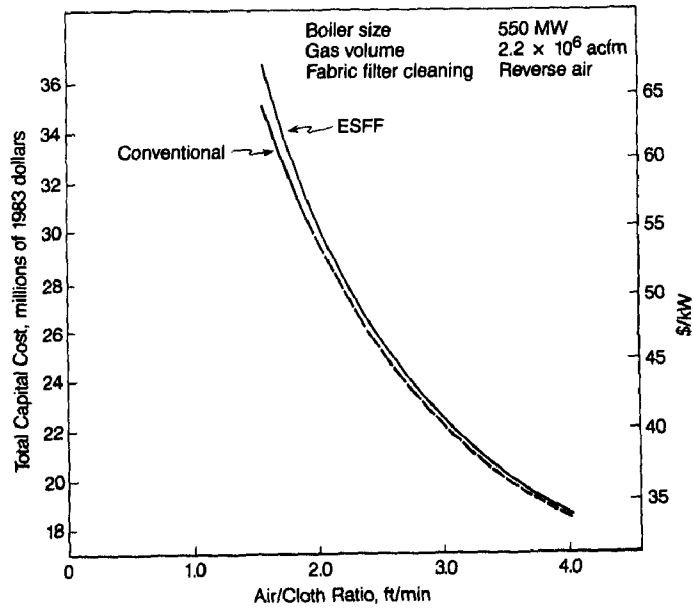


Figure 7. Total capital cost versus air/cloth ratio.

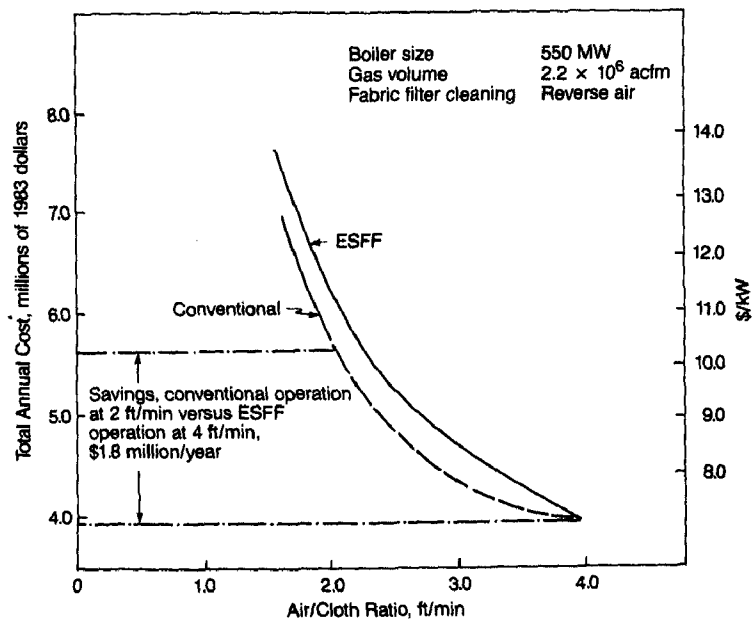


Figure 8. Total annual cost versus air/cloth ratio.

TABLE 2. SUMMARY OF COST COMPARISON OF ESFF VERSUS CONVENTIONAL
REVERSE-AIR FABRIC FILTRATION SYSTEMS

Air/cloth ratio, ft/min	Total capital cost (10 ⁶ 1983 \$)*		Total annual cost (10 ⁶ 1983 \$)*		Cost of electricity (10 ⁶ 1983 \$)†	
	ESFF	Conventional	ESFF	Conventional	ESFF	Conventional
1.56	36.4	35.5	7.50	6.45	0.48	0.67
2.3	27.4	26.8	5.51	5.07	0.26	0.33
3.1	21.8	21.3	4.47	4.21	0.31	0.42
4.0	18.6	18.5	3.92	3.88	0.39	0.58

* Calculated using a Chemical Engineering Plant Cost Index (CEPCI) of 310.0. To escalate to another time period, simply multiply the indicated numbers by the ratio of the CEPCI for another time period divided by 310.0.

† Calculated at 3¢/kWh.

pressure drop for ESFF operation. One interesting observation is the minimum in total electrical costs for both ESFF and conventional systems as a function of air/cloth ratio. This results from two competing effects. As the air/cloth ratio increases, the electrical costs increase due to the higher operating pressure drop. However, for a given gas flow rate (in the case of Table 2, 2.2×10^6 acfm), the number of baghouse modules decreases with increasing air/cloth ratio. This means less electricity for ash handling, hopper heaters (if required), and controls. The net result of the two competing effects is the observed minimum.

It is important to remember that ESFF reverse-air fabric systems can be operated at air/cloth ratios of at least 4.0 ft/min (and perhaps greater); whereas, conventional reverse-air systems cannot. Thus, the comparison shown in Figures 7 and 8 is only academic at air/cloth ratios above about 2.0 ft/min. In other words, Figures 7 and 8 show an imaginary comparison above about 2.0 ft/min. The most appropriate comparison to be made is between the highest air/cloth ratio at which ESFF can be operated (based on results at the SPS pilot unit, this is at least 4.0 ft/min) and the highest air/cloth ratio at which conventional reverse-air systems can be operated (about 2.0 ft/min). At 2.0 ft/min, the total annual cost for the conventional reverse-air system is about \$5.7 million (\$10.36/kW); whereas, for an ESFF system at 4.0 ft/min, the total annual cost is \$3.9 million (\$7.09/kW), a savings of 32 percent (\$3.27/kW).

3.2 RETROFIT COSTS

Assumptions made for the calculation of the retrofit installation of ESFF are:

Average pressure drop before ESFF	9.5 in. H ₂ O
Average pressure drop after ESFF	5.5 in. H ₂ O
Air/cloth ratio before and after ESFF installation (gross)	1.56 ft/min.

All other parameters are as given in Table 1 for a new installation. The values selected for the average pressure drop before and after ESFF are from Figure 6. It is assumed that the reduction in ΔP_{avg} resulting from the installation of ESFF may be approximated by finding in Figure 6 the air/cloth ratio at which ΔP_{avg} equals 9.5 in. H₂O (i.e., 4.0 ft/min) and reading down to find the corresponding ΔP_{avg} for ESFF. In the retrofit application of ESFF, the capital expenditure will be only the installed cost of the ESFF hardware itself. It is assumed that the existing fan and baghouse will remain in place.

The capital cost of the ESFF hardware can be calculated from the computer program used to develop the cost of a new ESFF system (4,5) and is found to be \$660,000. To this is added the engineering (20%) and contingency (20%) costs to obtain a total capital cost of \$924,000. For a retrofit, the cost will generally be higher than for a new installation due to limited access to space, site cleaning required, and interference with normal operations. As an estimate, it is assumed here that the retrofit cost will be 10 percent greater than the cost for a new installation (6). Thus, the total capital cost for the ESFF hardware for a baghouse as specified in Section 3.0 is (1.10)(\$924,000) or \$1,016,000 (\$1.85/kW).

To this installed hardware cost must be added the cost of the ESFF bags themselves. As discussed in Table 1, this cost is taken, somewhat arbitrarily, to be \$1.50/ft². For a baghouse flow rate of 2.2×10^6 acfm at an air/cloth ratio of 1.56 ft/min, the total filtration area is 1.41×10^6 ft², yielding a total cost for the ESFF bags of $\$2.11 \times 10^6$, or \$3.84/kW.

Thus, the total installed capital cost for the retrofit of ESFF to a 550-MW boiler is:

ESFF hardware		ESFF bags		Total	
(10 ³ \$)	(\$/kW)	(10 ³ \$)	(\$/kW)	(10 ³ \$)	(\$/kW)
1,016	1.85	2,110	3.84	3,126	5.68

The savings in operating costs with ESFF will result from the decreased pressure drop. Assuming that no additional operating labor would be needed for the ESFF, and that the bag life for the new ESFF bags (3 years) is the same as for the old conventional bags being replaced (which have a life of 4

years, and assuming they are replaced after 1 year, leaving a useful life of 3 years at that point), the total annual operating cost difference between the baghouse retrofit with ESFF and the baghouse before ESFF installation can be calculated from the difference in annual operating costs between a baghouse operating at a ΔP_{avg} of 9.5 in. H₂O (but without ESFF hardware or bags) and one operating at a ΔP_{avg} of 5.5 in. H₂O (but with the added annual costs associated with maintenance and capital recovery for the ESFF hardware and bags).

The cost program (4,5) has been executed for these two cases. The results are shown in Table 3. Note that the total electricity costs, calculated at 3¢/kWh, are \$197,000 per year less with ESFF than with continued operation at a pressure drop of 9.5 in. H₂O. However, the total annual cost is \$564,000 more for ESFF than continued high pressure drop operations. One consideration that is extremely important in evaluating the cost of an ESFF retrofit is not reflected in Table 3; i.e., if the conventional reverse-air baghouse is operating at a ΔP_{avg} of 9.5 in. H₂O, it is likely that the owner will have to undertake some capital improvement. The comparison in Table 3 is only between continued operation at 9.5 in. H₂O average pressure drop and adding ESFF. A more valid comparison would be between adding ESFF and some other expenditure designed to lower the pressure drop; (e.g., such as adding an additional conventional reverse-air compartment (which may be precluded by limited space, for example)). While it is beyond the scope of this paper to consider all the possible options, it can be said, based on Table 3, that ESFF would be less expensive than any option with a total annual cost (calculated under the same assumptions used in the cost program) of more than \$1.74 million. As a comparison, the approximate total annual cost to add enough compartments to reduce the pressure drop to 5.5 in. H₂O (equivalent to the effect of an ESFF retrofit), corresponding to an air/cloth ratio of about 3.0 ft/min (see Figure 6), is about \$2.6 million (see Figure 8).

Thus, it appears that the retrofit installation of ESFF may well result in a considerable electrical cost savings over continued operation at high pressure drop and, in addition, an ESFF retrofit may be less costly than adding conventional compartments in reducing excessive pressure drop.

4.0 SUMMARY OF RESULTS

The results of this study, in summary, are:

- Woven-electrode fiberglass fabric filter material has been woven and fabricated into commercial-scale bags. These bags have been installed and successfully operated for over 15 months with no premature failure and consistent pressure drop reduction of about 40 percent compared to the same bags without ESFF.
- The total annual cost (TAC) of installing ESFF at the demonstrated air/cloth ratio of 4.0 ft/min for a new 550-MW boiler is estimated

TABLE 3. COMPARISON OF ANNUAL COSTS BETWEEN RETROFIT ESFF AND HIGH PRESSURE DROP OPERATIONS

High pressure drop operation				Retrofit ESFF			
ΔP_{avg} , in. H ₂ O	Total elec- tricity costs* (10 ³ 1983 \$)	Annual oper- ating costs† (10 ³ 1983 \$)	Total annual cost‡	ΔP_{avg} , in. H ₂ O	Total elec- tricity costs* (10 ³ 1983 \$)	Annual oper- ating costs† (10 ³ 1983 \$)	Total annual cost‡
9.5	675	1,175	1,175	5.5	478	1,574	1,739

*Electricity costs calculated at 3¢/kWh.

†Annual operating costs include operating labor, maintenance labor and supplies, utilities (assumed to be only electricity), overhead, and insurance.

‡Total annual costs include annual operating costs plus capital recovery. For the high pressure drop operation, there are no additional capital costs; thus, the total annual cost and total operating costs are the same. For retrofit ESFF, there is a capital cost (for the ESFF hardware) of \$1,016,000 (see text). Thus, for retrofit ESFF only, there is a capital recovery cost of 16.275% (10%, 10 years) \times \$1,016,000 = \$165,000 added to the annual operating cost of \$1,574,000 for a total annual cost of \$1,739,000.

to be \$3.9 million (\$7.09/kW) with a total capital cost (TCC) of \$18.6 million (\$33.82/kW); whereas, the corresponding TAC and TCC for a conventional reverse air system operating at approximately the maximum demonstrated air/cloth ratio of 2.0 ft/min are \$5.7 million (\$10.36/kW) and \$30.0 million (\$54.55/kW), respectively, a TAC savings of 32 percent.

5.0 METRIC EQUIVALENTS

Readers more familiar with metric units may use the following to convert to that system.

<u>Non-metric</u>	<u>Times</u>	<u>Yields metric</u>
acfm	4.72×10^{-4}	am^3/s
ft	0.305	m
ft ²	9.29×10^{-2}	m ²
ft/min	5.08×10^{-3}	m/s
gr/scf	2.29	g/sm ³
in.	2.54	cm
in. H ₂ O	249	Pa
lb	0.454	kg
mil	2.54×10^{-5}	m
oz	2.83×10^{-2}	kg
oz/yd ²	3.39×10^{-2}	kg/m ²
W/ft ²	10.8	W/m ²
yd	0.914	m

6.0 REFERENCES

1. Lamb, G.E.R., and Costanza, P.A. 1977. Electrical Stimulation of Fabric Filtration. Textile Res. J., 47, May, pp. 372-80.
2. Ladd, K., Hooks, W., Kunka, S., and Harmon, D. 1982. SPS Pilot Baghouse Operation. In Vol. I, Third Symposium on the Transfer and Utilization of Particulate Control Technology, EPA-600/9-82-005a (NTIS No. PB83-149583). pp. 55-64.
3. Reynolds, J., Kreidenweis, S., and Theodore, L. Results of a Baghouse Operation and Maintenance Survey on Industry and Utility Coal-Fired Boilers. JAPCA, 33(4), April 1983. pp. 352-8.
4. Viner, A.S., and Ensor, D.S. Computer Programs for Estimating the Cost of Particulate Control Equipment. EPA-600/7-84-054 (NTIS PB84-183573). May 1984.
5. Severson, S.D., Horney, F.A., Ensor, D.S., and Markowski, G.R. Economic Evaluation of Fabric Filtration Versus Electrostatic Precipitation for Ultrahigh Particulate Collection Efficiency. Electric Power Research Institute report FP-775, June 1978.

6. Ensor, D.S., Hooper, R.G., and Scheck, R.W. Determination of the Fractional Efficiency, Opacity Characteristics, Engineering and Economic Aspects of a Fabric Filter Operating on a Utility Boiler. Electric Power Research Institute report FP-297, November 1976.

ESFF PILOT PLANT OPERATION AT HARRINGTON STATION

Richard Chambers
Southwestern Public Service Company
Amarillo, Texas 79170

James J. Spivey
Research Triangle Institute
Research Triangle Park, North Carolina 27709

Dale Harmon
Environmental Protection Agency
Research Triangle Park, North Carolina 27711

ABSTRACT

Under the direction of the Environmental Protection Agency, Southwestern Public Service (SPS) converted the pilot fabric filter system at Harrington Station to conduct electrostatic fabric filtration (ESFF) experiments. Research Triangle Institute was subcontracted by SPS to construct the ESFF power supply and to work with the vendors involved in developing a suitable ESFF fabric. As a result of this project, the first ESFF fabric with woven-in electrodes was constructed.

The results of the program to date, with the program over half-way through its original test plan, have been encouraging. The pilot has confirmed previous results obtained in small scale pilot units, in the laboratory, as well as demonstrations that indicate ESFF will work with fly ash from an operating utility boiler.

INTRODUCTION

The use of fabric filters to remove particles from gas streams is a well established industrial practice and is currently a cost-effective particulate control technique for many coal-fired electric utilities.

Electrostatic fabric filtration (ESFF) differs from conventional fabric filtration in the application of a non-ionizing electrostatic field at the fabric/dirty gas interface. ESFF can be achieved by applying a voltage across very fine stainless steel electrodes woven into the cloth in the warp direction or with external electrodes. The residual and operating pressure drops are reduced substantially with apparently no loss in collection efficiency. Previous laboratory and pilot-scale studies have consistently demonstrated this reduced pressure drop effect.

The original concept of ESFF was developed by Lamb and Costanza.¹ Continuing research under the sponsorship of the U.S. Environmental Protection Agency has encompassed:

- * Laboratory experiments at Textile Research Institute (TRI) and Research Triangle Institute (RTI) to develop a more basic understanding of the fundamental mechanisms of ESFF.
- * Pilot studies of pulse jet and reverse-air ESFF applied to an industrial boiler at a Du Pont facility in Waynesboro, Virginia.
- * In-house research on EPA facilities at the laboratory and small pilot unit scale.

As a logical extension of previous work, the application of ESFF to a large-scale electric utility pilot was undertaken. The purpose of this project is to determine the technical feasibility of ESFF applied to flue gas from a coal-fired electric utility boiler. Use of the SPS pilot fabric filter with its full scale bags, consistent operating conditions, and proven scale-up history has overcome many problems previously encountered with smaller pilot scale and laboratory work.

This project has accomplished two first-time achievements:

- 1) The first application of ESFF to a commercial-scale fabric filter bag.
- 2) The first demonstration of a woven-in electrode fiberglass filtration fabric for ESFF on a commercial scale.

DESCRIPTION OF THE PILOT UNIT

The pilot fabric filter at Harrington Station is a two-compartment baghouse filtering flue gas slip-streamed from the Unit 2 boiler. Each of the two compartments contains 6 filter bags (two rows of three), the same size as employed in the main baghouse (30 ft, 9 in.* by 11.5 in). The bags are suspended from shaker tubes by a J-hook and spring mechanism. The deflation fan is capable of providing sufficient flow to allow the unit to be used for either shake/deflate or reverse air cleaning studies.

Temperature control in the pilot unit is achieved by blending flue gas streams taken from before and after the air preheater (see Figure 1). The flow is then split into two separate streams where the flow rate is measured by individual venturi flow meters and controlled with butterfly valves.

CLEANING CYCLE AND OPERATING CONDITIONS

During the ESFF testing program, the cleaning cycle was set up to duplicate a typical reverse air collector. Operating specifications are listed below:

*Readers more familiar with metric units are asked to use the conversion factors at the end of this paper.

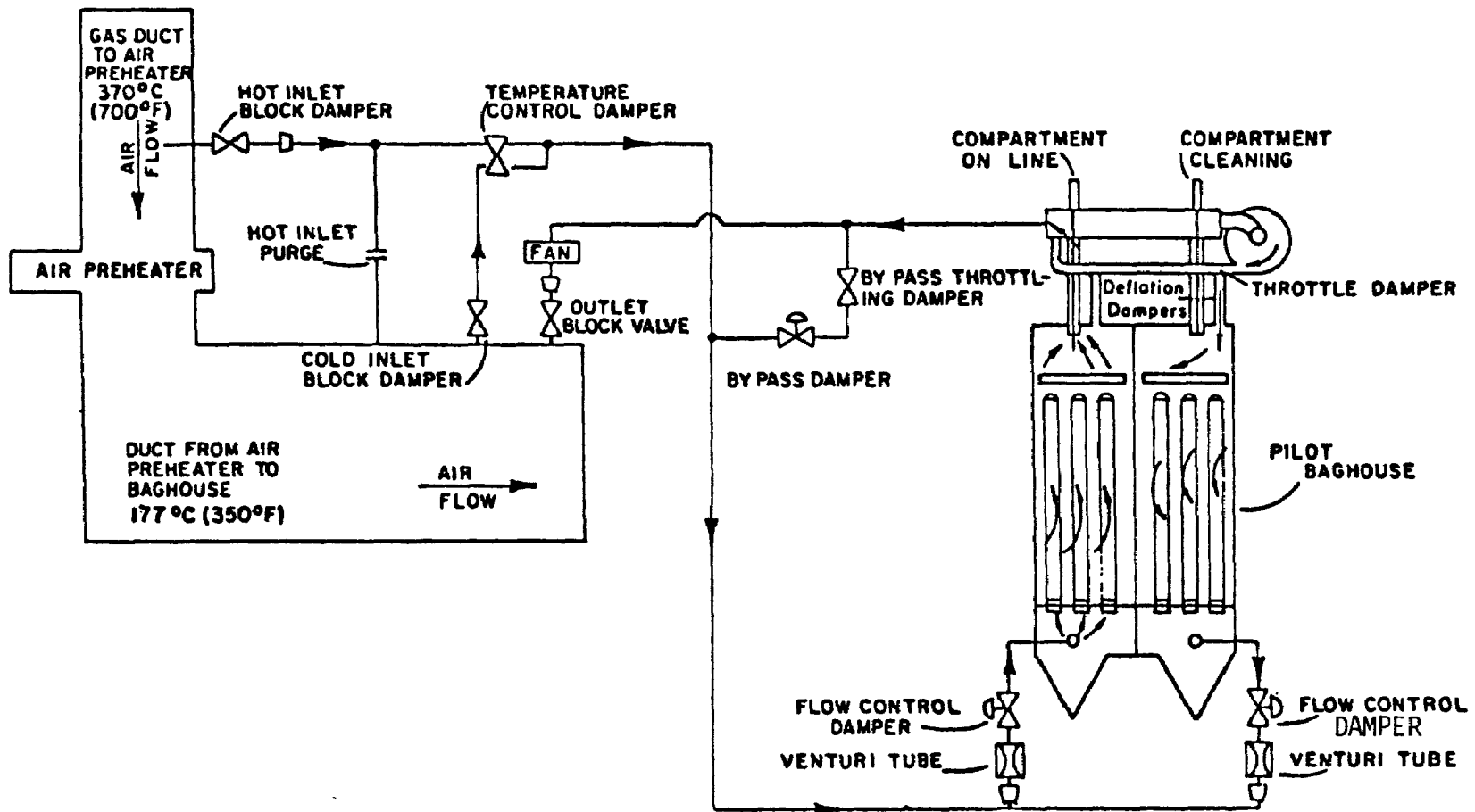


Figure 1. Schematic of Southwestern Public Service pilot fabric fiber unit.

First Settle	30 sec
Reverse Air (R/A)	45 sec
Second Settle	30 sec
R/A air-to-cloth	1.3-1.5
Filtration Cycle	60 min
Grain Loading	1.5-2.0 gr/scf
Inlet Temperature	400°F
Field Strength	2.4-2.6 kV/cm

ELECTRICAL SYSTEM DESIGN

A schematic of the electrical system arrangement is shown in Figure 2. The system has two power supplies rated -15 kV @ 10 mA. Each of the power supplies is attached to one row of three bags in the west compartment. The electrical control and monitoring systems include:

Continuous digital display and strip chart recording of the applied voltage and current for each power supply (i.e., each row of three bags).

Continuously, variably applied voltage control for each power supply.

The capability to measure independently, with a panel-mounted analog electrometer, the voltage applied to either row of bags.

The design of the electrical system incorporated a number of safety features to make sure that the operating and maintenance personnel were not exposed to high voltage. These included the following:

Removal of all high voltage when the baghouse access door is opened.

Removal of all high voltage when the power supply cabinet door is opened.

Short-circuiting of all high voltage leads to ground whenever the high voltage is turned off to discharge any static voltage remaining on the bags.

ELECTRICAL SYSTEM OPERATION

Power is applied to the bags after a 30-sec delay following the beginning of a filtering cycle. This delay allows the bags to become mechanically stable after the filtering cycle begins and is designed to prevent arcing between adjacent bags. Likewise, the power to the bags is turned off as soon as the cleaning cycle begins to avoid arcing as the bags collapse.

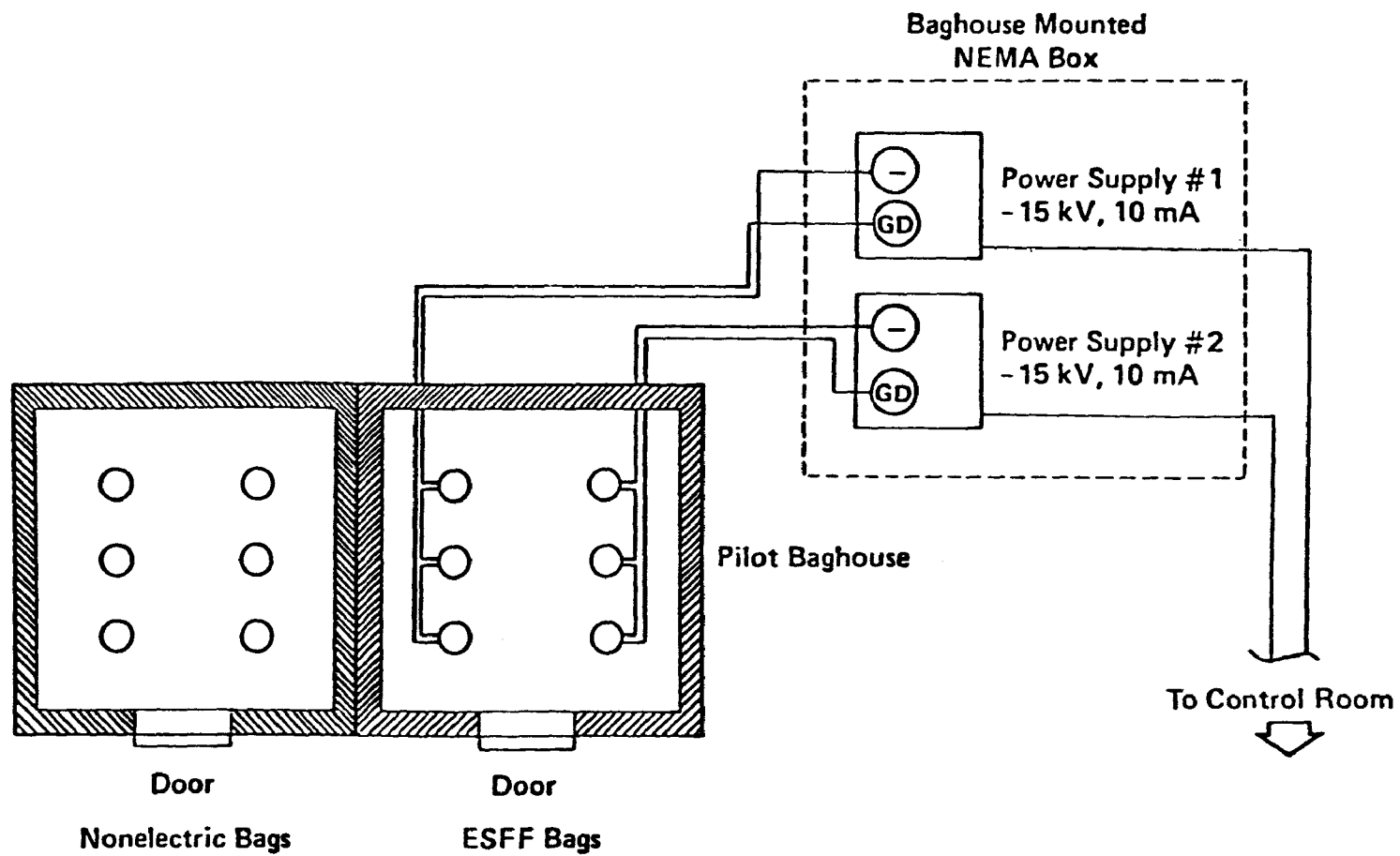


Figure 2. Electrical arrangement of bags.

ESFF FABRIC

The fabric chosen for use in this project was J. P. Stevens 648. This fabric was preferred because of its texturized warp and fill weave construction (warp - 37 1/0 T 37 1/0 F; fill - 75 1/3 T) since previous testing indicated that ESFF works better with highly texturized surfaces.

J. P. Stevens made approximately 200 yd (linear) of fabric with woven-in Bekaert VN22/1X90 stainless steel wire spaced at 2 cm intervals. The fabric was made into filter bags by Menardi-Southern Corporation in Torrance, California. After construction, a stainless steel braid was attached to the bag to electrically connect every other electrode at each end of the bag (see Figure 3). Thus, the braid at the top of the bag connected the odd electrodes, and the bottom braid connected the even ones. The bottom braid was connected to ground and the top braid to the power supply.

Two types of anticollapse rings were used in the bags. Solid Teflon O-rings were used in six of the bags and conventional 3/16-in. steel anticollapse rings covered with two envelopes of 30 mil TFE Teflon were used on the remaining six bags. Three Teflon-ringed bags and three steel-ringed bags were used in each compartment.

Bags for the control compartment were constructed in the same manner as the ESFF bags except that the steel electrode was not inserted in the cloth.

TEST PLAN

The goal of the ESFF project is to determine the technical feasibility of ESFF applied to low sulfur western coal. To this end, a test program was devised to measure ESFF performance at various air-to-cloth ratios over an extended period of time.

START-UP

In addition to normal start-up checkouts and system testing, the pilot unit was operated at several air-to-cloth ratios to get a feel for the performance of ESFF so that a high, low, and intermediate load could be assigned for further testing.

CONSTANT LOAD RUNS

The pilot was run for extended (2 to 4 weeks) periods at constant air-to-cloth ratios to establish performance under these conditions. The air-to-cloth ratios used, determined from start-up data, were 2.0, 3.0, and 4.0.

FIRST CYCLING TEST

To approximate actual utility boiler cycling conditions, the ESFF pilot unit was operated for 8 hr a day each at air-to-cloth ratios of 2.0, 3.0,

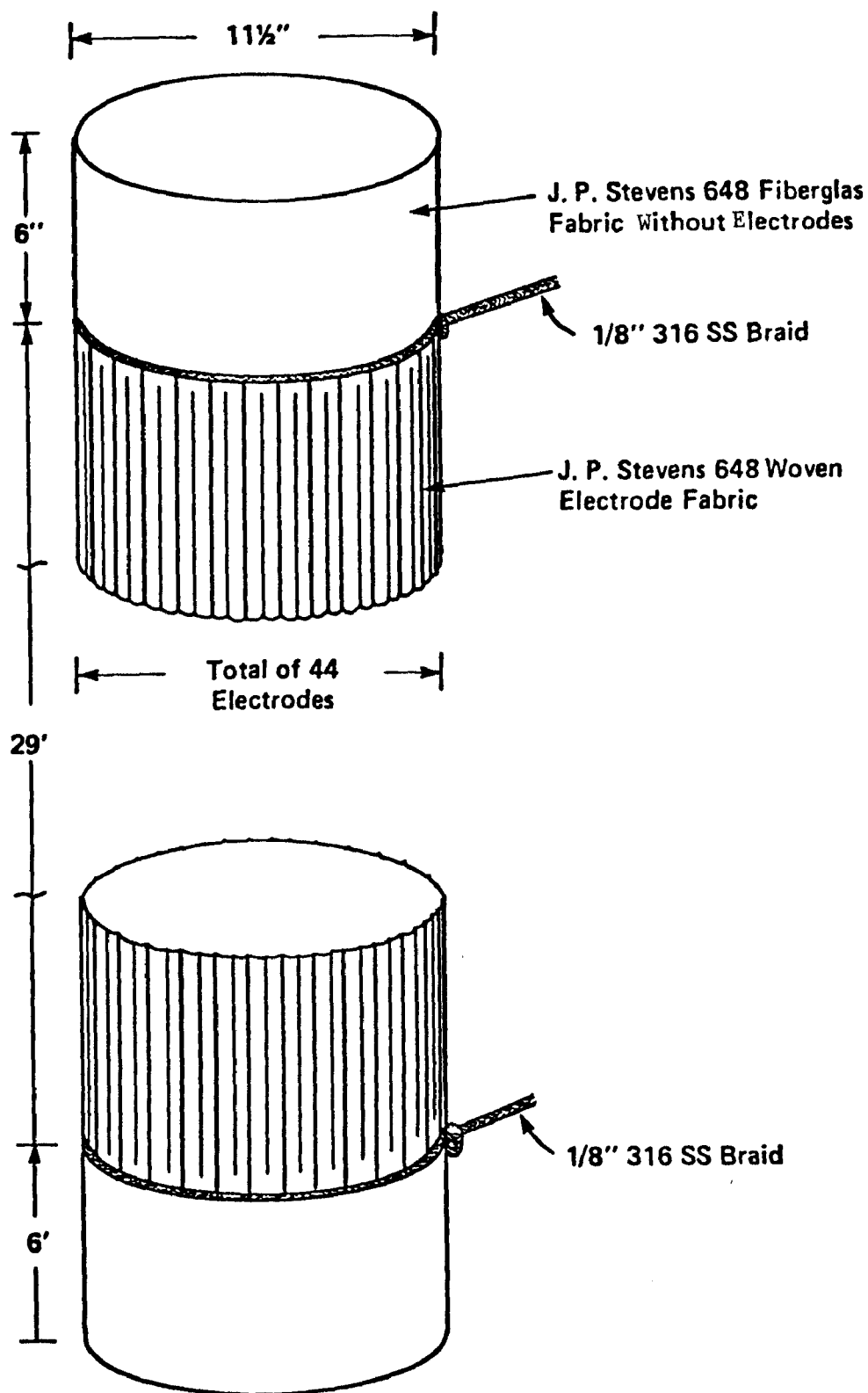


Figure 3. Construction of the woven electrode bags.

and 4.0 (corresponding roughly to low, intermediate, and high load conditions on the Unit 2 Harrington boiler). The first cycling test was scheduled for 16 weeks.

INTERMEDIATE CONSTANT LOAD RUN

Following the first cycling test, a constant air-to-cloth ratio test will be repeated to measure any change in performance that might take place since the first constant load runs.

SECOND CYCLING TEST

The second cycling test calls for a duplication of the first cycling test over the same time period. This phase of the test plan has not been finalized.

FURTHER TESTING

Additional testing is allocated by the test plan to allow time to study phenomena occurring in the program that might warrant further study. The time period allowed will depend on funding constraints and testing requirements.

ESFF TESTING TO DATE

Start-up of the pilot unit began on May 12, 1983. Testing was done at several air-to-cloth ratios between 2.0 and 4.0 (both the ESFF and nonelectric compartments were always operated at the same air-to-cloth ratio). Several trends were apparent from the limited data taken during start-up.

The residual pressure drop, ΔP_R , for the ESFF filter bags was less than for the nonelectric bags. This was true at each of the air-to-cloth ratios between May 13 and 16, namely 2.0, 3.0, and 4.0 ft/min. At air-to-cloth ratios of up to 4.0, the residual pressure drop was about 2 in. H_2O on the ESFF bags and about 4 in. H_2O on the nonelectric bags.

A higher air-to-cloth ratio caused higher power supply current. Although this effect was small (for example, the current at 2.0 ft/min and at a voltage of about -5 kV on the west row of three ESFF bags was about 6.7 mA; under identical conditions but at 4.0 ft/min, the current was 7.5 mA), the trend was nonetheless consistent, repeatable, and reversible.

The instantaneous ratio of pressure drop readings for the ESFF compartment to that of the nonelectric compartment was about 0.5 to 0.6. (This value could generally be obtained at any point in the filtration cycle.)

The slope of the "linear" portion of the pressure drop/time curve for the ESFF compartment divided by that of the nonelectric compartment

was about 0.5 to 0.7.

After several weeks of testing to determine appropriate operating conditions at air-to-cloth ratios of 2.0, 3.0, and 3.4 ft/min, 24-hr tests were made at each of these three conditions. (The upper air-to-cloth ratio was limited to 3.4 at this point -- several weeks after start-up; i.e., late May 1983 -- due to the capacity of the pilot unit fan. Table 1 shows the results of these initial tests, which indicate that:

For both the ESFF and nonelectric bags, the effective pressure drop (ΔP_E), the terminal pressure drop (ΔP_T), and the specific dust cake resistance (K_2) increase with air-to-cloth ratio, as expected. ΔP_E is the value of the pressure drop at the beginning of the filter cycle as obtained from extrapolation of the ΔP vs. time curve to zero time (i.e., the beginning of filter cycle).

The values of ΔP_E , ΔP_T , and K_2 are lower for the ESFF bags than for the nonelectric bags at each air-to-cloth ratio.

The ratio of $(K_2)_{\text{ESFF}} / (K_2)_{\text{nonelectric}}$ is about 0.58 (varying from 0.55 to 0.60) at each air-to-cloth ratio. This value is lower than similar values obtained in pilot tests at Waynesboro (approximately 0.70) for limited runs on different fly ash. The 0.58 value means that the average rate of rise of pressure drop during a filtering cycle is about 70 percent ($1/0.58 = 1.72$) greater for the nonelectric bags than for the ESFF bags.

TABLE 1. COMPARISON OF ESFF AND NONELECTRIC FILTRATION
AT VARIOUS AIR-TO-CLOTH RATIOS^a

A/C ^b ft/min	ESFF $P_{E H_2O}$ in. H ₂ O	Nonelec. $P_{E H_2O}$ in. H ₂ O	ESFF K_2^c	Nonelec. K_2^c	ESFF $\Delta P_{T H_2O}$ in. H ₂ O	Nonelec. $\Delta P_{T H_2O}$ in. H ₂ O
2.1	1.35	2.28	9.9	17.8	1.69	2.89
3.1	2.23	4.14	13.5	22.4	3.27	5.25
3.4	2.97	5.77	15.0	27.0	4.46	8.44

^aData taken 6/7-6/10/83, field strength = 2.4-2.6 kV/cm, filtering cycle=1hr
^bAir-to-cloth ratio. The value was limited by the baghouse fan capacity to 3.4

CONSTANT LOAD TESTS

Subsequent to these tests at three air-to-cloth ratios, an extended test was run at the following conditions:

Air-to-cloth ratio: 3.0 ft/min
Cleaning cycle: 1 hr

Field strength: 2.4-2.6 kV/cm

The test was run for a total of 1,076 hours (approximately 45 days). The results are shown in Figure 4. The drop in ΔP at day 21 was due to failure of the pilot plant ID fan (equipment unrelated to the ESFF test effort, but which forced the pilot baghouse unit off-line). Results from this extended test may be summarized as follows:

The ESFF pressure drop readings, both ΔP_E and ΔP_T , were lower than those for the nonelectric bags throughout the entire test. The ESFF pressure drop averaged about 50 to 55 percent of the nonelectric pressure drop.

For both the ESFF and the nonelectric bags, the pressure drop readings (both ΔP_T , and, more importantly, ΔP_E) appeared to rise with time throughout the test.

Subsequent to the extended test at 3.0 air-to-cloth ratio, a test of about 370 hours duration at 2.0 air-to-cloth ratio was performed. The field strength and cleaning cycle were the same as for the test at 3.0. The results for this trial are shown as the lower pair of curves in Figure 5 and may be summarized as follows:

As with the previous test, at a 2.0 air-to-cloth ratio, ΔP_E and ΔP_T are less for the ESFF bags than for the nonelectric bags. The pressure drop rise during the filtering cycle, $\Delta P_T - \Delta P_E$, is also less for the ESFF bags than of the nonelectric bags.

It appears that the pressure drop is stable with time.

It was also observed that, at a constant power supply setting, the field strength was slightly higher and the current slightly lower at 2.0 ft/min than at 3.0 ft/min. This may be due to less electrical conductance attributable to a presumably thinner dust cake at the lower air-to-cloth ratio.

Subsequent to the tests at the 2.0 air-to-cloth ratio, the pilot unit was taken off-line on August 9, 1983, to inspect the bags for wear and to take fabric samples for analysis. The following observations were made:

Dust was present in both compartments on the clean side of the fabric, although there was a slightly heavier deposit of dust in the nonelectric compartment than in the ESFF compartment.

The solid Teflon O-rings in the west (ESFF) compartment as well as the east (nonelectric) compartment were substantially deformed. The Teflon rings toward the bottom of the bag were deformed more than the upper ones, presumably since they cooled first.

On the ESFF bags, every other electrode appeared to be clean from the outside of the bag where dust had been deposited. This clean electrode was determined to be grounded.

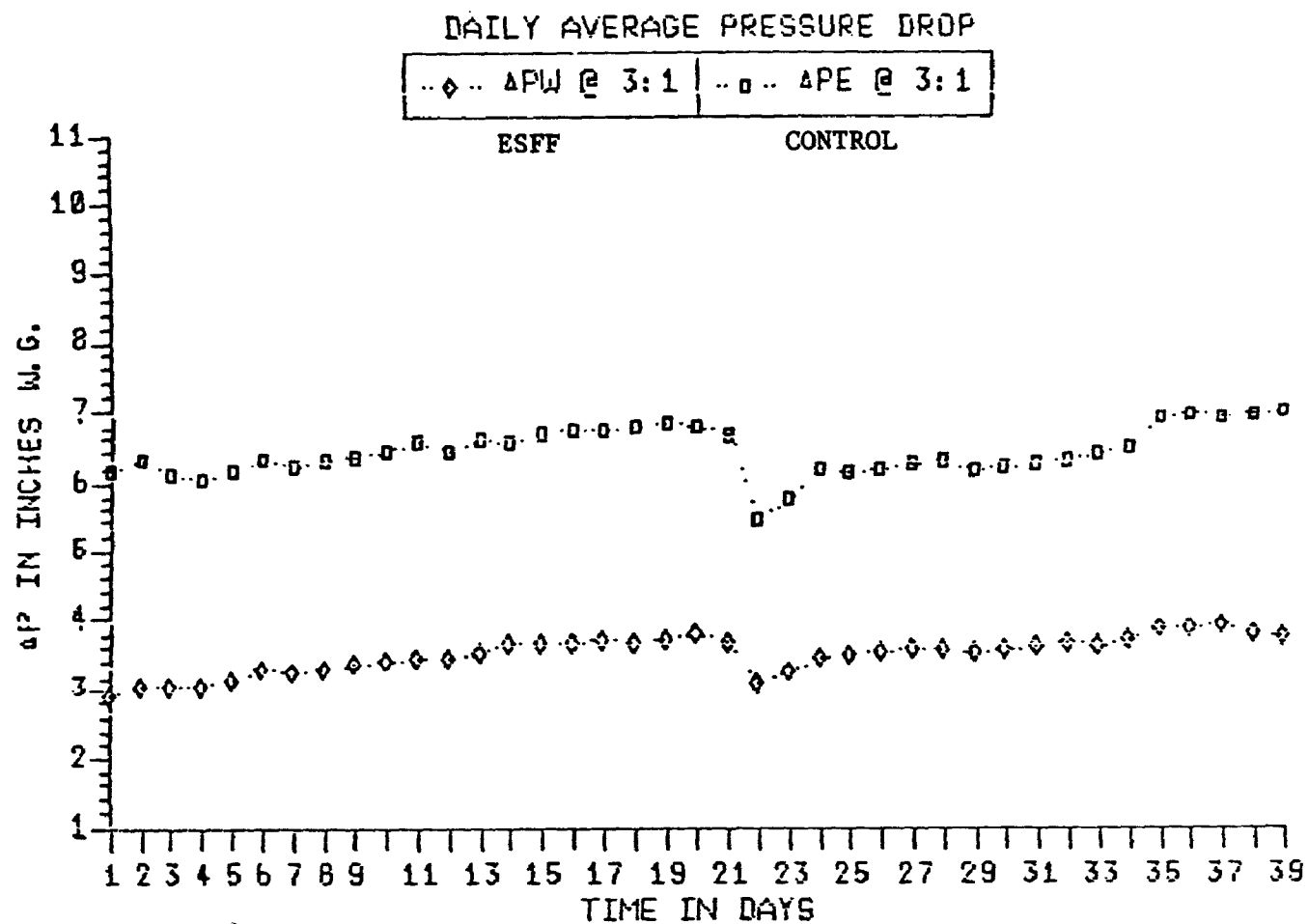


Figure 4. Constant Load Runs 3:1

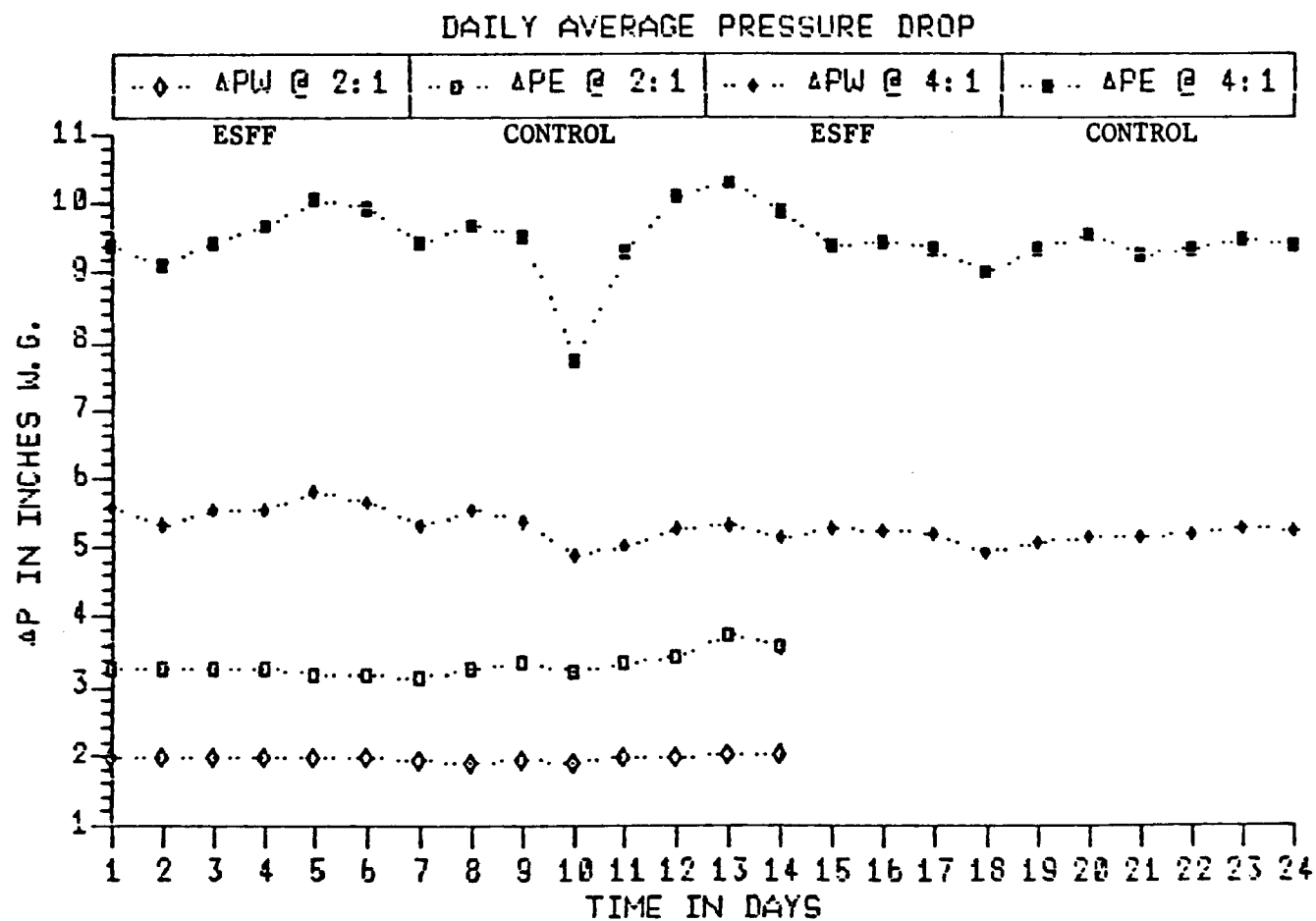


Figure 5. Constant Load Runs 2:1 and 4:1

The solid Teflon-ringed ESFF bags had less outside dust deposit than the steel-ringed bags. This may be due to the collapsing of the Teflon rings as they cooled.

There were no tears or pinholes apparent in a visual inspection of all bags. Neither were there areas where adjacent bags appeared to have rubbed against one another.

There was no visible wear around the electrodes in the ESFF bags.

Next, dust samples were taken from both the ESFF and nonelectric bags. The following items were noted:

On the ESFF and the nonelectric bags, the residual dust loadings (these bags were taken off-line immediately after the cleaning cycle) were much greater at the upper end of the bag than at the lower end.

The residual dust loading on the ESFF bag was substantially less than on the nonelectric bag. The gross weights of the ESFF and nonelectric bags (excluding the weights of the small samples that were taken), including the Teflon anti-collapse rings, were 32 and 56 lb, respectively. The residual dust loading for these bags was:

<u>Bag Type</u>	<u>Residual dust load, lb/ft²</u>
ESFF	0.16
Nonelectric	0.42

On August 10, 1983, the pilot unit was restarted. Inadvertently, the air flow rate was set at 2,184 cfm, corresponding to an air-to-cloth ratio of 4.8 ft/min. The unit ran at this higher air-to-cloth ratio for about 6 hr. Although the data are very limited, the following observations were made at this air-to-cloth ratio before the flow rate was lowered to 1,830 cfm (corresponding to an air-to-cloth ratio of 4.0 ft/min, cleaning cycle at 1 hr):

<u>Elect. Fld</u>	<u>East Row (3 ESFF bags)</u>	<u>West Row (2 ESFF bags)</u>	<u>ΔP (in. w.g.)</u>	<u>ESFF</u>	<u>Nonelectric</u>
kV	5.91	5.60	P_T	7.7	10.0
mA	0.82	1.40	P_E	5.6	8.0

The air-to-cloth ratio for the pilot unit was reset at 4.0 ft/min and continued to operate at this air-to-cloth ratio through the end of August. These data are shown as the upper pair of curves in Figure 5. On the tenth day of testing, the unit was forced off line, accounting for the drop in average ΔP in Figure 5. The pressure drop does not appear to be increasing with time, and the ESFF effect continues to reduce pressure drop substantially.

CYCLING TESTS

Subsequent to a scheduled outage of the Unit 2 boiler from the end of August through the end of October, the pilot unit baghouse was restarted on October 25 and run in a cycling mode aimed at simulating realistic boiler load swings. The air-to-cloth ratio was varied as follows:

<u>Air-to-cloth ratio, ft/min</u>	<u>Period of time during which air-to-cloth ratio is maintained, hr.</u>
4.0	8
3.0	8
2.0	8

The cycle is repeated continuously to approximate the normal air-to-cloth variation of the main baghouse resulting from the normal variation in boiler load.

The results from this cyclical testing are shown in Figures 6 and 7. As shown, the daily average pressure drop (calculated as the time-averaged pressure drop over the course of a 1-hr filter cycle, with 24 such hourly values being averaged to give the average pressure drop for the day) is less for the ESFF bags than for the nonelectric bags at all air-to-cloth ratios. Also important is the observation that the nonelectric compartment average pressure drop appears to be increasing with time at all air-to-cloth ratios, while the average pressure drop appears stable for the ESFF bags. The mean values of the daily average pressure drop for the period October 25, 1983, through February 20, 1984, are shown in Table 2.

TABLE 2. MEAN DAILY AVERAGE PRESSURE DROPS FOR ESFF
AND NONELECTRIC BAGS

Air-to-cloth ratio, ft/min	Daily ΔP_{avg} , averaged over the period 10/25/83-02/20/84, in. w.g.		Ratio of ΔP 's, in. w.g.
	Nonelectric	ESFF	
4.0	9.55	5.77	0.60
3.0	5.80	3.40	0.59
2.0	2.41	1.58	0.66

The values above show the distinct reduction in the average pressure drop for the ESFF bags, averaging about 40 percent. If casing losses of 1.5 to 2.5 in. w.g. are added to the cell plate pressure drops shown above, a full scale fabric filter operating under these conditions might be expected to have a pressure drop of 7.3-8.3 in. w.g. at an air-to-cloth ratio of 4.0. Correspondingly, at air-to-cloth ratios of 2.0 and 3.0, the expected pressure drops would be 3.08-4.08 and 4.9-5.9 in. w.g., respectively. Further extended tests, such as those to be done during the cycling tests,

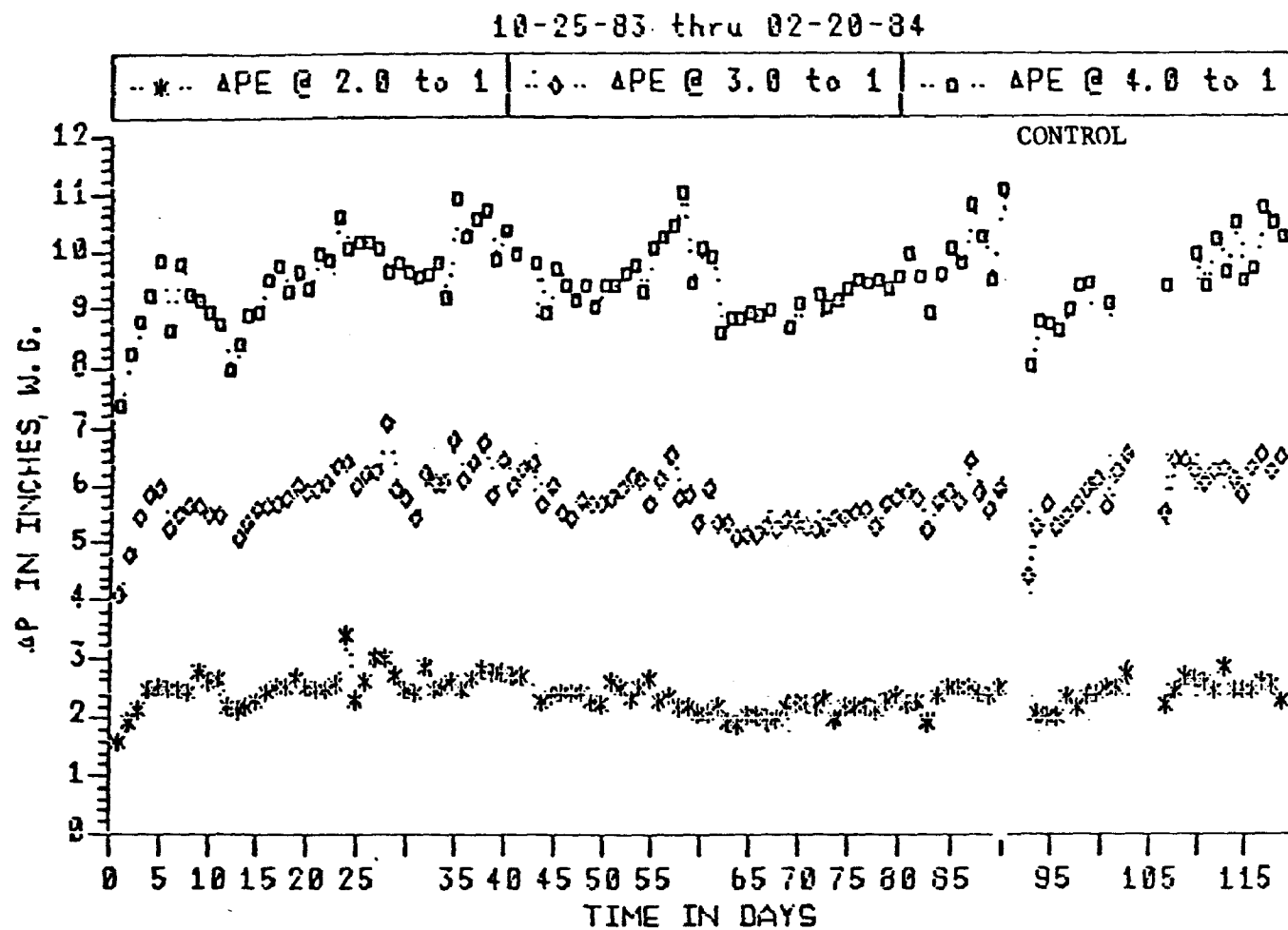


Figure 6. Cyclic Load Test Control

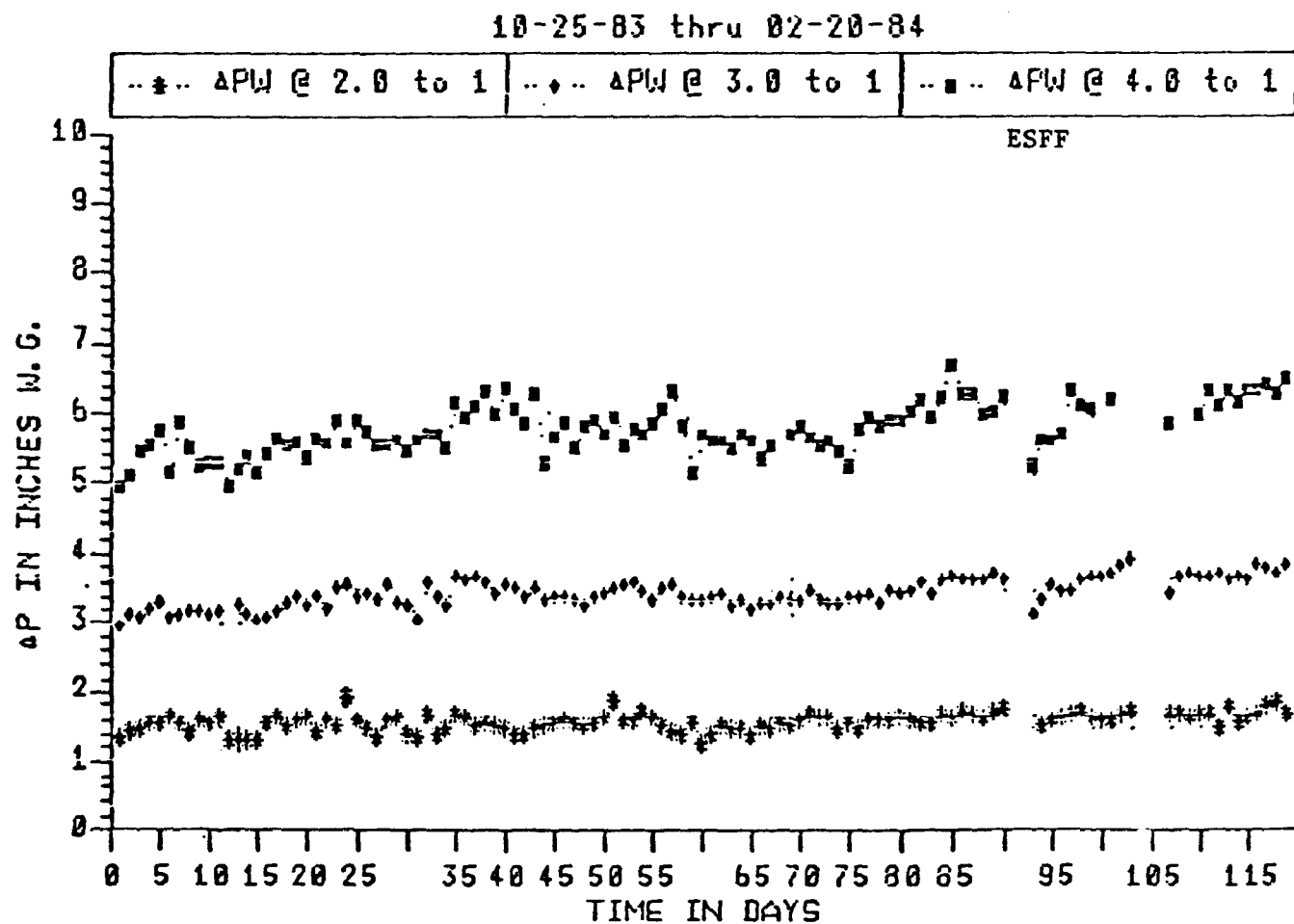


Figure 7. Cyclic Load Test ESFF

will be necessary to determine if the pressure drop for the ESFF bags is stable with time. Also, additional large-scale tests on other ashes will be needed to determine the applicability of ESFF: although, pilot and bench-scale tests on other ashes have consistently shown reduced pressure drop, albeit to varying degrees (VanOsdell and Furlong²; and Lamb and Costanza¹).

REFERENCES

- ¹Lamb, G. E.R., P.A. Costanza, "Electrical Stimulation of Fabric Filtration," Textile Res. J., 47, May 1977, PP. 372-80.
- ²VanOsdell, D.W., D.A. Furlong, Electrostatic Augmentation of Fabric Filtration: Reverse-Air Pilot Unit Experience, EPA-600/7-84-085 (NTIS PB84-230002), U.S. EPA, Research Triangle Park, NC, August 1984.

METRIC EQUIVALENTS

Readers more familiar with metric units may use the following to convert to the system.

<u>Nonmetric</u>	<u>Times</u>	<u>Yields Metric</u>
cfm	4.719×10^{-4}	m^3/s
ft	0.3048	m
ft/min	5.08×10^{-3}	m/s
°F	$(°F-32)/(1.8)$	°C
gr/scf	2.29	g/sm^3
in.	2.54	cm
in. H ₂ O	249	Pa
lb	0.454	kg
lb/ft ²	4.882	kg/m^2
mil	2.54×10^{-5}	m
yd	0.914	m